12th european symposium on vascular biomaterials

NEW ENDOVASCULAR TECHNOLOGIES | FROM BENCH TEST TO CLINICAL PRACTICE

esvb 2021

Biomaterials, Education and Digital Technologies for Patient Management in Vascular Surgery

- Robotics, non-X-Ray guidance, and latest trends in per-operative imaging technologies
- Updates in endovascular surgery: aortic and peripheral
- Compliance
- Education
- Infection
- The near future

Editors :

Nabil Chakfé | Strasbourg, France

Frédéric Heim | Mulhouse, France

Gert J. de Borst | Utrecht, The Netherlands

Ulf Hedin | Stockholm, Sweden

Wolfgang Meichelboeck | Pentenried, Germany

Biomaterials, Education and Digital Technologies for Patient Management in Vascular Surgery

Robotics, non-X-Ray guidance, and latest trends in per-operative imaging technologies
Updates in endovascular surgery: aortic and peripheral
Compliance
Education
Infection
The near future

Editors

Nabil CHAKFÉ
Department of Vascular Surgery and Kidney Transplantation,
University Hospital of Strasbourg, Strasbourg, France
& Groupe Européen de Recherche sur les Prothèses Appliquées à la Chirurgie Vasculaire (GEPROVAS),
Strasbourg, France

Frédéric HEIM
Laboratoire de Physique et Mécanique Textiles, ENSISA,
Mulhouse, France
& Groupe Européen de Recherche sur les Prothèses Appliquées à la Chirurgie Vasculaire (GEPROVAS),
Strasbourg, France

Ulf HEDIN
Department of Vascular Surgery, Karolinska University Hospital,
Stockholm, Sweden

Gert J. de BORST
Department of Vascular Surgery, University Medical Center Utrecht,
Utrecht, The Netherlands

Wolfgang MEICHELBOECK
Pentenried, Germany

This volume was published at the time of the 12 th edition of the European Symposium of Vascular Biomaterials, which took place in Strasbourg from 4 th to 6 th of November 2021

Organized by the GEPROVAS

The **GEPROVAS**-Groupe Européen de Recherche sur les Prothèses Appliquées à la Chirurgie Vasculaire-is a **unique and pioneer organization. Only independent platform of vascular explant analysis in the world,** the GEPROVAS was established out of a common will from Pr. Nabil CHAKFÉ, vascular surgeon (Strasbourg) and from Pr. Bernard DURAND (Laboratoire Physique et Mécanique des Textiles, ENSISA, Mulhouse) to **understand and characterize a certain number of complications occurring on vascular prostheses, in particular tearing and rupture phenomenon that could be observed after several years of implantation in patients.** Strong from an intensive collaboration between the Department of Vascular Surgery and Kidney Transplantation from Strasbourg and the laboratory of textile physic and mechanic in the person of Pr. Frédéric HEIM, the GEPROVAS quickly became a reference in the field.

Henceforth **major actor in vascular medical device appraisal and analysis,** the GEPROVAS has an innovative and multidisciplinary approach covering the life cycle of a medical device from the innovation to explant analysis, clinical follow-up but also the **training of vascular surgeons** from all over Europe in our new René KIENY Simulation Training Center in Strasbourg, France.

This year was highly important for the GEPROVAS, since we decided to merge all surgical specialties to share their experiences according to the Cycle of the Implant. We are creating a large place for innovation, research, patient safety and education inside an Institute whose name will be given very soon. We hope to welcome you in with unique in our future building.

More than ever, the Institute will be a global open place for all of you who would like to be part of the story we are writing.

Professor Nabil CHAKFÉ and Professor Frédéric HEIM

For more information, visit our website www.geprovas.org

Contributors

Mohamed Ahmed ABDELHALIM

Academic Department of Vascular Surgery,
Guy's and St Thomas' NHS Foundation Trust and
King's College London, School of Cardiovascular
Medicine and Sciences, St Thomas' Hospital,
London, United Kingdom

Saber Ben ABDESSALEM

Textile Materials and Processes Research Unit
(MPTex), ENIM, University of Monastir,
Monastir, Tunisia

Yogesh ACHARYA

Western Vascular Institute, Department of Vascular
and Endovascular Surgery, University Hospital,
National University of Ireland Galway,
Galway, Ireland
& Department of Vascular Surgery and Endovascular
Surgery, Galway Clinic, Doughiska, Royal College of
Surgeons in Ireland and National University
of Ireland, Galway affiliated Hospitals,
Galway, Ireland

Sara ALLIEVI

Vascular Surgery Department,
Fondazione IRCCS Ca' Granda Ospedale
Maggiore Policlinico,
Milan, Italy

Dimitri AMIRAS

Department of Surgery
and Cancer, Imperial College London
and Department of Radiology,
Imperial College Healthcare NHS Trust,
London, United Kingdom

Christian APEL

Dept. of Biohybrid & Medical Textiles (BioTex),
Applied Biomedical Engineeering,
RWTH Aachen University,
Center for Biohybrid Medical Systems (CBMS),
Aachen, Germany

Mélissandre ASFAZADOURIAN

LVTS, INSERM U 1148, Université de Paris,
Université Sorbonne Paris Nord,
Villetaneuse, Paris, France

Ferdinando AURICCHIO

Department of Civil Engineering and
Architecture (DICAr), University of Pavia,
Pavia, Italy

Hualong BAI

Department of Vascular and Endovascular Surgery,
First Affiliated Hospital of Zhengzhou University,
Henan, China
& Key Vascular Physiology and Applied Research
Laboratory of Zhengzhou City,
Henan, China

Marc A. BAILEY

Leeds Institute of Cardiovascular and Metabolic
Medicine, School of Medicine, University of Leeds,
Leeds, United Kingdom
& Leeds Vascular Institute, Leeds General Infirmary,
Leeds Teaching Hospitals NHS Trust,
Leeds, United Kingdom

Frederico BASTOS GONÇALVES

Department of Angiology and Vascular Surgery,
Centro Hospitalar Universitário de Lisboa Central,
Hospital de Santa Marta,
Lisbon, Portugal
& NOVA Medical School,
Universidade NOVA de Lisboa,
Lisbon, Portugal

Isabelle BATAILLE

LVTS, INSERM U 1148, Université de Paris,
Université Sorbonne Paris Nord,
Villetaneuse, Paris, France

Hannah S. BAUER

Xeltis BV, De Lismortel 31,
Eindhoven, The Netherlands

Cécile BEBEAR

Université de Bordeaux, USC EA 3671,
Mycoplasma and chlamydia human infections,
Bordeaux, France
& CHU de Bordeaux, Bacteriology Department,
Bordeaux, France

Volker C. BEHR

Clinic for Radiology and Nuclear Medicine,
University Hospital Schleswig Holstein,
Campus Lübeck,
Lübeck, Germany

Christian-Alexander BEHRENDT

Department for Vascular Medicine,
Vascular Surgery – Angiology - Endovascular Therapy,
University Heart & Vascular Center,
University Medical Center Hamburg-Eppendorf,
Hamburg, Germany

Michael BELL

Leeds Institute of Cardiovascular and Metabolic
Medicine, School of Medicine, University of Leeds,
Leeds, United Kingdom

Xavier BERARD

CHU de Bordeaux, Vascular Sugery Department,
Bordeaux, France

Daniele BIANCHI

Civil Engineering and Architecture Department,
Università degli Studi di Pavia,
Pavia, Italy

Jean BISMUTH

Houston Methodist DeBakey Heart
and Vascular Center,
Houston, Texas, USA

Daniele BISSACCO

Vascular Surgery Department,
Fondazione IRCCS Ca' Granda Ospedale
Maggiore Policlinico,
Milan, Italy

Thorsten A. BLEY

Clinic for Radiology and Nuclear Medicine,
University Hospital Schleswig Holstein,
Campus Lübeck,
Lübeck, Germany

Christian BOEHM

Dept. of Biohybrid & Medical Textiles (BioTex),
Applied Biomedical Engineeering,
RWTH Aachen University,
Center for Biohybrid Medical Systems (CBMS),
Aachen, Germany

Tristan BOURCIER

GEPROVAS (Groupe Européen de Recherche sur
les Prothèses Appliquées à la Chirurgie Vasculaire),
Strasbourg, France
& UNISIMES (UNIté de SIMulation Européenne
en Santé),
Strasbourg, France
& Department of Ophthalmology,
University Hospital of Strasbourg,
Strasbourg, France

Stefano CASARIN

Department of Surgery, Houston Methodist Hospital,
Houston, Texas, USA
& Center for Computational Surgery,
Houston Methodist Research Institute,
Houston, Texas, USA
& Houston Methodist Academic Institute,
Houston, Texas, USA

Charles CAZANAVE

CHU de Bordeaux,
Infectious and Tropical Diseases Department,
Bordeaux, France
& Université de Bordeaux, USC EA 3671,
Mycoplasma and chlamydia human infections,
Bordeaux, France

Nabil CHAKFÉ

Department of Vascular Surgery and Kidney Transplantation, University Hospital of Strasbourg, Strasbourg, France
& GEPROVAS (Groupe Européen de Recherche sur les Prothèses Appliquées à la Chirurgie Vasculaire), Strasbourg, France
& UNISIMES
(UNIté de SIMulation Européenne en Santé), Strasbourg, France

Frédéric CHAUBET

LVTS, INSERM U 1148,
Université de Paris, Université Sorbonne Paris Nord, Villetaneuse, Paris, France

Arindam CHAUDHURI

Bedfordshire–Milton Keynes Vascular Centre, Bedfordshire Hospital NHS Foundation Trust, Bedford, United Kingdom

Claudio CHIASTRA

Laboratory of Biological Structure Mechanics (LaBS), Department of Chemistry, Materials and Chemical Engineering "Giulio Natta", Politecnico di Milano, Milan, Italy
& PoliToBIOMed Lab, Department of Mechanical and Aerospace Engineering, Politecnico di Torino, Turin, Italy

Roberto CHIESA

Division of Vascular Surgery,
IRCCS San Raffaele Scientific Institute,
Milan, Italy

Marc COGGIA

Department of Vascular Surgery,
Ambroise Paré University Hospital, AP-HP,
Boulogne-Billancourt, France
& Faculté de Médecine Paris-Ile de France-Ouest,
UFR des sciences de la santé Simone Veil,
Université Versailles Saint-Quentin en Yvelines,
Montigny-le-Bretonneux, France

Monika COLOMBO

Laboratory of Biological Structure Mechanics (LaBS), Department of Chemistry, Materials and Chemical Engineering "Giulio Natta", Politecnico di Milano, Milan, Italy
& Institute for Chemical and Bioengineering, Department of Chemistry and Applied Biosciences, ETH Zürich, Switzerland

Michele CONTI

Department of Civil Engineering and Architecture (DICAr), University of Pavia, Pavia, Italy

Anna CORTI

Laboratory of Biological Structure Mechanics (LaBS), Department of Chemistry, Materials and Chemical Engineering "Giulio Natta", Politecnico di Milano, Milan, Italy

Raphaël COSCAS

Department of Vascular Surgery,
Ambroise Paré University Hospital, AP-HP,
Boulogne-Billancourt, France
& Faculté de Médecine Paris-Ile de France-Ouest,
UFR des sciences de la santé Simone Veil,
Université Versailles Saint-Quentin en Yvelines,
Montigny-le-Bretonneux, France
& GEPROVAS (Groupe Européen de Recherche sur les Prothèses Appliquées à la Chirurgie Vasculaire), Strasbourg, France
& UMR 1018, Inserm-Paris11-CESP,
Versailles Saint-Quentin-en-Yvelines University,
Paris-Saclay University, Paul Brousse Hospital,
Villejuif, Paris, France

Martijn. A. J. COX

Xeltis BV, De Lismortel 31,
Eindhoven, The Netherlands

Alan DARDIK

Vascular Biology and Therapeutics Program,
and Department of Surgery,
and Department of Cellular and Molecular Physiology, Yale School of Medicine,
New Haven, Connecticut, USA

Gert J. de BORST

Department of Vascular Surgery,
University Medical Center,
Utrecht, The Netherlands

Eike Sebastian DEBUS

Department for Vascular Medicine,
Vascular Surgery – Angiology - Endovascular Therapy,
University Heart & Vascular Center, University
Medical Center Hamburg-Eppendorf,
Hamburg, Germany

Marina DIAS-NETO

Department of Vascular Surgery,
McGovern Medical School at
The University of Texas Health Science Center,
Houston, Texas, USA

Maurizio DOMANIN

Vascular Surgery Department,
Fondazione IRCCS Ca' Granda Ospedale
Maggiore Policlinico,
Milan, Italy
& Clinical and Community Sciences Department,
Università degli Studi di Milano,
Milan, Italy

Jonas EIBERG

Department of Vascular Surgery, Rigshospitalet,
Copenhagen, Denmark
& Copenhagen Academy for Medical Education
and Simulation, Centre for HR and Education
and The Capital Region of Denmark,
Copenhagen, Denmark

Mohammed S. EL-KURDI

Xeltis BV, De Lismortel 31,
Eindhoven, The Netherlands

Joshua EVES

Imperial Vascular Unit,
Imperial College Healthcare NHS Trust,
London, United Kingdom

Gábor FAZEKAS

Department of Vascular Surgery,
Medical School, University of Pécs,
Pécs, Hungary

Alicia FERNÁNDEZ-COLINO

Dept. of Biohybrid & Medical Textiles (BioTex),
Applied Biomedical Engineeering,
RWTH Aachen University,
Center for Biohybrid Medical Systems (CBMS),
Aachen, Germany

Rita Soares FERREIRA

Department of Angiology and Vascular Surgery,
Centro Hospitalar Universitário de Lisboa Central,
Hospital de Santa Marta,
Lisbon, Portugal
& NOVA Medical School,
Universidade NOVA de Lisboa,
Lisbon, Portugal

Aloke V. FINN

CVPath Institute,
Gaithersburg, Maryland, USA
& University of Maryland, School of Medicine,
Baltimore, Maryland, USA

Diego GALLO

PolitoBIOMed Lab, Department of Mechanical
and Aerospace Engineering, Politecnico di Torino,
Turin, Italy

David GARBAISZ

Semmelweis University,
Department of Vascular and Endovascular Surgery,
Budapest, Hungary

Mitchell J. GEORGE

Department of Vascular Surgery,
McGovern Medical School at The University
of Texas Health Science Center,
Houston, Texas, USA

Elizabeth L. GEORGE

Division of Vascular Surgery,
Stanford Hospitals and Clinic,
Stanford, California, USA

Lucie GERNEZ

LVTS, INSERM U 1148,
Université de Paris, Université Sorbonne Paris Nord,
Villetaneuse, Paris, France

K. Jane GRANDE-ALLEN

Department of Bioengineering, Rice University,
Houston, Texas, USA

Constantjin E.V.B. HAZENBERG

Department of Vascular Surgery,
University Medical Center Utrecht,
Utrecht, The Netherlands

Ulf HEDIN

Department of Vascular Surgery,
Karolinska University Hospital,
Stockholm, Sweden

Frédéric HEIM

Laboratoire de Physique et Mécanique Textiles (LPMT), ENSISA, Université de Haute Alsace,
Mulhouse, France
& GEPROVAS (Groupe Européen de Recherche sur les Prothèses Appliquées à la Chirurgie Vasculaire),
Strasbourg, France

Stefan HERZ

Clinic for Radiology and Nuclear Medicine,
University Hospital Schleswig Holstein,
Campus Lübeck,
Lübeck, Germany

Niamh HYNES

Department of Vascular Surgery and Endovascular Surgery, Galway Clinic, Doughiska, Royal College of Surgeons in Ireland and National University of Ireland, Galway affiliated Hospitals,
Galway, Ireland

Gábor JANCSÓ

Department of Vascular Surgery,
Medical School, University of Pécs,
Pécs, Hungary

Emily JANUS-BELL

Université de Strasbourg, INSERM, EFS Grand-Est,
Strasbourg, France

Jérémie JAYET

Department of Vascular Surgery,
Ambroise Paré University Hospital, AP-HP,
Boulogne-Billancourt, France
& Faculté de Médecine Paris-Ile de France-Ouest,
UFR des sciences de la santé Simone Veil, Université Versailles Saint-Quentin en Yvelines,
Montigny-le-Bretonneux, France
& GEPROVAS (Groupe Européen de Recherche sur les Prothèses Appliquées à la Chirurgie Vasculaire),
Strasbourg, France
& Laboratoire de Physique et Mécanique Textiles (LPMT), ENSISA, Université de Haute Alsace,
Mulhouse, France
& UMR 1018, Inserm-Paris11-CESP, Versailles Saint-Quentin-en-Yvelines University, Paris-Saclay University, Paul Brousse Hospital,
Villejuif, Paris, France

Hiba JAZIRI

Textile Materials and Processes Research Unit (MPTex), ENIM, University of Monastir,
Monastir, Tunisia

Hiroyuki JINNOUCHI

CVPath Institute,
Gaithersburg, Maryland, USA

Stefan JOCKENHOEVEL

Dept. of Biohybrid & Medical Textiles (BioTex),
Applied Biomedical Engineeering,
RWTH Aachen University,
Center for Biohybrid Medical Systems (CBMS),
Aachen, Germany
& Aachen-Maastricht-Institute for Biobased Materials (AMIBM), Maastricht University,
Brightlands Chemelot Campus,
Geleen, The Netherlands

Andrea KAHLBERG

Division of Vascular Surgery,
IRCCS San Raffaele Scientific Institute,
Milan, Italy

Fabien KAWECKI

Université de Bordeaux, Inserm, BIOTIS, UMR1026,
Bordeaux, France

Jurre KLAASSEN

Department of Vascular Surgery,
University Medical Center Utrecht,
Utrecht, The Netherlands

Netanel KORIN

Department of Biomedical Engineering Technion,
Israel Institute of Technology,
Haifa, Israel

Yevgeniy KRIENIN

Department of Biomedical Engineering Technion,
Israel Institute of Technology,
Haifa, Israel

Salomé KUNTZ

GEPROVAS (Groupe Européen de Recherche sur
les Prothèses Appliquées à la Chirurgie Vasculaire),
Strasbourg, France
& Department of Vascular Surgery and Kidney
Transplantation, University Hospital of Strasbourg,
Strasbourg, France
& UNISIMES
(UNIté de SIMulation Européenne en Santé),
Strasbourg, France

Nicolas L'HEUREUX

Université de Bordeaux, Inserm, BIOTIS, UMR1026,
Bordeaux, France

John LANGFORD

Vascular Biology and Therapeutics Program,
and Department of Surgery,
Yale School of Medicine,
New Haven, Connecticut, USA

Jason T. LEE

Division of Vascular Surgery,
Stanford Hospitals and Clinic,
Stanford, California, USA

Anne LEJAY

Department of Vascular Surgery and Kidney
Transplantation, University Hospital of Strasbourg,
Strasbourg, France
& GEPROVAS (Groupe Européen de Recherche sur
les Prothèses Appliquées à la Chirurgie Vasculaire),
Strasbourg, France
& UNISIMES
(UNIté de SIMulation Européenne en Santé),
Strasbourg, France

Léa LEPOIX

Université de Lorraine, faculté de droit de Nancy,
Nancy, France

Didier LETOURNEUR

LVTS, INSERM U 1148,
Université de Paris, Université Sorbonne Paris Nord,
Villetaneuse, Paris, France

Diletta LOSCHI

Division of Vascular Surgery,
IRCCS San Raffaele Scientific Institute,
Milan, Italy

Giulia LURAGHI

Laboratory of Biological Structure Mechanics (LaBS),
Department of Chemistry, Materials and Chemical
Engineering "Giulio Natta", Politecnico di Milano,
Milan, Italy

Fatima M'ZALI

Université de Bordeaux,
UMR 5234 CNRS, Aquitaine microbiologie,
Bordeaux, France

Robroy MACIVER

Children's Hospitals and Clinics of Minnesota,
Minneapolis, Minnesota, USA

Louis MAGNUS

Houston Methodist DeBakey Heart
and Vascular Center,
Houston, Texas, USA
& Department of Vascular Surgery and Kidney
Transplantation, University Hospital of Strasbourg,
Strasbourg, France
& GEPROVAS (Groupe Européen de Recherche sur
les Prothèses Appliquées à la Chirurgie Vasculaire),
Strasbourg, France

Pierre H. MANGIN

Université de Strasbourg, INSERM, EFS Grand-Est,
Strasbourg, France

Josè Felix Rodriguez MATAS

Laboratory of Biological Structure Mechanics (LaBS),
Department of Chemistry, Materials and Chemical
Engineering “Giulio Natta”, Politecnico di Milano,
Milan, Italy

Germano MELISSANO

Division of Vascular Surgery, IRCCS San Raffaele
Scientific Institute,
Milan, Italy

Gábor MENYHEI

Department of Vascular Surgery,
Medical School, University of Pécs,
Pécs, Hungary

Bijan MODARAI

Academic Department of Vascular Surgery,
Guy’s and St Thomas’ NHS Foundation Trust and
King’s College London, School of Cardiovascular
Medicine and Sciences, St Thomas’ Hospital,
London, United Kingdom

Francesco MIGLIAVACCA

Laboratory of Biological Structure Mechanics (LaBS),
Department of Chemistry, Materials and Chemical
Engineering “Giulio Natta”, Politecnico di Milano,
Milan, Italy

Sofiene MOKHTAR

Textile Materials and Processes Research
Unit (MPTex), ENIM, University of Monastir,
Monastir, Tunisia

Jonathan M. MORRIS

Medical Director of Anatomic Modeling Unit
Mayo Clinic, Department of Radiology,
Division of Neuroradiology
Rochester, Minnesota, USA

Srinidhi NAGARAJA

G. Rau Inc., Scotts Valley,
California, USA

Leizl Joy NAYAHANGAN

Copenhagen Academy for Medical Education and
Simulation, Centre for HR and Education
and The Capital Region of Denmark,
Copenhagen, Denmark

Nicole NEUMANN

GEPROVAS (Groupe Européen de Recherche sur
les Prothèses Appliquées à la Chirurgie Vasculaire),
Strasbourg, France

Gustavo S. ODERICH

Department of Vascular Surgery,
McGovern Medical School at The University
of Texas Health Science Center,
Houston, Texas, USA

Alan R. PELTON

G. Rau Inc., Scotts Valley, California, USA

Sabine PEREYRE

Université de Bordeaux, USC EA 3671,
Mycoplasma and chlamydia human infections,
Bordeaux, France
& CHU de Bordeaux, Bacteriology Department,
Bordeaux, France

Elena REDAELLI

Laboratory of Biological Structure Mechanics (LaBS), Department of Chemistry, Materials and Chemical Engineering “Giulio Natta”, Politecnico di Milano, Milan, Italy

Tiago RIBEIRO

Department of Angiology and Vascular Surgery, Centro Hospitalar Universitário de Lisboa Central, Hospital de Santa Marta, Lisbon, Portugal
& NOVA Medical School, Universidade NOVA de Lisboa, Lisbon, Portugal

Enrico RINALDI

Division of Vascular Surgery, IRCCS San Raffaele Scientific Institute, Milan, Italy

Anne-Florence ROUBY

GEPROVAS (Groupe Européen de Recherche sur les Prothèses Appliquées à la Chirurgie Vasculaire), Strasbourg, France
& Department of Vascular Surgery and Kidney Transplantation, University Hospital of Strasbourg, Strasbourg, France
& UNISIMES (UNIté de SIMulation Européenne en Santé), Strasbourg, France

Payman SAFFARI

Engage Medical Device Services, Inc., Newport Beach, California, USA

Atsushi SAKAMOTO

CVPath Institute, Gaithersburg, Maryland, USA

Annarita SANTORO

Division of Vascular Surgery, IRCCS San Raffaele Scientific Institute, Milan, Italy

Yu SATO

CVPath Institute, Gaithersburg, Maryland, USA

Adeline SCHWEIN

Houston Methodist DeBakey Heart and Vascular Center, Houston, Texas, USA
& Department of Vascular Surgery and Kidney Transplantation, University Hospital of Strasbourg, Strasbourg, France
& GEPROVAS (Groupe Européen de Recherche sur les Prothèses Appliquées à la Chirurgie Vasculaire), Strasbourg, France

Luigia SCUDELLER

Department of Clinical Epidemiology and Biostatistics, IRCCS Ca’ Granda Ospedale Maggiore Policlinico, Milan, Italy

Joseph SHALHOUB

Imperial Vascular Unit, Imperial College Healthcare NHS Trust, London, United Kingdom
& Department of Surgery & Cancer, Imperial College London, London, United Kingdom

Toshiharu SHINOKA

Nationwide Children’s Hospital, The Ohio State University Medical Center Columbus, Ohio, USA

Anthal I.P.M. SMITS

Department of Biomedical Engineering, Eindhoven University of Technology, Eindhoven, The Netherlands
& Institute for Complex Molecular Systems (ICMS), Eindhoven University of Technology, Eindhoven, The Netherlands

Abhilash SUDARSANAM

Imperial Vascular Unit, Imperial College Healthcare NHS Trust, London, United Kingdom

Ga-Young SUH

Department of Biomedical Engineering,
California State University,
Long Beach, California, USA

Sherif SULTAN

Western Vascular Institute, Department of Vascular and Endovascular Surgery, University Hospital Galway, National University of Ireland,
Galway, Ireland
& Department of Vascular Surgery and Endovascular Surgery, Galway Clinic, Doughiska, Royal College of Surgeons in Ireland and National University of Ireland, Galway affiliated Hospitals,
Galway, Ireland

Zeeshan H. SYEDAIN

Departments of Biomedical Engineering and Chemical Engineering,
Minneapolis, Minnesota, USA

Zoltan SZEBERIN

Semmelweis University,
Department of Vascular and Endovascular Surgery,
Budapest, Hungary

Jörg TESSAREK

Department of Vascular and Endovascular Surgery,
Bonifatius Hospital Lingen,
Lingen, Germany

Radu-Ionut TOADER

Department for Vascular Medicine,
Vascular Surgery – Angiology - Endovascular Therapy,
University Heart & Vascular Center, University Medical Center Hamburg-Eppendorf,
Hamburg, Germany

Giovanni Federico TORSELLO

Department of Radiology, Charité Campus Virchow-Klinikum, Charité University Medicine Berlin,
Berlin, Germany

Giovanni Battista TORSELLO

Institute for Vascular Research, Franziskus Hospital,
Münster, Germany

Robert T. TRANQUILLO

Departments of Biomedical Engineering and Chemical Engineering and Materials Science
University of Minnesota,
Minneapolis, Minnesota, USA

Lucille TREIL

GEPROVAS (Groupe Européen de Recherche sur les Prothèses Appliquées à la Chirurgie Vasculaire),
Strasbourg, France
& Department of Vascular Surgery and Kidney Transplantation, University Hospital of Strasbourg,
Strasbourg, France
& UNISIMES
(UNIté de SIMulation Européenne en Santé),
Strasbourg, France

Santi TRIMARCHI

Vascular Surgery Department,
Fondazione IRCCS Ca' Granda Ospedale Maggiore Policlinico,
Milan, Italy
& Clinical and Community Sciences Department,
University of Milan,
Milan, Italy

Jochen ULMER

Euroflex, GmbH,
Pforzheim, Germany

Paweł TULINSKI

BIOASTER,
Lyon, France

Joost A. Van HERWAARDEN

Department of Vascular Surgery,
University Medical Center Utrecht,
Utrecht, The Netherlands

Dragoslava P. VEKILOV

Department of Bioengineering, Rice University,
Houston, Texas, USA

Ramon VILA COLL

Department of Vascular Surgery, Hospital
Universitari de Bellvitge,
Barcelona, Spain

Régis VILLET

BIOASTER,
Lyon, France

Renu VIRMANI

CVPath Institute,
Gaithersburg, Maryland, USA

Patrick VOGEL

Clinic for Radiology and Nuclear Medicine,
University Hospital Schleswig Holstein,
Campus Lübeck,
Lübeck, Germany

F. WOLF

Dept. of Biohybrid & Medical Textiles (BioTex),
Applied Biomedical Engineeering,
RWTH Aachen University,
Center for Biohybrid Medical Systems (CBMS),
Aachen, Germany

Jianbiao XU

Vascular Biology and Therapeutics Program,
Yale School of Medicine,
New Haven, Connecticut, USA

Acknowledgements

The main idea of the European Symposium on Vascular Biomaterials was established out of a strong desire to bring together in a same place people from different backgrounds: research, clinical or industry to discuss, share ideas, collaborate on different topics related to vascular biomaterials. The first event was organised in 2001, in the city of Mulhouse, high place of the textile industry, with communication and collaborations as first objectives.

Edition after edition, the European Symposium of Vascular Biomaterials evolved, bringing together even more scientists, medical doctors, young researchers and industries to share and discuss together. Since 2005, this event takes place in the capital of Alsace, a high place of vascular surgery in the beginning of the 20th century with René LERICHE and René FONTAINE.

The 11th edition was our last meeting before the COVID era. Many things have changed in our practice, in our way of thinking and sharing knowledge.

The 12th edition is also the 20th anniversary of the meeting that becomes now a young adult. It is also the first edition in post-COVID era. We need to meet, to share and keep on working together for a better practice for our patients.

It is focusing on hot topics in the field as robotics, non-X-Ray guidance, latest trends in per-operative imaging technologies, but also updates in endovascular surgery: aortic and peripheral, infection, compliance, and on what could be the near future. Moreover, we dedicate a large room for education that we believe to be a cornerstone for patient safety.

We wish you a fruitful European Symposium on Vascular Biomaterials in terms of discussion, networking, idea-sharing and beginnings of collaboration. Have a pleasant time reading this ESVB 2021 Congress Book which gathers all the presentations occurring during this event edition! For the first time, we privilege an e-book to contribute in preserving the environment.

We want to thank all the members of the clinical, biological and mechanical departments of GEPROVAS. All the team has been fully involved in this event that reflects the philosophy of GEPROVAS. This year was a new year in terms of development with a new building and new human resources involved in this nice story we are writing. We also thank Arborescence for the realization of this congress e-book and the commitment of their team Frédéric JACQUET and Véronique OEUVRARD.

We also thank our institutional partners who supported this symposium through their advice, guidance, logistics and financial support: BioValley France, University of Strasbourg, University of Haute-Alsace, Strasbourg – Eurométropole, Council of the Grand-Est region, as well as the label Alsace.

Strasbourg, October 2021

Professor Nabil CHAKFÉ

Professor Frédéric HEIM

Contents

Education

1 | **3D Printing in Aortic Endovascular Therapies: a review** 20
Mitchell J. GEORGE, Marina DIAS-NETO, Gustavo S. ODERICH, Jonathan M. MORRIS

2 | **The Role of Industry in Vascular Education in Europe Introducing a ESVS wide survey** 30
Radu-Ionut TOADER, Eike Sebastian DEBUS, Christian-Alexander BEHRENDT

3 | **The role of industry in Vascular Education in North America** 35
Elizabeth L. GEORGE, Jason T. LEE

4 | **What does independence and conflict of interest mean for the lawyer?** 39
Léa LEPOIX

5 | **Education in Vascular Surgery: the ESVS academy experience** 45
Ramon VILA COLL, Jonas EIBERG, Leizl Joy NAYAHANGAN

6 | **The Vascupedia experience** 55
Giovanni Federico TORSELLO, Giovanni Battista TORSELLO

7 | **Which curriculum for trainees' education in vascular surgery? The GEPROVAS experience** 57
Anne-Florence ROUBY, Nicole NEUMANN, Lucille TREIL, Salomé KUNTZ, Anne LEJAY, Tristan BOURCIER, Nabil CHAKFÉ

Navigation

8 | **Effect of radiation on vascular surgeons: State of the art** 70
Mohamed Ahmed ABDELHALIM, Bijan MODARAI

9 | **Endovascular navigation with Fiber Optic RealShape (FORS) technology** 76
Jurre KLAASSEN, Constantjin E V B. HAZENBERG, Joost A. Van HERWAARDEN

10 | **Magnetic Particle Imaging-guided Stenting** 80
Stefan HERZ, Volker C BEHR, Thorsten A BLEY, Patrick VOGEL

11 | **Augmented reality in vascular and endovascular surgery: a scoping review** 86
Joshua EVES, Abhilash SUDARSANAM, Joseph SHALHOUB, Dimitri AMIRAS

Peripheral

12 | New technologies of the last two years: a critical appraisal 104
Jörg TESSAREK

13 | Systematic review on femoral artery stents fractures; A comprehensive study 113
Salomé KUNTZ, Anne LEJAY, Nabil CHAKFÉ

14 | Review and Analysis of Nitinol Trans Aortic Valve Repair Devices 123
Alan R. PELTON, Srinidhi NAGARAJA, Ga-Young SUH, Payman SAFFARI, Jochen ULMER

15 | Fully bioresorbable vascular scaffolds: lessons learned and future directions 131
Atsushi SAKAMOTO, Hiroyuki JINNOUCHI, Yu SATO, Renu VIRMANI, Aloke V. FINN

16 | Is there a future for polymeric braided stents? 144
Saber Ben ABDESSALEM, Hiba JAZIRI, Sofiene MOKHTAR, Frédéric HEIM, Nabil CHAKFÉ

17 | Thrombosis on medical implants: a focus on the importance of hemodynamics 152
Emily JANUS-BELL, Yevgeniy KRIENIN, Netanel KORIN, Pierre H. MANGIN

18 | Identification of patients at risk of secondary cardiovascular events despite using antiplatelet therapy 163
Gert J. de BORST

Aortic

19 | Functional Imaging of the Aortic Wall 168
Michael BELL, Marc A. BAILEY

20 | Post endograft implantation syndrome: review of mechanisms and signification 179
Rita Soares FERREIRA, Tiago RIBEIRO, Frederico BASTOS GONÇALVES

21 | What do we actually know about the mechanical properties of guide wires used in endovascular practice? 192
Arindam CHAUDHURI

22 | Fenestration state of the art: When, Who and How? 201
Jérémie JAYET, Frédéric HEIM, Jennifer CANONGE, Marc COGGIA, Nabil CHAKFÉ, Raphaël COSCAS

Infection

23 | **European Society for Vascular Surgery (ESVS) 2019 clinical practice guidelines on the management of Vascular Graft and Stent Graft infections with endorsement of the European Association of Nuclear Medicine (EANM)** 211
Nabil CHAKFÉ

24 | **Vascular biomaterials: the (experimental) truth about infectability?** 214
Mathilde PUGES, Fatima M'ZALI, Sabine PEREYRE, Cécile BEBEAR, Charles CAZANAVE, Xavier BERARD

25 | **All you need to know about biofilm** 235
Paweł TULINSKI, Régis VILLET

26 | **Aortic Endograft Infections** 245
Diletta LOSCHI, Annarita SANTORO, Enrico RINALDI, Andrea KAHLBERG, Roberto CHIESA, Germano MELISSANO

27 | **Cryopreserved allografts in vascular infection** 258
David GARBAISZ, Zoltan SZEBERIN

28 | **Investigation of Decellularized Porcine Biograft** 267
Gábor FAZEKAS, Gábor MENYHEI, Gábor JANCSÓ

29 | **Versatility of Pericardial Patches in Vascular Surgery** 276
John LANGFORD, Jianbiao XU, Hualong BAI, Alan DARDIK

Compliance

30 | **A systematic review of stent-graft materials "PTFE *vs.* Polyester" in endovascular repair of abdominal aortic aneurysms** 287
Yogesh ACHARYA, Niamh HYNES, Sherif SULTAN

31 | **Compliance mismatch and flow pattern in endovascular aortic repairs** 296
Anna RAMELLA, Elena REDAELLI, Francesco MIGLIAVACCA, Giulia LURAGHI

32 | **Modifications in aortic stiffness after endovascular or open aortic repair: a systematic review and meta-analysis** 305
Daniele BISSACCO, Michele CONTI, Maurizio DOMANIN, Daniele BIANCHI, Luigia SCUDELLER, Sara ALLIEVI, Ferdinando AURICCHIO, Santi TRIMARCHI

The Future

33 | **Venous wall mechanical properties change after deep vein thrombosis: an experimental model** 317
Dragoslava P. VEKILOV, Adeline SCHWEIN, Louis MAGNUS, Nabil CHAKFÉ, Jean BISMUTH, K. Jane GRANDE-ALLEN

34 | **Mechanics of small diameter arteries and dedicated vascular grafts: a short review** 327
Lucie GERNEZ, Mélissandre ASFAZADOURIAN, Didier LETOURNEUR, Isabelle BATAILLE, Frédéric CHAUBET

35 | **Tissue Engineering Vascular Graft: current status and clinical application** 338
Toshiharu SHINOKA

36 | **Xeltis: towards grafts from supramolecular materials** 348
Martijn. A. J. COX, Hannah S. BAUER, Mohammed S. EL-KURDI

37 | **Bioresorbable synthetic Heart Valves to induce *In Situ* tissue regeneration: recent advances and current challenges** 359
Anthal I.P.M. SMITS

38 | **Tissue-Engineered Vascular Grafts: the promise of the Textile-Inspired approach** 369
Fabien KAWECKI, Nicolas L'HEUREUX

39 | **Biohybrid Vascular Graft – Reduction of production time through the integration of textile reinforcement systems** 378
Alicia FERNÁNDEZ-COLINO, Christian APEL, Christian BOEHM, F. WOLF, Stefan JOCKENHOEVEL

40 | **Relationship between hemodynamics and in-stent restenosis in femoral arteries** 384
Anna CORTI, Monika COLOMBO, Diego GALLO, Josè Felix Rodriguez MATAS, Francesco MIGLIAVACCA, Stefano CASARIN, Claudio CHIASTRA

41 | **Growth assessment of Engineered Vascular Grafts and Heart Valves** 394
Zeeshan H. SYEDAIN, Robroy MACIVER, Robert T. TRANQUILLO

Education

- 3D Printing in Aortic Endovascular Therapies: a review 20
- The Role of Industry in Vascular Education in Europe Introducing a ESVS wide survey 30
- The role of industry in Vascular Education in North America 35
- What does independence and conflict of interest mean for the lawyer? 39
- Education in Vascular Surgery: the ESVS academy experience 45
- The Vascupedia experience 55
- Which curriculum for trainees' education in vascular surgery? The GEPROVAS experience 57

3D Printing in Aortic Endovascular Therapies: a review

1

Mitchell J. GEORGE, Marina DIAS-NETO, Gustavo S. ODERICH, Jonathan M. MORRIS

Endovascular treatment of aortic disease like aneurysm or dissection is expanding at a rapid pace. Often the specific patient anatomy in these cases is complex. Additive manufacturing, also known as three-dimensional (3D) printing, is especially useful in the treatment of aortic disease due to its ability to manufacture physical models of complex patient anatomy. Compared to other surgical procedures, endovascular aortic repair can readily exploit the advantages of 3D printing with regards to operative planning and pre-operative training. To date there have been numerous uses of 3D printing in the treatment of aortic pathology as an adjunct in pre-surgical planning and as a basis for training modules for fellows and residents. In this review, we summarize these current uses of 3D printing in the endovascular management of aortic disease. We also review the process of producing these models, the limitations of these applications, and future directions of 3D printing in this field.

Introduction

Three-dimensional (3D) printing, also known as additive manufacturing, was developed in parallel by three American inventors in the 1980's. In 1986 Charles Hull patented a method to cure a liquid resin layer by layer with an ultra-violet laser. His novel method was termed stereolithography (SLA) and he later founded the company 3D Systems. In 1988 Carl Deckard from the University of Texas patented selective laser sintering – where solid powder is cured in layers by an argon laser. In 1989 Scott Crump patented fused deposition modelling and founded the company Stratasys based on this technology. The primary advantage of additive manufacturing over standard manufacturing processes is the ability to iterate quickly, freely integrate highly complex geometry, and create one-off parts or models without significant production costs. These attributes make additive manufacturing especially useful in the endovascular treatment of aortic disease where each patient is unique.

3D printing in surgery can be divided into three broad domains – surgical planning, *in vivo* use, and more recently – surgical training. Surgical planning or construction of anatomical models using 3D printing was made possible by parallel advances in high-quality cross-sectional imaging like magnetic resonance imaging or multi-detector computed tomography. In addition, powerful rendering software platforms like Rhinoceros (McNeel & Associates, Seattle WA) and Materialise Mimics (Materialise, Leuven, Belgium) allow creation or refinement of patient specific digital models prior to physical construction. *In vivo* use of 3D printed parts includes surgical guides, instrumentation, implants, or prosthetics. The most common *in vivo* use of 3D printing in surgery is surgical guides with intra-operative uses in orthopedics, neurosurgery, general surgery, dental surgery, spinal surgery, and maxillofacial surgery[1]. For example, complex maxillo-facial surgery has proven benefit from 3D printing for construction of implants in oncologic resections[2]. 3D printed surgical instruments have also proved feasible for use in general surgical applications like hernia repair[3]. 3D printing in surgical training is especially useful

since it allows gain of experience without harm to patients. Benefits from surgical training using 3D printed models outside of the operating room include reduction in operative time [4], reduced exposure to radiation [5], and simulation of patient specific or lesion specific anatomy [6]. Compared to other training models like human cadavers, 3D printed models are reusable and without risk of biohazard exposure [7].

This article gives an overview of the applications of 3D printing in aortic endovascular therapies. We focused on applications of the technology in the field, types of printers, material issues, limitations of 3D printing, the build process, cost considerations, and future directions. This topic is important because the use of 3D printing in aortic endovascular disease is expanding at a rapid pace and training programs for aortic surgery are uniquely positioned to exploit the advantages of 3D printing.

3D Printing Applications in Aortic Disease, what has been done so far

Two primary areas of application for additive manufacturing in endovascular treatment of aortic disease exist: surgical planning and modelling for training. When used for surgical planning, these models offer improved visualization of complex aortic anatomy for planning case specific like visceral vessel fenestration placement. When used for training, these 3D printed aortic models allow improvement in clinical metrics like operative time and fluoroscopy.

Modelling for Surgical Planning

3D printing has expanded planning and conceptualization of complex aortic anatomy in anticipation of open or endovascular repair. A three-dimensional visualization of a patient's disease has proven beneficial for the purposes of planning the appropriate intervention. Early efforts in 3D printed vascular structures were time intensive and still involved lost-wax techniques to produce the final model [8]. More recently surgical teams around the world have begun to use 3D printing to aid in surgical planning of endovascular treatment of aortic disease in a number of ways.

Physician modified endografts are one method to incorporate visceral vessels in thoracoabdominal aortic aneurysm. Koleilat *et al.* employed 3D printed aortic models to evaluate the accuracy of premeasured visceral vessel location and orientation for physician modified endograft planning [9]. They compare standard vessel measurements for fenestration done by three different blinded reviewers with measurements from a 3D printed aortic model. They found significant differences in the reviewer visceral vessel measurements compared to the 3D printed aortic model. This study is relevant because it suggests that standard preoperative planning measurements could lead to higher than anticipated rates of vessel shuttering and decreased graft patency requiring future interventions. Leotta *et al.* demonstrated that 3D printed aortic models could be used to guide fenestration placement in the operating room during a physician modified endograft case [10]. An aortic phantom was scanned with computed tomography (CT) and a template with cut outs of the visceral vessels was 3D printed. This template was used to guide fenestration placement in a custom graft. The graft was then deployed in the aortic phantom with fluoroscopic confirmation of correct graft alignment. This paper is significant because this method potentially saves time during a physician modified endograft case. Rather than manually measuring fenestration location on an endograft, the surgeon can simply mark the fenestration using the template as a guide. Another paper with a similar technique of printing aortic phantoms for planning endovascular aortic repair was written by Taher *et al.*[11]. In their study, Taher demonstrates that aortic phantoms or models can guide design of custom fenestrated endografts. Their group changed design of endografts 20% of the time based on fit of the graft within a 3D printed model.

3D printing is advantageous in cases with complex anatomy or rare pathology. For example, Tam et al 3D printed an infra-renal aortic model in a patient with a 90-degree neck angulation to assist in visualization of ostial origins and selection of a proper stent-graft [12]. Schmauss *et al.* 3D printed an aortic model of a patient with aneurysmal degeneration of their distal aortic arch. Calcifications made visualization on CT scan difficult and a printed model allowed the team to plan a frozen elephant trunk repair and with post-operative modeling for second stage endovascular repair [13]. In the case of a patient with hypoplastic aortic arch, Valverde *et al.* printed an aortic model from a previous magnetic resonance imaging (MRI) to practice the case and test stent sizing and placement in a hybrid operating room. Their team found that the printed model accurately replicated the patient's anatomy [14]. Other teams have employed similar approaches for difficult patient anatomy including type B dissections and thoracic aneurysm [15,16].

Modelling for Training

One of the earliest uses of additive manufacturing for training in endovascular treatment of aortic disease was by Chong *et al.* in 1997 [17]. Using an SLA printer, they built an acrylic replica of a patient's abdominal aortic aneurysm and use light projection through the model instead of radiation to mimic an actual repair. They perfuse the system with a glycerol solution using a mechanical pulsatile pump to mimic blood flow. This demonstrated the first embodiment of the necessary requirements for an endovascular aortic training system which include minimal to no radiation exposure, reusability, and patient specific.

More recently, Karkkainen *et al.* demonstrated that endovascular aortic repair simulation using 3D printed models was useful in distinguishing skill levels of trainees [18]. One advantage they noticed in their study was the durability of the aortic model that allowed multiple uses and thus a standardized scenario for all participants. Operator's previous experience correlated well with overall performance metrics like total operative time, fluoroscopy time, and time to device deployment.

Training suites for simulating endovascular aortic therapy using 3D printed aortas have been commercialized. One example of this is the ANGIO Mentor (Simbionix, Airport City, Israel). Saratzis *et al.* used the ANGIO Mentor to study the usefulness of simulation-based training amongst residents. They demonstrate that after 4 simulation-based training sessions their quality metrics improve across the board including mean procedure time, limb cannulation time, and presence of endoleak upon completion. Although this study does not directly apply to live patient procedures, it is useful to demonstrate how an endovascular training suite can improve performance of trainees.

The clinical benefits of these realistic models have been proven. These benefits include things like shorter operative time and fluoroscopy time. Torres *et al.* demonstrated the feasibility of pre-operatively practicing endovascular aortic repair on 3D printed aortic models of actual patients. They compared residents that performed aortic repair on actual patients under supervision from a senior vascular surgeon with and without preoperative practice on a 3D printed aortic model [19]. Residents with the preoperative practice demonstrated significant decreases in fluoroscopy time, procedure time, and time to device deployment.

Process of production of Aortic Models, from conception to end user

The basic procedure for medical 3D printing consists of three steps: (I) pre-processing (from the medical imaging to a virtual object on computer-aided design (CAD) software); (II) printing the model or device; (III) post-processing according to the intended use. After these steps, the model is ready for surgical use or planning [20].

Pre-processing

While in other fields of manufacturing models are created primarily in CAD software, in medicine, 3D printing involves reverse engineering of "objects" that already exist physically in the patient [21]. For the that reason, the first step is to convert the Digital Imaging and Communications in Medicine (DICOM) data from computed tomography and magnetic resonance into a STereoLithography (STL) file format readable by a CAD software. Using visualizations software like the open source OsiriX and MeshLab or the non-open source TeraRecon, anatomical information is extracted from the combination of image slices often by the use of 3D reconstructions. This image still needs to undergo segmentation, that is, the creation of thresholds in the image based upon density, in order to create volumes of interest. This allows the selective reconstruction of specific anatomical structures. This segmentation process can be performed by manual selection of the 2D regions of interest. Semi-automated or completely automated segmentation have been attempted in order to speed up this step [22]. More and more, visualizations softwares contain automatic tools for manipulating DICOM data. For example, a threshold tool allows one to set a range of tissue density values to be retained, while ignoring data that fall outside a specified range [23]. Another tool is seed-based region growing, where the operator selects a starting point or seed and choose the voxel density parameter so adjacent voxels are added if they meet the criteria. Finally, in order to make it suitable for printing, the image must undergo smoothing on the surface, finding connections between continuous voxels and correct errors in the digital mesh, removing unnecessary details to reduce printing time and but keeping its accuracy [24].

3D Printing Modalities and Materials

Stereolithography

SLA is the dominant printing modality in aortic modelling. In SLA printers, coherent light sources (usually lasers emitting in the UV-range) are used to induce polymerization and cross-linking, and thus hardening, of the initially liquid polymers, ceramics, composites, and hydrogels [25,26]. Light exposure is performed sequentially by scanning the laser beam within the plane on the surface of the photosensitive material. SLA allows for a high spatial resolution that is provided by the spot size of the laser beam and this is one of its main advantages. The time necessary to produce one slice of the structure depends on the speed with which the laser beam is scanned and on the illuminated area. It allows for the fabrication of a computer drawing to a solid 3D object within hours. The main time-consuming step in SLA is the deposition of the new layer of photosensitive material. Furthermore, it sometimes requires a high-temperature postprocessing step [27]. The viscosity of the material also plays an important role. Very often nonreactive additives or solvent must be used to decrease the viscosity of the photopolymer resin.

Selective Laser Sintering

Selective Laser Sintering (SLS) relies on irradiation with a laser beam over plastic, ceramic, polymer, or metal powder which solidifies into layers. This method generates complex 3D structures resulting in fusion of the powder particles into a rigid layer; individual layers are then stacked onto one another and again fused together by laser illumination to fabricate a 3D shape [28]. This process does not require a high-temperature postprocessing step, and comes with a wide range of applicable materials, such metal, plastic, and ceramic [29]. SLS printers are more expensive. The final product porosity may be undesired, and it has lower dimensional accuracy compared to SLA [26]. The surface finish can be rough, requiring more post processing than in other methods.

Inkjet

Inkjet techniques use methods similar to 2D desktop inkjet printers. Like SLS, inkjet printing uses powder where the printer places droplets of a binder solution, causing the powder to congeal, or directly places curable droplets to form the desired structures [30]. Rather than using laser irradiation, this modality uses piezoelectric, electromagnetic, or thermal methods.
Like conventional inkjet printers that can use different color cartridges, 3D inkjet printers can apply various solutions to construct objects in a wide range of applicable materials and the fabrication is rapid and not expensive. Nevertheless, the objects have low resolution [26] and in general the parts are not as durable as with SLS [23].

Fused Deposition Modeling

Fused deposition modeling (FDM) uses a heat-controlled nozzle to extrude a semisolid filament onto a base, that becomes solid and forms a layer [29,31]. The base is then lowered, or the nozzle is elevated so that the next layer can be deposited. Since the nozzle can move horizontally and vertically, it allows the placement of the melted material at any position and it is able to originate highly uniform and geometrically complex structures. FDM can use biodegradable polymers with sufficiently high melting points that harden as soon as the polymers are extruded. But the choice of materials is limited (the list includes acrylonitrile butadiene styrene and other thermoplastics) and the resolution of the structures is low [32].

Post-processing

After printing, models often require post-processing to smooth rough surfaces and to remove any excess material. The degree of postprocessing needed often depends on the type and quality of 3D printer, and the materials used. An advantage of SLS and inkjet over other 3D printing processes is that they do not require support structures during printing of the models [33]. Despite being manually removed after the model has been cured, these structures, often leave a rough surface that may require cleaning and smoothing. Unlike SLS and inkjet, parts made with FDM may require support structures depending on their build orientation [23].

Implementation of Aortic Models for Training

Our group recently built and implemented an endovascular aortic simulator [18]. An SLA Objet500 Connex3 printer (Stratasys, Eden Prairie, MN) built the model which was based on a patient with an infra-renal aortic aneurysm. A rigid material, VeroClear, composed the inner core and a softer material, Agilus, composed the softer outer shell. Support material was washed out with a sodium hydroxide bath and a water jet. A fluid pump cycled water from the proximal aorta to the visceral and iliac vessels and emptied via connector tubing (Figure 1). The system was placed on a standard angiography table and

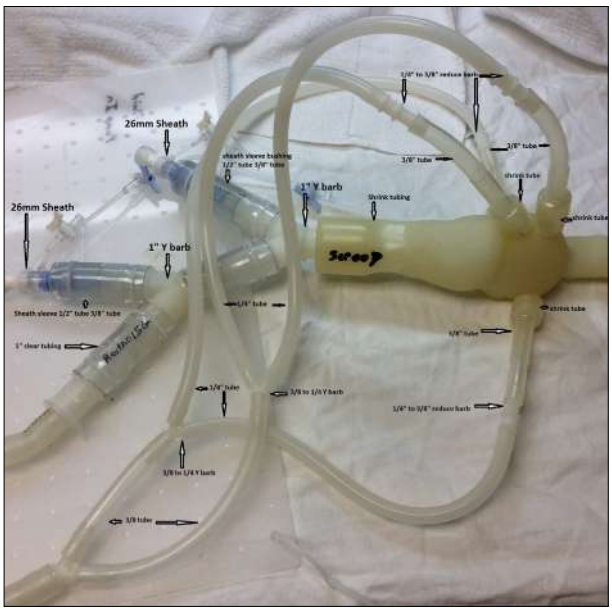

Figure 1: A 3D printed aortic model is attached to silicon tubing to allow flow of water through the visceral branches. A fluid pump cycles water in a pulsatile manner through the system. Barb connectors allow attachment of sheaths to mimic operative conditions and arterial access.

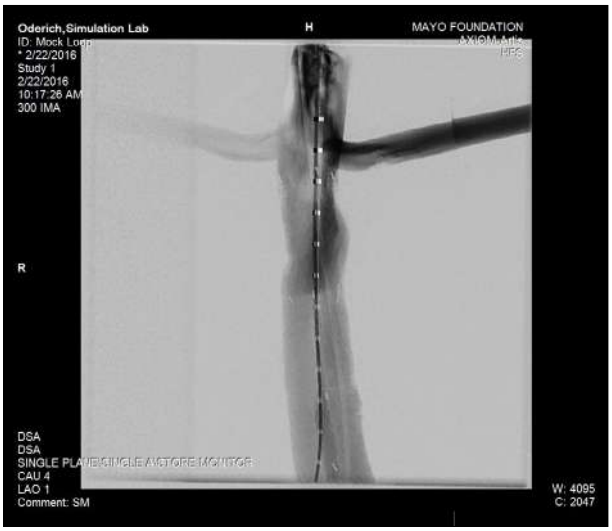

Figure 2: Digital subtraction angiography allows visualization of visceral branches prior to catheterization and stenting.

Figure 3: Deployment of a stent graft within the aortic model.

access was provided by Gore Dryseal sheaths. Digital subtraction angiography was performed (Figure 2), and standard instrumentation was used to deploy an appropriately sized endograft (Figure 3). After the case the system could be disassembled and the endograft recovered for repeat use (Figure 4).

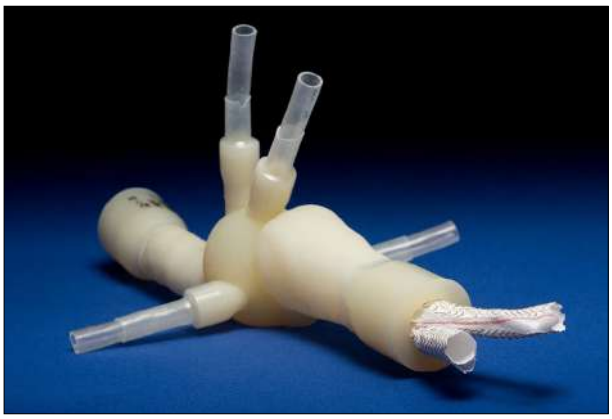

Figure 4: The entire system can be disassembled after simulation to retrieve and reuse the stent graft for continued training.

Limitations

Time spent in segmentation

One factor that limits the growth of 3D printing is the amount of time and effort required to isolate the areas of interest during postprocessing of the data. For example, tissues like bone, fat or muscle must be manually digitally removed from the 3D model created from the source imaging. Time spent on this stage affects the cost-effectiveness of using the model and reduces its usefulness in cases requiring urgent intervention. There is a pressing need to speed up these steps and many companies are developing software that allow users to easily perform segmentation and 3D reconstruction [34]. One example of this are functions that remove tissue like bone automatically from a 3D model.

Materials and Mechanical Constraints

Materials used to build models for training must be non-porous and devoid of free-floating bodies. Besides this, the texture of the materials currently used for models does not accurately imitate that of human tissue, a feature that may change in the future with the development of novel biomaterials. It is conceivable that, in the future, training would be possible on models made of actual living tissue [35].

There are mechanical limitations inherent to the 3D printing processes, that increase the risk of build inaccuracies. One is that a number of 3D printing parameters have been shown to significantly impact the physical characteristics of the final manufactured device, such as laser beam energy density, scanning speed, deposition velocity, and humidity within the build environment [36], meaning that quality measures are needed to ensure consistency. Second, device variations can result from the position of the device layout within the build platform, so that devices built in unfavorable positions such as the platform edges are at increased risk of warping [37]. Third, it was shown that 3D-printed devices can have only 15% tensile strength in the axis of the build direction, especially in laser sinter systems [38].This is thought to be due to anisotropy introduced between print layers and is especially applicable to devices with complex structures. In general, these limitations do not hamper the success of the artic models used for planning and training. Nevertheless, for printable implantable devices, it is expected that FDA require that all printing parameters and processes to be included in the Investigational Device Exemption application [36].

Accuracy of 3D Printed Models

Whether they are used for planning, training or implantation, 3D printed aortic models for training or surgical planning must be accurate and precise. Dorweiler *et al.* demonstrated that 3D printed aortic models can achieve a high degree of accuracy. Using Materialise Mimics (Materialise, Leuven, Belgium), they isolate the aorta and its branches and print it using an FDM and SLA printer. The aortic model was then scanned using computed tomography and subjected to accuracy and deviation analysis compared to the original STL file. Their primary finding was that globally the wall thickness was increased by 5%, possibly due to integration of support material. However, printing accuracy was well within the established 1 mm accuracy limit set by the imaging error [39].

Lack of a randomized control trials

Most of the studies about the 3D printed applications reported in this review are case studies and review articles. Despite this body of evidence, further research is needed to establish the effect of 3D printing on patient outcomes. Moreover, the cost-effectiveness of using 3D models as part of a treatment plan is also currently unknow, that is, whether the extra cost required to produce 3D models is offset by saving in reduced operation time, reduced revisions, and decreased length of hospital stay.

Cost

The costs for the use of 3D printing in aortic therapies must combine the 3D printer, the consumable inks and eventual sterilization, along with medical imaging acquisition and processing. The cost of commercially available 3D printers has decreased, with most in the range of $1,000-$5,000, and the consumable inks vary according to the materials used (for example, $20-$100/kg for plastics and $100-$200/L for resins) [26]. Despite this drop in prices, high-resolution commercial machines might still cost tens of thousands of dollars [12]. Plus, most institutions may not produce the volume of 3D models needed to justify the cost of an in-house printer. Many institutions pool resources and share 3D printing resources amongst other departments to offset the high cost of production.

Future Directions

The use of 3D printing in medicine is an evolving concept and is rapidly advancing in several fronts: the production of ready-for-use devices; the generation of scaffolds composed of biodegradable materials onto which cells can adhere, migrate, and proliferate; and the deposition of living cells, themselves, in stereotyped patterns, a process also known as bioprinting [40].
Endovascular devices are more and more tailored to specific patients. A stent to treat an iliac stenosis may require a different diameter, length and material comparing to the one needed to treat a popliteal aneurysm. This is even more challenging for aortic diseases, often poorly suited for off-the-shelf designs, where the endoprosthesis vary not only in size but also in the adaptations needed to accommodate the visceral aortic vessels. Besides the current use of printed products as aortic models for planning and training, one might expect the future production of implantable devices.

As for ancillary material, addictive manufacturing might provide an alternative to large and costly inventories of catheters and sheaths. Antibiotic and chemotherapeutic drugs might also be combined with constructs in different combinations of strength, versatility, and enhanced drug deliveries [41] using a 3D printing system. The way materials can be sterilized is also a matter of research. In the study of Perez *et al.* [42], nine FDM materials were tested using four methods of sterilization: autoclave, ethylene oxide, hydrogen peroxide, and gamma radiation. The majority of the materials were sterilizable by all four methods while deformations were caused by autoclaving.

As to fabrication of human tissues, the construction of microvascular beds was proposed by Lee *et al.* [35]. This group developed a 3D printing method to construct (fluidic vascular channels (lumen size of ~1mm) and to create adjacent capillary network through a natural maturation process, thus providing a feasible solution to connect a capillary network to large perfused vascular channels. Furthermore, implantation of 3D-printed grafts containing endothelial-cell-lined lumens was shown to induce spontaneous, geometrically guided generation of collateral circulation in ischaemic settings [43]. In rodent models of hind-limb ischemia and myocardial infarction, the vascular patches rescued perfusion of distal tissues, preventing capillary loss, muscle atrophy and loss of function. Finally, a triple-layer vascular graft was also designed to simulate the structures and functions of natural blood vessels, by combining E-jet 3D printing and electrospinning techniques [44]. The biocompatible triple-layer graft was used for *in vivo* implantation, and results demonstrated that the longitudinally-aligned fibers within the lumen of the graft could enhance the proliferation and migration of endothelial cells, while maintained good mechanical properties.

References

1. Tack P, Victor J, Gemmel P, Annemans L. 3D-printing techniques in a medical setting: a systematic literature review. *Biomed Eng Online* 2016; 15: 115.

2. Shengwei H, Zhiyong W, Qingang H, Wei H. Combined use of an anterolateral thigh flap and rapid prototype modeling to reconstruct maxillary oncologic resections and midface defects. *J Craniofac Surg* 2014; 25: 1147-9.

3. George M, Aroom KR, Hawes HG, Gill BS, Love J. 3D Printed Surgical Instruments: The Design and Fabrication Process. *World J Surg* 2017; 41: 314-9.

4. Tam MD, Latham TR, Lewis M, Khanna K, Zaman A, Parker M, *et al.* A Pilot Study Assessing the Impact of 3-D Printed Models of Aortic Aneurysms on Management Decisions in EVAR Planning. *Vasc Endovascular Surg* 2016; 50: 4-9.

5. Ghisiawan N, Herbert CE, Zussman M, Verigan A, Stapleton GE. The use of a three-dimensional print model of an aortic arch to plan a complex percutaneous intervention in a patient with coarctation of the aorta. *Cardiol Young* 2016; 26: 1568-72.

6. Ryan JR, Almefty KK, Nakaji P, Frakes DH. Cerebral Aneurysm Clipping Surgery Simulation Using Patient-Specific 3D Printing and Silicone Casting. *World Neurosurg* 2016; 88: 175-81.

7. Al-Ramahi J, Luo H, Fang R, Chou A, Jiang J, Kille T. Development of an Innovative 3D Printed Rigid Bronchoscopy Training Model. *Ann Otol Rhinol Laryngol* 2016; 125: 965-9.

8. Knox K, Kerber CW, Singel SA, Bailey MJ, Imbesi SG. Stereolithographic vascular replicas from CT scans: choosing treatment strategies, teaching, and research from live patient scan data. *AJNR Am J Neuroradiol* 2005; 26: 1428-31.

9. Koleilat I, Jaeggli M, Ewing JA, Androes M, Simionescu DT, Eidt J. Interobserver variability in physician-modified endograft planning by comparison with a three-dimensional printed aortic model. *J Vasc Surg* 2016; 64: 1789-96.

10. Leotta DF, Starnes BW. Custom fenestration templates for endovascular repair of juxtarenal aortic aneurysms. *J Vasc Surg* 2015; 61: 1637-41.

11. Taher F, Falkensammer J, McCarte J, Strassegger J, Uhlmann M, Schuch P, *et al.* The influence of prototype testing in three-dimensional aortic models on fenestrated endograft design. *J Vasc Surg* 2017; 65: 1591-7.

12. Tam MD, Laycock SD, Brown JR, Jakeways M. 3D printing of an aortic aneurysm to facilitate decision making and device selection for endovascular aneurysm repair in complex neck anatomy. *J Endovasc Ther* 2013; 20: 863-7.

13. Schmauss D, Juchem G, Weber S, Gerber N, Hagl C, Sodian R. Three-dimensional printing for perioperative planning of complex aortic arch surgery. *Ann Thorac Surg* 2014; 97: 2160-3.

14. Valverde I, Gomez G, Coserria JF, Suarez-Mejias C, Uribe S, Sotelo J, *et al.* 3D printed models for planning endovascular stenting in transverse aortic arch hypoplasia. *Catheter Cardiovasc Interv* 2015; 85: 1006-12.

15. Yuan D, Luo H, Yang H, Huang B, Zhu J, Zhao J. Precise treatment of aortic aneurysm by three-dimensional printing and simulation before endovascular intervention. *Sci Rep* 2017; 7: 795.

16. Ho D, Squelch A, Sun Z. Modelling of aortic aneurysm and aortic dissection through 3D printing. *J Med Radiat Sci* 2017; 64: 10-7.

17. Chong CK, Brennan J, How TV, Edwards R, Gilling-Smith GL, Harris PL. A prototype simulator for endovascular repair of abdominal aortic aneurysms. *Eur J Vasc Endovasc Surg* 1997; 13: 330-3.

18. Karkkainen JM, Sandri G, Tenorio ER, Alexander A, Bjellum K, Matsumoto J, *et al.* Simulation of Endovascular Aortic Repair Using 3D Printed Abdominal Aortic Aneurysm Model and Fluid Pump. *Cardiovasc Intervent Radiol* 2019; 42: 1627-34.

19. Torres IO, De Luccia N. A simulator for training in endovascular aneurysm repair: The use of three dimensional printers. *Eur J Vasc Endovasc Surg* 2017; 54: 247-53.

20. Hangge P, Pershad Y, Witting AA, Albadawi H, Oklu R. Three-dimensional (3D) printing and its applications for aortic diseases. *Cardiovasc Diagn Ther* 2018; 8(Suppl 1): S19-S25.

21. Baradeswaran A, Selvakumar J, Priya P. Reconstruction of Images into 3D Models using CAD Techniques. *Eur J Appl Engineer Sci Res* 2014: 3: 1-8.

22. Massoptier L, Casciaro S. A new fully automatic and robust algorithm for fast segmentation of liver tissue and tumors from CT scans. *Eur Radiol* 2008; 18: 1658-65.

23. Marro A, Bandukwala T, Mak W. Three-Dimensional Printing and Medical Imaging: A Review of the Methods and Applications. *Curr Probl Diagn Radiol* 2016; 45: 2-9.

24. Gall M, Xing L, Xiaojun C, Schmalstieg D, Egger J. Computer-aided planning and reconstruction of cranial 3D implants. *Annu Int Conf IEEE Eng Med Biol Soc* 2016; 2016: 1179-83.

25. Ligon SC, Liska R, Stampfl J, Gurr M, Mulhaupt R. Polymers for 3D Printing and Customized Additive Manufacturing. *Chem Rev* 2017; 117: 10212-90.

26. Sheth R, Balesh ER, Zhang YS, Hirsch JA, Khademhosseini A, Oklu R. Three-Dimensional Printing: An Enabling Technology for IR. *J Vasc Interv Radiol* 2016; 27: 859-65.

27. Melchels FP, Feijen J, Grijpma DW. A review on stereolithography and its applications in biomedical engineering. *Biomaterials* 2010; 31: 6121-30.

28. Mazzoli A. Selective laser sintering in biomedical engineering. *Med Biol Eng Comput* 2013; 51: 245-56.

29. Seol Y, Kang T, Cho D. Solid free form fabrication technology applied to tissue engineering with various biomaterials. *Soft Matter* 2012; 8: 1730–5.

30. Minemawari H, Yamada T, Matsui H, Tsutsumi J, Haas S, Chiba R, *et al.* Inkjet printing of single-crystal films. *Nature* 2011; 475: 364-7.

31. Patel R, Patel S, Patel J. A review on optimization of process peramater of fused deposition modeling for better dimentional accuracy. IJEDR 2014; 2: 1620-4.

32. Korpela J, Kokkari A, Korhonen H, Malin M, Närhi T, Seppälä J. Biodegradable and bioactive porous scaffold structures prepare dusing fused deposition modeling. *J Biomed Mater Res Part B Appl Biomater* 2013; 101: 610–9.

33. Levy RA, Guduri S, Crawford RH. Preliminary experience with selective laser sintering models of the human temporal bone. *AJNR Am J Neuroradiol* 1994; 15: 473-7.

34. Lambrecht JT, Berndt DC, Schumacher R, Zehnder M. Generation of three-dimensional prototype models based on cone beam computed tomography. *Int J Comput Assist Radiol Surg* 2009; 4: 175-80.

35. Lee VK, Lanzi AM, Haygan N, Yoo SS, Vincent PA, Dai G. Generation of Multi-Scale Vascular Network System within 3D Hydrogel using 3D Bio-Printing Technology. *Cell Mol Bioeng* 2014; 7: 460-72.

36. Morrison RJ, Kashlan KN, Flanangan CL, Wright JK, Green GE, Hollister SJ, *et al.* Regulatory Considerations in the Design and Manufacturing of Implantable 3D-Printed Medical Devices. *Clin Transl Sci* 2015; 8: 594-600.

37. Soe S, Eyers D, Setchi R. Assessment of non-uniform shrinkage in the laser sintering of polymer materials. *Int J Adv Manuf Technol* 2013; 68: 111-25.

38. B C, PE M, S L. Dependence of mechanical properties of polyamide components on build parameters in the SLS process. *J Mater Proc Tech* 2007; 182: 477-88.

39. Dorweiler B, Baque PE, Chaban R, Ghazy A, Salem O. Quality Control in 3D Printing: Accuracy Analysis of 3D-Printed Models of Patient-Specific Anatomy. *Materials (Basel)* 2021; 14: 1021.

40. Xu T, Zhao W, Zhu JM, Albanna MZ, Yoo JJ, Atala A. Complex heterogeneous tissue constructs containing multiple cell types prepared by inkjet printing technology. *Biomaterials* 2013; 34: 130-9.

41. Weisman JA, Nicholson JC, Tappa K, Jammalamadaka U, Wilson CG, Mills DK. Antibiotic and chemotherapeutic enhanced three-dimensional printer filaments and constructs for biomedical applications. *Int J Nanomedicine* 2015; 10: 357-70.

42. Perez M, Block M, Espalin D, Winker R, Hoppe T, Medina F, *et al*. Sterilization of FDM-manufactured parts. 23rd Annual International Solid Free form Fabrication Symposium-An Additive Manufacturing Conference, SFF2012 University of Texas at Austin. 2012: 285-96.

43. Mirabella T, MacArthur JW, Cheng D, Ozaki CK, Woo YJ, Yang M, *et al*. Author Correction: 3D-printed vascular networks direct therapeutic angiogenesis in ischaemia. *Nat Biomed Eng* 2020; 4: 572.

44. Huang R, Gao X, Wang J, Chen H, Tong C, Tan Y, *et al*. Triple-Layer Vascular Grafts Fabricated by Combined E-Jet 3D Printing and Electrospinning. *Ann Biomed Eng* 2018; 46: 1254-66.

The Role of Industry in Vascular Education in Europe Introducing a ESVS wide survey

2

Radu-Ionut TOADER, Eike Sebastian DEBUS, Christian-Alexander BEHRENDT

A better care for patients with vascular disease has been obtained through the development of new treatment options in the past decades. Vascular surgeons faced new training and research challenges in acquiring new skills and learning how to use new medical devices.

The industry has played a key role in the evolution of surgical training so far. Through the organisation and financial support of medical congresses, training seminars, debates, peer teaching, expert panels workshops and master classes it has created a field of learning on its own. Even though it is at times skeptically seen because of bias issues and resulting potential risks, it is indisputably a contributing aspect of modern-day learning. Nevertheless, an integration in the standard curriculum is warranted, as many of vascular procedures are device-driven with the need for specific deployment training. Bias issues raise concern and a clear standardisation of the independence of learning material, should be implemented through a professional medical society.

Vascular surgical training could be vastly improved through a proper standardisation of industry sponsored training using a proper evaluation platform that could offer real time data for longer periods of time. Better insight into possible research ideas that could derive from a society controlled and low biased industry sponsored training can be obtained.

Introduction

Vascular surgery has evolved significantly in the last 15 years, especially with the incorporation of endovascular treatment opportunities. This has allowed patients to get a better care for their underlying vascular disease and has offered a new pathway to training and research. This however needs a mandatory training of vascular surgeons, which needs to include acquiring new skills and learning how to use new medical devices as well as keeping up-to-date with the latest research and therapy guidelines. The number of open surgical procedures and derived experience relevant to the vascular surgical training was as a result subsequently reduced.

According to European law, the limitation of working hours to prioritise personal well-being and avoid stress related disorders represented an increase in quality of life but on the contrary it amounted for a serious limitation in training time. A need for a separate training curriculum was noticed among vascular trainees in some small studies.[1] This corroborated with the increasing age and number of patients with vascular diseases were some of the possible factors that led to the paradigm shift in the early 2000s, when vascular surgery became a specialty on its own in many countries.

Adapting vascular surgical training to fit the needs stipulated above, led to the development and implementation of new teaching tools. This was achieved with means such as medical simulation (through skill training or scenario-based models), professional video platforms or self-assessment and benchmark tools. Many companies, including Johnson&Johnson, Autosuture, Getinge and many others have driven these developments by creating and introducing teaching institutes, implementing virtual trainings and hands on teaching in living animals and cadavers as well. Alternative teaching tools like podcasts, virtual reality classes, smart phone-based learning and industry sponsored training show massive potential and benefit despite lack of big data evidence. Recently, the European Society for Vascular Surgery (ESVS) has introduced a comprehensive virtual training platform collating material from life and life in the box events (such as the ESVS masterclasses), trainings and courses from its e-academy and the invention of a virtual textbook (Virtual Vascular).[2] Global challenges like the COVID-19 pandemic also played a part in further augmenting surgical training with the creation or maturing of existing eLearning platforms.
The efforts to create and implement a high quality vascular surgical training are directly related to the teaching challenges and time resources. As such the endeavour of teaching experts to build better surgical training programs should also be shouldered by the trainees, whose feedback is essential in evaluating new and existing teaching methods.

The industry has played a key role in the evolution of medical training so far. Through the organisation and financial support of medical congresses, training seminars, debates, peer teaching, expert pannels workshops and master classes it has created a field of learning on its own. This situation applies for many other specialties, as e.i. cardiology.[3] Although many physicians look skeptically at research derived from this area because of bias issues and resulting potential risks, it is indisputably a contributing aspect of modern-day learning.[1] The Society for Vascular Surgery has therefore published a statement paper for guidance in the management of relationships with industry[4]. European countries follow different strategies and policies in industry support, and a harmonization between at least European countries should be aimed for.

Materials and Methods

In order to find a way to approach the standardisation of industry sponsored vascular surgical training we aimed to obtain feedback from physicians that have attended or would like to attend sponsored courses. For this reason, a questionnaire was created, which was approved by the ESVS executive committee to send to the ESVS vascular community. The target group that we addressed was comprised of vascular surgeons, cardiac or general surgeons that still perform vascular surgery procedures as well as angiologists or interventional radiologists that perform peripheral endovascular procedures.
Even though main focus were surgical trainees we also included specialists divided into sub groups with more than five years of training or less than five years of training. Additionaly, medical chiefs, head of departments or head of divisions as a separate group were included.

The first part of the survey contained 6 single-choice questions that collected demographic data including gender and country where the participants actively practiced medicine. Information regarding the actual academic degree of the participants was requested and divided as follows: MD, PhD, associate professor, full Professor, other. Details about the type of institution where the participants practice medicine was asked and divided these into public or non-profit making medical centres, University medical centres, medical practices and other. The emphasis at the end of the first part of the survey will be whether the participants already took part in an industry sponsored training or not.

Question text	Mandatory	Choice
What is your gender?	X	1: male, 2: female, 3: diverse
In which country do you work regularly?	X	Free text (or single country choice)
What is your clinical experience in vascular surgery?	X	1: in training, 2: specialist after training <5 years, 3: specialist after training ≥5 years, 4: head of department or division
What is your highest academic degree?	X	1: medical degree/license, 2: MD, 3: PhD, 4: Associate professor (reader, docent, etc. usually employed by a hospital), 5: Full professor (main employer is a university), 6: Other (please specify)
Please indicate the type of institution/ hospital of your main working place	X	1: Public (community) or non-profit making medical centres (with or without teaching assignment), 2: University medical centre, 3: Other (please specify)
Have you previously attended in any industry-sponsored vascular surgical training activity?	X	1: yes, 2: no

The second part represents nine affirmations to which the participants answer using a four item Likert Scale ranging from strongly agree, agree, disagree or strongly disagree (the typical balance point or neutral value was intentionally omitted). If the participants have not undergone industry sponsored vascular training, the first two feedback questions regarding to a past participation will not be registered.

Text	Mandatory	Choice			
Please vote:		1 Strongly disagree	2 Disagree	3 Agree	4 Strongly agree
Through Industry sponsored vascular training i have improved my clinical/operating skills.	X				
More than half of the vascular surgical training courses that I attended so far have been sponsored by industry	X				
Financial and other support of vascular surgical training activity leads to biased learning content	X				
Bias issues and competing interests can be reduced through a clear transparency code and institutional review boards	X				
Scientific medical societies should organise and administer funding for industry-sponsored vascular surgical training activities	X				

Scientific medical societies should review and approve the content of industry-sponsored vascular surgical training activities	X				
Industry-sponsored activities can improve the vascular surgical training	X				
Industry-sponsored activities Should be integral part of curricula in vascular surgical training	X				
I am more likely to participate in industry-sponsored activities if the institution I work for is organising the funding	X				

The survey is compiled using the online survey site “Survey monkey” and is distributed via Internet web link through the ESVS newsletter and on discussion channels with the help of other vascular trainees’ associations. We ran the survey in a preliminary phase for a month. After that the results were pooled in with the help of the survey site “Survey Monkey” and analysed in a quantitative and qualitative fashion using SPSS. The data recorded was interpreted using the ... Test.

Discussion

Industry sponsored vascular surgical training plays a pivotal role in vascular education, especially in endovascular skills and techniques. A national needs assessment using a standardised Delphi method identified a list of procedures that are highly suitable and may provide the basis for future simulation-based training programs for vascular surgeons in training.[6]
The perceived effectiveness in such trainings is high. Novice vascular trainees achieve skills and competencies in open aortic repair in a simulated setting with dedicated supervision and feedback and can become ready for supervised surgery on real patients.[6] Learning rates are individual, and it is important to construct training programs with emphasis on proficiency and not merely attending a course.[7] Vascular training can benefit from industry sponsor training and it is needed. A possible integration in the standard curriculum is therefore necessary. This needs specific standards for transparence and content, as well as an independent co-convenor. Accordingly, the Union Européenne edes Médecins Spécialistes (UEMS) has developed detailed standards in collaboration with ESVS, to create an optimal benefit out of industry supported training.

Furthermore, there is a need for a better standardisation of International Society for Vascular Surgeons in Training (ISVST) regarding the informational content, reducing possible bias and fund access. A possible solution is through task force groups overseen by specialty organisations like the ESVS, or other national organisations.[1] Bias issues regarding informational content remain a concern for trainees and specialists alike. Therefore, it is of great importance that a standardised consensus regarding the independence of learning material, should be implemented and overseen through the ESVS and / or national societies, faculty or staff members according to existing regulation.[8]

In addition, we propose the creation of a feedback platform that could facilitate ease of access to direct feedback among vascular surgical trainees to insure the better evaluation of future possible alternative teaching tools. Systematically and periodically answered surveys about learning research in the vascular training could have an important contribution in data generation. Such programs could be spearheaded by workgroups such as the ESVT or could be integrated in the ESVS smartphone application or website. As a way of encouraging the active participation in such programs we could use a rewarding point-based system from which the participants could benefit from tax reduction to workshops or congresses or mentorship sessions with leading experts in the field of teaching research.

Prospectively we agree that vascular surgical training could be vastly improved through a proper standardisation of industry sponsored training combined with a proper evaluation platform that could offer real time data for longer periods of time. In doing so we could better understand future ramifications and development possibilities of the training curriculum. Better insight into possible research ideas that could derive from a society controlled and low biased industry sponsored training could be obtained.

Conclusion

Industry supported education plays an important role with presumably different impact in different countries. To avoid bias in constant and support/attendance, regulations and transparency is needed. This should be developed with independent societies like ESVS and / or national societies. This way, industry sponsored training should become a mandatory part of vascular education.

References

1. Irfan W, Sheahan C, Mitchell EL, Sheahan MG. The pathway to a national vascular skills examination and the role of simulation-based training in an increasingly complex specialty. *Semin Vasc Surg* 2019; 32: 48-67.

2. https://ESVS.org

3. Harrington RA, Califf RM. There is a role for industry-sponsored education in cardiology. *Circulation* 2010; 121: 2221-7.

4. https://vascular.org

5. Nayahangan LJ, Konge L, Schroeder TV, Paltved C, Lindoff-Larsen KG, Nielsen BU, et al. A national needs assessment to identify technical procedures in vascular surgery for simulation based training. *Eur J Vasc Endovasc Surg* 2017; 53: 591-9.

6. Bandyk DF. Vascular surgery resident education and hands-on training in vascular laboratory testing. *Sem Vasc Surg* 2019; 32: 41-7.

7. Lawaetz J, Nayahangan LJ, Strom M, de la Motte L, Rordam P, Grondal N, et al. Learning curves and competences of vascular trainees performing open aortic repair in a simulation-based environment. *Ann Vasc Surg* 2021; 72: 430-9.

8. Dua A, Rothenberg K, Lee JT. The role of industry in vascular surgery trainee education. *Semin Vasc Surg* 2019; 32: 30-2.

The role of industry in Vascular Education in North America

3

Elizabeth L. GEORGE, Jason T. LEE

Vascular and endovascular surgery has emerged as a field highlighted by a lifelong learning process where new devices and techniques will continue to develop. Industry partnership can provide a safe learning environment for trainees with a focus on maximizing learning opportunities during fellowship or residency. Unlike other specialties, vascular surgery requires its trainees to become competent both in open and image-guided endovascular interventions, requiring two unique, but often complementary, skill sets to become a contemporary vascular surgeon in 2021. Due to the rapid growth of technology and innovations, industry partnerships enhance and maximize the learning experience of the trainee by often providing the products, education, research support, and financial assistance. This can come in the form of innovative and educational activities including simulation, exposure to key opinion and thought leaders, attendance at conferences and workshops, and one-on-one assistance with cases. We review in this chapter the role that industry can serve in vascular education to support budding vascular surgeons through exposure and repetition as they lay down the fundamentals of their careers.

Introduction

The endovascular revolution was launched in 1990 when Dr Parodi performed the first endovascular abdominal aortic aneurysm repair.[1] In the following 26 years, the shift of the additional skills required for a competent vascular surgeon added significantly to the base skill set required which in turn forced a new paradigm for vascular trainees in the form of multiple pathways to be trained in vascular surgery. The field embraced endovascular solutions for all their traditional operations, and every year new graft technology, new deployment systems, new platforms, new sizing parameters, and new indications are brought to market for every aspect of vascular surgery. With this surge of novel endovascular techniques, vascular fellows and residents along with their program directors have a unique challenge to master not only what is already in the field but what is to come; discarding old data or devices and replacing them with updated technology quickly, safely, and efficiently so patients can immediately benefit. This daunting task would be even more challenging without the support of industry in vascular surgery education.

Prior to the 0+5 training programs, vascular surgeons of this era only came from a general surgery background through fellowships, which initially found creative ways with ensuring adequate training in both open and endovascular techniques over a short period.[2] Fortunately this was recognized just 20 years ago when most programs increased to two years for traditional fellowship, and with issues related to work-force and interest in vascular surgery, the addition of integrated vascular surgery residencies provided learners even more time to gain competency in vascular and endovascular surgery.[3,4] This need for increased education and training comes with a cost, however, both in terms of infrastructure and finances. While trainees are supported primarily by accreditation council for graduate medical education (ACGME) funds, the overwhelming amount of technology and skills that vascular surgeons need to master requires additional support.

Since industry initially partnered with academic medicine in the form of research grants in the 1970s,[5] the United States government support for biomedical research and development has decreased significantly, while industry increased their contributions from 32% to 62%.[6] Though these partnerships are often critiqued due to concerns for conflict of interest, there are ways to appropriately utilize these collaborations in a synergistic way that continues to encourage education and research. Moving forward, conflict of interest and full disclosure is important in maintaining some separation of the business and educational sides of our industry partners.

Exposure to Industry

Vascular trainees begin their journey often with little to no exposure to endovascular training and a relatively short period in which to acquire skill and comfort. Before a trainee can even start understanding endovascular procedures, it is imperative to have a grasp of the building block and technical fundamentals. Once competency of the fundamentals has occurred, the trainee can go to the next stage which involves practicing or repeating the approaches until ultimate mastery.

One of the major contributions of industry is its support both educationally and financially for trainees to gain exposure to endovascular technology and open surgical techniques *before* they enter formal training by our national society meetings.[7] Industry partners have long funded through grant support educational activities at these meetings that allow attendance by multiple learner groups. Identifying what the appropriate level and purpose of each type of meeting is an important current project at the level of the Association of Program Directors in Vascular Surgery (APDVS) to assure that needs are aligned with offerings.

In addition to allowing access to many national meetings, most of our regional and national societies in the USA will partner with the industry to create educational experiences to recruit surgically-minded students and general surgery residents. These programs include dedicated simulation sessions with hands-on training so future trainees may gain exposure, opportunities for mentorship and networking, and lectures on various vascular surgery topics. At the Society of Clinical Vascular Surgery, there is a separate incoming fellows program, fellows program, and program for young faculty all with various agendas and mix of hands on, didactic lectures, panel discussions, and what to expect for each learner level. Particularly for the young trainee, gaining exposure to wires, catheters, grafts, stents and other basic building blocks of endovascular approaches can alleviate some of the initial anxiety associated with learning a new skill.[7] Both the Society for Vascular Surgery (SVS) and Vascular and Endovascular Surgery Society (VESS) also have robust opportunities for trainees of all experiences and backgrounds, and focus on different aspects of their learning. These programs are well supported by our industry partners.

Industry can also provide a forum where global thought leaders can be directly exposed to trainees at an early stage. Trainees need to be exposed often from mentors outside of their home institution to truly grasp the multiple types of solutions that our specialty thrives on. Active and spirited debates about the decision to approach something endovascularly versus with open techniques give trainees unique perspectives. Sessions with thought leaders discussing the pros and cons of different approaches are often highly rated educational experiences. When a industry supports a lecturer who fairly debates the utility of a device or technique, it highlights the merits of a particular technology.[7] Industry also heavily supports regulatory clinical trials to show the endovascular approach is safe and effective for the disease process. Multiple studies are performed across the globe comparing one technology to another to provide the safest options for use and aid in appropriate patient selection and some of these important studies that serve as the basis for training would not be feasible without industry support.

Repetition of Skills and Simulation

Once the vascular trainee has begun training and gained initial exposure, repetition is paramount to success and ultimate mastery. For both open and endovascular procedures, preoperative planning is paramount, and especially for endovascular can be creative and complex in multiple facets and would include understanding imaging software, device selection, sizing, deployment steps, and actual implementation in the hybrid operating room. To become facile with these elements repetition is necessary and herein lies another contribution of industry to vascular surgery education in the form of simulation. Medical simulation systems allow surgeons to gain experience and confidence in a realistic, safe environment, while providing the opportunity to practice many technical and problem-solving skills in a short period of time. Simulation training has been shown to improve residents' endovascular techniques,[8,9] and could ultimately be a great tool for evaluation, however creating and maintaining these labs with realistic machines and educators who can provide sound feedback can be costly and time-consuming.[10,11]

Industry has embraced simulation and hands-on approaches and therefore maintains involvement in training by introducing new products and providing a safe training environment in which to enhance skill. The augmenting of trainee education is done both in a one-on-one interaction where industry partners can actively participate in the planning and sizing of endovascular devices, and certainly support simulation exercises that allow for actual practice runs of cases. These simulated training sessions done on high-fidelity platforms, table top demos, or even on cadavers are invaluable to trainees as they serve as repetitive, practice sessions that cause no harm to patients and a safe space for a trainee to master techniques.

During a simulation session, learners are encouraged to independently plan and carry out each step of a procedure. They may encounter problems with any portion of the procedure including catheter positioning, guidewire placement, or difficulties in selecting balloon size — challenges they may not have faced in the operating room. Simulation faculty can help to foresee potential pitfalls and teach trainees how to trouble-shoot those concerns intraoperatively from their experience with different operators. This is invaluable experience that afford trainees the opportunity to learn from others experience and mistakes. Errors in case simulations also highlight certain problems that the trainee may not have appreciated, such as the need to think about procedures in an organized way and the need to plan ahead. Simulation may also reveal bad habits, such as the excessive use of fluoroscopy without the detrimental impact of being radiated. Although simulation takes place in a risk-free environment, it is not a stress-free environment. Something as simple as having the mentoring physician stand quietly behind the trainee, observing the simulated procedure, can introduce a level of stress that helps the trainee accept the reality of the exercise. Obviously, the advantages of this educational experience would be wonderful for all learners to have full and unlimited access to, but the cost of these sessions often can be prohibitive. This again is where industry partners can share in the financial impact to individual programs, and therefore in partnership really augment the educational environment. For example, at the Top Gun fellows' competition through the Society for Clinical Vascular Surgery (SCVS),[12] trainees certainly have appreciated the value of such training model, both endovascular and open skills, and these sessions allows trainees to also see how they fare compared to their peers.[7]

Research Support

Industry interest in educational also comes in the form of research support, as they often partner with academic institutions by supporting trials or development of medications or devices, or in providing grants and scholarships in support of research.[5,13] By partnering with the industry, researchers and learners

can get seed funding or confirmatory projects that might be more challenging through traditional funding mechanisms.[14] Vascular surgical society meeting partnerships with the industry support research by providing scholarships and grants for learners to attend and present their work, and again to help with early concept ideas, particularly to assist young faculty researchers. This again highlights the interest our industry partners have in both research and education. The VESS has been particularly generous with both trainee and early faculty seed grant programs, again also generously supported by our industry partners. Without grants like these, many government and non-commercial resources are unable to allow young, prior non-funded investigators, to get started in a research career.[13]

Conclusion

In summary, vascular surgery education and lifelong learning is unique in that the skills required of the vascular trainee change dramatically in very short periods of time. Vascular surgery is heavily technology dependent on the endovascular revolution and continued refinement of open procedures that is dwindling in number. Providing a safe, reliable, and effective method by which to efficiently educate vascular trainees is imperative to success of the profession. Industry partners therefore serve an important adjunct in providing the products, education, research and financial assistance necessary for trainees to engage in innovative and education activities. This fosters the maximal learning experience, and provides resources to our budding vascular surgeons as they lay down the fundamentals of their careers by educating them on new techniques and maximizing their time in training by enhancing the learning process with simulation and one-on-one tutorials and exposure to thought leaders that may contribute to their educational experience.

References

1. Veith FJ, Marin ML, Cynamon J, Schonholz C, Parodi J. 1992: Parodi, Montefiore, and the first abdominal aortic aneurysm stent graft in the United States. *Ann Vasc Surg* 2005; 19: 749-51.
2. Reed AB. Advanced Training in Vascular Surgery: How Does it Need to Change? *Semin Vasc Surg* 2006; 19: 191-3.
3. Yan H, Maximus S, Kim JJ, Smith B, Kim D, Koopmann M, *et al.* General surgery resident vascular operative experience in the era of endovascular surgery and vascular fellowships. *Am Surg* 2015; 81: 1093-6.
4. Lee JT, Teshome M, de Virgilio C, Ishaque B, Qiu M, Dalman RL. A survey of demographics, motivations, and backgrounds among applicants to the integrated 0+5 vascular surgery. *J Vasc Surg* 2010; 51:496-503.
5. Bauer EA, Cohen DE. The changing roles of industry and academia. *J Invest Dermatol* 2012; 132: 1033-6.
6. Moses III H, Martin JB. Academic Relationships With Industry. *J Am Med Assoc* 2015; 285: 933-5.
7. Verhoeven E, Lee JT, Benenati JF, Dubenec S. A Model for Industry-Supported Physician Education. *Endovasc Today, Suppl* 2012; March: 15-8.
8. Dawson DL. The Benefits of Simulation Training for Fellows and Residents. *Endovasc Today, Suppl* 2005; September: 20-2.
9. Robinson WP, Doucet DR, Simons JP, Wyman A, Aiello FA, Arous E, *et al.* An intensive vascular surgical skills and simulation course for vascular trainees improves procedural knowledge and self-rated procedural competence. *J Vasc Surg* 2017; 65: 907-15.e3.
10. Munz Y. Role of industry in development of surgical simulation centres: A medical education perspective. *Surgeon* 2011; 9: S28-S29.
11. Duran C, Shames M, Bismuth J, Lee JT. Validated assessment tool paves the way for standardized evaluation of trainees on anastomotic models. *Ann Vasc Surg* 2014; 28: 115-21.
12. Bismuth J, Lumsden AB. The Fellows Top Gun Challenge. *Endovasc Today* 2009; July: 1-2.
13. DuVal G. The benefits and threats of research partnerships with industry. *Crit Care* 2005; 9: 309-10.
14. Chen J, Pickett T, Langell A, Trane A, Charlesworth B, Loken K, *et al.* Industry-academic partnerships: An approach to accelerate innovation. *J Surg Res* 2016; 205: 228-33.

What does independence and conflict of interest mean for the lawyer?

4

Léa LEPOIX

The objective is to assess the legal strategies put in place by the legislator in order to prevent (part I) and repress conflict of interest (part II) in the medical field. As legal texts are not special medical law, the applicable provisions are mainly governed by common law.

The drafting method is the traditional methodology of legal sciences, by exposing the legal texts governing offenses, then the constituent elements and finally their repression.

The Mediator case brought to light the problem of conflicts of interest in health. Consequently, the legislator has multiplied the instruments for combating conflict of interest. It has focused more on prevention by instituting ethics and the publication of public declarations of interest rather than on the aggravation of repressive texts. Indeed, a more moral regulation of the links of interest is to be favored rather than instituting a stricter law concerning the links of interest.

Introduction

Integrity is an unclear notion which can be defined in various ways depending on the field or even on relationships. Indeed, intellectual integrity is very different from professional, religious, friendly or romantic integrity.

As such, there is no such thing as an integrity, but there are many forms of integrity that would offer a range of definitions in the shadow of its numerous synonyms: fiscal probity, interpersonal loyalty and moral integrity. All fall under the unalike behaviors of a single person.

Integrity is usually defined as a human quality which refers to a person with good faith or with a behavior which is in compliance with morals and virtue: is considered to be upright someone who does not let himself be corrupted and therefore reliable.

The legal definition of integrity does not exist and the notion is not used in its current form in French legislation.

The notion of integrity, despite not being verbatim mentioned, is expressed through the law. We can provide the instance of the pieces of information found in « sworn statement of tax declaration. » As evidenced by article 103 of French criminal procedure code: « witnesses swear to say the whole truth and nothing but the truth. »

The three-part adage honor-transparency- truth seems to appear to lead us to our subject. At the crossroads of law, morality and politics, according to Emilie DEBAETS, the notion of conflict of interests was first mentioned only in its punitive aspect. It is only later, bit by bit, that the establishment of a law aiming for preventive actions came to be. The loi Bertrand of 2011 established a new book within the French public health regulations, entitled « Règles déontologiques et expertise sanitaire » and puts forward transparency and self-declaration as the main tools to fight against conflict of interests.

Fear that a decision which has to be made may be influenced by personal interests of the decision-maker to the detriment of common good is not something new. In Roman law, the adage « Nemo in rein suam auctor esse potest » (no one can officiate in his own cause) forbade to all policy officers to have the facts when these facts would likely concern his own personal interests.

According to article 431-12 of the French penal code « is a conflict of interest all situation where a public interest and other public or private interests overlap to jeopardize or possibly jeopardize the independent, neutral and unbiased exertion of one's function. » The following article, applied to agents working in public institutions, decrees the same facts.

To have a conflict of interest is not illegal in itself, but abstaining yourself from reporting it or using it as an advantage turn it into a criminal offense. The most media covered criminal offenses are those of influence peddling and of illegal conflict of interest.

In special criminal law, is an illegal conflict of interest the fact that a person entrusted with a public service mission in charge of an operation, takes, receives or keeps any interest in the aforesaid operation. This conflict of interest can either be direct or indirect and this interest can be material, pecuniary or moral (like favoring an acquaintance)

On the other hand, corruption or bribery is a double offense as acceptance of bribes involves the occupation of the corrupted and bribery involves the corrupting.

Bribery consists in offering or accepting to give advantages to a public official — for himself or for someone else — for him to fulfill a deed regarding his functions to use his genuine or alleged influence in order to obtain a favorable decision.

Acceptance of bribes is, for a public official or a person entrusted with a public service mission, to have accepted or requested the proposal. In law, acceptance of bribes is also known under the name of influence peddling.

The criminal offense is observed even if no material elements are produced. Indeed, the mere fact of requesting of accepting the proposal is seen as corruption.

In 1993, France adopted preventive measures against conflicts of interests in the health sector via the Medical Drug Agency by forbidding its members to be involved in the decisions of the committees when they had any bonds of personal interests with the file. In order to insure the minimum respect of this rule, the agency compels its members to declare any bonds of interest with the companies of the sector which are published in the annexes to the annual status report of the agency. Over the years, the agency provided itself with a deontological hub[1].
Those same measures were taken by the law of July 1st, 1998 and were gradually applied to the agencies later created : ANSM, Agence Nationale de Santé et du Médicament (French Agency for the Safety of Health Products), ANSES, agence nationale de sécurité sanitaire et des aliments, de l'environnement et du travail (French Agency for Food, Environmental and Occupational Health & Safety), the French agency of biomedicine and then to the ARS, Agence Régionales de Santé[2].

Following the Mediator trial, legislations turned out to become deeply stepped up towards more verifications.

Now that the terms have been defined, a first part will be dedicated to prevention whilst a second part will tackle repression.

Prevention

In France, the independence of liberal professions is a fundamental component [3] (cf. article R. 4127-5 CSP: the doctor cannot give up in professional independence in any form whatsoever). With regard to this, the French Medical Council, which is bound to ensure the reputation of the profession, witnesses the law seize the deontological mission.

The DPI (public declaration of interest): the law of December 29th, 2011 — also known as the loi Bertrand — extended the obligation to fill up a public declaration of interest. According to the Ministry of Social Affairs and Health, the DPI meets two main purposes:

→ The first aim is to strengthen the transparency of public prosecution by ensuring that the bonds of interests held by decision-makers and health experts are publicized.

→ The second aim is to allow the administration to guarantee the impartiality of the people involved in the decision-making process and in the health expert assessments by proceeding beforehand to the analysis of the declared bonds of interests regarding the study cases or the profession practiced.

In fact, according to article L1453-1 from the French public health regulations, companies making, selling products or providing a service related to the sold products are bound to unveil the precise object, the date, the direct beneficiary as well as the final beneficiary and the amounts of the deals achieved between health professionals and students, health professionals' association and consumers of the healthcare system, healthcare facilities, academies, foundations, learned societies, council societies or organism, legal entities insuring or participating in formal or continuing education. Those companies are bound to publicize any amount, exceeding the threshold set by decree, paid to any of the legal entities aforementioned.

As for health professionals, they must submit a declaration of interest. It must mention any bonds of any sort, directly or indirectly or through another person that the declarant had or had for the last five years preceding his assumption of duties with companies, establishments or organizations which sphere of activities, techniques or products enter the scope of practice of health authorities within which the declarant practices or within the advisory body he is part of, or with the companies or advisory bodies taking part in the same sectors.

This declaration must be update at the initiative of the declarant. To omit or to do a dishonest declaration is an offense punished by article 1452-2 of the French public health regulations : « is punished by a fine of €30000 the fact, for people mentioned in I and II of articles L.1451-1 and L.1452-3, to deliberately omit — in conditions established by this article — to make or to modify a declaration of interest in order to update data featured or to provide false information that scathe the honesty of the declaration. »

Furthermore, people subjected to those measures cannot take part to works, committees and votes of the bodies they are part of unless the declaration is done or updated.

In case of a later revealed conflict of interest, the decision can be overturned after the examination of the litigation by the administrative judge (instance of February 11th, 2011 : French food safety agency went to overturn a decision of the Health Minister as he refused an authorization for a method of water treatment or even the instance of April 27th, 2011, to annul a recommendation of the French Health Authority (HAS) as declarations of interest of members of the group of work were missing) [4].

However, a report from the Court of Audit [5] highlighted the flaws of that system and particularly targets the lack of control of the declared information, the criminal sanctions without real significance and the very restrictive reading of the agreed advantages provided by industrialists to health professionals. In 2016, a second wave which wanted to be, in theory, more strict installed deontological hubs in many institutions (Assistance Publique-Hôpitaux de Paris, French Health Authority (HAS), French national blood service (EFS)). [6]

Regarding the anti-gift measures created by law n° 93-121 of January 27th, 1993 then standardized by article L1453-3 of the French public health regulations: « is prohibited the fact, for people mentioned in article L. 1453-4, of receiving cash or natural advantages in any form whatsoever, directly or indirectly, offered or provided by people mentioned in article L. 1453-5.

This prohibition is also applied to health professionals, psychotherapists, osteopaths, chiropractic students, associations gathering those people and their trainers.

However, it is possible, through exemption and on conditions to allow remuneration, compensation and defrayal of research work, valorization of research, scientific assessment, advisement, service delivery, trade promotion, as soon as payment is in proportion to the service rendered and that the defrayal does not exceed the cost incurred by individuals. It is also possible to allow gifts and munificences, in cash or in kind, intended to exclusively finance research activities, valorization if research or scientific assessments, the hospitality shown, directly or indirectly, during professional or scientific events exclusively or during product launch events or performances as soon as this hospitality is within reason and as long as the financing or the financial participation to professional training activities or career development keep on going.

Until 2017, « as part of pharmaceuticals promotion of medicines to people entitled to prescribe or deliver them, it was tolerated to grant, to offer or promise to those people a bonus, a financial advantage or a benefit in kind unless those are of negligible values » (defined by decree, L-5122-10 CSP).

Due to the vagueness of the law — the decree reckons the amount of €10 — and before the difficulty to arbitrate and the risk of legislative bypass, it was decided to forbid all « gift » whatever its value.

Article 5122-9 from the French public health regulations reckons the free medicines samples cannot be handed to people entitled to prescribe or dispense medications within the scope of pharmacies for internal use on **their request**.
« Those samples cannot contain substances classified as psychotropic or narcotics, or to which narcotics regulations are applied in whole or in part ».
« They must be identical to the proprietary medicines concerned and bear the words “free sample” ».

Moreover, there are different legal obligations, such as the obligation to communicate any contract signed during the practice of their craft:

- The legal obligation stated in article L4113-9 of the French public health regulations : « doctors, dental surgeons, working midwives as well as people applying to registration on the list of the medical order, of dental surgeons or midwives must communicate to the departmental board — of the order they are a part of — all contracts or additional clauses linked to the practice of their craft as well as, if they are not the owners of the equipment nor of the premises in which they practice or will practice, all contracts or additional clauses insuring the use of these equipment or premises. The communication hereinabove expected must be done in the following month after the conclusion of contact or additional clause. The same obligations apply to contracts and additional clauses aiming to pass down on resolutive condition the ownership of equipment and premises.

- R. 4127-105 al.2 of French public health regulation : « a doctor cannot accept a expertise mission in which his own interests are at stake, those of one of his patients, those of one of his kins, of his friends or of a group which usually call on his services ».

- Finally, article L4113-13 decrees to professionals who wish to express themselves during written, televisual or public demonstrations to declare the bonds of interest that tie them with the product or they will be subjected to disciplinary actions.

Repression

Many authors consider that deontology is not efficient enough against the sirens of big groups and that one of the reasons why the Mediator affair was not avoided is because of the very weak self-regulation. Consequently, the law takes the reins in order to prevent similar scandals[7].

Authors agree wholeheartedly with this: « the normative mechanism of the control of conflict of interest enacts rules not in order to make meaning, to make sense, but rather to solve practical difficulties » which leads to a multitude of rules and instances that cannot even totally include each other.[8]

As regards to the conflict of interest, « an individual must detain an interest, direct or indirect, material or moral, which is known thanks to his declaration of interest » and that the latter is in conflict with his mission[9]. This conflict of interest must be quite important for a doubt to exist.

In addition to criminal penalties and flat-fee fines of half a million of euros, or with an amount that can be doubled to the product concerned with the offense, individuals who have put forward their own interests before those of the entrusted mission can be inflicted with ancillary punishments displayed in article 432-17 of French public health regulations.

For the cases provided by the current chapter, the following ancillary punishments can be given:

- Loss of civil, civic and family rights.
- Ban on the exercise of public functions or to exercise the professional or social activity in the pursuit or in connection with the pursuit of the activity in which the offense was observed.
- Forfeiture of the amounts or objects improperly received by the perpetrator
- The display or the publication of the pronounced decision.

In addition to that, a disciplinary action can be executed on the basis of these following articles and lead to the removal of the offender from the council's list.

We can point out some provisions at the disposal of the Medical Council.

- Article R.4127-5: the doctor cannot give up in professional independence in any form whatsoever
- Article R.4127-24: are prohibited for a doctor : entreaty or acceptance of in cash or in kind benefits in any form whatsoever, directly or indirectly, for a prescription or any medical act.
- Article R.4127-27: It is prohibited to a doctor who carries out an elective mandate or an administrative function to use that as a mean to increase his customer base.

Civil actions, in readiness for compensation to injured parties, can also be executed.

Yet, not many decisions are annulled after a conflict of interest: the mechanism of prevention restricts some cases but it is mainly the automatic refusal of the administrative judge to annul all act or decision confronted to the issue of conflict of interest, the latter reckons that such an ideology would strengthen the feeling of widespread suspicion.

Conclusion

The legal and regulatory texts deal with conflict of interest: conflicts of interest exist in each company. For a long time, this type of offense known as white-collar crime was little retained and few trials have taken place on this legal basis. Concerning the conflict of interest in the field of health, but it is only since 2011 and the case of the Mediator that this problem interests the authorities and that they have put in place prevention mechanisms by setting up place of ethics officers and the open-date publication of public declarations of interests.

The legal texts remain common laws for all fields (health, education, food, cosmetology, etc.). These texts do not target the specific problems encountered in the field of health. Conversely, specific texts exist in politics (addition of certain specificities in the criminalization text). However, it is not certain that the law is the best tool in the fight against conflicts of interest in health, and it is probable that the current texts are sufficient. Indeed, the best way to fight against conflicts of interest is to opt for more transparency in the links of interest rather than toughening repression. A better circulation of information, use of pedagogy and a change in practices seem more effective than an unused law.

Finally, it is necessary to wonder if all the links of interest are necessarily reprehensible or even necessarily bad. Cooperation, particularly financial, is essential in the field of health to carry out research projects and innovate under good conditions when public funds do not allow funding of this type of project.

Special thanks

I would like to thank Saaed HENDEI for the time and effort he took to translate this. I am truly grateful for what he did for me.

References

1. Emilie Debaets, Publicité des processus décisionnels: l'exemple de la prévention des conflits d'intérêt en matière sanitaire, *RDSS* 2017.
2. Anne Laude, Xavier Bioy, Didier Tabuteau, Droit de la santé, Presse Universitaires de France - *P.U.F*, 2012, p.102-105
3. Translated from : Définir les conflits d'intérêts – Joël Moret-Bailly – D. 2011. 1100
4. Anne Laude, Xavier Bioy, Didier Tabuteau, Droit de la santé, Presses Universitaires de France - *P.U.F*, 2012, p.102-105
5. La transparence : un outil au service de la prévention des conflits d'intérêts dans le secteur de la santé – David Ginocchi – *RDSS* 2018. 117
6. Les déontologues dans les institutions de santé – Olivier Renaudie – *RDSS* 2018. 91
7. Markus, Conflits d'intérêts et déontologie : l'échec des déontologies existantes et l'improbable (?) succès de la loi Médecine & Droit Volume 2014, Issue 124, January–February 2014, Pages 9-22
8. Taillefait, Le développement contemporain des régimes juridiques des conflits d'intérêts : l'exemple du secteur de la santé, Méd. et droit 1/2014, no 124, p. 3.
9. La transparence : un outil au service de la prévention des conflits d'intérêts dans le secteur de la santé – David Ginocchi – *RDSS* 2018. 117

Education in Vascular Surgery: the ESVS academy experience

5

Ramon VILA COLL, Jonas EIBERG, Leizl Joy NAYAHANGAN

ESVS Academy was founded in 2017 as an evolution of the Education and training Committee with the objective to redesign the way that educational activities were or-ganized during the Annual Meeting (AM). Long courses with traditional lectures were replaced by short hands-on workshops with clear and concise educational objectives. The experience was very successful and the number of workshops and attendees keep growing reaching its peak in Hamburg's AM where the program included 57 work-shops, 112 tutors and more than 900 attendees.

After that the Academy had to go on-line due to Covid pandemic and in 2020 orga-nized 20 interactive sessions during the virtual ESVS month and in 2021 has organized 20 online workshops including remote hands-on on vascular anastomosis and planning and sizing aortic aneurysms.

ESVS Academy has organized its educational activities in disease oriented pathways, such as carotid disease or peripheral arterial disease, offering workshops for different levels of expertise.

To ensure that training is targeted to current trainee needs, the Academy supported a Delphi process among key opinion leaders from 34 countries across Europe to reach consensus on the list of technical procedures suitable for simulation training that should be included in the curriculum of any trainee. Most of these techniques are cov-ered in the Academy workshops during the AM.

To complete the educational circle, the ESVS Academy has promoted the establish-ment of a certification system in vascular ultrasound and the development of an objec-tive system to evaluate practical and theoretical competence.

Introduction

The recently revamped mission and vision statements of the European Society for Vascular surgery (ESVS) define that the Society has the mission of improving vascular health for the public benefit and to achieve this, the vision is to be the leading training organisation with standardised and recognised education pathways.

Education and training have always been the core of ESVS. More than 10 years ago, a dedicated committee was established with the responsibility to organise the workshops at the Annual Meeting (AM) and also workshops and symposia throughout the year. The activity of this education and training committee grew rapidly and in January 2017, an extensive rethink of the ESVS educational program and the activities of this committee especially during the AM was conducted. The committee was renamed "ESVS Academy" and the cornerstone of its innovative program was the fundamental principles that every ESVS attendee should be able to create his/her individualised training program, that small interactive workshops are better than lectures in auditoria, and that hands-on training, including simulation, is better than theory alone.

In parallel to training activities, the Academy supports educational research studies to ensure evidence-based training programs. We started with a needs assessment involving European key opinion leaders to achieve consensus regarding the technical procedures that should be included in future simulation-based curricula in vascular surgery. As a follow-up, an on-going study is exploring how these procedural skills are taught in various countries and what the barriers and facilitators are that might play a role in the implementation of simulation-based training in Europe.

To complete the education and training circle, the Academy has also embraced an initiative to assess skills and competences after training. This path started with the certification of competence in vascular ultrasound (CCVUS) which will be explained below. We will continue to establish certification programs for other basic skills such as basic vascular anastomosis.

Evolution of the ESVS Academy

ESVS Annual Meeting, Lyon 2017

In 2017, the educational ambitions in connection with the Annual Meeting were revised, and the ESVS Academy was founded. One of its main objectives was to replace the training courses held during the AM which mostly included long traditional lectures with short and dedicated hands-on workshops or interactive case discussions with clear learning objectives.

The ESVS Academy was founded with the commitment to provide premium education in the fields of vascular medicine and vascular surgery (endovascular and open) and offer training in seven educational tracks or areas: endovascular, open, venous, diagnostics, human relations, science, and vascular medicine. Within each area, the ESVS Academy provides short workshops with several levels of complexity (basic to advanced) for trainees and young and senior consultants who want to see, touch, and ask questions about products and participate in detailed simulations or interactive case discussions. Clear objectives are defined for each workshop and the number of participants is kept small. Passionate educators share their knowledge and expertise, including tips and tricks during these fundamentally interactive sessions. Each educational area is organised and overseen by the ESVS Academy. ESVS Academy workshops are organised in collaboration with the industry, offering high quality education with minimal commercial bias, and in compliance with both Union Européenne des Médecins Spécialistes (UEMS) standards and the MedTech Code of Ethical Business Practice. The annual ESVS meeting in Lyon 2017, with >30 workshops and an attendee rate of 90%, reflected the success of this new training strategy of the ESVS Academy. Compared to the European Training Committee in 2016, the numbers of workshops, available seats, and participants have increased in 2017's Academy by 500%, 400%, and 350% respectively, making the ESVS Academy one of the fastest growing educational events for (endo) vascular enthusiasts in the world. The overall experience in Lyon was positive[1].

ESVS Annual Meeting, Valencia 2018

In 2018, the ESVS Academy arranged 44 workshops that were attended by delegates from nearly 60 nations, more than half were under 40 years and a trainee to specialist ratio of 2:3 was observed. There is no doubt that the ESVS Academy has had a significant impact on the rejuvenation of the Annual Meetings witnessed over the last years[2].

ESVS Annual Meeting, Hamburg 2019

The focus on education by the ESVS continued to strengthen during the Annual Meeting in Hamburg. ESVS Academy held the largest educational programme so far, with 57 workshops and interactive case discussions delivered within 48 hrs (Wednesday and Thursday). The workshops and case discussions were run in eight dedicated rooms situated in a separate hall next to the scientific lecture and Exhibition halls (Figure 1). This huge offering involved 112 experienced and dedicated convenors from all over Europe and beyond and was very well attended by more than 900 delegates.

Figure 1: Hands on workshop in Hamburg.

ESVS Annual Meeting, 2020 and 2021

In 2020, the Academy prepared a program with 56 sessions (45 workshops and 11 interactive case discussions with more than 1000 seats and the involvement of more than 100 tutors, however the COVID-19 pandemic forced the cancellation of any in-person event and therefore, we went online, organizing 20 interactive sessions scheduled before or after the main sessions of the ESVS Month. These educational sessions were based on clinical case discussions and educational contents that covered the full spectrum of the seven Academy tracks. Delivering these educational sessions online allowed us to increase the capacity of attendees with an average of 30 viewers per session who stayed connected during the full session (average of 56 minutes per session).

In 2021, the willingness to organise an onsite event and the unpredictable extent of regulations that would be in place led the ESVS to prepare an Annual Meeting with limited audience, which reduced the ESVS Academy program accordingly. This year, the Academy program will consist of 10 on-site hands-on workshops and 6 online sessions of interactive case discussions.

Other ESVS Academy-supported courses

ESVS Academy is continuously evolving and still has a lot to learn and will constantly seek renewal and improvement. The activities and workshops of the Academy not only attract young colleagues to the meetings, but also vascular surgeons with various levels of expertise. It allows the exchange of ideas in a relaxed ambiance, and the possibility of learning of new techniques and finding new opportunities. Additionally, the workshops provide a unique chance to get more people involved in training, to network, and to create powerful contacts and hopefully long-term friendships.

Apart from organizing the educational programs at the Annual Meeting, the Academyhas maintained the organization of longer courses focused on other relevant specialty-specific topics that were not covered by other existing courses. These include the vascular ultrasound courses in Copenhagen and Barcelona and the course on Aortic rupture in Zurich. These are practical courses, with short lectures and extensive hands-on and practical sessions that last 2-3 days and allow participants to gain in depth knowledge of the topic and set the basis for further development of the skills by attendee on his/her own. Most of these courses have reached 10 editions, but in 2020 and 2021, these were cancelled due to the pandemic or were converted to online seminars.

Table 1: Evolution of Academy's activity at ESVS Annual Meetings 2016-2019

ESVS ACADEMY	Copenhagen 2016	Lyon 2017	Valencia 2018	Hamburg 2019
Workshops	9	31	43	57
Participants	85	≈200	631	913
Team	≈36	≈58	70+	112

ESVS Academy Educational Pathways

Looking at the comprehensive list of workshops that were organised, and to help attendees to define or focus the selection of workshops they wanted to attend based on a specific disease or educational objective, the Academy started to define educational pathways. A pathway is a selection of workshops that deal with disease of an anatomical sector or system. This suggested grouping started in Valencia and was more openly announced in Hamburg (Figure 2). We defined 5 clinical pathways and 2 paths to prepare for the Fellow European Board of Vascular Surgery (FEVBS) and CCVUS exams. The clinical pathways were: Aorta, Peripheral artery disease (PAD), venous, carotid and vascular access. Special attention was placed when scheduling the workshops to allow attendees to follow the paths and avoiding crashes or overlaps.

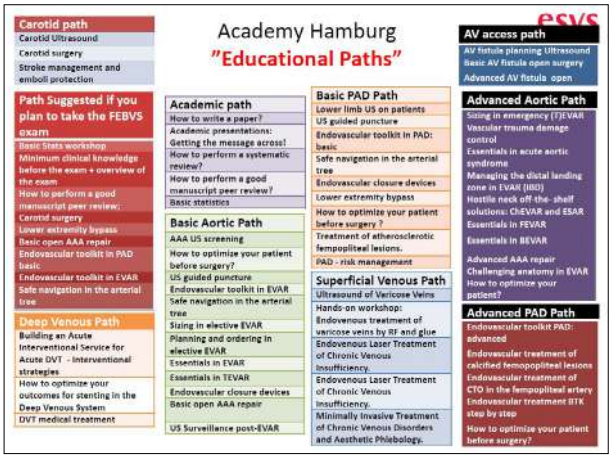
Academy Hamburg
"Educational Paths"
esvs
Carotid path
Carotid Ultrasound
Carotid surgery
Stroke management and emboli protection
Path Suggested if you plan to take the FEBVS exam
Basic Stats workshop
Minimum clinical knowledge before the exam + overview of the exam
How to perform a good manuscript peer review:
Carotid surgery
Lower extremity bypass
Basic open AAA repair
Endovascular toolkit in PAD basic
Endovascular toolkit in EVAR
Safe navigation in the arterial tree
Deep Venous Path
Building an Acute Interventional Service for Acute DVT - Interventional strategies
How to optimize your outcomes for stenting in the Deep Venous System
DVT medical treatment
Academic path
How to write a paper?
Academic presentations: Getting the message across!
How to perform a systematic review?
How to perform a good manuscript peer review?
Basic statistics
Basic Aortic Path
AAA US screening
How to optimize your patient before surgery?
US guided puncture
Endovascular toolkit in EVAR
Safe navigation in the arterial tree
Sizing in elective EVAR
Planning and ordering in elective EVAR
Essentials in EVAR
Essentials in TEVAR
Endovascular closure devices
Basic open AAA repair
US Surveillance post-EVAR
Basic PAD Path
Lower limb US on patients
US guided puncture
Endovascular toolkit in PAD: basic
Safe navigation in the arterial tree
Endovascular closure devices
Lower extremity bypass
How to optimize your patient before surgery ?
Treatment of atherosclerotic fempopliteal lesions.
PAD - risk management
Superficial Venous Path
Ultrasound of Varicose Veins
Hands-on workshop: Endovenous treatment of varicose veins by RF and glue
Endovenous Laser Treatment of Chronic Venous Insufficiency.
Endovenous Laser Treatment of Chronic Venous Insufficiency.
Minimally Invasive Treatment of Chronic Venous Disorders and Aesthetic Phlebology.
AV access path
AV fistula planning Ultrasound
Basic AV fistula open surgery
Advanced AV fistula open
Advanced Aortic Path
Sizing in emergency (T)EVAR
Vascular trauma damage control
Essentials in acute aortic syndrome
Managing the distal landing zone in EVAR (IBD)
Hostile neck off-the- shelf solutions: ChEVAR and ESAR
Essentials in FEVAR
Essentials in BEVAR
Advanced AAA repair
Challenging anatomy in EVAR
How to optimize your patient?
Advanced PAD Path
Endovascular toolkit PAD: advanced
Endovascular treatment of calcified femopopliteal lesions
Endovascular treatment of CTO in the fempopliteal artery
Endovascular treatment BTK step by step
How to optimize your patient before surgery?

Figure 2: Hamburg's pathways.

In response to the shift to online courses because of the COVID-19 pandemic, the Academy prepared a year-long program of more than 30 online workshops focused on three educational pathways (Table 2): Aorta, PAD and venous disease. Each pathway included workshops on diagnosis, medical treatment and open and endovascular treatment. Duplex workshops were performed with live transmissions of an ultrasound exam and discussion among tutors and attendees of the pitfalls of each examination. To train on venous laser ablation, we organised a live transmission from an operating room with the possibility to directly interact with the surgeon. And to deliver hands-on online, we organised two series of workshops that allowed the participants to attend the workshop and perform the activities from their homes under the remote supervision of tutors. The first series was devoted to train on planning and sizing aortic aneurysms using dedicated software that delegates had to install in their computer and that tutors could remotely control to guide them through the different steps of the procedure. The other series of 4 workshops were dedicated to train basic anastomosis skills using simulation models. In this case, the remote training was achieved by sending kits to the attendee's home or hospital (Figure 3). These kits included instruments, a surgical model (arterial bifurcation with plaque inside), graft segments and sutures. During the online sessions, attendees were divided in small groups and were asked to

Table 2: 2021 Annual program of ESVS Academy

ESVS ACADEMY PROGRAM 2021											
January	February	March	April	May	June	July	August	September Annual Meeting	October	November	December
AORTIC DISEASE PATHWAY											
		Importance of Duplex in Aorto-iliac disease: screening to treatment & follow up		**Endovascular toolkit** for endovascular aortic procedures				Essentials in elective EVAR			
		Planning and sizing How to use software	**Planning and sizing** Elective EVAR	**Planning and sizing** Emergent EVAR	**Planning and sizing** TEVAR Elective, emergent, dissection			Essentials in complex endovascular aortic procedures			
	MARZ 10th anniversary							Trauma Damage Control			
								Percutaneous Access for EVAR/TEVAR: femoral, axillar, brachial		Open Aortic Surgery (basic)	
								Open Aortic Surgery (complex)			
VENOUS DISEASE PATHWAY											
	Patient with CVD Presentation, examination, treatment planning		**EVLA** How to do it safely and efficiently	**Patient with CVD** Which method should you choose for the treatment				**Deep veins stenting** How to do it safely and efficiently	**Glue/RF** How to do it safely and efficiently	**Management of DVT and PTS** Interventional and conservative treatment	**MOCA** How to do it safely and efficiently
								Venous US (development of 1st webinar from Venous pathway)			
PAD PATHWAY											
		Optimizing medical treatment for chronic PAD (ICD)		**Endovascular toolkit** for PAD	Best medical treatment postintervention			**Safe navigation** in the arterial tree		**BTK Endovascular treatment** Tips and tricks	
			Open Surgery Toolkit	Basic Vascular anastomosis	Basic Vascular anastomosis			Lower limbs arterial duplex	Basic Vascular anastomosis		
								Endovascular *treatment* of complex calcified/CTO lesions			

focus their cameras on the model and to perform the technique with the help of a local assistant. This allowed tutors to watch what the attendees were doing and advise or teach how to perform it properly. This advice was shared among the participants of the small group. The key to success of these courses were to make small groups of 3-4 attendees per tutor which allowed for close supervision and interaction. This first experience of online delivery of hands-on training has been extremely successful and will probably be maintained as an adjunctive system to deliver education and training to people unable to attend the Annual meeting. It can also be pre-learning that can be further developed and improved during the in-person meeting. This "extended" Academy program with workshops organized along the year and not only during the Annual Meeting fostered the implementation of the Educational Pathways that had been proposed since 2018. The Academy programme for 2021 has covered only three pathways (aorta, PAD and venous) and for 2022 the plan is to start the remaining two (Carotid and vascular access).

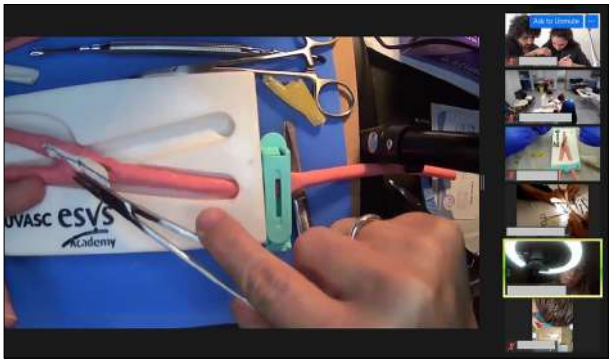

Figure 3: Image of the online hands-session of the Basic Anastomosis Workshop.

Defining curricular content for simulation-based education in vascular surgery

The selection and development of the comprehensive training programs of the Academy have always been based on intuitive or subjective criteria of the educational track leads and the available simulation equipment. To ensure that training is targeted to current trainee needs, there was a need to achieve consensus amongst key opinion leaders on a prioritized list of technical procedures that should be developed as simulation-based training programs and would define a simulation curriculum for in vascular surgery.

Simulation, defined as a situation in which a particular set of conditions is created artificially to experience something that could exist in reality, has gained popularity in surgery since the early 1990s. Learning open vascular and endovascular skills outside an operating theatre, hybrid, or angio suite allows trainees to develop skills in a non-threatening stress-free environment, without distraction, in a structured manner, free of adverse consequences to actual patients. Over the last two decades, several specialties have embraced simulation technology for clinical skills training to comply with patient safety concerns, reduce medical and surgical errors, and observe cost effective patient centered care [3,4].

The current European healthcare system is faced with several challenges in terms of delivery of effective vascular surgical education especially that vascular surgery has evolved into an independent specialty with highly technical and complex procedures [5]. Furthermore, vascular surgeons in training need to cope with the introduction of the European Working Time Directive, shortened residency training time, and the recent surge of endovascular procedures and decreasing number of open procedures. New training strategies have been introduced to address these challenges and ensure efficient training for vascular surgeons [6]. It is critical to implement structured and efficient educational strategies to ensure that vascular surgeons are proficient in open and endovascular procedures.

The development of an efficient curriculum should follow a systematic approach instead of relying on available simulators, on the training lead's specialty or interests, or merely by coincidence. It should start with problem identification and a general needs assessment (GNA) to identify training needs. This process helps to identify the procedures that should be taught before defining how to teach them.

In 2018, a Delphi process was initiated among 189 key opinion leaders (KOL) from 34 countries across Europe who were identified according to their positions in the ESVS, the European Journal of Vascular and Endovascular Surgery (EJVES), and the UEMS Section and Board of Vascular Surgery [7]. The modified Delphi method consisted of a three-round online iterative survey questionnaire: Round 1 was a brainstorming phase to identify technical procedures that a newly qualified vascular surgeon should be able to perform. Round 2 investigated how frequent the identified procedures are performed, the number of vascular surgeons that should be able to perform these procedures, whether the procedures pose a risk to the patients, and whether simulation-based education is feasible. Round 3 was elimination and re-ranking of the procedures. Consensus agreement was defined as procedures gaining more than 70% support were to be included. An international steering group consisting of open and endovascular surgeons and medical educators governed the process.

The final result after the three rounds was a prioritized list included 30 technical procedures for simulation. The top five procedures focus on basic open vascular skills, basic endovascular skills, vascular imaging interpretation, femoral endarterectomy, and open peripheral bypass. The list of procedures that were finally selected is presented in Table 3, highlighting those that are covered in the Academy's program.

Table 3: List of procedures identified in the GNA for simulation training.
(Highlighted in yellow are already covered in Academy's workshops)

Basic open skills (anastomosis training, instruments, sutures, prosthesis, clamping techniques, patches)
Basic endovascular skills (endovascular tools, radiation safety, US access, arteriography)
Vascular imaging interpretation (arteriography, CTA and MRA)
Femoral endarterectomy (profunda plasty, patch)
Open embolectomy of upper and lower limb
Peripheral bypass (Infrainguinal, above knee, below knee, crural, intraoperative flow measurement)
Aortoiliac angioplasty
Basic EVAR and sizing
Carotid thromboendarterectomy (CEA)
Open AAA resection (tube or bifurcated graft)
Above knee angioplasty
Basic vascular ultrasound (aorta, varicose veins, DVT, fem-pop, bypass, pseudoaneurysms)
Open management of ruptured AAA
Endovascular closure devices
Vascular access surgery, hemodialysis (radiocephal fistula, brachiocephal fistula, fistula thrombectomy)
Endovascular management of ruptured AAA (EVAR, REBOA)
Endovenous management of varicose veins
Open management of vascular trauma
Open management of varicose veins
Basic TEVAR (aneurysm) and sizing
Minor amputations (finger, toe, forefoot)
Aorto-bifemoral, aorto-biiliacal and iliac-femoral bypass due to occlusive disease
Fasciotomy
Below knee angioplasty
Extra anatomical bypass lower limb (fem-fem, axillo fem, obturator)
Open resection of femoral and popliteal aneurysms (medial/posterior approach)
Open management of pseudoaneurysms
Endovascular management of pseudoaneurysms (trombin injection, covered stent)
Endovascular management of vascular trauma
Angioplasty of vascular access for hemodialysis

Most of the techniques that were identified as suitable for simulation training have been included in the workshops of the Academy, and the few remaining will be included in the next few years. It is acknowledged that a short workshop does not cover the needs for simulation training of trainees but it could be very helpful to start such program in the attendees' institution. The kits provided for the current online hands-on workshops can be used many times and could also help to establish simulation-based training programs without the need for big facilities in countries or institutions where it would have never been possible.

Currently, the same research group that performed the general needs assessment in 2018 is conducting a study to explore the current training environment in vascular surgery in Europe, including the availability of simulation-based education, and to expose facilitators and barriers associated with its implementation.

Certification of competence in vascular ultrasound

The ESVS Academy is committed to improve and expand the knowledge and quality of performance in Vascular Ultrasound (US) by organizing accredited workshops to facilitate the training and education of vascular health professionals in Europe. This is in response to vascular ultrasound becoming a cornerstone in vascular surgery and an essential part of screening programs, preoperative work-up, intraoperative quality control, and postoperative follow-up. Well-trained and competent vascular US operators are needed to ensure correct diagnosis derived from high quality examinations and interpretations. Structured training and assessment of competence are imperative. The need for training basic vascular US was identified in the needs assessment that were performed in Denmark [10] and across Europe [7]. At current, trainees learn vascular US during their daily clinical practice while under supervision. However, a major gap in training is how to ensure that the operator has achieved a defined level of competence both in knowledge and technical skills to be able to acquire high sonographic quality, image optimization and interpretation. Assessment of competence is critical to ensure that a trainee progresses from the training environment to the clinical setting where patients are at stake.

The need to certify operators who meet the minimum requirements to perform basic vascular ultrasound has become a priority of the ESVS Academy. In 2018, we initiated a certification program to assess basic vascular ultrasound competences and ensure that an operator is ready to progress towards independent practice, the certification of competence in vascular ultrasound (CCVUS). To qualify for the exam, the candidates should submit a logbook that provides an overview of supervised and independent US examinations.

The CCVUS examination consists of two parts- a theoretical and practical tests. For this purpose, the Assessment of basic Vascular Ultrasound Expertise (AVAUSE) tool was developed by five vascular US experts, which includes both theoretical and practical tests covering the most important US examinations within the vascular curriculum. [11] The first part is a 50-item theoretical test (multiple choice test) with focus on physics, haemodynamics, technology and US instrumentation, and the second part is a practical exam in which two examiners evaluate the applicant's practical skills according to an objective scoring system. CCVUS is a high-stakes international certification with potential consequences for both the trainees and their future patients. Solid validity evidence was therefore gathered to support the proposed use of AVAUSE and ensure that the interpretation of scores and decisions based on the results were trustworthy, defensible, and repeatable over time. Pass-fail score for each of the component to support decisions for certification were also established.

Validity investigation for the theoretical test and two practical tests- carotid and superficial venous incompetence (SVI) ultrasound examinations- was performed during the ESVS Annual meeting in Hamburg in 2019 (Figure 4). Vascular surgeons, vascular surgical trainees, sonographers and nurses with varying experience levels took the CCVUS. The theoretical test was held in the auditorium and were supervised by members of the Academy. The participants worked on individual computers and were given 60 minutes to complete the test. For the practical test, two stations were set for carotid examinations and two for SVI. Eight raters were assigned in pairs in each station. The theoretical pass-fail score was 29 out of 50. The rater-set pass-fail scores were 3.0 points for carotid and 3.0 points for

SVI examinations. In total, 10 participants passed both the theoretical and practical tests and were certified. The results showed that the AVAUSE is a useful tool system to assess competences in basic vascular ultrasound, demonstrating that operators can progress towards independent practice.

Participants must pass all three components (theoretical test and two practical tests) to be an ESVS certified operator in basic vascular US. A certification in basic vascular US indicates that the experienced operator is able to demonstrate satisfactory technical skills, is able to scan without direct supervision, and has the decision-making skills to call on expert supervisors when needed.

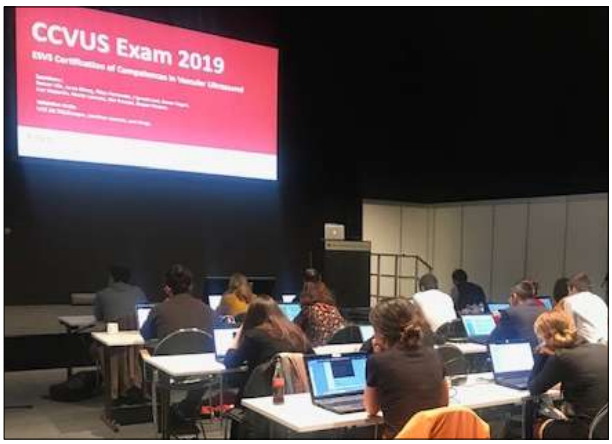

Figure 4: Certification of Competence in Vascular Ultrasound Exam 2019.

Since its implementation in 2018, the CCVUS examination has only been held two times and only 21 candidates have been granted the Certificate of competence in Vascular Ultrasound. The editions of 2020 and 2021 were cancelled due to the pandemic. We look forward to being able to organise a CCVUS examination during the ESVS Annual Meeting of 2022.

Conclusions

ESVS Academy is one of the most active committees of the ESVS. Since 2017, its offer of simulation-based training grew exponentially until it was interrupted by the COVID-19 pandemic. Despite this, the Academy has found ways to continue delivering education and even virtual hands-on training by establishing structured programs for the whole year. These are organised in educational pathways to extend and provide continuity to the education delivered during the Annual Meeting. Following the general needs assessment performed and published in 2019, the ESVS Academy is also in full-support and is helping to explore the current training situation in Europe, to seek ways on how to improve it, and to expose barriers and facilitators to implementation. Going even further, it has started to implement a certification system of competence in vascular Ultrasound as a first step towards a comprehensive system of skills certification in Vascular Surgery.

References

1. Eiberg J, van Herzeele I. From European training Committee to ESVS Academy: the start of a new paradigm in ESVS education. *Eur J Vasc Endovasc Surg* 2018; 56: 157-8.

2. Eiberg J, Vila R, van Herzeele I, The ESVS Academy is Growing. *Eur J Vasc Endovasc Surg* 2019; 58: 1-2

McGaghie WC, Issenberg SB, Cohen ER, Barsuk JH, Wayne DB. Does simulation-based medical education with deliberate practice yield better results than traditional clinical education? A metaanalytic comparative review of the evidence. *Acad Med* 2011; 86: 706-11.

3. Khamis NN, Satava RM, Alnassar SA, Kern DE. A stepwise model for simulation-based curriculum development for clinical skills, a modification of the six-step approach. *Surg Endosc* 2016; 30: 279-87.

4. Mitchel EL, Arora S, Moneta GL. Ensuring vascular surgical training is on the right track. *J Vasc Surg* 2011; 53: 517-25.

5. Goldstone J, Wong V. New training paradigms and program requirements. *Semin Vasc Surg* 2006; 19: 168-71.

6. Nayahangan L, Van Herzeele I, Konge L, Konkar I, Cieri E, Mansilha A, *et al.* Achieving consensus to define curricular content for simulation-based education in vascular surgery: a European wide needs assessment initiative. *Eur J Vasc Endovasc Surg* 2019; 58: 284-91

7. Eiberg J, Konge L, Vila R, Sillesen H. How vascular surgeons can learn ultrasound. *Semin Vasc Surg* 2019; 32: 33-40.

8. Eiberg JP, Hansen MA, Gronvall Rasmussen JB, Schroeder TV. Minimum training requirement in ultrasound imaging of peripheral arterial disease. *Eur J Vasc Endovasc Surg* 2008; 36: 325-30.

9. Nayahangan LJ, Konge L, Schroeder TV, Paltved C, Lindorff-Larsen KG, Nielsen BU, *et al.* A national needs assessment to identify technical procedures in vascular surgery for simulation based training. *Eur J Vasc Endovasc Surg* 2017; 53: 591-9.

10. Nayahangan L, Vila R, Lawaetz J, Leal Lorenzo JI, Bredahl K, Lawaetz M, *et al.* European Society for Vascular Surgery (ESVS) Certification of Theoretical and Practical Competences in Basic Vascular Ultrasound: Validity Investigation of the Assessment Tools. *Eur J Vasc Endovasc Surg* 2020; 60: 933-41.

The Vascupedia experience

6

Giovanni Federico TORSELLO, Giovanni Battista TORSELLO

With the advent of online learning, vascular education evolves from textbooks and lectures to a more flexible form of gathering information. Today, educational material is dispersed via the web to physicians, regardless of where they practice or how much money they can spend on education.

The aim of Vascupedia (www.vascupedia.com) is to boost the vascular educational level with evidence-based medicine and to contribute to patient's safety and well-being.

During the last 3 years, vascular specialists from 181 countries, mostly from Europe and USA but also from Latin America and Asia, used the platform to gain free and state of the art information on vascular topics.

Introduction

A well-trained vascular specialist is an important premise for a safe and effective patient treatment. Due to the rapid development of new technologies and to the increasing complexity of vascular procedures, education and training in Vascular Medicine becomes an import role.

In the past, attending congresses or reading scientific journal or books were the traditional way of medical education. Today, due to the continuous introduction of new techniques and technologies modern disease management requires a quick update of knowledge. Vascular specialists need a specific and comprehensive answer to a specific question around a vascular problem. The solution should be industry-independent, easily accessible and 24/7 available.

Vascupedia – Structure of the e-learning platform

In 2018 a multidisciplinary vascular team created a global educational e-learning platform in order to cover questions about patient management, troubleshooting, complications and non-product related decision making. Vascupedia was introduced for helping vascular specialist treating their patients in a safe and effective way.

The internet platform consists of three virtual rooms (Figure 1): Main Arena, CME Corner and Exhibition Area.

In the *Main Arena* users can found scientific presentations as PowerPoint or Video file. The contributions undergo a review process before they are uploaded. The presentations are in English, worldwide accessible and free for everyone. Registered users can upload scientific materials and make comments or report on their own experience.

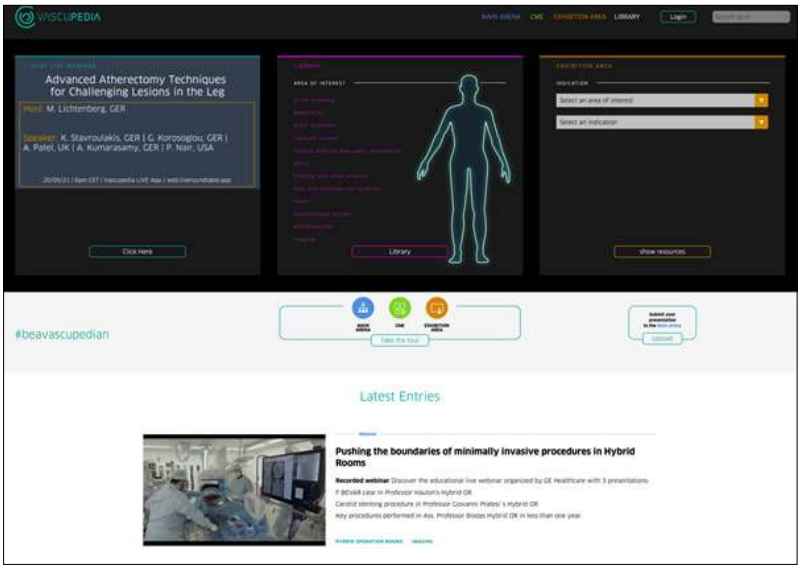
VASCUPEDIA
Advanced Atherectomy Techniques for Challenging Lesions in the Leg
#beavascupedian
Latest Entries
Pushing the boundaries of minimally invasive procedures in Hybrid Rooms

Figure 1: Structure of the internet platform Vascupedia.com

In the Continuing Medical Education *(CME) corner* the users can find courses on different topics planned and implemented in accordance with the accreditation requirements and policies of European authorities. The target audience for this CME activity is the physician who specializes in vascular surgery, interventional radiology, vascular medicine, cardiothoracic surgery, and interventional cardiology.

Upon completion of the course the participants should be able to reach predefined educational objectives and correctly answer the questions of the self-assessment. This is achieved by a quiz which consists of multiple-choice questions. For each question one answer is the best one. Each question is allocated equal marks and no negative marking will be made. To pass the quiz it is needed to answer 70% of questions correctly. If the learner has not met the pass mark, he may take the quiz again. The time limit is 30 minutes.

As accredited provider of continuing medical education, VASCUPEDIA requires to obtain the disclosure of any financial interests in biotech, medical device, or pharmaceutical companies. The faculty involved in the CME activity may not receive payment directly from a commercial interest. Additionally, faculty are required to disclose to learners when products or procedures being discussed are off-label, unlabeled, experimental, and/or investigational and any limitations on the information that is presented, such as data that are preliminary or that represent ongoing research, interim analyses, and/or unsupported opinion. At the end of the course participants should complete a feedback form.

Finally, in the *Exhibition Area* registered companies provide a comprehensive and credible product information according to the indication for use. All companies are equally presented in alphabetical order. Hence, every Vascupedian has a fair overview of all manufacturers regardless the size of the company or number of the products.

Conclusion

After three years 69.550 users from 181 countries visited the website and more then 4000 healthcare professionals were registered. The numbers show that Vascupedia is filling a relevant gap in the daily practice of vascular specialists worldwide keeping a complementary role to the traditional way of education.

Which curriculum for trainees' education in vascular surgery? The GEPROVAS experience

7

Anne-Florence ROUBY, Nicole NEUMANN, Lucille TREIL, Salomé KUNTZ, Anne LEJAY, Tristan BOURCIER, Nabil CHAKFÉ

The "Groupe Européen de recherche sur les PROthèses appliquées à la chirurgie VASculaire", GEPROVAS, works on four platforms about implantable medical devices (IMD): test and research, education, clinical follow-up and explants.

Education is a crucial part of GEPROVAS' activities since vascular surgeons, trainees and confirmed surgeons must be familiar with an increasing number of IMD and evolving intra-operative technologies.

Although simulation has proven its efficiency in many fields as aeronautics, medical simulation is still young. However, studied showed a major interest of simulation for technical procedures. In addition to its educational program based on endovascular simulation, the GEPROVAS is now focusing on four development axes: promoting clinically-relevant academic programs, rediscovering training in open surgery, optimization of assessment and stress management in surgery or well-being in education.

GEPROVAS

The "Groupe Européen de recherche sur les PROthèses appliquées à la chirurgie VASculaire », GEPROVAS, created in 1993, is a non profit association first dedicated to the study and analyse of implantable medical devices (IMD) used in vascular surgery. The group mainly focused its expertise on explanted vascular grafts and endografts analysis. In the 2010's, the group became more professional being ISO 9001 and ISO 13485 certified, and introduced the concept of the "cycle of IMD" that became the cornerstone of the project. The cycle of IMD concept is based on the necessity to have a global approach associating: 1. Test platforms, 2. Education, 3. Post-market clinical studies, 4. Explants analysis. (Figure 1)

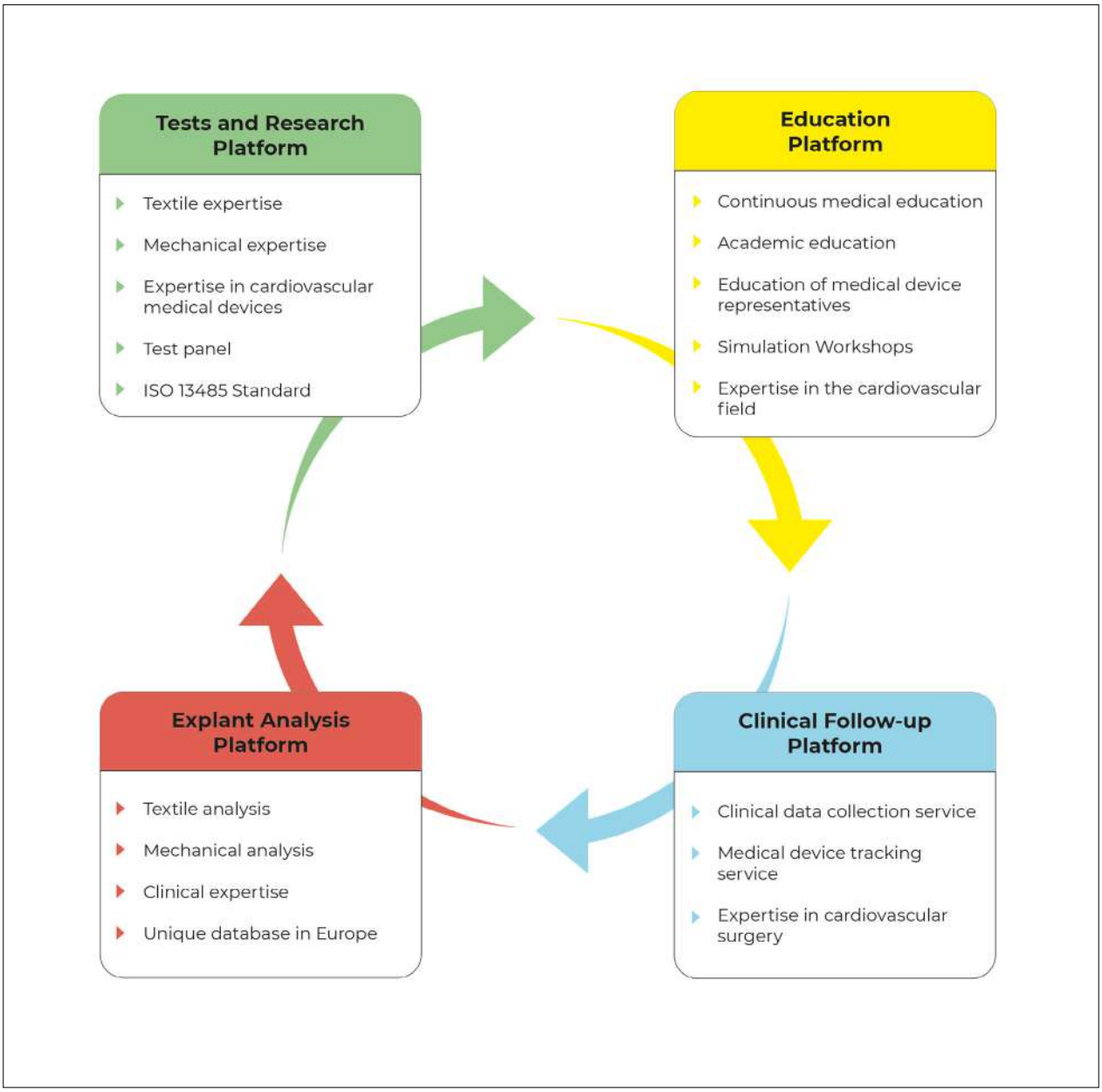

Figure 1: The cycle of implantable medical devices developped by GEPROVAS.

Including education is mandatory since vascular surgeons must be familiar with an increasing number of IMD for more complex procedures, particularly for endovascular procedures. During their whole curriculum and professional activities, vascular surgeons need to update their knowledges on IMD and sophisticated intra-operative technologies.

Simulation in vascular education

Simulation has proven its efficiency in many technical fields. First simulators have been developed for the aeronautic industry at the beginning of the 20th century[1]. Real flight hours are still performed during pilot training but simulators are mandatory to train for rare scenarios and maintain the pilot skills.

In the medical field, teaching was based for centuries on companionship at the patient's bed rather than simulation. In order to avoid direct training on patients, simulation provides a safe and controlled environment to apply theoretical knowledge, to develop practical skills and to build trainee's confidence. By confronting the trainee to a wide range of scenarios, simulation makes it possible to master procedures in a shortened period.

Simulation has proven to be particularly efficient for technical procedures such as central venous catheter placement, emergency airway management, laparoscopic surgery, bronchoscopy or pleural drainage[2-7].

Further than pure technical skills, simulation enables to learn non-technical skills in high-fidelity environment: operative planning and decision-making, effective communication for teamwork and leadership, resources organization and stress management in standard procedures or crisis.

As in aeronautics, medical simulation cannot fully replace the actual operating room (OR) experience, especially concerning the lack of emotional impact on the machine compared with a real patient. However, the improvement of simulator technology and Virtual Reality (VR) makes it possible to build simulation-training programs going from trainees learning the basic skills for handling guidewires and catheters to experienced surgeons seizing the opportunity to practice difficult cases with patient-specific procedures.

Trainees' formation has drastically evolved in the past decades due to the European Working Time Directive and the growing technical innovations. Endovascular procedures take a major place, creating the need for adequate training programs to acquire the endovascular skill set . The rapidly evolving field of endovascular devices and procedures makes it necessary for vascular surgeons to regularly update their skills. Despite acquiring basic technical skills, simulation also allows to shorten the learning curve in endovascular procedures, such as EndoVascular Aortic Repair (EVAR), Thoracic EndoVascular Aortic Repair (TEVAR), renal artery stenting or carotid artery stenting[9-15].

Simulation-based training programs are implemented in trainees' education to ensure the residents own appropriate technical skills at the end of their curriculum[16-18]. Numerous studies proved that VR simulation in a standardized practice[11,19-22] improves surgeons' performance concerning procedure time, fluoroscopy time and contrast volume[23]. Even with the cost associated with VR simulators, the proven benefice of simulation led to fund this kind of program as soon as affordable by institutions, allowing 56% of vascular surgery programs in the US to be equipped[17,24].

To ensure efficient education curricula across Europe, a consensus for simulation-based education was defined in 2019. This consensus defines a list of procedures to prioritize for simulation-based education[25]. In order to assess trainees' performance on simulators, a model of Fundamentals of EndoVascular Surgery (FEVS) was developed that gathers the minimal skill set required to become a modern vascular surgeon[7,17]. The FEVS model successfully differentiates proficient and non-proficient surgeons on performance measures.

To conclude it is actually time to embrace similation in vascular surgical training.[7]

The GEPROVAS appraisal

The GEPROVAS educational program started in 2010.
In addition of its original purpose, four main subjects are being integrated in the program:

- Promoting clinically-relevant academic programs
- Rediscovering training in open surgery
- Optimization of assessment
- Stress management in surgery and well-being in education

Promoting clinically-relevant academic programs

During curricullum, trainees must first acquire basic technical skills related to open or endovascular surgery. Often, basic technical skills training does not require VR simulator. For instance, the Clock Face was developed to train on aortic anastomosis (Figure 2) or the FEVS simulator, ANGIO Mentor TM (Simbionix®, Cleveland, OH, USA) to acquire basic endovascular skills (Figure 3).[26,27]

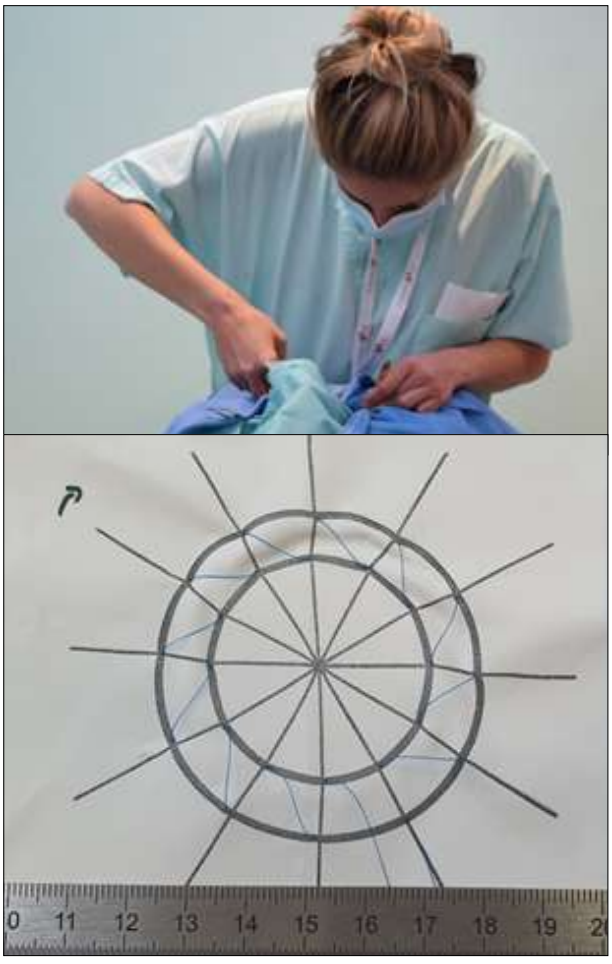

Figure 2: The ClockFace suture exercise.

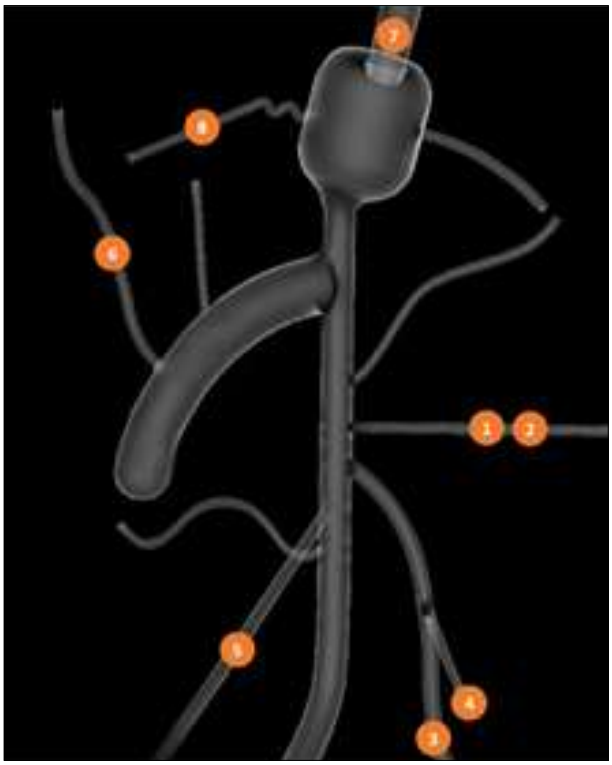

Figure 3: FEVS model providing 8 fundamental tasks to be performed within a limited time: **(1)** Cannulation of the right angle branch (3 min); **(2)** Stable catheter exchange (4 min); **(3)** Navigation up and over a bifurcation (5 min); **(4)** Cannulation of a second order branch (4 min); **(5)** Cannulation of an anterior branch (4 min); **(6)** Cannulation of an arch branch (4 min); **(7)** Gate cannulation (4 min) and **(8)** Cannulation of the branch off of the aneurysmal segment (5 min).

Once the basic skills are reached by a trainee, knowledge of the sequences workflow of specific procedures is mandatory to perform safe clinical procedures. In this second phase, a VR environment is advisable to mimic the OR conditions for trainees and to reproduct clinical procedures. Trainees are assessed with a validated Objective Structures Assessment of Technical Skills (OSATS) files (Figure 4). OSATS evaluates trainees on each procedural phase. In the VR environment, all procedures are recorded to perform a debriefing session at the end. Recordings include hands and back positions of the trainee, fluroroscopy screen and simulator screen (Figure 5).

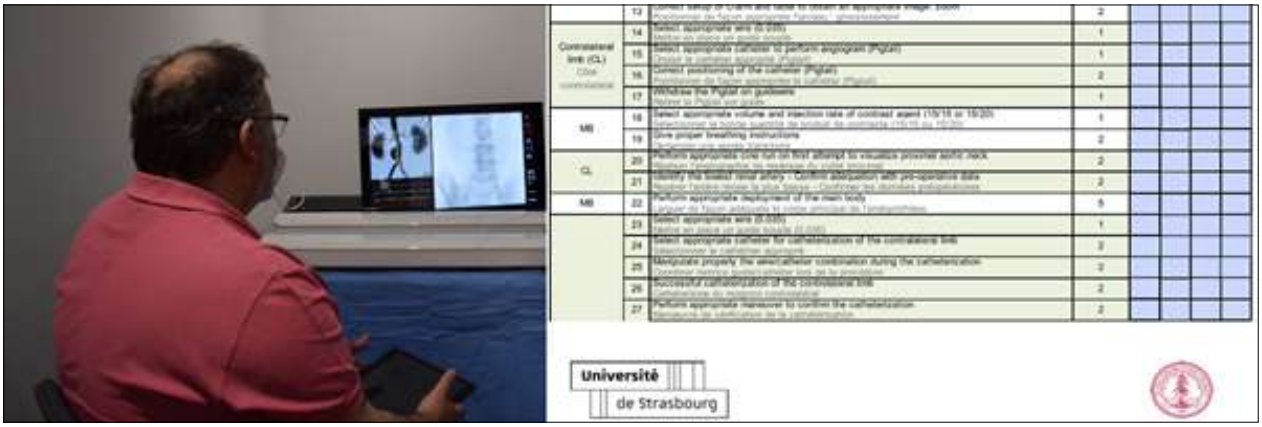

Figure 4: Example of an assessment file developped in collaboration with the department of Vascular surgery at Stanford, Jason T Lee.

Figure 5: Example of a sceenshot during an assessment. Simulataneous recording of the trainee's hands (Left up corner), the trainee's back (rigth up corner), the simulator screen (left down corner) and the fluoroscopic screen (rigth down corner).

The GEPROVAS experience found tasks specific checklist usefull as they allow to evaluate skill acquisition as well as procedural flow knowledge. OSATS combined with video recording allow to point trainees' shortcomings.

For both steps (skills and sequences), lessons alternate with independent evaluation of each trainee at the end of each lesson cycle. At the end, each trainee has an identified learning curve and personnalized points to focus on.

Rediscovering training in open surgery

Since the early 90's, vascular surgery has evolved and endovascular procedures have become the first option for most vascular diseases [8]. This new paradigm raises concerns about trainees being insufficiently prepared for open vascular surgery (OVS) [28, 29].

Then, OVS simulation appears to be a fundamental part of trainees education. Fewer open OR exposition needs to be compensated with adequat simulation to guarantee good clinical outcomes in the future. A good translation of the technical skills learned during OVS simulation is to be expected [30] but it requires expert supervision [31].

Focusing on OVS, there is a multitude of simulators: from simple suture bench [32] to high-fidelity models. These high-fidelity models can be cadaveric [33], animal [34], pulsatile pumps to simulate bloodflow in the makeshift vessel [35, 36] or even in cadavers [37]. The obstacle for high-fidelity model implementation remains their cost and the need for supervision by a trained professional on the simulator in addition to supervising surgeon.

OVS simulation allows trainees to decrease their time to complete an anastomosis, to decrease the number of technical errors during the exercise [38] and to improve their movement process measures such as wrist rotation [32].

Altough, long term retention and long term translation of technical skills in the OR are still to be adressed, it has been put forward that the translation of technical skills in the OR is only partial [30]. This can be explained by the lack of simulation centers reproducing an OR-like environnement. With the GEPROVAS experience, we chose low-fidelity simulators adaptable to several exercises and placed them in an immersive environment mimicking the OR. The objective is to create affordable simulators, which could be upgraded in the future thanks to technology avancements.

As in endovascular simulation, the current standard for trainees' evaluation is the OSATS checklist. However, a study conducted in collaboration with Louisiana State University exposed a significative intra-evaluator and inter-evaluator variability [39]. We submitted 287 pictures of completed Clock Face sutures to be reviewied by 4 experienced surgeons. Then, we asked them to grade the sutures all again with the order of the pictures randomly rearranged. For each picture, scores by each evaluators were correlated (Figure 6) but with a significant variability ($p<0.001$). As shown on Figure 7, the same variability was observed with each evaluator between the two times they evaluated the same picture ($p<0.001$).

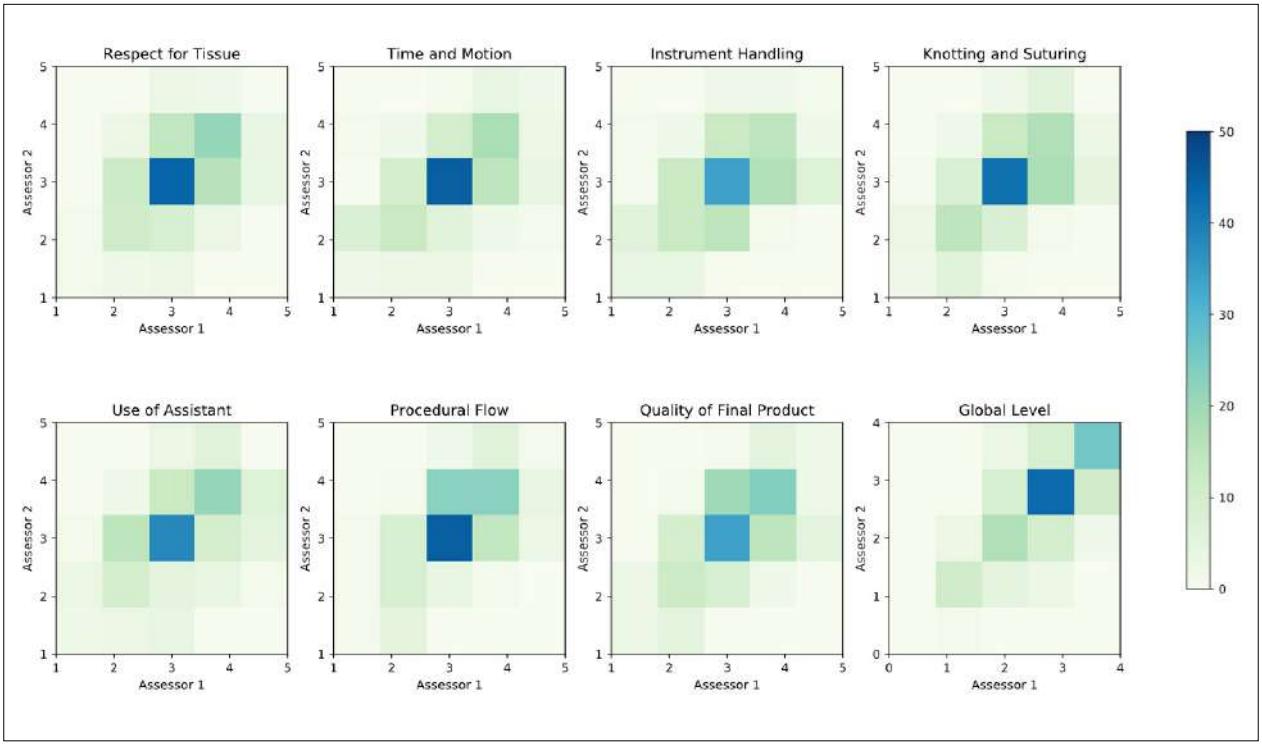

Figure 6: Score distribution between both assessors for the 7 items of the OSATS checklist and the Global Level.

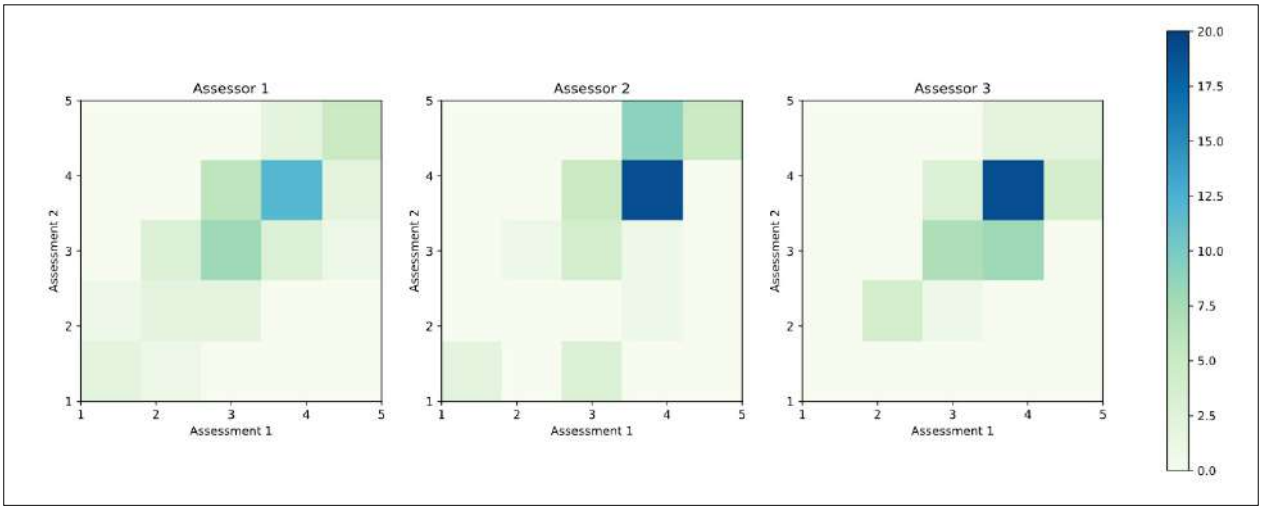

Figure 7: Score distribution for the double assessment by three senior vascular surgeons of 50 randomly chosen ClockFace sutures.

To avoid this variability, we tested a semi-automated process to mesure errors in the Clock Face suture and found a correlation with the score obtained for quality of final product in the OSATS checklist ($p<0.001$).

This has enouraged us to develop objective metrics to measure skills acquisition in trainees.

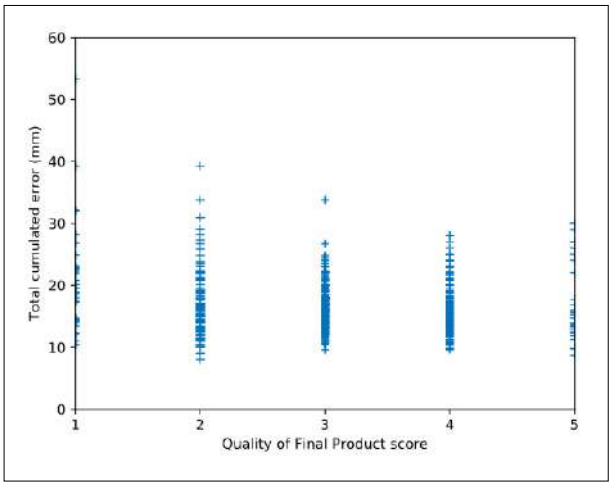

Figure 8: Total cumulated error as a function of the Quality of Final score given by the initial assessor.
This has enouraged us to develop objective metrics to measure skills acquisition in trainees.

Optimization of access to training

In our experience, during unsupervised simulation sessions, trainees tend to make a game out of the case rather than simulating a work scenario. Unconsciously, trainees tend to take shortcuts to go straight to the objective, without taking all the necessary steps to ensure safe and efficient procedures. To provide the best training with the best results, simulation requires a direct contact between the trainee and the expert. To obtain this contact is often the most difficult considering busy and unpredictable clinical schedules on both parts. Most of the time, it is a challenge to free up time for a trainee or for an expert and moreover for both at the same time. If the expert's presence is essential during teaching activities, we believe that his presence can be removed during assessment sessions or skills training. From now on, trainees will be able to come independently to train on the skill lab to enhance its performances between teaching or assessment sessions. With our connected skill lab, the expert (a surgeon from the GEPROVAS network) will be notified of his trainee's independent sessions. The expert will grade these sessions to point progresses and points to focus on on a dedicated app.

Nowadays, multiple simulation devices and training courses are offered by industries. However, these simulators are sold without any follow-up which reduces their long-term use. In order not to consider these highly technological tools as video games, GEPROVAS optimizes their use by constantly adapting them to the environment and by creating and maintaining personalized training courses over time.

Stress and well-being in education

Surgeon stress has wide repercussions going from physician welness to clinical performances. This is a fundamental aspect to study since stress in the OR can lead to errors and undermine patient outcomes. [40-43]. However, stress remains a plural phenomenon with lots of intricated variables from physiologic aspects and cognitive constructs to cultural and environmental considerations.

When facing emotional stimuli, the Autonomic Nervous System (ANS) activates to increase the vigilance. Sympathetic and parasympathetic nervous systems compose the ANS. Heart Rate Variability (HRV) is a noninvasive measure of ANS cardiac control. Pain, fear or anxiety result in a decrease of HRV high frequency indicating decrease of the parasympathetic activity. HRV is transformed into a numeric scale called ANI. Instantaneous ANI values were computed as a function of time by the ANI V2 monitor, commercialized by MDoloris Medical Systems (Lille, France) [40, 44]. Requiring only an electrocardiogram as an entry point, this monitor acquires the ANI signal thanks to a disposable self-adhesive pair of electrodes, one of which is placed on the right shoulder while the other is put at the apex of the heart. ANI was developed for pain evaluation during general anesthesia. ANI can be considered as a vagal tone index, which allows to obtain both a quantitative and qualitative measurement of HRV. De Jonckheere *et al.* demonstrated that a negative stimulus is associated with a decreased ANI and confirmed it as an efficient tool to observe changes in the emotional status. [44]

We studied if simulation could allow residents to reach experienced surgeons' results on fundamental technical skills of endovascular surgery. In order to study surgeons' emotional response during simulation, ANI (Analgesia Nociception Index) was monitored 5 minutes before and during the whole procedure. To guarantee a broader observation of surgeons stress, this physiological metric was studied alondside a self-evaluation questionnaire (the Lickert scale). [45]

In our study, stress self-evaluation was similar in each group with low degree of anxiety. However, ANI monitoring reported significantly different results between groups, showing a significantly lower level of stress for novices and a growing level of stress with experience. Most importantly, stress level at baseline varied significantly between surgeons, regardless of their group or experience. However, everyone presented with the same stress peaks during each task. (Figure 9). Patterns of stress could be identified within the participants' group, especially for the 4th task that is splited into two parts. For each participant, the instanteneous ANI increased at the end of the first part, which means that the level of stress was decreasing, and, as soon as the second part was announced by the simulator, the ANI suddendly descreased.

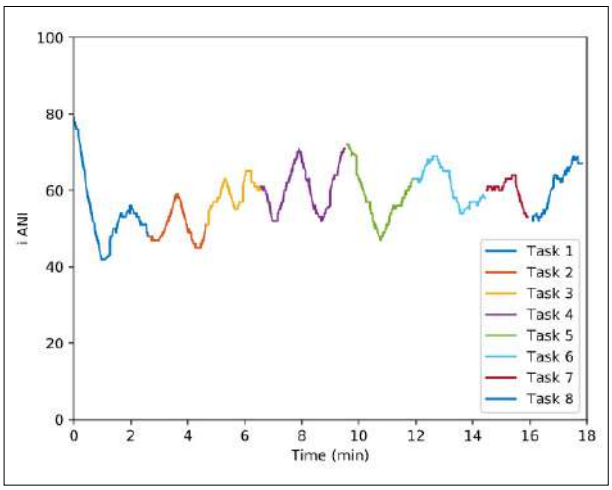

Figure 9: Instantaneous ANI as a function of time for one participant where the ANI during each task is depicted in a different color.

Our results suggested that the discovery of a simulation environment did not impact the subjective and objective level of stress. Indeed, both novice residents and seniors practiced for the first time on this simulator while advanced residents beneficiated from 5 sessions. ANI monitoring showed the lowest stress level among novice residents suggesting that discovering the simulating environment does not induce stress. ANI monitoring among advanced residents suggested that knowledge of the simulating environment and protocol does not protect from stress.

Stress generates positive and negative effects. Reaching an optimal level of vigilance and stress would improve the surgeon's ability but high levels of stress would lead to decreased efficiency and could cause complications. In our study, surgical performance is inversely correlated to stress level, suggesting a positive effect of stress among seniors. These results suggest that with growing experience, levels of vigilance and awareness rise to face the surgery, even in a simulated environment. Seniors have internalized potential complications which could cause their higher objective stress results without altering their subjective evaluations. By contrast, with less real life exposure in the OR and complicated experiences, trainees seem to perform simulation as a game.

Conclusion

In order to practice safer and more controlled procedures, simulation will become a mandatory step in a vascular surgeon curriculum, during the formation and throughout the entire career due to constant technological changes.

Vascular surgery benefits of two complementary therapeutic options: open and endovascular surgery. Each surgery must be mastered to become a 21st century vascular surgeon, having every tool to hold its place in a concurential landscape. In the future, simulation is the only way to achieve this prerequisite for young trainee with less access to OR and more legal implications.

With tremendous simulation possibilities, both in endovascular and open surgery, vascular surgeons can become pioneers of medical simulation and lead other surgical specialties in this field. With an increasing number of studies showing clear trainees' progression after simulation, further studies are mandatory to observe impacts of simulation in the OR and clinical practice.

Furthermore, to guarantee an homogeneous level of practice in a region, a country or even a continent, structured simulation courses need to be implemented by our vascular societies.

Acknowledgments

The authors would like to thank the Eurometropole de Strasbourg and the Région Grand'Est for their financial support.

References

1. Dibley H, Desmorat G. *Petite histoire des simulateurs d'entraînement dans l'aéronautique, Risque Sécurité Environnement* 2011 : 9-13,.

2. Barsuk JH, McGaghie WC, Cohen ER, Balachandran JS, Wayne DB. Use of Simulation-based Mastery Learning to Improve the Quality of Central Venous Catheter Placement in a Medical Intensive Care Unit. *J Hosp Med* 2009; 4: 397-403.

3. Mayo PH, Hackney JE, Mueck JT, Ribaudo V, Schneider RF. Achieving house staff competence in emergency airway management: results of a teaching program using a computerized patient simulator. *Crit Care Med* 2004; 32: 2422-7.

4. Andreatta PB, Woodrum DT, Birkmeyer JD, Yellamanchilli RK, Doherty GM, Gauger PG, *et al*. Laparoscopic skills are improved with LapMentor training: results of a randomized, double-blinded study," *Ann Surg* 2006; 243: 854-60.

5. Blum MG,Powers TW, Sundaresan S .Bronchoscopy simulator effectively prepares junior residents to competently perform basic clinical bronchoscopy. *Ann Thorac Surg* 2004; 78: 287-91.

6. Wayne DB, Barsuk JH, O'Leary KJ, Fudala MJ,McGaghie MC. Mastery learning of thoracentesis skills by internal medicine residents using simulation technology and deliberate practice. *J Hosp Med* 2008; 3: 48-54.

7. Boyle JR, Ghuysen A, d'Orio V, Vega de Ceniga M, Chakfé N. Time to Embrace Simulation in Vascular Surgical Training: Little Things Matter. *Eur J Vasc Endovasc Surg* 2019; 58: 161-2.

8. Schanzer A, Steppacher R, Eslami M, Arous E, Messina L, Belkin M. Vascular surgery training trends from 2001-2007: A substantial increase in total procedure volume is driven by escalating endovascular procedure volume and stable open procedure volume. *J Vasc Surg* 2009; 49: 1339-44.

9. van Herzeele I, O'Donoghue KGL, Aggarwal R, Vermassen F, Darzi A, Cheshire NJW. Visuospatial and psychomotor aptitude predicts endovascular performance of inexperienced individuals on a virtual reality simulator. *J Vasc Surg* 2010; 51: 1035-42.

10. van Herzeele I, Aggarwal R, Malik I, Gaines P, Hamady M, Darzi A, *et al.* EVEResT. Validation of video-based skill assessment in carotid artery stenting. *Eur J Vasc Endovasc Surg* 2009; 38: 1-9.

11. Dawson DL,Meyer J, Lee ES, Pevec WC. Training with simulation improves residents' endovascular procedure skills. J Vasc Sur 2007; 45: 149-54.

12. Desender L, Rancic Z, Aggarwal R, Duchateau J, Glenck M, Lachat M, *et al.* Patient-specific rehearsal prior to EVAR: a pilot study. *Eur J Vasc Endovasc Surg* 201; 45: 639-47.

13. Neequaye SK, Aggarwal R, Brightwell R,van Herzeele I, Darzi A, Cheshire NJW. Identification of skills common to renal and iliac endovascular procedures performed on a virtual reality simulator. *Eur J Vasc Endovasc Surg* 2007; 33: 525-32.

14. Aggarwal R, Black SA, Hance JR, Darzi A, Cheshire NJW. Virtual reality simulation training can improve inexperienced surgeons' endovascular skills. *Eur J Vasc Endovasc Surg* 2006,; 31: 588-93.

15. Vento V, Cercenelli L, Mascoli C, Gallitto E, Ancetti S, Faggiolo G. The Role of Simulation in Boosting the Learning Curve in EVAR Procedures. *J Surg Educ* 2018; 75: 34-40.

16. Bismuth J, Donovan MA, O'Malley MK, El Sayed HF, Naoum JJ, Peden EK, *et al.* "Incorporating simulation in vascular surgery education. *J Vasc Surg* 2010; 52: 1072-80.

17. Sheahan MG, Duran C, Bismuth J. National Simulation-Based Training of Fellows: The Vascular Surgery Example," *Surg Cin North Am* 2015; 95: 781-90.

18. Robinson WP, Doucet DR, Simons JP, Wyman A, Aiello FA, Arous E, *et al.* An intensive vascular surgical skills and simulation course for vascular trainees improves procedural knowledge and self-rated procedural competence. *J Vasc Surg* 2016; 65: 907-15.

19. Seymour NE, Gallagher AG, Roman SA, O'Brien MK, Bansal VK, Andersen DK, *et al.* Virtual reality training improves operating room performance: results of a randomized, double-blinded study. *Ann Surg* 2002; 236: 458-63.

20. van Herzeele I, Aggarwal R, Neequaye S, Hamady M, Cleveland T, Darzi A, *et al.* Experienced endovascular interventionalists objectively improve their skills by attending carotid artery stent training courses. *Eur J Vasc Endovasc Surg* 2008; 35: 541-50.

21. van Herzeele I, Aggarwal R, Choong A, Brightwell R, Vermassen FE, Cheshire NJ. Virtual reality simulation objectively differentiates level of carotid stent experience in experienced interventionalists. *J Vasc Surg* 2007; 46: 855-63.

22. Bech B, Lönn L, Falkenberg M, Bartholdy NJ, Räder SB, Schroeder TV. Construct validity and reliability of structured assessment of endoVascular expertise in a simulated setting. *Eur J Vasc Endovasc Surg* 201; 42: 539-48.

23. See KWM, Chui KH, Chan WH, Wong KC, Chan YC. Evidence for Endovascular Simulation Training: A Systematic Review. *Eur J Vas Endovasc Sur* 2016; 51: 441-51.

24. Robertson V, Davies R. Provision of simulation-based training (SBT) within UK vascular surgery training programmes. *Surgeon* 2019; 17: 321-25.

25. Nayahangan LJ, van Herzeele I, Konge L, Koncar I, Cieri E, Mansilha A, *et al.* Achieving Consensus to Define Curricular Content for Simulation Based Education in Vascular Surgery: A Europe Wide Needs Assessment Initiative. *Eur J Vasc Endovasc Surg* 2019; 58: 284-91.

26. Belvroy VM, Murali B, Sheahan MG, O'Malley MK, Bismuth J. In the Fundamentals of Endovascular and Vascular Surgery model motion metrics reliably differentiate competency. *J Vasc Surg* 2020; 72: 2161-65.

27. Duran C, Estrada S, O'Malley M, Sheahan MG, Shames ML, Lee JT, Bismuth J. The model for Fundamentals of Endovascular Surgery (FEVS) successfully defines the competent endovascular surgeon. *J Vasc Surg* 2015; 62: 1660-6.

28. Aziz F. Vascular Surgery Trainees Still Need to Learn How to Sew: Importance of Learning Surgical Techniques in the Era of Endovascular Surgery. *Front Surg* 2015; 2: 16.

29. Bath J, Lawrence P. Why we need open simulation to train surgeons in an era of work-hour restrictions. *Vascular* 2011; 19: 175-7.

30. Datta V, Bann S, Beard J, Mandalia M, Darzi A. Comparison of bench test evaluations of surgical skill with live operating performance assessments. *J Am Coll Surg* 2004; 199: 603-6.

31. Robinson WP, Baril DT, Taha O, Schanzer A, Larkin AC, Bismuth J, *et al.* Simulation-based training to teach open abdominal aortic aneurysm repair to surgical residents requires dedicated faculty instruction. *J Vasc Surg* 2013; 58: 247-53.

32. Bann SD, Khan MS, Darzi AW. Measurement of surgical dexterity using motion analysis of simple bench tasks. *World J Surg* 2003; 27: 390-4.

33. Sidhu RS, Park J, Brydges R, MacRae HM, Dubrowski A. Laboratory-based vascular anastomosis training: A randomized controlled trial evaluating the effects of bench model fidelity and level of training on skill acquisition. *J Vasc Surg* 2007; 45: 343-9.

34. Price J, Naik V, Boodhwani M, Brandys T, Hendry P, Lam BK. A randomized evaluation of simulation training on performance of vascular anastomosis on a high-fidelity in vivo model: The role of deliberate practice. *J Thorac Cardiovasc Surg* 2011; 142: 496-503.

35. Tavlasoglu M, Durukan AB, Gurbuz HA, Jahollari A, Guler A. Skill acquisition process in vascular anastomosis procedures: a simulation-based study. *Eur J Cardiothorac Surg* 2015; 47: 812-8.

36. Duschek N, Assadian A, Lam nt PM, Klemm K, Schmidli J, Mendel H, *et al.* Simulator training on pulsatile vascular models significantly improves surgical skills and the quality of carotid patch plasty. *J Vasc Surg* 2013; 57: 1148-54.

37. Delpech PO, Danion J, Oriot D, Richer JP, Breque C, Faure JP. SimLife a new model of simulation using a pulsated revascularized and reventilated cadaver for surgical education. *J Visc Surg* 2017; 154: 15-20.

38. Okhah Z, Morrissey P, Harrington DT, Cioffi WG, Charpentier KP. Assessment of surgical residents in a vascular anastomosis laboratory. *J Surg Res* 2013; 185: 450-4.

39. Treil L, Neumann N, Chanes N, Rouby AF, Lejay A, Bourcier T, *et al.* Objective evaluation of clockface suture compared to OSATS checklist. EJVES Vasc Forum. submitted

40. McQueen S, Hammond Mobilio M, Moulton CA. Fractured in surgery: Understanding stress as a holistic and subjective surgeon experience. *Am J Surg* 2020, 0002-9610,.

41. Weenk M, Alken APB, Engelen LJLPG, Bredie SJH, van de Belt TH, van Goor H. Stress measurement in surgeons and residents using a smart patch. *Am J Surg* 2018; 216: 361-8.

42. Quick JA, Bukoski AD, Doty J, Bennett BJ, Crane M, Randolph J, *et al.* Case Difficulty, Postgraduate Year, and Resident Surgeon Stress: Effects on Operative Times. *J Surg Educ* 2019; 76: 354-61.

43. Abdullayev R, Yildirim E, Celik B, Topcu Sarica L. Analgesia Nociception Index: Heart Rate Variability Analysis of Emotional Status. *Cureus* 2019; 11: e4365.

44. de Jonckheere J, Rommel D, Nandrino JL, Jeanne M, Logier R. Heart rate variability analysis as an index of emotion regulation processes: interest of the Analgesia Nociception Index (ANI). In Annual International Conference of the IEEE Engineering in Medicine and Biology Society, San Diego, 2012.

45. Rouby AF, Neumann N, Ayer S, Paris, H, Vento V, Bismuth J, *et al.* Importance of trainees' simulation in endovascular surgery and evaluation of surgeon's stress during procedures. EJVES Vasc Forum submitted

Navigation

- Effect of radiation on vascular surgeons: State of the art 70
- Endovascular navigation with Fiber Optic RealShape (FORS) technology 76
- Magnetic Particle Imaging-guided Stenting 80
- Augmented reality in vascular and endovascular surgery: a scoping review 86

Effect of radiation on vascular surgeons: State of the art

8

Mohamed Ahmed ABDELHALIM, Bijan MODARAI

The effects of chronic low dose radiation exposure are not well known. Estimates suggest that the average background population radiation exposure, in the UK as an example, is 2.7mSv. This compares with a dose of 6.6mSv for a single CT scan of the chest. Patients undergoing EVAR receive a dose of 10-100mSv during the procedure, while the vascular surgeon is estimated to receive a dose of 36-345μSv depending on the complexity of the procedure. Experienced operators may perform more than 1000 EVARs during their career, accumulating a significant radiation exposure. There is evidence suggesting an increased radiation-related cancer risk in patients undergoing EVAR compared with open aortic aneurysm repair. In operators, markers of DNA damage and repair have been observed to rise after performing an EVAR. It is therefore possible that endovascular surgeons are also at a greater risk of radiation-related malignancy and longitudinal studies are required to investigate this. Establishing the utility of biological dosimetry at low doses may be the first step in delineating the true long-term effects of radiation exposure on vascular surgeons.

Introduction

Much of our knowledge of the effects of ionizing radiation has been established from studies on the survivors of the atomic bombs of Hiroshima and Nagasaki and after nuclear accidents such as Chernobyl. The Life Span Study, which examined the cohort of survivors of the atomic bombings in Japan, is perhaps the most reliable source of information about the long-term health effects of radiation exposure[1]. Since the two cities were bombed non-selectively, the cohort is a true representation of the populations. Furthermore, based on the survivors' distance and level of shielding at the time of the explosions, individual radiation doses were estimated and studied, ranging from zero to the highest survivable levels.

Exposure to large doses of radiation over a short period of time leads to acute radiation syndrome (ARS) Services[2]. The severity and presentations of ARS vary significantly with dose. Equivalent doses of greater than 10Gy cause destructive and irreparable changes to the gastrointestinal tract leading to gastrointestinal bleeding, infections and electrolyte imbalances. This is invariably fatal. Doses of 2-10Gy cause the bone marrow syndrome with the hallmarks of infections, nausea, vomiting and haemorrhaging. Fatality rates range from 10-60%, rising with increasing dose. Exposure to doses of 0.5-2Gy causes a mild radiation intoxication and a limited bone marrow syndrome including a fall in white blood cell count, however this is usually survivable. The effect of exposure to doses below 0.5Gy is less well established[3].

Individuals who survive acute radiation exposures and those who accumulate a series of significant but asymptomatic exposures then risk the long-term consequences of their exposure. The carcinogenic nature of ionising radiation is well established. Leukaemia and most solid cancers have been linked to radiation in a linear relationship with dose [4]. As well as cancer, low doses of ionising radiation have also been associated with development of cataracts, cardiovascular disease, and long-term psychological consequences [5-7].

Low-dose ionising radiation and cancer

Exposure to low doses of ionising radiation is normal and unavoidable, coming mainly in the form of natural background radiation from the earth and cosmic rays. The amount of background radiation varies widely depending on geographic location. Public Health England has calculated that in the United-Kingdom (UK), the average background exposure is 2.7mSv per year [8]. Furthermore, some segments of the population are exposed to additional doses from medical exposures or from occupational exposures, such as nuclear power plant workers and healthcare professionals. For comparison, in the same study, Public Health England calculated that an average computed tomography (CT) scan of the chest exposes the patient to a dose of 6.6mSv [8]. The Health and Safety Executive in the UK has set an annual exposure limit of 20mSv for radiation workers, including healthcare professionals [9].

Although the evidence for detrimental effects at doses above 100mSv is well studied and clear, the cancer risks at lower doses of radiation are normally less well established and normally extrapolated downwards from studies of higher dose exposures. This is known as the linear no-threshold (LNT) model. In essence, the LNT model assumes that any exposure to radiation carries a risk of malignancy and that the linear relationship between dose and risk continues uniformly below 100mSv. Therefore, the model suggests that there is no 'safe' dose of ionising radiation [10]. Supporting this theory are studies of the less severely exposed survivors of nuclear incidents and studies on medical and occupational exposures, which have been used to create dose response curves for cancer at lower doses [4]. An excess risk of colon cancer has been detected at radiation exposures as low as 5mSv [11]. It must be noted, however, that although official radiation protection guidelines are currently based on the LNT model, there remains a great degree of controversy surrounding it. Some authors reject this model and believe that exposure to low doses of radiation is in fact protective, a theory known as radiation hormesis [12, 13].

Radiation exposure associated with EVAR

Background

A patient undergoing an endovascular aneurysm repair will almost certainly have had a pre-operative computed tomography (CT) scan. The procedure, under X-ray guidance, will then add a radiation dose that will vary depending on procedure duration and complexity. They will then progress to a follow-up stage that will likely involve an annual CT scan to monitor for complications and graft integrity. Complications of endovascular aneurysm repair (EVAR), such as endoleaks and aneurysm sac expansion, are usually treated with further endovascular procedures and of course each of these reinterventions confers an additional radiation dose to the patient. Repeated radiation exposures such as this have previously been shown to have an additive effect on overall effective dose [14]. It is clear that depending on the complexity of an EVAR and post-operative events, there is a large and significant range of possible patient radiation exposures.

Estimating dose – Monte Carlo modelling

Published estimates of effective dose from the EVAR procedure alone are typically in the range of 10-100mSv[15-18]. All of these estimates have been obtained by using the Monte Carlo code PCXMC (STUK, Helsinki, Finland)[19]. Monte Carlo modelling uses a computational algorithm to simulate the known probabilities of penetrance, absorbance and scatter of each X-ray particle from a given radiation source. Since the probability of each X-ray particle's fate is known, the algorithm is able to simulate a model of a radiation exposure from the specified source to a phantom model of the human body. Based on this simulation, an overall effective dose can then be estimated.

Relative risk of cancer in patients after EVAR

Another approach to investigating the radiation associated with EVAR is to examine the pathological end points in a cohort of patients undergoing this procedure. Attempts have been made to estimate the risk of radiation-related malignancy associated with endovascular interventions by retrospectively studying these patient cohorts. A recent study used the Hospital Episode Statistics (HES) database to compare the cancer outcomes of patients undergoing EVAR with those undergoing open aneurysm repair[20]. The authors reported an increased risk of abdominal cancers in the EVAR group, with a hazard ratio of 1.14. Although the findings of such studies are often interesting, they are confounded by the fact that nonhomogeneous populations are compared. The EVAR group is invariably older and more comorbid than the open surgery group and therefore inherently has a higher risk of malignancy. Specifically, this study could not distinguish between de novo and recurrent cancers and therefore is it likely that some patients already had their primary cancer at the time of radiation exposure for EVAR. Despite attempts at accounting for confounding factors, it is difficult to be certain that any differences observed are related to radiation. In order to clarify this question, further studies using more reliable databases are required, or of course ideally, a large prospective multi-centre observational study.

Radiation exposure to the operator associated with EVAR

Background

In a standard hybrid suite, the positioning of the patient on a mobile operating table between an X-ray source and an image intensifier (receiver) allows maximum mobility to achieve the widest possible range of X-ray angles while allowing access to the patient's groins for the operator performing the procedure. As previously described, each X-ray particle (or photon) emitted from the source has one of three fates: it may be absorbed by the patient's tissues, it may penetrate and reach the image intensifier to create the image, or it may be scattered by the objects between the source and image intensifier (*i.e.* the operating table or the patient's body). Scattered X-ray particles then become a source of ionising radiation to any personnel in the room. Given that the primary operator is usually standing immediately next to the patient and X-ray source, it follows that he/she would have the highest exposure to this scatter radiation.

Experienced operators may perform more than 1000 EVARs during their career, and therefore will have accumulated a significant dose of occupational radiation. There are many variables determining the dose of radiation absorbed by the operator during an endovascular procedure. These include the variability in procedure duration and complexity, the variability in use of personal protective equipment, and the

variability in operator positioning and behaviours. Accurate measurement of exposure becomes difficult as a result of this variation. However, repeated exposures to small radiation doses have been shown to contribute in an additive manner to overall effective dose [14]. At present, staff are issued with TLD dosimeters to be worn at chest level, under protective lead, and analysed regularly for overexposure. However, these dosimeters only record under lead dose at a specific point and rely on a high level of compliance by the operator. They do not offer any information on overall effective dose, or dose to exposed areas such as the legs, arms and head. To the best of our knowledge, there are no studies in the literature accurately measuring the effective dose of radiation absorbed by the operator during EVAR.

Real-time dosimetry

Accurate measurement of the effective dose of radiation received by interventionalists is complicated by varying use of dosimeters and protective equipment. The DoseAware system (Phillips) is a real-time dosimeter providing a simple method of estimating effective dose during endovascular procedures. The operator wears a personal dose meter, which calculates the personal dose equivalent, also known as the Hp(d). From this, an estimate of effective dose can be made with the assumption that the personal dose meter is worn on an area of the body representative of overall exposure and that there is a uniform whole-body exposure. Although these assumptions give rise to obvious flaws in the method, it is thought to be sufficiently accurate for radiation protection purposes.

Comparing exposure in aortic and coronary interventions

Studies using the DoseAware system have estimated a mean per procedure operator effective dose of 0.5μSv for coronary angioplasties and 3.1μSv for peripheral arterial interventions [21]. Using the same system during EVAR, an operator dose of 36μSv has been reported for simple EVAR, while the more complex fenestrated (FEBAR) and branched (BEVAR) BEVAR procedures gave an operator dose of 345μSv [22]. From these studies, it is clear that operator doses accrued from endovascular aortic procedures are significantly higher than from coronary procedures.

Cytogenetic techniques have previously been used to demonstrate radiation-related chromosomal abnormalities in cardiologists performing coronary interventions [23,24]. These studies reported an annual dose of 1.7 -24.5mSv in cardiologists performing these X-ray guided procedures. Such a study has never been performed in vascular surgeons performing EVAR. However, the comparatively many fold radiation doses involved in EVAR raise concerns that the annual dose would be much higher for a vascular surgeon.

Individual variability

Although the risks associated with radiation exposure rise linearly with dose, there is a degree of inter-individual variability in biological responses. Exposure to the same dose of radiation has been shown to elicit different degrees of desoxyribonucleic acid (DNA) damage in different individuals [25]. These variations are most pronounced at low doses and reduce significantly as dose increases. Inter-observer variability at low doses adds even more uncertainty to the ultimate effect of radiation on vascular operators.

Quantification of γH2AX in operators

It is well established that ionising radiation causes genetic damage in the form of DNA double strand breaks. These breaks are always followed by phosphorylation of the histone H2AX by kinases such as ataxia telangiectasia mutated (ATM) to form γH2AX, which is the first step in recruiting and localising DNA repair proteins [26-28]. The level of γH2AX is directly proportional to the number of DNA double strand breaks and therefore correlates with the absorbed dose of radiation.

Peak levels of γH2AX are observed half an hour after exposure with a return to baseline levels within 48 hours. Our group has used flow cytometry to demonstrate this phenomenon in vascular surgeons and interventional radiologists performing EVAR, comparing them to surgeons performing open operations as unexposed controls[29]. The rise in γH2AX observed in these vascular interventionalists indicates that performing EVAR procedures exposes them to doses of radiation high enough to induce DNA damage. While γH2AX is important in demonstrating acute radiation exposure, it offers no information about residual DNA damage accumulating over years of chronic exposure as a career vascular interventionalist. There are currently no studies in the literature reporting on chronic markers of radiation exposure in vascular interventionalists.

Conclusion

Defining the risk of radiation exposure to vascular interventionalists is important as it will inform the guidance and regulations surrounding the use of protective equipment, operative workload, and the set-up of hybrid theatres and angiography suites. This information is also important for future service planning and avoidance of potential litigation. Investigating the inter-individual variability in sensitivity to radiation may be a first step toward individualised radiation dose limits for radiation workers. The current dose limits are usually monitored through TLD dosimeters, which are inaccurate and often worn only intermittently. Establishing the utility of biological dosimetry at low doses of radiation may facilitate a more accurate, novel method of monitoring radiation dose limits in healthcare works.

References

1. Ozasa K, Grant EJ, Kodama K. Japanese Legacy Cohorts: The Life Span Study Atomic Bomb Survivor Cohort and Survivors' Offspring. *J Epidemiol* 2018; 28: 162-9.
2. US Department of Health and Human Services. *A Brochure for Physicians: Acute radiation syndrome* 2017.
3. Squillaro T, Galano G, De Rosa R, Peluso G, Galderisi U. Concise Review: The Effect of Low-Dose Ionizing Radiation on Stem Cell Biology: A Contribution to Radiation Risk. *Stem Cells* 2018; 36: 1146-53.
4. Gilbert IS. Ionising radiation and cancer risks: What have we learned from epidemiology? *Int J Rad Biol* 2009; 85: 467-82.
5. Ainsbury EA, Bouffler SD, Dorr W, Graw J, Muirhead CR, Edwards AA, *et al.* Radiation cataractogenesis: a review of recent studies. *Radiat Res* 2009; 172: 1-9.
6. Pastel RH. Radiophobia: long-term psychological consequences of Chernobyl. *Mil Med* 2002; 167: 134-6.
7. Sumner D. Health effects resulting from the Chernobyl accident. *Med Confl Surviv* 2007; 23: 31-45.
8. Public Health England. Ionising radiation exposure of the UK population: 2010 review. 2016.
9. Health and Safety Executive. Working with ionising radiation: Ionising radiation regulations 2017. *Health and Safety Executive* 2018.
10. National Research Council. Health Risks from Exposure to Low Levels of Ionizing Radiation: BEIR VII Phase 2: *The National Academies Press*; 2006.
11. Preston DL, Pierce DA, Shimizu Y, Cullings HM, Fujita S, Funamoto S, *et al.* Effect of recent changes in atomic bomb survivor dosimetry on cancer mortality risk estimates. *Radiat Res* 2004;162: 377-89.
12. Luckey TD. Radiation hormesis: the good, the bad, and the ugly. *Dose Response* 2006; 4: 169-90.
13. Sutou S. Black rain in Hiroshima: a critique to the Life Span Study of A-bomb survivors, basis of the linear no-threshold model. *Genes Environ* 2020; 42: 1.
14. Fazel R, Krumholz HM, Wang Y, Ross JS, Chen J, Ting HH, *et al.* Exposure to Low-Dose Ionizing Radiation from Medical Imaging Procedures. *New Engl J Med* 2009; 361: 849-57.
15. Howells P, Eaton R, Patel AS, Taylor P, Modarai B. Risk of Radiation Exposure during Endovascular Aortic Repair. *Eur J Vasc Endovasc Surg* 2012; 43: 393-7.
16. Kalef-Ezra JA, Karavasilis S, Ziogas D, Dristiliaris D, Michalis LK, Matsagas M. Radiation burden of patients undergoing endovascular abdominal aortic aneurysm repair. *J Vasc Surg* 2009; 49: 283-7.

17. Fossaceca R, Brambilla M, Guzzardi G, Cerini P, Renghi A, Valzano S, *et al.* The impact of radiological equipment on patient radiation exposure during endovascular aortic aneurysm repair. *Eur Radiol* 2012; 22: 2424-31.

18. Hertault A, Maurel B, Sobocinski J, Martin Gonzalez T, Le Roux M, Azzaoui R, *et al.* Impact of Hybrid Rooms with Image Fusion on Radiation Exposure during Endovascular Aortic Repair. *Eur J Vasc Endovasc Surg* 2014; 48: 382-90.

19. Tapiovaara M, Siiskonen, T. PCXMC: A Monte Carlo program for calculating patient doses in medical x-ray examinations. 2008.

20. Markar SR, Vidal-Diez A, Sounderajah V, Mackenzie H, Hanna GB, Thompson M, *et al.* A population-based cohort study examining the risk of abdominal cancer after endovascular abdominal aortic aneurysm repair. *J Vasc Surg* 2019; 69: 1776-85.

21. Ingwersen M, Drabik A, Kulka U, Oestreicher U, Fricke S, Krankenberg H, *et al.* Physicians' Radiation Exposure in the Catheterization Lab. *JACC: Cardiovasc Interv* 2013; 6: 1095-102.

22. De Ruiter QMB, Jansen MM, Moll FL, Hazenberg CEVB, Kahya NN, Van Herwaarden JA. Procedure and step-based analysis of the occupational radiation dose during endovascular aneurysm repair in the hybrid operating room. *J Vasc Surg* 2018; 67: 1881-90.

23. Vellingiri B, Shanmugam S, Subramaniam MD, Balasubramanian B, Meyyazhagan A, Alagamuthu K, *et al.* Cytogenetic endpoints and Xenobiotic gene polymorphism in lymphocytes of hospital workers chronically exposed to ionizing radiation in Cardiology, Radiology and Orthopedic Laboratories. *Ecotoxicol Environ Saf* 2014; 100: 266-74.

24. Zakeri F, Assaei RG. Cytogenetic monitoring of personnel working in angiocardiography laboratories in Iran hospitals. *Mutat Res* 2004; 562: 1-9.

25. Pajic J, Rakic B, Rovcanin B, Jovicic D, Novakovic I, Milovanovic A, *et al.* Inter-individual variability in the response of human peripheral blood lymphocytes to ionizing radiation: comparison of the dicentric and micronucleus assays. *Radiat Environ Biophys* 2015; 54: 317-25.

26. Lobrich M, Rief N, Kuhne M, Heckmann M, Fleckenstein J, Rube C, *et al. In vivo* formation and repair of DNA double-strand breaks after computed tomography examinations. *Proc Natl Acad of Sci USA* 2005; 102: 8984-9.

27. Rogakou EP, Pilch DR, Orr AH, Ivanova VS, Bonner WM. DNA Double-stranded Breaks Induce Histone H2AX Phosphorylation on Serine 139. *J Biol Chem* 1998; 273: 5858-68.

28. Rothkamm K, Lobrich M. Evidence for a lack of DNA double-strand break repair in human cells exposed to very low x-ray doses. *Proc Natl Acad of Sci USA* 2003; 100: 5057-62.

29. El-Sayed T, Patel AS, Cho JS, Kelly JA, Ludwinski FE, Saha P, *et al.* Radiation-Induced DNA Damage in Operators Performing Endovascular Aortic Repair. *Circulation* 2017; 136: 2406-16.

Endovascular navigation with Fiber Optic RealShape (FORS) technology

9

Jurre KLAASSEN, Constantjin E V B. HAZENBERG, Joost A. Van HERWAARDEN

In recent decades, there has been a major shift in vascular surgery from open to endovascular surgery. While this allows for less invasive surgical methods and new treatments for complex pathologies, the use of fluoroscopy also has disadvantages. The main disadvantage is that three-dimensional structures and endovascular devices are projected two-dimensionally onto the screens. Another major disadvantage is that prolonged exposure to fluoroscopy poses serious health risks. To overcome these disadvantages, the Fiber Optic RealShape (FORS) technology was developed. This technique uses light instead of X-rays to visualize specially designed fiber-integrated endovascular devices in 3D. The FORS technology therefore can limit X-ray exposure during the navigation phase of endovascular procedures. In addition, the three-dimensional visualization of the FORS devices improves spatial perception during procedures. Therefore, the scope of this review is to outline the potential and the current status of the FORS technology.

Introduction

Since the first endovascular treatment in 1964 by Charles Dotter [1], there has been a major shift in the treatment of most vascular surgical pathologies from open to endovascular treatment methods. [2,3] Besides the fact that these newly developed endovascular methods are less invasive compared to conventional open surgery, they also offer new treatment options for complex vascular pathologies. However, the treatment of these complex pathologies prolongs procedure times, resulting in high radiation doses for both the patient and the treatment team. [4,5]

During endovascular procedures, fluoroscopy is used to visualize the necessary medical devices. Although fluoroscopy is widely used in these procedures, its use also has disadvantages. The main disadvantage of fluoroscopy is that the three-dimensional structures are projected only as two-dimensional grayscale images onto screens. This eliminates the spatial perception of depth and tortuosity, making endovascular navigation more difficult and increasing the risk of procedural failure. To overcome this problem, so-called image fusion and 3D roadmap imaging tools have been developed over the past decade. [6–9] These imaging tools project 3D Computed Tomography Angiography (CTA) or Magnetic Resonance Angiography (MRA) segmentations onto real-time 2D fluoroscopy images and have been shown to reduce radiation dose, procedural time and amount of contrast medium used. [8,9] However, these imaging tools are limited to projecting a 3D outline of anatomical structures and therefore the devices used are still projected in 2D. In addition, viewing angles are limited due to mechanical limitations of the fluoroscopy system. As a result, it is not always possible to view the anatomy from the optimal angle during endovascular procedures. Another important disadvantage is that prolonged exposure to fluoroscopy can lead to DNA damage and long-term health effects. [10,11] The current radiation guidelines are therefore based on the “as low as reasonable achievable” (ALARA) principle which aims to achieve the lowest radiation exposure to perform a procedure safely. [12]

To overcome both mentioned disadvantages of using fluoroscopy for navigation during endovascular procedures, the Fiber Optic RealShape (FORS) technology (Philips Koninklijke N.V., Best, The Netherlands) was developed by Philips in close collaboration with clinical experts. This technology combines the image fusion and 3D roadmap imaging tools with specially designed 3D visualized fiber-integrated endovascular devices that use light instead of X-rays and therefore limits X-ray exposure and provides more spatial insight into the positioning of the endovascular devices during the procedure.

FORS Technology

The FORS system consist of four main parts: (1) Workstation, (2) trolley, (3) docking base and docking top and (4) workstation. Figure 1 shows an overview of the numbered parts. There are currently three purpose-designed single-use endovascular FORS devices with integrated multicore optical fibers: (1) 0.035 inch angle hydrophilic floppy guidewire, (2) 5.5 F Berenstein catheter, and (3) 5.5 F Cobra C2 catheter (Figure 2). The system sends laser light through the optical fibers. By analyzing the changes in the returning laser light spectrum caused by twisting and bending, the system can create a 3D reconstruction of the full length of the optical fiber within the devices in real time without the use of radiation.[13] To connect FORS compatible devices to the light source, the devices must first be placed in the docking top and subsequently connected to the docking base. The docking base is attached to the operating table preoperatively and provides a fixed-point relative to the changing position coordinates of the fluoroscopy system during procedures. During a so-called shape registration step, the coordinate systems of the fluoroscopy system and the FORS system are linked. The coupled coordinate systems allow the FORS system to calculate the spatial position of the FORS enabled devices with respect to x-ray and CT roadmaps.

Figure 1: Overview of the FORS system with **(1)** workstation, **(2)** trolley, **(3)** docking base and **(4)** docking top which connects FORS enabled devices. All FORS enabled devices are visualized in context of an anatomical roadmap of digital subtraction angiograph on the screen **(5)**. Copyright © (2020) Koninklijke Philips N.V. All rights reserved.

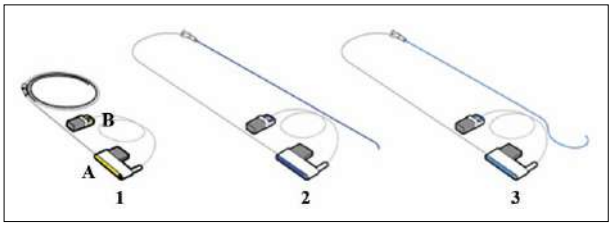

Figure 2: Overview of available FORS enabled devices: **(1)** 0.035 inch angle hydrophilic floppy guidewire, **(2)** 5.5 F Berenstein catheter and **(3)** 5.5 F Cobra C2 catheter. Devices are connected to the FORS system by placing the docking fin **(A)** into the docking top and subsequently connecting the optical connector **(B)** to the docking base. Copyright © (2020) Koninklijke Philips N.V. All rights reserved.

All FORS enabled devices are fully compatible with conventional devices and have comparable mechanical and radiopacity properties. Yet, due to the tethered connection to the docking top, the FORS guidewire is only front loadable. Moreover, the FORS enabled devices are visualized with 3D features such as shading and a white dot at the distal tip of the displayed device. Due to the white dot on the tip, it is clearly visible in which direction the guidewire and/or catheter are pointing. Nonetheless, without information about the surrounding anatomical structures, the use of the visualized FORS devices is limited. The FORS technology is therefore always used in combination with a Philips fluoroscopy system, such as Philips Azurion 7 FD20 system or Philips Allura Xper FD20 system (Philips Koninklijke NV, Best, The Netherlands), allowing FORS users to use a roadmap consisting of preoperative CTA imaging or perioperative X-ray imaging (*i.e.* digital subtraction angiography imaging, single shot exposure or fluoroscopy) for anatomical context during navigation.

Clinical implementation

Currently, two studies have been published describing the use of FORS technology: (I) Preclinical results as described by Jansen *et al.*[14] and (II) First in human clinical results as described by Van Herwaarden *et al.*[15]. The preclinical study described by Jansen *et al.*[14] mainly looked at the accuracy and safety of the FORS technology. For this study, three vascular surgeons and three interventional radiologists performed different navigation tasks in a phantom and a porcine model. Tip-to-tip distance measurement outcomes returned a mean ± standard deviation of 2.7 ± 2.2 mm. However, distance measurements were performed in a two-dimensional image and therefore may underestimate the actual distance in a three-dimensional space. No side effects or potential hazards were identified during this study, indicating that the technique can be used safely. In addition, the participating specialists indicated that the system felt safe and intuitive to use and that it could be a potential clinical improvement due to its three-dimensional representation and radiation reduction.

Subsequently, a first in human clinical study was performed at UMC Utrecht.[15] In this study, FORS was used during the navigation phase of treatment in 21 patients (13 endovascular aortic repairs and 7 repairs of peripheral lesions). Of the described navigation tasks, 90.9% was successfully performed with the use of at least one FORS enabled device. In addition, in 76% of the procedures FORS enabled image guiding was scored as “better than standard guidance”. In particular, FORS’ unrestricted viewing angles were considered a major advantage, as it provides the ability to overcome the limitations of C-arm positioning during navigation (Figure 3).

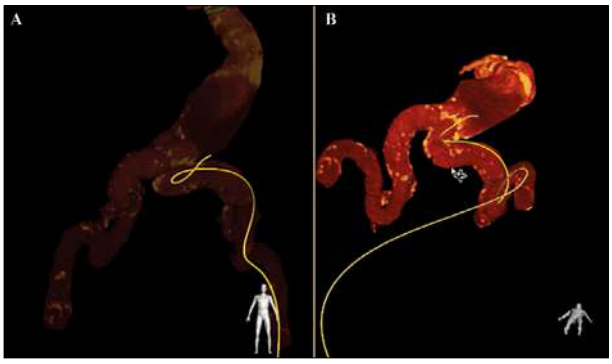

Figure 3: Example of unlimited viewing angles and use of the FORS system’s biplane view mode during catheterization of a tortuous iliac artery. Biplane view consists of an **(A)** anteroposterior view and a **(B)** caudocranial view that improves three-dimensional understanding of the tortuous anatomy during insertion and advancement of the FORS enabled guidewire (yellow) into the iliac artery.

Although the use of FORS technology is expected to reduce the amount of radiation required for successful completion of the navigation phase of endovascular procedures, this has not yet been demonstrated in the studies mentioned. On the other hand, the first in human study[15] shows that it is possible to perform certain tasks with little or no exposure to X-rays. However, to objectively quantify the X-ray reduction and added value of FORS-guided imaging, it is necessary to obtain more data from less heterogeneous pathologies and more participating centers. This data is currently

being collected as part of the FORS Learn Registry study at three centers in Europe * and two in the United States **. Ultimately, the goal is to increase the number of participating centers to ten (five in Europe and five in the United States). The purpose of this registry is both to demonstrate the effect on X-ray exposure and to build a baseline cohort against which future research results can be compared. The FORS system has CE mark approval and is Food and Drug Administration (FDA) 510(k) cleared. Development continues, especially on expansion of the platform of different catheters and wires that can be visualized with FORS. For example, Philips is currently developing a 3D catheter agnostic guidance solution for the FORS system that will allow compatible *** conventional catheters to be visualized without fluoroscopy. In addition, new guidewires with a longer working length and thinner diameters are being developed, making FORS technology even more widely applicable. Ultimately, this technology should become the best option for navigation during endovascular procedures offering improved 3D visualization while reducing health risks for both patient and medical staff.

* University Medical Center Utrecht, Utrecht, Netherlands
Maastricht University Medical Center, Maastricht, Netherlands
University Heart Center Hamburg, Hamburg, Germany

** UMass Memorial Medical Center, Massachusetts, United States
Beth Israel Deaconess Medical Center, Boston, United States

*** A compatible catheter has a Luer lock complying with [Standard.80369-7], a length of equal or less than 95cm and an ID compatible with a 0.035" OD guide wire. In layman terms, it means that most standard 0.035" Sos, Cobra, Berenstein catheters etc. should be able to run over our FORS 0.035" navigation wire.

References

1. Dotter CT, Judkins MP. Transluminal Treatment of Arteriosclerotic Obstruction. *Circulation* 1964; 30: 654-70.

2. Volodos NL. The 30th Anniversary of the First Clinical Application of Endovascular Stent-grafting. *Eur J Vasc Endovasc Surg* 2015; 49: 495-7.

3. Friedman SG. Charles Dotter and the fiftieth anniversary of endovascular surgery. *J Vasc Surg* 2015; 61: 556-8.

4. Thakor AS, Winterbottom A, Mercuri M, Cousins C, Gaunt ME. The radiation burden from increasingly complex endovascular aortic aneurysm repair. *Insights Imaging* 2011; 2: 699-704.

5. Ketteler ER, Brown KR. Radiation exposure in endovascular procedures. *J Vasc Surg* 2011; 53: 35S-38S.

6. Jones DW, Stangenberg L, Swerdlow NJ, Alef M, Lo R, Shuja F, *et al.* Image Fusion and 3-Dimensional Roadmapping in Endovascular Surgery. *Ann Vasc Surg* 2018; 52: 302-11.

7. Ahmad W, Obeidi Y, Majd P, Brunkwall JS. The 2D-3D Registration Method in Image Fusion Is Accurate and Helps to Reduce the Used Contrast Medium, Radiation, and Procedural Time in Standard EVAR Procedures. *Ann Vasc Surg* 2018; 51: 177-86.

8. Ahmad W, Hasselmann H-C, Galas N, Majd P, Brunkwall S, Brunkwall JS. Image fusion using the two-dimensional-three-dimensional registration method helps reduce contrast medium volume, fluoroscopy time, and procedure time in hybrid thoracic endovascular aortic repairs. *J Vasc Surg* 2019; 69: 1003-10.

9. Doelare SAN, Smorenburg SPM, van Schaik TG, Blankensteijn JD, Wisselink W, Nederhoed JH, *et al.* Image Fusion During Standard and Complex Endovascular Aortic Repair, to Fuse or Not to Fuse? A Meta-analysis and Additional Data From a Single-Center Retrospective Cohort. *J Endovasc Ther* 2021; 28: 78-92.

10. Ko S, Kang S, Ha M, Kim J, Jun JK, Kong KA, *et al.* Health Effects from Occupational Radiation Exposure among Fluoroscopy-Guided Interventional Medical Workers: A Systematic Review. *J Vasc Interv Radiol* 2018; 29: 353-66.

11. Tang FR, Loganovsky K. Low dose or low dose rate ionizing radiation-induced health effect in the human. *J Environ Radioact* 2018; 192: 32-47.

12. Hertault A, Maurel B, Midulla M, Bordier C, Desponds L, Saeed Kilani M, *et al.* Editor's Choice – Minimizing Radiation Exposure During Endovascular Procedures: Basic Knowledge, Literature Review, and Reporting Standards. *Eur J Vasc Endovasc Surg* 2015; 50: 21-36.

13. Froggart ME, Klein JW, Gifford DK, Kreger ST. Optical position and/or shape sensing. US 8773650 B2, 2014.

14. Jansen M, Khandige A, Kobeiter H, Vonken EJ, Hazenberg C, van Herwaarden J. Three Dimensional Visualisation of Endovascular Guidewires and Catheters Based on Laser Light instead of Fluoroscopy with Fiber Optic RealShape Technology: Preclinical Results. *Eur J Vasc Endovasc Surg* 2020; 60: 135-43.

15. van Herwaarden JA, Jansen MM, Vonken EPA, Bloemert-Tuin T, Bullens RWM, de Borst GJ, *et al.* First in Human Clinical Feasibility Study of Endovascular Navigation with Fiber Optic RealShape (FORS) Technology. *Eur J Vasc Endovasc Surg* 2021; 61: 317-25.

Magnetic Particle Imaging-guided Stenting

10

Stefan HERZ, Volker C. BEHR, Thorsten A. BLEY, Patrick VOGEL

Magnetic Particle Imaging (MPI) is a promising tomographic imaging technique using magnetic fields to determine the spatial distribution of tracer agents based on superparamagnetic iron oxide nanoparticles (SPIONs). MPI is very promising for vascular imaging and non-X-ray guidance, especially due to its high sensitivity for detecting small amounts of tracer agents, the avoidance of nephrotoxic contrast agent and the capability of real-time imaging. This chapter provides an overview of the current status of MPI-guided stenting.

Introduction

The rapid development of minimally invasive cardio-vascular interventions is based on high-resolution real-time imaging. Currently, X-ray fluoroscopy and digital subtraction angiography (DSA) are considered the gold standard for a variety of these interventional procedures. However, X-rays can be associated with high doses of ionizing radiation, which poses a risk of subsequent cancer to patients and clinical staff [1-3]. Another disadvantage is the use of potentially allergenic and nephrotoxic iodine-containing contrast agents [4].

In this book chapter, we present a basic overview of Magnetic Particle Imaging (MPI), a new radiation-free tracer-based tomographic imaging technique. We discuss the great potential for vascular and interventional imaging with a focus on experimental MPI-guided stenting along with current limitations and future directions.

Magnetic Particle Imaging

MPI is a magnetic field-based tomographic imaging technique that visualizes the spatial distribution of superparamagnetic iron oxide nanoparticles (SPIONs). Although some hardware and imaging concepts from magnetic resonance imaging (MRI) are used in MPI, the principles of the two imaging modalities are different [5]. MPI is based on the nonlinear response of SPIONs to external magnetic fields and was introduced by Gleich and Weizenecker in 2005 [6]. In a simplified scanner concept (Figure 1), two opposing permanent magnets create a small field-free point (FFP) in the center of a strong magnetic field gradient.

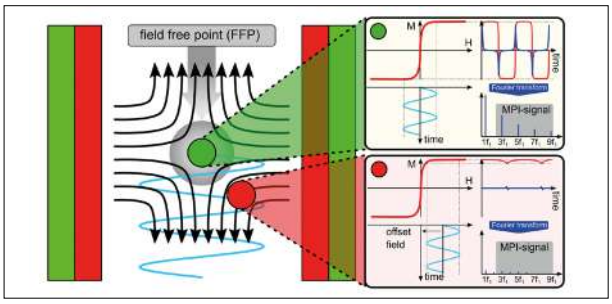

Figure 1: Basic principle of magnetic particle imaging (MPI).

Left: Two opposing permanent magnets create a so-called field-free point (FFP) in their center. Two SPION-samples are depicted in (green dot) and outside (red dot) of the FFP. The blue sinusoidal wave stands the excitation signal (frequency $f1$).

Top right: The magnetization of SPIONs in the vicinity of the FFP (green dot) show a nonlinear response on time-varying magnetic fields due to their magnetization curve resulting in higher harmonics $1f1 \ldots 9f1$ (Fourier transformation), the MPI signal.

Bottom right: The magnetization of SPIONs outside of the FFP (red dot) are saturated and do not produce an MPI signal.

SPIONs located in the vicinity of the FFP show a non-linear magnetization response on time-varying magnetic fields resulting in higher harmonics (Fourier transformation). The magnetization of SPIONs that are not in the immediate proximity of the FFP saturates and does not generate an MPI signal. For multidimensional spatial encoding additional drive-coils are used to steer the FFP rapidly on specific trajectories through the FOV, scanning the probe point-by-point.

MPI is characterized by very fast [7-9] and highly sensitive [10] imaging with high signal-to-noise ratio (SNR) and enables, imaging with almost no depth attenuation [5,11]. Intravenously (i.v.) administered SPION-based tracer agents are used to visualize the vascular system similar to conventional DSA. An important feature of MPI is that the background structures do not produce any visible signal or relevant image artifacts. SPIONs have already been used as i.v. MRI contrast agents in certain applications in humans, *e.g.* in liver imaging or in the detection of lymph node metastases [12-14]. Unlike iodine-containing X-ray and computed tomography (CT) contrast agents, SPIONs are non-nephrotoxic.

In principle, MPI enables imaging at molecular level with nanomolar sensitivity and submillimeter spatial resolution [6,15-17]. Real-time image reconstructions and visualization [8,18] have been shown. The MPI signal is linear to the particle concentration and thus is directly dependent on the number of SPIONs in the blood volume [11].

Experimental studies have shown that visualization of interventional instruments, such as guidewires or catheters, is possible by signal cancellation by the instruments themselves, or alternatively by marking them with SPIONs, such as applied in the form of lacquers, or processed in the coating material [19-21]. Initial studies in vessel phantoms assessing vascular pathologies such as aneurysms in 4D high-resolution imaging [22,23], or stenoses [24-26] as well as MPI-guided percutaneous transluminal angioplasty [27,28] have been demonstrated recently. In small animal experiments, MPI has been used to image the beating heart of a mouse in real-time [29,30], as well as perfusion deficits in a murine model of ischemic stroke [31].

Magnetic Particle Imaging-guided stenting

Here we discuss MPI-guided stenting as has been reported previously [32]. Imaging and experimental vascular interventions were performed on a custom-built traveling wave MPI scanner (isotropic resolution ~ 2 mm, gradient strength 3T/m). The inner diameter of the bore was 29 mm, the length of the tunnel 227 mm. The field of view (FOV) in the center of the scanner was 29 mm in diameter and 65 mm in length [33,34]. An accelerated reconstruction algorithm using standard PC hardware allowed for interventional guidance in real-time at a rate of 8 frames/s with very short latency time (~ 115 ms) [9,35,36].

Polyvinyl chloride (PVC) tubes with an inner diameter of 8 mm prepared with a centrally aligned easy to break cable tie were used as vascular stenosis phantoms. Standard interventional balloon catheters (FoxCross, Abbott Vascular, Redwood City, CA, USA) and guidewires (0.035-inch Radifocus M hydrophilic guidewire, Terumo, Tokyo, Japan) for angioplasty and stenting were prepared with custom-made SPION-based (Ferucarbotran, Bayer Pharma, Berlin, Germany) dot-like lacquer (water-based clear coat) markers for MPI visibility (Figure 2).

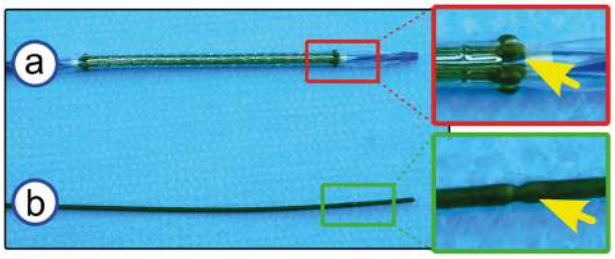

Figure 2: Customized magnetic particle imaging visible interventional instruments:

(a) Stainless steel stent mounted on a balloon catheter. Both ends of the stent are labeled with custom-made SPION-based lacquer markers (yellow arrow).

(b) Guidewire (0.035 inch) prepared with custom-made SPION-lacquer (yellow arrow).

An MPI angiography (MPA, injection of diluted Ferucarbotran) visualized the stenosis in the vessel phantom. A guidewire was advanced through the stenosis followed by positioning of an over-the-wire balloon catheter in the area of the stenosis. Balloon angioplasty and stent placement were performed by manually inflating the balloon catheter with diluted Ferucarbotran (Figure 3). The SPION lacquer markers at the ends of the interventional instruments allowed for precise positioning in real-time. After deployment of a stent, the markers at the ends were clearly visible by MPI. In this experimental setting the applied lacquer markers did not relevantly alter the sliding properties of the interventional instruments and withstood friction during the experiments. Final MPA confirmed successful stenosis treatment. Because the SPION signal from the lacquer markers was significantly lower than the injected tracer agent, the in-stent lumen could be visualized without interference from the signal from the markers.

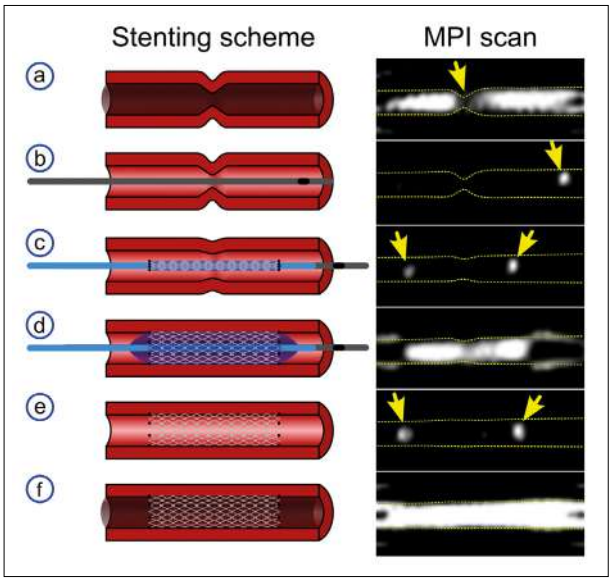

Figure 3: Magnetic particle imaging (MPI)-guided stenting in a vascular stenosis phantom. **Left column:** Scheme of the stenting procedure. **Right column:** Original reconstructed MPI scan (8 frames/s, latency time between data acquisition and visualization ~ 115 ms). Arrows indicate MPI visible markers of endovascular devices.
(a) MPI angiography of the vascular stenosis phantom. The dotted yellow line depicts the inner boundaries of the vessel phantom.
(b) The guidewire is passed through the stenosis.
(c) Positioning of the stent delivery system in the area of stenosis (two point markers at both ends).
(d) Balloon inflated to deliver the stent.
(e) Expanded stent (two markers at both ends).
(f) Post-interventional visualization of the in-stent lumen.

Discussion

MPI-guided experimental angioplasty with stent placement was feasible using highly accelerated visualization algorithms for real-time tracking of the endovascular instruments and visualization of the vasculature. With frame rates of up to 8 frames/s (latency time to image visualization ~ 115 ms) MPI provided image visualization in the range of clinical systems where frame rates of 7.5 frames/s in fluoroscopy and frame rates of 1–2 frames/s in DSA are customary [37]. This visualization speed remains the fastest reported for MPI-guided interventions so far.

SPION markers on interventional devices and stents did not hamper lumen visualization, which is in line with other published studies evaluating coronary, endovascular and flow diverter stents [38-40]. During post-interventional angiography, the markers on the deployed stents temporarily faded due to concentration differences to the injected tracer agent, which greatly facilitated the assessment of the in-stent lumen and possible in-stent stenosis. An interesting imaging approach in this context is the concept of multi-color MPI, which enables the differentiation of two different SPIONs and has been applied for a marked guidewire and a vessel phantom filled with SPIONs [41,42].

During interventions stripe-like artifacts occurred at both ends of the catheter balloons, which were caused by the highly accelerated reconstruction algorithm. Refined reconstruction algorithms should be able to reduce these artifacts. Further research is necessary to clarify the underlying cause of artifacts in MPI.

Due to the basic imaging methodology of MPI, the surrounding structures such as the vascular phantom material, similar to a conventional DSA, were not visualized. On the downside, the advantage of MPI as a strictly tracer-based imaging modality lacks spatial and anatomical information. Proof-of-concept studies have introduced hybrid imaging systems combining MPI with MRI or CT that may overcome these limitations [43,44].

Current limitations and future directions

So far, the spatial resolution of MPI is significantly lower than the submillimeter resolution of state of the art X-ray fluoroscopes. Since MPI scanners are still in an early stage of development, further advances such as higher spatial resolution, larger FOV, optimized SPIONs, and dedicated interventional instruments are most likely. To date, only few small animal scanners have been built worldwide and the number of preclinical applications is still small [45]. Currently, the up-scaling of MPI scanners to human size remains a technological challenge especially due to issues in specific absorption rate (SAR) and peripheral nerve stimulation (PNS). Recently, a first scanner suitable for head imaging in humans has been presented [46].

Labeling of interventional instruments for in-vivo MPI is challenging, because the coating of the devices has to retain gliding abilities, be thin enough to retain maneuverability and still provide sufficient signal [19,20]. Potential applications in small animals or humans would require a biocompatible hydrophilic polymer coating for low friction maneuverability.

Interventional instruments commonly contain ferromagnetic materials. A recent study evaluating the heating behavior of stents in alternating magnetic fields in MPI concluded that safe use of endovascular stents (stainless steel, nitinol, platinum-chromium, cobalt-chromium) is possible with only few exceptions [47]. Further research has to focus on safety aspects of MPI-guided interventions especially concerning PNS and SAR [5,11].

Conclusion

MPI is a promising imaging technique for vascular imaging and non-X-ray guided interventions. In phantom models MPI-guided stenting with real-time tracking of endovascular instruments was feasible. These results encourage further investigations with preclinical MPI-guided interventions.

References

1. Modan B, Keinan L, Blumstein T, Sadetzki S. Cancer following cardiac catheterization in childhood. *Int J Epidemiol* 2000; 29: 424-8.

2. Roguin A, Goldstein J, Bar O, Goldstein JA. Brain and neck tumors among physicians performing interventional procedures. *Am J Cardiol* 2013; 111: 1368-72.

3. Pitton MB, Kloeckner R, Schneider J, Ruckes C, Bersch A, Düber C. Radiation exposure in vascular angiographic procedures. *J Vasc Interv Radiol*. 2012; 23: 1487-95.

4. Bartorelli AL, Marenzi G. Contrast-induced nephropathy. *J Interv Cardiol* 2008; 21: 74-85.

5. Saritas EU, Goodwill PW, Croft LR, Konkle JJ, Lu K, Zheng B, *et al*. Magnetic particle imaging (MPI) for NMR and MRI researchers. *J Magn Reson* 2013; 229: 116-26.

6. Gleich B, Weizenecker J. Tomographic imaging using the nonlinear response of magnetic particles. *Nature* 2005; 435: 1214-7.

7. Vogel P, Ruckert MA, Klauer P, Kullmann WH, Jakob PM, Behr VC. Superspeed Traveling Wave Magnetic Particle Imaging. *IEEE Trans Magn* 2015; 51: 1-3.

8. Vogel P, Ruckert MA, Kampf T, Herz S, Stang A, Wockel L, *et al.* Superspeed Bolus Visualization for Vascular Magnetic Particle Imaging. *IEEE Trans Med Imaging* 2020; 39: 2133-9.

9. Vogel P, Rückert MA, Klauer P, Herz S, Kampf T, Bley TA, *et al.* Real-time 3D Dynamic Rotating Slice-Scanning Mode for Traveling Wave MPI. *IJMPI* 2017; 3: 7.

10. Graeser M, Knopp T, Szwargulski P, Friedrich T, von Gladiss A, Kaul M, *et al.* Towards Picogram Detection of Superparamagnetic Iron-Oxide Particles Using a Gradiometric Receive Coil. *Sci Rep* 2017; 7: 6872.

11. Zheng B, Vazin T, Goodwill PW, Conway A, Verma A, Saritas EU, *et al.* Magnetic Particle Imaging tracks the long-term fate of *in vivo* neural cell implants with high image contrast. *Sci Rep* 2015; 5: 14055.

12. Lawaczeck R, Bauer H, Frenzel T, Hasegawa M, Ito Y, Kito K, *et al.* Magnetic Iron Oxide Particles Coated with Carboxydextran for Parenteral Administration and Liver Contrasting. *Acta Radiologica* 1997; 38: 584-97.

13. Wang YX, Hussain SM, Krestin GP. Superparamagnetic iron oxide contrast agents: physicochemical characteristics and applications in MR imaging. *Eur Radiol* 2001; 11: 2319-31.

14. Harisinghani MG, Barentsz J, Hahn PF, Deserno WM, Tabatabaei S, van de Kaa CH, *et al.* Noninvasive detection of clinically occult lymph-node metastases in prostate cancer. *N Engl J Med* 2003; 348: 2491-9.

15. Weizenecker J, Borgert J, Gleich B. A simulation study on the resolution and sensitivity of magnetic particle imaging. *Phys Med Biol* 2007; 52: 6363-74.

16. Vogel P, Ruckert MA, Jakob PM, Behr VC. µMPI-Initial Experiments With an Ultrahigh Resolution MPI. *IEEE Trans Magn* 2015; 51: 1-4.

17. Vogel P, Rueckert MA, Kemp SJ, Khandhar AP, Ferguson RM, Herz S, *et al.* Micro-Traveling Wave Magnetic Particle Imaging-Sub-Millimeter Resolution With Optimized Tracer LS-008. *IEEE Trans Magn* 2019; 55: 1-7.

18. Molwitz I, Ittrich H, Knopp T, Mummert T, Salamon J, Jung C, *et al.* First magnetic particle imaging angiography in human-sized organs by employing a multimodal ex vivo pig kidney perfusion system. *Physiol Meas* 2019; 40: 105002.

19. Haegele J, Panagiotopoulos N, Cremers S, Rahmer J, Franke J, Duschka RL, *et al.* Magnetic Particle Imaging: A Resovist Based Marking Technology for Guide Wires and Catheters for Vascular Interventions. *IEEE Trans Med Imaging* 2016; 35: 2312-8.

20. Haegele J, Rahmer J, Gleich B, Borgert J, Wojtczyk H, Panagiotopoulos N, *et al.* Magnetic particle imaging: visualization of instruments for cardiovascular intervention. *Radiology* 2012; 265: 933-8.

21. Haegele J, Biederer S, Wojtczyk H, Gräser M, Knopp T, Buzug TM, *et al.* Toward cardiovascular interventions guided by magnetic particle imaging: first instrument characterization. *Magn Reson Med* 2013; 69: 1761-7.

22. Sedlacik J, Frölich A, Spallek J, Forkert ND, Faizy TD, Werner F, *et al.* Magnetic Particle Imaging for High Temporal Resolution Assessment of Aneurysm Hemodynamics. Sznitman J, editor. *PLoS ONE* 2016; 11: e0160097.

23. Franke J, Lacroix R, Lehr H, Heidenreich M, Heinen U, Schulz V. MPI Flow Analysis Toolbox exploiting pulsed tracer information -an aneurysm phantom proof. *Int J Mag Part Imag* 2017; 3: 5.

24. Vaalma S, Rahmer J, Panagiotopoulos N, Duschka RL, Borgert J, Barkhausen J, *et al.* Magnetic Particle Imaging (MPI): Experimental Quantification of Vascular Stenosis Using Stationary Stenosis Phantoms. *PLoS ONE* 2017; 12: e0168902.

25. Herz S, Vogel P, Kampf T, Rückert MA, Veldhoen S, Behr VC, *et al.* Magnetic Particle Imaging for Quantification of Vascular Stenoses: A Phantom Study. *IEEE Trans Med Imaging* 2018; 37: 61-7.

26. Dietrich P, Vogel P, Kampf T, Ruckert MA, Behr VC, Bley TA, *et al.* Near real-time magnetic particle imaging for visual assessment of vascular stenosis in a phantom model. *Phys Med* 2021; 81: 210-4.

27. Salamon J, Hofmann M, Jung C, Kaul MG, Werner F, Them K, *et al.* Magnetic Particle / Magnetic Resonance Imaging: In-Vitro MPI-Guided Real Time Catheter Tracking and 4D Angioplasty Using a Road Map and Blood Pool Tracer Approach. *PLoS ONE* 2016; 11: e0156899.

28. Herz S, Vogel P, Dietrich P, Kampf T, Ruckert MA, Kickuth R, *et al.* Magnetic Particle Imaging Guided Real-Time Percutaneous Transluminal Angioplasty in a Phantom Model. *Cardiovasc Intervent Radiol* 2018; 29: 424-6.

29. Vogel P, Rückert MA, Klauer P, Kullmann WH, Jakob PM, Behr VC. First *in vivo* traveling wave magnetic particle imaging of a beating mouse heart. *Phys Med Biol* 2016; 61: 6620-34.

30. Weizenecker J, Gleich B, Rahmer J, Dahnke H, Borgert J. Three-dimensional real-time *in vivo* magnetic particle imaging. *Phys Med Biol* 2009; 54: L1–L10.

31. Ludewig P, Gdaniec N, Sedlacik J, Forkert ND, Szwargulski P, Graeser M, *et al.* Magnetic Particle Imaging for Real-Time Perfusion Imaging in Acute Stroke. *ACS Nano* 2017; 11: 10480-8.

32. Herz S, Vogel P, Kampf T, Dietrich P, Veldhoen S, Ruckert MA, *et al.* Magnetic Particle Imaging-Guided Stenting. *J Endovasc Ther* 2019; 29: 512-9.

33. Vogel P, Klauer P, Rückert MA, Bley TA, Kullmann WH, Jakob PM, *et al.* Dynamic Linear Gradient Array for Traveling Wave Magnetic Particle Imaging. *IEEE Trans Magn* 2018; 54: 1-9.

34. Vogel P, Ruckert MA, Klauer P, Kullmann WH, Jakob PM, Behr VC. Traveling wave magnetic particle imaging. *IEEE Trans Med Imaging* 2014; 33: 400-7.

35. Vogel P, Herz S, Kampf T, Rückert MA, Bley TA, Behr VC. Low Latency Real-time Reconstruction for MPI Systems. *Int J Mag Part Imag* 2017; 3: 1-8.

36. Vogel P, Kampf T, Rückert MA, Behr VC. Flexible and Dynamic Patch Reconstruction for Traveling Wave Magnetic Particle Imaging. *Int J Mag Part Imag* 2016; 2: 1-11.

37. Abdelaal E, Plourde G, MacHaalany J, Arsenault J, Rimac G, Déry JP, *et al.* Effectiveness of low rate fluoroscopy at reducing operator and patient radiation dose during transradial coronary angiography and interventions. *JACC Cardiovasc Interv* 2014; 7: 567-74.

38. Herzberg M, Dorn F, Dietrich P, Rückert MA, Kampf T, Bley TA, *et al.* Magnetic particle imaging for artifact-free imaging of intracranial flow diverter stents: A phantom study. *Phys Med* 2021; 88: 65-70.

39. Wegner F, Friedrich T, Gladiss von A, Grzyska U, Sieren MM, Lüdtke-Buzug K, *et al.* Magnetic Particle Imaging: Artifact-Free Metallic Stent Lumen Imaging in a Phantom Study. *Cardiovasc Intervent Radiol* 2020; 43: 331-8.

40. Wegner F, Gladiss von A, Haegele J, Grzyska U, Sieren M, Lüdtke-Buzug K, *et al.* Stent Lumen Quantification of 21 Endovascular Stents with MPI. *Int J Mag Part Imag* 2020; 6.

41. Rahmer J, Halkola A, Gleich B, Schmale I, Borgert J. First experimental evidence of the feasibility of multi-color magnetic particle imaging. *Phys Med Biol* 2015; 60: 1775-91.

42. Haegele J, Vaalma S, Panagiotopoulos N, Barkhausen J, Vogt FM, Borgert J, *et al.* Multi-color magnetic particle imaging for cardiovascular interventions. *Phys Med Biol* 2016; 61: N415-26.

43. Vogel P, Markert J, Ruckert MA, Herz S, Keßler B, Dremel K, *et al.* Magnetic Particle Imaging meets Computed Tomography: first simultaneous imaging. *Sci Rep* 2019; 9: 12627.

44. Vogel P, Lother S, Ruckert MA, Kullmann WH, Jakob PM, Fidler F, *et al.* MRI Meets MPI: a bimodal MPI-MRI tomograph. *IEEE Trans Med Imaging* 2014; 33: 1954-9.

45. Panagiotopoulos N, Duschka RL, Ahlborg M, Bringout G, Debbeler C, Graeser M, *et al.* Magnetic particle imaging: current developments and future directions. *Int J Nanomedicine* 2015; 10: 3097-114.

46. Graeser M, Thieben F, Szwargulski P, Werner F, Gdaniec N, Boberg M, *et al.* Human-sized magnetic particle imaging for brain applications. *Nat Commun* 2019;10: 1936.

47. Wegner F, Friedrich T, Panagiotopoulos N, Valmaa S, Goltz JP, Vogt FM, *et al.* First heating measurements of endovascular stents in magnetic particle imaging. *Phys Med Biol* 2018; 63: 045005.

Augmented reality in vascular and endovascular surgery: a scoping review

11

Joshua EVES, Abhilash SUDARSANAM, Joseph SHALHOUB, Dimitri AMIRAS

Technological advances have transformed vascular intervention over recent decades. Augmented reality (AR) is a subject of growing interest within surgery, with potential to improve the clinicians' understanding of 3D anatomy and their processing of real-time information. The aim of this review was to summarise the fundamental concepts of these technologies and to systematically assess the literature currently applying AR to vascular surgery.

A systematic literature review of 'Medline,' 'Scopus' and 'Embase' was performed according to PRISMA guidelines. Studies were selected by a blinded process between two investigators and assessed with data quality tools.

AR technologies have had a number of applications across vascular and endovascular surgery. The majority of studies use 3D imaging (*e.g.*) CT angiogram derived images of vascular anatomy to augment the clinicians anatomical understanding during procedures. A wide range of AR technologies have been employed with 'heads up' fusion imaging and AR head-mounted displays the most commonly clinically applied. AR applications have included guiding open, robotic and endovascular surgery while minimising dissection, improving procedural times and reducing radiation and contrast exposure. Additionally, AR has been successfully applied to surgical training, with scope to improve technical and team communication skills.

AR has shown promising developments in the field of vascular and endovascular surgery, with potential benefits to surgeons and patients alike. These include reductions in patient risk and operating times as well as contrast and radiation exposure for radiological interventions. While more technological advances are required to overcome current limitations, it is likely that AR will be a regular feature of vascular surgery clinical practice and training in the future.

Introduction

Emerging technologies are transforming vascular surgery at a rapid pace. In particular the introduction of endovascular techniques has opened the way for a Cambrian explosion of technological evolution, in terms of both hardware[1] and software[2].

One such technology is augmented reality (AR), which aims to enhance the clinicians' ability by offering intuitive augmentation of the real environment with computer-generated real-time input of virtual information. AR lies on the continuum from virtual reality (VR), in which the user is immersed in a completely virtual setting, to real-life. AR allows minimal interaction between virtual and real worlds, whereas mixed reality (MR) involves a combination of the real and virtual worlds, where both elements are able to interact[3].

Currently, available literature on the applicability of AR in vascular surgery is limited,[4] though theoretical benefits to the field are significant. A recent review on the applicability of head mounted displays (HMDs) and smart glasses in vascular surgery demonstrates potential uses in anatomical teaching, surgical training, tele-mentoring, pre-surgical planning and data collection[4].
Complications in vascular surgery, such as wound infections, have associations with the extent of dissection, size of the wound and duration of surgery[5]. Anatomical localisation with AR may help in reducing complications and improving overall outcomes. Whilst the Getting It Right First Time (GIRFT) program used a principle of standardisation across vascular surgery to improve outcomes in the United Kingdom (UK)[6], AR has promise in allowing both personalisation, taking into account individual patient anatomy and pathology whilst standardising the technical approach by providing intraprocedural guidance.

Surgical AR technology utilizes a range of technology, including everyday smartphone devices[7], however commercial products such as Magic Leap (Magic Leap, Plantation, FL, USA) and Microsoft HoloLens (Microsoft, Redmond, WA, USA), have more sophisticated optical systems and software to readily apply advanced computer vision techniques. These augmented reality head-mounted-displays (AR HMD) offer developers flexibility, allowing clinicians to experience virtual content that is overlaid directly into the present reality[3].

Across a number of subspecialties, the potential for AR as an important training tool has been identified[8]. With increasingly specialist surgical practice, more comorbid patients, and prevalent ethical challenges for surgical training, trainees have become increasingly reliant on simulation. Simulation has been demonstrated to effectively reduce training risk and costs[9]. Both VR and AR have been applied to surgical simulation successfully[10], however the superimposition of real-time information into the real world, and the flexibility offered by AR could make it a more realistic and adaptable simulation tool[11].

Methods

Search design

A systematic search of “MEDLINE”, “SCOPUS” and “EMBASE” was performed in accordance with the Preferred Reporting Items on Systematic Reviews and Meta-analysis (PRISMA) guidelines[12]. All studies written in English from inception until 8th of January 2021 were included in the search. Combinations of the following keywords were used in the systematic search string: *(‘augmented reality’ OR ‘hololens’ OR ‘image overlay’ OR ‘daqri’ OR ‘magic leap’ OR ‘immersive reality’ OR ‘extended reality’ OR ‘mixed reality’ OR ‘head mounted display’) AND (‘vascular surgery’ OR ‘endovascular’).*

First, a blinded and independent process of selection based on title and abstract was made without collusion by two authors (AS and JE) with a third author (JS) consulted with regards to discrepancies. Next, a selection of eligible studies was performed by analysing full texts. Inclusion criteria were: (1) studies in the English language; (2) minimum of level V Evidence using the Oxford Centre for Evidence-Based Medicine 2011 Levels of Evidence; (3) AR was used in vascular or endovascular surgery, and (4) applicability was reported. Exclusion criteria were (1) review articles, or conference abstracts; (2) non-English language articles; (3) articles lacking an available full-text; (4) AR was used outside of vascular or endovascular surgery, and (5) only VR was used.

The quality of data was evaluated using the Cochrane risk of bias tools (ROB-2) for randomised trials and (ROBINS-1) for non-randomised trials[13,14]. For those studies which included human participants but did not meet criteria for the aforementioned scoring tools, the Johanna Briggs Institute Critical Appraisal Checklist (JBI CAC) was used, with a score derived based on the checklist. A score of 1 was assigned for ‘Yes’, 0.5 for ‘unclear’ and 0 for ‘no’. Results were given as percentages.

Results

Thirty-two articles applicable to vascular surgery met criteria for inclusion (Figure 1). Included articles were sorted into categories: open vascular surgery; endovascular surgery (subdivided into aortic, visceral, peripheral and venous where applicable); and training (Table 1).

Quality assessment could only be performed in cases where human study populations were evaluated, which was 13 out of 32 (41%). The Cochrane risk of bias assessment was not used as no randomized trials were included in our search. Among the clinical studies, two [15,16] were cohort studies which were found to have a moderate risk of bias according to the Cochrane risk of bias tool for non-randomised trials (ROBIN-113). One was a case-control study [17] with a score of 55% according to the JBI CAC, seven were case-series [18–23] with an average score of 67% (range 50-80%) and three were case reports [22,24,25] with an average score of 65% (range 40-80%).

Articles are presented further subdivided into studies focused on concept and design to reflect the early stage of this technology in vascular surgery, and those which conducted research directly applied to surgery, training and or simulation.

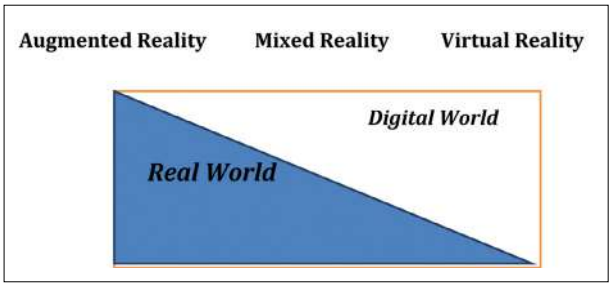

Figure 1: The location of augmented reality, mixed reality and virtual reality-on a spectrum of interplay between digital and real-world realities.

Table 1: Included studies applicable to augmented reality in vascular surgery

Article author	Title	Year	Category	Applied/ Concept and design	Clinical study type (No. patients)
Grinshpoon A *et al.* 2018	Hands-free augmented reality for vascular interventions	2018	Endovascular	Concept and design	N/A
Cheng I *et al.* 2014	An augmented reality framework for optimization of computer assisted navigation in endovascular surgery	2014	Endovascular	Concept and design	N/A
Parrini S *et al.* 2014	Augmented reality system for freehand guide of magnetic endovascular devices	2014	Endovascular	Applied	N/A
Wang J *et al.* 2012	Augmented reality during angiography: Integration of a virtual mirror for improved 2D/3D visualization	2012	Endovascular	Concept and design	N/A
Swerdlow N.J *et al.* 2019	Three-dimensional image fusion is associated with lower radiation exposure and shorter time to carotid cannulation during carotid artery stenting	2019	Endovascular	Applied	Cohort (116)
Van Den Berg J.C. 2013	Three-dimensional image overlay to assist endovascular procedures	2013	Endovascular	Applied	N/A

Groher M *et al.* 2009	Deformable 2D-3D registration of vascular structures in a one view scenario.	2009	Endovascular	Concept and design	N/A
Kilian-Meneghin J *et al.* 2018	Evaluation of Methods of Displaying the Real-Time Scattered Radiation Distribution during Fluoroscopically-Guided Interventions for Staff Dose Reduction.	2018	Endovascular	Concept and design	N/A
Schulz CJ *et al.* 2016	Fusion Imaging to Support Endovascular Aneurysm Repair Using 3D-3D Registration.	2016	Endovascular	Applied	Cohort (101)
Rynio P *et al.* 2019	Holographically-Guided Endovascular Aneurysm Repair.	2019	Endovascular	Applied	Case report (1)
Dumenil A *et al.* 2016	A versatile intensity-based 3D/2D rigid registration compatible with mobile C-arm for endovascular treatment of abdominal aortic aneurysm.	2016	Endovascular – Aortic	Concept and design	N/A
Koutouzi *et al.* 2015	EVAR Guided by 3D Image Fusion and CO2 DSA: A New Imaging Combination for Patients With Renal Insufficiency.	2015	Endovascular – Aortic	Applied	Case Series (3)
Carrell *et al.* 2010	Feasibility and limitations of an automated 2D-3D rigid image registration system for complex endovascular aortic procedures.	2010	Endovascular – Aortic	Applied	N/A
Kaladji *et al.* 2019	Fusion Imaging for EVAR with Mobile C-arm.	2019	Endovascular – Aortic	Applied	Case-control (54)
García-Vázquez *et al.* 2018	Navigation and visualisation with HoloLens in endovascular aortic repair.	2018	Endovascular – Aortic	Applied	N/A
Goudeketting *et al.* 2018	The use of 3D image fusion for percutaneous transluminal angioplasty and stenting of iliac artery obstructions: validation of the technique and systematic review of literature.	2018	Endovascular – Peripheral	Applied	Case series (11)
Schwein *et al.* 2017	Magnetic resonance venography and three-dimensional image fusion guidance provide a novel paradigm for endovascular recanalization of chronic central venous occlusion.	2017	Endovascular – Venous	Applied	Case Series (4)
Pietrabissa A *et al.* 2009	Mixed reality for robotic treatment of a splenic artery aneurysm.	2009	Endovascular – Visceral	Applied	Case report (1)
Haxthausen F.V *et al.* 2019	Catheter pose-dependent virtual angioscopy images visualized on augmented reality glasses.	2019	Endovascular-Aortic	Concept and design	N/A

Chaoyang Shi *et al.* 2016	*In vitro* three-dimensional aortic vasculature modelling based on sensor fusion between intravascular ultrasound and magnetic tracker.	2016	Endovascular-Aortic	Concept and design	N/A
Dumenil A *et al.* 2015	Safety and accuracy of endovascular aneurysm repair without pre-operative and intra-operative contrast agent.	2015	Endovascular-Aortic	Applied	Case Series (6)
Rolls A.E *et al.* 2016	A Comparison of Accuracy of Image-versus Hardware-based Tracking Technologies in 3D Fusion in Aortic Endografting.	2016	Endovascular-Aortic	Applied	N/A
Fukuda T *et al.* 2013	Evaluation of automated 2D-3D image overlay system utilizing subtraction of bone marrow image for EVAR: Feasibility study.	2013	Endovascular-Aortic	Applied	Case series (20)
Koutouzi *et al.* 2017	3D Image Fusion to Localise Intercostal Arteries During TEVAR.	2017	Endovascular-Aortic	Applied	Case series (7)
Lu W *et al.* 2020	Augmented reality navigation to assist retrograde peroneal access for the endovascular treatment of critical limb ischemia.	2020	Endovascular-Peripheral	Applied	Case report (1)
Mochizuki *et al.* 2016	New simple image overlay system using a tablet PC for pinpoint identification of the appropriate site for anastomosis in peripheral arterial reconstruction.	2016	Open	Applied	Case series (11)
Aly, Omar 2020	Assisting Vascular Surgery with Smartphone Augmented Reality.	2020	Open	Applied	N/A
Mangina E *et al.* 2018	3D modelling for augmented reality systems in novel vascular models.	2018	Training	Concept and design	N/A
Burke E *et al.* 2017	Augmented reality EVAR training in mixed reality educational space.	2017	Training	Concept and design	N/A
Bartesaghi S *et al.* 2017	Spatial augmented reality and simulations to improve abdominal aortic aneurysm diagnosis and monitoring.	2017	Training	Concept and design	N/A
Rudarakanchana N *et al.* 2014	Endovascular repair of ruptured abdominal aortic aneurysm: Technical and team training in an immersive virtual reality environment.	2014	Training	Applied	N/A
Anderson J *et al.* 2002	Virtual reality training in interventional radiology: The Johns Hopkins and Kent Ridge digital laboratory experience.	2002	Training	Concept and design	N/A

Concept and design

Basic design and concept

AR in surgery mostly relies on the registration of a virtual image or object onto the real patient, using a tracking method, which can trace the real environment and place virtual objects in the correct position and orientation. As Table 2 demonstrates, 29 of 32 included studies involved deriving digital structures of blood vessels from clinical imaging, including non-contrast computer tomography (CT), CT angiography, cone-beam CT, magnetic resonance angiography (MRA), conventional ultrasound (US), intravascular US and 3D US. The most used modality is CT angiography (CTA) (Figure 2), with cone-beam CT often used in registration process with patient in the operating suite.

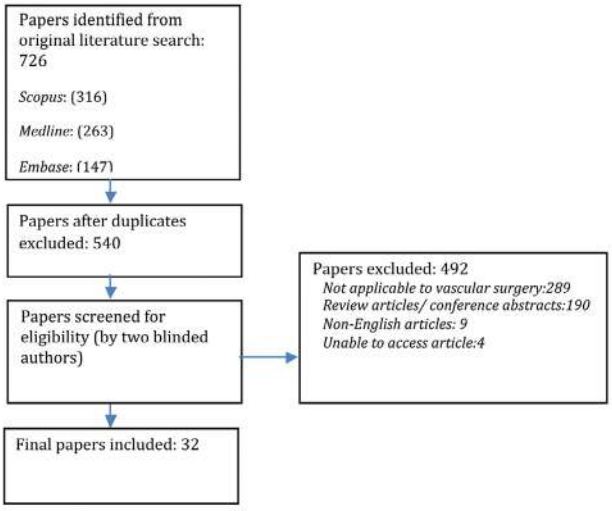
Papers identified from original literature search: 726
Scopus: (316)
Medline: (263)
Embase: (147)
Papers after duplicates excluded: 540
Papers screened for eligibility (by two blinded authors)
Papers excluded: 492
Not applicable to vascular surgery:289
Review articles/ conference abstracts:190
Non-English articles: 9
Unable to access article:4
Final papers included: 32

Figure 2: Systematic search of 'MEDLINE,' 'SCOPUS,' and 'EMBASE,' PRISMA flowchart.

Table 2: Included studies showing image, registration/tracking and display type

Article author	Title	Year	Image Type	Registration/ Tracking Type	Type of display	Outcome
Grinshpoon A *et al.* 2018	Hands-free augmented reality for vascular interventions	2018	3D model of heart	Human pose estimation	AR HMD (Hololens)	Interaction with 3D model using voice and head rotations
Cheng I *et al.* 2014	An augmented reality framework for optimization of computer assisted navigation in endovascular surgery	2014	Live ultrasound registered on 3D model derived from pre-scanned CT images	Electromagnetic (EM) and GPS tracking	Monitor	AR simulator prototype allowing robotic control of catheter inside 3D models of aorta with live ultrasound imaging
Parrini S *et al.* 2014	Augmented reality system for freehand guide of magnetic endovascular devices	2014	3D US derived model	Marker tracking (fiducial)	AR HMD	Proof of concept-10 users able to guide capsule through phantom vessel using external magnets.
Wang J *et al.* 2012	Augmented reality during angiography: Integration of a virtual mirror for improved 2D/3D visualization	2012	CT angiography (CTA) derived models used to derive 2D 'mirror' overlaid onto 2D fluoroscopic images	Fusion image overlay software (2D-3D)	Monitor	10 clinicians, 5 R+D engineers and 9 computer scientists concurred that 2D mirror could be useful during endovascular intervention

Swerdlow N.J *et al.* 2019	Three-dimensional image fusion is associated with lower radiation exposure and shorter time to carotid cannulation during carotid artery stenting	2019	3D models from CTA/ MRA with superimposed CBCT	'VesselNavigator' computer-based image fusion	Monitor	3D image fusion associated with shorter fluoroscopy time, lower radiation exposure and shorted CCA cannulation times
Van Den Berg J.C. 2013	Three-dimensional image overlay to assist endovascular procedures	2013	3D image overlay using rotational XR/ CBCT	'VesselNavigator' computer-based image fusion	Monitor	Cone-beam CT potential for 3D image registration
Groher M *et al.* 2009	Deformable 2D-3D registration of vascular structures in a one view scenario.	2009	CBCT and preoperative CTA	Fusion image overlay software (2D-3D)	Monitor	Improvement in image fusion registration for deformable structures
Kilian-Meneghin J *et al.* 2018	Evaluation of Methods of Displaying the Real-Time Scattered Radiation Distribution during Fluoroscopically-Guided Interventions for Staff Dose Reduction.	2018	Computer generated scatter beams	Microsoft Kinect (RGB and Depth) optical tracking	Monitor	Survey results indicate that scatter distribution displays helpful in managing staff dose
Schulz CJ *et al.* 2016	Fusion Imaging to Support Endovascular Aneurysm Repair Using 3D-3D Registration.	2016	Pre-operative CTA registered with non-contrast Cone Beam CT (nCBCT)	Fusion image overlay software (3D-3D)	Monitor	Fusion imaging with EVAR repair. Fluoroscopy required to confirm accurate image overlay
Rynio P *et al.* 2019	Holographically-Guided Endovascular Aneurysm Repair	2019	Pre-operative CTA onto 2D fluoroscopy	Optical Simultaneous localisation and mapping (SLAM) (CarnaLife Holo)	AR HMD (Hololens)	Hologram useful during EVAR. Limitations with binocular vision, battery life, inability to manipulate hologram
Dumenil A *et al.* 2016	A versatile intensity-based 3D/2D rigid registration compatible with mobile C-arm for endovascular treatment of abdominal aortic aneurysm	2016	Preoperative CTA onto fluoroscopy	Intensity-based image overlay software (2D-3D)	Monitor	Initial tests show registration system compatible with EVAR workflow and can be used throughout procedure
Koutouzi *et al.* 2015	EVAR Guided by 3D Image Fusion and CO2 DSA: A New Imaging Combination for Patients With Renal Insufficiency.	2015	nCBCT fused with preoperative CTA and overlaid onto fluoroscopy	Intensity-based registration image overlay software (3D-3D)	Monitor	Reduces iodine-contrast exposure. Contrast fluoroscopy advised to verify placement
Carrell *et al.* 2010	Feasibility and limitations of an automated 2D-3D rigid image registration system for complex endovascular aortic procedures.	2010	Pre-operative CTA onto fluoroscopy	Intensity-based registration image overlay software (2D-3D)	Monitor	Poor registration in highly angulated aortas due to deformation with device insertion
Kaladji *et al.* 2019	Fusion Imaging for EVAR with Mobile C-arm.	2019	Pre-operative CTA	Intensity based registration image overlay software (2D-3D)	Monitor	Shorter operation times and reduced contrast agent. Feasible to use fusion imaging with mobile c-arm.

García-Vázquez *et al.* 2018	Navigation and visualisation with HoloLens in endovascular aortic repair.	2018	3D models derived from 3D Ultrasound and CTA	Feature-based registration with electromagnetic tracking (EM)	AR HMD (Hololens)	Promising study on US model to overcoming need for radiation/ constrast during EVAR
Goudeketting *et al.* 2018	The use of 3D image fusion for percutaneous transluminal angioplasty and stenting of iliac artery obstructions: validation of the technique and systematic review of literature.	2018	Contrast enhanced MRA (CE MRA) registered onto CBCT	Intensity based registration image overlay software (3D-3D)	Monitor	Minimal fusion displacement of iliac arteries caused by insertion of catheters
Schwein *et al.* 2017	Magnetic resonance venography and three-dimensional image fusion guidance provide a novel paradigm for endovascular recanalization of chronic central venous occlusion.	2017	MRV and CBCT registered to each other. Overlaid onto 2D fluoroscopy	Intensity-based registration image overlay software (2D-3D)	Monitor	Image fusion feasible for stenting central venous occlusion and could improve success, safety and surgical confidence
Pietrabissa A *et al.* 2009	Mixed reality for robotic treatment of a splenic artery aneurysm	2009	CTA derived 3D model	Infrared optical tracking	AR HMD	Robotic exclusion of a splenic artery aneurysm assisted by AR
Haxthausen F.V *et al.* 2019	Catheter pose-dependent virtual angioscopy images visualized on augmented reality glasses	2019	CTA derived 3D model	Feature-based registration with electromagnetic tracking	AR HMD-Hololens	Feasibility of EM tracking of catheter tip with 3D model demonstrated on phantom
Chaoyang Shi *et al.* 2016	*In vitro* three-dimensional aortic vasculature modelling based on sensor fusion between intravascular ultrasound and magnetic tracker.	2016	Intravascular ultrasound derived 3D model	Electromagnetic tracking with hybrid motion sensor	Monitor	Proof of concept prototype built and tested successfully
Dumenil A *et al.* 2015	Safety and accuracy of endovascular aneurysm repair without pre-operative and intra-operative contrast agent.	2015	Unenhanced CT derived 3D model fused with CBCT	Intensity based registration with image overlay software (3D-3D)	Monitor	Successful aneurysm repair on 6 patients without contrast, with good placement confirmed on post-operative CT and intraoperative duplex
Rolls A.E *et al.* 2016	A Comparison of Accuracy of Image-versus Hardware-based Tracking Technologies in 3D Fusion in Aortic Endografting	2016	CTA and CBCT derived 3D model fusion with 2D fluoroscopy	Image based vs Hardware based tracking	Monitor	Significant reduction in overlay error using image-based tracking
Fukuda T *et al.* 2013	Evaluation of automated 2D-3D image overlay system utilizing subtraction of bone marrow image for EVAR: Feasibility study	2013	CTA and CBCT derived 3D model with 2D fluoroscopy	Feature based registration image overlay software (2D-3D)	Monitor	Series of 20 patients confirm feasibility of '3D roadmap' use in EVAR to reduce maneuvres and radiation required. 50% accuracy of registration of iliac bifurcation and renal arteries despite deformation with insertion of instruments.

Koutouzi *et al.* 2017	3D Image Fusion to Localise Intercostal Arteries During TEVAR.	2017	CBCT and preoperative CTA fused onto 2D fluoroscopy	Intensity based registration with image overlay software (2D-3D)	Monitor	Successfully used in 7 procedures. Overlay not always accurate and should be checked with angiography in high precision cases
Lu W *et al.* 2020	Augmented reality navigation to assist retrograde peroneal access for the endovascular treatment of critical limb ischemia	2020	Preoperative CTA	Manual tracking by lining up markers on patients and glasses	AR HMD	Successful and feasible approach. Learning curve for user to ensure overlapping of markers and to follow AR projected trajectory
Mochizuki *et al.* 2016	New simple image overlay system using a tablet PC for pinpoint identification of the appropriate site for anastomosis in peripheral arterial reconstruction.	2016	Preoperative CTA	Fiducial marker landmark-based registration and optical (RBG) tracking	Tablet PC	Successful identification of 11 target branches. On missed by 10mm, due to incorrect marker tracking
Aly, Omar 2020	Assisting Vascular Surgery with Smartphone Augmented Reality.	2020	Preoperative CTA to derive 3D model	Optical (RBG) augmented with gyroscopic tracking	Mobile phone	Good initial results from combined optical tracking with gyroscopic data. Limitations of lack of deformability of model
Mangina E *et al.* 2018	3D modelling for augmented reality systems in novel vascular models	2018	Preoperative CTA to derive 3D Model	N/A	N/A	Using opensource software inc UNITY and PROENGINEER, a 3D model was created and sliced for use in VR or AR applications
Burke E *et al.* 2017	Augmented reality EVAR training in mixed reality educational space	2017	3D model derived from CTA and 3D printed model	Optical fucidial marker tracking	Mobile phone	Good initial user feedback. Further development required for realism. HMD devices to be used to improve user experience
Bartesaghi S *et al.* 2017	Spatial augmented reality and simulations to improve abdominal aortic aneurysm diagnosis and monitoring	2017	CTA derived model	Optical fucidial marker tracking (ARToolkit)	Projector	Successful creating of model from CTA which was projected onto a mannequin for simulated EVAR.
Rudarakan-chana N *et al.* 2014	Endovascular repair of ruptured abdominal aortic aneurysm: Technical and team training in an immersive virtual reality environment	2014	VR rAAA from CTA derived models	ORCAMP simulated angiosuite	Monitor	Feasibility of immersive angiosuite for emergency EVAR demonstrated. Specialists performed significantly faster than trainees.
Anderson J *et al.* 2002	Virtual reality training in interventional radiology: The Johns Hopkins and Kent Ridge digital laboratory experience	2002	3D models of blood vessels	Simulated user interface with real guidewires- (hardware tracking)	Monitor	Positive feedback from peripheral and neurological interventionalists

This data is processed into a virtual object and displayed to the clinician on a screen, projector, monitor or augmented reality head mounted display (ARHMD.) A number of steps are required to complete processing, including segmentation to reduce the model to the area of interest (*e.g.* aorta) often by thresholding a Hounsfield scale, and then using a 3D computer generated mesh to unify the model and to fill holes/ defects, and a slicer to break up the model aorta into its different anatomical sections [26].

The type of display will depend on the application, and a range of display types were included, with HoloLens the most used AR HMD (see Figure 3).
Registration and tracking are essential components of AR, allowing alignment of the virtual and real data in a usable way. Registration is commonly performed using markers, where a particular pattern or anatomical landmark in the real world is used as a reference, corresponding to a virtual marker derived from medical imaging [11]. This can be performed manually, or by the use of trackers. Marker less tracking can be performed patterns in real and virtual data are corresponded [27]. Integrated or external optical sensors (Infrared (IR) or colour (RGB)) can be used to track markers or recognised patterns from a patient's anatomy. In recent years RBG-D (depth) cameras which track both depth and colour simultaneously allow contemporaneous tracking of the real-world [28]. Electromagnetic (EM) tracking is a useful method for tracking instruments deep to the surface [29]. In many cases, such as with Microsoft HoloLens, a variety of sensor inputs are used for hybrid tracking [30].

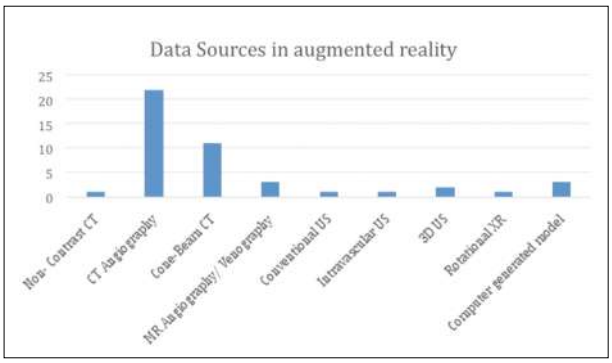

Figure 3: Majority of included studies derived data from 3D clinical imaging which can be overlaid into real-world.

Challenges with these techniques include the deformability of anatomy, for example when stiff endovascular devices are inserted into blood vessels. These changes can cause registration errors which can be clinically significant *i.e.* with complex visceral anatomy in EVAR. Groher *et al.* [31] has proposed computational algorithms for allowing some accurate deformability of three dimensional (3D) models for registration with two dimensional (2D) fluoroscopy. Another innovative tracking solution combating this problem involves electromagnetic trackers on the tips of angiography catheters which can give accurate information on 3D position and orientation of the catheter in space such as those used by Garcia-Vasquez *et al.* [32].
Alternatively, intravascular US on the tip of catheters can be used to create the 3D model of blood vessels during endovascular procedures, with magnetic trackers to orientate the catheter in real-time as proposed by Chaoyang Shi *et al.* [33]. Parrini *et al.* [34] tested the use of freehand external magnets as a means of guiding magnetic endovascular devices to their targets with AR vessel models on a phantom.

Endovascular procedures

Given the inherent reliance of endovascular procedures on imaging, the potential benefits of AR were identified early. In particular, to improve clinician understanding of 3D anatomy during critical steps as well as to reduce time, radiation and contrast exposure [35]. Image overlay techniques are used for complex endovascular work worldwide, and usually rely on merging live fluoroscopy with 2D or 3D images from X-ray/ CT or MRI.

Endovascular aneurysm repair (EVAR) and aortic disease

Endovascular aneurysm repair (EVAR) is increasingly being performed for the repair of both complex and conventional infrarenal abdominal aortic aneurysms in the elective and emergency setting.

AR visualisation has now been used in planning and EVAR navigation, with a case report by Rynio *et al.*[24] describing the use of an AR head mounted display (AR HMD) to project the aortic aneurysm and bones (vertebral column lying posterior to the aneurysm) as a 3D hologram which responds to gestures and voice commands.

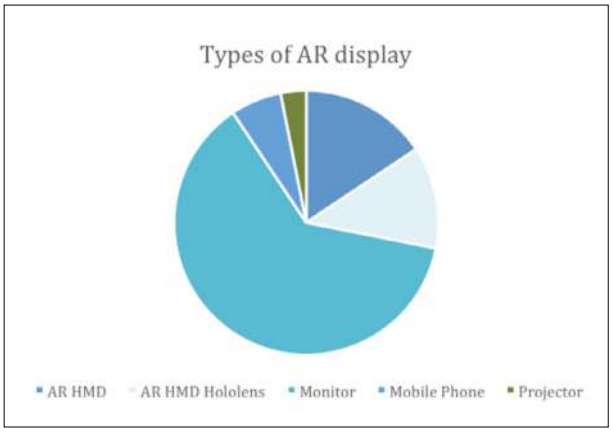

Figure 4: Types of augmented reality displays. A monitor was the most frequently used type of display, often used for image fusion in interventional procedures.

Published in 2013, a '3D Roadmap' was developed by Fukuda *et al.*[36] using pre-operative CT imaging where bone marrow subtraction and the use of the iliac crest and lumbar vertebrae as landmarks resulted in the creation of an image overlay to guide aortic endografting. This reduced the need for digital subtraction angiography and its associated risks, ultimately giving rise to fusion imaging.

Fusion imaging has been used for endovascular navigation in hybrid vascular operating theatres, particularly in complex fenestrated endovascular aneurysm repairs. This uses pre-operative 3D CT imaging to overlay vascular structures onto peri-operative 2D fluoroscopy images with the aim of reducing fluoroscopy time, contrast agent dosing and overall operating time. This may also be used in a conventional operating theatre with a mobile C-arm with good results for conventional aortic endografting, as reported by Kaladji *et al.*[17]. Koutouzi *et al.*[18] modified this modality to require C02 digital subtraction angiography (DSA) to confirm accurate registration of the CT-derived 3D vascular overlay to avoid iodinated contrast in patients with poor renal function or contrast allergies.

Kaladji *et al.*[37] went on to successfully demonstrate the use of fusion imaging to undertake EVAR without the use of any iodinated contrast in the pre or peri-operative phase in a case-series of 6 patients. Patients with severe chronic kidney disease underwent unenhanced CT imaging. Centrelines for EVAR planning were manually drawn out and key anatomical points / landing zones marked following segmentation and processing. A pre-operative 3D image overlay reconstruction with these markers was then projected onto 2D fluoroscopy imaging to guide placement of the aortic endograft without the use of contrast agent. No endoleaks were noted during post-operative duplex surveillance, with minimal error in positioning of the aortic endograft on post-operative CT imaging and no significant reduction in renal function.

A series of 101 patients by Schulz *et al.*[15] in 2016 tested the use of image overlay alone in patients undergoing conventional infrarenal EVAR. Fusion image overlay utilising images from pre-operative CTA with images obtained from an intra-operative CBCT, was compared with intra-operative DSA. Whilst < 5 mm accuracy was seen in most patients (68% of patient cohort), significant deviations were noted in some patients including significant caudal deviation in 9 patients (9% of the patient cohort) which would have resulted in coverage of the lowest lying renal artery, rendering significant operative morbidity. Therefore, contrast injection study for cannulation of the lowest lying visceral vessel was advocated. (Figure 5)

Koutouzi *et al.*[19] described a technique which aims to use image overlay to reduce the risk of covering intercostal arteries during TEVAR and causing paraparesis. Intraoperative CBCT is used to perform 3D/3D registration with the preoperative CTA in order to enhance accuracy. Once calibrated onto live fluoroscopy, this overlaid 3D model is used to guide the TEVAR and avoid pre-planned intercostal arteries. A case series of seven was reported without spinal cord injury.

A common problem with image overlay techniques is the non-deformability of a rigid 3D model created from a pre-operative CT scan. Garcia-Vasquez *et al.*[32] attempt to overcome this problem through the use of 3D ultrasound to create a real-time model of the patients anatomy visible to a clinician wearing the AR HMD. Coupled with the electromagnetic catheter tip tracking system used by von Haxthausen *et al.*[29] this concept has been proposed to perform EVAR completely free of radiation and contrast, and tested on a phantom model with a 3D model of an aortic aneurysm [32]. The concept showed promising progress, however issues around registration accuracy still remain. (Figure 6)

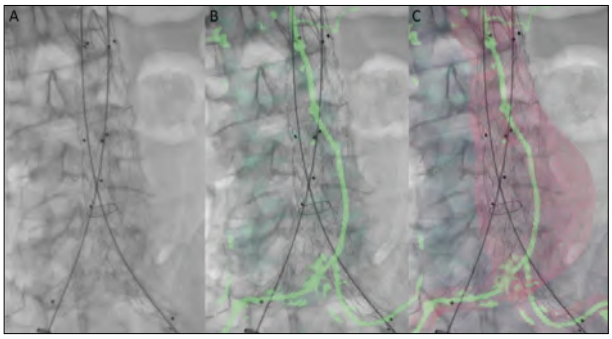

Figure 5: During the procedure, different information was overlaid onto the native 2D fluoroscopic image to guide instrument placement **(A)** None **(B)**. Centerlines and keys points can be projected **(C)**, artificially enhanced aortic volume.
Kaladji A, Dumenil A, Mahé G, Castro M, Cardon A, Lucas A, *et al.* Safety and Accuracy of Endovascular Aneurysm Repair Without Pre-operative and Intra-operative Contrast Agent. *Eur J Vasc Endovasc Surg* 2015;49(3):255–61.

Figure 6: View from Hololens display of 3D vasculature from 3D ultrasound being projected onto phantom
(Haxthausen, F. Von, Jäckle, S., Strehlow, J., Ernst, F. & García-Vázquez, V. Catheter pose-dependent virtual angioscopy images visualized on augmented reality glasses. *Curr. Dir. Biomed. Eng.* 5, 289–291 (2019))

Endovascular arterial disease

Endovascular techniques are being applied to increasingly complex surgical problems in comorbid patients. The potential to reduce radiation and contrast exposure while navigating tortuous vessels makes the application of AR technology more attractive.

Lu *et al.* [25] described successful retrograde peroneal access through an AR system with CTA image derived overlay of fluoroscopy images. AR glasses were worn by the operator to guide needle trajectory. The case report highlighted technical difficulties, including the need for manual registration, with the having to align virtual dots on their AR HMD with fiducial markers on the patients' leg. Additionally, aligning the trajectory of the needle path on the AR HMD required acquisition of new technical skills.

The work of Goudeketting *et al.*[20] focused on the accuracy of image fusion based on preprocedural contrast enhanced MRA during percutaneous angioplasty of iliac lesions. They found that guidewires and endovascular catheters did not cause significant vessel displacement to influence the image fusion according to angiographic experts.

Swerdlow *et al.*[16] retrospectively compared carotid stenting with 2D-3D image fusion (46 patients) and without (70 patients.) MRI or CTA images were overlaid onto real-time 2D fluoroscopy. They found significantly improved cannulation times and reduced radiation exposure using this technique.

Endovascular - venous disease

Endovascular venous work compared to arterial can be more challenging because of the lack of landmarks from calcifications and thicker vessel walls. Schwein *et al.*[21] used image fusion techniques with magnetic resonance venography (MRV) to successfully recanalize four patients with central venous occlusion. It was felt that MRV image fusion improved clinician confidence and safety of difficult venous endovascular navigation.

Open Surgery

'Traditional' open vascular surgery has increasingly been replaced by novel endovascular techniques, which, in combination with problems with tissue deformation as previously described may explain why AR less well researched in this field.

The use of a new image overlay system has been demonstrated successfully in lower limb revascularisation surgery by Mochazuki *et al.*[23]. This system used pre-operative CT imaging to help locate the target distal anastomotic site, and plan a limited incision accordingly, using a branch artery as a reference point. (Figure 7)

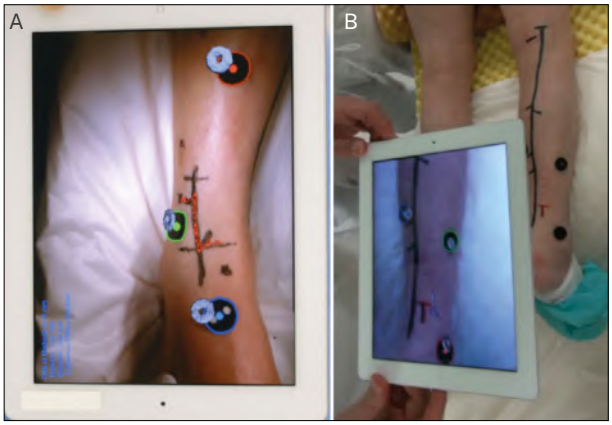

Figure 7: CT-derived 3D model is superimposed onto camera images. Doughnut shaped fiducial markers on the limb help to match images so that the target artery and its branches can be overlaid onto the limb as red (A) or blue (B) lines.
Mochizuki Y, Hosaka A, Kamiuchi H, Nie JX, Masamune K, Hoshina K, *et al.* New simple image overlay system using a tablet PC for pinpoint identification of the appropriate site for anastomosis in peripheral arterial reconstruction. *Surg Today* 2016;46(12):1387–93.

Modern day mobile phones have multiple sensors which may be used for AR assisted surgery (ARAS). The benefits of easy accessibility (most operators have access to a mobile phone) and cost make them an attractive option. An ARAS system was developed by Aly *et al.*[7] to provide 3D guidance during vascular procedures. CTA derived images were used by the smartphone to produce a 3D guidance model fused with the patient's anatomy, and rotational and positional tracking compared for planning an ilio-femoral bypass as well as an endovascular sheath placement in the common femoral artery. (Figure 8)

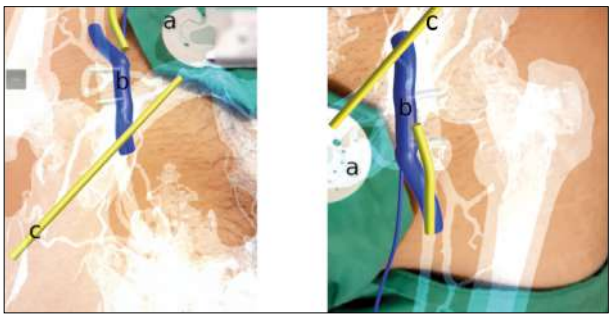

Figure 8: Screen capture of ARAS system developed by Aly *et al.* (2020). Fiducial marker (sterile suture pack) used for registration and tracking with 3D model derived from CT angiogram superimposed from mobile phone.
a) Tracking marker ;
b) Common femoral vein ;
c) Inguinal ligament
Aly O. Assisting Vascular Surgery with Smartphone Augmented Reality. *Cureus* 2020;12

Robotic Surgery

The use of AR with robotic-assisted surgery is of increasing academic interest worldwide. Pietrabissa *et al.*[22] successfully used an AR HMD to superimpose a surgical anatomy from CT angiography onto the patients' body for pre-operative planning, in order to guide trocar placement and to guide dissection so as to minimize disruption

using the da Vinci surgical system (Intuitive Surgical Inc. (Sunnyvale CA.)) While robotic assisted surgery is becoming increasingly common for vascular interventions, the use of AR is in early stages of adoption and investigation.

Training and simulation

Published work on AR vascular and endovascular training was limited in our search to five papers, while one paper applied this to training vascular surgeons, four focused on design concepts.
Mangina *et al.*[26] tested the concept of creating a 3D model of the aorta from CTA images using a number of programming tools and platforms including UNITY, ARToolKit and PROENGINEER. A model aorta was created, with the potential to be merged with VR and AR tracking technologies to create an accurate training and educational tool, for application to both open and endovascular training.

Bartesaghi *et al.*[38] used similar techniques to create a 3D model of the aorta, projected onto a mannequin, to allow 3D AR simulation of an EVAR repair. The original model was derived from CTA images, and segmentation with meshing performed to create the model. Software was optimised for interplay between the simulation and a hardware mannequin, allowing surgical trainees to learn the steps of an EVAR.

Similarly, Anderson *et al.*[39] described the development of a personal computer based AR simulation system for interventional radiology. This system allows real time manipulation of catheters and guidewires through a tactile user interface device which creates hand-eye coordinated realism of the movement of instruments over 3D generated models of vessels. Extra enhancements have been built in including the administration and subsequent washout of contrast and control of the c-arm. The paper reports good initial feedback from neuro and peripheral vascular interventionalists who felt it had 75% of desired functionality and was useful for educational simulation, with further work required to achieve sufficient realism for pre-operative planning. (Figure 9)

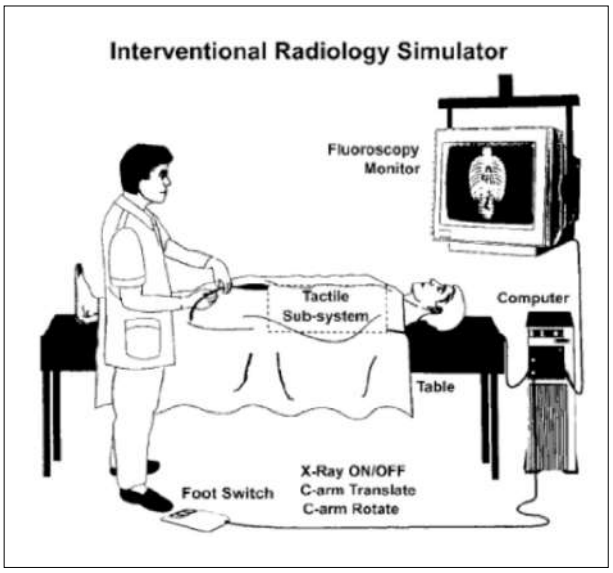

Figure 9: AR Interventional simulator design
(Anderson, J. *et al.* Virtual reality training in interventional radiology: The Johns Hopkins and Kent Ridge digital laboratory experience. *Seminars in Interventional Radiology* vol. 19 179–185 (2002))

Crowley *et al.*[40] built on the work of Mangina *et al.* further exploring the concept of EVAR mixed reality simulation. They found that creation of a solid 3D printed model of an aortic aneurysm through which real instruments (guidewires, catheters, delivery devices) can be placed and manipulated, gave the simulation tactile realism. A mobile device provides the user with fluoroscopic data, through an AR software (ARToolKit, Daqri), while haptic feedback was provided by the 3D model. Limitations of 3D printed models include the lack vascular wall deformability, and realism of feedback from catheter tips against the model wall. The system's usability was tested by medical students and university lecturers.

An AR system for US guided endovascular surgical training was devised by Cheng *et al.*[41]. Live ultrasound images were transferred to a pre-scanned phantom model of the aorta and iliac arteries, which was extended to a computer assisted remote endovascular surgery model. The user is able to navigate an endovascular catheter by a robotic device, with computer-generated images to augment 3D

understanding of the catheter in space. The phantom provides both haptic and visual feedback aiming to be as realistic as possible.

Rudarakanchana *et al.*[42] applied the concept of simulation to the pressured setting of ruptured EVAR. This was achieved through VR simulators being integrated into a simulated angiosuite, with a whole team present. Ten teams were tested, five led by interventional specialists, and five by trainees. The study measured time to achieve proximal control, total procedure and fluoroscopy times. Experts were significantly faster than trainees, using reduced fluoroscopy time, suggesting that the simulation model had good applicability to real-life experience. In particular the value of the simulation for improving team communication and human factor skills were highlighted by feedback, suggesting that AR and mixed reality simulation could be a useful adjunct to improving ruptured EVAR outcomes.

Limitations

While we have demonstrated that there is a wide range of applicability of AR to vascular surgery, at this stage there is a lack of clinical trials proving benefit. Image overlay technology has shown a lot of promise, with many options available, but problems remain with the accuracy of image registration, especially with more complex anatomy[15]. A common problem is the deformation of vascular structures with respiration, surgical manipulation or 'stretching out' of vessels with rigid stent delivery systems. Robust deformable registration algorithms or intraoperative real-time 3D scanners are potential solutions to assist AR guided surgery on soft/ deformable structures. These would demand high levels of data transmission and processing which must be met by technology to prevent lag[43].

There have been a number of reports of AR HMD use in vascular surgery and early promise that they can reduce the need for radiation and contrast exposure[32]. AR HMD's such as HoloLens still have a few technical concerns which could restrict their usefulness. Their weight (500g-645g depending on device and manufacturer), can cause discomfort and fatigue over long procedures. AR HMD processing capacity and memory are limited, which can restrict certain applications. The immersive experience can be limited by a restricted field of view and projection size, image quality and computational time will improve as the technology evolves. There is not yet consensus on the optimal methods for merging and displaying virtual and real information so that depth perception/ focus and visual clutter do not distract the wearer[4,44].

Conclusions

A significant proportion of studies we identified are preclinical and demonstrate proof-of-concept findings. Nevertheless, AR solutions are applicable a wide spectrum of fields within vascular surgery, including those highlighted in this systematic review.

AR has been shown potential to enhance accuracy, reduce procedural time, radiation exposure and contrast dose in a range of vascular surgery applications by digitally augmenting the clinicians' procedural ability, reducing surgical risk and improving patient outcomes. Clinicians, who demand high levels of accuracy and safety for use on patients, should be aware of potential technical pitfalls when using AR technology on patients as well as open to the potential benefits. AR has also been shown to be an increasingly valuable tool in surgical simulation and education. As technology improves, it can be expected that AR will become an arrow in the surgical quiver that is increasingly relied upon, and that more applications will be found for AR which could benefit the clinician. Future development and studies should assess whether the use of AR affords improvements in the patient experience and in clinical and cost effectiveness.

References

1. Cheng SWK. Novel endovascular procedures and new developments in aortic surgery. *Br J Anesth* 2016; 117: ii3-ii12.

2. Bedi VS, Sharma N. Game changers in vascular and endovascular surgery. *Indian J Vasc EndovascSurg* 2020; 7: 13-7.

3. Rahman R, Wood ME, Qian L, Price CL, Johnson AA, Osgood GM. Head-Mounted Display Use in Surgery: A Systematic Review. *Surg Innov* 2020; 27: 88-100.

4. Lareyre F, Chaudhuri A, Adam C, Carrier M, Mialhe C, Raffort J. Applications of Head-Mounted Displays and Smart Glasses in Vascular Surgery. *Ann Vasc Surg* 2021; 75: 497-512.

5. Groin wound infection after vascular exposure (GIVE) multicentre cohort study group .Groin wound infection after vascular exposure (GIVE) multicentre cohort study. *Int WoundJ* 2021; 18: 164-75.

6. Gray WK, Day J, Horrocks M. Editor's Choice–Volume–Outcome Relationships in Elective Abdominal Aortic Aneurysm Surgery: Analysis of the UK Hospital Episodes Statistics Database for the Getting It Right First Time (GIRFT) Programme. *Eur J Vasc EndovascSurg 2*020; 60: 509-17.

7. Aly O. Assisting Vascular Surgery with Smartphone Augmented Reality. *Cureus* 2020; 12: e8020.

8. Lahanas V, Georgiou E, Loukas C. Surgical Simulation Training Systems: Box Trainers, Virtual Reality and Augmented Reality Simulators. *Int J Adv Robot Automn* 2016; 1: 1-9.

9. Aggarwal R, Mytton OT, Derbrew M, Hananel D, Heydenburg M, Issenberg B, *et al*. Training and simulation for patient safety. *Qual Saf Health Care* 2010;19:ci34-43.

10. McKnight RR, Pean CA, Buck JS, Hwang JS, Hsu JR, Pierrie SN. Virtual Reality and Augmented Reality—Translating Surgical Training into Surgical Technique. *Curr Rev Musculoskelet Med* 2020; 13: 663-74.

11. Lungu AJ, Swinkels W, Claesen L, Tu P, Egger J, Chen X. A review on the applications of virtual reality, augmented reality and mixed reality in surgical simulation: an extension to different kinds of surgery. *Expert Rev Med Devices* 2021; 18: 47-62

12. Page MJ, McKenzie JE, Bossuyt PM, Boutron I, Hoffmann TC, Mulrow CD, *et al*. The PRISMA 2020 statement: An updated guideline for reporting systematic reviews. *BMJ* 2021; 372: n71.

13. Sterne JA, Hernán MA, Reeves BC, Savović J, Berkman ND, Viswanathan M, *et al*. ROBINS-I: A tool for assessing risk of bias in non-randomised studies of interventions. *BMJ* 2016; 355: i4919.

14. Mayhew AD, Kabir M, Ansari MT. Considerations from the risk of bias perspective for updating Cochrane reviews. *Syst Rev* 2015: 4: 136.

15. Schulz CJ, Schmitt M, Böckler D, Geisbüsch P. Fusion Imaging to Support Endovascular Aneurysm Repair Using 3D-3D Registration. *J Endovasc Ther* 2016; 23: 791-9.

16. Swerdlow NJ, Jones DW, Pothof AB, O'Donnell TFX, Liang P, Li C, *et al*. Three-dimensional image fusion is associated with lower radiation exposure and shorter time to carotid cannulation during carotid artery stenting. *J Vasc Surg* 2019; 69: 1111-20.

17. Kaladji A, Villena A, Pascot R, Lalys F, Daoudal A, Clochard E, *et al*. Fusion imaging for EVAR with mobile c-arm. *Ann Vasc Surg* 2019; 55: 166-75.

18. Koutouzi G, Henrikson O, Roos H, Zachrisson K, Falkenberg M. EVAR guided by 3D image fusion and CO DSA: A new imaging combination for patients with renal insufficiency. *J Endovasc Ther* 2015; 22: 912-7.

19. Koutouzi G, Sandström C, Skoog P, Roos H, Falkenberg M. 3D Image Fusion to Localise Intercostal Arteries During TEVAR. EJVES Short Reports 2017; 35: 7-10.

20. Goudeketting SR, Heinen SG, Van Den Heuvel DA, Van Strijen MJ, De Haan MW, Slump CH, *et al*. The use of 3D image fusion for percutaneous transluminal angioplasty and stenting of iliac artery obstructions: Validation of the technique and systematic review of literature. *J Cardiovasc Surg (Torino)* 2018: 59: 26-36.

21. Schwein A, Lu T, Chinnadurai P, Kitkungvan D, Shah DJ, Chakfe N, *et al*. Magnetic resonance venography and three-dimensional image fusion guidance provide a novel paradigm for endovascular recanalization of chronic central venous occlusion. *J Vasc Surg Venous Lymphat Disord* 2017; 5: 60-9.

22. Pietrabissa A, Morelli L, Ferrari M, Peri A, Ferrari V, Moglia A, *et al*. Mixed reality for robotic treatment of a splenic artery aneurysm. *Surg Endosc* 2010; 24: 1204.

23. Mochizuki Y, Hosaka A, Kamiuchi H, Nie JX, Masamune K, Hoshina K, *et al*. New simple image overlay system using a tablet PC for pinpoint identification of the appropriate site for anastomosis in peripheral arterial reconstruction. *Surg Today* 2016; 46: 1387-93.

24. Rynio P, Witowski J, Kamiński J, Serafin J, Kazimierczak A, Gutowski P. Holographically-Guided Endovascular Aneurysm Repair. *J Endovasc Ther* 2019; 26: 544-7.

25. Lu W, Wang L, Zhou W, Fu W. Augmented reality navigation to assist retrograde peroneal access for the endovascular treatment of critical limb ischemia. *J Vasc Surg Cases Innov Tech* 2019; 5: 518-20.

26. Mangina E, Almaksy A, Campbell A. 3D modeling for augmented reality systems in novel vascular models. ACM International Conference Proceeding Series. *Association for Computing Machinery* 2017: 93-7.

27. Andrews CM, Henry AB, Soriano IM, Southworth MK, Silva JR. Registration Techniques for Clinical Applications of Three-Dimensional Augmented Reality Devices. *IEEE J Transl Eng Heal Med* 2021; 9: 4900214.

28. X W, S H, N N. Inverse visualization concept for RGB-D augmented C-arms. *Comput Biol Med* 2016; 77: 135-47

29. Haxthausen F Von, Jäckle S, Strehlow J, Ernst F, García-Vázquez V. Catheter pose-dependent virtual angioscopy images visualized on augmented reality glasses. *Curr Dir Biomed Eng* 2019; 5: 289-91.

30. Horn M, Ernst F, Kuhlemann I, Stahlberg E, Goltz JP, Wiedner M, *et al.* Experimental Visualization of Vascular Structures with Microsoft Hololens–Set-Up for Navigated Contrast Agent and Radiation-Sparing Endovascular Procedures (NAV-CARS EVAR). *Eur J Vasc Endovasc Surg* 2019; 58: e104.

31. Groher M, Zikic D, Navab N. Deformable 2D-3D registration of vascular structures in a one view scenario. *IEEE Trans Med Imaging* 2009; 28: 847-60.

32. Garciá-Vázquez V, Von Haxthausen F, Jäckle S, Schumann C, Kuhlemann I, Bouchagiar J, *et al.* Navigation and visualisation with HoloLens in endovascular aortic repair. *Innov Surg Sci* 2020; 3: 167-77.

33. Shi C, Tercero C, Ikeda S, Ooe K, Fukuda T, Komori K, *et al. In vitro* three-dimensional aortic vasculature modeling based on sensor fusion between intravascular ultrasound and magnetic tracker. *Int J Med Robot Comput Assist Surg* 2012; 8: 291-9.

34. Parrini S, Cutolo F, Freschi C, Ferrari M, Ferrari V. Augmented reality system for freehand guide of magnetic endovascular devices. *Annu Int Conf IEEE Eng Med Biol* 2014; 2014: 490-3.

35. Three-Dimensional Image Overlay to Assist Endovascular Procedures. *Vasc Dis Man* 2013; 10: E&èç-E184.

36. Fukuda T, Matsuda H, Doi S, Sugiyama M, Morita Y, Yamada M, *et al.* Evaluation of automated 2D-3D image overlay system utilizing subtraction of bone marrow image for EVAR: Feasibility study. *Eur J Vasc Endovasc Surg* 2013; 46: 75-81.

37. Kaladji A, Dumenil A, Mahé G, Castro M, Cardon A, Lucas A, *et al.* Safety and Accuracy of Endovascular Aneurysm Repair Without Pre-operative and Intra-operative Contrast Agent. *Eur J Vasc Endovasc Surg* 2015; 49: 255-61.

38. Bartesaghi S, Colombo G, Morone S. Spatial Augmented Reality and Simulations to Improve Abdominal Aortic Aneurysm Diagnosis and Monitoring. *Computer-Aided Design & Applications* 2015; 12: 803-10.

39. Anderson J, Chui CK, Cai Y, Wang Y, Li Z, Ma X, *et al.* Virtual reality training in interventional radiology: The Johns Hopkins and Kent Ridge digital laboratory experience. *Semin Intervent Radiol* 2002:179-85.

40. Burke E, Felle P, Crowley C, Jones J, Mangina E, Campbell AG. Augmented reality EVAR training in mixed reality educational space. *IEEE Global Engineering Education Conference* 2017; 1571-9.

41. Cheng I, Shen R, Moreau R, Brizzi V, Rossol N, Basu A. An augmented reality framework for optimization of computer assisted navigation in endovascular surgery. *Ann Int Conf IEEE Eng Med Biol Soc* 2014; 2014: 5647-50.

42. Rudarakanchana N, Van Herzeele I, Bicknell CD, Riga C V., Rolls A, Cheshire NJW, *et al.* Endovascular repair of ruptured abdominal aortic aneurysm: Technical and team training in an immersive virtual reality environment. *Cardiovasc Intervent Radiol* 2014; 37: 920-7.

43. Ferrari V, Carbone M, Condino S, Cutolo F. Are augmented reality headsets in surgery a dead end? *Expert Rev Med Devices* 2019; 16: 999-1001.

44. Park BJ, Hunt SJ, Martin C, Nadolski GJ, Wood BJ, Gade TP. Augmented and Mixed Reality: Technologies for Enhancing the Future of IR. *J Vasc Interv Radiol* 2020; 31: 1074-82.

Peripheral

- New technologies of the last two years: a critical appraisal 104
- Systematic review on femoral artery stents fractures; A comprehensive study 113
- Review and Analysis of Nitinol Trans Aortic Valve Repair Devices 123
- Fully bioresorbable vascular scaffolds: lessons learned and future directions 131
- Is there a future for polymeric braided stents? 144
- Thrombosis on medical implants: a focus on the importance of hemodynamics 152
- Identification of patients at risk of secondary cardiovascular events despite using antiplatelet therapy 163

New technologies of the last two years: a critical appraisal

12

Jörg TESSAREK

Since the 2019 ESVB meeting a variety of innovative tools have reached the marked or CE and FDA approval. Noticeably, during the last two years the focus of innovation has been on peripheral occlusive disease and critical limb threatening ischemia treatment, not on aneurismal or cerebrovascular disease.

This survey based on a literature research presents new treatment options and tools that might further change the daily routine in the cathlab but also in the operating theatre. It includes devices already available but also innovations in the process for approval or with published or accessible data from the last two years.

The development or launching of innovative and effective tools for endovascular treatment allowed continuous procedural and outcome improvements, which will further challenge the value of surgical procedures. Fortunately, the negative side effects of endovascular treatment, which irradiation and contrast associated complications, are also in the focus of improvements.

Introduction

The amount of new materials and methods in the endovascular segment was immense through the last two decades provoking many controversial and emotional discussions. With the publication of the BASIL results in 2005 and 2010 [1,2] comparing simple plain old balloon angioplasty (POBA) to open bypass surgery for patients with critical limb ischemia (CLI) the endovascular community developed an even stronger sense of mission. This was later supported by the publication of UK results from femoropopliteal bypass surgery [3] in 2019, which showed a significant decline limb salvage and overall outcome. Not surprisingly, further surgical domains, the common femoral artery, the eccentric calcified stenosis of the popliteal artery and more have become a routine part of the endovascular portfolio, although direct comparison is lacking in many fields [4,5]. Even for the last challenges of “endo”, which is severe calcification, atherectomy is propagated as the gamechanger, either with POBA or drug coated devices [6]. But the reported success rates of atherectomy 95-96% [7,8] or endovascular bypass demand a closer inquiry.

Method

The data for this chapter, that does not claim for completeness were collected based on a literature research including publications or presentations publicly available from 2019 to 2021. Innovations in the different vascular fields, which are already available on the market or new materials with available study results were included. Unpublished but accessible data were also considered, if the device seemed to offer beneficial effects for future treatment options.

Results: The new focus, peripheral artery disease treatment

After reviewing plenty of data it can be stated, that the focus for endovascular innovation was in the peripheral segments, which is reflected in this chapter leaving aside carotid and aneurismal disease. New devices for carotid or aneurismal disease treatment or relevant data were not presented during the last two years. One publication describing *in situ* fenestration for arch involving aneurysms in the emergency and elective setting showed interesting results [9]. The withdrawal of the Navion™ endograft (Medtronic Inc., USA) and the strong recommendation for a closer follow up of treated patients after ascertainment of material fatigue indicated, that further device miniaturization has reached a limit.

Intraoperative imaging

Image guidance using x-ray and contrast media does not always represent minimal invasive treatment. The application of iodinated contrast media as well as high energy radiation represent relevant risks for patient and staff [10]. The growing complexity in all fields of endovascular procedures is associated with increasing amounts of contrast and radiation dose. Exemplary the rendez-vous techniques in peripheral arterial disease (PAD) have to be mentioned. In most operative settings, the operator is working in close vicinity to the radiation source and therefore strongly exposed.

The perhaps most interesting innovation in the field of image guidance is the FORS™ (Fiber Optic Reality Shaped) system (Royal Philips b.v., The Netherlands) [11]. FORS™ uses the combination of image fusion, x-ray hardware, software solutions and a growing number of dedicated catheters and configurations with fiber optic inlays to implement these devices in a virtual reality making radiation redundant for many steps of a procedure. Contrast media would still be necessary for completion angiography, but the hardware platform allows to integrate intravascular ultrasounds (IVUS), which could replace angiographic guidance. The radiation dose in T/EVAR can be reduced for 96% with zero contrast and no change of procedural pathways or quality [12]. IVUS could already achieve better safety and long-term outcome PAD treatment superior to angiographic imaging. The 12-month restenosis rate in aortoiliac procedures was 0% for IVUS *vs.* 18% for angiographic guidance [13]. The meta-analysis of eight trials with 93551 patients with a mean follow-up (FU) of 24,2 ± 15 months published by Sheik *et al.* [14] in 2020 also showed excellent results. The lesion outcome for IVUS and angiographic guidance did not differ, but IVUS guided interventions showed a significant lower rate of adverse events (p=0,006) and perioperative complications (p=0,013). IVUS did also show superior outcomes to angiographic imaging in terms of mortality and morbidity, cardiovascular death, stent thrombosis and restenosis in coronary interventions [15].

The Track Cath™ catheter (Medyria, Switzerland) is another innovative device also giving direction to radiation reduction. It has sensors placed in the shaft to detect even faint turbulences and flux change to recognize and cannulate aortic side branches without contrast application and minimal use of fluoroscopy [16].

Innovations in the field of catheters and sheaths

Miniaturization of endovascular devices had to compromise with visibility and sufficient material stability. But further progress could be achieved in terms of puncture or access trauma. An example for successful downsizing of the outer diameter with constant inner lumen is represented by the Glide Sheath Slender® (Terumo Interventional Systems, Tokyo, Japan). The sheath is available with 5F, 6F und 7F inner diameter and a shaft length of 10 or 16cm, but due to thinner wall layers the outer diameter is

1F smaller than standard sheaths. Below-the-knee (BTK) retrograde access or even pedal access for rendez-vous techniques has become a routine procedure [17] and the low profile sheaths would allow to maintain angiographic control making the rendezvous technique and a second access site redundant. Until now, safety and feasibility data of the sheath are available only regarding the radial approach for coronary interventions [18].

Beside coronary interventions radial puncture [19,20,21] is discussed also for lower limb interventions and the manufacturers responded to these demands planning to offer 90 and 125 cm low profile sheaths.

Stearable sheath and guiding catheters

Deflectable sheaths are not new, but the indication for use now also includes complex peripheral interventions. Beside the unidirectional Oscor Destination Twist™ (Oscor Inc., USA) which is available with 6.5-13.8F, lumen and 0-190° deflectable, the Oscor Destino™ and Destino reach™ (8.5-12F, 0-180°) offer a bidirectional steering mechanism with working lengths of 45,55,65 and 90 cm similar to the AGILIS™ NXT (Abbott Global Inc., USA), which has a 55mm bending radius. The Fustar™ (LaMed, Oberhaching, Deutschland) is another unidirectional 5-10F deflectable sheath with a maximal bend of 0-160° available with a length of 55,70 und 90cm. Beside the maximal bending extent the bending radius and the bending force are important for the handling in small vessels and in stenotic lesions. The Destination Twist™ can be ordered with different bending radius diameters (9 to 33mm) to adapt to different vessel diameters. Due to the robustness of the bending mechanism the Oscor sheath can be used with the dilator inside to penetrate hard plaques or neointimal fibrosis without guiding catheter, then followed by direct wire and adjunctive device insertion.

Beside deflectable sheaths steerable microcatheters have also been launched over the last two years. The 2.7F SwiftNINJA® (Merit Medical Inc., USA) steerable microcatheter is available since 2018, but clinical reports are rare and coming mainly from coronary interventions [22] and embolization procedures [23]. In 2020 the BENDIT™ 2.1F neuro microcatheter (Benditttech Inc., Israel) had received FDA approval. Meanwhile a 2.7F catheter is available with approval for peripheral interventions. Steerability means better controllability, reduced procedure time and a higher success rate [24]. The widespread clinical and economic evaluation has to follow.

New guidewires

Guidewires play an important role and sometimes even the leading part during an intervention to achieve access to the distal vessel lumen. The material composition but also its fabric determine the properties of a wire and new manufacturing techniques allow to reduce the thickness without loss of stability or flexibility. This could reduce the need for wire exchange thus reducing the procedure time and manipulation related complications.

Although having a reduced outer diameter the new allrounder wires show higher bending resistance than standard and stiff wires. One of the representative devices is the 0.0018” Glide wire Advantage™ (Terumo Interventional Systems, Japan). The smaller wire thickness allows to use a smaller passing profile for the balloon and a smaller sheath. The passing profile of a standard 0.0035” balloon system is about 4.8F. The 0.0018” balloons have a passing profile of 2.9 to 3.5F, which might have an influence on the puncture trauma.

The 0.0035” Marsman Speedwire® (Mermaid Medical, Hilversum, The Netherlands) is a dedicated 70cm starter wire with a pre-bended shaft and a soft J-tip to facilitate antegrade access to the superficial femoral artery by preventing the via falsa into the profunda artery. The preshaped wire has the tendency to turn to the anterior wall of the femoral artery.

Re-Entry Systems

Safe intraluminal wire position distal to the target lesion is crucial for procedural success in PAD treatment. The OUTBACK Elite™ and LTD™ systems from Cardinal Health (Cardinal Health, Germany) are the primal representatives of this re-entry device family [25] and good results have been recently reported for the use in the popliteal and BTK vessels with antegrade and retrograde access [26,27]. In 2020, a new multipurpose re-entry system, the GoBack® Crossing & Re-entry catheter (Upstream Peripheral Technologies Ltd., Israel) was launched. This catheter is available with 80cm or 120cm shaft length. The passing profile is 2.9F running over an 0.0014" or 4F for a 0.0018" non-hydrophilic wire. The curved needle can be used either to penetrate antegrade or sideward, depending on the extent of protrusion.

Innovations in the field of „active" devices

The term „active" refers to those devices that are used to treat vessel pathology, let it be balloons, stents or atherectomy devices.

Balloons

For a long time, the development of balloons aimed for higher inflation pressure, lower passing profiles and, especially for the coronary and cerebral vasculature, for reduced deflation time. Prolonged dilatation with a standard balloon could make stenting redundant [28] and drug application could reduce the probability of recurrent stenosis. Recent balloon design developments aimed for a more effective vessel preparation by directly changing the plaques consistency towards a more compressible microstructure, either mechanically or using ultrasound.

The Serranator™ balloon (Cagent Vascular, USA) was first presented in 2017 and the promising trial results of the PRELUDE trial were published in 2019 [29], showing a lesser need for stent use and higher lumen gain compared to POBA alone.

A second innovation in this field is the XO score™ system (Transcient Scientific, USA), which received FDA approval in 2020. Strictly speaking, the device is a Nitinol mesh placed at the tip of a catheter with 65 to 145cm length, that is expanded from inside using a standard balloon introduced into the already placed catheter. The circumferential cutting depth of the mesh is 0,25-0,50mm with a range of usable balloon sizes from 2 to 7mm diameter and a balloon length of 20 to 120mm with 6F passing profile. Balloon diameters of 4 to 8mm with a length of 20 to 40mm require a 7F sheath.

The risk of using such robust devices is significant vessel injury and flow limiting dissection, especially in case of unintentional device dislodgement during inflation. To avoid such risks, engineers developed a „non slip element" placed on the balloon (NSE Alpha™, B.Braun, Germany). The trial results from 2020 showed a significant reduction of dissection depth (8.8% *vs.* 29.7%, p=0.027) and length (11.5±12.8 *vs.* 35.7±24.1 mm, p=0.027), which reduced the need for bail out stenting from 40.5% *vs.* 17.6% (p=0.035) [30].

Drug coated balloons

The controversial discussion initiated by Katsanos *et al.* in 2018 [31] is ongoing and the results from studies remain conflicting. The new drug coated balloons (DCB) represent an alternative for focal drug application. In 2020 the Magic Touch™ Sirolimus coated balloon (Concept Medical Inc., USA) received approval and a variety of balloon sizes has become available for peripheral and arteriovenous fistula intervention. The active drug transfer is mediated by nanotechnology and the results from the TRANSFORM I trial showed promising results [32]. Sirolimus compounds as the antiproliferative drug until today have not shown any effect on mid or long-term mortality. They have a strong antiproliferative and anti-inflammatory effect [33] without known toxicity [34].

Stents

The common attitude towards stenting in femoropopliteal and BTK PAD interventions seems to have undergone significant changes from a „must have“ to a „must avoid“, represented by the “leave nothing behind” philosophy [35]. But flow limiting residual stenosis or dissections after POBA still mandate a mechanical solution, if prolonged dilatation remains ineffective. The TACK™ system (Intact vascular Inc., USA) with short Nitinol stents in a row loaded inside a catheter allows spot stenting of angiographically relevant lesions without covering long segments and thereby reduce the amount of thrombogenic material inside the vessel. TACK™ could achieve promising results with POBA and DCB [36,37], but it remains unclear, how the target lesions are diagnosed best and how to define the exact parameters for treatment. IVUS instead of angiography with multiple projections and injections might be the more effective technique in these situations. Surprisingly, the FDA has determined that a residual stenosis of more than 30% after POBA, which represents the typical stent indication, is a contraindication for the system [38].

The new Jaguar™ stent (Balton Inc., Poland), launched in Europe in 2020, is a single Nitinol wire endless woven device. It is 0.0035” wire compatible and available with sizes from 4 to 14mm diameter and 20 to 150mm length with 6-8F passing profile. 5 year FU after popliteal placement showed zero stent fracture [39]. The primary patency at 5 years was 68% and 61% for three and two-vessel run off, respectively. The mesh design adapts to changing diameters and results in a defined elongation (outlined on the package for 1 and 2mm oversizing each).

The other innovative device is the NiTiDES™ selfexpandable stent (Alvimedica, Turkey) with Amphilimus™ as the active drug, a patented compound of Sirolimus and fatty acids. The drug is stored in small abluminal reservoirs at the strut crossings. The fatty acid results in a planar diffusion into the inner vessel wall creating a circumferentially all embracing distribution og the drug. The multicentric ILLUMINA study with 24 months FU could show a primary patency of 89,3% after 12 and 83,4% after 24 months. The freedom from target lesion revascularization (TLR) was 91.3% for a mean lesion length of 72.54±37.99mm [40].

Atherectomy devices

Severely calcified lesions do still represent a real challenge for endovascular PAD treatment and a variety of techniques have been tested or propagated, like the „pave and crack” technique [41], which requires to access sites and expensive covered stents. Atherectomy allows plaques removal instead of compression but it was not a stand-alone solution in the majority of cases requiring adjunctive treatment, such as POBA or DCB use, but it could reduce the need for stenting [42,43].

Notably, in the EASE study with the Phoenix™ device (Royal Philips b.v., The Netherlands) the mean lesion length was 34mm [44] while in the ByCross™ CE approval trial [45] this was 124.7mm. Both systems showed 95.1% technical success in the trials. A closer look to the unpublished ByCross data shows a mean lesion length of 53.6mm and 229.2mm in the two participating center. Adjunctive POBA was used in 92% and 94.1% with a stenting rate of 28% in in complex lesions (Table 1). Short lesions required stenting in 12% of the cases and 52.94% for the long lesions up to 450mm. Six-month freedom from TLR and target vessel revascularization (TVR) was 88.0% and 86.1%, respectively for the EASE study [44] and 100% and 95.24% for the ByCross CE approval study (unpublished data, [45]).

Table 1: The table shows lesion characteristics and results from three atherectomy trials.
* In the EASE trial circumferential calcification and in the VISION moderate to severe calcification was an exclusion criterion. In the ByCross study calcification severity was scored according to the PACCS [46] but did not represent an exclusion criterion.

	Center 1	Center 2	ByCross	EASE	VISION
N	25	17	42	128	158
PACSS	3.5	2.5	3.1	Max. 2*	Max.1*
Mean lesion length mm	53.6	229.2	124.7	34	53
Mean degree of stenosis %	94.4	99.4	96.4	89.5	78.7
Mean residual stenosis %	8.3	0.8	5.7	10.5	22.4

Alternative revascularization techniques

The DETOUR I trial (PQBypass™, USA) recruited complex femoropopliteal lesions [47]. The primary patency (PP) and assisted PP at 12 months were 71% and 80%, respectively. The mean lesion length was 370mm with 96% chronic occlusions and 81% severely calcified lesions. The technique demands implantation of covered stents and the cost effectiveness still has to be evaluated.

For diabetic or thrombendangiitis obliterans patients with no run off vessel the Limflow™ system [48] offers an endovascular solution for retrograde arterialization. The PROMISE I trial recruited only patients with Rutherford 5 or 6. The technical success rate and the above ankle amputation free survival at 6 months was 100%, each, with a PP rate of 90% at 30days and 40% at 6 months [49]. A health economic evaluation is mandatory.

Discussion

The trend for going endovascular is still in progress and open surgery is losing ground. A publication from 2019 documented the decline of bypass surgery outcome. Despite a significant decrease of perioperative mortality and morbidity (22% *vs.* 45%, p=0,005) since 2005, the amputation free survival decreased from 62% to 28% (p= 0,007). The limb salvage rate decreased from 85% to 69% (p=0,02) and the survival rate from 69% to 35% (p=0.05) with an increase of major adverse limb events (47% to 67%, p=0.01) [3]. Contrary, the endovascular studies scored with better long-term patency and limb salvage.
The German IDOMENEO registry [50] is collecting nationwide real life data from surgical and endovascular procedures and will allow to take a closer look on the results also for innovative techniques outside studies performed in high volume centers.

The manufacturers have responded to the remaining challenges for “endo”. Compact hard-and software solutions with integration of non-radiation-based techniques are available, offering multiple options for angiographic and 3D imaging on table with optimal radiation protection. The Azurion™ system (Royal Philips b.v., The Netherlands) does represent such a solution with integrated IVUS and 3D computed tomography scan software, thus offering optional contrast free 3D imaging prior to and after treatment, but also conventional angiography. The influence of virtual reality will increase while more dedicated FORS catheters are developed. The highly probable reduction of lifetime radiation might, as a side effect, convince experienced staff members to stay in the department [11].

The use of innovative wires, scoring balloons or atherectomy systems will make treatment of severely calcified vessels more effective. This will reduce operating time and material consumption.
The discussion about the usefulness of stents or avoiding implants will continue while new, nonhazardous drug coated devices are available for preventing recurrent stenosis. There has been a warning signal [31] and it has to be kept in mind, that cytotoxic drugs like paclitaxel remaining in the vessel wall for months or being washed off as downstream emboli do represent a considerable bit more than "nothing left behind". This seems to be underrecognized.
Independent from this discussion, the last domains of bypass surgery or surgical reconstruction have not yet fallen, but the decline of surgical outcomes [3] and the ongoing improvement.

Acknowledgements

Jörg Tessarek has received research grants from COOK AI and Abbott Global Inc. and presentation honoraria from abmedica Germany, plusmedica, Abbott Global Inc., Philips b.v., Lombard Inc.

References

1. Adam DJ, Beard JD, Cleveland T, Bell J, Bradbury AW, Forbes JF, *et al.* Bypass *vs.* angioplasty in severe ischaemia of the leg (BASIL): multicentre, randomised controlled trial. *Lancet* 2005; 366: 1925-34.

2. Bradbury AW, Adam DJ, Bell J, Forbes JF, Fowkes FGR, Gillespie I, *et al.* Bypass *vs.* Angioplasty in Severe Ischaemia of the Leg (BASIL) trial: An intention-to-treat analysis of amputation-free and overall survival in patients randomized to a bypass surgery-first or a balloon angioplasty-first revascularization strategy. *J Vasc Surg* 2010; 51: 5S-17S.

3. Meecham L, Popplewell M, Bate G, Patel S, Bradbury AW. Contemporary (2009-2014) clinical outcomes after femoropopliteal bypass surgery for chronic limb threatening ischemia are inferior to those reported in the UK Bypass *vs.* Angioplasty for Severe Ischaemia of the Leg (BASIL) trial (1999-2004). *J Vasc Surg* 2019; 69: 1840-47.

4. Sauguet A, Philippart R, Honton B. Directional atherectomy with antirestenotic therapy for the treatment of no-stenting zones. *J Cardiovasc Surg (Torino)* 2019; 60: 198-204.

5. Goueffic Y, Della Schiava N, Thaveau F, Rosset E, Favre JP, Salomon du Mont L, *et al.* Stenting or Surgery for De Novo Common Femoral Artery Stenosis. *JACC Cardiovasc Interv* 2017; 10: 1344-54.

6. Lichtenberg M, Korosoglou G. Atherectomy plus antirestenotic therapy for SFA lesions: evolving evidence for better patency rates in complex lesions. *J Cardiovasc Surg (Torino)* 2019; 60: 205-11.

7. Gandini R, Pratesi G, Merolla S, Scaggiante J, Chegai F. A Single-Center Experience With Phoenix Atherectomy System in Patients With Moderate to Heavily Calcified Femoropopliteal Lesions. *Cardiovasc Revasc Med* 2020; 21: 676-81.

8. Teßarek J. 6 Month results of a atherectomy device CE approval study. 2020; LINC Leipzig.

9. Li HL, Chan YC, Jia HY, Cheng SW. Methods and clinical outcomes of *in situ* fenestration for aortic arch revascularization during thoracic endovascular aortic repair. *Vascular* 2020; 28: 333-341.

10. Katsogridakis E, Lea T, Yap T, Batchelder A, Saha P, Diamantopoulos A, *et al.* Acute kidney injury following endovascular intervention for peripheral artery disease. *Br J Surg* 2021; 108: 152-9.

11. van Herwaarden JA, Jansen MM, Vonken EPA, Bloemert-Tuin T, Bullens RWM, de Borst GJ, *et al.* First in Human Clinical Feasibility Study of Endovascular Navigation with Fiber Optic RealShape (FORS) Technology. *Eur J Vasc Endovasc Surg* 2021; 61: 317-25.

12. Teßarek J. IVUS in EVAR. EVC presentation; Maastricht 2021

13. Buckley CJ, Arko FR, Lee S, Mettauer M, Little D, Atkins M, *et al.* Intravascular ultrasound scanning improves long-term patency of iliac lesions treated with balloon angioplasty and primary stenting. *J Vasc Surg* 2002; 35: 316-23.

14. Sheikh AB, Anantha-Narayanan M, Smolderen KG, Jelani QU, Nagpal S, Schneider M, *et al.* Utility of Intravascular Ultrasound in Peripheral Vascular Interventions: Systematic Review and Meta-Analysis. *Vasc Endovascular Surg* 2020; 54: 413-22

15. Darmoch F, Alraies MC, Al-Khadra Y, Moussa Pacha H, Pinto DS, Osborn EA. Intravascular Ultrasound Imaging-Guided Versus Coronary Angiography-Guided Percutaneous Coronary Intervention: A Systematic Review and Meta-Analysis. *J Am Heart Assoc* 2020; 9: e013678.

16. Floros N, Schelzig H, Kölbel T, Schmidt A, Branzan D, Kalder J, *et al.* First-in-man Clinical Application of the Trackcath System in Endovascular Repair of Aortic Aneurysms ; A Prospective Multi-centre Clinical Trial. *Eur J Vasc Endovasc Surg* 2019; 58: 723-4

17. Ruzsa Z, Bellavics R, Nemes B, Huttl A, Nyerges A, Sotonyi P, *et al.* Combined Transradial and Transpedal Approach for Femoral Artery Interventions. *JACC Cardiovasc Interv* 2018; 11: 1062-71.

18. El-Sayed H, Bennett ME, Loh TM, Davies MG. Retrograde Pedal Access and Endovascular Revascularization: A Safe and Effective Technique for High-Risk Patients with Complex Tibial Vessel Disease. *Ann Vasc Surg* 2016; 31: 91-8.

19. Michael TT, Alomar M, Papayannis A, Mogabgab O, Patel VG, Rangan BV, *et al.* A randomized comparison of the transradial and transfemoral approaches for coronary artery bypass graft angiography and intervention: the RADIAL-CABG Trial (RADIAL Versus Femoral Access for Coronary Artery Bypass Graft Angiography and Intervention). *JACC Cardiovasc Interv* 2013; 6: 1138-44.

20. Aoun J, Hattar L, Dgayli K, Wong G, Bhat T. Update on complications and their management during transradial cardiac catheterization. *Expert Rev Cardiovasc Ther* 2019; 17: 741-51.

21. Harvey JA, Kim S, Ireson ME, Gulati R, Bell MR, Moran SL. Acute Upper-Limb Complications Following Radial Artery Catheterization for Coronary Angiography. *J Hand Surg Am* 2020; 45: 655 e1-e5.

22. Kassimis G, Kontogiannis N, Raina T. Steerable microcatheters for complex percutaneous coronary interventions in octogenarians: from Venture to Swift Ninja. *J Geriatr Cardiol* 2019; 16: 54-9.

23. Hinrichs JB, Marquardt S, Wacker FK, Meyer BC. Coil embolization of reversed-curve hepatointestinal collaterals in radioembolization: potential solutions for a challenging task. *Radiol Case Rep* 2017; 12: 529-33.

24. Soyama T, Yoshida D, Sakuhara Y, Morita R, Abo D, Kudo K. The Steerable Microcatheter: A New Device for Selective Catheterisation. *Cardiovasc Intervent Radiol* 2017; 40: 947-52.

25. Gandini R, Fabiano S, Spano S, Volpi T, Morosetti D, Chiaravalloti A *et al.* Randomized control study of the outback LTD reentry catheter *vs.* manual reentry for the treatment of chronic total occlusions in the superficial femoral artery. *Catheter Cardiovasc Interv* 2013; 82: 485-92.

26. Diamantopoulos A, Santonocito S, Thulasidasan N, Gkoutzios P, Ahmed I, Zayed H *et al.* Initial Experience With the Outback Catheter for Targeted Reentry During Subintimal Angioplasty of the Infragenicular Arteries. *J Endovasc Ther* 2018; 25: 178-82.

27. Patrone L, Stehno O. Retrograde insertion of the outback reentry device from a tibial artery for complex infrainguinal recanalization. *CVIR Endovasc* 2019; 2: 47.

28. Horie K, Tanaka A, Taguri M, Kato S, Inoue N. Impact of Prolonged Inflation Times During Plain Balloon Angioplasty on Angiographic Dissection in Femoropopliteal Lesions. *J Endovasc Ther* 2018; 25: 683-91.

29. Holden A, Hill A, Walker A, Buckley B, Merrilees S, Nowakowski P, *et al.* PRELUDE Prospective Study of the Serranator Device in the Treatment of Atherosclerotic Lesions in the Superficial Femoral and Popliteal Arteries. *J Endovasc Ther* 2019; 26: 18-25.

30. Karashima E, Yoda S, Yasuda S, Kajiyama S, Ito H, Kaneko T. Usefulness of the "Non-Slip Element" Percutaneous Transluminal Angioplasty Balloon in the Treatment of Femoropopliteal Arterial Lesions. *J Endovasc Ther* 2020; 27: 102-8.

31. Katsanos K, Spiliopoulos S, Kitrou P, Krokidis M, Karnabatidis D. Risk of Death Following Application of Paclitaxel-Coated Balloons and Stents in the Femoropopliteal Artery of the Leg: A Systematic Review and Meta-Analysis of Randomized Controlled Trials. *J Am Heart Assoc* 2018; 7: e011245.

32. Ono M, Kawashima H, Hara H, Katagiri Y, Takahashi K, Kogame N *et al.* A prospective multicenter randomized trial to assess the effectiveness of the magic touch sirolimus-coated balloon in small vessels: Rationale and design of the TRANSFORM I trial. *Cardiovasc Revasc Med* 2021; 25: 29-35.

33. Parry TJ, Brosius R, Thyagarajan R, Carter D, Argentieri D, Falotico R, *et al.* Drug-eluting stents: sirolimus and paclitaxel differentially affect cultured cells and injured arteries. *Eur J Pharmacol* 2005; 524: 19-29.

34. Wessely R, Schomig A, Kastrati A. Sirolimus and Paclitaxel on polymer-based drug-eluting stents: similar but different. *J Am Coll Cardiol* 2006; 47: 708-14.

35. Karashima E, Yoda S, Yasuda S, Kajiyama S, Ito H, Kaneko T. Usefulness of the "Non-Slip Element" Percutaneous Transluminal Angioplasty Balloon in the Treatment of Femoropopliteal Arterial Lesions. *J Endovasc Ther* 2020; 27: 102-8.

36. Gray WA, Cardenas JA, Brodmann M, Werner M, Bernardo NI, George JC *et al.* Treating Post-Angioplasty Dissection in the Femoropopliteal Arteries Using the Tack Endovascular System: 12-Month Results From the TOBA II Study. *JACC Cardiovasc Interv* 2019; 12: 2375-84.

37. Brodmann M, Wissgott C, Brechtel K, Nikol S, Zeller T, Lichtenberg M, *et al.* Optimized drug-coated balloon angioplasty of the superficial femoral and proximal popliteal arteries using the Tack Endovascular System: TOBA III 12-month results. *J Vasc Surg* 2020; 72: 1636-47 e1

38. FDA. Tack Endovascular System® (6F) - P180034. Available from: https://www.fda.gov/medical-devices/recently-approved-devices/tack-endovascular-systemr-6f-p180034. [cited June 2021]

39. Takacs T, Mihalovits G, Varadi R, Palasthy Z. Early experience with self-expanding flexible stent for the treatment of atherosclerotic diseases in the popliteal artery. *Orv Hetil* 2020; 161: 588-93.

40. Scheinert D. Innovative siroLimus seLf Expanding drUg-eluting Stent for the treatMent of perIpheral Disease: Evaluation of Safety aNd efficAcy. *The ILLUMINA Study (ILLUMINA) presentation* 2020; LINC; Leipzig

41. Dias-Neto M, Matschuck M, Bausback Y, Banning-Eichenseher U, Steiner S, Branzan D *et al.*. Endovascular Treatment of Severely Calcified Femoropopliteal Lesions Using the "Pave-and-Crack" Technique: Technical Description and 12-Month Results. *J Endovasc Ther* 2018; 25: 334-42.

42. Schwindt AG, Bennett JG Jr, Crowder WH, Dohad S, Janzer SF, George JC, Tedder B *et al.* Lower Extremity Revascularization Using Optical Coherence Tomography-Guided Directional Atherectomy: Final Results of the EvaluatIon of the PantheriS OptIcal COherence Tomography ImagiNg Atherectomy System for Use in the Peripheral Vasculature (VISION) Study. *J Endovasc Ther* 2017; 24: 355-66.

43. Janas A, Milewski K, Buszman P, Kolarczyk-Haczyk A, Trendel W, Pruski M, *et al.* Comparison of long-term outcomes after directional *vs.* rotational atherectomy in peripheral artery disease. *Postepy Kardiol Interwencyjnej* 2020; 16: 76-81.

44. Davis T, Ramaiah V, Niazi K, Giessler HM, Crabtree T. Safety and effectiveness of the Phoenix Atherectomy System in lower extremity arteries: Early and midterm outcomes from the prospective multicenter EASE study. *Vascular* 2017; 25: 563-75.

45. CE Approval study of the ByCross rotational atherectomy device. *ClinicalTrials.gov* NCT03724279)

46. Rocha-Singh KJ, Zeller T, Jaff MR. Peripheral Artery Calcification:Prevalence, Mechanism, Detections and Clinical Implications Catheter *Cardiovasc Interv* 2014; 83: E212-20.

47. Krievins DK, Halena G, Scheinert D, Savlovskis J, Szopinski P, Kramer A, *et al.* One-year results from the DETOUR I trial of the PQ Bypass DETOUR System for percutaneous femoropopliteal bypass. *J Vasc Surg* 2020; 72: 1648-58 .

48. Schmidt A, Schreve MA, Huizing E, Del Giudice C, Branzan D, Unlu C, *et al.* Midterm Outcomes of Percutaneous Deep Venous Arterialization With a Dedicated System for Patients With No-Option Chronic Limb-Threatening Ischemia: The ALPS Multicenter Study. *J Endovasc Ther* 2020; 27: 658-65.

49. Mustapha JA, Saab FA, Clair D, Schneider P. Interim Results of the PROMISE I Trial to Investigate the LimFlow System of Percutaneous Deep Vein Arterialization for the Treatment of Critical Limb Ischemia. *J Invasive Cardiol* 2019; 31: 57-63.

50. https://innovationsfonds.g-ba.de/projekte/versorgungsforschung/idomeneo-studie-ist-die-versorgungsrealitaet-in-der-gefaessmedizin-leitlinien-und-versorgungsgerecht.8, downloaded June 20th, 2021.

Systematic review on femoral artery stents fractures; A comprehensive study

13

Salomé KUNTZ, Anne LEJAY, Nabil CHAKFÉ

Primary stenting for long superficial femoral artery (SFA) lesions remains controversial because of the high risk of stent fracture (SF). This study aims to summarize current knowledge on SF from randomized control trials about femoral stenting.

A systematic review of the Medline database was performed by a combined strategy of MeSh terms: "femoral artery", "superficial femoral artery", "stenting" and "stent fracture", with no time-limit.

The literature search identified 16 publications; 2 studies addressed covered stents (CS), 7 drug-eluting stents (DES) and 7 bare metal stents (BMS). Data were extracted from 3067 patients; median age was 67,9 years (IQR 25th-75th, 66,7 - 69 years) and 71,4 % were male patients. Median lesion length was 81mm (IQR 25th-75th, 69,5 - 114,5 mm) with a median chronic total occlusion of 32,8% (IQR 25th-75th, 24,9 – 56,8%). For CS, 230 were enrolled and 116 patients were treated with CS. SF rates in CS were low and ranged from none to 2,6% at 36 months and there was no clinical correlation. For DES, 1464 patients were enrolled, including 1355 patients who were treated with DES. SF were relatively low in big cohort ranging from 0% at 12 months to 1,9% at 60 months, in more little cohorts they ranged from 12,5% at 6 months to 36% at 18 months, with no clinical repercussion. For BMS, 1155 patients were enrolled, including 801 patients who were treated with BMS. SF rates in BMS ranged from 2% to 27,1% at 12 months and from 1,9% to 32,7% at 24 months, with no relationship with bad clinical outcomes.

SF in CS were very rare; SF rate in DES was low and SF were quite common in BMS, although none of them were linked to clinical repercussions. Stent design refinement might lead to less SF in the future. Mild or moderate fractures seemed to be a benign condition in the majority of the patients, although a longer follow-up is needed to assess their clinical insignificance.

Introduction

With an aging population, endovascular interventions are now considered the first-line strategy for the treatment of peripheral obstructive artery disease, however achieving long-term patency is still a very challenging goal, especially in the superficial femoral artery (SFA).[1,2] Even though lesions are more distal and longer, the technical success does not seem to be altered. Successful recanalization of TASC C and D lesions exceeds 80%, but endovascular treatment of long femoropopliteal lesions require ongoing surveillance and longer follow-up.[3]

Controversies exist on whether SFA treatment should be restricted to transluminal percutaneous angioplasty (PTA) or is best achieved with stent implantation.[4] The use of angioplasty with stents may improve patency rates over angioplasty without stents.[5] Nevertheless, primary stenting for longer femoropopliteal lesions is controversial because of the high risk of stent fracture (SF).[6]

Therefore, in this chapter we chose to discuss SF of femoropopliteal lesions (including common femoral artery (CFA)), with a systematic literature review of available data from randomized control trials (RCT) about femoral stenting in order to expand our knowledge on SF in the SFA and also the perspective and advances in the field.

Materials and methods

The systematic literature review was performed following previously published guidelines for the reporting of reviews.[7]

Eligibility criteria for the selection of the publication

Studies included were full text English language publications without any chronological limit. All RCTs reporting SF in the femoral artery were included (SFA and CFA). The main outcome of interest was the presence of SF and their clinical implications. Same studies at a different time point were excluded, duplicating the same data.

Information sources and search strategy

The Medline and Embase databases were searched with a combined strategy using the medical terms, “femoral artery”, “superficial femoral artery”, “stenting”, “stent fracture”, with no time-limit. One investigator (SK) screened all titles and abstracts collected from the search strategy for relevance. When a relevant article was found, full text articles were retrieved. Studies that did not meet the inclusion criteria were excluded. The reference lists of included studies were searched, and the first 20 related items in MEDLINE were scanned for relevant studies. The full texts of all relevant articles were obtained and reviewed.

Study records and data items

We extracted data using a standardized form. This was done in duplicate to increase accuracy and to reduce assessment bias. Data extracted included year of publication, type of devices and study design, clinical characteristics of patients (age, gender, indication of endovascular treatment), device type and characteristics, average stented length, percentage of occlusion, type of fracture analysis, rate of fracture and clinical outcomes associated to these fractures. The presence of SF was classified as type 1 to 5: type 1: a single strut fracture; type 2: 2 or more strut fractures without deformation; type 3: 2 or more strut fractures with deformation; type 4: multiple strut fractures with acquired transection but without gap; and type 5: multiple strut fractures with acquired transection with gap in the stent body.[8]

Results

Knowledge learned about SF have been summarized on the basis of a systematic review of the literature. A flowchart shows the selection criteria for inclusion for our review in Figure 1. Data extraction led to the evaluation of 186 publications; 19 publications met the inclusion criteria; three studies were excluded due to duplicate information.[9–11] Out of these, all of them were RCTs. Two studies addressed covered stents (CS).[12,13]. Seven studies addressed drug-eluting stents (DES).[14–20] Seven studies addressed bare-metal stents (BMS) only.[4,21–26]

Data were extracted from 3067 patients; median age was 67,9 years (IQR 25th-75th, 66,7 - 69 years) and 71,4 % were male patients. Median lesion length was 81mm (IQR 25th-75th, 69,5 - 114,5 mm) with a median chronic total occlusion of 32,8% (IQR 25th-75th, 24,9 – 56,8%). All the SF diagnosis were made using biplane radiography. A descriptive presentation of the data was performed. The paucity of the available data did not enable a proper meta-analysis.

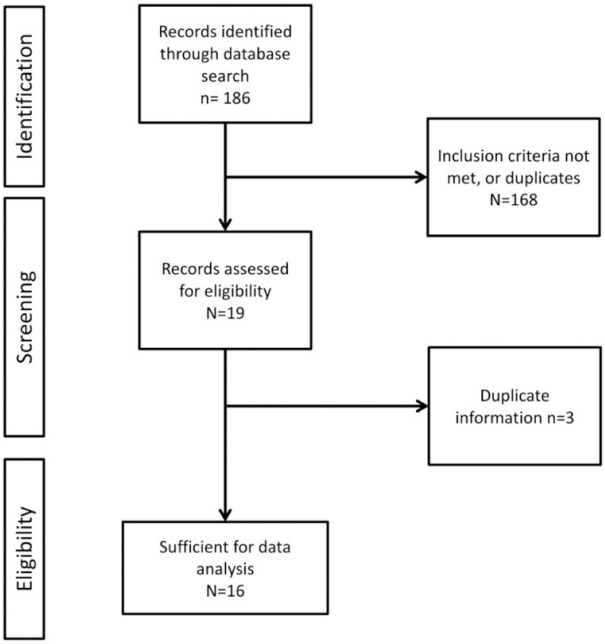

Figure 1: Flowchart of the systematic review.

Stent fracture with covered stents in the femoral artery

A total of 2 publications addressed femoral CS with the endoprosthesis VIABAHN®, (GORE®, Flagstaff, AZ, USA) and reporting on SF (Table 1).[12,13] VIABAHN® CS are self-expanding endoprosthesis covered with ePTFE with an external nitinol open-cell support along its entire length.

Table 1. Studies including stent fractures with covered stenting in the femoral artery.

Auteur	Design	Age	Male	Patients	Type of implant	Details	Average lesion length, cm	Chronic total occlusion, %	Stent fracture	Type	Total number of fracture per subject and time point	Outcome	Details
Bosiers	Covered stent vs PTA	68	72	44	Covered stents	Viabahn®	173	23	None	/	0 at 12 months	None	
		67	74,4	39			190	25	/	/			
Geraghty	Covered stent vs BMS	69	62,5	72	Covered stents	Viabahn®	72	61,1	Present	/	2,1% at 12 months, 4,7% à 24-months and 2,6 at 36 months	/	
		64	64,5	76	Self-expanding stents	Bare nitinol stents, unspecified models	76	56,6	Present	Higher severity in bare nitinol stents	32,7%% at 12 months, 48,9% à 24-months and 50 at 36 months	/	Fracture is associated with stented length

Two hundred and thirty patients were enrolled in these studies, and one hundred and sixteen patients were treated with CS, with a median age of 67,5 years (IQR 25th-75th, 66,3 – 68,8 years) and 68,3% male patients (IQR 25th-75th, 63,0–73,8 years). The average lesion length treated was 127,8 mm with an average 41,4 % of chronic total occlusion. SF rates in CS were low and ranged from none to 2,6% at 36 months.

The first study by Geraghty *et al.* reported the results of CS with the VIABAHN® endoprosthesis *versus* nitinol BMS for complex SFA lesions.13 The average treated lesion measured 18 ± 8 cm in length, and 58.8% of chronic total occlusion. At 3 years, primary patency rates did not significantly differ between patients treated with the VIABAHN® endoprosthesis and those who received a nitinol BMS (24.2% *vs.* 25.9%; p=0,3). SF were diagnosed with biplane radiography, and significantly more common BMS (50.0%) than in the VIABAHN® endoprostheses (2.6%) and associated with longer treated segment. SF severity was significantly greater for BMS than for VIABAHN® endoprostheses: only type 1 and 2 for VIABAHN® endoprosthesis *vs.* all types of SF including 3 and 4 for nitinol BMS; they did not correlate with bad outcomes.

The second study by Bosiers *et al.* compared the outcome of the treatment of in-stent restenotic or reoccluded lesions in the femoropopliteal arteries, by comparing the treatment of the VIABAHN® with a standard PTA treatment.[12] The average lesion length was 181,5 cm with a 24% of chronic total occlusion. The 12-month primary patency rates were 74.8% for the VIABAHN® group and 28.0% for the PTA group (p<0.001). The primary patency rate for the 24-month follow-up was 58.40% in the VIABAHN® group and 11.60% in the PTA group (p<0.001). There were no SF observed through 12 months.

Stent fracture with drug-eluting stents in the femoral artery

A total of 7 publications addressed SF in DES in the femoral artery (Table 2).[14–20] Three different stents were studied: the ZilverPTX®,(COOK Medical®, Bloomington, IN, USA) which is an open-cell self-expanding nitinol stent coated with paclitaxel, the ELUVIA®, (Boston Scientific®, Malborough, MA, USA) which is an open-cell self-expanding nitinol stent coated with paclitaxel and SMART®, (Cordis®, Santa Clara, CA, USA), which is an open-cell self-expanding nitinol stent coated with sirolimus.

Table 2: Studies including stent fractures with drug-eluting stenting in the femoral artery.

Date	Auteur	Design	Age	Male	Patients	Type of implant	Average lesion length, cm	Chronic total occlusion, %	Stent fracture	Type	Total number of fracture per subject and time point	Outcome	Details
2020	*Gouëffic*	BMS vs PES	68	73	91	Misago®	76	30	Present	Type 3 and 4	2,4% at 24 months	None	
			71	72	90	Zilver PTX®	69	33	Present	Type 4	1,7% at 24 months	None	
2020	*Bosiers*	DES vs Bypass	69	72	113	Zilver PTX®	241	92	None	/	0% at 12 months	/	
			67	76	107	PTFE Dacron	252	97,2	/	/	/	/	
2018	*Gray*	Eluvia vs ZilverPTX	68,5	66	294	ELUVIA®	86	31	Present	Type 3	0,3% at 12 months	None	
			67,8	67	146	ZILVER PTX®	81	30	None	/	/	/	
2017	*Miki*	ZilverPTX 6mm vs 8mm	76,6	90	10	ZILVER PTX® 6mm	78	NC	None	/	/	/	
			74,5	80	10	ZILVER PTX® 8mm	70	NC	Present	Type 1	12,5% at 6 months	None	
2016	*Dake*	ZilverPTX vs PTA	67,7	63,5	238		63,2	27,4	/	/	/	/	
			67,9	67,9	236	ZILVER PTX®	66,4	32,8	Present	/	0,9% at 6 months, 1,9% at 36 months, 1,9% at 60 months	None	
2006	*Duda*	DES vs BMS	66,3	66	47	SMART® sirolimus	85	69	Present	/	36% at 18 months	Vessel ulceration, covered-stent graft placement	
			65,9	78	46	SMART®	81	57	Present	/	20% at 18 months		
2002	*Duda*	DES vs BMS	65	61	18	SMART® sirolimus	82,8	56,3	Present	/	16,7% at 6 months	None	Occured when 3 overlapping stents
			66	88	18	SMART®	88,6	58,8	Present	/	16,7% at 6 months	None	Occured when 3 overlapping stents

A thousand four hundred and sixty-four patients were enrolled in these studies, including 1355 patients who were treated with DES, with a median age of 67,8 years (IQR 25th-75th, 66,4 – 70,5) and 69,9 % male patients (IQR 25th-75th, 66,0 – 77,5%). The average lesion length treated was 104,6 mm with an average

52,7 % of chronic total occlusion. SF rate in DES was relatively low in big cohort ranging from 0% at 12 months to 1,9% at 60 months, in more little cohorts they range from 12,5% at 6 months to 36% at 18 months.

Studies involving the ZilverPTX® stents reported a SF rate ranging from 0 at 12 months to 1,9% at 60 months.[14–18] The highest rate reported was 12,5% at 6 months by Miki *et al.*[17] None of the SF were associated with clinical events not bad outcomes.

Two studies involved sirolimus coated stents.[19,20] Both studies reported relatively high SF rates, ranging from 16,7% at 6 months to 36% at 18 months. Although in the study comparing BMS and sirolimus stents with the same design (SMART® stents), the rate was similar between the two groups.[19] In the concerned lesions, SF occurred in the region when 3 stents were overlapping. In the more recent study of Duda *et al.* the SF rate increased to 36% at 18 months, providing evidence that the SF rate increased minimally and slowly with longer follow-up.[20] Although all of the patients were clinically asymptomatic, but 1 patient was hospitalized for prophylactic placement of a CS owing to a 12-mm vessel ulceration at the site of a SF.

Studies involving the Eluvia® stent reported a very low SF rate, 0,3% at 12 months.[15] Only one of 319 implanted Eluvia stents had grade 3 SF (Eluvia® 150 mm length) identified via radiography and verified by comparison with angiographic images. The patient's vessel was patent, and they had no major adverse events at 12 months of follow-up.

Stent fracture with bare metal stents in the femoral artery

A total of 11 publications addressed BMS SF in the femoral artery (Tables 1, 2 and 3).[4,13,16,19–26] They included different BMS: SMART®, (Cordis®, Santa Clara, CA, USA) stents, which were open-cell self-expanding nitinol stents, Lifestents®, (Bard®, New Providence, NJ, USA) which is an open-cell self-expanding

Table 3: Studies including stent fractures with bare metal stenting in the femoral artery.

Date	Auteur	Design	Age	Male	Patients	Type of implant	Details	Average lesion length, cm	Chronic total occlusion, %	Stent fracture	Type	Total number of fracture per subject and time point	Outcome
2019	*Ko*	Spot vs long stenting	70	70,3	59	SES	SMART®	245	89,8	Present	Type 1 to 3	8,0% at 12 months	No relationship between SF and ouctcomes
			89,8	81,8	66	SES	SMART®	238	87,9	Present	Type 1 to 3	20,8% at 12 months	No relationship between SF and ouctcomes
2019	*Iida*	SES vs PTA	73	67	51	/	/	32	13	/	/	/	/
			74	71	52	SES	SMART®	35	29	Present	NC	1,9% at 36 months	None
2017	*Laird*	Tigris vs Lifestent	66,7	71,6	197	SES	Tigris®	107	42,1	None	/	/	/
			67,9	70	70	SES	LifeStent®	117	37,1	Present	Type 4 and 5	27,1% at 12 months, 32,7% at 24 months	None
2017	*Gouëffic*	Stenting vs surgery for CFA	68	84	58	/	/	/	23	/	/	/	/
			68	86	54	BES	Stainless steel	/	36	Present	Type 3	1,9% at 24 months	/
2012	*Laird*	Nitinol vs PTA	68	70,9	134	SES	LifeStent®	70	17	Present	Type 1 and 4	3,1% at 12months and 4,1% at 18 months	No relationship between SF and ouctcomes
			66	66,7	72	/	/	64,1	18,5	/	/	/	/
2007	*Krankenberg*	Nitinol vs PTA	67	66,2	123	SES	Luminexx®	45,2	36,6	Present	NC	12% at 12 months	Not correlated with restenosis
			66	75,2	121			44,5	24,8	/	/	/	/
2007	*Schillinger*	Primary stenting vs PTA/optional stenting	64	59	46	SES	Dynalink® and Absolute®	112	41	Present	NC	2% at 6 months and 2% at 12months	None
			67	46	52	/	/	96	31	/	/	/	/

nitinol stent, the TIGRIS®, (Gore®, Flagstaff, AZ, USA) which is an open-cell self-expanding nitinol stent covered with Carmeda Bioactive Heparin Surface, the Luminexx®, (Bard®, New Providence, NJ, USA) which is an open-cell self-expanding nitinol stent, the Absolute®, (Abbott®, Chicago, IL, USA), the Misago®, (Terumo®, Tokyo, Japan), an open-cell self-expanding nitinol stent and Dynalink®, (Guidant®, Santa Clara, CA, USA) which is also an open-cell self-expanding nitinol stent.

Six thousand and eighty-two patients were enrolled in these studies, including 2984 patients who were treated with BMS, with a median age of 67,9 years (IQR 25th-75th, 66,5–69 years) and 70,9 % male patients (IQR 25th-75th, 66,1–75,6 years). The average lesion length treated was 100,2 mm with an average 42,7% of chronic total occlusion. SF rates in BMS ranged from 2% to 27,1% at 12 months and from 1,9% to 32,7% at 24 months.

Four studies included SMART® stents.[19–22] The first study involved long *versus* spot stenting in long femoropopliteal lesions, in order to compare the efficiency of stenting in long lesions.[21] They both reported a low SF rate without clinical implications. The presence of SF was evaluated at 12 months in 49 patients (24 patients in the long stenting group and 25 patients in the spot stenting group). Among them, 5 patients (20.8 %) in the long stenting group and 2 patients (8.0 %) in the spot stenting group showed SF (p=0.247) Stented length, not lesion length, was found to be an independent predictor of restenosis. SF rate was not different between the spot stenting and long stenting groups and was not associated with restenosis. The second study compared SMART® stents to PTA in the long-term treatment of short femoropopliteal lesions. The primary patency rate at 3 years was significantly higher in the SMART group than in the PTA group [73% (9 5% CI 60 % to 84 %) *vs.* 51 % (95% CI, 38 % to 64 %), p=0.033]. The rates of freedom from clinically driven target-vessel revascularization (TVR) and target-lesion revascularization (TLR) were not significantly different between the groups. There was 1 type I SF without restenosis. In Duda *et al.* studies, the SMART® SF ranged from 16,7 % at 6-months to 20 % at 18 months, without clinical repercussions, but occurred when 3 stents were overlapping.[19,20]

Two studies included LifeStent® stents.[23,25] Both reported SF; the rate ranging from 3,1% to 27,1% at 12 months. The first study compared two treatment strategy PTA *vs.* stenting in intermediate femoropopliteal lesions (< 15 cm).[25] It demonstrated that for moderate-length lesions (up to 15 cm) in the SFA and/or proximal popliteal artery, use of the nitinol LifeStent® provided better outcomes at 12 months compared to PTA. Patients with stents underwent radiographic evaluation for SF analysis at 6-, 12-, and 18-months post procedure. At 18 months, the radiography core laboratory evaluated 291 stents in all phases and arms of the RESILIENT study; they found 12 SF in 11 patients. Only 3 new SF were identified from the 12-to 18-month radiographs. Six stents in 6 patients had type 1 SF, 5 stents in 4 patients had type 4 SF, and 1 stent in 1 patient had both type 1 and type 4 SF. The overall incidence of SF was low (4.1 %; 12 fractures/291 stents), but some observations were possible. For instance, all stents with type 4 SF were elongated more than 10% at the time of deployment, 4 of 6 were deployed in lesions that were moderately to severely calcified, and 4 of 6 type 4 SF occurred proximal or distal to a point of stent overlap. A posthoc subset analysis of patients with SF *vs.* patients with stents that did not fracture demonstrated no relationship between SF and clinical outcome. None of the patients with SF experienced a revascularization procedure through 24 months, and the freedom from TLR in the SF group at 36 months was estimated by Kaplan-Meier analysis at 90%. The second study compared LifeStent® to Tigris® stents in intermediate femoropopliteal lesions and reported that Tigris® stent and LifeStent® were similarly effective for the treatment of intermediate lesions in the femoropopliteal lesions, although there were no SF in the Tigris group at 12 and 24 months.[23] It should be noted that 1 study device was determined to have a type 1 SF immediately after implantation; however, no SF could be seen in subsequent follow-up images of this subject's stent. The LifeStent® group had a significantly higher SF rate of 32.7 % at 24 months (p<0.001), with the majority of SF being high grade (class 4 and 5).

Two other studies compared BMS to PTA.[4,26] First study compared the Luminexx® stent in short femoro-popliteal lesions.[4] In this RCT of implantation of a single Luminexx 3 nitinol stent *versus* stand-alone PTA in 244 patients with a SFA lesion up to 10 cm in length (mean 4.5 cm), no statistically significant difference was found between the 2 treatment modalities in the primary end point of ultrasound-assessed binary restenosis at 12 months. Stent integrity at 12 months was assessed in 83 of 101 patients; SF were detected in 10 of 83 patients (12 %). The binary restenosis rate in patients with SF was statistically not different from that in patients without SF (20.0 % *versus* 28.8 %, respectively; p=0.719). The second study reported that at 2 years, primary stenting with self-expanding nitinol stents (Dynalink®) for the treatment of SFA obstructions yields a sustained morphological benefit and a trend toward clinical benefit compared with balloon angioplasty with optional stenting.[26] They reported at SF rate of 2% at 6 months and 12-months, the 2-year results showed no new SF.

Others BMS including the Misago® stents were studied. Goueffic *et al.* reported a Misago® SF rate of 2,4% at 24 months, with no clinical repercussion, despite type 3 and 4 SF.[16] In Geraghty's paper, comparing BMS to VIABAHN®, SF rate in BMS were higher than in the CS group.[13] Although details of the type of BMS were not disclosed, SF rate was 32,7 % at 12-months, 48,9 % at 24-months and 50% at 36-months and was associated with the stented length. Furthermore, SF severity was significantly greater for bare nitinol stents than for VIABAHN® endoprostheses.

The last RCT reporting on BMS SF is the study from Goueffic *et al.* in the CFA.[24] In patients with de novo atherosclerotic lesions of the CFA, the perioperative morbidity and mortality rate was significantly lower among patients who underwent endovascular therapy by stenting compared with surgery, whereas clinical, morphological, and hemodynamic outcomes were comparable at mid-term. Even though concerns were raised for SF due to this high-mobility region and further surgical approaches. Surprisingly enough, among the stenting group, 1 SF was observed at 24 months. The SF was a type 3. Despite the SF no restenosis was observed, and no reintervention was required.

Discussion

The main findings in our literature review on femoral stents RCTs were: 1) SF in CS in femoral artery were very rare and did not lead to any clinical repercussions 2) SF rate in DES was low, except for sirolimus SMART® stent, although very few led to clinical repercussions, 3) SF were quite common in BMS, although few of them were linked to restenosis in RCTs.

The femoropopliteal arterial segment is known to be exposed to special mechanical influences. This may have a negative impact on vessel patency after both angioplasty and stenting.[6] The superficial course of the artery with crossing of flexion points as well as interaction with the surrounding musculature, potentially exposes the artery to relevant external forces, including compression, torsion, and elongation. The *in vitro* study from Nakanorov *et al.* showed that commercially available stents exhibit a variable ability to withstand chronic deformation *in vitro*, and their response is highly dependent on the type of deformation applied.[27] The highest rates of fracture were observed in the Luminexx® and LifeStent FlexStar® stents, at 80 % and 50 %, respectively. Protégé EverFlex® and S.M.A.R.T. Control® exhibited the lowest (0 fractures in 5 stents). The highest rates of SF were observed in the Luminexx®, Protégé EverFlex®, and S.M.A.R.T. Control®, all of which exhibited 100% SF rates (5 of 5 stents). The lowest SF rate was observed in LifeStent FlexStar® (0 fractures in 4 stents). When axial and bending deformation fatigue data were combined, the Absolute stent had the lowest composite rate of SF (3 %). The primary mode of BMS patency loss was the ingrowth of intimal hyperplasia through the stent interstices, a process that appeared to be potentiated by nitinol SF in the mobile SFA territory.[6] Although quite common in BMS,

the RCTs did not seem to find any clinical repercussion to SF, in the contrary to Scheinert *et al.* who reported a considerable risk of SF after long segment femoral artery stenting, associated with a higher in-stent restenosis and reocclusion rate.[6] One of the potential explanations of the low rates of SF but furthermore the rare clinical significance might be explained by the "short" follow-up of these RCTs; none of them include a follow-up greater than 36-months. Later on, we did find some late SF complications, such as pseudoaneurysm formations, as described in few case reports.[28–30] Stent perforation has also been described by Lewitton *et al.* leading to a large, compressive intramuscular hematoma with deep venous thrombosis. The patient returned to the catheterization laboratory where the SF and perforation were successfully treated by the deployment of another stent across the SF site.[31] Restenosis has been also associated with SF in several case reports, after few months but also decade after the first treatment.[32,33] Concerning the CFA, we also reported on a fractured CS in this segment.[34] The explant analysis revealed that the coverage was broken and the angle formed by the struts was in correspondence with the membrane perforation; however there was no clinical repercussion as well. Although a recent study by Tijani *et al.* demonstrated that the CFA is a fixed segment during the movements of extension and flexion of the hip and stent implantation did not modify this observation.[35]

Stent design also played a role in SF, and SF rate seemed to decrease over time. Müller-Hülsbeck *et al.* compared in an *ex vivo* study different nitinol stent designs intended for the SFA with regard to the appearance of fracture.[36] The 7 SFA stents showed differences in the incidence of high strain zones, which indicates a potential for SF, as demonstrated by the mechanical fatigue tests. The Misago®, LifeStent® and Absolute® stents presented no zones of high strain during bending tests; in the torsion test, the Smart® stent also had no zones of high strain. Macroscopic evaluation after mechanical bending indicated that the LifeStent®s performed the best (no SF after 650,000 cycles). Misago®s and Absolute®s stents showed SF at 536,000 cycles and 456,667 cycles, respectively (range 320,000–650,000 cycles). After compression and torsion testing, Misago® showed no SF after 650,000 cycles. The worst performing stent was Luminexx® during all test cycles. Differences in stent design might play a major role in the appearance of stent strut fracture related to restenosis and reocclusion.

Considering we only included RCT, we left off the SUPERB trial which reported long-term outcomes of an interwoven nitinol stent design (Supera®, IDEV Technologies®, Inc, Webster, TX, USA) in popliteal obstructive arterial disease, which achieved an excellent primary patency and maintaining the durability of the stent through 36 months, but moreover SF were distinctly uncommon with this stent with a single SF event in the 36-month follow-up period.[37] The idea behind the Supera® was to design a stent flexible enough to mimic the reticular structure of native collagen and elastin within vessels, emphasizing radial strength, flexibility, and kink resistance. More recently, we worked on explanted femoral stents and we reported that SF were observed in 3 cases, and only 1 resulted in failure from thrombosis, identified only by micro-computed tomography.[38] The Supera® stents in our study, placed in distal SFA or proximal popliteal artery showed in-stent restenosis but no SF despite a duration of implantation > 1 year.

We need to also to gather more data on SF, not only in femoral arteries but also on stented visceral vessels, especially in endovascular thoraco-abdominal procedures. In Grimme *et al.* study, SF were seen in 10.3 % of uncovered stents and two CS (1.2 %). SF significantly reduced stent patency rate ($p<0.01$).[39] In total, 41 stenoses or occlusions occurred in 254 stents. In 22 cases with stenosis or occlusion, an in-stent kink was present (53.7 %), and in five cases, the stent was fractured (12.2 %). In the other 14 stents, there were no evident changes in stent configuration. The authors explained that the polytetrafluoroethylene layers in the CS might create a higher radial strength by connecting the stent struts, thereby providing strong fixation of the CS to the visceral arteries, without compromising flexibility, and therefore CS might be less prone to fatigue fracture.

Conclusion

In conclusion, SF occur frequently after long segment femoral artery stenting, especially with BMS. Mild or moderate fractures seemed to be a benign condition in the majority of the patients, although a longer follow-up is needed to assess the clinical insignificance of the SF.

References

1. Aboyans V, Ricco J-B, Bartelink M-LEL, Björck M, Brodmann M, Cohnert T, *et al.* Editor's Choice – 2017 ESC Guidelines on the Diagnosis and Treatment of Peripheral Arterial Diseases, in collaboration with the European Society for Vascular Surgery (ESVS). *Eur J Vasc Endovasc Surg* 2018; 55: 305-68.

2. Conte MS, Bradbury AW, Kolh P, White JV, Dick F, Fitridge R, *et al.* Global vascular guidelines on the management of chronic limb-threatening ischemia. *J Vasc Surg* 2019; 69: 3S-125S.e40.

3. Davaine JM, Azéma L, Guyomarch B, Chaillou P, Costargent A, Patra P, *et al.* One-year Clinical Outcome after Primary Stenting for Trans-Atlantic Inter-Society Consensus (TASC) C and D Femoropopliteal Lesions (The STELLA "STEnting Long de L'Artère fémorale superficielle" Cohort). *Eur J Vasc Endovasc Surg* 2012; 44: 432-41.

4. Krankenberg H, Schlüter M, Steinkamp HJ, Bürgelin K, Scheinert D, Schulte KL, *et al.* Nitinol Stent Implantation Versus Percutaneous Transluminal Angioplasty in Superficial Femoral Artery Lesions up to 10 cm in Length: The Femoral Artery Stenting Trial (FAST). *Circulation* 2007; 116: 285-92.

5. Conroy RM, Gordon IL, Tobis JM, Hiro T, Kasaoka S, Stemmer EA, *et al.* Angioplasty and Stent Placement in Chronic Occlusion of the Superficial Femoral Artery: Technique and Results. *J Vasc Interv Radiol* 2000; 11: 1009-20.

6. Scheinert D, Scheinert S, Sax J, Piorkowski C, Bräunlich S, Ulrich M, *et al.* Prevalence and clinical impact of stent fractures after femoropopliteal stenting. *J Am Coll Cardiol* 2005; 45: 312-5.

7. Moher D, Liberati A, Tetzlaff J, Altman DG, PRISMA Group. Preferred reporting items for systematic reviews and meta-analyses: the PRISMA statement. *BMJ* 2009; 339: b2535.

8. Nakazawa G, Finn AV, Vorpahl M, Ladich E, Kutys R, Balazs I, *et al.* Incidence and Predictors of Drug-Eluting Stent Fracture in Human Coronary Artery. *J Am Coll Cardiol* 2009; 54: 1924-31.

9. Dake MD, Ansel GM, Jaff MR, Ohki T, Saxon RR, Smouse HB, *et al.* Paclitaxel-Eluting Stents Show Superiority to Balloon Angioplasty and Bare Metal Stents in Femoropopliteal Disease: Twelve-Month Zilver PTX Randomized Study Results. *Circ Cardiovasc Interv* 2011; 4: 495-504.

10. Laird JR, Katzen BT, Scheinert D, Lammer J, Carpenter J, Buchbinder M, *et al.* Nitinol Stent Implantation Versus Balloon Angioplasty for Lesions in the Superficial Femoral Artery and Proximal Popliteal Artery: Twelve-Month Results From the RESILIENT Randomized Trial. *Circ Cardiovasc Interv* 2010; 3: 267-76.

11. Bosiers M, Deloose K, Callaert J, Verbist J, Hendriks J, Lauwers P, *et al.* Superiority of Stent-Grafts for In-Stent Restenosis in the Superficial Femoral Artery: Twelve-Month Results From a Multicenter Randomized Trial. *J Endovasc Ther* 2015; 22: 1-10.

12. Bosiers M, Deloose K, Callaert J, Verbist J, Hendriks J, Lauwers P, *et al.* Stent-grafts are the best way to treat complex in-stent restenosis lesions in the superficial femoral artery: 24-month results from a multicenter randomized trial. *J Cardiovasc Surg (Torino)* 2020; 61: 617-25..

13. Geraghty PJ, Mewissen MW, Jaff MR, Ansel GM, VIBRANT Investigators. Three-year results of the VIBRANT trial of VIABAHN® endoprosthesis *versus* bare nitinol stent implantation for complex superficial femoral artery occlusive disease. *J Vasc Surg* 2013; 58: 386-395.e4.

14. Bosiers M, Setacci C, De Donato G, Torsello G, Silveira PG, Deloose K, *et al.* ZILVERPASS Study: ZILVER PTX Stent *vs.* Bypass Surgery in Femoropopliteal Lesions. *J Endovasc Ther* 2020; 27: 287-95.

15. Gray WA, Keirse K, Soga Y, Benko A, Babaev A, Yokoi Y, *et al.* A polymer-coated, paclitaxel-eluting stent (Eluvia) *versus* a polymer-free, paclitaxel-coated stent (Zilver PTX) for endovascular femoropopliteal intervention (IMPERIAL): a randomised, non-inferiority trial. *Lancet* 2018; 392:1541-51.

16. Gouëffic Y, Sauguet A, Desgranges P, Feugier P, Rosset E, Ducasse E, *et al.* A Polymer-Free Paclitaxel-Eluting Stent Versus a Bare-Metal Stent for De Novo Femoropopliteal Lesions. *JACC Cardiovasc Interv* 2020; 13: 447-57.

17. Miki K, Fujii K, Shibuya M, Fukunaga M, Imanaka T, Kawai K, *et al.* Impact of stent diameter on vascular response after self-expanding paclitaxel-eluting stent implantation in the superficial femoral artery. *J Cardiol* 2017; 70: 346-52.

18. Dake MD, Ansel GM, Jaff MR, Ohki T, Saxon RR, Smouse HB, *et al.* Durable Clinical Effectiveness With Paclitaxel-Eluting Stents in the Femoropopliteal Artery: 5-Year Results of the Zilver PTX Randomized Trial. *Circulation* 2016; 133: 1472-83.

19. Duda SH, Pusich B, Richter G, Landwehr P, Oliva VL, Tielbeek A, *et al.* Sirolimus-Eluting Stents for the Treatment of Obstructive Superficial Femoral Artery Disease: Six-Month Results. *Circulation* 2002; 106: 1505-9.

20. Duda SH, Bosiers M, Lammer J, Scheinert D, Zeller T, Oliva V, *et al.* Drug-Eluting and Bare Nitinol Stents for the Treatment of Atherosclerotic Lesions in the Superficial Femoral Artery: Long-term Results From the SIROCCO Trial. *J Endovasc Ther* 2006; 13: 701-10.

21. Ko YG, Ahn CM, Rha SW, Yu CW, Park SH, Lee SJ, *et al.* Comparison of Spot *versus* Long Stenting for Femoropopliteal Artery Disease. *Ann Vasc Surg* 2019; 58: 101-7.

22. Iida O, Urasawa K, Komura Y, Soga Y, Inoue N, Hara H, *et al.* Self-Expanding Nitinol Stent *vs.* Percutaneous Transluminal Angioplasty in the Treatment of Femoropopliteal Lesions: 3-Year Data From the SM-01 Trial. *J Endovasc Ther* 2019; 26: 158-67.

23. Laird JR, Zeller T, Loewe C, Chamberlin J, Begg R, Schneider PA, *et al.* Novel Nitinol Stent for Lesions up to 24 cm in the Superficial Femoral and Proximal Popliteal Arteries: 24-Month Results From the TIGRIS Randomized Trial. *J Endovasc Ther* 2018; 25: 68-78.

24. Gouëffic Y, Della Schiava N, Thaveau F, Rosset E, Favre JP, Salomon du Mont L, *et al.* Stenting or Surgery for De Novo Common Femoral Artery Stenosis. *JACC Cardiovasc Interv* 2017; 10: 1344-54.

25. Laird JR, Katzen BT, Scheinert D, Lammer J, Carpenter J, Buchbinder M, *et al.* Nitinol stent implantation *vs.* balloon angioplasty for lesions in the superficial femoral and proximal popliteal arteries of patients with claudication: three-year follow-up from the RESILIENT randomized trial. *J Endovasc Ther* 2012; 19: 1-9.

26. Schillinger M, Sabeti S, Dick P, Amighi J, Mlekusch W, Schlager O, *et al.* Sustained Benefit at 2 Years of Primary Femoropopliteal Stenting Compared With Balloon Angioplasty With Optional Stenting. *Circulation* 2007; 115: 2745-9.

27. Nikanorov A, Smouse HB, Osman K, Bialas M, Shrivastava S, Schwartz LB. Fracture of self-expanding nitinol stents stressed *in vitro* under simulated intravascular conditions. *J Vasc Surg* 2008; 48: 435-40.

28. Bilman V, Ardita V, Grandi A, Chiesa R, Bertoglio L. Symptomatic superficial femoral artery pseudoaneurysm due to late stent fracture. *J Vasc Surg Cases Innov Tech* 2020; 6: 106-9.

29. Rahimi M, Robertson B, Doctor LM, Bath J. Successful Management of Arterial Pseudoaneurysm Caused by Stent Fracture. *Ann Vasc Surg* 2017; 41: 281.e11-281.e14.

30. Sirignano P, Citone M, Menna D, Mansour W, Montelione N, Capoccia L, *et al.* Superficial Femoral Artery Stent Disruption Treated by Peripheral Endograft. *Ann Vasc Surg* 2015; 29: 1661.e5-8.

31. Lewitton S, Babaev A. Superficial femoral artery stent fracture that led to perforation, hematoma and deep venous thrombosis. *J Invasive Cardiol* 2008; 20: 479-81.

32. Park JY, Jeon YS, Cho SG, Jin CI, Kim KR, Shin WY, *et al.* Stent fractures after superficial femoral artery stenting. *J Korean Surg Soc* 2012; 83: 183-6.

33. Tsujimura T, Ishihara T, Iida O, Fujita M, Okamoto S, Uematsu M. A case complicated by floating fractured stent 141 months after nitinol stent implantation in the superficial femoral artery. *J Cardiol Cases* 2017; 16: 38-40.

34. Bonnin E, Lermusiaux P, Chakfé J, Dion D, Heim F, Chakfé N, *et al.* Disruption of a Covered Nitinol Self Expanding Stent Graft Implanted in the Common Femoral Artery. *EJVES Vasc Forum* 2020; 47: 55-9.

35. Tijani Y, Burgaud M, Hamel A, Raux M, Nasr B, Gouëffic Y. The Common Femoral Artery Is a Fixed Arterial Segment. *Ann Vasc Surg* 2021; 73: 51-4.

36. Müller-Hülsbeck S, Schäfer PJ, Charalambous N, Yagi H, Heller M, Jahnke T. Comparison of Second-Generation Stents for Application in the Superficial Femoral Artery: An *In Vitro* Evaluation Focusing on Stent Design. *J Endovasc Ther* 2010; 17: 767-76.

37. Garcia LA, Rosenfield KR, Metzger CD, Zidar F, Pershad A, Popma JJ, *et al.* SUPERB final 3-year outcomes using interwoven nitinol biomimetic supera stent: SUPERB Final 3-Year Outcomes Using Interwoven Supera Stent. *Catheter Cardiovasc Interv* 2017; 89: 1259-67.

38. Kuntz S, Torii S, Jinnouchi H, Cornelissen A, Sakamoto A, Sato Y, *et al.* Pathology and Multimodality Imaging of Acute and Chronic Femoral Stenting in Humans. *J Am Coll Cardiol Interv* 2020; 13: 418-27.

39. Grimme FAB, Zeebregts CJ, Verhoeven ELG, Bekkema F, Reijnen MMJP, Tielliu IFJ. Visceral stent patency in fenestrated stent grafting for abdominal aortic aneurysm repair. *J Vasc Surg* 2014; 59: 298-306.

Review and Analysis of Nitinol Trans Aortic Valve Repair Devices

14

Alan R. PELTON, Srinidhi NAGARAJA, Ga-Young SUH, Payman SAFFARI, Jochen ULMER

Transcatheter aortic valve (TAV) replacement is a key advancement in the cardiovascular device industry that provides patients suffering from severe symptomatic aortic stenosis an alternative to an open surgical procedure. It is important for this high-risk device that durability of the TAV frame is thoroughly assessed. As such, a comprehensive device durability approach is recommended that incorporates worst-case boundary conditions, computational stress/strain analyses, and benchtop fatigue testing. In particular, the TAV frame is subjected to complex biomechanical deformations *in vivo* that need to be critically evaluated during device design to ensure durability of the TAV frame. For example, pressure loading from blood flow, compressive forces from aortic root contraction, and torsion of the TAV frame may occur during systole. Furthermore, TAV frame may be loaded by transvalvular pressure gradient, inward bending of the commissure posts, and torsion during diastole. Another important consideration for structural durability is selection of the optimal material and manufacturing methods to withstand these potentially severe stress/strain conditions on the TAV frame for at least 400 million duty cycles. Therefore, this review article summarizes biomechanical deformations of the aortic valve and presents a case study on the use of standard and high purity Nitinol in a TAV frame subjected to a variety of biomechanical motions.

Introduction

There are four valves in the heart: aortic, pulmonary, mitral, and tricuspid valves. The boundary conditions and functions of each of these heart valves are unique and therefore must be considered separately. Inadequate understanding of the biomechanical environment for heart valve replacement devices may lead to adverse events such as regurgitation, implant migration, leaflet failure, and/or frame fracture(s). The aortic valve is located above the left ventricular outflow tract and below the sinotubular junction of the aorta (Figure 1). As a treatment of severe aortic stenosis, transcatheter aortic valve implantation (TAVI) is a promising therapeutic option with minimal incision without sternotomy, shorter operation, and faster post-operative recovery as compared to surgical valve replacement.

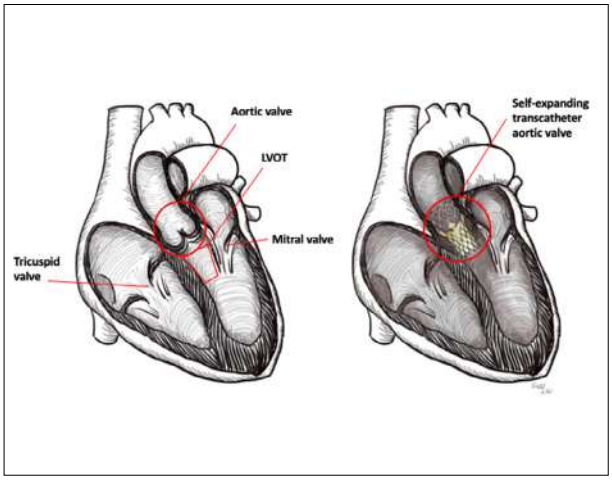

Figure 1: Anatomy of heart valves (left) and a self-expanding TAV frame implanted in the aortic valve (right).

A commonly used material for percutaneous heart valve (PHV) frames is Nitinol, a nearly equiatomic nickel-titanium alloy known for its unique shape memory, superelastic response, and biocompatibility. This material has proved particularly successful in cardiovascular applications such as vascular stents over the past two decades1. With substantially higher recoverable strains compared to traditional metals, Nitinol enables minimally invasive procedures and thereby reduces unnecessary patient trauma[1,2]. Nitinol PHV frames are manufactured in their open configuration, compressed into a much smaller delivery catheter (the superelastic effect), and then pushed out of the catheter where they expand against the vessel wall upon release and exposure to body temperature (the shape memory effect)[4]. Nitinol-based TAVI devices such as the Medtronic CoreValve have had clinical success [1-4]; however, some studies have raised concern regarding the long-term performance and adverse outcomes after TAVI. Gotzmann, *et al.* reported three-year outcomes after TAVI with the self-expanding transcatheter aortic valves. Eigthy-five of 150 patients exhibited paravalvular regurgitation. Aortic valve area increased right after TAVI, and slightly decreased during the 3-year period[5]. Sheleger *et al.* and Chen *et al.* reported paravalvular regurgitation after Medtronic CoreValve PHV implantation, which was induced by malapposition of the valve[6]. Although paravalvular regurgitation has been observed clinically, there is only one published case report of a frame fracture for the Medtronic CoreValve[7].

PHVs require the highest demonstration of safety and effectiveness based on their patient risk (US FDA Class III). Therefore, failure modes with potential severe patient sequelae such frame fatigue fractures need to be critically evaluated during design evaluation and regulatory approval. Accurate lifetime predictions of PHV structural components to >108 cycles under relevant *in vivo* conditions is imperative for heart valve replacement and repair devices. Therefore, it is critical to understand the relationship of the PHV devices with its dynamic vascular environment to prevent frame fractures. In fact, FDA expressed concern with the proper identification of boundary conditions for non-clinical benchtop testing, and with the use of materials such as Nitinol in the dynamic environment of heart valve implantation sites[8]. Consequently, the latest ISO 5840 standard provides heightened rigor for testing and analysis of PHV frames, especially under severe anatomical and physiological conditions. Fatigue assessment of a heart valve frame provides a relative assessment of the likelihood of structural component fracture during *in vivo* operation. Multiple contributions must be considered, as outlined in Figure 2, based on ISO 5840-1:2021[9]. This comprehensive device fatigue approach incorporates computational analyses of worst-case *in vivo* boundary conditions from literature, animal and/or cadaver studies and clinical implantations to obtain critical stresses and strains on the frame. These inputs guide the Material Fatigue Analysis and Fatigue Demonstration benchtop testing to provide device-specific Fatigue Safety Factors (FSFs).

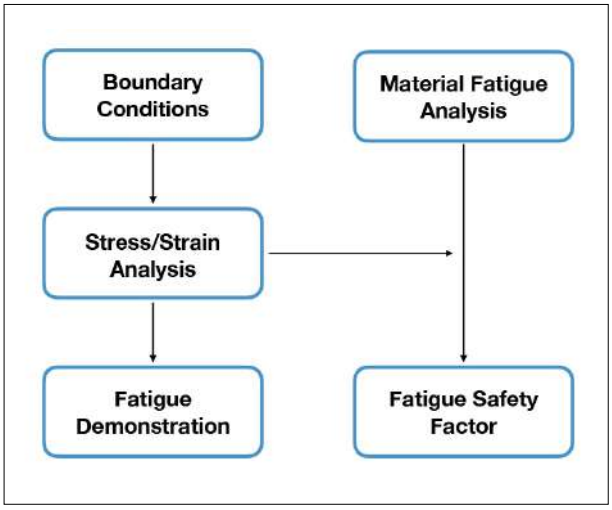

Figure 2: Requirements to determine device fatigue safety adapted ISO 5840-1:2021 Figure K.1 (9)

Aortic Valve Boundary Conditions

The aforementioned FDA perspective article on PHVs emphasized the importance of establishing "a consistent and conservative approach to determine the *in vivo* boundary conditions for each device."[8]. As such, it is critical for a comprehensive assessment of the *in vivo* boundary conditions during PHV development to insure devices are durable for the intended environment. Due to potential adverse outcomes, assessment of aortic annulus geometry and deformations are important for procedural strategy and evaluating long-term performance.

In order to characterize aortic root anatomy and provide essential data for surgical planning, imaging modalities such as multidetector Computed Tomography (CT) and transesophageal echocardiography have been commonly utilized[10, 11]. Studies using these imaging modalities have discovered that cross-sections of the aortic root where the self-expanding TAVs are implanted are commonly non-circular shape, accompanied by incomplete stent frame expansion[12]. Specifically, Schultz and colleagues quantified the major and minor diameters at four distinct locations along the length of the Medtronic CoreValve device, and found non-circular conformations at all four locations of the device with the ellipse aspect ratio (major to minor axis) ranging from 1.04 (commissures) to 1.24 (ventricular end). Another study performed geometric analysis of post-deployment dimension of CoreValve Prosthesis using fluoroscopic images. 27 of 50 patients exhibited incomplete stent frame expansion at the inflow portion after TAVI, yet, no significant difference in the aortic valve area, pressure gradients, or incidence of regurgitation with respect to complete expansion. Also, 31 of 50 patients exhibited incomplete stent frame expansion at the outflow portion, and the authors noted that aortic regurgitation grade seemed to increase with respect to the degree of under-expansion in the outflow portion[13]. Eccentric cross-sectional configuration of TAV frame as well as incomplete frame expansion may impact not only the strain distribution within the Nitinol frame, but also the stresses on the leaflets[14-16]. Gunning and colleagues investigated the impact of eccentric deployment of a Nitinol TAV frame on leaflet strains using dual-camera stereophotogrammetry, and found significantly higher leaflet commissure strains in eccentric valves compared to circular valves[17].

In addition to TAV frame deformations due to non-circular conformations, cyclic multi-axial motions can produce an aggressive biomechanical environment for the Nitinol frame. The ISO 5840-1:2021[9] standard recommends consideration of the following loading conditions for durability testing of heart valve frames: (1) Differential pressures across the valve, (2) Stent post deflection, (3) Transient stresses occurring during opening and closing, (4) Radial dilatation and compression, (5) Torsion, (6) Bending, (7) Axial tension, (8) Axial compression, and (9) Linear/transverse compression (*e.g.*, crushing). Understanding these *in vivo* deformations of the native and post-operative PHV is crucial to evaluate the mechanical durability of TAV frames. Several studies documented the *in vivo* deformations of the aortic root throughout the cardiac cycle using CT or MRI. Cheng *et al.* provided systematic review of aortic root deformation from the level of aortic annulus to the commissures, and observed four modes of deformation: circumferential deformation at the base, circumferential deformation at the commissures, longitudinal deformation, and torsion deformation, during the cardiac phase of isovolumic contraction, ejection, isovolumic relaxation, and filling[18]. They observed asymmetric deformation in circumferential and longitudinal directions, along with torsion during ejection and isovolumic relaxation, and recoil during filling. Further, Bertaso *et al.* and Hamdan *et al.* noted that, from diastole to systole, the cross-sectional area was increased by 11.2 ± 5.4% (normal aortic valves) and 6.2 ± 4.8% (calcified valves) owing to lower compliance in stenotic aortic valves[19, 20].

When the TAV frame is implanted in a highly dynamic environment, various deformations on the frame may arise during the cardiac cycle such as ejection of blood or at valve closure (Figure 3).

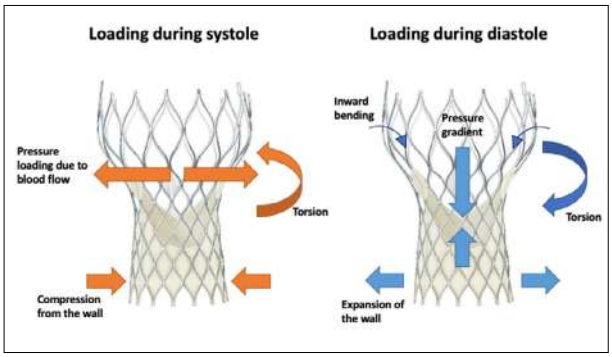

Figure 3: Possible loading on the TAV frame during systole (left) and diastole (right).

During systole, the leaflets open resulting in pressure loading on the TAV frame and compressive forces from the aortic root during contraction as blood is ejected into the ascending aorta. Also, the TAV frame may be subjected to counter-clockwise torsion based on native aortic root dynamics during systole. During diastole, the valve is closed and the TAV frame is loaded by the transvalvular pressure gradient, approximately 72.1 - 87.8 mmHg in patients with aortic valve stenosis [3, 21]. In addition, ISO 5840 provides peak aortic pressure gradients up to 165 mmHg for individuals with severe hypertension [9]. The TAV frame may also be subject to clockwise torsion during the diastole. Another important TAV deformation mode is the cyclic inward bending of the frame commissure posts. Such bending may occur due to pulling by the leaflets while the valve is loaded by the transvalvular pressure gradient.

Computational Simulation of TAV Biomechanical Motions

As an example of a stress/strain analysis for device durability, we present the results of a finite element analysis (FEA) of a generic Nitinol TAV frame (Figure 4). Whereby the frame was subjected to the the following boundary conditions simulating loading conditions throughout the cardiac cycle: (1) TAV frame was shape set to 25mm outer diameter at the annulus level, (2) TAV frame radially sheathed to 15 Fr (5mm diameter), (3) TAV frame deployed inside a 22mm diameter annulus with 3% radial distension during the cardiac cycle, (4) Commissures were pulled inwards with 1mm cyclic motion, and (5) 100 mmHg pressure gradient acting axially on the TAV frame. It is important to note that the displacements applied in this simulation are not necessarily based on clinical data, rather intended to provide a framework for durability analysis. The highest strains in TAV frames are typically observed during the sheathing process; Figure 5 illustrates the location and magnitude of the resultant sheathing strains.

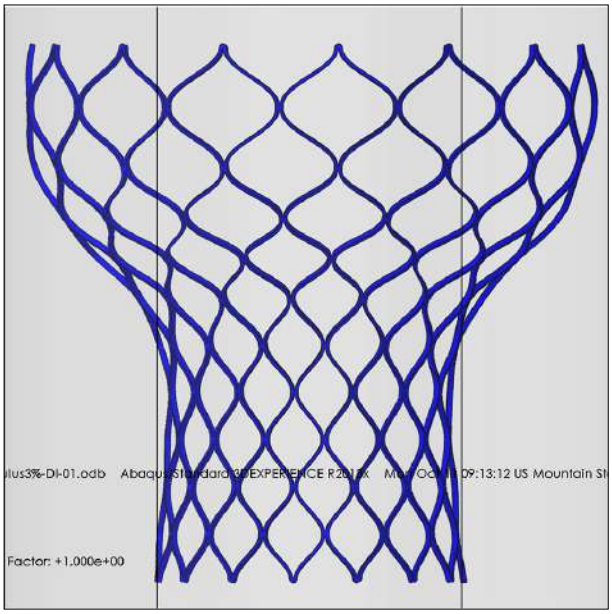

Figure 4: Image of generic transcatheter aortic heart valve frame.

The maximum sheathing strains are greater than 9% for this example. Once implanted in the annulus, the combination of cyclic deformations as described above result in radial deformations on the frame as shown in Figure 6. Note that the greatest strains (red) are located at the commissure posts where the leaflets attach. Per the model, the displacement magnitudes are 1mm. The corresponding strain amplitudes from this combined motion is illustrated in Figure 7. The maximum strain amplitude for this case is 0.57% located at three commissure post regions of the frame. The “point cloud” that displays the mean strain and corresponding strain amplitude for every element of the model is shown in Figure 8.

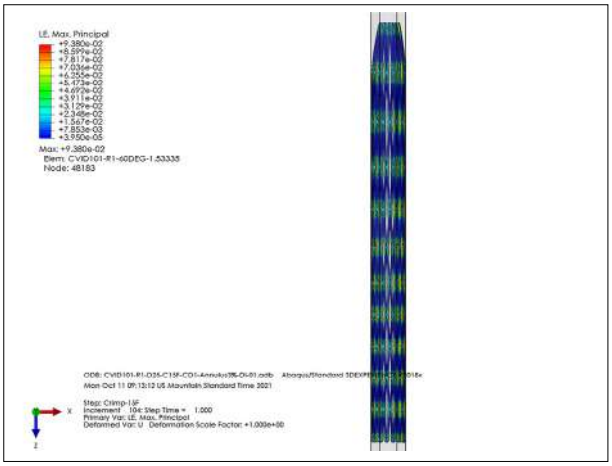

Figure 5: Strain distribution in generic TAV frame in compressed state after sheathing to 15Fr.

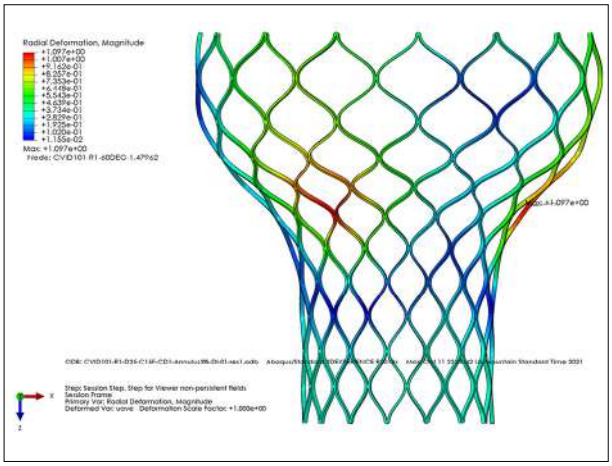

Figure 6: Radial deformation distribution after loading conditions were applied to the generic TAV frame.

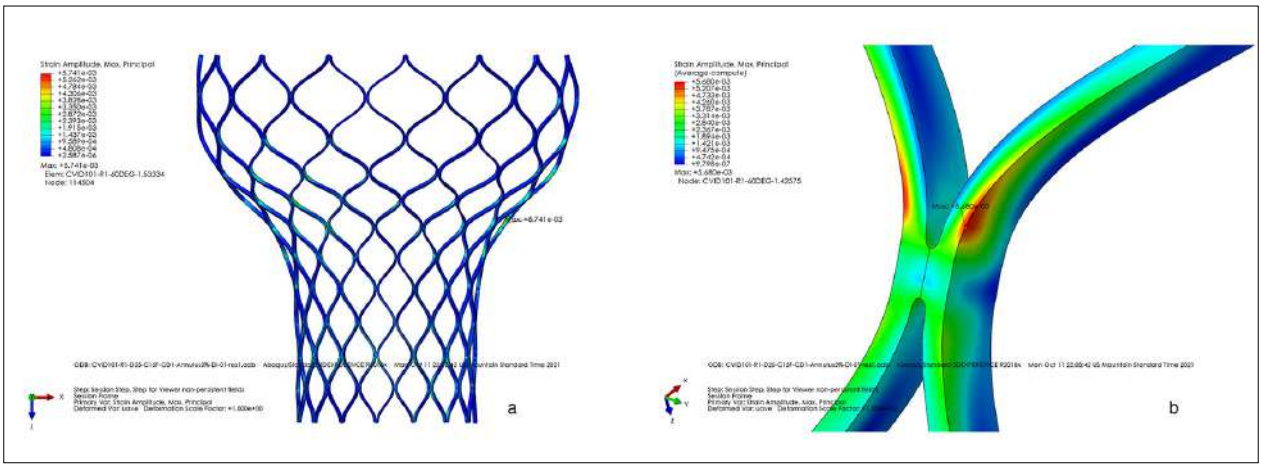

Figure 7: Strain amplitude distribution on generic TAV frame after applied cyclic combined loading (a) and maximum strain amplitude location at commissure post (b).

The maximum mean strain is 4.2% located in the annular region from oversizing a 25mm diameter TAV in the 22mm native annulus. Note that the highest strain amplitude element is not located in the annulus. In this region, the corresponding strain amplitude is approximately 0.1%. In contrast, the commissure post region has a mean strain of approximately 0.5%. Consequently, there is a wide range of mean strains and strain amplitudes throughout the frame due to the combined loads. These cyclic displacements/strains may lead to fatigue damage including fracture depending upon the magnitude of the strains and the Nitinol material characteristics. This will be discussed in further detail in the next section.

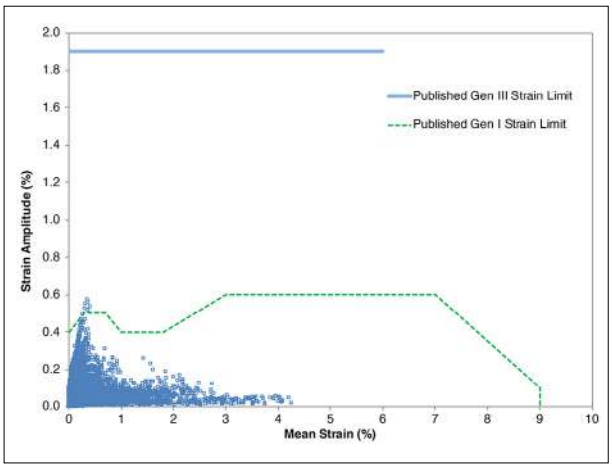

Figure 8: FEA "point cloud: analysis of the mean strains and strain amplitudes for the generic TAV frame subjected to cyclic loads. The published fatigue limits for Generation I and Generation III Nitinol are displayed in green and black, respectively.

TAV Frame Durability

Durability assessment of cardiovascular devices is an essential element of design evaluation and regulatory submission process. The confidence to predict lifetimes of cardiovascular devices to ~ one billion fatigue cycles under relevant *in vivo* conditions has grown due to the incorporation of the "test-to-fracture" methods outlined in ASTM F3211[22] as well as the general guidance from ISO 5840:2021[9] as discussed above. These methodologies incorporate the use of a complete implant or a subcomponent ("extracted cell") of the device or coupons as test specimens. Accordingly, benchtop fatigue testing is conducted at a range of hyper-physiologic forces/displacements in order to determine the boundary between device fracture and survival. Fatigue is defined as the progressive localized permanent structural damage that occurs as a result of cyclic stresses and strains. This damage accumulation may lead to the initiation of microcracks, crack propagation and potentially to fracture[23].

Recent publications have summarized benchtop testing methods, Nitinol material selection, and strategies to obtain a robust profile of durability[24-28]. It is essential to mimic the full set of forces and displacements that the device undergoes from shape setting, sheathing, and deployment into the anatomical location. For Nitinol devices, especially those that undergo large sheathing strains (often on the order of 8-12%), it is important to conduct the cyclic displacements on the unloading plateau to account for the residual stresses and microstructural changes[29-32].

The most important aspects that govern device durability for a given device design and *in vivo* boundary conditions is "micro-purity" of Nitinol. The previous section outlined the boundary conditions for a generic aortic TAV design and indicated the complex nature of device-anatomy interactions, especially with the leaflet motions. This section will focus on a review of the effects of purity on Nitinol fatigue behavior.

Early cardiovascular peripheral vascular implants were manufactured with so-called "Generation I" Nitinol. During the past decade, manufacturers have accelerated the pace to provide "ultra-clean" Nitinol to the medical device industry. The key to these improvements is the reduction in oxide and carbide inclusion size and volume fraction[25, 27, 33, 34]. Recent presentations summarized the evolution in commercially available Nitinol and highlighted the direct correlation between inclusion characteristics of the final wire or tubing and fatigue strain limits of the Nitinol. The original Nitinol materials (Generation I) have

the largest (~ 100µm) and greatest volume fraction (~ 1.5%) of internal impurities (oxide and carbide inclusions). Consequently, these materials have the lowest fatigue strain limits under relevant cardiovascular device testing conditions. With the advent of the highest purity Nitinol (Generation III), there has been a decrease in the overall inclusion size (~ 5µm) as well as the volume fraction (~0.5%).

Robertson, *et al.* reported on the improvements in bending fatigue with increased purity Nitinol by testing superelastic wires and diamond-shaped stent surrogates from five different mill product suppliers[25]. This study was recently extended to the highest micro-purity Nitinol manufactured from an Electron Beam Refinement process[26,27]. These materials were subjected to identical final manufacturing processes typical for many PHV frames. The fatigue strain limit (FSL) for the Nitinol with large inclusions was determined to be about 0.4% at the low mean strain region, whereas the FSL for the small inclusion-low volume fraction Nitinol showed a substantial increase to about 2% strain amplitude.

Conclusion

This fatigue data comparison is quite revealing and demonstrates that not all Nitinol material is the same with respect to fatigue properties. Furthermore, the fourfold increase in FSL for Generation III Nitinol has a direct implication on the fatigue safety factor (FSF) of the finished PHV.

The effects of FSF can be seen the FEA scatter plot in Figure 8. For these conditions, the greatest fatigue strain amplitude is 0.57%, which can be compared to the FSL from Generation I material (0.4%) (dotted green line). As discussed in reference[28], the FSF can be calculated as $\frac{\varepsilon}{FSL} = \frac{0.4\%}{0.57\%} = 0.7$

With a FSF < 1.0, there is a greater probability of fatigue fracture with the Generation I Nitinol. However, if the highest purity Nitinol is used in the same design and under the identical conditions, the FSL is ~ 1.9% (solid blue line) so that the FSF is $\frac{1.9\%}{0.57\%} = 3.3$

Generation III Nitinol therefore provides an enhanced probability of long term durability due to the significantly smaller and lower volume fraction of inclusions. Therefore, considerations of modern high purity Nitinol provides a solution for environments with complex and severe boundary conditions such as in the aortic PHV.

References

1. Barbanti M, Petronio AS, Ettori F, Latib A, Bedogni F, De Marco F, *et al.* 5-Year Outcomes After Transcatheter Aortic Valve Implantation With CoreValve Prosthesis. *JACC Cardiovasc Interv* 2015; 8: 1084-91.
2. Barker CM, Reardon MJ. The CoreValve US pivotal trial. *Semin Thorac Cardiovasc Surg* 2014; 26: 179-86.
3. Grube E, Buellesfeld L, Mueller R, Sauren B, Zickmann B, Nair D, *et al.* Progress and current status of percutaneous aortic valve replacement: results of three device generations of the CoreValve Revalving system. *Circ Cardiovasc Interv* 2008; 1: 167-75.
4. Ussia GP, Barbanti M, Petronio AS, Tarantini G, Ettori F, Colombo A, *et al.* Transcatheter aortic valve implantation: 3-year outcomes of self-expanding CoreValve prosthesis. *Eur Heart J* 2012; 33: 969-76.
5. Gotzmann M, Czauderna A, Hehnen T, Aweimer A, Lind A, Kloppe A, *et al.* Three-Year Outcomes After Transcatheter Aortic Valve Implantation With the CoreValve Prosthesis. *Am J Cardiol* 2014; 114: 606-11.
6. Schleger S, Kasel M, Vogel J, Lieber M, Antoni D, Hoffmann E, *et al.* Successful Transapical Implantation of an Edwards Sapien Valve Within an Insufficient Aortic CoreValve Prosthesis: An Initial Experience. *Ann Thorac Surg* 2013; 95: 1070-2.
7. Chen M, Feng Y, Tang H, Xu Y-n, Wei X, Huang D-j. Strut fractures of CoreValve frames. *Int J Cardiol* 2013; 163: e42-e3.
8. Aguel F, Hillebrenner M, Stewart SFC, Swain J, Hampshire V, Zuckerman B. U.S. Regulatory Considerations for Heart Valves Implanted by Minimally Invasive Surgery. *Cardiovasc Eng Technol* 2011; 2: 62-5.
9. ISO. ISO 5840:2021 Cardiovascular implants - Cardiac valve protheses. 2021.

10. Kasel AM, Cassese S, Leber AW, von Scheidt W, Kastrati A. Fluoroscopy-guided aortic root imaging for TAVR: "follow the right cusp" rule. *JACC Cardiovasc Imaging* 2013; 6: 274-5.

11. Clavel MA, Malouf J, Messika-Zeitoun D, Araoz PA, Michelena HI, Enriquez-Sarano M. Aortic valve area calculation in aortic stenosis by CT and Doppler echocardiography. *JACC Cardiovasc Imaging* 2015; 8: 248-57.

12. Schultz CJ, Weustink A, Piazza N, Otten A, Mollet N, Krestin G, *et al.* Geometry and Degree of Apposition of the CoreValve ReValving System With Multislice Computed Tomography After Implantation in Patients With Aortic Stenosis. *J Am Coll Cardiol* 2009; 54: 911-8.

13. Jilaihawi H, Chin D, Spyt T, Jeilan M, Vasa-Nicotera M, Mohamed N, *et al.* Comparison of Complete Versus Incomplete Stent Frame Expansion After Transcatheter Aortic Valve Implantation With Medtronic CoreValve Bioprosthesis. *Am J Cardiol* 2011; 107: 1830-7.

14. Abbasi M, Azadani AN. The Synergistic Impact of Eccentric and Incomplete Stent Deployment on Transcatheter Aortic Valve Leaflet Stress Distribution. *Transcatheter Therapies* 2015. p. B253.

15. Sun W, Li K, Sirois E. Simulated elliptical bioprosthetic valve deformation: implications for asymmetric transcatheter valve deployment. *J Biomech* 2010; 43: 3085-90.

16. Gunning PS, Vaughan TJ, McNamara LM. Simulation of self expanding transcatheter aortic valve in a realistic aortic root: implications of deployment geometry on leaflet deformation. *Ann Biomed Eng* 2014; 42: 1989-2001.

17. Gunning PS, Saikrishnan N, Yoganathan AP, McNamara LM. Total ellipse of the heart valve: the impact of eccentric stent distortion on the regional dynamic deformation of pericardial tissue leaflets of a transcatheter aortic valve replacement. *J R Soc Interface* 2015; 12: 20150737.

18. Cheng A, Dagum P, Miller DC. Aortic root dynamics and surgery: from craft to science. *Philos Trans R Soc Lond B Biol Sci* 2007; 362: 1407-19.

19. Bertaso AG, Wong DT, Liew GY, Cunnington MS, Richardson JD, Thomson VS, *et al.* Aortic annulus dimension assessment by computed tomography for transcatheter aortic valve implantation: differences between systole and diastole. *Int J Cardiovasc Imaging* 2012; 28: 2091-8.

20. Hamdan A, Guetta V, Konen E, Goitein O, Segev A, Raanani E, *et al.* Deformation dynamics and mechanical properties of the aortic annulus by 4-dimensional computed tomography: insights into the functional anatomy of the aortic valve complex and implications for transcatheter aortic valve therapy. *J Am Coll Cardiol* 2012; 59: 119-27.

21. Lamb HJ, Beyerbacht HP, de Roos A, van der Laarse A, Vliegen HW, Leujes F, *et al.* Left ventricular remodeling early after aortic valve replacement: differential effects on diastolic function in aortic valve stenosis and aortic regurgitation. *J Am Coll Cardiol* 2002; 40: 2182-8.

22. ASTM. F3211–17 Standard Guide for Fatigue-to-Fracture (FtF) Methodology for Cardiovascular Medical Devices. 2017.

23. Manson SS, Halford GR. Fatigue and Durability of Structural Materials. *ASM International* 2006.

24. Pelton AR, Schroeder V, Mitchell MR, Gong XY, Barney M, Robertson SW. Fatigue and Durability of Nitinol Stents. *J Mech Behav Biomed Mater* 2008; 1: 153–64.

25. Robertson SW, Launey M, Shelley O, Ong I, Vien L, Senthilnathan K, *et al.* A statistical approach to understand the role of inclusions on the fatigue resistance of superelastic Nitinol wire and tubing. *J Mech Behav Biomed Mater* 2015; 51: 119-31.

26. Pelton AR, Pelton SM, Ulmer J, Niedermaier D, Plaskonka K, Mitchell MR, *et al.* The use of next generation Nitinol for medical implants. In: Chakfé N, Heim F, Meichelboeck W, editors. European Symposium on Vascular Biomaterials; October 12-14 2017; Strasbourg, France: Geprovas; 2017. p. 35-44.

27. Pelton AR, Pelton SM, Jörn T, Ulmer J, Niedermaier D, Plaskonka K, *et al.* The Quest for Fatigue-Resistant Nitinol for Medical Implants. In: Mitchell MR, Berg BT, Woods TO, Jerina KL, editors. STP1616: Fourth Symposium on Fatigue and Fracture of Metallic Medical Materials and Devices. West Conshohocken, PA: ASTM International; 2019. p. 1-30.

28. Pelton AR. Evaluation of Mechanical Fatigue and Durability. H*andbook of Vascular Motion: Elsevier* 2019. p. 313-35.

29. Pelton AR, Clausen B, Stebner AP. *In Situ* Neutron Diffraction Studies of Increasing Tension Strains of Superelastic Nitinol. *Shape Memory and Superelasticity* 2015; 1: 375-86.

30. Stebner AP, Paranjape HM, Clausen B, Brinson LC, Pelton AR. In-situ Neutron Diffraction Studies of Large Monotonic Deformations of Superelastic Nitinol. *Shape Memory and Superelasticity* 2015; 1: 252-267.

31. Stebner AP, Vogel SC, Noebe RD, Sisneros TA, Clausen B, Brown DW, *et al.* Micromechanical quantification of elastic, twinning, and slip strain partitioning exhibited by polycrystalline, monoclinic nickel–titanium during large uniaxial deformations measured via in-situ neutron diffraction. *J Mech Phys Solids* 2013: 2302-30.

32. Launey M, Ong I, Pelton AR. On the life fatigue of superelastic Nitinol. SMST 2013; Prague, Czech Republic 2013.

33. Urbano MF, Cadelli A, Sczerzenie F, Luccarelli P, Beretta S, Coda A. Inclusions Size-based Fatigue Life Prediction Model of NiTi Alloy for Biomedical Applications. *Shape Memory and Superelasticity* 2015; 1: 240-51.

34. Launey M, Robertson SW, Vien L, Senthilnathan K, Chintapalli P, Pelton AR. Influence of microstructural purity on the bending fatigue behavior of VAR-melted superelastic Nitinol. *J Mech Behav Biomed Mater* 2014; 34: 181-6.

Fully bioresorbable vascular scaffolds: lessons learned and future directions

15

Atsushi SAKAMOTO, Hiroyuki JINNOUCHI, Yu SATO, Renu VIRMANI, Aloke V. FINN

The technology of percutaneous coronary intervention (PCI) is constantly being refined in order to overcome the limitations of present-day devices. Although the performance of current generation metallic drug-eluting stents (DES) is quite acceptable in the short-term, concerns still exist about their long-term efficacy.table Fully bioresorbable scaffolds (BRS) were designed to surmount the shortcomings of metallic DES, which permanently cage the vessel wall, thereby restricting normal coronary vasomotor function, impede bypass grafting and can provoke long-term foreign body responses. The Absorb Bioresorbable Vascular Scaffold (Absorb-BVS; Abbott Vascular) was the first U.S.FDA-approved BRS. This device represented the most advanced attempt to fulfill the dream of interventional cardiologists, *i.e.* a transient scaffolding which would eventually disappear and therefore would not hamper further treatment options. Early, small studies and even large randomized control trials showed acceptable short-term outcomes up to 1 year of follow-up, however, longer-term results over 1 year have not been satisfactory with increased rates of scaffold thrombosis and target lesion revascularization. The inherent characteristics of Absorb-BVS such as thicker struts, greater vessel surface area coverage, and less radial force versus contemporary DES seemed to lead adverse mid-term outcomes. As a result, almost one year after its initial approval by the FDA, this device was withdrawn from the market due to declining devisce utilization driven by the concerns about scaffold thrombosis seen in both early and late time points. In this chapter, we summarize the preclinical and clinical data available for Absorb-BVS to understand how the vascular biological reactions to this device differ from that to metallic DES and how these responses translate into clinical outcomes. Also, we discuss next generation BRS and outline modifications that are needed to improve the long-term outcomes for the treatment of coronary artery disease.

Introduction

Contemporary metallic drug-eluting stents (DES) with thin struts, biocompatible polymer coating, and feasible drug-elution profile improved their safety and efficacy profiles and made them the first choice for the percutaneous treatment of symptomatic coronary artery disease (CAD) which is a leading cause of morbidity and mortality worldwide [1]. However, intrinsic disadvantages of DES implantation still exist such as the development of neoatherosclerosis caused by chronic foreign body reaction, limitation of normal vasomotion and adaptive arterial remodelling (Glagov effect), and preclusion of bypass surgery due to metallic caging [2,3]. Indeed, the long-term outcome of 2nd-generation durable-polymer DES regarding death and non-fatal myocardial infarction (MI) was not different from that of bare metal stent (BMS), and clinical events continue to occur in BMS as well as DES [4]. To overcome these limitations, the concept of totally bioresorbable vascular scaffold/stent (BRS) was launched with the idea that by eliminating long-term exposure of the vessel wall to drug, metal, and polymer we could better maintain long-term

vessel wall physiology. The ideal material for this concept might have appropriate temporal radial strength to resist recoil, flexibility, biocompatibility and be resorbed without massive inflammation or systemic toxicities. Thus far, there are two major categories of material which are used in BRS: polymer and bioerodible metallic alloy (Table 1).

Table 1. Features of bioresorbable scaffold/stent

Device	Manufacturer	Backbone	Coating	Eluted drug	Strut thickness (μm)	Complete resorption (months)
Absorb BVS*	Abbott Vascular	PLLA	PDLLA	Everolimus	157	36–42
Absorb BVS gen 2	Abbott Vascular	PLLA	PLGA	Everolimus	<99	36
DESolve Nx*	Elixir Medical	PLLA	Polylactide-based polymer	Novolimus	150	24
DESolve Cx*	Elixir Medical	PLLA	Polylactide-based polymer	Novolimus	120	24
DESolve NXT*	Elixir Medical	PLLA	Polylactide-based polymer	Novolimus	120	24
Fantom*	REVA Medical	PTD-PC	PTD-PC	Sirolimus	125	36
ART-Pure*	Arterial Remodeling Technologies	PDLLA	none	none	170	12
MeRes 100*	Meril Life Science	PLLA	PDLL A	Sirolimus	100	24
Mirage	Manli Cardiology	PLLA	PLL A	Sirolimus	125–150	14
FORTITUDE	Amaranth Medical	UHMW-PLLA	PDLLA	Sirolimus	150	12–24
APTITUDE	Amaranth Medical	UHMW-PLLA	PDLLA	Sirolimus	115	>36
MAGNITUDE	Amaranth Medical	UHMW-PLLA	PDLLA	Sirolimus	98	24–36
Firesorb	MicroPort	PLLA	PDLLA	Sirolimus	100–125	36
XINSORB	HuaAn Biotechnology	PLLA	PDLLA	Sirolimus	160	24–36
NeoVas	Lepu Medical Technology (Beijing)	PLLA	PDLLA	Sirolimus	170	36
Magmaris*	Biotronik	Magnesium	PLLA	Sirolimus	150	9–12
DREAMS 3G	Biotronik	Magnesium	PLLA	Sirolimus	99, 117, 147	9–12
IBS	Lifetech Scientific	Iron	PDLLA	Sirolimus	70	>12

Abbreviations: BVS=bioresorbable vascular scaffold, IBS=iron bioresorbable scaffold, PDLLA=poly-d, l-lactide, PLGA=poly-lactic-co-glycolic acid, PLLA=poly-l-lactide, PTD-PC=desaminotyrosine polycarbonate, UHMW=ultra-high molecular weight. *Device has received CE marking approval.

However, the Absorb-bioabsorbable vascular scaffold (Absorb-BVS, Abbott Vascular), the most comprehensively tested BRS, did not show the ideal clinical performance as it demonstrated higher adverse events due to greater frequency of scaffold thrombosis *versus* contemporary metallic DES in several clinical trials [5,6], suggesting further drastic refinements need to be achieved to establish BRS with acceptable safety and efficacy. In this regards, careful analysis of the promises and pitfalls of the Absorb-BVS may allow us to understand how to better design the next generation BRS which has the potential to revolutionize the interventional treatment of coronary artery disease.
In this chapter, we summarize prior experience with BRS, mainly focused on the Absorb-BVS, and discuss future directions of this field from pre-clinical, pathologic and clinical points of views.

Absorb-BVS: development and testing

Absorb-BVS, a non-metallic scaffold made of poly-l-lactic acid (PLLA) backbone coated by a poly-d,l-lactide (PDLLA) with the antiproliferative agent everolimus was the most widely utilized BRS. Fundamentally, material of PLLA has lower tensile and mechanical strength, stiffness and ductility compared with metals (*e.g.*, stainless steel or cobalt-chromium [CoCr]) used in the current coronary stents. Therefore, scaffolds made from PLLA need to have thicker (Absorb-BVS=157μm) and wider strut profile *versus* metallic stents to improve tensile and radial strength, but these parameters in Absorb-BVS are still nearly half of metallic stent [7]. Thus, because of its strut thickness, Absorb-BVS struts occupy on average 27% of the vessel wall area, while most metallic DES occupy only 13% [8]. This type of strut topography and surface coverage area is well known to lead flow disturbances especially in smaller vessels due to flow disturbances and to impede endothelial coverage of the device [9].

Preclinical evaluation

We previously reported the histopathologic comparison between Absorb-BVS and CoCr-everolimus eluting stent (CoCr-EES, Xience, Abbot Vascular) implanted arteries at various time points using 136 healthy swine (total 263 Absorb-BVS and 72 CoCr-EES) [10]. In the assessment of angiography and intravascular ultrasound, Absorb-BVS implanted arteries showed significantly smaller minimal lumen diameter *versus* CoCr-EES implanted arteries up to 6 months. However, from 12 months to 42 months, only Absorb-BVS implanted arteries showed the progressive enlargement of lumen area at the site of scaffold beyond reference lumen area (*i.e.*, vascular positive remodeling). Such change was not observed in CoCr-EES implanted arteries [11]. In line with the imaging-based assessment, histopathologic analysis revealed significantly greater percent area stenosis in Absorb-BVS at 1 and 6 months, however, at 30, 36, and 42 months, percent stenosis was significantly lower with Absorb-BVS than with CoCr-EES10. Complete strut coverage with neointimal tissue was achieved at 1-month in both devices, while the inflammation around strut was significantly greater in the Absorb-BVS than CoCr-EES, beginning at 6 months after implantation, peaking at 12 months and remaining significantly greater at 18 months. The inflammation in the Absorb-BVS decreased thereafter but continued to be significantly greater than that in the CoCr-EES at 30, 36, and 42 months.

Stent designs influence endothelial turnover and its functional status by altering wall shear stress and blood-flow dynamics (Figure 1) [12]. Kolandaivelu *et al.* reported using an swine coronary model, bare metal stent (BMS) with thick struts (162μm) increased thrombogenicity 1.6-fold as compared to BMS with thin struts (81μm) (p=0.004) at 3-day post-implantation [13]. In our *ex vivo* arteriovenous swine shunt model comparing Absorb-BVS with other competitors, significantly greater thrombogenicity was observed in Absorb-BVS *versus* either thin-strut, biodegradable polymer DES (Biomatrix; Biosensors [120μm] and Synergy; Boston Scientific [74μm]) or a BMS (Omega Platinum–Chromium; Boston Scientific [81μm]) [14] (Figure 2A). Low shear stress around large struts also inhibits re-endothelialization [15] (Figure 1).

Figure 1: Alteration of blood flow dynamics and thrombogenicity in the vicinity of thin or thick stent struts. Stent-induced flow disturbances affect thrombogenicity and re-endothelialization following stent implantation.

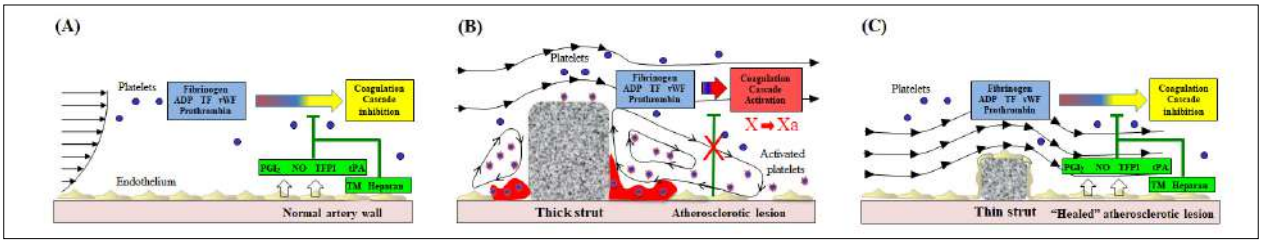

(A): Healthy endothelium in the normal artery wall expresses anticoagulant and antithrombotic molecules, including NO, PGI2, TFPI, tPA, TM, and heparin-like molecules.

(B): Stent placement results in local endothelial denudation, which leads to activation of the coagulation cascade. Stents, especially thicker strutted ones, may promote non-streamlined flow separation in regions proximal and distal to struts. Accelerated blood flow (high shear) over the strut edges can activate platelets through the release of thromboxane A2 and ADP, whereas flow recirculation zones with low shear rates are associated with inhibition of re-endothelialization, potentially enabling procoagulant and proinflammatory elements to accumulate, which contribute to thrombus formation.

(C): A thin strut geometry reduces flow separation and low shear, leading to the inhibition of platelet activation. Moreover, the generation of recirculation zones proximal and distal to thin struts will be minimized, resulting in the reduced thrombogenicity. Undisturbed flow proximal and distal to streamlined struts promotes re-endothelialization, which further helps to maintain hemostatic balance and prevent thrombosis. *Modified and reprinted with permission from Jimenez JM, et al. Ann. Biomed. Eng. 2009; 37: 1483-94, and Sakamoto A, et al. Bioengineering (Basel). 2018; 5: 71.*

Abbreviations: ADP; adenosine diphosphate, AR; aspect ratio, CFD; computed flow dynamics, NO; nitric oxide, PGI2; prostacyclin, TF; tissue factor, TFPI; tissue factor pathway inhibitor, TM; thrombomodulin, tPA; vWF; von Willebrand factor.

Figure 2: Acute thrombogenicity and delayed endothelial coverage of Absorb-BVS in experimental models.

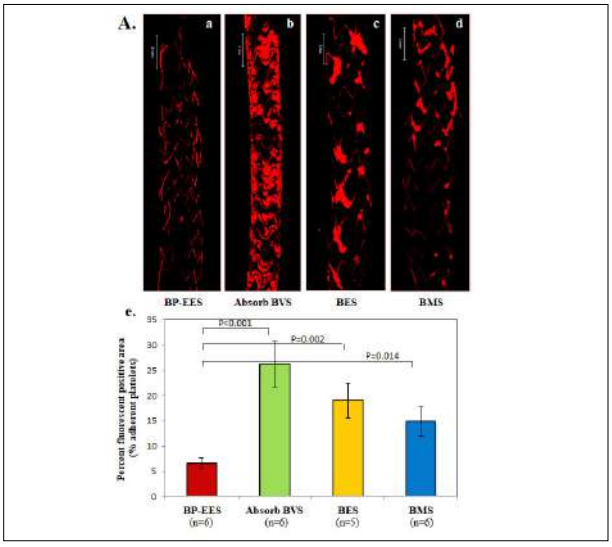

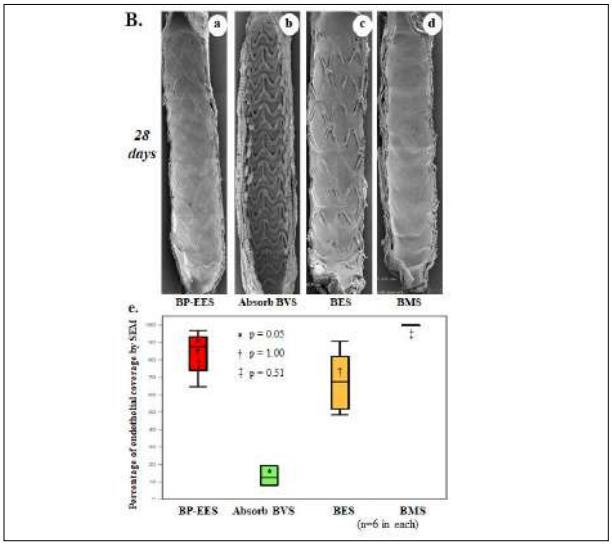

(A): *Ex vivo* arteriovenous porcine shunt model. Representative images derived from confocal microscopy after 1 hour in a swine *ex vivo* shunt model. Platelets were stained with anti-CD61 and CD42b primary antibody and red-fluorescent secondary antibody. (a) Biodegradable polymer everolimus-eluting stent (BP-EES); (b) fully bioabsorbable everolimus-eluting scaffold (Absorb-BVS); (c) biodegradable polymer biolimus-eluting stent (BES); and (d) bare metal stent (BMS). (e) Percent fluorescent positive area based on percentage of fluorescent positive staining against CD61 and CD42b within the entire stented segment. Values are expressed as mean ± SD in each group. BP-EES, Absorb-BVS, and BMS included n=6 stents in each group, whereas BES included n=5 stents. One BES was incompletely expanded and therefore excluded in the analysis.

(B): Rabbit model. Representative images of endothelial coverage assessed by scanning electron microscopy (SEM) at 28 days. Low magnification (15×) SEM images provide an overview of the luminal surface of the bisected segment from proximal (top) to distal (bottom). (a) BP-EES, (b) Absorb-BVS, (c) BES, and (d) BMS. (e) Relative percentage of endothelial coverage above struts assessed by scanning electron microscopy is shown in box and whisker diagrams on the right. Values represent median with lower (25th percentile) and upper quartiles (75th percentile) and whiskers for minimum and maximum value. Each group has n=6, respectively. *Modified reprinted from Koppara T, et al. Circ Cardiovasc Interv 2015; 8: e002427 and Sakamoto A, et al. Bioengineering (Basel). 2018; 5: 71.*

Palmatz *et al.* showed, using their *in vitro* flow chamber model at physiologic wall shear stress (15 dynes/cm^2), that obstacle heights of 100µm or greater had significantly less coverage of endothelial cells than those which were 25µm[16]. Our observation for strut endothelialization by scanning electron microscopy in a rabbit model also showed lower endothelialization with the Absorb-BVS than with either DES or BMS[14] (Figure 2B).

Result of clinical trials

Absorb-BVS received CE mark in 2010 based on the result of ABSORB clinical trial[17,18]. Following the result of large scale ABSORB III trial[19], the U.S.FDA approved the clinical use of the Absorb-BVS in 2015. In the ABSORB III, 2,008 patients with stable or unstable angina were randomly allocated to the Absorb-BVS (n=1,322) or the CoCr-EES arm (n=686) with a primary end point of a 4.5% margin of noninferiority for target-lesion failure (TLF; a composite of cardiac death, target-vessel MI or ischemia-driven target lesion revascularization [TLR]) at 1 year. The incidence of TLF between Absorb-BVS (7.8%) and CoCr-EES (6.1%) met the requirement for noninferiority (absolute difference of 1.7%, p<0.007)[19]. However, a meta-analysis involving six trials including 3,738 patients underwent PCI treatment with either an Absorb-BVS (n=2,337) or a CoCr-EES (n=1,401) showed higher rates of definite or probable stent thrombosis in the Absorb-BVS than CoCr-EES group (OR 1.99, 95% CI 1.00–3.98, p=0.05) in a median follow-up of 12 months[20]. The highest risk was found at 1–30 days after implantation (OR 3.11, 95% CI 1.24–7.82, p=0.02)[20]. The incidence of TVR was also relatively higher in the Absorb-BVS group (p=0.08)20. The 3 years result of ABSORB II trial involving 501 patients with myocardial ischemia and one-or two-vessel disease assigned for the treatment of either an Absorb-BVS (n=335) or a CoCr-EES (n=166) was presented in 2016[5]. The incidence of device-oriented composite end point (cardiac death, target-vessel MI, and clinically indicated TLR) was significantly higher in the Absorb-BVS *versus* the CoCr-EES (10.4% *vs.* 4.9%; HR 2.17, 95% CI 1.01–4.69, p=0.043)[5]. In March 2017, the AIDA clinical trial including 1845 patients undergoing PCI randomly allocated to receive either a Absorb-BVS (924 patients) or a metallic stent (921 patients) revealed significantly higher incidence of device-oriented definite/probable thrombosis in the Absorb-BVS than the CoCr-EES at a median follow-up of 707 days (2 years cumulative event rates of 3.5% *versus* 0.9%; HR 3.87, 95% CI 1.78–8.42, p<0.001)[6]. Subsequently, a meta-analysis of 2 years outcomes of seven randomized clinical trials showed significantly greater incidence of device-oriented outcomes (cardiac mortality, target-vessel-related MI and ischemia-driven TLR) and device thrombosis in Absorb-BVS than CoCr-EES[21]. Accordingly, clinical use of the Absorb-BVS never gained enough momentum to justify the costs of production, and Abbott Vascular withdrew this device from the market in September 2017. In 2019, Stone GW *et al.* reported the time-varying clinical outcomes with the Absorb-BVS for 5 years follow-up[22]. 3384 patients from four trials of Absorb-BVS *versus* CoCr-EES were included in this meta-analysis. Through 5-year follow-up, treatment with Absorb-BVS compared with CoCr-EES was associated with greater incidence of TLF (14.9% *vs.* 11.6%; HR 1.26, 95% CI 1.03-1.54, p=0.03) and device thrombosis (2.5% *vs.* 0.8%; HR 2.87, 95% CI 1.46-5.65, p=0.002). Between 0 to 3 years, greater incidence of TLF and device thrombosis were observed in Absorb-BVS *versus* CoCr-EES (TLF: 11.6% *vs.* 7.9%, HR 1.42, 95% CI 1.12-1.80, device thrombosis: 2.4% *vs.* 0.6%, HR 3.86, 95% CI 1.75-8.50). However, between 3 to 5 years, the outcomes of TLF and device thrombosis were comparable between two groups (TLF: 4.3% *vs.* 4.5%, HR 0.92, 95% CI 0.64-1.31, device thrombosis: 0.1% *vs.* 0.3%, HR 0.44, 95% CI 0.07-2.70)[22]. More recently, the final 5 years clinical outcome of AIDA trial was published[23]. Accordingly, there was no difference in TVF between Absorb-BVS *versus* CoCr-EES through 5 years (17.7% *vs.* 16.1%, HR 1.31, 95% CI 0.90-1.41, p=0.302). Overall incidence of definite/probable device thrombosis was greater in Absorb-BVS than CoCr-EES (4.8% [43 patients] *vs.* 1.5% [13 patients], HR 3.32, 95% CI 1.78-6.17, p<0.001). Between 3-to 4-years, device thrombosis occurred 6 in Absorb-BVS *versus* 3 in CoCr-EES. The incidence between 4-to 5-years was 3 in Absorb-BVS *versus* 2 in CoCr-EES (note 2/3 cases in Absorb-BVS occurred at the lesion treated with stent [CoCr-EES]-in-scaffold during index procedure). The authors concluded that the excess risk of Absorb-BVS on late adverse events, particularly device thrombosis, in routine PCI continues up to 4-years and seems to plateau afterwards[23].

Mechanisms of scaffold thrombosis

A multi-center observational study by Puricel *et al.* reported the causal relationship between the risk of scaffold thrombosis and inappropriate procedural techniques during device placement [24]. Appropriate implantation technique was proposed as a method to reduce scaffold thrombosis (*i.e.*, the concept of PSP; optimal pre-dilatation, vessel and device sizing, and post-dilatation) [25]. Nevertheless, based upon the inherent characteristics of the Absorb-BVS device, not all scaffold thrombosis can be prevented by adapting the proper device implantation technique and sizing (Figure 3). Prior clinical studies suggested different mechanisms for scaffold thromboses within and beyond 1 year. In cases of 1-year device implantation, thrombotic events were largely related to the thick strut device being placed into small vessels (reference vessel diameter <2.40mm) [26], whereas scaffold thromboses >1-year following deployment were mainly due to intraluminal scaffold dismantling caused by discontinuity of uncovered scaffold strut [27]. Sotomi *et al.* reported possible mechanisms of scaffold thrombosis from previously published imaging-based case reports including 43 cases of scaffold thrombosis (acute or subacute thrombosis, n=17; late or very late thrombosis, n=26) [28]. The most frequent cause in the acute and subacute thrombosis was malapposition (23.5%), followed by uncovered struts (17.6%), strut under-deployment (11.8%), acute scaffold disruption (5.9%), overlapping stents (5.9%) and acute scaffold recoil (5.9%). In the late or very late phases, strut malapposition remained the most common mechanism (34.6%), followed by late scaffold discontinuity (30.8%), peri-strut low-intensity areas (19.2%), uncovered or under-deployed struts (15.4%), incomplete lesion coverage or scaffold recoil (11.5%), restenosis (7.7%), neoatherosclerosis (3.8%) and bifurcation (3.8%). Yamaji and colleagues reported 36 cases (38 lesions) of very late scaffold thrombosis (median 20 [16-27] months) who underwent OCT evaluation during urgent revascularization at 19 centers [27]. The underlying mechanisms of very late scaffold thrombosis were scaffold discontinuity (42.1%), malapposition (18.4%), neoatherosclerosis (18.4%), under expansion or scaffold recoil (10.5%), uncovered struts (5.3%), and edge-related disease progression (2.6%) [27]. Although OCT has difficulties for detecting some of these phenomena (*e.g.*, mistaking struts with attached fibrin/thrombus as endothelialized covered struts), these findings suggest variety of the underlying pathologic mechanisms for scaffold thrombosis, made even more important because of the lack of large autopsy data. We briefly discuss each of the major causes of scaffold thrombosis as below.

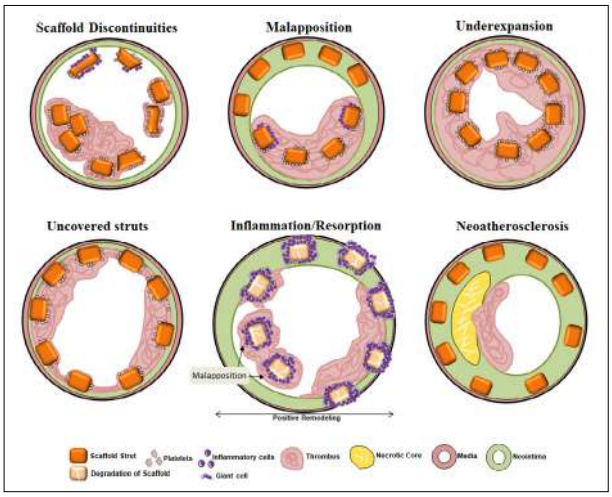

Figure 3: Mechanisms of very late scaffold thrombosis. The figure shows the most likely causes of scaffold thrombosis on the basis of clinical and preclinical studies: scaffold discontinuities, malapposition, underexpansion, uncovered struts, inflammation and neoatherosclerosis. *Reprinted from Jinnouchi H, et al. Nat Rev Cardiol. 2019;16:286-304.*

Scaffold discontinuity

Fracture or discontinuity of scaffold struts has been commonly reported in Absorb-BVS with increasing incidence over time after implantation (25% of lesions at 2 years and 42% at 3 years) [29]. Discontinuity does not mean the normal absorption process of the polymer, but the dismantling of the scaffold structure caused by the mechanical fragility. Once struts are covered by neointima, late scaffold disruption and disintegration may occur safely. In such case, the disrupted strut is trapped with surrounding tissues and has been isolated from circulating blood. However, if neointimal coverage of scaffold struts is delayed,

the fractured struts will protrude into the vessel lumen, causing blood-flow turbulence and generating a nidus for thrombus formation[28]. Preclinical studies of Absorb-BVS in healthy swine coronary arteries have shown multiple strut discontinuities observed at 3 and 6 months after implantation, especially assessed by micro-CT[30] (Figure 4). Scaffold discontinuities by micro-CT observation was found in 50% of the scaffolds at 3 month, which increased up to 100% at 6 month, with >10 discontinuities per scaffold[30]. According to the pharmacokinetics of Absorb-BVS scaffold polymer in healthy swine, approximately 20% of molecular weight loss occurs at 6 months by hydrolysis, and only <10% of mass loss of polymer is achieved at 6 months[10]. These data suggest that scaffold discontinuities seen at these time points are unrelated to the resorption process, because very little breakdown has occurred by then. Due to inherent biases of cross-sectional observation as well as the limited resolution of imaging, the incidence of scaffold disruption reported in OCT studies in humans and histological studies in pigs is much lower than that which we have observed in micro-CT studies in pigs. The advantage of micro-CT is that it allows the entire length and circumference of the stent to be examined by from different angles, something not possible by histology or OCT. Therefore, the likelihood of missing scaffold fractures is high in OCT-or histology-based studies.

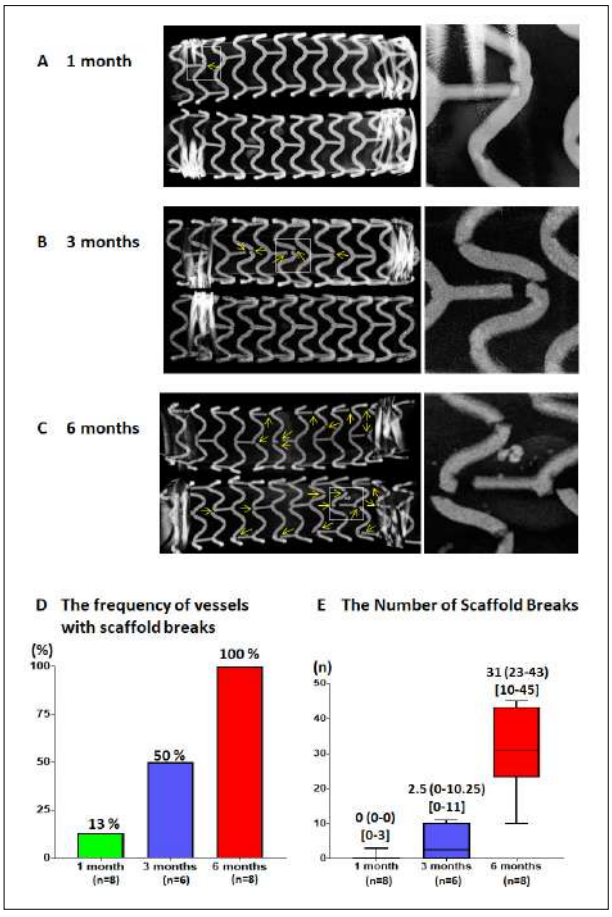

Figure 4: Micro-CT images after implantation of the Absorb-BVS in pig coronary arteries. The Absorb Bioresorbable Vascular Scaffold (Absorb-BVS; Abbott Vascular) was cut longitudinally, and both halves are shown in the images on the left, accompanied by corresponding high magnification images from the white boxed areas. Yellow arrows indicate scaffold discontinuities.

A: At 1 month after implantation, scaffold discontinuities were rarely observed.

B: At 3 months, the number of scaffold discontinuities had increased.

C: At 6 months, scaffold discontinuities were very frequent.

D: Bar graph showing the frequency of scaffold discontinuities detected with the use of micro-CT at 1 month, 3 months and 6 months after scaffold implantation. Discontinuities were observed in all vessels at 6 months.

E: Box plot graph showing the number of scaffold breaks detected with the use of micro-CT at 1 month, 3 months and 6 months after scaffold implantation. Data show the median (25–75% interquartile range) [minimum and maximum]. *Reprinted from Jinnouchi H, et al. Nat Rev Cardiol. 2019;16:286-304.*

Malapposition

Malapposition is one of the major causes of stent/scaffold thrombosis in view of local blood flow disturbance, increased thrombogenicity, as well as delayed endothelialization. Foin *et al.* revealed the positive correlation between the degree of flow disturbance around strut and the extent of malapposition (100–500μm) estimated by fluid dynamics model [31]. Pooled *in vivo* OCT data of human coronary artery at 6 month after DES implantation revealed full strut coverage with initial malapposition <100μm, however, malapposition of 100–300μm showed 6.1% uncovered struts, and malapposition of 300–500μm exhibited 13.7% uncovered struts, suggesting greater malapposition distance had a negative influence on the speed of strut coverage [31]. The impact of malapposition and uncovered struts would be much greater in Absorb-BVS than that of contemporary metallic DES [27,32]. Iannaccone and colleagues performed a meta-analysis of 13 studies using OCT to determine the incidence of uncovered struts, malapposition and the degree of neointimal coverage according to stent or scaffold type at 6–12 months of follow-up[33]. The Absorb-BVS showed the highest incidence of strut malapposition (3.8%), followed by biolimus-eluting stent (2.7%), sirolimus-eluting stent (2.1%), paclitaxel-eluting stent (2.2%), CoCr-EES (0.9%), first generation zotarolimus-eluting stent (0.1%) and BMS (0.1%). The higher incidence of malapposition with the Absorb-BVS suggested the requirement for longer duration of dual antiplatelet therapy in order to compensate for the much longer healing time. Additionally, relatively aggressive pre- and post-dilatation at the site of scaffold implantation might be performed to avoid incomplete strut expansion and malapposition. This procedure potentially causes greater arterial wall damage, exposing sub-endothelial collagen which initiates coagulation cascade via binding to platelet[34] and pro-coagulation tissue factor within the necrotic core [35] to blood stream. These device features and implantation procedures may directly and/or indirectly elevate the thrombogenicity at the site of scaffold.

Uncovered struts

Several factors affect the speed of endothelial struts coverage, *e.g.*, strut thickness, type of polymer, drug type and/or dose of anti-proliferative agent, extent of vessel injury, and type of underlying plaques. Strut thickness is one of the most important factors regarding disturbance of wall shear stress and blood flow dynamics [9,12]. Therefore, the strut thickness of Absorb-BVS (157 m) has an innate disadvantage for endothelialization. In the ABSORB-STEMI TROFI II OCT study involving patients with Absorb-BVS (n=95) and CoCr-EES (n=96) implantation, the rate of strut coverage at 6-month evaluated by OCT was equivalent between Absorb-BVS and CoCr-EES (99.4±1.0% *versus* 99.1±1.8%; p=0.27), with a favorable healing score in Absorb-BVS [36]. However, OCT studies have an inherent limitation for the assessment of strut coverage, *i.e.*, OCT may not distinguish neointima from surface fibrin or thrombus, the two hallmarks of delayed and incomplete healing. Given the thick struts of Absorb-BVS, it is hard to understand how neointimal coverage and healing could have been equivalent or superior to that with the CoCr-EES. In our preclinical experiments in rabbits, delayed neointimal coverage of the Absorb-BVS was obvious over SYNERGY (*i.e.* a thin-strut metallic DES) stents at both 28 and 120 days post-implantation [30]. Since the healing of healthy animal vessels are much faster than diseased human artery, delayed healing at 120 days in normal rabbit artery suggesting the full strut coverage at 6 months after implantation of Absorb-BVS in patients with atherosclerotic disease seems difficult.

Inflammation

During the degradation process and biological reaction against an implanted foreign material, an inflammatory reaction is provoked after BRS implantation. Infiltration of macrophages, giant cells and lymphocytes occurs during the normal resorption process and is usually limited to areas surrounding the struts. Histological study of swine revealed that inflammation with the Absorb-BVS peaks at 12 months

post-implantation and stays higher than that with the CoCr-EES at a time when positive remodeling of the vessel wall occurs. Nevertheless, our knowledge for the feature of the inflammatory response to Absorb-BVS in human coronary artery is quite limited because, at present, only a small number of cases with histological evidence have been reported. Raber L *et al.* previously reported four thrombus aspirates of Absorb-BVS scaffold thrombosis [37]. Inflammation, especially the presence of giant cells, was observed around the strut of scaffold at 113 days after implantation, with focal strut coverage by smooth muscle cells in one of the four autopsy cases. In addition, two of the four patients who presented with thrombosis at 19 months after implantation also showed areas of inflammation and platelet-rich thrombus around the scaffold. Thus, inflammation and fibrin deposition around struts could be another mechanism of late scaffold thrombosis in Absorb-BVS.

Late acquired coronary evagination between strut, reviously highlighted as a risk factor for late stent thrombosis in 1st-generation DES, was also reported in patients receiving Absorb-BVS. Gori *et al.* analyzed the OCT and angiographic follow-up data of 90 cases (102 scaffolds) who underwent Absorb-BVS implantation [38]. The result showed more than half (54%) of the Absorb-BVS cases had at least 1 or more evaginations at 12-months follow-up and evaginations were strongly associated with the presence of malapposition and strut fracture. Also, 18% of cases showed peri-strut contrast staining. Since evagination and peri-strut contrast staining in 1st-generation DES were thought to result from a chronic inflammatory response, this finding suggested that Absorb-BVS potentially causes inflammatory reaction during polymer degrading process. Although this device is no longer commercially available, patients with Absorb-BVS implantation need to be carefully followed up.

Neoatherosclerosis

Is was expected for Absorb-BVS that at the end of degradation the vessel would return to its native state with preserved vasomotion/vasodilation resulting in protection from neoatherosclerosis. However, imaging-based observations have already been reported the presence of neoatherosclerosis in Absorb-BVS implanted site. In the INVEST registry, which included cases of very late scaffold thrombosis, a 28% incidence of neoatherosclerotic changes in neointimal tissue was reported at a median of 4.7 years [27]. Moriyama and colleagues reported 5-year follow-up OCT data of Absorb-BVS in 20 patients (22 lesions)[39]. At 1 and 5 years serial OCT follow-up, significant differences in the prevalence of in-scaffold lipid-laden neointima (17% *versus* 61%; p=0.04), calcification (28% *versus* 94%; p<0.01), neovascularization (6% *versus* 78%; p<0.01), and thin-cap fibroatheroma (0% *versus* 22%; p=0.02) were observed. On the other hand, no significant differences in plaque prevalence between 1 and 5 years was found in native vessel segment [39]. Although the number of cases was relatively small, this serial observation gives us important insights into the short-and long-terms biologic response to Absorb-BVS. The development of neoatheroscrerosis in Absorb-BVS segment is not surprising because augmentation of vascular endothelial permeability by anti-prolirefative agent (*e.g.*, rapamycin or its analogues) is a key pathophysiologic change for the development of neoatherosclerosis [40]. In-scaffold neoatherosclerosis should be considered as a potential cause of late scaffold failure events and long-term follow-up should be conducted in patients receiving BRS implantation.

Vasomotion after complete degradation of biodegradable scaffold

One of the anticipated benefits of Absorb-BVS was the return of endothelium-dependent coronary vasomotion which is linked to vascular health. Several early small clinical trials suggested recovery of endothelium-dependent vasomotion in patients who underwent Absorb-BVS implantation for stable coronary disease, which assessed by acetylcholine intra-coronary acetylcholine infusion at 1 and 2 year after deployment [41-43]. However, at 3-year follow-up of the ABSORBII, no difference of vasoreactivity between Absorb-BVS and CoCr-EES was observed [5]. Four-year follow-up of this cohort did not report

the results of acetylcholine-derived vasodilatation [44]. Furthermore, sub-analysis data of TROFI II trial at 3 years comparing the performance of Absorb-BVS *versus* CoCr-EES in patients with ST-segment elevation MI did not show any benefit of Absorb-BVS regarding endothelium-dependent vasoreactivity[45]. Furthermore in preclinical models Absorb-BVS showed lack of return of healthy endothelium-dependent vasoreactivity. To justify what is likely to be their higher cost, clear-cut benefit in endpoints such as long-term vasomotion with Absorb-BVS need to be shown.

Next generation of BRS and future perspectives

For generating ideal BRS, further innovation in material and design need to be achieved. To date, several bioabsorbable scaffolds based on polymers are in development (Table 1). All of currently developing polymer BRS are limus-eluting scaffolds. In order for polymer based BRS to be successful, a reduction of the strut profile while maintaining radial strength needs to be demonstrated in order to overcome the above mentioned shortages observed in Absorb-BVS.

The most widely used materials for BRS are polymers such as PLLA, however, bioerodible metallic alloys are also anticipated material for ideal BRS and being investigated. One of the most advanced systems is the magnesium resorbable scaffold and Magmaris (Biotronik). Magmaris is composed of a magnesium-based alloy which has low elastic recoil, minimal shortening after inflation, and high collapse pressure with the ability of complete degradation by 12 months [46]. In BIOSOLVE-II and III clinical trials, comparable outcomes between Magmaris and 2nd generation DES was demonstrated low rates of TLF (6.4%) and clinically-driven revascularization (3.7%) at 36 months follow-up without any stent thrombosis events [47]. BIOSOLVE-IV trial, a large-scale international registry including 1075 patients, is now ongoing and 12- and 24-month TLF were reported as 4.3% and 6.6%, respectively [48,49]. At present, no increase in scaffold thrombosis between 12-month and 24-month follow up was reported. The follow up will be continued for 5 years. The strut thickness of Magmaris (150μm) is similar to Absorb-BVS, however, our group previously reported, in the *ex vivo* porcine AV-shunt model, that Magmaris has higher thromboresistance as compared to Absorb-BVS and thin-strut Osiro DES (strut thickness, 60μm) (Biotronik) [50]. Currently, 3rd generation magnesium-based BRS (DREAMS 3G, Biotronik) with thinner strut than Magmaris (99μm [2.5mm diameter], 117μm [3.0-3.5mm diameter], and 147μm [4.0mm diameter]) is ready to start clinical trials and first-in-man study BIOMAG-1 (NCT 04157153) is now enrolling patients [51]. Further studies are desired to confirm the feasibility of magnesium-based BRS for short-and long-term clinical outcomes.

Conclusion

BRS technology is potentially able to improve long-term clinical outcomes by complete platform resorption after implantation. However, our initial experience of Absorb-BVS told us that further innovation of material and strut design (*i.e.*, thinner strut with optimal degradation profiles maintaining initial radial strength) is indispensable to establish this technology in a clinical setting. In this regard, currently new magnesium based BRS and newer generation PLLA-based BRSs are on the way to development. Further efforts to generate ideal BRS are essential for improving clinical outcomes of PCI treatment.

References

1. Dai H, Much AA, Maor E, Asher E, Younis A, Xu Y, *et al.* Global, regional, and national burden of ischemic heart disease and its attributable risk factors, 1990-2017: Results from the global burden of disease study 2017. *Eur Heart J Qual Care Clin Outcomes* 2020: qcaa076

2. Serruys PW, Garcia-Garcia HM, Onuma Y. From metallic cages to transient bioresorbable scaffolds: Change in paradigm of coronary revascularization in the upcoming decade? *Eur Heart J* 2012; 33: 16-25b.

3. Nakazawa G, Otsuka F, Nakano M, Vorpahl M, Yazdani SK, Ladich E, *et al.* The pathology of neoatherosclerosis in human coronary implants bare-metal and drug-eluting stents. *J Am Coll Cardiol* 2011; 57: 1314-22.

4. Bønaa KH, Mannsverk J, Wiseth R, Aaberge L, Myreng Y, Nygård O, *et al.* Drug-eluting or bare-metal stents for coronary artery disease. *N Engl J Med* 2016; 375: 1242-52.

5. Serruys PW, Chevalier B, Sotomi Y, Cequier A, Carrié D, Piek JJ, *et al.* Comparison of an everolimus-eluting bioresorbable scaffold with an everolimus-eluting metallic stent for the treatment of coronary artery stenosis (absorb ii): A 3 year, randomised, controlled, single-blind, multicentre clinical trial. *Lancet* 2016; 388: 2479-91.

6. Wykrzykowska JJ, Kraak RP, Hofma SH, van der Schaaf RJ, Arkenbout EK, AJ IJ, *et al.* Bioresorbable scaffolds *versus* metallic stents in routine pci. *N Engl J Med* 2017; 376: 2319-28.

7. Onuma Y, Serruys PW. Bioresorbable scaffold: The advent of a new era in percutaneous coronary and peripheral revascularization? *Circulation* 2011; 123: 779-97.

8. Ormiston JA, Webber B, Ubod B, Darremont O, Webster MW. An independent bench comparison of two bioresorbable drug-eluting coronary scaffolds (absorb and desolve) with a durable metallic drug-eluting stent (ml8/xpedition). *EuroIntervention* 2015; 11: 60-7.

9. Simon C, Palmaz JC, Sprague EA. Influence of topography on endothelialization of stents: Clues for new designs. *J Long Term Eff Med Implants* 2000; 10: 143-51.

10. Otsuka F, Pacheco E, Perkins LE, Lane JP, Wang Q, Kamberi M, *et al.* Long-term safety of an everolimus-eluting bioresorbable vascular scaffold and the cobalt-chromium xience v stent in a porcine coronary artery model. *Circ Cardiovasc Interv* 2014; 7: 330-42.

11. Lane JP, Perkins LE, Sheehy AJ, Pacheco EJ, Frie MP, Lambert BJ, *et al.* Lumen gain and restoration of pulsatility after implantation of a bioresorbable vascular scaffold in porcine coronary arteries. *JACC Cardiovasc Interv* 2014; 7: 688-95.

12. LaDisa JF, Jr., Olson LE, Douglas HA, Warltier DC, Kersten JR, Pagel PS. Alterations in regional vascular geometry produced by theoretical stent implantation influence distributions of wall shear stress: Analysis of a curved coronary artery using 3d computational fluid dynamics modeling. *Biomed Eng Online* 2006; 5: 40.

13. Kolandaivelu K, Swaminathan R, Gibson WJ, Kolachalama VB, Nguyen-Ehrenreich KL, Giddings VL, *et al.* Stent thrombogenicity early in high-risk interventional settings is driven by stent design and deployment and protected by polymer-drug coatings. *Circulation* 2011; 123: 1400-09.

14. Koppara T, Cheng Q, Yahagi K, Mori H, Sanchez OD, Feygin J, *et al.* Thrombogenicity and early vascular healing response in metallic biodegradable polymer-based and fully bioabsorbable drug-eluting stents. *Circ Cardiovasc Interv* 2015; 8:e 002427.

15. Jiménez JM, Davies PF. Hemodynamically driven stent strut design. *Ann Biomed Eng* 2009; 37: 1483-94.

16. Palmaz JC, Bailey S, Marton D, Sprague E. Influence of stent design and material composition on procedure outcome. *J Vasc Surg* 2002; 36: 1031-9.

17. Onuma Y, Serruys PW, Ormiston JA, Regar E, Webster M, Thuesen L, *et al.* Three-year results of clinical follow-up after a bioresorbable everolimus-eluting scaffold in patients with de novo coronary artery disease: The absorb trial. *EuroIntervention* 2010; 6: 447-53.

18. Serruys PW, Onuma Y, Ormiston JA, de Bruyne B, Regar E, Dudek D, *et al.* Evaluation of the second generation of a bioresorbable everolimus drug-eluting vascular scaffold for treatment of de novo coronary artery stenosis: Six-month clinical and imaging outcomes. *Circulation* 2010; 122: 2301-12.

19. Ellis SG, Kereiakes DJ, Metzger DC, Caputo RP, Rizik DG, Teirstein PS, *et al.* Everolimus-eluting bioresorbable scaffolds for coronary artery disease. *N Engl J Med* 2015; 373: 1905-15.

20. Cassese S, Byrne RA, Ndrepepa G, Kufner S, Wiebe J, Repp J, *et al.* Everolimus-eluting bioresorbable vascular scaffolds *versus* everolimus-eluting metallic stents: A meta-analysis of randomised controlled trials. *Lancet* 2016; 387: 537-44.

21. Ali ZA, Serruys PW, Kimura T, Gao R, Ellis SG, Kereiakes DJ, *et al.* 2-year outcomes with the absorb bioresorbable scaffold for treatment of coronary artery disease: A systematic review and meta-analysis of seven randomised trials with an individual patient data substudy. *Lancet* 2017; 390: 760-72.

22. Stone GW, Kimura T, Gao R, Kereiakes DJ, Ellis SG, Onuma Y, *et al.* Time-varying outcomes with the absorb bioresorbable vascular scaffold during 5-year follow-up: A systematic meta-analysis and individual patient data pooled study. *JAMA Cardiol* 2019; 4: 1261-9.

23. Kerkmeijer LSM, Renkens MPL, Tijssen RYG, Hofma SH, van der Schaaf RJ, Arkenbout KE, *et al.* Long-term clinical outcomes of everolimus-eluting bioresorbable scaffolds *versus* everolimus-eluting stents: Final 5-year results of the aida randomized clinical trial. *EuroIntervention* 2021; EIJ-D-21-00419.

24. Puricel S, Cuculi F, Weissner M, Schmermund A, Jamshidi P, Nyffenegger T, *et al.* Bioresorbable coronary scaffold thrombosis: Multicenter comprehensive analysis of clinical presentation, mechanisms, and predictors. *J Am Coll Cardiol* 2016; 67: 921-31.

25. Ortega-Paz L, Capodanno D, Gori T, Nef H, Latib A, Caramanno G, *et al.* Predilation, sizing and post-dilation scoring in patients undergoing everolimus-eluting bioresorbable scaffold implantation for prediction of cardiac adverse events: Development and internal validation of the psp score. *EuroIntervention* 2017; 12: 2110-7.

26. Ellis SG, Steffenino G, Kereiakes DJ, Stone GW, van Geuns RJ, Abizaid A, *et al.* Clinical, angiographic, and procedural correlates of acute, subacute, and late absorb scaffold thrombosis. *JACC Cardiovasc Interv* 2017; 10: 1809-15.

27. Yamaji K, Ueki Y, Souteyrand G, Daemen J, Wiebe J, Nef H, *et al.* Mechanisms of very late bioresorbable scaffold thrombosis: The invest registry. *J Am Coll Cardiol* 2017; 70: 2330-44.

28. Sotomi Y, Suwannasom P, Serruys PW, Onuma Y. Possible mechanical causes of scaffold thrombosis: Insights from case reports with intracoronary imaging. *EuroIntervention* 2017; 12: 1747-56.

29. Onuma Y, Serruys PW, Muramatsu T, Nakatani S, van Geuns RJ, de Bruyne B, *et al.* Incidence and imaging outcomes of acute scaffold disruption and late structural discontinuity after implantation of the absorb everolimus-eluting fully bioresorbable vascular scaffold: Optical coherence tomography assessment in the absorb cohort b trial (a clinical evaluation of the bioabsorbable everolimus eluting coronary stent system in the treatment of patients with de novo native coronary artery lesions). *JACC Cardiovasc Interv* 2014; 7: 1400-11.

30. Jinnouchi H, Torii S, Sakamoto A, Kolodgie FD, Virmani R, Finn AV. Fully bioresorbable vascular scaffolds: Lessons learned and future directions. *Nat Rev Cardiol* 2019; 16: 286-304.

31. Foin N, Gutiérrez-Chico JL, Nakatani S, Torii R, Bourantas CV, Sen S, *et al.* Incomplete stent apposition causes high shear flow disturbances and delay in neointimal coverage as a function of strut to wall detachment distance: Implications for the management of incomplete stent apposition. *Circ Cardiovasc Interv* 2014; 7: 180-9.

32. Onuma Y, Sotomi Y, Shiomi H, Ozaki Y, Namiki A, Yasuda S, *et al.* Two-year clinical, angiographic, and serial optical coherence tomographic follow-up after implantation of an everolimus-eluting bioresorbable scaffold and an everolimus-eluting metallic stent: Insights from the randomised absorb japan trial. *EuroIntervention* 2016; 12: 1090-101.

33. Iannaccone M, D'Ascenzo F, Templin C, Omedè P, Montefusco A, Guagliumi G, *et al.* Optical coherence tomography evaluation of intermediate-term healing of different stent types: Systemic review and meta-analysis. *Eur Heart J Cardiovasc Imaging* 2017; 18: 159-66.

34. Lippi G, Franchini M, Targher G. Arterial thrombus formation in cardiovascular disease. *Nat Rev Cardiol* 2011; 8: 502-12.

35. Toschi V, Gallo R, Lettino M, Fallon JT, Gertz SD, Fernández-Ortiz A, *et al.* Tissue factor modulates the thrombogenicity of human atherosclerotic plaques. *Circulation* 1997; 95: 594-9.

36. Sabaté M, Windecker S, Iñiguez A, Okkels-Jensen L, Cequier A, Brugaletta S, *et al.* Everolimus-eluting bioresorbable stent *vs.* Durable polymer everolimus-eluting metallic stent in patients with st-segment elevation myocardial infarction: Results of the randomized absorb st-segment elevation myocardial infarction-trofi ii trial. *Eur Heart J* 2016; 37: 229-40.

37. Räber L, Brugaletta S, Yamaji K, O'Sullivan CJ, Otsuki S, Koppara T, *et al.* Very late scaffold thrombosis: Intracoronary imaging and histopathological and spectroscopic findings. *J Am Coll Cardiol* 2015; 66: 1901-14.

38. Gori T, Jansen T, Weissner M, Foin N, Wenzel P, Schulz E, *et al.* Coronary evaginations and peri-scaffold aneurysms following implantation of bioresorbable scaffolds: Incidence, outcome, and optical coherence tomography analysis of possible mechanisms. *Eur Heart J* 2016; 37: 2040-9.

39. Moriyama N, Shishido K, Tanaka Y, Yokota S, Hayashi T, Miyashita H, *et al.* Neoatherosclerosis 5 years after bioresorbable vascular scaffold implantation. *J Am Coll Cardiol* 2018; 71: 1882-93.

40. Habib A, Karmali V, Polavarapu R, Akahori H, Cheng Q, Pachura K, *et al.* Sirolimus-fkbp12.6 impairs endothelial barrier function through protein kinase c-α activation and disruption of the p120-vascular endothelial cadherin interaction. *Arterioscler Thromb Vasc Biol* 2013; 33: 2425-31.

41. Serruys PW, Onuma Y, Dudek D, Smits PC, Koolen J, Chevalier B, *et al.* Evaluation of the second generation of a bioresorbable everolimus-eluting vascular scaffold for the treatment of de novo coronary artery stenosis: 12-month clinical and imaging outcomes. *J Am Coll Cardiol* 2011; 58: 1578-88.

42. Serruys PW, Ormiston JA, Onuma Y, Regar E, Gonzalo N, Garcia-Garcia HM, *et al.* A bioabsorbable everolimus-eluting coronary stent system (absorb): 2-year outcomes and results from multiple imaging methods. *Lancet* 2009; 373: 897-910.

43. Brugaletta S, Heo JH, Garcia-Garcia HM, Farooq V, van Geuns RJ, de Bruyne B, *et al.* Endothelial-dependent vasomotion in a coronary segment treated by absorb everolimus-eluting bioresorbable vascular scaffold system is related to plaque composition at the time of bioresorption of the polymer: Indirect finding of vascular reparative therapy? *Eur Heart J* 2012; 33: 1325-33.

44. Chevalier B, Cequier A, Dudek D, Haude M, Carrie D, Sabaté M, *et al.* Four-year follow-up of the randomised comparison between an everolimus-eluting bioresorbable scaffold and an everolimus-eluting metallic stent for the treatment of coronary artery stenosis (absorb ii trial). *EuroIntervention* 2018; 13: 1561-4.

45. Gomez-Lara J, Brugaletta S, Ortega-Paz L, Vandeloo B, Moscarella E, Salas M, *et al.* Long-term coronary functional assessment of the infarct-related artery treated with everolimus-eluting bioresorbable scaffolds or everolimus-eluting metallic stents: Insights of the trofi ii trial. *JACC Cardiovasc Interv* 2018; 11: 1559-71.

46. Campos CM, Muramatsu T, Iqbal J, Zhang YJ, Onuma Y, Garcia-Garcia HM, *et al.* Bioresorbable drug-eluting magnesium-alloy scaffold for treatment of coronary artery disease. *Int J Mol Sci* 2013; 14: 24492-500.

47. Haude M, Ince H, Kische S, Abizaid A, Toelg R, Lemos P, *et al.* Tct-188 safety and clinical performance of the drug-eluting absorbable metal scaffold in the treatment of subjects with de novo lesions in native coronary arteries at 36-month follow-up: Biosolve-ii and biosolve-iii. *Transcatheter Cardiovascular Therapeutics (TCT)* 2019; 92: E502–E511.

48. Verheye S, Wlodarczak A, Montorsi P, Torzewski J, Bennett J, Haude M, *et al.* Biosolve-iv-registry: Safety and performance of the magmaris scaffold: 12-month outcomes of the first cohort of 1,075 patients. *Catheter Cardiovasc Interv* 2021; 98: E1-E8.

49. Tozewski J. Safety and performance of magmaris at 24-month follow-up of biosolve-iv. virtual EuroPCR 2021.

50. Waksman R, Lipinski MJ, Acampado E, Cheng Q, Adams L, Torii S, *et al.* Comparison of acute thrombogenicity for metallic and polymeric bioabsorbable scaffolds: Magmaris *versus* absorb in a porcine arteriovenous shunt model. *Circ Cardiovasc Interv* 2018; 10: e004762.

51. Forrestal B, Case BC, Yerasi C, Musallam A, Chezar-Azerrad C, Waksman R. Bioresorbable scaffolds: Current technology and future perspectives. *Rambam Maimonides Med J* 2020; 11: e0016.

Is there a future for polymeric braided stents?

16

Saber Ben ABDESSALEM, Hiba JAZIRI, Sofiene MOKHTAR, Frédéric HEIM, Nabil CHAKFÉ

Polymeric stents were developed as an alternative to replace commercial metallic ones presenting several failures caused especially by the used metals. Among those materials, the polyethylene terephthalate (PET) have been used to develop stents since PET is suitable for several biomedical uses such as vascular prosthesis. Braiding technique was used since it provides flexible structures. In this review, the different studies held about polymeric non-biodegradable stents are summarized for comparison purposes. Then the methods and materials for the development and characterization of PET braided stents were given and the main results were highlighted. Results bring out that PET braided stents show very promising structural and mechanical performances comparing to metallic stents. They guarantee in particular a good flexibility and stability to cyclic loadings predicting their long-term behavior. As a conclusion, PET-braided vascular stents show a huge potential to replace commercial stents but their manufacturing parameters should be carefully chosen.

Introduction

Despite advances in cardiovascular stent materials and designs to decrease post-deployment complications, starting from the "Wallstent" implanted in 1986[1] until today, problems such as corrosion, structural failure and fractures causing inflammation, early thrombosis and in-stent re-stenosis are still existing[2,3-7].

These complications are mainly due to the metallic material used as well as to the structure itself, more precisely, to a poor tolerance of the organism to their long-term presence, to an excessive rigidity causing a high mechanical stress on the vessel wall, to a lack of flexibility especially in tortuous arteries or to a low resistance to fatigue caused by *in vivo* cyclic displacements due to the blood flow, etc. For this, stents are classified by the European authorities as the most implantable medical devices showing important risks of local and general complications after implantation.

Research is advancing on all fronts, especially towards the use of other materials. Among the solutions that could be promising in reducing complications related to commercial stents, several research groups developed and characterized polymeric vascular stents, braided or knitted, using non-biodegradable polymers such as polyethylene terephthalate (PET), polypropylene (PP), polyurethane (PUR), polyamide (PA), etc.[6,8-12]. From the results, PET-braided stents are found to be the best candidates to replace metallic stents.

This study gives a review about polymeric non-biodegradable stents, and then summarizes and discusses the main findings about PET-braided vascular stents.

Materials and Methods

A literature review was performed in order to compare between findings of the different studies held about non-biodegradable polymeric stents. First of all, we should point on the main problems encountered with commercial stents.

Weaknesses of commercial stents

Bare metallic stents (BMS) have been largely used over the last decades to treat successfully vascular diseases like stenosis. Generally, 316L stainless steel and Nitinol Ni-Ti alloy stents are the most common commercial ones. 316L stainless steel is used because it is cheap and easily processed [13] and Nitinol is well known for its shape memory effect and flexibility which is 10 to 20 times greater than stainless steel [2].

Although metallic stents remain the gold standard for vascular treatment, they are subjected to chemical and mechanical fatigue inducing *in vivo* complications after a certain time of implantation. Studies have proved the possibility of immunologic reactions of the host tissues to the significant release of metallic ions [5, 14]. Corrosion, fretting wear and fracture have been also found in metallic stents [14]. In fact, due to *in vivo* cyclic displacements, some Nitinol self-expanding stents showed fracture occurrences of up to 50% after one year especially on the superficial femoral artery [4]. Moreover, deformations have been observed in stainless steel stents due to the lack of flexibility [2].

Metallic Drug Eluting Stents (DES) were then developed in order to reduce early in-stent restenosis rates found in BMS. However, they have shown increased stent thrombosis and endothelial dysfunction when compared with BMS [15]. Also, they could delay healing of the vascular wall, which have raised concerns about the long-term safety [16].

Currently, bioresorbable stents are under development to reduce complications of previous stents. Bioresorbable polymeric stents (BRS) [15] and biodegradable magnesium alloy stents (BMgS) were developed, with the idea that they would gradually disappear after providing healing of the arterial wall. Multiple clinical trials confirmed an increased rate of thrombosis and myocardial infarctions with BRS [17,18]. Observations report that BRS problems may be partially explained by relatively weak bioresorbable polymer material, low radial strength leading to strut disruption [17], asymmetric material degradation from local stress concentration and microstructural damage from stent crimping and implantation. Magnesium alloys offer superior mechanical properties and uniform degradation behavior to polymeric materials. However, they are prone to the same asymmetric strains and degradation introduced by crimp[18].

Towards non-biodegradable polymeric stents

Several research studies have been carried out with the aim of avoiding the complications encountered with commercial vascular stents in use today. According to the literature, the development of non-biodegradable polymeric stents is one of the most promising avenues. Indeed, synthetic non-biodegradable polymers used for medical purposes have proven their effectiveness in various medical applications (vascular prosthesis, sutures, artificial ligaments, etc.) thanks to their interesting properties, namely good biocompatibility, the possibility of modifying their composition and their physical and mechanical properties, their low friction coefficients, the possibility of modifying their surface chemically or physically, etc. Furthermore, they do not cause carcinogenicity, immunogenicity, teratogenicity or toxicity. In addition, polymers are less rigid than metallic materials, which would limit the long-term stress exerted on the vessel wall, and consequently reduce the risk of restenosis.

In this axis, several research groups have studied the potential of non-biodegradable polymeric stents, braided or knitted, in polyethylene terephthalate (PET) [6, 8 - 10, 19], in polypropylene (PP) [6, 11], polyurethane (PUR) [12, 20] and polyamide PA [6]. These studies are summarized in Table 1.

Table 1: Studies reporting the development of non-biodegradable polymeric vascular stents.

Authors	Year	Material and technique used
Van der Giessen *et al.* [8]	1992	PET-braided stent for coronary arteries.
Irsale and Adanur [9]	2006	PET-braided stents, tubular for the coronary arteries and bifurcated for the aneurysm.
Yuksekkaya and Adanur [10]	2009	PET-braided stents.
Schreiber *et al.* [12]	2010	PUR-braided stent.
Freitas *et al.* [11]	2010	PP braided and knitted stents for coronary arteries.
Singh and Wang [20]	2015	Knitted stent composed of elastic parts in PUR and rigid parts in PET.
Rebelo *et al.* [6]	2015	PET, PA and PP braided stents for coronary arteries.
Jaziri *et al.* [19]	2019	PET-braided stents for peripheral arteries.

After the analysis of the results described by these studies, we can conclude that braiding technique and PET polymer are the most suitable to develop non-biodegradable vascular stents. In fact, braided stents had the best results in terms of dimensional stability, lateral strength and recovery of the original shape than knitted stents [11]. In addition, the most significant disadvantage of knitted stents is the difficulty of their removal from the human body. When placed in an organ, it is difficult to bend and remove the dilated knitted stent [21]. Singh and Wang [20] also developed a knitted stent composed of elastic parts in PUR and rigid parts in PET in order to improve their mechanical behavior. However, the problem detected when using PUR is that it has shown phenomena that should be minimized, namely relaxation and creep stresses. Also, because of its mechanical properties much lower than those of Nitinol, PUR must be used with thicker fibers [6]. Rebelo *et al.* [6] demonstrated that PET braided stent showed better mechanical performances than PA and PP stents, comparable to those of commercial Nitinol stents.

For all these reasons, we will focus on the materials and methods used to develop and characterize PET-braided stents.

Development of PET-braided vascular stents

The objective is to develop PET braided vascular stents able to replace metallic stents in use today and able to maintain the integrity of their structure and physical and mechanical properties in short and long term.

Braided stents were manufactured using a vertical or horizontal braiding machine. The possible braiding parameters to vary in order to obtain the ideal stent design are the wire (monofilament) diameter, the stent internal diameter (or more precisely the mandrel diameter which is a cylindrical support for the produced braid), the braiding angle, the braiding pattern and the number of wires in the braid. After braiding, PET stents should be stabilized in a heat-setting machine in order to fix the filament helical geometry in the stent.

Evaluation of stents key performances

In order to compete with commercial stents, PET-braided stents should meet certain criteria. They should have the capacity to support the arterial wall while avoiding all the risks and complications encountered with commercial stents. In fact, they have to be enough flexible, elastic, resistant to radial and longitudinal compression and fairly stable structurally and mechanically over the whole period of its implantation. Table 2 summarizes the key performances to be assessed.

Table 2: Stents main performances and their *in vitro* assessment methods.

Studied performance	Measurement method	Measured characteristic
Ability to adapt to the anatomy of the implantation site and uniformity of the stent	Cover factor calculation [6]	Cover factor
Flexibility	3 points bending test, *(ASTM F2606-08)* Measurement of the bending diameter [6]	Bending force Bending stiffness Percentage of unchanged bending diameter
Crush resistance	Compression between parallel plates test *(ISO 25539-2:2012)*	Lateral compression force
Resistance to longitudinal compression	Longitudinal compression test [22]	Longitudinal compression force
Elongation	Longitudinal elongation test [22]	Elongation Longitudinal rigidity
Resistance to radial compression	Static and dynamic radial compression tests *(ASTM F3067–14)*	Static and dynamic maximal radial forces Percentage of radial force change after dynamic compression Percentage of the diameter's elastic recovery
Fatigue resistance	Accelerated fatigue test	Percentage of radial force loss after fatigue Percentage of the diameter's elastic recovery after fatigue

The cover factor $CF_{\%}$ of a vascular stent is defined as the ratio between the stent area covered by the material used and the total stent area [6,23]. In other words, it is the amount of fibrous material deposited on the surface of the mandrel during the braiding operation. Vascular stents should have a cover factor between 20 and 30 % (*i.e.*, porosity of approximately 70-80 %) [24,25] to minimize surface thrombosis [26]. The $CF_{\%}$ is calculated as follows:

$$\mathbf{CF\%} = \left[\, \mathbf{1} - \left(\mathbf{1} - \frac{\emptyset_f \, \mathbf{N}}{\mathbf{2\pi}\, \emptyset_s \, \mathbf{cos\alpha}}\right)^{\mathbf{2}} \right] \times \mathbf{100} \qquad \textbf{Eq.1}$$

With: $Ø_f$: Monofilament diameter (mm) ; N : Number of wires ; α : Braiding angle (°) : It represents the angle between the wires and the longitudinal axis of the braided structure [6] and measured by image processing (Figure 1).

Flexibility is one of the main performances for vascular stents since they could be subjected to bending actions, especially when implanted in the peripheral arteries [27-29]. For this, they must show a minimum bending stiffness which is measured via a three-point bending test *(ASTM F2606-08)* (Figure 2A), and they must have the ability to maintain at least 75% of the original diameter when flexed [6, 30]. For that, the percentage of the unchanged bending diameter is calculated as the ratio between the diameter at the midpoint of the bent section (Figure 2B) and the initial stent diameter.

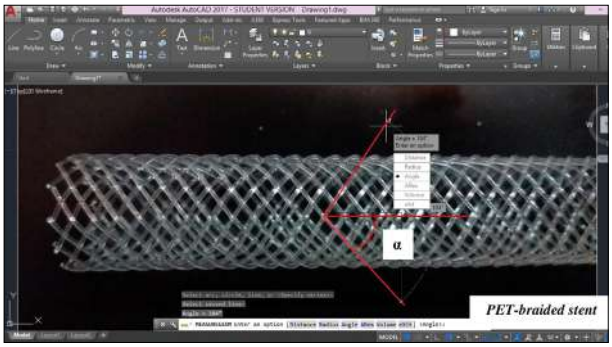

Figure 1: PET-braided stent showing the braiding angle α.

The lateral compression strength should be sufficient to prevent the stent crush after implantation, so in order to measure it, a lateral compression between plates test is performed *(ISO 25539-2:2012)* (Figure 2C). In addition, stents should be resistant to longitudinal compression otherwise they will be easily compressed at their ends and should be elastic enough. For purpose, longitudinal compression and extension tests were performed according to recommendations of *"GoreMedical®"* [22] (Figure 2D.E).

Additionally, the radial compression behavior should be assessed in particular the radial force and the diameter's elastic recovery. In fact, the radial force is the load the stent can sustain before permanent deformation occurs or the stent is completely destroyed [13]. Furthermore, every stent should recover 100% of its initial diameter after radial loading. For those reasons, a radial compression test using a dedicated radial compression machine is performed *(ASTM F3067–14)* (Figure 2F). The long term behavior of PET-braided stents could be predicted by performing a dynamic radial compression test and an *in vitro* axial fatigue test (Figure 2F.G).

Figure 2: Characterization methods: **(A)** Three points bending test **(B)** Unchanged bending diameter measurement **(C)** Parallel plates compression test **(D)** longitudinal compression test **(E)** Elongation test **(F)** Radial compression test **(G)** Accelerated fatigue test.

Results and Discussion

All studies about PET-braided stents have demonstrated the huge influence of the braiding parameters on the stents performances [6, 9, 10, 19, 31]. The cover factor of PET-braided stents is an important parameter that must be taken into account when designing the stent [10] and could be in the same range as the metallic braided stents if the braiding parameters were chosen correctly [6, 19]. Jaziri *et al.* [19], developed a PET stent having a cover factor of 35 %, larger than what is obtained for a metallic braid (20%) used as reference in order to have similar radial strength. Actually, polymer material being less stiff than Nitinol, it is necessary to increase the quantity of material involved in the braid to obtain a similar radial strength. For that purpose, it is necessary to increase either the diameter of the filaments involved in the braid or the number or filaments over the circumference, or the braid angle which all contribute to increasing the cover factor.

Regarding the bending behavior of PET-braided stents, bending stiffness can be between 10 and 20 times less stiff than Nitinol braided metallic stents. With respect to the bending diameters, different PET-braided stents were characterized by values around 95% of the nominal diameter (above the 75% minimum expected for commercial peripheral stents) [19].

Lateral and longitudinal compression forces are highly dependent on manufacturing parameters. Furthermore, the braiding angle has been found to be the braiding parameter which directly influences the mechanical properties of the developed braids [6, 9, 31]. Stents with a higher braiding angle are more resistant to lateral compression. For higher braiding angles, the wires are deposited more and more towards the transverse axis, resulting in greater resistance to transverse forces acting during lateral compression [31]. In addition, a higher braiding angle also improved the cover factor and compactness of the stent resulting in a higher resistance to lateral forces [6]. In addition, stents with larger monofilament diameter have a higher longitudinal compression force due to their high flexural rigidity, as in longitudinal compression stents are also subjected to flexion and buckling [6]. Also, stents with higher elongation showed lower longitudinal rigidity [31].

Comparing with commercial Nitinol stents [22], developed PET stent show lateral and longitudinal compression forces and percentage of elongation in the same range of commercial stents and even higher in some cases [31].

All of the previously mentioned studies have investigated the structural and mechanical properties of developed PET stents only in a static state, which can predict their behavior only in the short term (during and immediately after implantation). However, the investigation of the PET-braided stents behavior under cyclic loadings, in particular their behavior to dynamic radial compression and to *in vitro* fatigue, have been reported only with Jaziri *et al.* [19, 32]. Results of cyclic radial compression tests showed that the PET-braided stents present a 100% elastic recovery after 20 % diameter compression over 2000 repetitive loading cycles despite the friction that occurs in the braid. Regarding the radial force, it is highly influenced by the stent design and the braiding angle in particular. Furthermore, it came out that radial strength remains stable after long term repeated fatigue stress up to 100.000 cycles with no wire breakage. Compared to metallic braided stents, it was observed that polymeric stents are more flexible and less subjected to inter-wire wear due to friction [32].

Conclusion

This study demonstrates that PET braided stents have the potential to mimic the mechanical performance of commercial metallic stents, if all of their design and manufacturing parameters are carefully chosen. In fact, the combination between PET and braiding could guarantee flexibility and radial strength at the same time. PET admits a low stiffness compared to metals (elastic modulus of PET of 2500 MPa against 80 GPa for Nitinol), and it is widely used in medical applications because of its interesting characteristics. Braiding technique can increase the flexibility of stents, especially in mobile environments such as the superficial femoral artery and could limit the crushing of stents in a tortuous implantation environment, or what is called as the "kinking phenomenon". This could be a promising solution especially in the stenting of peripheral arteries which remains a challenging surgical procedure. Further work is now necessary to determine the most suitable stent design and further animal tests are important in the next step in order to assess *in vivo* long-term behavior of these devices.

References

1. Sigwart U, Puel J, Mirkovitch V, Joffre F, Kappenberger L. Intravascular stents to prevent occlusion and restenosis after transluminal angioplasty. *N Engl J Med* 1987; 316: 701-6.
2. Duerig T, Pelton A, Stöckel D. An overview of nitinol medical applications. *Mater Sci Eng A* 1999; 273: 149-60.
3. Marrey RV, Burgermeister R, Grishaber RB, Ritchie RO. Fatigue and life prediction for cobalt-chromium stents: A fracture mechanics analysis. *Biomaterials* 2006; 27: 1988-2000.
4. Pelton AR, Schroeder V, Mitchell MR, Gong XY, Barney M, Robertson SW. Fatigue and durability of Nitinol stents. *J Mech Behav Biomed Mater* 2008; 1: 153-64.
5. Kapnisis KK, Halwani DO, Brott BC, Anderson PG, Lemons JE, Anayiotos AS. Stent overlapping and geometric curvature influence the structural integrity and surface characteristics of coronary nitinol stents. *J Mech Behav Biomed Mater* 2013; 20: 227-36.
6. Rebelo R, Vila N, Fangueiro R, Carvalho S, Rana S. Influence of design parameters on the mechanical behavior and porosity of braided fibrous stents. *Mater Des* 2015; 86: 237-247.
7. Dordoni E, Petrini L, Wu W, Migliavacca F, Dubini G, Pennati G. Computational Modeling to Predict Fatigue Behavior of NiTi Stents: What Do We Need? *J Funct Biomater* 2015; 6: 299-317.
8. Giessen WJ van der, Slager CJ, Beusekom HMMV, Schenau DSVI, Huijts RA, Schuurbiers JC, *et al.* Development of a Polymer Endovascular Prosthesis and its Implantation in Porcine Arteries. *J Interv Cardiol* 1992; 5: 175-86.
9. Irsale S, Adanur S. Design and Characterization of Polymeric Stents. *J Ind Text* 2006; 35: 189-200.
10. Yuksekkaya ME, Adanur S. Analysis of Polymeric Braided Tubular Structures Intended for Medical Applications. *Text Res J* 2009; 79: 99-109.
11. Freitas AFDP, de Araujo MD, Zu WW, Fangueiro RME. Development of weft-knitted and braided polypropylene stents for arterial implant. *J Text Inst* 2010; 101: 1027-34.
12. Schreiber F, Schuster P, Borinski M, Vogt F, Blindt R, Gries T. Improving the mechanical properties of braided shape memory polymer stents by heat setting. *Autex Res J* 2010; 10: 73-6.
13. Liu Y, Yang J, Zhou Y, Hu J. Structure Design of Vascular Stents. In: *"Multiscale simulations and mechanics of biological materials"*, Li S, Qian D (eds.), John Wiley & Sons, 2013.
14. Høl PJ, Gjerdet NR, Jonung T. Corrosion and metal release from overlapping arterial stents under mechanical and electrochemical stress - An experimental study. *J Mech Behav Biomed Mater* 2019; 93: 31-5.
15. Balla S, Aggarwal K, Nistala R. Bioabsorbable coronary stents--are these the next big thing in coronary angioplasty? *Recent Pat Cardiovasc Drug Discov* 2010; 5: 86-90.
16. El-Mokadem M, El-Ramly M, Hassan A, Boshra H, AbdelWahab A. Comparison between catheter-based delivery of paclitaxel after bare-metal stenting and drug-eluting stents in coronary artery disease patients at high risk for in-stent restenosis. *Cardiovasc Revasc Med* 2017; 18: 596-600.
17. Omar WA, Kumbhani DJ. The Current Literature on Bioabsorbable Stents: a Review. *Curr Atheroscler Rep* 2019; 21: 1-9.
18. Chen C, Chen J, Wu W, Shi Y, Jin L, Petrini L, *et al. In vivo* and *in vitro* evaluation of a biodegradable magnesium vascular stent designed by shape optimization strategy. *Biomaterials* 2019; 221: 119414.
19. Jaziri H, Mokhtar S, Chakfé N, Heim F, Abdessalem SB. Elastic recovery of polymeric braided stents under cyclic loading: Preliminary assessment. *J Mech Behav Biomed Mater* 2019; 98: 131-6.

20. Singh C, Wang X. A biomechanically optimized knitted stent using a bio-inspired design approach. *Text Res J* 2016; 86: 380-92.

21. Shomura Y, MD. Composite Material Stent Comprising Metallic and Non-metallic Materials. In: *"Advances in Composite Materials for Medicine and Nanotechnology"*, Attaf B (ed.), IntechOpen, Croatia, 2011.

22. Mechanical Properties of Nitinol Stents and Stent-grafts. Comparison of 6 mm Diameter Devices. Available from: https://docplayer.net/14090234-Mechanical-properties-of-nitinol-stents-and-stent-grafts-comparison-of-6-mm-diameter-devices.html

23. Kyosev Y, Aurich M. Investigations about the braiding angle and the cover factor of the braided fabrics using Image Processing and Symbolic Math Toolbox of Matlab. In: *"Advances in Braiding Technology"*, Kyosev Y (ed.), Woodhead Publishing, 2016.

24. Hoi Y, Ionita CN, Tranquebar RV, Hoffmann KR, Woodward SH, Taulbee DB, *et al.* Flow modification in canine intracranial aneurysm model by an asymmetric stent: studies using digital subtraction angiography (DSA) and image-based computational fluid dynamics (CFD) analyses. *Proc SPIE Int Soc Opt Eng* 2006; 6143: 61430J.

25. Rebelo R, Vila N, Fangueiro R, Carvalho S, Henriques M. Development of braided fiber-based stents. *Stud Health Technol Inform* 2014; 207: 135-44.

26. Schampaert E, Moses JW, Schofer J, Schlüter M, Gershlick AH, Cohen EA, *et al.* Sirolimus-Eluting Stents at Two Years: A Pooled Analysis of SIRIUS, E-SIRIUS, and C-SIRIUS With Emphasis on Late Revascularizations and Stent Thromboses. *Am J Cardiol* 2006; 98: 36-41

27. Kim JH, Kang TJ, Yu WR. Mechanical modeling of self-expandable stent fabricated using braiding technology. J Biomech 2008; 41: 3202-12.

28. Zhao S, Liu X (Cheryl), Gu L. The Impact of Wire Stent Fabrication Technique on the Performance of Stent Placement. *J Med Devices* 2012; 6: 011007.

29. Maleckis K. Comparison of femoropopliteal artery stents under axial and radial compression, axial tension, bending, and torsion deformations. *J Mech Behav Biomed Mater* 2017; 75: 160-8.

30. Biomechanical Forces in the Femoropopliteal Arterial Segment. Endovascular Today. Available from: https://evtoday.com/articles/2005-june/EVT0605_F3_Smouse.html

31. Jaziri H, Mokhtar S, Aguir K, Ben Abdessalem S. Investigation of PET-Braided Vascular Stents Potential Compared with Commercial Metallic Stents. In: *"Narrow and Smart Textiles"*, Kyosev Y, Mahltig B, Schwarz-Pfeiffer A (eds.), Springer International Publishing, 2018.

32. Jaziri H, Mokhtar S, Ben Abdessalem S, Heim F. Behavior of Polymeric Braided Vascular Stents Under Cyclic Loading. In: The Fiber Society's Fall 2019 Technical Meeting and Conference Revitalizing the Textile Industry Through Innovative Research, Education, and Entrepreneurship. Austin, United States, 2019. Available from: https://hal.archives-ouvertes.fr/hal-03106618

Thrombosis on medical implants: a focus on the importance of hemodynamics

17

Emily JANUS-BELL, Yevgeniy KRIENIN, Netanel KORIN, Pierre H. MANGIN

Medical implants such as stents, endovascular prostheses, artificial heart valves and left ventricular assist devices are used worldwide to treat cardiovascular pathologies and help to restore body functions, improve the quality of life of patients, and saved millions of lives. However, since they are in direct contact with flowing blood, their use is linked to complications, with thrombosis being one of the most dangerous. Thrombus formation on the medical devices can hinder the function of the device which becomes a major medical concern. In addition, thrombosis can also result in life-threatening ischemic events at the site of device implantation or at distance. There is no doubt that artificial surfaces remain thrombogenic and despite significant improvements, the thrombotic events have not been eliminated. In addition, there is compelling evidence that implantation of medical devices modifies the local hemodynamics and generates disturbed flows promoting thrombosis. This article describes the basic concepts of hemodynamics and highlights how normal and pathological flows regulate platelet function and coagulation in hemostasis and arterial thrombosis. It also provides clinical and experimental evidence showing that blood flow modifications of currently used medical implants affect local hemodynamics and precipitate thrombosis.

Introduction

Medical implants are composed of biological or artificial materials which are inserted or grafted into patients. Amongst the artificial devices used to treat cardiovascular diseases, one finds stents, synthetic vascular grafts, left ventricular assist device (LVAD) and artificial heart valves which benefit to millions of patients and have significantly reduced the rate of mortality and morbidity. Thrombosis is one of the most serious complication occurring after implantation of cardiovascular devices, and represents a common cause of failure [1]. Thrombi, which result from the direct contact of blood with the device, are made up of platelets, red blood cells (RBCs) and fibrin. Anticoagulants and antiplatelet agents are commonly used to treat or prevent thrombosis on medical devices. Their use is however associated with an increased risk of bleeding which can be particularly deleterious. A thorough understanding of the mechanism underlying thrombosis on implanted medical devices is crucial to clinicians to adapt the antithrombotic therapy in order to improve the prevention of acute thrombosis while minimizing the risk of bleeding [2]. It is well accepted that the material composing the medical devices is itself a major cause of blood activation and thrombosis [1]. Indeed, artificial surfaces can adsorb biologically active plasma proteins and in turn recruit circulating blood cells, mainly platelets, but also leukocytes to initiate thrombosis. In addition, they can activate the contact pathway of coagulation and facilitate the generation of thrombin, which forms fibrin and potently activates platelets to promote thrombus formation [1]. Therefore, a significant effort has been made to improve medical devices in the last two decades through the use of less thrombogenic material, reducing the interface between the device and blood and even coating the device with low thrombogenic components [3]. These technical improvements

have reduced, but have not eliminated the risk of thrombosis. As a consequence, they have not modified the guidelines recommending antithrombotic drugs to manage patients, and have therefore not reduced the hemorrhagic risk. It is very challenging and probably near impossible to develop devices with no thrombogenic surface. In addition, hemodynamics is critical, independently of the material, and can promote thrombotic events under certain conditions [4]. Some modifications of the blood flow regime impact on homeostasis. For instance, low shear pockets or regions of stagnation facilitate platelet adhesion and initiate the coagulation cascade. On the other hand, high shear unfolds von Willebrand factor (vWF) precipitating platelet adhesion, activation and aggregation [5]. If a lot of attention has been brought to reduce the thrombogenicity of artificial surfaces of medical devices, their impact on the local hemodynamic has been much less investigated and has not been a major focus of most manufacturers. In this review, we: i) provide basic concepts on hemodynamics; ii) describe the process of hemostasis and thrombosis; iii) highlight the importance of hemodynamics in regulating platelet function, coagulation, hemostasis and arterial and venous thrombosis; iv) provide a literature review and some computational fluid dynamics (CFD) results on the impact of implants on hemodynamics; and v) conclude and suggest future directions to improve the biocompatibility of medical implants by reducing their impact on generating pathological flows.

Basic concepts on hemodynamics

Hemodynamics represents the dynamics of blood flow, which follows the laws governing mass and momentum of fluids, and modulates the interactions between blood and the vascular wall under health and disease conditions. Since hemostasis, but also pathological events such as inflammation, occur at the interface of the vessel wall, blood dynamics near the wall plays a key role in regulating these processes. The flow near the wall directly affects: 1) transport kinetics of material and 2) mechanical forces exerted on the wall and on flowing elements interacting with each other and with the wall. Two commonly used parameters to define these flow characteristics are: the wall shear rate (WSR) and the wall shear stress (WSS).

The WSR is the radial gradient of the velocity near the wall which describes the rate at which the flow increases when moving away from the vessel wall, where velocity is assumed to be zero. The WSR is an indicator of the axial velocity near the wall that controls the convective mass transport along the wall interface. An increased WSR, represents a higher velocity near the wall, which results in a higher influx of material interacting with the wall (such as platelets and proteins), at the same time a high WSR also implies a short residence time and a rapid washout of material from the wall (such as agonists at an injury site). While the WSR directly affects the mass transport near the wall, it also governs the WSS. The WSS is the tangential frictional force per area generated by blood flow on the vessel wall, which can be derived by the product of WSR and kinematic viscosity of the fluid. The relationship between WSR and WSS is not completely proportional in blood, due to the non-Newtonian nature of the latter. The frictional shear force at the wall affects the adhesion of cells and proteins as well as their conformation and state (*e.g.*; platelet activation, endothelial phenotype, vWF unfolding, ligands conformation) [6]. Thus, these two linked parameters, WSR and WSS, are important hemodynamic parameters that are tightly regulated throughout the human circulation system [7]. Consequently, both too low and too high WSR and WSS are associated with pathological conditions [8].

More generally, from a fluid mechanics perspective, these and other flow features which describe the local dynamics near the wall are derived from the global flow field within a defined geometry under controlled perfusion conditions. In the case of a long, undeformable tube, under laminar flow conditions (where friction forces in the fluid are high enough to ensure a layered flow, as opposed to turbulent flow) the WSR can be assumed constant and can be estimated by: $\gamma = 4Q/\pi r^3$, where Q is the volumetric flow

rate and r is the tube's radius. The fact that WSR, under these conditions, is inversely proportional to the cube of the radius, highlights the key role geometry has on the WSR. Although the WSR (and WSS) may be assumed constant in this simplified case, this is not the case for more complex geometries and/or under pulsatile flow. Areas of narrowing, bifurcation, bending and curvature can result in complex irregular flow patterns, termed disturbed flow, that can produce shear gradients, recirculation zones and stagnation areas, which have profound effects on transport and forces near the wall as well as in the bulk flow[8]. For example, in a stenotic (narrowed) blood vessel, high WSR form at the apex where the fluid accelerates, while low WSR exists past the stenosis at recirculation zones that may form, when the fluid decelerates and flow detachment occurs, see Figure 1[9]. It is also worth noting that besides the WSR value, shear gradients under such conditions also produce forces on flowing cells and molecules affecting their conformation and activity. Moreover, the effect of fluid based mechanical forces on cells and molecules under flow depends on the duration at which different forces are applied on the flowing element (cell/molecule) and hence a more comprehensive understanding of the hemodynamics and its effect on blood elements is needed when studying disease conditions as well as designing medical implants that interact with flowing blood.

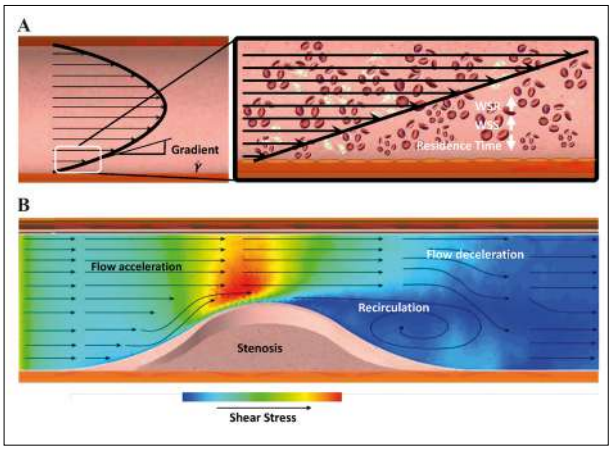

Figure 1: Hemodynamics affects the transport kinetics and forces in healthy and diseased blood vessels.

A. The WSR, the radial gradient of the velocity near the wall, is an important parameter of transport kinetics and forces applied near the wall. Increasing the WSR, increases the influx and outflux of material near the wall while reducing their residence time (RT). Additionally, increasing the WSR directly increases the WSS.

B. In a stenotic artery, complex flow patterns can exist which can produce high WSS at the apex (see WSR colormap derived from CFD simulation), where the fluid accelerates, and low WSR, recirculating flows past the stenosis. Such flow features have profound biomechanical effects on pathophysiological process at sites of arterial thrombosis.

Hemostasis and thrombosis

Hemostasis is the physiological process which maintains vascular integrity and arrests bleeding. The first step, also known as primary hemostasis, occurs immediately after vessel wall injury and relies on platelet adhesion, activation and aggregation at the lesion site to form a hemostatic plug. Platelets stick to one another through bonds ensured by adhesive plasma proteins such as vWF, fibrinogen and fibronectin. Secondary hemostasis, or coagulation, is a cascade of enzymatic reactions involving clotting factors, which occurs in close vicinity of the lesion and results in thrombin generation. Two main pathways co-exist to trigger the coagulation cascade, which are known as the extrinsic or tissue factor (TF) pathway and the intrinsic or contact pathway[10]. The TF pathway is central in blood clotting during hemostasis and most likely in many different types of thrombosis. In contrast, the contact pathway involving FXI and FXII, is believed not to be central in physiological hemostasis but rather playing a role in venous and arterial thrombosis. Furthermore, the contact pathway is generally triggered when blood is in contact with artificial surfaces, implants for example, leading to thrombosis. These two pathways join in the common pathway to ultimately generate the serine protease thrombin which cleaves fibrinogen, present throughout the plug generating an insoluble fibrin network to stabilize the clot and stop blood loss.

Arterial thrombosis is a pathological process taking place in diseased arteries presenting an atherosclerotic plaque, which is the result of a chronic and inflammatory disease named atherosclerosis. At an advanced stage, the plaque grows within the lumen of the artery causing a vessel stenosis [11]. The plaque profoundly modifies the local rheology generating thrombogenic flows such as shear gradients and elongational flows in the pre-stenotic region, extremely high shear in the stenosis throat and regions of disturbed flow with eddies and recirculation events in the post-stenotic zone [4]. It is assumed that the flow exerts forces on the plaque which can result in its erosion or rupture exposing a thrombogenic material with lipids, reactive adhesive proteins such as collagen, fibronectin or laminins as well as elevated amounts of TF to initiate coagulation. This promotes an efficient platelet recruitment, thrombus growth and thrombin generation which lead to acute thrombosis directly on the plaque to form an occlusive thrombus responsible for ischemic pathologies such as myocardial infarction. The thrombus can also embolize to occlude smaller arteries located downstream such as in the cerebral bed when thrombosis occurs within a carotid artery causing an ischemic stroke.

The molecular mechanisms involved in hemostasis and arterial thrombosis are very similar. The initial trigger is a vessel lesion which exposes adhesive proteins in the subendothelium, many of them being able to adsorb plasma vWF, notably collagen, fibronectin or laminins. vWF supports the recruitment of circulating platelets through an interaction with the glycoprotein (GP) Ib-IX complex. The GPIb-IX/vWF interaction is the only bond able to form at WSR above 1,000 s^{-1} and is therefore essential to ensure platelet capture at sites of injury in an artery [12]. At lower WSR, integrins of the β1 (α2β1, α5β1 and α6β1) and β3 (αvβ3, αIIbβ3) families can also contribute and ensure stable platelet adhesion. This facilitates the interaction of GPVI with a number of subendothelial proteins including collagen, which initiates platelet activation and the release of soluble agonists, such as adenosine diphosphate (ADP) and thromboxane A2 (TxA2). These agonists amplify the process of platelet activation and notably the conversion of αIIbβ3 from a low to a high affinity state for plasma fibrinogen facilitating platelet aggregation and thrombus growth and stability. Some platelets become pro-coagulant allowing the recruitment of coagulation factors at their surface to facilitate enzymatic reactions and promote local thrombin generation.

Venous thromboembolism (VTE) is a serious condition including deep-vein thrombosis which occurs when a blood clot forms, generally in large veins of the legs or pelvis. The clot is generated as the result of an imbalance between thrombogenic stimuli and protective factors [13]. The thrombogenic factors were initially proposed by Rudolf Virchow in 1847 and comprise blood hypercoagulability, endothelial injury, and dysregulation of blood flow such as stasis or turbulence. As for arterial thrombosis, the clot can embolize and reach the arteries of the lungs inducing its main complication, pulmonary embolism. Despite improvement in the managing of VTE, it remains a major health and financial burden worldwide.

The importance of blood flow in regulating platelet function, hemostasis and thrombosis

Blood flow plays a central role in the regulation of platelet function during hemostasis and arterial thrombosis. Following injury of a healthy vessel, the initial step of the formation of a hemostatic plug is the adhesion of platelets to the subendothelial proteins. This initial step can occur over a wide range of blood flow conditions ranging from low WSR in veins (100 s^{-1}) up to elevated WSR in small arteries and in the microcirculation (2,500 s^{-1}) [15]. To ensure interaction with the large array of adhesive proteins found in the subendothelium, platelets are equipped with several adhesion receptors. Platelets express integrins of the β1 and β3 families ensuring platelet capture and stable adhesion. However, these integrins are unable to capture flowing platelets at arterial WSR exceeding 1,000 s^{-1}. For such conditions, platelets use

an exclusive receptor, the GPIb-IX complex, which interacts with its ligand vWF to ensure platelet recruitment under low but also very elevated WSR (100 s^{-1} up to 10,000 s^{-1}) [12]. Plasma vWF carries many functions and for instance can rapidly adsorb to many subendothelial proteins allowing platelet capture in every physiological situation *i.e.* to distinct matrices exposed in different vessel types with various flow conditions (Figure 2).

Once adhered, platelets become activated, which is another important step of the hemostatic process. Platelet activation is initiated by receptor-ligand processes inducing a signalling cascade which ultimately leads to morphological changes of platelets, the release of soluble agonists and the up-regulation of integrin αIIbβ3 allowing platelet aggregation. Activation is initiated by adhesive proteins such through the GPIb-IX complex, integrins and the collagen receptor GPVI. It has also been reported that some of these receptors, namely the GPIb-IX complex and integrin αIIbβ3, present mechanoreceptor properties allowing the forces of the blood flow to regulate this initial trigger of platelet activation [16]. This initial signal promotes the release of soluble agonists such as adenosine triphosphate, ADP and TxA2, which bind to their receptors at the platelet surface to amplify platelet activation. Blood flow regulates this activation step through its ability to dilute soluble agonists in the blood stream avoiding excessive activation (Figure 2). A similar effect is achieved for the coagulation cascade, which is initiated at site of TF exposure. As coagulation is a cascade of enzymatic reactions composed of soluble mediators, flow limits their action by diluting them in the blood stream.

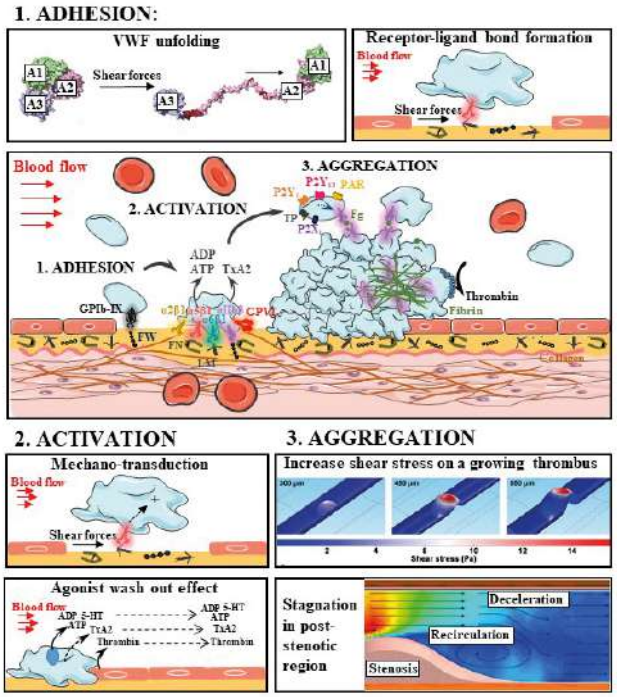

Figure 2: Blood flow regulates platelet adhesion, activation and aggregation.

1. Adhesion: the forces generated by the blood flow favour vWF unfolding and platelet attachment through GPIb-IX, while they also tend to prevent receptor-ligand bond formation;

2. Activation: the shear forces of the flow promote platelet activation through their ability to initiate signalling through some platelet receptors such as P2X1, GPIb-IX or αIIbβ3, a process called mechano-transduction.

3. Aggregation: as a thrombus grows, the shear stress increases on the top of the thrombus generating elevated forces on receptor-ligand bonds which tends to avoid thrombus progression and vessel occlusion. Under pathological conditions, the flow disturbances occurring in the post-stenotic region were shown to enhance platelet aggregation (adapted from Crawley *et al.*, 2011).

The flow is also playing a major role in the regulation of arterial thrombosis. This event usually takes place in a diseased artery presenting an atherosclerotic plaque. At an evolved stage plaque growth within the lumen creates a stenosis which profoundly modifies the local geometry. Flow accelerations found within the pre-stenotic region facilitate vWF unfolding allowing it to become active and pro-thrombogenic [17]. At the apex of the stenosis, extremely high WSR can take place with values reaching couple of 10,000 s^{-1}, exceeding the level at which vWF unfolds in bulk flow (around 5,000 s^{-1}) [4,19]. As a consequence, in both pre- and post-stenotic regions, vWF unfolding exposes cryptic sites allowing platelet binding and initiating the formation of a thrombus. Finally, it has been described that disturbed flow takes place in the post-stenotic region, with a reciprocating, low shear flow, region of recirculation and stagnation points which exert a range of pro-thrombotic properties [19]. This is achieved by increasing the residence time of platelets, plasma proteins such as vWF and fibrinogen, soluble agonists released by platelets and coagulation factors, thereby favouring thrombus growth (Figure 2).

Blood flow has also a direct impact on VTE which has been reported to be initiated in pocket of stasis where the coagulation cascade can be initiated to form a thrombus composed mainly of RBCs and fibrin. Since the thrombus increases the pressure within the vessel, the forces exerted by the flow can break off the clot and a part of it moves to the lungs where it blocks smaller arteries and provokes the most serious complication of VTE, pulmonary embolism.

The impact of implants on local hemodynamics and potential pro-thrombotic effects

For this review we focused on four medical implants including stents, endovascular prosthesis, prosthetic aortic valves and LVADs.

Stents

Angioplasty and cardiovascular stenting is the treatment of choice in situations of arterial stenosis resulting from the growth of an atherosclerotic plaque in the vessel lumen. Its main objective is to relieve the stenosis to restore vessel patency and normalization of the flow thereby allowing the downstream tissues to be properly irrigated with blood. This approach has been a breakthrough advance in reducing mortality and morbidity related to arterial thrombosis [20]. It has been improved over the past 40 years through the development of better devices including the second generation of drug-eluting stents and the more recent bioresorbable scaffolds, which are more biocompatible and allow better vascular healing and re-endothelialization of the stent. This has also helped to reduce stent thrombosis, which remains a major drawback of angioplasty and a clinical concern [21].

In-stent restenosis is defined as a reduction in the vessel lumen occurring after percutaneous intervention (PCI) and represents its most frequent complication. For drug-eluting stent, in-stent restenosis is generally the consequence of late stent thrombosis which is rare but extremely dangerous. A study reported that stent thrombi from 253 patients, either from early or late stent thrombosis, were mostly rich in platelets and fibrin as platelets represent 57% of thrombus area. Leukocytes were also found in stent thrombi, even more than on acute myocardial infarction native thrombi use as control [22]. Stent thrombosis has various causes including insufficient vascular re-endothelialization, a hypersensitivity to polymer coating, and an increased deposition of fibrin on the stent due to chronic inflammation. In addition, flow disturbances due to stent implantation are also considered as a major trigger of stent thrombosis. Numerical and experimental approaches have provided evidence that the design and geometry of stents impact on the fluid mechanical environment of an artery after implantation [23]. For instance, the use of CFD has shown that intracranial stent implantation can promote stagnant as well as disturbed flow [24]. While stagnation could facilitate platelet adhesion and activation of coagulation, disturbed flow could favour platelet activation. As shown in Figure 3, the flow appears particularly altered around the stent struts which could be a likely trigger to initiate stent thrombosis. In addition, incomplete stent apposition or suboptimal expansion also result in major hemodynamic disturbances after PCI [25]. They promote flow alterations resulting in high shear stress known to unfold vWF and support platelet attachment initiating thrombosis. Flow disturbances have also been described in clinical studies and correlate with both stent suboptimal expansion and malapposition [26]. Some studies even suggest that the stent-induced flow disturbances might be a much more important determinant of stent thrombosis than the composition or coating of the stent which rather precludes thrombosis[27]. Finally, the effect of shear modifications on

stent thrombosis might also be the consequence of alterations of the integrity of the RBCs, which could result in lysis and release of pro-thrombotic factors, including ADP, a major platelet agonist [28]. Together, these studies highlight the important hemodynamic modifications of the local blood flow after stent positioning with optimal or suboptimal implantation and identify them as major triggers of thrombotic events.

Endovascular prosthesis

Endovascular prosthesis, also called endovascular stent grafts, are used to treat weakened arteries in two main pathologies: aneurysm and arterial dissection. Concerning aneurysm, endovascular grafts exclude the aneurysmal portion of the artery from the circulation and reinforce the vascular wall, thereby limiting the expansion of the aneurysm and the risk of rupture. Concerning arterial dissections, mostly occurring in the aorta, endovascular prosthesis seals the lesion of the vessel wall. Endovascular flow prosthesis are composed of a vascular conduit (the graft) serving as a barrier to create a synthetic new vascular wall, supported by a metal mesh (the stent) serving as a support for the graft [29].

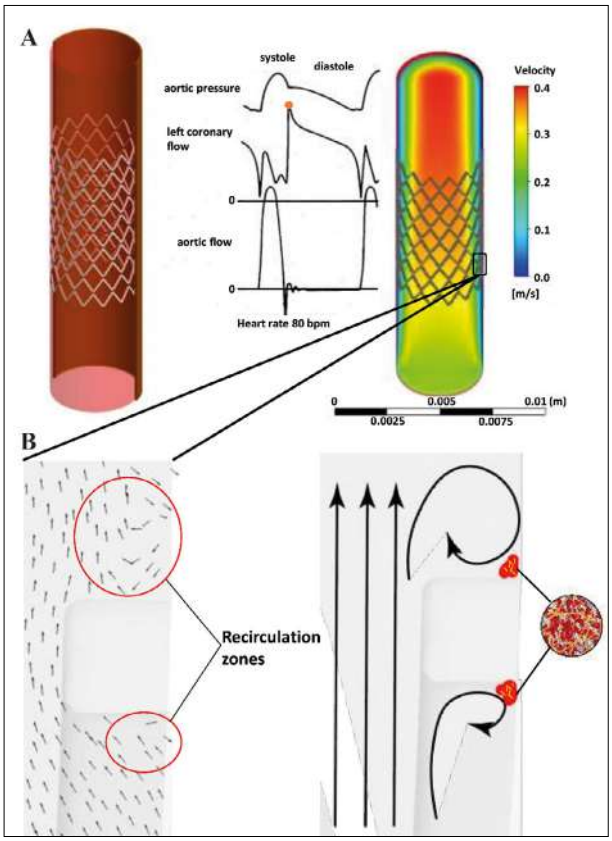

Figure 3: Biorheology of stent thrombosis.

A. A stent placed in an artery (left: the 3D computerized geometry) is subjected to an arterial pulse (middle: the pulse of a coronary artery). The stent that reopens the vessel allow the flow to return to it basal flow profile (CFD results on right).

B. On the microscale, in the areas of the stent struts complex flow patterns form (left: CFD streamlines between struts) which include recirculation zones that can promote thrombosis (right: illustration of thrombosis between struts).

One of the main endovascular flow prosthesis complication is thrombosis. In abdominal aortic aneurysm stent graft, approximately one patient over six presents thrombus deposition in the graft lumen at early time points following the procedure[30]. Thrombus composition of graft thrombosis is not well known but platelets seem to play a major role since antiplatelet agents reduce thrombosis. The origin of thrombus formation is not fully elucidated, but likely depends on the graft material itself, despite recent improvement of biocompatibility. The very important surface area (>100 cm^2) of the graft enhances the probability of blood interaction with the artificial surface. As a result, adhesive proteins can adsorb to the graft and initiate platelet adhesion and thrombus formation. In addition to the material, local flow disturbances also appear to dictate graft thrombosis. While one objective of grafts is to restore a normal blood flow, this is not always the case and that pro-thrombotic flows can occur [31,22]. Thrombi forming on grafts are usually clinically silent, but some rare cases of life-threatening thromboembolic complications have been reported and interestingly they appear to result from a device infolding which is linked to flow disturbances [33]. Another case of graft shape modification inducing a kink formation might also be the cause of an almost occlusive thrombus formation, which further highlight the importance of blood flow modifications on graft thrombosis[34]. These examples illustrate the occurrence of disturbed flow in grafted arteries and their link with thrombosis. They also highlight the need to develop new endovascular prosthesis design to reduce graft thrombosis.

Prosthetic aortic valves

Aortic valve stenosis is a highly prevalent and progressive pathology occurring when the left ventricular outflow tract narrows due to calcification and thickening, and which can ultimately result in heart failure or sudden cardiac death. While, surgical aortic valve replacement has been the standard of care for patients for many years, the minimally invasive transcatheter aortic valve replacement (TAVR) has been introduced 10 years ago and is increasingly used even in intermediate and low risk patients. The two main types of prosthetic valves are the mechanical valves (MVs) and bioprosthetic valves which both exhibit pro-thrombogenic features. The MVs are the most thrombogenic with a mortality rate above 10%, and since patients are treated with anticoagulants for life, their implantation is also accompanied by bleeding complications [35]. The bioprosthetic valves have a better biocompatibility, but are not devoid of thrombotic risk and experience a limited durability due to tissue degeneration. The use computed tomography identified subclinical leaflet thrombosis with an unexpected high prevalence reaching nearly 1 in 5 patients post-TAVR [36]. Composition of prosthetic aortic valve thrombus seems to depend on the localisation of the valve: on the right side of the heart (tricuspid and pulmonic valves), coagulation seems to play a major role; whereas on the left side of the heart (aortic and mitral valves), platelets and fibrin seem to play a major role [37]. These subclinical thrombotic events are a medical concern as they were shown to result in valve failure due to structural deterioration and they are also associated with an almost 3-fold increase in the risk of stroke [38].

The fluid dynamics around prosthetic aortic valves have been extensively studied. Their deployment creates a neosinus in which pro-thrombotic flows with stagnation regions and vortices are occurring, highlighting that artificial surfaces exposed to the blood are clearly not the only trigger of prosthetic valve thrombosis [39] (Figure 4). In addition, heart valves also induce high shear and turbulence proposed to harm blood cells directly by activating platelets or indirectly by promoting hemolysis with the release of platelet agonists, and thereby precipitate thrombosis [40]. Using anatomical data from patients, a study has established a link between flow stasis and valve thrombosis [41]. It has also been reported that post-procedural aortic regurgitation which occurs in almost 20% of patients undergoing TAVR is linked to a defect in high molecular weight vWF and to an increase in mortality rate [42]. This clinical observation indicates that pathological flows around prosthetic valves promote vWF unfolding and thereby its cleavage by a disintegrin and metalloprotease with thrombospondin type I repeats-13 (ADAMTS-13) which can contribute to bleeding[43]. On the other hand, vWF unfolding is also a trigger of thrombosis as this event exposes cryptic sites which allow platelet adhesion and activation. In summary, clinically-used prosthetic valves generate a panel of flow conditions which are pro-thrombogenic but can also result in bleeding complications, and developing new valves which would limit high shear and with improved washing outs of stagnant flow regions would undoubtedly reduce the thrombogenicity and reduce bleeding events linked to these implants and therefore improve the management of the patients.

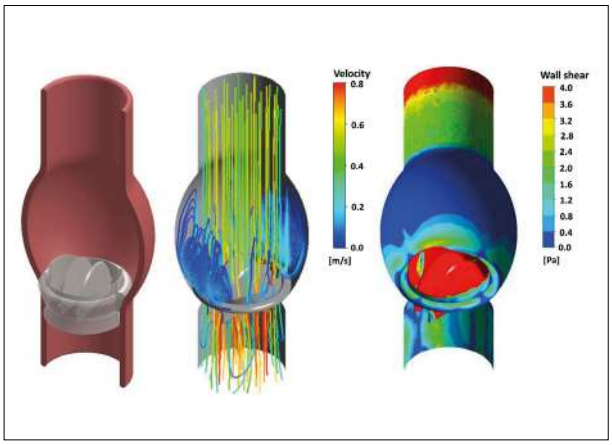

Figure 4: Biorheology of heart valve thrombosis. An aortic mechanical heart valve in its open configuration (lef: 3D model, middle: CFD streamline results, right: WSS map). High WSS are found near the valve leaflets while recirculating flows and stagnation zones are found around the valve and at the sinus region of the aortic root. This disturbed flow pattern, which include high shear forces and low shear recirculation zones, provokes platelet activation and thrombosis.

Left ventricular assistance devices

Left ventricular assistance device (LVAD) is a surgically implantable mechanical circulation support device, maintaining blood flow in the organism when the left ventricle of the heart is weakened and not able to pump blood adequately, such as in case of heart failure. They are used for patients waiting for heart transplant or as long term treatment if patients are not eligible [44]. Around 2,700 LVADs were implanted in the United-States in 2015. They are composed of a pump connecting the apex of the left ventricle to the ascendant aorta, allowing a sufficient continuous blood flow in the systemic circulation to extend survival and improve quality of life [45]. The first generation of LVAD used a pulsatile flow mechanism, but induced severe adverse events such as thrombosis and valve failure [46]. Ameliorations led to a second and a third generation of continuous-flow pumps, of which three have been approved for clinical use: HeartWare HVAD, HeartMate II and HeartMate 3 [46].

Despite significant improvements, patients implanted with LVADs frequently experience adverse events reaching 70% after 1 year [47]. They can be due to a malfunction of the pump or issues related to the heart that has a hard time adapting to the device. An additional reported adverse effect of LVADs implantation is thrombosis. It occurs in the pump and thrombus can be either red or white depending on the area of formation. Red thrombi, rich in red blood cells and fibrin develop in areas of low shear, recirculation zones as inlet stator for example. White thrombi, rich in platelets and fibrin, rather develop in high shear area such as outlet stator [48]. The last-generation LVAD (HeartMate 3) uses a centrifugal flow pump designed to reduce device-induced thrombosis. Indeed, the pump is composed of a rotating disk magnetically elevated which does not generate frictions and reduce flow perturbations as it passes through pump, as assessed by CFD [49]. This pump is also able to decrease and increase the rotor speed every 2 seconds, creating a partial pulsatility that allows reduction of stasis areas and reduction of in-pump thrombosis[49]. Beside the pump itself, the outflow graft linking the heart to ascending aorta represents another element of the LVAD which can generate disturbed flow and increase the risk of thrombosis [50]. LVAD patients can also develop acquired von Willebrand disease. Indeed, the pump is increasing blood flow which creates local turbulences inducing high vWF multimer to extend, leading to vWF cleavage by ADAMTS13 [51]. vWF is then not able to adhere at sites of vascular trauma and cannot not induce platelet recruitment, leading to bleeding. These studies highlight the flow perturbations induced by LVADs and suggests that pump design amelioration to reduce in-pump stasis, frictions and out-flow perturbations could improve thrombosis and increase patient survival.

Conclusions and future perspectives

Implantable medical devices have significantly improved human life expectancy and are increasingly used. Amongst the limitations of these devices, thrombosis stands out as it does not only impair the function of the implants, but can also precipitate life-threatening ischemic pathologies. Intensive research has helped to improve the biocompatibility of implantable devices in order to reduce their potential to activate blood components and maintain homeostasis thereby avoiding an imbalance of the hemostatic system and prevent bleeding events as well as thrombotic complication. Despite these improvements, thrombotic events persist with all the medical devices implanted today. One reason relies in the artificial surfaces requiring further ameliorations such as a coating with active biomolecules locally reducing blood activation, or ideally promoting complete re-endothelialization to maintain native? homeostasis. In addition to the nature of the artificial surfaces, the local hemodynamics are another determinant of thrombosis as they can generate highly thrombogenic flows such as stagnation regions, recirculation events or high shear. It is therefore critical to conceive new medical devices which would restore the fluid dynamics found in healthy vessels.

A thorough understanding of the events underlying thrombotic complications linked to disturbed flow generated by implanted medical devices appears as critical step in the quest of developing safer medical implants. However, this remains challenging as this clinical issue requires a combined expertise in different fields including fluid mechanics, platelet and coagulation biology and hematology, with experts who seldom get together and are not naturally prone to communicate. It therefore appears critical to create conditions for exchanges in order to speak a common language and better understand the cellular and molecular mechanisms of medical device-induced thrombosis and its link to pathological flows. In the end, this will create the conditions for the production of new devices which would better respect the hemodynamic of healthy vessels to avoid thrombotic events.

References

1. Jaffer IH, Fredenburgh JC, Hirsh J, Weitz JI. Medical device-induced thrombosis: what causes it and how can we prevent it? *J Thromb Haemost* 2015; 13 Suppl 1: S72-81.
2. Baron TH, Kamath PS, McBane RD. Management of antithrombotic therapy in patients undergoing invasive procedures. *N Engl J Med* 2013; 368: 2113-24.
3. Bluestein D, Chandran KB, Manning KB. Towards non-thrombogenic performance of blood recirculating devices. *Ann Biomed Eng* 2010; 38: 1236-56.
4. Nesbitt WS, Mangin P, Salem HH, Jackson SP. The impact of blood rheology on the molecular and cellular events underlying arterial thrombosis. *J Mol Med* 2006; 84: 989-95.
5. Siedlecki CA, Lestini BJ, Kottke-Marchant KK, Eppell SJ, Wilson DL, Marchant RE. Shear-dependent changes in the three-dimensional structure of human von Willebrand factor. *Blood* 1996; 88: 2939-50.
6. Kroll MH, Hellums JD, McIntire LV, Schafer AI, Moake JL. Platelets and shear stress. *Blood* 1996; 88: 1525-41.
7. Ku DN. Blood flow in arteries. *Annu Rev Fluid Mech* 1997; 29: 399-434.
8. Wootton DM, Ku DN. Fluid mechanics of vascular systems, diseases, and thrombosis. *Annu Rev Biomed Eng* 1999; 1: 299-329.
9. Bluestein D, Niu L, Schoephoerster RT, Dewanjee MK. Fluid mechanics of arterial stenosis: relationship to the development of mural thrombus. *Ann Biomed Eng* 1997; 25: 344-56.
10. Versteeg HH, Heemskerk JWM, Levi M, Reitsma PH. New fundamentals in hemostasis. *Physiol Rev* 2013; 93: 327-58.
11. Libby P, Ridker PM, Hansson GK. Progress and challenges in translating the biology of atherosclerosis. *Nature* 2011; 473: 317-25.
12. Savage B, Saldívar E, Ruggeri ZM. Initiation of platelet adhesion by arrest onto fibrinogen or translocation on von Willebrand factor. *Cell* 1996; 84: 289-97.
13. Bruni-Fitzgerald KR. Venous thromboembolism: An overview. *J Vasc Nurs* 2015; 33: 95-9.
14. López JA, Chen J. Pathophysiology of venous thrombosis. *Thromb Res* 2009; 123 Suppl 4: S30-34.
15. Panteleev MA, Korin N, Reesink KD, Bark DL, Cosemans JMEM, Gardiner EE, *et al.* Wall shear rates in human and mouse arteries: Standardization of hemodynamics for *in vitro* blood flow assays: Communication from the ISTH SSC subcommittee on biorheology. *J Thromb Haemost* 2021; 19: 588-95.
16. Goncalves I, Nesbitt WS, Yuan Y, Jackson SP. Importance of temporal flow gradients and integrin alphaIIbbeta3 mechanotransduction for shear activation of platelets. *J Biol Chem* 2005; 280: 15430-7.
17. Receveur N, Nechipurenko D, Knapp Y, Yakusheva A, Maurer E, Denis CV, *et al.* Shear rate gradients promote a bi-phasic thrombus formation on weak adhesive proteins, such as fibrinogen in a VWF-dependent manner. *Haematologica* 2020; 105: 2471-83.
18. Hariri N, Russell T, Kasper G, Lurie F. Shear rate is a better marker of symptomatic ischemic cerebrovascular events than velocity or diameter in severe carotid artery stenosis. *J Vasc Surg* 2019; 69: 448-52.
19. Nesbitt WS, Westein E, Tovar-Lopez FJ, Tolouei E, Mitchell A, Fu J, *et al.* A shear gradient-dependent platelet aggregation mechanism drives thrombus formation. *Nat Med* 2009; 15: 665-73.
20. Pradhan A, Vishwakarma P, Sethi R. Landmark Trials in Cardiology in 2017-Celebrating 40 Years of Angioplasty. *Int J Angiol* 2018; 27: 167-73.
21. Wayangankar SA, Ellis SG. Bioresorbable Stents: Is This Where We Are Headed? *Prog Cardiovasc Dis* 2015; 58: 342-55.
22. Riegger J, Byrne RA, Joner M, Chandraratne S, Gershlick AH, Ten Berg JM, *et al.* Histopathological evaluation of thrombus in patients presenting with stent thrombosis. A multicenter European study: a report of the prevention of late stent thrombosis by an interdisciplinary global European effort consortium. *Eur Heart J* 2016; 37: 1538-49.
23. Balossino R, Gervaso F, Migliavacca F, Dubini G. Effects of different stent designs on local hemodynamics in stented arteries. *J Biomech* 2008; 41: 1053-61.
24. Tanemura H, Ishida F, Miura Y, Umeda Y, Fukazawa K, Suzuki H, *et al.* Changes in hemodynamics after placing intracranial stents. *Neurol Med Chir (Tokyo)* 2013; 53: 171-8.

25. Foin N, Gutiérrez-Chico JL, Nakatani S, Torii R, Bourantas CV, Sen S, *et al.* Incomplete stent apposition causes high shear flow disturbances and delay in neointimal coverage as a function of strut to wall detachment distance: implications for the management of incomplete stent apposition. *Circ Cardiovasc Interv* 2014; 7: 180-9.

26. Fujii K, Carlier SG, Mintz GS, Yang Y, Moussa I, Weisz G, *et al.* Stent underexpansion and residual reference segment stenosis are related to stent thrombosis after sirolimus-eluting stent implantation: an intravascular ultrasound study. *J Am Coll Cardiol* 2005; 45: 995-8.

27. Kolandaivelu K, Swaminathan R, Gibson WJ, Kolachalama VB, Nguyen-Ehrenreich K-L, Giddings VL, *et al.* Stent thrombogenicity early in high-risk interventional settings is driven by stent design and deployment and protected by polymer-drug coatings. *Circulation* 2011; 123: 1400-9.

28. Kapnisis K, Seidner H, Prokopi M, Pasias D, Pitsillides C, Anayiotos A, *et al.* The effects of stenting on hemorheological parameters: An *in vitro* investigation under various blood flow conditions. *Clin Hemorheol Microcirc* 2019; 72: 375-93.

29. Eliason JL, Upchurch GR. Endovascular abdominal aortic aneurysm repair. Circulation 2008; 117: 1738-44.

30. Mestres G, Maeso J, Fernandez V, Allegue N, Constenla I, Matas M. Incidence and evolution of mural thrombus in abdominal aortic endografts. *Ann Vasc Surg* 2009; 23: 627-33.

31. Raptis A, Xenos M, Spanos K, Kouvelos G, Giannoukas A, Matsagkas M. Endograft Specific Haemodynamics After Endovascular Aneurysm Repair: Flow Characteristics of Four Stent Graft Systems. *Eur J Vasc Endovasc Surg* 2019; 58: 538-47.

32. Liu MY, Jiao Y, Liu J, Zhang S, Li W. Hemodynamic Parameters Predict In-stent Thrombosis After Multibranched Endovascular Repair of Complex Abdominal Aortic Aneurysms: A Retrospective Study of Branched Stent-Graft Thrombosis. *Front Cardiovasc Med* 2021; 8: 654412.

33. Marone EM, Kahlberg A, Tshomba Y, Logaldo D, Chiesa R. Surgical conversion for intragraft thrombosis following endovascular repair of traumatic aortic injury. *J Vasc Surg* 2012; 55: 538-41.

34. Alvarez B, Constenla I, Maeso J, Matas M. Late thrombosis of a thoracic aorta stent graft: Therapeutic management. *J Vasc Surg* 2009; 49: 774-7.

35. Ranasinghe MP, Peter K, McFadyen JD. Thromboembolic and Bleeding Complications in Transcatheter Aortic Valve Implantation: Insights on Mechanisms, Prophylaxis and Therapy. *J Clin Med* 2019; 8: E280.

36. Ruile P, Minners J, Breitbart P, Schoechlin S, Gick M, Pache G, *et al.* Medium-Term Follow-Up of Early Leaflet Thrombosis After Transcatheter Aortic Valve Replacement. *JACC Cardiovasc Interv* 2018; 11: 1164-71.

37. Dangas GD, Weitz JI, Giustino G, Makkar R, Mehran R. Prosthetic Heart Valve Thrombosis. *J Am Coll Cardiol* 2016; 68: 2670-89.

38. Chakravarty T, Søndergaard L, Friedman J, De Backer O, Berman D, Kofoed KF, *et al.* Subclinical leaflet thrombosis in surgical and transcatheter bioprosthetic aortic valves: an observational study. *Lancet* 2017; 389: 2383-92.

39. Midha PA, Raghav V, Sharma R, Condado JF, Okafor IU, Rami T, *et al.* The Fluid Mechanics of Transcatheter Heart Valve Leaflet Thrombosis in the Neosinus. *Circulation* 2017; 136: 1598-609.

40. Dasi LP, Simon HA, Sucosky P, Yoganathan AP. Fluid mechanics of artificial heart valves. *Clin Exp Pharmacol Physiol* 2009; 36: 225-37.

41. Singh-Gryzbon S, Ncho B, Sadri V, Bhat SS, Kollapaneni SS, Balakumar D, *et al.* Influence of Patient-Specific Characteristics on Transcatheter Heart Valve Neo-Sinus Flow: An In Silico Study. *Ann Biomed Eng* 2020; 48: 2400-11.

42. Van Belle E, Rauch A, Vincent F, Robin E, Kibler M, Labreuche J, *et al.* Von Willebrand Factor Multimers during Transcatheter Aortic-Valve Replacement. *N Engl J Med* 2016; 375: 335-44.

43. Bortot M, Ashworth K, Sharifi A, Walker F, Crawford NC, Neeves KB, *et al.* Turbulent Flow Promotes Cleavage of VWF (von Willebrand Factor) by ADAMTS13 (A Disintegrin and Metalloproteinase With a Thrombospondin Type-1 Motif, Member 13). *Arterioscler Thromb Vasc Biol* 2019; 39: 1831-42.

44. Pinney SP, Anyanwu AC, Lala A, Teuteberg JJ, Uriel N, Mehra MR. Left Ventricular Assist Devices for Lifelong Support. *J Am Coll Cardiol* 2017; 69: 2845-61.

45. Rogers JG, Pagani FD, Tatooles AJ, Bhat G, Slaughter MS, Birks EJ, *et al.* Intrapericardial Left Ventricular Assist Device for Advanced Heart Failure. *N Engl J Med* 2017; 376: 451-60.

46. Prinzing A, Herold U, Berkefeld A, Krane M, Lange R, Voss B. Left ventricular assist devices-current state and perspectives. *J Thorac Dis* 2016; 8: E660-6.

47. Kirklin JK, Naftel DC, Kormos RL, Stevenson LW, Pagani FD, Miller MA, *et al.* Fifth INTERMACS annual report: risk factor analysis from more than 6,000 mechanical circulatory support patients. *J Heart Lung Transplant* 2013; 32: 141-56.

48. Rowlands GW, Pagani FD, Antaki JF. Classification of the Frequency, Severity, and Propagation of Thrombi in the HeartMate II Left Ventricular Assist Device. *ASAIO J* 2020; 66: 992-9.

49. Bourque K, Cotter C, Dague C, Harjes D, Dur O, Duhamel J, *et al.* Design Rationale and Preclinical Evaluation of the HeartMate 3 Left Ventricular Assist System for Hemocompatibility. *ASAIO J* 2016; 62: 375-83.

50. Aliseda A, Chivukula VK, Mcgah P, Prisco AR, Beckman JA, Garcia GJM, *et al.* LVAD Outflow Graft Angle and Thrombosis Risk. *ASAIO J* 2017; 63: 14-23.

51. Geisen U, Heilmann C, Beyersdorf F, Benk C, Berchtold-Herz M, Schlensak C, *et al.* Non-surgical bleeding in patients with ventricular assist devices could be explained by acquired von Willebrand disease. *Eur J Cardio-Thorac Surg* 2008; 33: 679-84.

Identification of patients at risk of secondary cardiovascular events despite using antiplatelet therapy

18

Gert J. de BORST

Platelets play a pivotal role in the progression of atherosclerosis and related cardiovascular events (CVE). Since the introduction of aspirin treatment for the prevention of secondary manifestations of atherosclerotic vascular disease, a drop in recurrence events has been observed. With the development of alternative and supplementary platelet-aggregation inhibitors such as clopidogrel, the prevention of recurrent CVE has become even more effective. Antiplatelet therapy (APT) with aspirin as monotherapy or the combination of aspirin and clopidogrel as dual therapy (DAPT) has become the standard treatment for the primary, secondary and periprocedural prevention of CVE.

However, patients treated with a protocol of aspirin and clopidogrel may still develop CVE. Suggested causes of the impaired efficacy of APT are non-compliance, APT intolerance, high platelet turnover, and non-response.

An estimated 40% of patients with coronary artery, cerebrovascular or peripheral arterial disease treated with clopidogrel have inadequate platelet inhibition. This phenomenon is called high on-treatment platelet reactivity (HTPR). HTPR is associated with a 2.8-fold higher risk of CVE compared to patients with adequate platelet inhibition. Strategies to counter the added thrombotic risk of HTPR vary from an alteration of dosage, switching antiplatelet agents or combining antithrombotic drugs for a synergistic effect. Early identification of patients with HTPR may allow for timely medical intervention and improvement of the treatment decision process.

Platelet function tests (PFT) can be used to both identify HTPR and monitor thrombotic risk. The therapeutic platelet activity window consists of HTPR at the one end of the spectrum and low platelet reactivity (LPR) at the other. Hypothetically, this allows for tailored antiplatelet therapy to lower residual platelet activity (*e.g.*, a higher dose or different drug) to reduce thrombotic risk.

Laboratory testing to identify those patients at increased risk of secondary CVE or post-procedural thrombotic events could aid in optimizing APT and lead to adequate individualized treatment. To date, a great number of tests that measure different aspects of platelet function have been described in the literature. However, considerable variability in the response to APT has been demonstrated between the tests, with high on-aspirin platelet reactivity (HAPR) being reported in 5–45% of patients and high on-clopidogrel platelet reactivity (HCPR) in 4–30%. Furthermore, many platelet-function tests measure platelet reactivity with limited specificity for the applied APT. To our knowledge, no studies have been published that have compared the predictive value of these tests. Clinically, identifying patients at risk of developing secondary CVE despite the use of an APT protocol might be more relevant than identifying genuine resistance to APT.

Differences in patient cohorts, study types, study quality and cardiovascular endpoint definitions complicate a baseline platelet-reactivity test comparison. As a result, there is still no consensus on which HPR test offers the highest predictive value for future CVE.

Genotyping

Clopidogrel is a prodrug, which is transformed into its active metabolite by hepatic cytrochome P450 enzymes. The most important gene to cause reduced clopidogrel effectiveness is the *CYP2C19* gene. Polymorphisms of the CYP2C19-gene have been shown to influence the efficacy of several drugs, including clopidogrel. CYP2C19 enzymes convert clopidogrel into its active metabolite. The active metabolite irreversibly inhibits the P2Y12 receptor on platelets, resulting in inhibition of platelet aggregation. However, clopidogrel-treated patients demonstrate a substantial individual response variability. Carriers of *CYP2C19* loss-of-function (LoF) alleles are at an increased risk of thrombotic events. This has prompted the United State Food and Drug Administration and the European Medicines Agency to add a boxed warning to the label, describing that clopidogrel might not be effective in poor metabolizers.

More than 30 gene alleles have been identified. The *CYP2C19 *1* is the most prevalent (60–70% of the population) and is regarded as the allele causing normal activity. The *CYP2C19*17* is regarded as a gain-of-function allele by many. Based on these assumptions, patients are divided into four different phenotype categories. However, *CYP2C19*17* is not independently associated with clopidogrel response. Furthermore, data on the influence of the *CYP2C19*17* allele on clinical outcomes are inconsistent and its clinical relevance is therefore questionable.

Despite the better efficacy of the stronger $P2Y_{12}$ inhibitors, clopidogrel remains the most utilized platelet inhibitor of the three. The reduced risk of bleeding and reduced costs, especially in non-western countries, probably plays an important part in this. In addition to the introduction of the stronger $P2Y_{12}$ inhibitors, the introduction of newer generation stents have caused a dramatic decrease in thrombotic events, which has shifted attention to the prevention of bleeding complications. This has spurred on research that tries to combine the improved efficacy of the stronger $P2Y_{12}$ inhibitors in patients that are unable to metabolize clopidogrel with the reduced risk of bleeding in patients that react properly to clopidogrel. This can be achieved in two ways, either by using proof from platelet function testing or from genetic testing. Furthermore, it is possible to either chose a strategy in which these tests are used to escalate a strategy from clopidogrel to the stronger $P2Y_{12}$ inhibitors or a de-escalation strategy from the stonger $P2Y_{12}$ inhibitors to clopidogrel.

Platelet function testing

A 2017 literature search in MEDLINE and EMBASE identified 3882 studies. After screening of the titles and abstracts of the papers reporting these studies, 266 were selected for full-text evaluation. On the basis of the exclusion criteria, 164 studies were rejected. A total of 102 studies reporting on 44 098 patients were thus included in the meta-analysis.

Of the 102 studies, 55 (22 441 patients) reported on HAPR, 59 (34 776 patients) on HCPR, and 10 (2864 patients) on HDPR. We identified 97 prospective cohort studies (55 aspirin, 59 clopidogrel, and nine dual treatment) and 5 randomized controlled trials (4 aspirin, 4 clopidogrel, and 1 dual treatment). A number of these studies investigated more than one type of HPR and/or more than one drug.

Study quality, as assessed with the structural checklist, was variable and only a few achieved the maximum score (5 aspirin, 9 clopidogrel, and 1 dual treatment). In most studies, blinding of clinicians and adjudication of clinical events by independent clinicians was either poorly implemented or not described. Thirty-six of 55 studies on HAPR scored 'low risk of bias' on eight or more of the 11 items, and were thus classified as 'good-quality' studies. This was found for 37 of the 59 studies on HCPR.

Regardless of APT, there was significant heterogeneity between selected studies in patient cohorts, treatment of atherosclerotic disease, laboratory methods, percentage of males, proportion of patients with HPR, endpoints, and follow-up.

The review and meta-analysis showed that HAPR, HCPR and HDPR are associated with an increased risk of cardiovascular endpoints. Increasing APT intensity in all patients is associated with an increased risk of bleeding, further emphasizing the need for good risk stratification.

Several laboratory methods for determining HAPR were investigated, and 11 of them predicted an increased CVE risk. PFA-100 and/or VerifyNow were studied most frequently, and had a larger sample size than other HAPR tests. VerifyNow-defined HAPR showed a higher RR of CVEs than PFA-100-defined HAPR, but this difference did not reach statistical significance. On the basis of RR, therefore, none of the tests is superior to the others. Furthermore, there was no difference in the proportion of HAPR between VerifyNow-defined HAPR and PFA-100-defined HAPR. As long as there is no evidence for superiority of one of the HAPR tests, the choice of test should be based on cost, laboratory expertise, equipment, and personal preference.

Of the 14 HCPR tests, 10 predicted increased cardiovascular risk in patients with HCPR. Studies that compared multiple HCPR tests directly did not show superiority of a specific HCPR test. The HCPR tests PFA-100 and VASP did, however, identify high proportions of patients with HCPR.

Most platelet-function tests are either non-specific platelet-function tests or are restricted to a single platelet-activation pathway. It remains unclear whether HPR is caused by genuine APT resistance or by other factors that influence platelet reactivity, such as diabetes mellitus, inflammation, or severity of cardiovascular disease. Only when the cause of HPR is identified will targeted treatment of HPR be achieved. To determine the cause of HPR, there is a need for more sensitive and more specific tests to assess intrinsic platelet reactivity and the effect of APT. Such tests will improve both risk prediction and treatment strategies.

The prevalence of HAPR in our meta-analysis was 29.0%, which is comparable to the 26% that was found in a meta-analysis on the prevalence of aspirin resistance. Potential explanations for HAPR are non-adherence to aspirin therapy, severity of cardiovascular disease, genetics, inflammation and non-platelet sources of thromboxane, sex, aspirin dose, interacting drugs, and tachyphylaxis. HAPR can be improved by addressing non-adherence and by stopping the use of interacting drugs. Furthermore, the optimal regulation of diabetes mellitus, the management of tachyphylaxis and smoking cessation may further improve HAPR. Even though there is no consensus on the definition of HAPR, the available tests suggest that treatment of patients with HAPR might reduce CVE risk.

As users of high doses of aspirin (≥ 300 mg daily) show a lower HAPR prevalence than users of low doses (≤ 100 mg), increasing the aspirin dose may reduce the number of HAPR patients. It is debatable, however, whether improvement of HAPR with a higher aspirin dose reduces CVE risk. No reduction in the number of CVEs was found in a substudy of a large clinical trial comparing an aspirin dose of ≤ 100 mg with a dose of > 100 mg in patients with cardiovascular disease. Similarly, there was no improvement in CVE incidence when APT was adjusted, *i.e.* when the aspirin dose was increased as compared with standard aspirin treatment. Further research on the reduction of CVE incidence with increased aspirin dosage in patients with documented HAPR is required for definitive conclusions to be drawn.

The review found that 38.5% of the patients receiving clopidogrel were classified as having HCPR. The $P2Y_{12}$ receptor-blocking effects of clopidogrel are affected by non-adherence to clopidogrel therapy, high body mass index, diabetes mellitus, acute coronary syndrome, possible drug–drug interactions, insufficient absorption, insufficient metabolic activation, and reduced biological activity. Moreover, a significant amount of variability can be attributed to genetic polymorphisms. HCPR can be improved by reducing non-adherence to clopidogrel therapy and by stopping the use of possible interacting drugs. This can then be followed by adjustment of the APT.

Increasing the clopidogrel dose reduces HCPR. Switching to prasugrel, ticlopidine, ticagrelor or cilostazol has the same effect. However, none of these options is suitable for the treatment of HCPR in all patients. Increasing the clopidogrel dose was less effective in reducing platelet activity than the use of alternative platelet inhibitors, such as prasugrel, ticagrelor, or cilostazol.

Given the conflicting results, which are partly explained by the large variability in study characteristics, it remains unclear which monitoring strategy should be followed. Future research should focus on optimizing HCPR detection and treatment strategies in different clinical settings, in order to maximize the clinical benefit of platelet testing, and to reduce the numbers of both CVEs and bleeding events.

Key take home points

1) Patients with HTPR are prone to a higher thrombotic risk.
2) Both PFT's and genotyping have been proposed as tools to guide antiplatelet therapy.
3) Personalised antiplatelet therapy based on platelet function testing in patients undergoing percutaneous coronary intervention proved non-inferior compared to genotype-guided APT.
4) There is a wide variety of PFT assays available, but the reproducibility, predictive value and ease of use vary greatly. Moreover, the optimal time for testing residual platelet activity is still unknown.
5) Fundamental knowledge concerning the pharmacodynamics of antiplatelet therapy over time is needed to interpret PFT results.
6) not all of the numerous platelet tests are able to identify patients at increased risk for CVE, and each test has a unique predictive value

References

The above text has been derived based on papers by Peter Paul Wisman, the important work by prof Jur ten Berg and his team in the St Antonius Hospital Nieuwegein, and more recently by Aarent Brand in the UMC Utrecht. See below:

Leunissen TC, Wisman PW, van Holten TC, de Groot PG, Korporaal SJ, Koekman AC, et al. The effect of $P2Y_{12}$ inhibition on platelet activation assessed with aggregation-and flow

Leunissen TC, Gijsberts CM, Wisman PP, Huisman A, Berg MT, Asselbergs FW, et al. Lower Platelet Reactivity Is Associated with Presentation of Unstable Coronary Artery Disease. *Int J Angiol* 2016; 25: 210-8.

P Wisman PP, Teraa M, de Borst GJ, Verhaar MC, Roest M, Moll FL. Baseline Platelet Activation and Reactivity in Patients with Critical Limb Ischemia. *PLoS One* 2015; 10: e0131356.

Brand AR, Houben E, Bezemer ID, Visseren FLJ, Bots ML, Mc Herings R , et al. Platelet aggregation inhibitor prescription for newly diagnosed peripheral arterial disease in the Netherlands: a cohort study. *BMJ Open* 2021; 11: e041715.

Ipema J, Brand AR, De Borst GJ, De Vries JP, ÜnlÜ C. Antiplatelet and anticoagulation therapy after revascularization for lower extremity artery disease: a national survey and literature overview *J Cardiovasc Surg (Torino)* 2021; 62: 59-70.

Aortic

- Functional Imaging of the Aortic Wall 168
- Post endograft implantation syndrome: review of mechanisms and signification 179
- What do we actually know about the mechanical properties of guide wires used in endovascular practice? 192
- Fenestration state of the art: When, Who and How? 201

Functional Imaging of the Aortic Wall

19

Michael BELL, Marc A. BAILEY

Diagnostic imaging has evolved and developed to accurately stratify subjects and inform clinicians on the correct course of intervention. The development of functional imaging techniques, where biological remodelling can be quantified, has improved our understanding of disease pathologies as well as diagnosing subjects and facilitating a personalised medicine approach. Functional Positron Emission Tomography (PET) methods such as metabolic profiling of tumours using 2-[^{18}F]-FDG and arterial spin labelling Magnetic Resonance Imaging (MRI) sequences to trace blood flow have enhanced our understanding of the biological processes underlying disease. Functional imaging techniques have been extensively used in the detection of abnormalities in the arterial wall caused by aneurysms, atherosclerotic plaques and peripheral arterial disease. This chapter explores the range of different functional imaging techniques used in detecting changes in the arterial wall and the potential to implement these strategies into the clinic.

Introduction

Modern medicine has evolved significantly over the last 50 years and successfully incorporated medical imaging modalities into the clinical diagnostic pathway to guide and personalise the diagnosis and management of patients. Imaging methods have enhanced our understanding, along with classical laboratory techniques such as immunohistochemistry, polymerase chain reaction (PCR) and immune based assays, of the change in the biological environment by onset of remodelling caused by external or local factors. This is well documented in oncology with hallmarks of cancer imaged include apoptosis, angiogenesis and hypoxia. Use of medical imaging modalities, namely computed tomography (CT), positron emission tomography (PET) and magnetic resonance imaging (MRI) allow visualisation of the internal organs to study disease and functionality. Imaging technologies are associated with their own functional imaging biomarkers to discriminate quantitatively between healthy and diseases states. Implemented imaging biomarkers are useful in the detection of cardiovascular disease.

Diseases of the aortic wall encompass a large proportion of cardiovascular disease burden. The aorta is the largest blood vessel in mammals and faces a large haemodynamic burden due to blood pressure and velocity [1]. The aorta is composed of three layers; a) a thin layer of endothelial cells and elastic lamella called the intima, (b) a densely packed multilayer of vascular smooth muscle cells (VSMCs) and extracellular matrix named the tunica, (c) the adventitia composed of small vessels and nerves. Breakdown of the aortic wall initiated through elastin and collagen degradation, VSMCs remodelling and influx of inflammatory mediators are key hallmarks of aortic wall degradation in abdominal aortic aneurysm (AAA) and atherosclerosis [2].

This chapter is focussed on the advances made in the last 10-15 years in imaging functional changes in the aortic wall in aneurysmal and atherosclerotic disease focussing on promising development of PET radiotracers in preclinical and clinical settings.

Positron Emission Tomography

PET is a powerful imaging modality that detects biological function through specialised radiotracers. The most common radiotracer used in the clinic is 2 [^{18}F] fluorodeoxyglucose (2-[^{18}F]-FDG), an analogue of glucose which reflects regions of high metabolic activity, for example within an actively growing tumour. Each radiotracer is radiolabelled with a positron emitting probe, named radionuclide. The administered radiotracer accumulates in diseased regions and becomes trapped. As the radionuclide decays and emits a positron, it reacts with an electron causing an annihilation event. The product of this event is two colinear 511 kEv gamma rays which are detected by the PET gantry. PET scanners are normally coupled with CT, to provide anatomical localisation of the annihilation event, or in some cases MRI.

Abdominal Aortic Aneurysm

An AAA is defined as a focal dilation of the abdominal aorta >1.5 times the normal diameter. The incidence in Europe is around 4 % in the elderly population (>65 years of age), whereas in the UK, incidence is around 1 %[3,4]. The diameter of a healthy abdominal aorta is 1-2 cm depending on patient sex and body habitus. A 3 cm aortic diameter is diagnostic for AAA. Surgical repair is considered when the aneurysm reaches 5.5 cm in diameter to prevent aneurysm rupture. Patients are considered for interventional treatment to repair the aneurysm through endovascular repair (EVAR) or open surgical repair (OSR) once the intervention threshold of 5.5 cm is reached[5]. The typically quoted rupture risk at 5.5 cm is 2% per year alongside a mortality risk from repair of 1-2% with EVAR and 2-3% with OSR in well selected patients[6]. However, longitudinal analysis from the NHS AAA screening programme (NAAASP) in the UK suggests the risk of rupture at 5.0-5.5cm is actually 0.4% per year in contemporary patients[7]. Based on MASS trial data, patients enter an ultrasound (US) screening programme after confirmed AAA diagnosis[8]. Aneurysm growth rate is typically 2 mm per year however growth is heterogenous and not necessarily linear between patients[9]. The risk factors associated with AAA include gender, smoking, family history and age. Diabetes is protective against AAA formation and growth[10].

Diagnosis of AAA through medical imaging is achieved through US-based screening programmes (in countries where this is available) or incidentally via imaging performed for other reasons. US-based screening programs have been implemented in the UK, USA and Sweden, with dedicated studies in Australia, New Zealand, Denmark, Finland and Norway[11]. In the UK subjects are invited for an abdominal US when they reach the age of 65 and enter the national screening programme if measured aortic diameter is > 3cm[7]. Aortic diameter is measured in the anterior to posterior direction to make a diagnosis. Between screening programmes, different measurements of aortic diameter are chosen. These include outer to outer diameter (OTO), inner to inner diameter (ITI) and leading edge to leading edge (LELE)[12]. The UK small aneurysm trial used OTO method however in both Sweden and the MASS trial, ITI is preferred. This has led to concerns over interobserver measurement reproducibility and standard US probe placement. Using the MASS guidelines, subjects are monitored and treated according to data shown in Table 1. US measurements are advantageous in screening programs as it is cheap, non-ionising and a high throughput of subjects can be scanned. However, data from the RESCAN study demonstrated that for subjects to reach the intervention threshold of 5.5 cm from a 3.0 cm starting diameter can take anywhere between 7 and 13 years[13]. In addition, small aneurysm rupture has been reported occasionally. The RESCAN trial authors argued for relaxation of the follow up period for patients with an aneurysm of 3 cm. This has not been implemented clinically and there are arguments to suggest this leaves both a large scanning burden on hospitals as well as the underlying heterogenous nature of AAA growth. Considerable effort in exploring new imaging biomarkers, as well as serum biomarkers, is currently being undertaken in the hope of finding a complementary method to stratify subjects and offer a personalised medicine approach to this patient population.

Table 1: Summary of MASS guidelines for ultrasound based screening monitoring of subjects [8].

Aortic Diameter	Follow up criteria
< 3 cm	No rescan
3 cm – 4.4 cm	Rescan at year interval
4.5 cm – 5.4 cm	Rescan at 3 month interval
> 5.5 cm	Refer to surgery

Pathology

Much of our initial understanding to the pathophysiology of aneurysm formation stemmed from analysis of surgical samples obtained from OSR – which occurs many years after the aneurysm first formed and grew. As a result, the reported biological pathophysiology may relate to end stage AAA as opposed to the overall remodelling that occurs earlier in the disease process and relates to aneurysm growth. From these studies, key hallmarks of AAA disease were described: infiltration of macrophages and other inflammatory cells, vascular smooth muscle cell loss, angiogenesis and breakdown of elastic lamellae[14]. Use of murine models have indicated two early markers of aneurysm formation; an inflammatory response due to an influx of macrophages and vascular smooth muscle cell (VSMC) remodelling as a cellular response to atherosclerosis [15,16]. Although the atherosclerosis risk in communities (ARIC) study concluded that subjects with atherosclerotic plaques have an increased risk of developing AAA, there are studies which contradict this statement [17,18].

Atherosclerosis

Atherosclerosis is a leading cause of vascular disease worldwide. Biological and non-biological risk factors of atherosclerosis include high plasma lipid levels, diabetes, hypertension, aging and smoking[19]. Atherosclerosis is a slowly progressive disease and presents clinically due to reduced blood supply to target organs (*e.g.* angina, intermittent claudication) or at plaque rupture causing sudden occlusion (*e.g.* myocardial infarction (MI), stroke, limb threatening ischaemia). The formation of atherosclerotic plaques is initiated when lipid containing lipoproteins, mainly low-density lipoproteins (LDLs) accumulate in the intima and activate the endothelium. An inflammatory response follows through recruitment of leukocytes and growth factors. The formation of dense cholesterol lipid lesions in the intimal layer (also referred to as plaques) are seen within the wall of major arteries including the coronary, carotid, femoral arteries and the aorta.

Classic hallmarks of atherosclerotic plaque progression, which provide functional imaging targets, include microcalcification, angiogenesis and inflammation [20]. Microcalcification formation, linked with plaque progression and vulnerability, is driven by inflammation, cholesterol and lipotoxicity [21]. Release of inflammatory cytokines promotes osteogenic switching of VSMC. Presence of microcalcification deposits is linked with plaque instability and VSMC death.

In comparison with AAA, 2-[^{18}F]-FDG and Sodium Fluoride (Na[^{18}F]F) has been studied widely in atherosclerosis disease to look at functional changes. Other markers of inflammation and angiogenesis have also been studied in atherosclerosis. However, much of the PET data analysis of atherosclerosis disease has relied on post-hoc analysis of full body scan data acquired for other diseases (*e.g.* oncology indications). Therefore, there could be a lack of specificity shown in the reported data.

Markers of inflammation

Matrix Metalloproteinases

An early manifestation of aortic wall disease is the loss of elastin and collagen in the aortic wall due to secretion of matrix metalloproteinases (MMPs) [2]. Serum levels of MMPs, in particular MMP-2 and MMP-9, have been detected in both atherosclerosis and AAA subjects. Although molecular markers for MMPs in AAA have been shown in MRI studies [22], radiotracers have only been tested in atherosclerosis models. [^{68}Ga]Ga DOTA TCTP 1 was developed to look at expression levels of MMP-2 and MMP-9 in a murine atherosclerosis model [23]. Although ex vivo autoradiography demonstrated a 1.8-fold increased uptake in atherosclerotic plaque compared to healthy vessel wall, radiotracer uptake was not visible on PET/CT scans due to a low target to background ratio. Alternatively, [^{18}F] radiolabelled (R) 2 (4 (4 Fluorobenzamido)phenylsulfonamido)-3-(1*H*-indol-3-yl)propanoic acid has shown specific binding to MMP-2 and MMP-9 in an ex vivo autoradiography analysis of human atherosclerotic plaque sections [24]. A wide range of radiotracers have been developed for MMP visualisation in other disease which could be applicable. It is unclear whether the reported MMP radiotracers are viable options to study functional wall remodelling in arterial disease.

Macrophages

Much of the work in studying functional remodelling of the arterial wall has focussed on applying 2-[^{18}F]-fluorodeoxyglucose (2-[^{18}F]-FDG) as a marker of metabolically active immune cells to study macrophage infiltration in response to arterial wall injury and inflammation. 2-[^{18}F]-FDG is a radioactive labelled analogue of glucose and localisation reflects hypermetabolic cells. 2-[^{18}F]-FDG is transported through GLUT4 and is not phosphorylated, thus accumulating in hypermetabolic regions. It should be noted that in this context, 2-[^{18}F]-FDG is assumed to report inflammation but the effects of hypoxia and uptake from other metabolically active and remodelling cells in the aortic wall (*e.g.* VSMC) should be considered [25].

The data reported in the literature on 2-[^{18}F]-FDG uptake in AAA and atherosclerosis is confounding. In 2-[^{18}F]-FDG positive AAA subjects (n=8), uptake was correlated with detection of inflammatory leukocytes in the adventitia and smooth muscle cell and collagen loss in the media [26]. This could relate to the weakening of the aortic wall during AAA progression. In asymptomatic AAA subjects (n=12), histological staining demonstrated an increase in the presence of T and B lymphocytes, located in the adventia and media, in the absence of 2-[^{18}F]-FDG uptake [27]. In contrast 2 [^{18}F] FDG can discriminate between symptomatic (n=3) and asymptomatic (n=12) AAA subjects which correlated with differing histological findings. Symptomatic AAA in this study were defined as presenting with aneurysm specific abdominal pain. Symptomatic subjects demonstrated a higher density of macrophages, MMP-9 expression and a reduction of collagen and smooth muscle cells in histological staining when compared to asymptomatic AAA tissue. Standard uptake value (SUV) has also been correlated with changes in aortic diameter. In a 9 month follow up study, AAA subjects (n=9) presenting with low 2-[^{18}F]-FDG uptake at baseline had an increase in aortic diameter [28]. Alternatively, both an inverse correlation (n=25) and no correlation (n=36) has been shown between SUV and aortic diameter. Discrepancies in 2-[^{18}F]-FDG AAA reports could be a result of small study sizes and comparing symptomatic AAA subjects with asymptomatic subjects [29,30].

In atherosclerosis, early studies demonstrated the value of 2-[^{18}F]-FDG in detecting inflammation in carotid plaques [31]. 2-[^{18}F]-FDG was able to discriminate between symptomatic and asymptomatic lesions in carotid atherosclerosis subjects (n=8) [32]. Regions of 2-[^{18}F]-FDG uptake correlated with an increase in macrophage accumulation, similar to some results in AAA. High risk carotid structures identified by CT (remodelling, low attenuation and luminal irregularity) and macrophage infiltration correlated

with an increase in 2-[18F]-FDG [33]. Although the evidence suggests, in atherosclerosis, 2-[18F]-FDG could detect functional changes in the arterial wall, similar confounding results have been reported. A large multicentre study showed there was no correlation between macrophage infiltration in carotid plaques and 2-[18F]-FDG uptake [34]. A comparison of CT derived features and 2 [18F]-FDG uptake in atherosclerosis subjects are defined as two separate events in lesion remodelling [35]. Similar to AAA, studies in atherosclerosis tend to have a small sample size and rely on data sets acquired for other clinical indications (*i.e.* full body oncology PET scans) for data analysis. In addition, a murine lineage tracing study demonstrated cells contributing to atherosclerosis development that were believed to be macrophages were VSMC derived [36]. Although this study may not truly reflect human pathology, it could be suggested in atherosclerosis 2-[18F]-FDG could be detecting remodelled VSMCs.

Although 2-[18F]-FDG data in atherosclerosis is contradictory, promising results have been shown to detect functional changes due to macrophage infiltration using [68Ga] labelled radiotracers. The VISION study demonstrated [68Ga]-DOTATATE, when compared to 2-[18F]-FDG, could discriminate between high and low risk lesions in coronary imaging due to macrophage specificity [37]. Future studies to detect inflammatory mediates in the arterial wall may lie with more specific radiotracers against markers of macrophages or other inflammatory mediates.

Microcalcification

The formation of calcification deposits within the structure of the aorta have been attributed to a response to extracellular remodelling and inflammation. Microcalcification, defined as deposits of calcium hydroxyapatite on the extracellular matrix, reflects active remodelling and is linked with increased instability of the arterial wall. On the other hand, macrocalcification is linked with stable calcium plaques (*e.g.* the 'porcelain aorta').

Na[18F]F is a marker of microcalcification and has been shown to differentiate between micro- and macrocalcification. Accumulation of Na[18F]F occurs through exchange of [18F]-and hydroxyl ions (OH-) in the hydroxyapatite structure. In a mouse model of atherosclerosis and in *in vitro* models of calcification suggested that Na[18F]F uptake reflects developing microcalcification devoid of CT contrast[38]. Autoradiography studies demonstrated that Na[18F]F bound freely to regions of microcalcification in carotid plaque sections, correlating with alizarin red staining [39]. Including studies in atherosclerosis and AAA, Na[18F]F has shown to be a valuable radiotracer to detect changes in the vasculature.

A post hoc analysis of 1,930 calcified plaques revealed that 12% of plaques displayed prominent Na[18F]F uptake [40]. Atherosclerotic Na[18F]F imaging has, however, shown to be able to discriminate between subjects with culprit and non-culprit plaques as well as symptomatic and asymptomatic subjects [41,42]. High uptake in culprit plaque correlated with remodelling, microcalcification and necrosis [43]. Definition of the PET metric used to define functional changes in the aortic wall as a result of atherosclerosis may need to be determined. Incubation dose per gram (% Inc/g) defined measurements of excised carotid plaques in stroke subjects was unable to discriminate Na[18F]F signal in culprit and non-culprit plaques[44]. Measuring the maximal tissue to background ratio (TBR_{max}) in the most diseased plaque segment allowed differentiation between culprit and non-culprit plaques independent of other factors (stenosis) [45]. Radiomic analysis could be used to define the most suitable metric to use in atherosclerotic plaques, similar to a study of Na[18F]F uptake from human AAA samples.

The Sodium Fluoride in Abdominal Aortic Aneurysm (SoFIA3) trial demonstrated that Na[18F]F uptake could predict patient outcome (end point rupture) and growth of AAA independent of classical risk factors (*e.g.* age) [46]. This is the first PET/CT trial in humans to demonstrate the use of functional imaging

in AAA in accurately stratifying subjects. Although the SoFIA[3] trial was conducted in end stage subjects, it would be beneficial to use Na[^{18}F]F in small, early stage aneurysms to see if similar results occur. In addition, studies utilising travelling subjects and multicentre PET scans should be considered.

The value of Na[^{18}F]F in vascular imaging has shown its benefits in predicting subjects who are at risk of restenosis when undergoing percutaneous transluminal angioplasty treatment for peripheral arterial hypertension (PAH) and subjects at risk of MI with coronary artery disease [47,48]. Further studies with Na[^{18}F]F to detect functional changes in arterial wall should be prioritised for translating into the clinic.

Angiogenesis

The formation of new vessels from existing vasculature is a feature of both AAA and atherosclerosis, with few PET/CT studies using radiotracers to analyse the functional change. Detection of angiogenesis is a histological feature of vascular disease, but is not fully understood in the progression of, for example, AAA.

The only human study to show the potential of angiogenic tracers in detecting changes in the vascular wall is the application of [^{18}F]-Fluciclatide in atherosclerotic subjects [49]. [^{18}F]-Fluciclatide binds to upregulated angiogenic integrin αvβ3 through an interaction with the amino acid sequence Ariginie-Glycine-Aspartate (RGD). Recruited subjects represented both stable (n=27) and unstable (n=19) carotid plaques. [^{18}F] Fluciclatide uptake was highest in unstable carotid plaques compared to stable carotid plaques (TBR_{max} = 1.29 vs 1.21 p=0.02). In addition, uptake correlated with common measures of atherosclerotic plaque including plaque volume and CT defined calcium score as well as histological features. An ex vivo AAA tissue study also determined uptake of [^{18}F]-Fluciclatide was highest when compared to other non-specific AAA radiotracers [50]. Another marker of αvβ3 upregulation, [^{18}F]-$FPPRGD_2$, was shown to discriminate between AngII induced AAA and sham operated murine models [51]. A positive correlation between radiotracer uptake and US defined aortic diameter was also found.

The study of the formation of new vessels in vascular disease using PET is in its infancy, however, there is promising data to suggest the application of these tracers could be beneficial. Further longitudinal studies in preclinical models would be beneficial to see how the detection of angiogenesis affects the functional remodelling of the aortic wall and if this is translatable into clinical practise.

Proliferation

In response to arterial injury and remodelling, a cellular proliferative event in response to inflammation, for example VSMC phenotypic switching showing upregulation of proliferation markers in AAA, has been shown (52). 3-[^{18}F]-Flurothymidine (3 [^{18}F] FLT) is a marker of cellular proliferation and has shown some promise in detecting vascular injury. In the AngII murine model of AAA, 3-[^{18}F]-FLT uptake was enhanced during the active aneurysm growth phase [53]. SUVmax peaked at day 14 post surgery and reduced at day 28. Uptake as well correlated with the upregulation of proliferative markers such as thymidine kinase 1 (TK-1). A similar finding was reported in idiopathic PAH subjects (n=8), where VSMC remodelling and proliferation is also a key part of the pathology [54]. 3-[^{18}F]-FLT uptake was distinguishable from control subject and isolated arteries showed an upregulation of TK-1. The promising results with 3-[^{18}F]-FLT in mice has driven calls for human investigation, in particular in AAA [55], with further exploration needed to study the potential role as a imaging biomarker.

Discussion

Functional imaging in the aortic wall has developed and advanced considerably over the last decade, with the application and development of new novel radiotracers for PET imaging, although has not yet transitioned into clinical practice. AAA diagnosis and monitoring tends to rely on anatomical imaging to measure aortic diameter and aneurysm growth. Although this allows monitoring of patients and referral for surgery at the intervention threshold of 5.5cm, it remains a blunt tool. Aortic diameter cannot predict longitudinal growth accurately or identify small AAA at risk of rupture [7,9]. On the other hand, atherosclerosis testing is reliant on diagnostic cholesterol tests and chest x-rays to name a few. Many of these interventions are too late for the patient and there is a need for a diagnostic test that can catch early manifestation of atherosclerosis plaque. PET imaging could provide an alternative route in stratifying and personalising patient care, as shown by the SoFIA^3 trial [46], as well as other 3D volumetric techniques [56], and further AI analysis of CT data [57].

Early studies in the field of functional imaging of the aortic wall have relied heavily on 2-[^{18}F]-FDG as it is widely available and is used routinely in PET centres. However, it is clear from the evidence reported in both atherosclerosis and AAA that the consensus on detecting changes is confounding. The attempt at correlating 2 [^{18}F] FDG with aortic growth in AAA has shown a variety of trends and the link between uptake and macrophage infiltration is tenuous. A similar trend has been shown in atherosclerosis, where uptake of 2-[^{18}F]-FDG may not necessarily reflect macrophage infiltration in plaques [34].

Research into imaging of functional changes in the aortic wall may benefit from focussing on radiotracers used in specific imaging pathways. The VISION trial showed [^{68}Ga]-DOTATATE specifically detected macrophage expressing somatostatin receptors on atherosclerotic plaque and differentiate between high-and low-risk plaques when compared to 2-[^{18}F]-FDG [37]. A study in AAA subjects to assess the feasibility of macrophage detection and its relationship with aortic growth could be beneficial. The SoFIA^3 trial demonstrated that uptake of Na[^{18}F]F in AAA subjects could predict patient outcome (risk of rupture) and aneurysm growth independent of classical AAA risk factors [46]. Further studies looking at how PET uptake reflects the longitudinal growth and changes in remodelling are required to understand the roles these tracers fully. In addition, evaluation of promising tracers such as 3-[^{18}F]-FLT [53] and [^{18}F]-FPPRGD$_2$ [51] are in human trials are warranted.

Within the research of the applicability of the radiotracers mentioned in this chapter, there are no at multicentre studies to further assess the roles of these tracers as imaging biomarkers in stratifying subjects as well as offering personalised medicine. Although these studies would need a large patient participant, careful monitoring of radiation dose and are expensive, it is important to determine the full clinical utility before translation into patient care.

To conclude, PET imaging of the functional wall has shown to be a viable option in determining aortic remodelling in response to disease. Further studies are required to evaluate the role of radiotracer uptake coupled with the underlying biological processes.

Table 2: Summary of radiotracers used to detect inflammation in vascular disease

Radiotracer	Vascular Disease	Summary	References
2-[^{18}F]-FDG	AAA	Evidence to support the use of 2-[^{18}F]-FDG as a marker of inflammation is confounding. Varying reports on correlation with histological staining of macrophages and with known clinical measures *e.g.* aortic diameter.	(26–30)
	Atherosclerosis	Conflicting reports on the ability of 2-[^{18}F]-FDG to detect vulnerable plaques. There is a suggestion that radiotracer uptake may reflect functional remodelling separate from features detected by CT.	(31–35)
[^{68}Ga]-DOTATATE	Atherosclerosis	VISION study showed [^{68}Ga]DOTATATE superiority in discriminating between high and low risk lesions compared to 2[^{18}F]FDG.	(37)

Table 3: Summary of Na[^{18}F]F detecting microcalcifications in vascular disease

Radiotracer	Vascular Disease	Summary	Reference
Na[^{18}F]F	AAA	The SoFiA^3 trial is the first PET/CT study to show Na[^{18}F]F detection in AAA is independent of AAA risk factors (*e.g.* age) and uptake is a predictor of aneurysm growth and endpoint (*e.g.* risk of rupture).	(46)
	Atherosclerosis	Na[^{18}F]F superior uptake has been able to discriminate between culprit and non-culprit plaques and symptomatic and asymptomatic subjects. Further work is required to define most suitable metric to report clinically.	(40–45)
	Peripheral Arterial Hypertension	Uptake of Na[^{18}F]F detected subjects at risk of restenosis after percutaneous transluminal angioplasty treatment.	(47)

Table 4: Summary of radiotracers used to detect angiogenesis in vascular disease

Radiotracer	Vascular Disease	Summary	Reference
[^{18}F]-Fluciclatide	Atherosclerosis	A small cohort study demonstrated that [^{18}F] Fluciclatide could discriminate between stable and unstable plaques. Uptake also correlated with CT scores.	(49)
	AAA	Ex vivo autoradiography of AAA human tissue showed superior binding of [^{18}F]Fluciclatide when compared to other tracers.	(50)
[^{18}F]-FPPRGD$_2$	AAA	Development of a novel arginine-glycine-aspartate binding radiotracer showed high uptake in a preclinical model of AAA compared to controls.	(51)

Table 5: Summary of 3-[^{18}F]-FLTF detecting proliferation in vascular disease

Radiotracer	Vascular Disease	Summary	Reference
3-[^{18}F]-FLT	AAA	Radiotracer uptake reflected the active growth phase in a preclinical model of AAA. Uptake also correlated with upregulation of proliferation transporters.	(53)
	Peripheral arterial hypertension	Idiopathic PAH subjects showed both an enhanced uptake and upregulation of proliferation transporters when compared to control subjects.	(54)

References

1. Bäck M, Gasser TC, Michel JB, Caligiuri G. Biomechanical factors in the biology of aortic wall and aortic valve diseases. *Cardiovasc Res* 2013; 99: 232-41.
2. Isselbacher EM. Thoracic and abdominal aortic aneurysms. *Circulation* 2005; 111: 816-28.
3. Sprynger M, Willems M, Van Damme H, Drieghe B, Wautrecht JC, Moonen M. Screening Program of Abdominal Aortic Aneurysm. *Angiology* 2019; 70: 407-13.
4. Kim LG, Sweeting MJ, Armer M, Jacomelli J, Nasim A, Harrison SC. Modelling the impact of changes to abdominal aortic aneurysm screening and treatment services in England during the COVID-19 pandemic. *PLoS One* 2021; 16: 1-13.
5. Swerdlow NJ, Wu WW, Schermerhorn ML. Open and endovascular management of aortic aneurysms. *Circ Res* 2019; 124: 647-61.
6. Sutzko DC, Mani K, Behrendt CA, Wanhainen A, Beck AW. Big data in vascular surgery: registries, international collaboration and future directions. *J Intern Med* 2020; 288: 51-61.
7. Oliver-Williams C, Sweeting MJ, Jacomelli J, Summers L, Stevenson A, Lees T, *et al.* Safety of Men with Small and Medium Abdominal Aortic Aneurysms under Surveillance in the NAAASP. *Circulation* 2019; 139: 1371-80.
8. Ashton HA, Buxton MJ, Day NE, Kim LG, Marteau TM, Scott RAP, *et al.* The Multicentre Aneurysm Screening Study (MASS) into the effect of abdominal aortic aneurysm screening on mortality in men: a randomised controlled trial. *Lancet* 2002; 360: 1531-9.
9. Bailey MA, Baxter PD, Jiang T, Charnell AM, Griffin KJ, Johnson AB, *et al.* Modeling the Growth of Infrarenal Abdominal Aortic Aneurysms. *Aorta* 2014; 1: 268-73.
10. Nordon IM, Hinchliffe RJ, Loftus IM, Thompson MM. Pathophysiology and epidemiology of abdominal aortic aneurysms. *Nat Rev Cardiol* 2011; 8: 92-102.
11. Stather PW, Dattani N, Bown MJ, Earnshaw JJ, Lees TA. International variations in AAA screening. *Eur J Vasc Endovasc Surg* 2013; 45: 231-4.
12. Matthews EO, Pinchbeck J, Elmore K, Jones RE, Moxon J V, Golledge J. The reproducibility of measuring maximum abdominal aortic aneurysm diameter from ultrasound images. *Ultrasound J* 2021; 13: 13.
13. Sweeting MJ, Thompson SG, Brown LC, Powell JT. Meta-analysis of individual patient data to examine factors affecting growth and rupture of small abdominal aortic aneurysms. *Br J Surg* 2012; 99: 655-65.
14. Golledge J. Abdominal aortic aneurysm: update on pathogenesis and medical treatments. *Nat Rev Cardiol* 2019; 16: 225-42.
15. Matthew Longo G, Xiong W, Greiner TC, Zhao Y, Fiotti N, Timothy Baxter B. Matrix metalloproteinases 2 and 9 work in concert to produce aortic aneurysms. *J Clin Invest* 2002; 110: 625-32.
16. Ward MR, Pasterkamp G, Yeung AC, Borst C. Arterial remodeling. Mechanisms and clinical implications. *Circulation* 2000; 102: 1186-91.
17. Yao L, Folsom AR, Alonso A, Lutsey PL, Pankow JS, Guan W, *et al.* Association of carotid atherosclerosis and stiffness with abdominal aortic aneurysm: The atherosclerosis risk in communities (ARIC) study. *Atherosclerosis* 2018; 270: 110-6.
18. Michel JB, Martin-Ventura JL, Egido J, Sakalihasan N, Treska V, Lindholt J, *et al.* Novel aspects of the pathogenesis of aneurysms of the abdominal aorta in humans. *Cardiovasc Res* 2011; 90: 18-27.
19. Mannarino E, Pirro M. Molecular biology of atherosclerosis. *Clin Cases Miner Bone Metab* 2008; 5: 57-62.
20. Ten Kate GL, Sijbrands EJG, Valkema R, Ten Cate FJ, Feinstein SB, Van Der Steen AFW, *et al.* Molecular imaging of inflammation and intraplaque vasa vasorum: A step forward to identification of vulnerable plaques? *J Nucl Cardiol* 2010; 17: 897-912.
21. Akers EJ, Nicholls SJ, Di Bartolo BA. Plaque calcification: Do lipoproteins have a role? *Arterioscler Thromb Vasc Biol* 2019; 39: 1902-10.

22. Makowski MR, Preissel A, von Bary C, Warley A, Schachoff S, Keithan A, *et al.* Three-Dimensional Imaging of the Aortic Vessel Wall Using an Elastin-Specific Magnetic Resonance Contrast Agent. *Invest Radiol* 2012; 47: 438-44.

23. Kiugel M, Hellberg S, Käkelä M, Liljenbäck H, Saanijoki T, Li XG, *et al.* Evaluation of [68Ga]Ga-DOTA-TCTP-1 for the detection of metalloproteinase 2/9 expression in mouse atherosclerotic plaques. *Molecules* 2018; 23: 1-11.

24. Selivanova S V., Stellfeld T, Heinrich TK, Müller A, Krämer SD, Schubiger PA, *et al.* Design, synthesis, and initial evaluation of a high affinity positron emission tomography probe for imaging matrix metalloproteinases 2 and 9. *J Med Chem* 2013; 56: 4912-20.

25. Folco EJ, Sheikine Y, Rocha VZ, Christen T, Shvartz E, Sukhova GK, *et al.* Hypoxia but not inflammation augments glucose uptake in human macrophages: Implications for imaging atherosclerosis with 18fluorine-labeled 2-deoxy-D-glucose positron emission tomography. *J Am Coll Cardiol* 2011; 58: 603-14.

26. Courtois A, Nusgens B V, Hustinx R, Namur G, Gomez P, Somja J, *et al.* 18F-FDG uptake assessed by PET/CT in abdominal aortic aneurysms is associated with cellular and molecular alterations prefacing wall deterioration and rupture. *J Nucl Med* 2013; 54: 1740-7.

27. Reeps C, Essler M, Pelisek J, Seidl S, Eckstein HH, Krause BJ. Increased 18F-fluorodeoxyglucose uptake in abdominal aortic aneurysms in positron emission/computed tomography is associated with inflammation, aortic wall instability, and acute symptoms. *J Vasc Surg* 2008; 48: 417-23.

28. Morel O, Mandry D, Micard E, Kauffmann C, Lamiral Z, Verger A, *et al.* Evidence of cyclic changes in the metabolism of abdominal aortic aneurysms during growth phases: 18F-FDG PET sequential observational study. *J Nucl Med* 2015; 56: 1030-5.

29. Barwick TD, Lyons OTA, Mikhaeel NG, Waltham M, O'Doherty MJ. 18F-FDG PET-CT uptake is a feature of both normal diameter and aneurysmal aortic wall and is not related to aneurysm size. Eur *J Nucl Med Mol Imaging* 2014; 41: 2310-8.

30. Kotze CW, Groves AM, Menezes LJ, Harvey R, Endozo R, Kayani IA, *et al.* What is the relationship between 18F-FDG aortic aneurysm uptake on PET/CT and future growth rate? *Eur J Nucl Med Mol Imaging* 2011; 38: 1493-9.

31. Arauz A, Hoyos L, Zenteno M, Mendoza R, Alexanderson E. Carotid plaque inflammation detected by 18F-fluorodeoxyglucose-positron emission tomography. Pilot study. *Clin Neurol Neurosurg* 2007; 109: 409-12.

32. Rudd JHF, Warburton EA, Fryer TD, Jones HA, Clark JC, Antoun N, *et al.* Imaging atherosclerotic plaque inflammation with [18F]-fluorodeoxyglucose positron emission tomography. *Circulation* 2002; 105: 2708-11.

33. Figueroa AL, Subramanian SS, Cury RC, Truong QA, Gardecki JA, Tearney GJ, *et al.* Distribution of inflammation within carotid atherosclerotic plaques with high-risk morphological features a comparison between positron emission tomography activity, plaque morphology, and histopathology. *Circ Cardiovasc Imaging* 2012; 5: 69-77.

34. Myers KS, Rudd JHF, Hailman EP, Bolognese JA, Burke J, Pinto CA, *et al.* Correlation Between Arterial FDG Uptake and Biomarks in Peripheral Artery Disease. *J Am Coll Cardiol Cardiovasc Imaging* 2012; 5: 38-45.

35. Dunphy MPS, Freiman A, Larson SM, Strauss HW. Association of vascular 18F-FDG uptake with vascular calcification. *J Nucl Med* 2005; 46: 1278-84.

36. Shankman LS, Gomez D, Cherepanova OA, Salmon M, Alencar GF, Haskins RM, *et al.* KLF4-dependent phenotypic modulation of smooth muscle cells has a key role in atherosclerotic plaque pathogenesis. *Nat Med* 2015; 21: 628-37.

37. Tarkin JM, Joshi FR, Evans NR, Chowdhury MM, Figg NL, Shah A V, *et al.* Detection of Atherosclerotic Inflammation by 68Ga-DOTATATE PET compared to [18F]FDG PET Imaging. *J Am Coll Cardiol* 2017; 69: 1774-91.

38. Creager MD, Hohl T, Hutcheson JD, Moss AJ, Schlotter F, Blaser MC, *et al.* 18F-fluoride signal amplification identifies micro-calcifications associated with atherosclerotic plaque instability in positron emission tomography/computed tomography images. *Circ Cardiovasc Imaging* 2019; 12: 1-11.

39. Irkle A, Vesey AT, Lewis DY, Skepper JN, Bird JLE, Dweck MR, *et al.* Identifying active vascular microcalcification by 18F-sodium fluoride positron emission tomography. *Nat Commun* 2015; 6: 1-11.

40. Derlin T, Richter U, Bannas P, Begemann P, Buchert R, Mester J, *et al.* Feasibility of 18F-sodium fluoride PET/CT for imaging of atherosclerotic plaque. *J Nucl Med* 2010; 51: 862-5.

41. Quirce R, Martínez-Rodríguez I, Banzo I, Jiménez-Bonilla J, Martínez-Amador N, Ibáñez-Bravo S, *et al.* New insight of functional molecular imaging into the atheroma biology: 18F-NaF and 18F-FDG in symptomatic and asymptomatic carotid plaques after recent CVA. Preliminary results. *Clin Physiol Funct Imaging* 2016; 36: 499-503.

42. Kitagawa T, Yamamoto H, Toshimitsu S, Sasaki K, Senoo A, Kubo Y, *et al.* 18F-Sodium Fluoride positron emission tomography for molecular imaging of coronary atherosclerosis based on computed tomography analysis. *Atherosclerosis* 2017; 263: 385-92.

43. Joshi N V., Vesey AT, Williams MC, Shah ASV, Calvert PA, Craighead FHM, *et al.* 18F-fluoride positron emission tomography for identification of ruptured and high-risk coronary atherosclerotic plaques: A prospective clinical trial. *Lancet* 2014; 383: 705-13.

44. Hop H, de Boer SA, Reijrink M, Kamphuisen PW, de Borst MH, Pol RA, *et al.* 18F-sodium fluoride positron emission tomography assessed microcalcifications in culprit and non-culprit human carotid plaques. *J Nucl Cardiol* 2019; 26: 1064-75.

45. Evans NR, Tarkin JM, Chowdhury MM, Le EPV, Coughlin PA, Rudd JHF, *et al.* Dual-tracer positron-emission tomography for identification of culprit carotid plaques and pathophysiology *in vivo*. *Circ Cardiovasc Imaging* 2020; 13: e009539.

46. Forsythe RO, Dweck MR, McBride OMB, Vesey AT, Semple SI, Shah ASV, *et al.* 18F–Sodium Fluoride Uptake in Abdominal Aortic Aneurysms: The SoFIA^3 Study. *J Am Coll Cardiol* 2018; 71: 513-23.

47. Chowdhury MM, Tarkin JM, Albaghdadi MS, Evans NR, Le EP V, Berrett TB, *et al.* Vascular Positron Emission Tomography and Restenosis in Symptomatic Peripheral Arterial Disease. A prospective clinical study. *J Am Coll Cardiol Cardiovasc Imaging* 2020; 13: 1008-17.

48. Kwiecinski J, Tzolos E, Adamson PD, Cadet S, Moss AJ, Joshi N, *et al.* Coronary 18F Sodium Fluoride Uptake Predicts Outcome in Patients with Coronary Artery Disease. *J Am Coll Cardiol* 2020; 75: 3061-74.

49. Jenkins WS, Vesey AT, Vickers A, Neale A, Moles C, Connell M, *et al. In vivo* alpha-V beta-3 integrin expression in human aortic atherosclerosis. *Heart* 2019; 105: 1868-75.

50. Tegler G, Estrada S, Hall H, Wanhainen A, Björck M, Sörensen J, *et al.* Autoradiography screening of potential positron emission tomography tracers for asymptomatic abdominal aortic aneurysms. *Ups J Med Sci* 2014; 119: 229-35.

51. Kitagawa T, Kosuge H, Chang E, James ML, Yamamoto T, Shen B, *et al.* Integrin-targeted molecular imaging of experimental abdominal aortic aneurysms by 18F-labeled Arg-Gly-Asp positron-emission tomography. *Circ Cardiovasc Imaging* 2013; 6: 950-6.

52. Ailawadi G, Moehle CW, Pei H, Walton SP, Yang Z, Kron IL, *et al.* Smooth muscle phenotypic modulation is an early event in aortic aneurysms. *J Thorac Cardiovasc Surg* 2009; 138: 1392-9.

53. Gandhi R, Cawthorne C, Craggs LJL, Wright JD, Domarkas J, He P, *et al.* Cell proliferation detected using [18F]FLT PET/CT as an early marker of abdominal aortic aneurysm. *J Nucl Cardiol* 2019.

54. Ashek A, Spruijt OA, Harms HJ, Lammertsma AA, Cupitt J, Dubois O, *et al.* 3'-Deoxy-3'-[18F]Fluorothymidine Positron Emission Tomography Depicts Heterogeneous Proliferation Pathology in Idiopathic Pulmonary Arterial Hypertension Patient Lung. *Circ Cardiovasc Imaging* 2018; 11: e007402.

55. Syed MBJ, Fletcher AJ, Dweck MR, Forsythe R, Newby DE. Imaging aortic wall inflammation. *Trends Cardiovasc Med* 2019; 29: 440-8.

56. Waduud MA, Kandavelu P, Reay M, Paradine K, Scott DJA, Baily MA. High frequency 3D lumen volume ultrasound is a sensitive method to detect early aneurysmal change in elastase induced murine abdominal aortic aneurysm. *Aorta* 2021.

57. Chandrashekar A, Handa A, Shivakumar N, Lapolla P, Uberoi R, Grau V, *et al.* A Deep Learning Pipeline to Automate High-Resolution Arterial Segmentation with or without Intravenous Contrast. *Ann Surg 2021 in press.*

Post endograft implantation syndrome: review of mechanisms and signification

20

Rita Soares FERREIRA, Tiago RIBEIRO, Frederico BASTOS GONÇALVES

Endovascular aneurysm repair (EVAR) can be associated to a systemic inflammatory response but there is still no consensus over the etiology, definition, incidence, associated factors, consequences, treatment and eventually prophylactic therapy of this syndrome.

To review the available literature reporting post endograft implantation syndrome (PIS), namely its incidence, mechanisms, clinical consequences, prevention and treatment.

A research was performed in MEDLINE and EMBASE databases for relevant studies with the following text word search: "endovascular" AND "aneurysm" AND ("postimplantation syndrome" OR "inflammation"). All studies reporting either incidence, etiology, clinical consequences, prophylaxis or treatment of PIS were included.

Forty-three studies were included in this review. The reported incidence of PIS in the literature varies widely (2-100%) and it occurs after EVAR but also after dissection and other aortic syndromes. The most common definition is a combination of fever and leukocytosis but some authors used fever and C reactive protein (CRP) elevation as diagnostic criteria. Several factors have been associated with the occurrence of PIS. The most well studied factor is endograft fabric: polyester, when compared to expanded polytetrafluoroethylene, results in a greater inflammatory reaction. Endovascular aneurysm sealing also associates to a reduced occurrence of PIS compared to EVAR. Clinical manifestations are similar to a flu syndrome with abdominal and/or lumbar pain and a rise in inflammatory markers (leukocyte count and CRP), but the cutoffs for diagnosis are not homogeneously defined. Procalcitonin appears to be a good laboratorial differentiator between PIS and postoperative infection. PIS is associated to a prolonged hospital stay and worse early quality of life but there is still no consensus over the possible effects on cardiovascular- and aneurysm-related complications. Prevention and treatment of this condition have been attempted with the use of steroids or nonsteroid anti-inflammatory drugs.

The most frequently reported incidence of PIS is 20-40%. Well-defined criteria for diagnosis may be established based on current evidence. Prospective longitudinal studies, preferably with blinded randomization, have to be designed to clarify the clinical consequences and the need to prophylactic or symptomatic treatment.

Introduction

Endovascular aneurysm repair (EVAR) can be associated to a systemic inflammatory response which is known by postimplantation syndrome (PIS)[1]. This syndrome is described since 1999 by Velazquez *et al.* as an association of fever and leukocytosis after aortic stent-graft implantation[2]. It was incidentally noted in clinical EVAR studies and its manifestations include fatigue or other constitutional (flu-like) symptoms, fever and laboratory findings of inflammation[2].

Experimental studies in animals confirmed a local peri-aortic inflammatory response to EVAR: macroscopic examination of the arterial wall revealed significant inflammatory peri-graft response with vascular thickening and adhesions around the grafts and microscopic examination, corresponding to a severe foreign-body response[3].
In spite of several publications addressing the topic, published since the 1990s, there is still no consensus over the ethiopatogeny, definition, incidence, associated factors, consequences, treatment and eventually prophylactic therapy of this syndrome.

The purpose of this article is to provide a comprehensive review of the available literature reporting PIS, namely its incidence, ethiopathogeny, clinical consequences, prophylaxis and treatment.

Materials and Methods

Data sources: A research was performed on 27th November 2020 in MEDLINE and EMBASE databases for relevant studies with the following text word search in the title: "endovascular" AND "aneurysm" AND ("postimplantation syndrome" OR "inflammation"), by one author (RSF). The bibliographies of included studies were also assessed. No language restriction was imposed.

Study selection: All studies reporting either incidence, etiology, clinical consequences, prophylaxis or treatment of PIS were included. Disagreements regarding inclusion were resolved by consensus of all three authors.

Data extraction: One author (RSF) collected data including details of the publication, demographics of the enrolled patients, description of the interventions used, outcome definitions and results. All the authors reviewed, compilated and summarized the extracted data.

Results

Forty-three studies were included in this review. The results are presented below by the following sub-topics: definition and incidence, ethiopathogeny, manifestations, clinical consequences and prevention/ treatment.

Definition and incidence

The most accepted definition for PIS is an association of constitutional symptoms, like fatigue and fever, and a rise in inflammatory biomarkers. However, which markers should be used and their cutoff values are not yet defined. Hence, in literature, there are several proposed combinations of fever, leukocytosis, and elevated C-reactive protein (CRP) used as definition for PIS. The most common definition is an adjustment of Systemic Inflammatory Response Syndrome (SIRS) criteria – combination of fever and leukocytosis – but some authors used fever and CRP elevation as criteria[1,2,4–11]. (Table 1)

Table 1: Incidence of PIS according to definition

Authors, Year of Publication, Journal	Study design	Number of included patients	Fever	Leukocyte count	CRP	Incidence of PIS
Unclear definition						
Blum *et al.*, 1997, New England Journal of Medicine[12]	Prospective	154	ns	ns	ns	56%
Chang *et al.*, 2014, Journal of Vascular Surgery[14]	Prospective	38	ns	ns	ns	47%
Georgiadis *et al.*, 2011, Journal of Vascular Surgery[15]	Prospective	77	ns	ns	ns	36,4%
Mazzaccaro *et al.*, 2016, Annals Vascular Surgery[16]*	Retrospective	10	ns	ns	ns	30%
Melissano *et al.*, 2015, Journal of Vascukar Surgery[17]**	Retrospective	42	ns	ns	ns	2%
Definition with leukocytosis and fever						
Arnaoutoglou *et al.*, 2011, Interact Cardiovasc Thorac Surg[4]	Prospective	162	>38°C	>12.000/ml	-	30.2%
Dosluoglu *et al.*, 2014, Journal Vascular Surgery[6]***	Retrospective	79	>37.8°C	>10.000/ml [a]	-	23%
Nano *et al.*, 2014, Annals Vascular Surgery[8]****	Retrospective	118	>38°C	>12.000//ml	-	20,3%
Kakisis *et al.*, 2014, Journal Vascular Surgery[18]	Retrospective	87	>38°C	>12.000//ml	-	39%
Arnaoutoglou *et al.*, 2014, European Jounal Cardiovascular Surgery[10]	Prospective	214	>38°C	>12.000//ml	-	36%
Sartipy *et al.*, 2015, Vasc Endovasc Surgery[19]	Prospective	45	>38°C	>12.000//ml	-	28%
Kwon *et al.*, 2016, Medicine[20]	Retrospective	204	>38°C	>12.000//ml	-	31,4%

Arnaoutoglou *et al.*,2016, Journal Vascular Surgery[21]	Prospective	182	>38°C	>12.000//ml	-	35.7%
Zhu *et al.*, 2019, Eur J Cardiothorac Surg.****	Retrospective	646	>38°C	>12.000//ml	-	31.6%
Definition with fever and CRP						
Voûte *et al.*, 2012, Journal Vascular Surgery[5]	Retrospective	149	>38°C	-	> 10 mg/L	38.9%
Gorla *et al.*, 2015, European Journal of Cardio-Thoracic Surgery[22] *****	Retrospective	133	>38°C	>12.000//ml	> 100 mg/L	15,8%
Soares Ferreira *et al.*, 2018, Angiologia e Cirurgia Vascular	Retrospective	106	>38°C		> 75 mg/L	31.6%
SIRS criteria with CRP instead of leukocyte count						
De la Motte *et al.*, 2014, Annals of Surgery[7]	Prospective, randomized, double-blind	76 (placebo group)	>38°C	-	> 75 mg/L	100%

*Only with Incraft® endograft **Only with Zenith Alpha® thoracic endografts
*** The sample only included percutaneous EVAR ****TEVAR for type B dissection
***** Only with Anaconda® endograft
[a] This group defined PIS as fever and leukocytosis and abdominal and/or back pain, or other nonspecific symptoms such as malaise or loss of appetite.

Blum *et al.*, in 1997, analyzed prospectively the clinical outcome of 154 patients that underwent EVAR with polyester-covered nitinol endograft [12]. In this study, 87 patients (56%) developed fever (38.0 to 39.7°C) during 4-10 days, without evidence of bacteremia or graft infection. Associated to fever, all patients showed leukocytosis (9.800-29.500/µL) and an elevation of CRP (4-34.1 mg/dL) in blood tests [12].

Two years after, despite a small sample, the first study concerning PIS was designed by Velazquez *et al.* They defined PIS as fever and leukocytosis after EVAR, but the cutoffs are not specified. They found leukocytosis in 58% (N=7) and fever in 83% (N=10). Any source of infection was excluded in 11 patients[2]. Gabriel *et al.* evaluated the inflammatory response after endovascular repair of abdominal (AAA), thoracic (TAA) and thoracoabdominal (TAAA) aortic aneurysms. Elevation of sedimentation velocity, CRP and interleukin-6 occurred at 7 postoperative days, while increase of leukocytes count occurred in premature phase and lymphocyte and platelet count in a late phase of follow-up. Fever raised mainly between 24 and 48 hours after the surgery. However, the authors did not define PIS neither evaluated its incidence [13].

Chang *et al.* also studied the systemic inflammation following endovascular TAAA repair in 38 patients. They hypothesized that endovascular repair of TAAA is associated to a severe form of PIS. 47% (N=18) of patients developed fever and all had statistically significant changes in leukocyte and platelet counts and prothrombin time [14]. Once again, neither the exact definition nor the incidence of PIS was stated.

Georgiadis *et al.*, in their prospective study comparing the results of Endurant® endoprosthesis in hostile and friendly necks, also analyzed PIS incidence and they found this syndrome in 36.4% of patients (9 patients in friendly neck group *vs.* 19 patients in hostile neck group; p=0,032). Nevertheless, the definition of PIS was also unclear [15].

Two other studies described PIS incidence but the definition used was not stated. In a retrospective study with 10 patients who underwent EVAR with Incraft® endograft, the incidence of PIS was 30% (N=3) [16]. Melissano *et al.* found an incidence of PIS of 2% (N=1) in a retrospective analysis of endovascular aortic repair of TAA, aortic ulcers and traumatic aortic rupture with Zenith Alpha® (Cook Medical Inc, Bloomington, IN, USA) [17].

Several studies described PIS as a combination of leukocytosis and fever. Arnaoutoglou *et al.* in their prospective study with 162 patients that underwent endovascular repair of AAA (N=148) or TAAA (N=14). The definition for PIS was according to the definition of SIRS: fever (continuous body temperature > 38°C) and leukocytosis (> 12,000/µl) despite antibiotic therapy and negative culture results. The incidence was 30,2% (N=49) and no differences were found between groups, regarding demographic and surgical characteristics [1]. In a subsequent prospective study of the same authors, with 40 patients, they found a similar incidence of PIS – 35% (N=14). A significant increase in IL-6 levels was observed in PIS patients and the decrease in platelets count and hs-CRP increase were greater in the PIS group. In this study, Anaconda grafts (Vascutek-Terumo Cardiovascular System Corp, Ann Arbor, MI, USA) had the highest incidence, with 100%, followed by Zenith grafts (Cook Medical Inc, Bloomington, IN, USA) with 50%, Talent grafts (Medtronic Vascular AVE, Medtronic Europe SA, Route du Molliau, Switzerland) with 37% and Excluder grafts (W.L. Gore & Associates, Inc, Flagstaff, AZ, USA) had the lowest incidence, with 12% [4].

Dosluoglu *et al.* studied the feasibility and safety of ambulatory percutaneous EVAR in a sample of 79 patients. PIS was defined as any combination of fever >37,8°C, white blood cell count >10.000/µl, abdominal and/or back pain, or other nonspecific symptoms such as malaise or loss of appetite. PIS occured in 23% of the patients, 19% in the same-day discharge group and in 26% in non-ambulatory group [6].

In another study, a retrospective analysis of 118 patients who underwent EVAR with Anaconda endograft, the chosen definition for PIS was leukocytosis (>12.000/µl) and temperature >38°C. The incidence was 20,3% (N=24) [8]. Another retrospective study with 87 patients, using the same definition for PIS, found an incidence of 39%. The incidence varied according to stent graft – 71% for Anaconda endograft and 13% for Excluder grafts [18].

With the same criteria for PIS, Arnaoutoglou *et al.*, in a prospective design, evaluated PIS after elective EVAR in 214 patients with AAA and investigated its association with clinical outcome during first 30 postoperative days. The incidence of PIS was 36% [10].

Sartipy *et al.* also studied the impact of stent graft material on the inflammatory response, in 45 patients undergoing standard elective EVAR. The global incidence of PIS was 28%, with criteria of fever and leukocytosis [19]. Another single-center, observational cohort study of 204 consecutive EVAR revealed an incidence of PIS of 31.4%, with the same definition [20]. Similarly, Arnaoutoglou *et al.*, in a more recent prospective study with 182 consecutive EVAR, diagnosed PIS in 65 patients (35.7%) [21].

Fewer studies used the criterion of CRP elevation instead of leukocytosis. Voûte *et al.* defined PIS as an association of fever (tympanic temperature > 38°C) and elevated serum CRP level (> 10 mg/L) after EVAR [22]. The incidence was 56.1% (N=46) for the woven polyester endografts and 17,9% (N=12) for the expanded polytetrafluoroethylene (ePTFE) ones (p=0.001) [5]. In a retrospective study with 106 patients, PIS was defined as fever (>38°C) and CRP higher than 75 mg/L after EVAR. The incidence was 31.6% [23].

In a randomized, double-blind, placebo-controlled trial, designed to analyze the effect of a single preoperative dose of 30 mg/kg of methylprednisolone as prophylaxis for PIS, the criteria used were the same as for SIRS, except that leukocytosis was replaced for CRP elevation (>75 mg/L). The incidence of PIS was 27% in the methylprednisolone group versus 100% in the placebo group[7].

Besides of PIS after EVAR, PIS after endovascular repair of acute aortic syndromes has also been studied. The incidence of PIS was analyzed after TEVAR due to type B acute aortic syndrome in a sample of 133 patients. PIS was defined as temperature >38°C, leukocytes >12.000/mL, CRP >10 mg/dL and negative blood cultures. An incidence of 15.8% was found[24].

Similarly, Zhu *et al.*, in their retrospective analysis of 646 patients who underwent thoracic endovascular aneurysm repair (TEVAR) for type B dissection in a single center, evaluated the incidence of PIS. The criteria used for diagnosis of PIS were fever lasting over 1 day after TEVAR and leukocytosis, when infectious complications were excluded. The overall incidence of PIS was 31.6% (N=204). Although the timing of TEVAR has been similar between PIS and non-PIS group (p=0.6), it is important to mark that 61% of the patients underwent TEVAR in acute phase and only 7% of the procedures occurred in chronic phase. Indeed, part of the patients were submitted simultaneously to aortic arch vessels bypass (23%), which revealed to be a predictor to PIS occurrence[25].
In two other studies the inflammatory response (leukocytes, CRP, interleucin-6 and interleucin-10) after TEVAR was analyzed, but the incidence of PIS was not evaluated neither the definition of this syndrome is stated[11,26].

More recent studies evaluated incidence of PIS after EVAR and endovascular aneurysm sealing (EVAS). Martinelli *et al.* in a retrospective study, that included 60 patients who underwent to EVAS and 110 to EVAR, found an overall incidence of 29.6% (N=50). The definition used for PIS was persistently high body temperature > 38°C, lasting for >1day, leukocyte count > 12.000/mL and hsPCR>10 mg/L.

Ethiopathogeny

Endograft material/modality: This is the best investigated risk factor; several studies compared the incidence of PIS or the difference in inflammatory response and endograft material or modality. The studies focus mainly on differences between polyester *vs.* ePTFE-based structures and EVAR *vs.* EVAS. The majority of the studies pointed to a higher incidence of PIS or a greater increase of inflammatory markers in polyester-based endografts[4,5,8,18,20,27].

Voûte *et al.* and Kakisis *et al.* constructed a multivariable risk model for PIS and only the type of endograft was independently associated with the development of PIS[5,18].

However, other three studies did not identify a significant statistical difference in the incidence of PIS incidence between polyester and ePTFE endografts[5,11,19]. The absence of statistical significance in these studies can be related to their reduced sample size.

Anaconda® endografts seem to have a particularly higher incidence of PIS[4,8,18,28]. Although Nano *et al.* reported a lower incidence (20.3%), a more intense clinical presentation was mentioned in this study[8].

In retrospective analysis of TEVAR for type B dissection, contrary to majority of publications, PIS was more frequent after ePTFE endografts implantation, but in multivariable model this is not a significant predictor. The possible explanation pointed by the authors for these different result is the fact that Ankura® are the unique ePTFE endografts implanted in this study[25].

Besides fabric, the stent structure may influence the occurrence of PIS. This topic was discussed by Voûte *et al.* The exposition amount of alloy, the exact balance between nickel and titanium (components of nitinol) or the way of cutting and polishing may differ between manufacturers and may influence the inflammatory reaction. However, the authors did not report results of these several factors.[5] But nitinol

has been broadly used in coronary and peripheral arterial "bare-metal" stents and no inflammatory response have been reported in these applications.[29]

Delivery systems may also influence PIS. Moulakakis *et al.* hypothesized that the introduction of the endograft through a sheath cause less injury to the endothelium. It can be one reason for Excluder® endograft have a milder postimplantation inflammation comparing to the others[28].

More recent studies compared the inflammatory reaction after EVAR and EVAS. Martinelli *et al.* compared retrospectively the incidence of PIS in EVAS (N=60) and ePTFE EVAR (N=110) in a single center. Among ePTFE devices, they also compared the incidence of PIS between AFX and the remaining ones, due to different characteristics of skeleton devices. PIS occurred significantly lower after EVAS than after EVAR (13.8 *vs.* 38.7%, p=0.001). Although less frequent after AFX implantation, the difference did not reach statistical significance (46.6 *vs.* 33.29%, p=0.333). EVAR patients had higher values of body temperature, hsCRP and leukocytes count. In their multivariable model, the use of Nellix device was the only independent factor to PIS, with an OR of 0.196 (p<0.001). The authors conjectured that the lower incidence of PIS in EVAS is due to absence of new-thrombus formation. The skeleton of EVAR devices did not seem to influence PIS occurrence[30].

Berg *et al.*, in a propensity score-matched design, also analyzed inflammatory response after EVAS *vs.* EVAR in a single center. Thirty-nine matched patients were included per group. PIS was defined as fever and leukocytosis and it occurred less often in EVAS group (5.1% *vs.* 20.5%, p=0.07). However, the sub analysis regarding endograft material revealed that incidence in EVAS group was higher than in ePTFE, with 0 cases of PIS in the latter group (0/13). Body temperature (p=0.05), leukocytes count (p=0.003) and hs-CRP (p<0.001) were lower in EVAS group comparatively to EVAR group. Despite of retrospective design and small sample limitations, the authors argued that besides graft composition, complete AAA sac thrombus sealing influence the systemic inflammatory response following endovascular AAA treatment[31].

Chronic mural/new-onset thrombus: Mural thrombus of aortic aneurysms contains high levels of IL-6, explaining the rationale for the hypothesis that the amount of pre-existing mural thrombus could be related to PIS development[32]. It was conjectured that thrombus manipulations, which undoubtedly occurred with wires and catheters during EVAR procedure, could release IL-6 and induce an inflammatory response. Nano *et al.* found an association between preoperative thrombus thickness and PIS after EVAR with Anaconda® endograft (p=0,001)[8]. But Kakisis *et al.* refuted this theory. They found that the volume of chronic mural thrombus did not affect any parameter of PIS[18]. Corroborating the latter one, Moulakakis *et al.* found that Anaconda® endograft had the highest inflammatory response and this endograft requires less thrombus manipulation during implantation than the other ones, since it has a magnet on the contralateral limb to facilitate its cannulation[28].

But, the explanation for PIS occurrence could be the new-onset thrombus instead of chronic mural thrombus[33]. Even though, the results about this topic were not consistent. Kakisis *et al.* found a significant correlation between the volume of new-onset thrombus and PIS parameters. In their multiple variable model, volume of new-onset thrombus and type of endograft were independently associated with the development of PIS[18]. Conversely, Vôute *et al.* also analyzed this hypothesis and found no significant correlation between new-onset thrombus and the rise in temperature (p=0,08) or CRP (p=0,17), with a larger patient sample[5]. Lastly, Arnaoutoglou *et al.* did not find differences in PIS incidence nor with preoperative endoluminal thrombus neither with the amount of newly formed thrombus[10].

On the other hand, studies described above that compared EVAR *vs.* EVAS favored the hypothesis that thrombus plays a role in inflammatory response, since with EVAS there is potentially less mural thrombus manipulation and there is no new-thrombus formation after aneurysm sealing.

Bacterial translocation: Bacterial translocation due to transient sigmoid ischemia after EVAR is another potential etiology for PIS. Thus, Kakisis *et al.* analyzed the association of inferior mesenteric artery patency to postoperative temperature and inflammatory markers and found no significant correlation[18]. Another trial, that studied the effect of antibiotic therapy in PIS is in agreement: there were no differences in parameters related to PIS, regardless of the duration of postoperative antibiotic therapy[26].

Contrast: A study suggested that contrast medium, iohexol, provokes neutrophil degranulation, which is greatly enhanced when combined with stent graft material, contributing to PIS occurrence[34]. More recent studies, however, did not find any correlation between contrast use or dosage and PIS parameters[5,8,18,28].

Other factors: Zhu *et al.* investigated predictors of PIS after TEVAR for type B aortic dissection in a stepwise multivariable model. The predictors found in this study to PIS occurrence were: age <60 years (OR=1.99, p=0.001), hypertension (OR=11.34, p>0.001), > 1 stent graft implanted (OR=1.97, p=0.002) and arch vessel bypass (OR=2.07, p=0.001). If any of these predictors were present in this population, the incidence of PIS was 0%. If one is present, the incidence was 18%, with two predictors, 31%, with 3 predictors 49% and with all predictors, the incidence was 67%[25].

In previous studies, factors like age, gender, aneurysm size, extent of aortic coverage, length of operation, blood loss or transfusion, intensive care unit, statin, chronic obstructive disease, ischemic heart disease and heart failure, were also evaluated and none revealed to be an important factor to PIS[5,8,9,14,18].

On the other hand, statins use revealed to a protective factor for PIS in two studies[23,25].

Manifestations and Diagnosis

This syndrome is characterized by flu-like symptoms, like fever, anorexia and fatigue, and abdominal or lumbar pain associated to laboratory changes, such as leukocytosis, CRP elevation, decrease in platelets count and/or coagulation abnormalities. Usually, it is a self-limited condition which resolves in about two weeks without significant sequela. However, severe complications of this syndrome are described, such as pulmonary dysfunction, cardiovascular events, renal insufficiency and multisystem organ failure[1,14,28].

Elevation of body temperature associates to a rise in laboratorial inflammatory markers and a drop in platelet count. Leukocytes count typically rises in the first postoperative day and CRP between first and third postoperative day[5,28, 26,35].

When it occurs, a work-up to exclude an infection is usually done[36]. Some authors advocate that this may be costly and unnecessary in clinical absence of an infection source[37]. Sartipy *et al.* designed a prospective study to evaluate the role of procalcitonin in diagnosis of PIS *vs.* infection after EVAR. They hypothesized that in PIS procalcitonin remains <0.5 ng/mL, conversely to infectious complications. PIS was defined as fever and leukocytosis (>12,000/mL) after EVAR with no other detected complication or any open surgical event explaining the inflammatory response. The global incidence of PIS in this trial was 17.5% (N=12). They confirmed that all PIS patients had levels of procalcitonin <0.5 ng/mL, as they hypothesized, whereas all showed an elevation on CRP >100 mg/L and leukocyte count > 12.000/mL[9].

Clinical consequences

Hospital Stay Duration/Readmissions: Several studies found an association of PIS to a prolonged hospital stay[4,6,8,10,20]. *(Predictors associated with an increased prevalence of postimplantation syndrome after thoracic endovascular aortic repair for type B aortic dissection).* Other ones described patients' readmissions due to moderate or severe presentation of PIS, including two cases that required intensive care admission and endovenous corticosteroids[1,6].

However, Moulakakis *et al.* did not find any clinical adverse events related to PIS neither readmissions in their study[11]. (Table 2)

Table 2: Influence of PIS on Clinical Outcomes

	Studies suggesting influence on prognosis (authors, design, no. patients)	**Studies suggesting no influence on prognosis** (authors, design, no. patients)
Hospital Stay/ Readmissions	1. Arnaoutoglou *et al.*[1], Prospective, n=162 2. Arnaoutoglou *et al.*[4], Prospective, n=40 3. Nano *et al.*[8], Retrospective, n=118 4. Arnaoutoglou *et al.*[10], Prospective, n=214 5. Kwon *et al.* 20, Retrospective, n=204	1. Moulakakis *et al.*[11], Prospective, n=30
Kidney Dysfunction	1. Chang *et al.*[14], Prospective, n=38	1. Moulakakis *et al.*[11], Prospective, n=30
Cardiovascular Events	1. Arnaoutoglou *et al.*[10], Prospective, n=214 2. Arnaoutoglou *et al.*[21], Prospective, n=182 3. Berg *et al.* Retrospective, n=78	1. Kwon *et al.*[20], Retrospective, n=204 2. Soares Ferreira *et al.*[41], Retrospective (149)
Aneurysm-related Complications	1. Gorla *et al.*[22], Retrospective, n=133 2. Kwon *et al.*[20], Retrospective, n=204 3. Jeong *et al.* Retrospective, n=168	1. Voûte *et al.*[5], Retrospective, n=149 2. Nano *et al.*[8], Retrospective, n=118 4. Arnaoutoglou *et al.*[21], Prospective, n=182 5. Soares Ferreira *et al.*[41], Retrospective (149)
Quality of Life	1. Nano *et al.*[8], Retrospective, n=118	-

Kidney Injury: Moulakakis *et al.* stated that kidney function was not influenced by the inflammatory response and no correlation was recognized between increased inflammatory markers and renal dysfunction[11].

Chang *et al.* analyzed systemic inflammation, coagulopathy and acute kidney injury (AKI) following endovascular TAAA repair. In this study, patients with postoperative AKI had higher changes in leukocytes and platelet count, compared with those that did not develop kidney failure. Their univariate logistic regression analysis revealed that each 5000cells/μL increase in leukocytes in the postoperative period was associated with 2.4-fold odds of postoperative AKI (p=0,02). For platelets, each decrease of 50.000 platelets/μL was associated with a 4.0-fold odd of postoperative kidney injury (p=0,02)[14].

Cardiovascular events: A study by Arnaoutoglou *et al.* analyzed the influence of inflammatory reaction after EVAR in 30-day outcomes. A multiple logistic regression model revealed that coronary artery disease (p=0.01), postoperative CRP (p=0,001) and duration of fever (p=0,02) independently predicted major cardiovascular events. For every additional day of fever after the first, the probability of a cardiovascular episode increased by 67.9% (p=0,017) and for every 10 units increase of CRP, it increased 15% (*p*=0.001). Postoperative CRP also revealed as an important predictor for AKI, readmission and death during the first 30 days. A cutoff value of 125mg/L was highly associated with an adverse event, with a sensitivity of 72% and specificity of 75%[10].

In a prospective study with 1-year follow-up after EVAR, with 182 patients, several adverse events were reported, such as major adverse cardiovascular events (MACE), acute kidney injury, readmission and death from any cause. Multiple logistic regression analysis showed that PIS was the only independent predictor of MACE (p=0,007) or any adverse event (p=0,005). Patients with the diagnosis of PIS were 4,5-times more likely to suffer MACE or another adverse event, compared to non-PIS patients[21].

In the same line, in the EVAS FORWARD IDE trial and Nellix EVAS FORWARD Global Registry a low all-cause mortality, mainly by fewer cardiac-related deaths, was found comparatively to EVAR patients. In the EVAS FORWARD IDE study, freedom from cardiovascular related mortality at 2 years was 99%. Since EVAS seems to have a lower incidence of PIS than EVAR, the authors argue that low cardiovascular mortality after EVAS may be related to the lower incidence of PIS. But the real reasons for these findings have yet to be established [38-40].

Berg *et al.* retrospectively compared EVAR and EVAS-associated adverse events, including MACE and secondary interventions for type I endoleaks in first 30 days after procedure. They also analyzed the influence of PIS on these complications. Adverse events (20% *vs.* 4%, p=0,12) and endoleak (20% *vs.* 3%, p=0,08) were proportionally higher in patients with PIS but did not achieve statistical significance [31]. Conversely, Kwon *et al.* stated that patients with and without PIS had similar long-term overall survival rates and other clinical outcomes, such as systemic or implant-related complications [20].
In a retrospective analysis with 149 patients with a longer follow up (median follow up of 6.4 years), the authors found that PIS has no major impact on cardiovascular prognosis or influence on survival. An increased rate of cardiovascular events during the first years was suggested but without statistical significance (one year freedom from cardiovascular events was 89% *vs.* 94% for non-PIS patients (p=0.32) and at two years it was 84% *vs.* 92% (p=0.17) [41].

Aneurysm-related complications: Know *et al.* found that PIS was significantly associated with a decreased risk of developing type II endoleaks (p=0,044) during postoperative period (44 months of follow up). In Kaplan-Meier survival analysis, rate of secondary procedures was significantly higher in the non-PIS group (p=0,049) [20]. An analysis of major adverse events (aortic rupture, need for reintervention and all-cause mortality) among patients that underwent TEVAR for acute aortic syndrome during a mean follow-up of 4.0±2.9 years revealed that they were more frequent in the PIS than in the non-PIS group (62.5 *vs.* 25.9%; p=0,004) [24].

Jeong *et al.* retrospectively evaluated sac behavior predictors after elective EVAR. Patients were divided in two groups: sac regression group and sac non-regression group. PIS was more common in the sac regression group (46.8% *vs.* 25.8%, p=0,005) and transient type II endoleaks occurred less often (8.9% *vs.* 27%, p=0,003) as persistent type II endoleaks (13.9% *vs.* 41.6%, p<0,001). Thrombus density within the sac was significantly lower in the sac regression group (43.1±9.6 *vs.* 48.9±11.4, *p*=0,001). Reintervention rate during follow-up (mean 44 months) was higher in the non-regression sac group (0 *vs.* 13.5%, p=0,001). No differences in mortality or secondary rupture were found. Multivariable analysis revealed that PIS (HR=1.68, *p*=0,023) was a positive predictor of sac regression and transient type II endoleaks (HR=0.43, p=0.037). Otherwise, higher-density thrombi (HR=.097, p=0,013) was a negative predictor of sac regression [42].

Conversely, in Voûte et al study, PIS did not correlate to postoperative endoleaks [5]. Nano *et al.* also established a benign character of PIS; no association between PIS and onset of early and/or long-term complications, namely endoleaks, was reported [8]. Arnaoutoglou *et al.* in a prospective study with a 1-year follow-up, also found no correlation between PIS and endoleak or other complication rates (p>0.05) [21].

In a retrospective analysis of 149 patients, all types of endoleaks were analysed and there were only differences for type II endoleaks, which were more common in non-PIS patients: 25 *vs.* 5 (p=0.005). All secondary interventions related to type II endoleaks also occurred in the non-PIS group. However, sac dynamics, using diameter or volume measurements, were similar between the groups [41].

Quality of Life: There is a study that assessed quality of life 1-month after surgery. PIS patients had their daily physical activities significantly limited and they were more emotionally discouraged and depressed/anxious about their state of health compared to non-PIS patients [8]. No long-term studies evaluating quality of life after PIS are available to date.

Prevention & treatment

Multiple therapeutic options for this condition have been studied. Akin *et al.* tested the extension of antibiotics during the postoperative time, but without any advantage in PIS incidence [26]. In a study of patients who underwent percutaneous ambulatory EVAR, one was readmitted due to severe PIS in third postoperative day. He was managed with hydration, pain control and anti-inflammatory drugs and was discharged 3 days after [6].
Other authors have evaluated corticotherapy-based regimen in treating and preventing this syndrome. In a study by Nano *et al.*, in case of PIS diagnosis, 1g of hydrocortisone was administered intravenously on the third postoperative day [8].

De la Motte *et al.* in a randomized, double-blind, placebo-controlled trial, analyzed the effect of a single preoperative dose of 30 mg/kg of methylprednisolone or placebo, administered 2 hours before surgery[7]. For diagnosis of PIS, they used SIRS criteria, except leukocytosis, that was changed to CRP elevation due to the influence of corticosteroids on leucocyte count. They obtained, with a single preoperative dose, a reduction in PIS from 100% in placebo group to 27%. Potential methylprednisolone side effects occurred in 10 patients (14%) [7]. Despite substantial difference in PIS incidence with a single preoperative dose of methylprednisolone, PIS was defined as having either fever or elevated CRP levels. Hence, possibly, the higher incidence of 100% in placebo group.

Kouvelos *et al.*, in a commentary, summarized the available evidence of PIS. The authors stated that in their practice they found favorable outcomes of oral non-steroid anti-inflammatory drugs (NSAID) in this group of patients [43].

Discussion

The reported incidence of PIS in the literature varies widely (2-100%) and it is described after endovascular exclusion of abdominal, thoracic and thoracoabdominal aneurysms and also after type B aortic dissections and other aortic syndromes. This variability occurs probably due to an absence of well-defined criteria for the diagnosis of this syndrome. Part of the studies do not specify PIS definition, others use the definition with leukocytosis and fever and few studies use a definition that includes CRP and fever. However, an incidence between 20 and 40% seems to be the most consensual in literature.
Ethiopathogeny is also unclear. Several factors have been pointed as reasons to PIS occurrence, namely endograft material and modality, chronic mural and new-onset thrombus, bacterial translocation, contrast use, age, number and extension of endografts used. The most studied factor is endograft fabric and polyester, when compared to ePTFE, results in a higher inflammatory reaction both *in vitro* and *in vivo* and this is well replicated in aortic endograft implants [44].

Indeed, EVAS also appears to provoke a lesser inflammatory reaction. The reasons for that are still unknown but some authors argued that it is related to absence of new-onset thrombus. However, the inflammatory response is not of the same magnitude in all patients treated with the same type of endograft. So, factors other than endograft related must also be responsible to the occurrence of PIS.

Manifestations of PIS are similar to a flu syndrome associated to abdominal and/or lumbar pain and a rise of inflammatory markers. The latter ones correspond to elevation of leucocytes count and CRP but cutoffs to diagnosis were not stablished yet. Hence, the diagnosis of PIS might be suspected in the presence of fever without source of infection in the immediate postoperative period after EVAR. With the current recognition of this condition, a full work-out to exclude an infection could be excessive in all situations, but a close observation is recommended, at least, due to devastating consequences of an early infection after EVAR. Of note, procalcitonin appears to be a good laboratorial differentiator between PIS and infectious complications, probably cheaper and faster than microbiologic culture tests.

The clinical consequences of this syndrome are not fully elucidated and more studies have to be performed. Yet, the evidence suggests that PIS is associated to a prolonged hospital stay and worse early quality of life for affected patients. There is no consensus among effects on cardiovascular-and aneurysm-related complications, but PIS appears to have no major effect on cardiovascular prognosis and mortality.

Concerning treatment, it seems reasonable to prevent this inflammatory reaction, since it can lead to prolonged hospitalization and/or readmission and even to more severe consequences. However, the routine administration of drugs like steroids or NSAID raises concerns due to side effects, mainly in patients with more severe comorbidities. Definitely, future studies are needed to clarify the benefits and risks of routine prophylaxis for this syndrome as well as symptom based anti-inflammatory therapy.

In conclusion, PIS is already a well-accepted inflammatory reaction that occurs after EVAR and also after aortic dissection and other aortic syndromes. Its incidence is probably between 20 and 40% but for a best knowledge of this, well-defined criteria for diagnosis might be stablished. Prospective studies, with larger samples, have to be designed to clarify the clinical consequences of this syndrome and the need to prophylactic and symptomatic treatment.

References

1. Arnaoutoglou E, Papas N, Milionis H, Kouvelos G, Koulouras V, Matsagkas MI. Post-implantation syndrome after endovascular repair of aortic aneurysms: need for postdischarge surveillance. *Interact Cardiovasc Thorac Surg* 2010; 11: 449-54.
2. Velázquez OC, Carpenter JP, Baum RA, Barker CF, Golden M, Criado F, *et al.* Perigraft air, fever, and leukocytosis after endovascular repair of abdominal aortic aneurysms. *Am J Surg* 1999; 178: 185-9.
3. Schürmann K, Vorwerk D, Bücker A, Neuerburg J, Klosterhalfen B, Muller G, *et al.* Perigraft inflammation due to Dacron-covered stent-grafts in sheep iliac arteries: correlation of MR imaging and histopathologic findings. *Radiology* 1997; 204: 757-63.
4. Arnaoutoglou E, Kouvelos G, Milionis H, Mavridis A, Kolaitis N, Papa N, *et al.* Post-implantation syndrome following endovascular abdominal aortic aneurysm repair: preliminary data. *Interact Cardiovasc Thorac Surg* 2011; 12: 609-14.
5. Voûte MT, Bastos Gonçalves FM, Van De Luijtgaarden KM, Klein Nulent CGA, Hoeks SE, Stolker RJ, *et al.* Stent graft composition plays a material role in the postimplantation syndrome. *J Vasc Surg* 2012; 56: 1503-9.
6. Dosluoglu HH, Lall P, Blochle R, Harris LM, Dryjski ML. Ambulatory percutaneous endovascular abdominal aortic aneurysm repair. *J Vasc Surg* 2014; 59: 58-64.
7. De La Motte L, Kehlet H, Vogt K, Nielsen CH, Groenvall JB, Nielsen HB, *et al.* Preoperative methylprednisolone enhances recovery after endovascular aortic repair: A randomized, double-blind, placebo-controlled clinical trial. *Ann Surg* 2014; 260: 540-9.
8. Nano G, Occhiuto MT, Stegher S, Malacrida G, Cova M, Righini P, *et al.* Postimplantation syndrome after endovascular aortic repair using the anacondaTM endograft. *Ann Vasc Surg* 2014; 28: 1409-15.
9. Sartipy F, Lindström D, Gillgren P, Ternhag A. The role of procalcitonin in postimplantation syndrome after evar: A pilot study. *Ann Vasc Surg* 2014; 28: 866-73.
10. Arnaoutoglou E, Kouvelos G, Papa N, Kallinteri A, Milionis H, Koulouras V, *et al.* Prospective Evaluation of Post-implantation Inflammatory Response After EVAR for AAA : In fl uence on Patients ' 30 Day Outcome. *Eur J Vasc Endovasc Surg* 2015; 49: 175-83.
11. Moulakakis KG, Sfyroeras GS, Papapetrou A, Antonopoulos CN, Mantas G, Kakisis J, *et al.* Inflammatory response and renal function following endovascular repair of the descending thoracic aorta. *J Endovasc Ther* 2015; 22: 201-6.
12. Blum U, Voshage G, Lammer J, Beyersdorf F, Töllner D, Kretschmer G, *et al.* Endoluminal Stent–Grafts for Infrarenal Abdominal Aortic Aneurysms. *N Engl J Med* 1997; 336: 13-20.
13. Gabriel EA, Locali RF, Romano CC, Duarte AJ, Palma JH, Buffolo E. Analysis of the inflammatory response in endovascular treatment of aortic aneurysms. *Eur J Cardio-thoracic Surg* 2007; 31: 406-12.
14. Chang CK, Chuter TAM, Niemann CU, Shlipak MG, Cohen MJ, Reilly LM, *et al.* Systemic inflammation, coagulopathy, and acute renal insufficiency following endovascular thoracoabdominal aortic aneurysm repair. *J Vasc Surg* 2009; 49: 1140-6.
15. Georgiadis GS, Trellopoulos G, Antoniou GA, Gallis K, Nikolopoulos ES, Kapoulas KC, *et al.* Early results of the Endurant endograft system in patients with friendly and hostile infrarenal abdominal aortic aneurysm anatomy. *J Vasc Surg* 2011; 54: 616-27.
16. Mazzaccaro D, Occhiuto MT, Stegher S, Righini P, Malacrida G, Nano G. Tips about the Cordis INCRAFT Endograft. *Ann Vasc Surg* 2016; 30: 205-10.
17. Melissano G, Tshomba Y, Rinaldi E, Chiesa R. Initial clinical experience with a new low-profile thoracic endograft. *J Vasc Surg* 2015; 62: 336-42.

18. Kakisis JD, Moulakakis KG, Antonopoulos CN, Mylonas SN, Giannakopoulos TG, Sfyroeras GS, *et al.* Volume of new-onset thrombus is associated with the development of postimplantation syndrome after endovascular aneurysm repair. *J Vasc Surg* 2014; 60: 1140-5.

19. Sartipy F, Lindsrom D. The impact of Stent Graft Material on the Inflammatory Response After EVAVR. *Vasc Endovascular Surg* 2015; 49: 1-5.

20. Kwon H, Ko GY, Kim MJ, Han Y, Noh M, Kwon TW, *et al.* Effects of postimplantation systemic inflammatory response on long-term clinical outcomes after endovascular aneurysm repair of an abdominal aortic aneurysm. *Medicine (Baltimore)* 2016; 95: e4532.

21. Arnaoutoglou E, Kouvelos G, Papa N, Gartzonika K, Milionis H, Koulouras V, *et al.* Prospective evaluation of postimplantation syndrome evolution on patient outcomes after endovascular aneurysm repair for abdominal aortic aneurysm. *J Vasc Surg* 2016; 63: 1248-55.

22. Soares Ferreira R, Bastos Gonçalves F. Postimplantation Syndrome after Endovascular Aneurysm Repair, Abdominal Aortic Aneurysm - From Basic Research to Clinical Practice. Koncar I, editor. *IntechOpen* 2018.

23. Soares Ferreira R, Bastos Gonçalves F, Abreu R, Camacho N, Nelson CJ, Correia R, *et al.* Síndrome Pós-Implante no EVAR. *Angiol e Cir Vasc* 2018; 14: 176-81.

24. Gorla R, Erbel R, Kahlert P, Tsagakis K, Jakob H, Mahabadi AA, *et al.* Clinical features and prognostic value of stent-graft-induced post-implantation syndrome after thoracic endovascular aortic repair in patients with type B acute aortic syndromes. *Eur J Cardio-thoracic Surg* 2016; 49: 1239-47.

25. Zhu Y, Luo S, Ding H, Liu Y, Huang W, Xie N, *et al.* Predictors associated with an increased prevalence of postimplantation syndrome after thoracic endovascular aortic repair for type B aortic dissection. *Eur J Cardiothorac Surg* 2019; 55: 998-1005.

26. Akin I, Nienaber CA, Kische S, Rehders TC, Ortak J, Chatterjee T, *et al.* Effect of antibiotic treatment in patients with postimplantation syndrome after aortic stent placement. *Rev Esp Cardiol* 2009; 62: 1365-72.

27. Ito E, Toya N, Fukushima S, Nishie R, Akiba T, Ohki T. Polyester Grafts Are a Risk Factor for Postimplantation Syndrome after Abdominal Endovascular Aneurysm Repair: Retrospective Analysis for Polyester Graft, Excluder®, and Endologix Powerlink®/AFX®. *Ann Vasc Dis* 2018; 11: 520-4.

28. Moulakakis KG, Alepaki M, Sfyroeras GS, Antonopoulos CN, Giannakopoulos TG, Kakisis J, *et al.* The impact of endograft type on inflammatory response after endovascular treatment of abdominal aortic aneurysm. *J Vasc Surg* 2013; 57: 668-77.

29. Stoeckel D, Pelton A DT. Self-expanding nitinol stents: material and design considerations. *Eur Radiol* 2004; 14: 292-301.

30. Martinelli O, Di Girolamo A, Irace L, Baratta F, Gossetti B, Gattuso R. Incidence of Post-Implantation Syndrome with Different Endovascular Aortic Aneurysm Repair Modalities and Devices and Related Etiopathogenetic Implications. *Ann Vasc Surg* 2020; 63: 155-61.

31. Berg P, Stroetges RA, Miller LE, Schoefferle J. A Propensity Score–Matched Analysis of Inflammatory Response With Endovascular Aneurysm Sealing *vs.* Endovascular Aneurysm Repair. *J Endovasc Ther* 2017; 24: 670-4.

32. Swartbol P, Truedsson L NL. Adverse reactions during endovascular treatment of aortic aneurysms may be triggered by interleukin 6 release from the thrombotic content. *J Vasc Surg* 1998; 28: 664-8.

33. Barba R, Di Micco P, Blanco-Molina A, Delgado C, Cisneros E VJ. Fever and deep venous thrombosis. Findings from the RIETE registry. *J Thromb Thrombolysis* 2011; 32: 288-92.

34. Videm V, Ødegård A MH. Iohexol-induced neutrophil myeloperoxidase release and activation upon contact with vascular stent-graft material: a mechanism contributing to the postimplantation syndrome? *J Endovasc Ther* 2003; 10: 958-67.

35. Abdelhamid MF, Davies RSM, Adam DJ, Vohra RK, Bradbury AW. Changes in thrombin generation, fibrinolysis, platelet and endothelial cell activity, and inflammation following endovascular abdominal aortic aneurysm repair. *J Vasc Surg* 2012; 55: 41-6.

36. Arnaoutoglou E, Kouvelos G, Koutsoumpelis A, Patelis N, Lazaris A, Matsagkas M. An Update on the Inflammatory Response after Endovascular Repair for Abdominal Aortic Aneurysm. *Mediators Inflamm* 2015; 2015: 945035.

37. Corfield L, Chan J, Chance T, Wilson N. Early pyrexia after endovascular aneurysm repair: Are cultures needed? *Ann R Coll Surg Engl* 2011; 93: 111-3.

38. Reijnen MMPJ, Holden A. Status of Endovascular Aneurysm Sealing After 5 Years of Commercial Use. *J Endovasc Ther* 2018; 25: 201-6.

39. Carpenter JP, Cuff R, Buckley C, Healey C, Hussain S, Reijnen MMPJ. Results of the Nellix system investigational device exemption pivotal trial for endovascular aneurysm sealing. *J VascSurg* 2015; 63: 23-31.

40. Thompson MM, Heyligers JM, Hayes PD, Reijnen MMPJ, Böckler D, Schelzig H. Endovascular Aneurysm Sealing: Early and Midterm Results From the EVAS FORWARD Global Registry. *J Endovasc Ther* 2016; 23: 685-92.

41. Soares Ferreira R, Oliveira-Pinto J, Ultee K, Voûte MT, Oliveira NFG, Hoeks S, *et al.* Long Term Outcomes of Post-Implantation Syndrome After Endovascular Aneurysm Repair. *Eur J Vasc Endovasc Surg* 2021, in press.

42. Jeong MJ, Kwon H, Ko GY, Gwon D Il, Kim MJ, Han Y, *et al.* New predictors of aneurysm sac behavior after endovascular aortic aneurysm repair. *Eur Radiol* 2019; 29: 6591-9.

43. Kouvelos G, Arnaoutoglou E, Giannoukas AD, Matsagkas M. Commentary: Postimplantation Syndrome: An Underrecognized EVAR Complication. *J Endovasc Ther* 2017; 24: 675-6.

44. Swartbol P, Truedsson L, Pärsson H, Norgren L. Tumor necrosis factor-alpha and interleukin-6 release from white blood cells induced by different graft materials *in vitro* are affected by pentoxifylline and iloprost. J Biomed Mater Res 1997; 997: 400-6.

What do we actually know about the mechanical properties of guide wires used in endovascular practice?

21

Arindam CHAUDHURI

The current endovascular revolution implies that many arteriovenous pathologies can be now treated without open surgery. A key technical component is lesion access using a guidewire that then 'creates the path' for the remaining devices that deliver definitive endovascular therapy. However, despite common guidewire use there is little work on this to add to the endovascular operator's knowledge and understanding of the wide range and relevant mechanical characteristics of the many guidewires that are currently available.

A search of Pubmed and Google Scholar was undertaken by the author using the phrase 'guidewire mechanical properties'. A narrative review is undertaken looking at the range of guidewires available for endovascular procedures and the literature specifically related to the mechanical properties thereof.

The author provides an overview of the information currently available on guidewires used in endovascular practice, with a review of the literature, insights into contemporary practice with a focus on available literature on the mechanical characteristics of guidewires in various application scenarios.

Guidewires are critical to obtaining access to the region of interest that is being treated by endovascular means, yet little information is actually present in the medical literature on the mechanical properties of these. More basic scientific research is needed to promote the understanding of guidewire characteristics, some of which could be provided by the manufacturers themselves.

Introduction

The endovascular revolution in vascular surgery has completed changed the treatment of vascular disease, whether it be occlusive, aneurysmal or otherwise, typified by endovascular aneurysm repair (EVAR) and peripheral arterial angioplasty. At the core is the improvement in guidewire (GW) technology which is fundamental to target vessel access and device delivery. Historically, the Seldinger technique[1] –specifically the catheter method for contrast angiography, as compared to direct injection of contrast via needle as described by Dos Santos-brought the guidewire (then described as a 'leader') concept into focus; the current form is effectively a wire with a tight coil wrap was used to provide the combination of strength (stiffness) and flexibility. The use of the "leader" GW was in fact preceded by use of silver wires by Jonsson in Stockholm [2]. This has of course continued to evolve, and despite much initial concern about the safety of guidewire-catheter techniques for angiography, including via open femoral access[2], this is now taken as granted as part of the armamentarium for undertaking minimally invasive

i.e. endovascular procedures. Effectively this has led to combinations of GWs that are in the working endovascular interventionists' jargon termed stiff/floppy, hydrophilic/non-hydrophilic. The key point is the choice of GW from the available range in order to negotiate vascular anatomy, and then allow 'carriage' of devices such as catheters, sheaths and stent-grafts. Other extensions of usage include assessing arterial tortuosity [3], or even straightening out tortuous vessels with multiple or pullthrough wires [4,5].

Yet, despite a plethora of GW designations, there is little information available/presented to the endovascular specialist in terms of the mechanical characteristics of such guidewires, and, ironically, endovascular practice continues in the absence of an exhaustive, relevant and available knowledge base. This includes company websites as well, which provide little information on this aspect [6]. This is comparable and even opposite to the process of buying a car: typically a bit of research is done on engine power, fuel economy, running costs, insurance, tax, environmental impact and so on before actual purchase. However, when it comes to a guidewire (GW), often it is a word of mouth recommendation from either a colleague or at a company stand, and a procedural trial before eventual use. This would be akin to buying a car after merely receiving a glossy brochure and undertaking a test drive or two, and raises the question about how much we actually we seek to know of guidewires in current endovascular practice before we start stocking them in our hybrid/angiography suites. Use of guidewires is also often dictated by local/historical choice rather than a clear examination of a range of wires in test scenarios, guided by an in-depth understanding of their mechanical properties, though a few attempts have been made as noted in the literature. This is despite endovascular interventions, and thus guidewire usage, becoming an integral part of the treatment armamentarium of vascular disease [7].

The purpose of this narrative review is to delve into the relevant literature regarding the mechanical properties of guidewires in order to consolidate the knowledge base on this matter.

Methods

Literature search strategy

A literature search was undertaken in PubMed and Google Scholar and also company websites. The search was focused using the phrase 'guidewire mechanical properties'. A review was undertaken focusing on how information is presented on the variety and mechanical characteristics of guidewires, scope of applications, extended applications and pitfalls with usage linked to the mechanical aspects.

A search focusing on 'guidewire mechanical properties' yielded 17, 700 results in Google Scholar and 37 in Pubmed. This was a clear reminder of the usage of guidewires in many fields such as urology, gastroenterology, orthopaedic interventions, and of course cardiology and not just as a guidewire but also with extra functions such as conductivity, as in pacemaker wires, non-fluoroscopy-guided interventions, and also in remote-sensing. References that did not allow citation, lacked abstracts, or had abstracts without summarising quantifying data, and also lacked Boolean connectivity between the terms in the search phrase (as noted in the Google Scholar search) were not included, as were references to non-vascular specialties, bar a few included that had direct relevance. This review thus effectively focuses on wires in common endovascular/interventional usage including for aortic *e.g.* endovascular aneurysm repairs (EVAR) which may be in the infrarenal, thoracic (TEVAR) [8] or thoracoabdominal (TAEVAR, including fenestrated/branched (F/BEVAR) aspects) aorta, and peripheral arteriovenous interventions.
Selected articles were populated into EndNote allowing elimination of duplicate references.

Results

There were 36 papers and one web article that could be selected based on the inclusion criteria; of these not all were papers that directly examined mechanical properties as such. Overall, there were few studies that looked specifically at wire stiffness, and even fewer looking at other mechanical characteristics. A flow chart outlining the study selection process is presented in Figure 1.

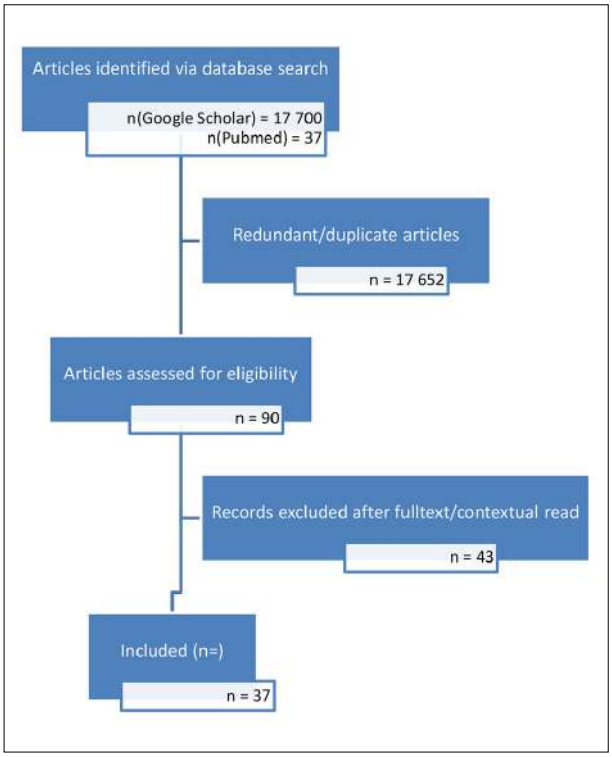

Figure 1: Flowchart illustrating selection process for inclusion of studies that related to the mechanical properties of guidewires.

Wire design and associated mechanical characteristics: a background

Wires are currently provided in a combination of designations based on *calibre* (and associated length), *materials* and *coating* (which determines whether hydrophilic or not), *stiffness*, which relates to *pushability/load/torquability* (strength-related) characteristics, and also *tip design*, relevant as this is the leading component of the GW. These characteristics are combined in various ways to provide an optimised wire for each interventional scenario, whether it be management of aneurysmal or occlusive disease. Other studies have looked at characteristics such *lag* and *whip*[9], which are linked to the properties of 'ideal' guidewires, but how this translates to effects in the clinical scenario is as yet unascertained on an experimental basis; it is understood that this would be linked to torquing characteristics of guidewires.

This chapter focuses on stiffness characteristics in particular, the reader will note that pushability (and to some extent tip) characteristics are particularly relevant in the context of wire applications in treatment of stenotic/occlusive vascular disease.

The current range of calibre for endovascular guidewires ranges from 0.018" to 0.035", though there are both finer and thicker wires outside this range in current use. As would be gathered, this is to accommodate the vessel being treated (*e.g.* distal lower limb vessels), the age group being treated (*e.g.* children as compared to adults), the pathology encountered (*e.g.* stenotic/occlusive or aneurysmal disease), the need to support appropriate catheters and devices, and also access, given the increasing use of upper limb vessels for many even non-coronary interventions, or pedal access, which drives the need for use of smaller sheaths *e.g.* 4F. From a materials standpoint, typically a mix of metals/alloys are employed including stainless steel (SS), nitinol (NT) with coatings of polymers such as PTFE which give the wire the hydrophilic designation that allows negotiation through blood vessels due to the reduced sliding friction coefficient[10]. Other metals including platinum-nickel[11] and other mixtures. The PTFE coating though common to many modern wires is not entirely non-thrombogenic as has been shown in studies[12], resulting in ongoing designs that include heparin-releasing GWs[13] for coronary application. This aspect is likely negated by the extensive use of unfractionated heparin during endovascular procedures. Representative wires are shown in Table 1.

Table 1: Representative guidewires in endovascular/interventional usage and applied mechanical characteristics (Length variations are not provided).

Name	***Manufacturer***	***Calibre***	***Materials***	***Lubricity designation***	***Stiffness application***	***Tip***	***Usage scenario***
Lunderquist Extra-stiff	Cook	.035”	PTFE-Coated SS	Non-hydrophilic	Supportive	Straight, Double curved, extended curved	EVAR
Bentson	Cook, Merit*	.018”, .025”, .035”	PTFE-Coated SS	Non-hydrophilic	Crossing/ navigating	Straight, floppy	EVAR, PA, venous
Rosen	Cook	.035”	PTFE-Coated SS	Non-hydrophilic	Supportive	J-tip	
Amplatz Super Stiff	Boston Scientific	.035”	Jacketed SS	Non-hydrophilic	Supportive	Straight, short, J-tip	EVAR, PA, CERAB
Hi-Torque Command	Abbott	.014”, .018”	Polymer-coated hybrid NT-SS	Hydrophilic	Crossing/ navigating	Straight, can loop	PA
Hi-Torque Connect	Abbott	.018”		Hydrophilic – hydrophobic hybrid	Crossing/ navigating	Straight, tapered, loaded tip	PA
Hi-Torque Proceed	Abbott	.014”	SS, Pt-Ni tip	Hydrophilic	Supportive	Straight, tapered	PA
Glidewire	Terumo	.018”, .025”, .032”, .035”	W-polyurethane jacketed NT	Hydrophilic	Crossing/ navigating	Straight/ Angled/ Shapeable	EVAR, CERAB, PA, venous
Glidewire Advantage	Terumo	.014”, .018”, .035”	PTFE-Coated NT	Hydrophilic	Crossing/ navigating/ supportive	Angled	EVAR, CERAB, PA
Glidewire Gold	Terumo	.018”	W-polyurethane jacketed NT	Hydrophilic	Crossing/ navigating	Angled	PA
Laureate	Merit	.018”, .025”, .035”, .038”	PTFE-coated NT	Hydrophilic	Crossing/ navigating	Angled, straight	EVAR, PA
InQwire	Merit*	.018”, .021”, .035”, .038”	PTFE-coated SS	Hydrophilic	Crossing/ navigating	J-tip, straight	EVAR, PA
Halberd	Asahi	.014”, .018”	Proprietary, not detailed	Hydrophilic, uncoated tip	Crossing/ navigating	Armoured tip	PA
Gladius	Asahi	.014”, .018”	Proprietary, not detailed	Hydrophilic, coated tip	Crossing/ navigating	Mini pre-shape	PA
Astato	Asahi	.014”, .018”	Proprietary, not detailed	Hydrophilic, uncoated tip	Crossing/ navigating	Loaded taper	PA

Abbreviations: SS= stainless steel; NT= nitinol; EVAR = endovascular aneurysm repair; PA = peripheral angioplasty; CERAB = covered endovascular reconstruction of the aortic bifurcation.
*= heparin-bonded version from Merit not currently CE-marked

Current status on biomechanical studies on guidewires

Historical studies

The reader is directed to a series of excellent historical studies by Schroder in 1993 [10, 14, 15]. In a series of 3 fundamental examinations of GW properties many relevant aspects are described. These effectively deal with three core mechanical issues: Stiffness and torsional strength, kink resistance, and sliding friction aspects. Many fundamental concepts are propounded in this trio of papers. Firstly, the stiffness of a wire is proportional to the 4th power of the core diameter (d^4) [14], but of course also varies depending on the wire material, be it SS (stiffer) or NT (less stiff). Secondly, whilst SS has kink resistance, an additional titanium alloy core provides increased kink resistance, *i.e.* stiffness [15]. Third, addition of a hydrophilic plastic coating reduces friction, notably PTFE which effectively halves the coefficient of friction [10], though modern studies indicate that this against a trade-off of thrombogenicity [12]. This series of three excellent papers, which to the author seem lost in time, examined >85 wires in each study and so provide in-depth analyses of the mechanical properties of guidewires even if historical.
Further studies, as exemplified by that from Nebesar *et al.* [16] have looked at the shaping of wire tips *e.g.* J-tip or widely curved tips, based on mechanical manipulation of wire design.

Recent studies

There have really been only few recent studies examining the mechanical properties of guidewires. Different modalities have been used to measure stiffness, such as flexural modulus (FM) [17], peak deformation force (PDF) as an index of radial stiffness [6], buckling force [18], and perhaps also unusually, tensile strength [19].

Stiffness is intrinsically linked to kink resistance[15] and this is relevant to choice of wire for device delivery at EVAR. An important study by Harrison *et al.* compared the stiffness of designated stiff wires [17] and indicated that the actual physical characteristics as measured in the laboratory have little correlation with the manufactures named designation of the wire wherein terms such as 'super-stiff', 'extra-stiff' or 'ultra-stiff' descriptors are used. Similar contradictions have been noted when examining common wires used for F/BEVAR [20], wherein the Rosen GW (Cook Aortic Interventions, Bloomington, USA) seemed stiff enough to justify its use to deliver stent-grafts at F/BEVAR, with deformation resistance higher than the Lunderquist Extra-Stiff GW (Cook Aortic Interventions) [Figure 2a]. Other specialties such as urology have also undertaken similar tests (excluding the Lunderquist) with the Amplatz Super-Stiff GW (Boston Scientific, Hemel Hempstead, UK) emerging as the most resistant to deformation [Figure 2b]. However,

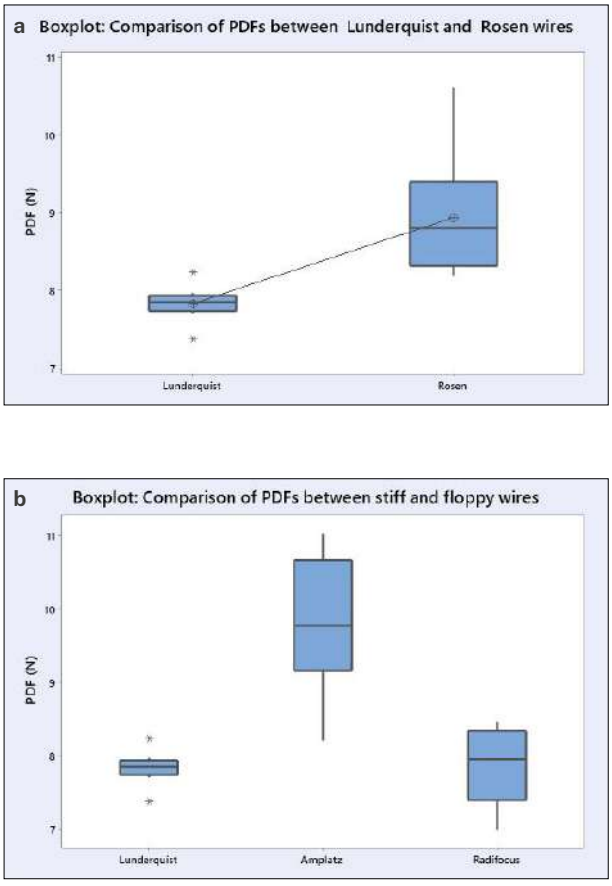

Figure 2: Box plots comparing the peak deformation forces (PDFs) between **(a)** between Rosen and Lunderquist wires. From Chaudhuri *et al.* [20] **(b)** stiff and floppy wires as indicated. From Chaudhuri *et al.* [6].

it would seem that despite the Lunderquist needing lower forces to deform it experimentally, it remains less flexible and thus justifies its use at EVAR[6]. These aspects may well be linked to the varied and complex constituent alloy profiles in these GWs[6].

However, with modern manufacturing techniques, a very high level of quality control and consistency in terms of at stiffness characteristics is to be expected, and this is borne out by recent studies, which also indicate the Lunderquist wire has minimum variation in it deformability characteristics, which supports its use in delivery large devices at EVAR/TEVAR/FEVAR[6]. This consistency is present despite any minor defects that have been noted elsewhere[21] and also the consideration of mixing of alloys used in wire construction[22]. Such studies therefore also suggest that the expected stiffness as borne out by the manufacturers' designation may not be in keeping with the stiffness characteristics when measured on the benchtop.

A previously unanswered question was about the tension exerted on a pullthrough wire (PTW) used at EVAR/TEVAR. Can different floppy wires 'stiffen' differently? The issue that therefore arises is the change in stiffness when a floppy, hydrophilic wire is tensioned as a PTW, thus functioning as a stiff wire[23]. A recent study by Chaudhuri *et al.* attempted to quantify the forces generating the appropriate tension to support large device delivery at EVAR for instance, with at least 38.3 ± 14.8 N tension [Figure 3a] sufficient to deliver a large device such as a sheath[5]. This also seems to be the case as borne by later experiments conducted by the same group using similar methodology, wherein different types of floppy wire tend to be also variably stiff as a PTW. This is graphically illustrated, as exemplified by the Radifocus M GW (Terumo, Bagshot, UK) in PTW configuration, demonstrating higher stiffness compared to conventional stiff wires [Figure 3b].

There seem to be very few studies that mechanically assess the lubricity of wires in the endovascular context. Bench tests of different coatings have been undertaken examining the need to keep wires hydrated[24], but little else noted in the vascular literature. There are studies in the *urology* literature that have undertaken studies – using frictional pull-out forces through sliced bologna-confirming the U-nite GW (Bard Urological, Covington, USA), which is not in common endovascular use, as having highest lubricity[25]. Latter studies using the same methodology affirm that the Glidewire Stiff GW (Terumo) was still not as slippery as other wires such as the Zipwire GW (Boston Scientific) and HiWire GW (Cook Medical); as these wires are not in endovascular use, studies need to be undertaken in the endovascular context.

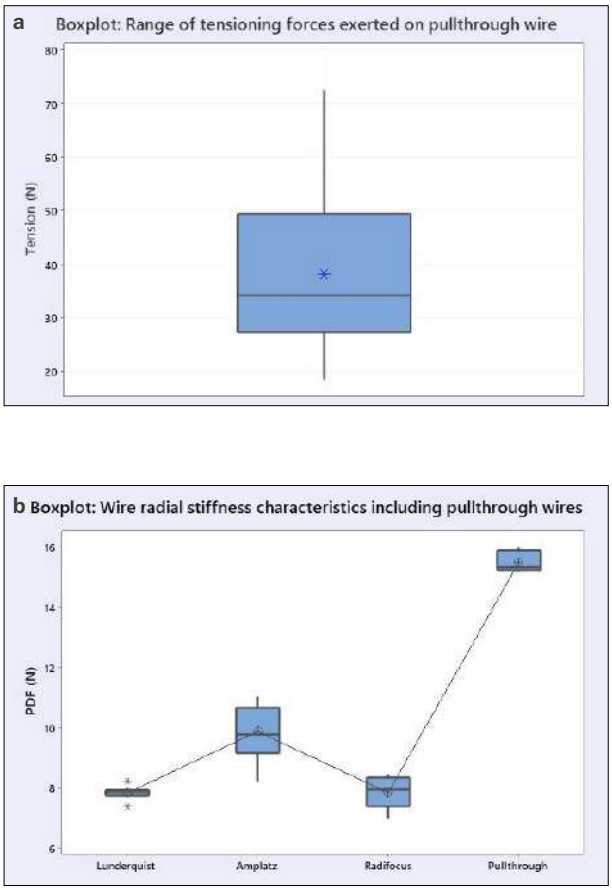

Figure 3: Box plots indicating **(a)** the range of tensions applied by the test group of vascular surgeons (*mean tension of 38.3 N, equivalent to 3.9kgf). From Chaudhuri *et al.*[5] **(b)** effective stiffness of pullthrough wires compared to standard stiff wires (unpublished work).

Discussion

Given the range of GWss available today, it is important for the endovascular operator to therefore have more than a passing acquaintance with the current range of GWs and their characteristics. What emerges is the data is largely based on stiffness; attempts to assess GW characteristics described, including guidewire tip radiopacity, lubricity, navigational characteristics, tip shape retention for instance have been studied, even though systematised well, using subjective response assessment [26]. A comprehensive review is provided by Lorenzoni *et al.* on GWs used for lower limb angioplasty [27], much like that by Khoynezhad et all on wires used during TEVAR [8]. This section also looks at extrapolations from the pure mechanical aspects of guidewires as below.

Mechanical complications related to guidewires

Complications with wires have been described across all specialties using GWs. These include transection [28] and breakage [29], with effects depending on the downstream vascular bed. Historical papers allude to plastic emboli from GWs [30], but such events are now rare and likely linked to improved manufacturing technology. Wire-knotting has also been described in the non-vascular [31] and vascular [32] literature, requiring ingenious salvage procedures.

Robotic and other applications

The issue with GWs is that visualisation is undertaken via fluoroscopy; with the push towards reducing radiation dosage based on the ALARA (As Low As Reasonably Achievable) principle, alternative imaging modalities drive the need for wires that are visualisable using non-fluoroscopic techniques. An emerging area that is yet to be fully developed are MRI-guided interventions with dedicated GWs required [33], but this is yet to become mainstream though technical applications are being explored [34]. Similarly, wires are simply not for tracking through vessel anatomy but can also be functional and be engineered, for pressure-sensing as an example [35], which could be applied across stenoses when treated, a familiar scenario when treating iliac stenotic disease. This potential is yet to be realised, and the mechanical properties yet to be characterised. However, robotic GW manipulation for peripheral angioplasty is now a reality at least from a feasibility standpoint [36].

Guidewires and training

As the mechanical characteristics of guidewires are integral to their function of traversing vascular structures (a function of stiffness-lubricity aspects and the implied trackability), research has also looked at modelling GW motion for simulation environments. This is relevant as modern technology lends itself to simulation training for endovascular procedures using virtual reality (VR) environments [37] and therefore simulation of 'feel', which is effectively related to the GW mechanical properties, becomes relevant.

Environmental impact

GWs are meant to be single-usage and therefore come in multi-layered packaging; there is however little data on the sustainability aspects in the manufacturing process and the environmental impact of GW disposal. This is a particular consideration also in less-developed countries where endovascular devices such as angioplasty balloons are re-sterilised and reused, raising the question around quality control if indeed the same is undertaken for GWs, given their propensity to retain debris as understood from studies of the surface properties [21]. These aspects need further emphasis and discussion, certainly with wire manufacturers. This then drives the potential consideration for the development of sustainable materials for GW themselves, and the ensuing need for the relevant analysis of the mechanical properties of such GWs were they to emerge.

Conclusion

The methods for assessing GW mechanical properties seem to vary in terms of methodology and experimental platform, so it is worth considering whether future tests are undertaken on a standardised platform. This would then guide a uniform designation of stiffness for instance, and would merit a multidisciplinary approach combining the insights of interested clinicians, biomechanical engineers and manufactures. This would then create a unified repository of knowledge that endovascular specialists can draw upon. There should be more standardised studies on *all* the mechanical characteristics of GWs, not just stiffness. For now, what is known that GW mechanical properties are seemingly well standardised and can accordingly be tailored to a wide range of endovascular interventions.

References

1. Seldinger SI. Catheter replacement of the needle in percutaneous arteriography; a new technique. *Acta radiol* 1953; 39: 368-76.
2. Doby T. A tribute to Sven-Ivar Seldinger. *AJR Am J Roentgenol* 1984; 142: 1-4.
3. Gokani VJ, Fishwick NG, Choke E, Bown MJ, Sayers RD. 'Trial of Stiff Guidewire': A Useful Adjunct to Determining Suitability for Endovascular Aneurysm Repair. *EJVES Extra* 2012; 24: e23-e4.
4. Kawatani Y, Nakamura Y, Hayashi Y, Taneichi T, Ito Y, Kurobe H, *et al.* Thoracic endovascular aortic repair of a severely angulated aorta using a double-wire technique. *J Surg Case Rep* 2016; 2016.
5. Chaudhuri A, Heim F, Chakfe N. Estimating the "Pull" on a Pullthrough Wire: A Pilot Study. *EJVES Vascular Forum* 2021; 50: 24-6.
6. Chaudhuri A, Heim F, Chakfe N. Are All Wires Created the Same? A Quality Assurance Study of the Stiffness of Wires Typically Employed During Endovascular Surgery Using Tension Dynamometry. *EJVES Vascular Forum* 2021: 20-4.
7. Fang TD. Ancillary Endovascular Equipment: Catheters, Guidewires, and Procedural Considerations. In: Fogarty TJ, White RA, editors. Peripheral Endovascular Interventions. New York, NY: Springer New York; 2010: pp. 165-79.
8. Khoynezhad A, Kruse MJ. Guidewires, Catheters, and Sheaths Used for Thoracic Endografting Procedures. *J Card Surg* 2009; 24: 113-9.
9. Shirazi RN, McGrath DJ, Clancy M, Higgins C, Mooney I, Dickenson RC, *et al.* The role of plasticity in combined torsion and bending of elastic–plastic guidewires. *Journal of the Mechanics and Physics of Solids* 2021; 151: 104405.
10. Schröder J. The mechanical properties of guidewires. *CardioVasc Interv Radiol* 1993; 16: 93-7.
11. Pelyhe L, Bán M, Bognár E. Kinking Resistance of Guidewires. *Materials Science Forum* 2013; 729: 476-81.
12. Pinto RS, Robbins E, Seidenwurm D. Thrombogenicity of Teflon versus copolymer-coated guidewires: evaluation with scanning electron microscopy. *Am J Neuroradiol* 1989; 10: 407-10.
13. Hanssen HJL, Koole LH. Heparin-releasing intravascular guidewires. *Med Device Technol* 2002; 13: 20-2.
14. Schröder J. The mechanical properties of guidewires. Part I: Stiffness and torsional strength. *CardioVasc Interv Radiol* 1993; 16: 43-6.
15. Schröder J. The mechanical properties of guidewires. Part II: Kinking resistance. *CardioVasc Interv Radiol* 1993; 16: 47-8.
16. Nebesar RA, Pollard JJ. A CURVED-TIP GUIDE WIRE FOR THORACIC AND ABDOMINAL ANGIOGRAPHY. *Am J Roentgenol Radium Ther Nucl Med* 1966; 97: 508-10.
17. Harrison GJ, How TV, Vallabhaneni SR, Brennan JA, Fisher RK, Naik JB, *et al.* Guidewire stiffness: what's in a name? *J Endovasc Ther* 2011; 18: 797-801.
18. Sarkissian C, Korman E, Hendlin K, Monga M. Systematic Evaluation of Hybrid Guidewires: Shaft Stiffness, Lubricity, and Tip Configuration. *Urology* 2012; 79: 513-7.
19. Schummer W, Trommer S, Kleemann F, Schummer C. Mechanical Properties of Seldinger Guidewires. *J Vasc Access* 2014; 15: 507-13.
20. Chaudhuri A, Heim F, Chakfe N. An Analysis of Deformation & Stiffness Characteristics of Guidewires Used at Fenestrated Endovascular Repair (FEVAR). *Eur J Vasc Endovasc Surg* 2019; 58: e856.
21. Anderson JH, Gianturco C, Wallace S, Dodd GD. A Scanning Electron Microscopic Study of Angiographic Catheters and Guide Wires. *Radiology* 1974; 111: 567-71.
22. Vannod J, Bornert M, Bidaux JE, Bataillard L, Karimi A, Drezet JM, *et al.* Mechanical and microstructural integrity of nickel–titanium and stainless steel laser joined wires. *Acta Materialia* 2011; 59: 6538-46.
23. Kawajiri H, Oka K, Yamasaki T, Koh E. Revisiting the brachiofemoral through-and-through wire technique for hybrid arch repair with a problematic elephant trunk. *J Thorac Cardiovasc Surg* 2015; 150: 250-2.

24. Guide Wire Coatings Put to the Test: Medical Design Briefs; 2015 [Available from: https://www.medicaldesignbriefs.com/component/content/article/mdb/features/technology-leaders/21837#.

25. Sarkissian C, Korman E, Hendlin K, Monga M. Systematic evaluation of hybrid guidewires: shaft stiffness, lubricity, and tip configuration. *Urology* 2012; 79: 513-7.

26. Shah A, Lau C, Stavropoulos SW, Nemeth A, Soulen MC, Solomon JA, *et al.* Comparison of Physician-rated Performance Characteristics of Hydrophilic-coated Guide Wires. *J Vasc Interv Radiol* 2008; 19: 400-5.

27. Lorenzoni R, Ferraresi R, Manzi M, Roffi M. Guidewires for lower extremity artery angioplasty: a review. *EuroIntervention* 2015; 11: 799-807.

28. Sakakura K, Taniguchi Y, Yamamoto K, Tsukui T, Jinnouchi H, Fujita H. Excessive Rotational Speed May Be Associated With the Transection of Guidewires in Rotational Atherectomy. *Am J Cardiol* 2020; 132: 172-3.

29. Datta G. Broken guidewire – A tale of three cases. *Indian Heart J* 2015; 67: S49-S52.

30. Kido DK, King PD, Manzione JV, Simon JH. The role of catheters and guidewires in the production of angiographic thromboembolic complications. *Invest Radiol* 1988; 23 Suppl 2: S359-65.

31. Joshi PM, Shivde SR, Dighe TA. Knotting of the guide wires: A rare complication during minimally invasive procedure on kidney-Lessons learnt. *J Minim Access Surg* 2008; 4: 114-6.

32. Koundouris C, Tornaris G, Charopoulos I, Vounasis A, Solomou G. Subclavian vein flexible guidewire knotting. A potential serious complication in hemodialysis patients. *Chirurgia (Bucur)* 2004; 99: 61-4.

33. Ladd ME, Zimmermann GG, McKinnon GC, von Schulthess GK, Dumoulin CL, Darrow RD, *et al.* Visualization of vascular guidewires using MR tracking. *J Mag Res Imaging* 1998; 8: 251-3.

34. Feng L, Dumoulin CL, Dashnaw S, Darrow RD, Guhde R, DeLaPaz RL, *et al.* Transfemoral Catheterization of Carotid Arteries with Real-time MR Imaging Guidance in Pigs. *Radiology* 2005; 234: 551-7.

35. Lum DP, Johnson KM, Paul RK, Turk AS, Consigny DW, Grinde JR, *et al.* Transstenotic Pressure Gradients: Measurement in Swine—Retrospectively ECG-gated 3D Phase-Contrast MR Angiography versus Endovascular Pressure-sensing Guidewires. *Radiology* 2007; 245: 751-60.

36. Behnamfar O, Pourdjabbar A, Yalvac E, Reeves R, Mahmud E. First Case of Robotic Percutaneous Vascular Intervention for Below-the-Knee Peripheral Arterial Disease. *J Invasive Cardiol* 2016; 28: E128-E31.

37. Alderliesten T, Konings MK, Niessen WJ. Modeling Friction, Intrinsic Curvature, and Rotation of Guide Wires for Simulation of Minimally Invasive Vascular Interventions. *IEEE Trans Biomed Eng* 2007; 54: 29-38.

Fenestration state of the art: When, Who and How?

22

Jérémie JAYET, Frédéric HEIM, Jennifer CANONGE, Marc COGGIA, Nabil CHAKFÉ, Raphaël COSCAS

Endovascular treatment with fenestrated endografts (FE) using reinforced nitinol ring fenestrations are the first-line endovascular option for juxta and pararenal abdominal aortic aneurysm. The standard use of FE is however limited by significant manufacturing delays, anatomic standards and procedure's cost. Physician-modified stent-graft (PMSG) and *in situ*.

Target vessel endoleaks rates up to 10% being the most common indication of reintervention following FE. Commercially available FE do not have the same design for fenestrations. In order to optimize the design of fenestrated devices, it is important to better understand the behavior of the connection between the covered stent graft (CSG) and the fenestrated graft itself. We have conducted a study to assess the mechanical performances of various commercially available FE. The radial strength of the fenestration as well as the branch pull out force were experimentally measured and compared between two designs of fenestration. Moreover, some fatigue tests were performed simulating the relative alternative flexure movement applied to the CSG in order to evaluate the behavior of the connection. The results point out differences between the devices at various levels: (1) the radial strength of the fenestration; (2) the pull out force necessary to extract a control branch from the fenestration; (3) the behavior under fatigue loading.

PMSG creation technique lacks standardization. Indeed, several surgical teams have reported various technical details to create a PMSG as selected stent-graft, the reinforcement material used, if used, the cutting material used, the suture and the stabilization with bridging stent. We compared various fenestration configurations in order to identify, which design parameters have a significant influence on the mechanical behavior of the fenestration. We demonstrated a better radial force and rupture resistance notwithstanding an elastic recoil decrease when using a Lasso double loop reinforcement associated to a polypropylene suture. These results could help to standardize the PMSG fenestration creation technique.

Finally, in an experimental work we have evaluated Laser ISF and compared it to Mechanical ISF regarding several features: (1) fenestration morphology, (2) fabric strength modification, (3) leakage through the connection, and (4) stability of the connection following *in vitro* or *in vivo* fenestration. We demonstrated that ISF locally modifies the fabric morphology, leading to strength loss and leakage at stent-fenestration interface. These modifications vary from one.

The performance of the fenestrations can be tuned by playing on the design of the fenestration. In term of mechanical performance, custom made fenestration remain the "gold standard". However, both PMSG and ISF techniques provided interesting alternative. Both could be improved with the standardization of the fenestration creation protocol.

Introduction

Endovascular treatment with fenestrated endografts (FE) using reinforced nitinol ring fenestrations are the first-line endovascular option for juxta and pararenal abdominal aortic aneurysm [1,2]. Commercially available FE include one to five reinforced fenestrations according to the number of target arteries (renal and/or visceral arteries) involved in the repair [3]. The reinforcement concept consists in the use of a nitinol-based wire ring surrounding the fenestrated zone on the fabric. The necessary crimping process to insert the FE in the delivery system theoretically induces sharp folds on the endograft. The shape memory of nitinol helps to recover the geometry of the fenestration after the device has been released from the delivery system. The wire strand includes radiopaque markers made off gold, silver or platinum for fenestration localization purpose [4].

The standard use of FE is however limited by significant manufacturing delays, anatomic standards and procedure's cost. The latter are not acceptable for patients at high surgical risk in association with emergent situations. To fulfill those therapeutics dead-ends, physicians have developed different alternatives to create the fenestration. Physician-modified stent-graft (PMSG) and *in situ* fenestration (ISF) have emerged to circumvent the restrictions raised by FE.

Both technique lacks standardization in the fenestration creation protocol [5,6]. Concerning PMSG, several surgical teams have reported various creation technical details to as selected stent-graft, the reinforcement material used, if used, the cutting material used, the suture and the stabilization with bridging stent [7]. One may wonder if the generalization of the PMSG results is accurate independently of the technical details. Moreover, the PMSG are used in many indications, mainly in aortic aneurysm and aortic dissection. Thus for example, we can see technical differences in aortic arch PSMG for aortic dissection compared to juxta-renal PSMG for aortic aneurysm [7].

In situ fenestration (ISF) represents an innovative and immediately available alternative for complex endovascular aneurysm repair. The ISF concept is based on covering the aortic branches involved in the repair with a standard endograft, to further puncture and dilate the fabric to maintain branches perfusion. This technique was first described by Mc Williams *et al.* to preserve the left subclavian artery during a thoracic aneurysm endovascular repair [8]. While ISF has been mainly reported at the level of the aortic arch, and currently emerged at the thoraco-abdominal level [9,10]. Two main methods can be considered to puncture the graft: (1) mechanical, generally using a needle (MISF) [11,12]; (2) physical, especially since laser catheters have been available [13]. Laser *In situ* fenestration (LISF) has been suggested to be technically simpler and faster, especially in antegrade approaches [14].

Fenestrated endografts mechanical performances

Clinical Achilles heel of the FE remains the endoleaks occurring in up to 30% after post-operative angiography completion [15]. Recent reports highlighted target vessel endoleaks rates up to 10% being the most common indication of reintervention following FE [16,17]. Target vessel endoleaks are mostly due to insufficient attachment, stent fracture, or inadequate seal [15]. Dedicated bridging covered stent grafts (CSG) in FE are still lacking in clinical practice. Torsello *et al.* have studied bridging CSG implanted in fenestrations testing different devices commercially available [18,19]. However, it is still difficult to conclude about the optimal graft/CSG combination.

The interaction between the balloon expandable CSG and the target vessel play an important role in the mechanical strength and in the sealing. If the resistance to radial expansion of the fenestration on the CSG is not high enough, leakage can occur at the connection and the CSG can easily migrate. Conversely, if the resistance to radial expansion is too high, the branch is locally compressed in the fenestration with a dog bone shape that generates flow restriction. In order to ensure that the lifetime of the device meets the clinical need, it is necessary to understand the behavior of a CSG inside the fenestration.

Commercially available FE do not have the same design for fenestrations. This observation raises the question about which design is better.
In that context, in order to optimize the design of fenestrated devices, it is important to better understand the behavior of the connection between the CSG and the fenestrated graft itself [20]. The mechanical strength of the assembling as well as its sealing performances must be controlled precisely to ensure the long-term performance of the device.
We have conducted a study to assess the mechanical performances of various commercially available FE. In particular, the radial strength of the fenestration as well as the branch pull out force were experimentally measured and compared between two designs of fenestration. Moreover, some preliminary fatigue tests were performed simulating the relative alternative flexure movement applied to the CSG in order to evaluate the behavior of the connection. The resulting modifications in the fenestration were analyzed Figure 1.

The results point out differences between the devices at various levels: (1) the radial strength of the fenestration; (2) the pull-out force necessary to extract a control branch from the fenestration; (3) the behavior under fatigue loading. It comes out that these differences can be directly related to the different designs, which could be identified.

Actually, the characteristics of both devices revealed differences in the fabric used to manufacture the cover, in the nitinol reinforcement design, as well as in the way how the nitinol was fixed to the fabric. The microscopic examination of the devices shows that the Anaconda fenestrations appear to be globally more rigid. Several features underline this difference. First, the higher density of the fabric around the fenestration (15% more yarns in warp direction) combined with the larger yarn diameter (by 15% on average), make that the Anaconda fabric is tighter. Our previous works highlighted that this fabric characteristic is directly related to the elastic recoil phenomenon [21]. As a consequence, the fenestration is consequently less deformable when radial deformation is applied to it, as the yarns mobility is limited within the weave. Second, this device is characterized by a the larger number of Nitinol laps (3 *vs.* 2 for the Cook device). As these laps are maintained together with stitches, the friction between the laps limits relative sliding and prevents the reinforcement loop to enlarge.

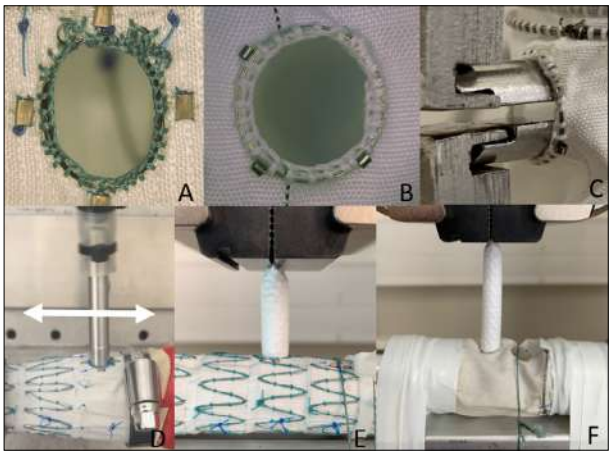

Figure 1

A: Microscopic view (*20) of the Cook fenestration

B: Microscopic view (*20) of the Anaconda fenestration

C: Illustration of the 0.1 N preload applied to an Anaconda fenestration sample.The two half cylinders were spaced at a 2mm vertical displacement

D: The calibrated cylinder was inserted into the fenestration (Cook)/ The white arrow represents the movement axis.

E: A Begraft CSG was inserted into the Cook fenestration

F: A Begraft CSG was inserted into the Anaconda fenestration

These design considerations explain why the radial strength is larger by nearly 60% in the Anaconda fenestration (54 N *vs.* 33 N) over a 2mm deformation range. Moreover, the global loading slope, which represents the radial rigidity of the fenestration, is also steeper. The number of fixing stitches appears to play only a limited role in that mechanism as the Cook fenestration is characterized by 30% more stitches (35 *vs.* 27) than the Anaconda fenestration, and is still more deformable (Figure 2).

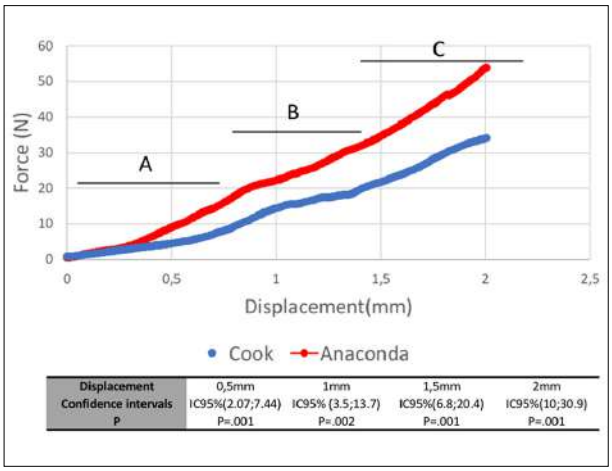

Figure 2: Load displacement curves obtained for both devices over the radial strength test
*N=Newton, mm=millimeters

Regarding the shape of the curves presented in Figure 2 this specific loading behavior can be explained with the different components that are involved in the fenestration design. One can assume that zone A corresponds to the deformability of the ring fixation thread, which is the first component undergoing extension. Once a force threshold is reached, the nitinol wire starts to slip at constant force within the threads, which could explain the plateau zone B. Finally, the yarns involved in the cover fibrous construction at the fenestration border start to be extended. In this latter configuration the deformation of the extended fenestration has reached the size of the initial textile hole before reinforcement which starts to deform itself.

The increased radial rigidity in the Anaconda fenestration was confirmed with the pull-out test. The pull-out force values were nearly twice as large for the Anaconda device. Basically, when the oversized control branch is inserted in a radially more rigid fenestration, the radial force value applied to the branch is greater. As the friction force applied to the branch over the extraction process is directly related to that radial force (Coulomb law), the pull-out force value is also larger.

With respect to the branch design difference, results bring out that the BeGraft CSG was easier to extract from the control fenestration than the V12 CSG as the pull-out force was reduced by nearly 70 % (from 6.75 N to 1.83 N on average). Actually, the BeGraft design is based on Cobalt-Chrome alloy (CoCr) stent segments which are linked together, while the V12 design is based on independent 316L SS segments. The elastic modulus of CoCr being higher (240 GPa *vs.* 200 GPa for steel) and the segments being not independent, the overall radial rigidity value of the BeGraft is higher. When the branch is released in the fenestration, it is therefore less deformed than the V12 design. In particular the “dog bone” shape induced is less pronounced. Consequently, it is easier to pull out the branch from the control tube with the BeGraft, which makes the assembling less stable. However, the design being less deformable, one can consider that once the branch is in position, the assembling is radially tighter and should induce limited leakage despite limited stability.
From a clinical point of view, considering a larger oversizing with the BeGraft design would be relevant to obtain both the tightness of the stent-fenestration junction and an increased “dog bone” shape for assembling stability purpose.

At last, regarding the fatigue tests, radial rigidity has also an influence on the long term behavior of the assembling. We observed that after already 7200 loading cycles, the morphology of the fenestration didn’t change for the Anaconda device while it changed for the Cook device. Actually, the movement amplitude as well as the frequency were largely exaggerated, reproducing extreme wearing conditions. Under these conditions, up to 25% deformation occurred in the Cook fenestration while the Anaconda fenestration size remained stable. The yarns being more mobile in the less tight Cook cover weave,

the fenestration size is less stable, especially under repeated load. One can predict from this result that the Cook device would tend to leak earlier at the CSG/graft interface. However, in all tests the fenestrations showed flexibility and maintained elastic recoil around the branch while no disconnection could observed in both devices.

Physician-modified stentgrafts: The little sister of fenestrated endografts?

As addressed in the introduction, the PMSG creation technique lacks standardization. Indeed, several surgical teams have reported various technical details to create a PMSG as selected stent-graft, the reinforcement material used, if used, the cutting material used, the suture and the stabilization with bridging stent [7]. One may wonder if the generalization of the PMSG results is accurate independently of the technical details. Moreover, the PMSG are used in many indications, mainly in aortic aneurysm and aortic dissection. Thus for example, we can see technical differences in aortic arch PSMG for aortic dissection compared to juxta-renal PSMG for aortic aneurysm [7]. Furthermore, the biomechanical consequences of the stent-graft modifications remain unknown and currently no data are available to determine the appropriate technique to design the fenestration.

We have conducted some experiments based our preliminary works on FE. This work aimed to optimize the technical PMSG characteristics by comparing the mechanical resistance of different fenestration configurations.

We compared various fenestration configurations in order to identify, which design parameters have a significant influence on the mechanical behavior of the fenestration. The radial strength of the fenestrations was measured in order to estimate the radial force applied on the CSG, which has a significant influence on the sealing between the 2 PMSG components. Balloon angioplasty was also carried out in the fenestrations with the intention of studying the permanent enlargement induced. Moreover, branch pull out tests as well fatigue tests were performed in order to assess the tightness and the stability of the assembling (Figure 3).

Significant differences could be observed between the samples tested. Among the main observations, which could be made, results obtained from the branch pullout test as well as from the enlargement test highlighted that reinforced fenestration is characterized by a larger radial stiffness. Actually, the edge of a non-reinforced fenestration is mainly constituted of fraying textile yarns belonging to the stent-graft cover. As these yarns are maintained individual

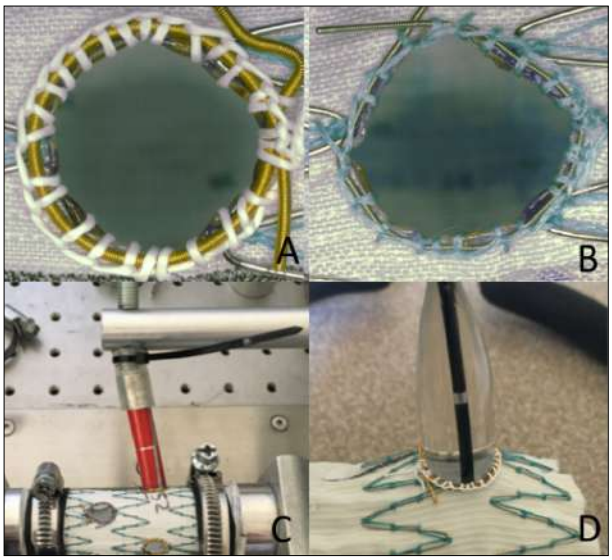

Figure 3

A: Magnification of a Lasso reinforced fenestration (*20)

B: Magnification of a Spartacore reinforced fenestration (*20)

C: Cyclical fatigue test inducing a cyclic linear movement to a 9mm diameter sample introduced in the fenestration

D: Balloon angioplasty test on a 8 mm Lasso-PTFE suture-ophtalmologic cautery fenestration

it is easy to make them move in the textile construction towards the enlargement of the fenestration. This happens when the caliber pin is inserted in the fenestration. The radial force applied by the fenestration on the pin is small, and the friction sliding force, which is directly related to the radial force is small as well. Conversely, when the fenestration is reinforced, the wire maintains the textile yarns together at the fenestration edge. It is more difficult in that case to enlarge the fenestration, as its radial stiffness is more important as can be concluded from the enlargement tests. The force required to extract the pin is consequently higher as well as can be observed with the pullout tests.

The significant role played by the reinforcement is confirmed when considering the double loop test. In Figure 4, one can observe that doubling the loop helps nearly doubling the radial strength of the fenestration.

With respect to the ultimate strength of the reinforcement, results showed an advantage for the Lasso system. Rupture tests confirmed these data. Figure 4 shows that the breakage threshold is smaller for the Spartacore reinforcement. It corresponded to the wire breakage.

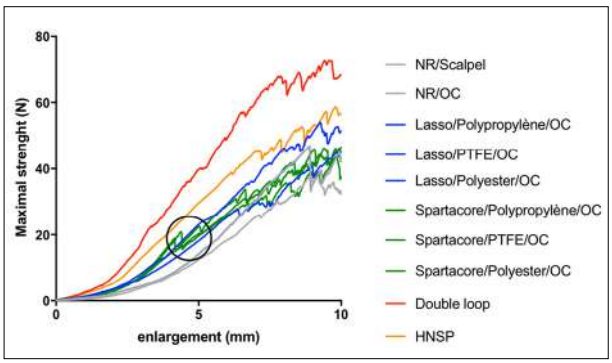

Figure 4: Rupture test : Maximal radial resistance strength (in Newton) by enlargement (in millimeters) for each fenestration category

NR : non reinforced

OC : ophtalmologic cautery

HNSP : high number of suture pass

Black circle : Spartacore rupture

When focusing on the non-reinforced fenestrations, one can observe that the fenestrations created with ophthalmologic cautery (OC) are characterized by increased radial stiffness compared to fenestrations created with scalpel or scissors. Actually, OC generates a local melting of the yarns' extremities, which tend to stick together along the circumference of the fenestration. The melted zones tend to block the movements of the yarns within the textile structure as soon as enlargement is generated, either with the pin or during the enlargement test. The radial stiffness of the fenestration consequently increases as well.

With respect to the fatigue tests, several observations can be made. First, results show that fatigue stress modifies the stiffness of the fenestration in all the fenestration designs. The phenomenon is more marked for the non-reinforced fenestration cut by knife or scissors. In this case, the recoil is very small (around 4%), showing that the geometry is enlarged in a permanent way. Actually, yarns are not maintained at their extremity in that configuration. As was already described above they are free to slide in the textile construction, towards fenestration enlargement. The mechanism is irreversible. In addition, some tearing could be observed in the textile located in the vicinity of the fenestration edge. It can be expected that these tears were initiated at the cutting step, and propagated over the fatigue process. Conversely, when the OC is used, the melting zones tend to block the extremities of the yarns and limit their movement. Under fatigue, yarns deform, the fenestration is deformed but in an elastic way, as the yarns tend to come back to their initial configuration.

Another observation is that the reinforcement appears to be less performant in terms of recoil compared to the OC non-reinforced fenestration. The recoil values are only between 15 to 30 % for reinforced samples. Actually, the cycling process induces repeated wire sliding within the loop, as the fenestration tends to enlarge. The reinforcement insufficient elasticity associated to the friction between the wire loops, the wires and the coil, the coil and the suture are responsible for the partial irreversibility of the deformation. The reinforcement loop size tends consequently to increase with fatigue, and the reinforcement can't come back to its original geometry.

Our study demonstrated a better radial force and rupture resistance notwithstanding an elastic recoil decrease when using a Lasso double loop reinforcement associated to a polypropylene suture. These results could help to standardize the PMSG fenestration creation technique.

In situ fenestration: The Ugly duckling

In an experimental work we have evaluated LISF and compared it to MISF regarding several features: (1) fenestration morphology, (2) fabric strength modification, (3) leakage through the connection, and (4) stability of the connection following in vitro or *in vivo* fenestration.

We demonstrated that ISF locally modifies the fabric morphology, leading to strength loss and leakage at stent-fenestration interface. These modifications vary from one fabric structure to the other, and depend on the fenestration technique.
Microscopic analysis highlighted substantial morphologic variations between fabrics following MISF and LISF. The hole created with MISF appears to separate textile yarns within the fabric to let the needle go through the textile thickness. Conversely, LISF generates a hole characterized by burned edges. Although not significant, it appears that laser puncture tends to weak the materials in a larger way. The study was completed following cutting balloon enlargement, which represents a key step in fenestration creation. In fact, reported experiences with *in situ* fenestration highlighted that it could be difficult to enlarge the initial hole. Cutting balloons clearly represent the most attractive option [22]. Besides, the use of a cutting balloon intends to obtain the target diameter and to prevent stent stenosis[23]. Our results here show that the cutting balloon tends to degrade the membrane in both MISF and LISF configurations (Figure 5).

Even though MISF seemed to preserve textile yarns, the technique was not generally considered in the literature via an antegrade approach because the non-availability of steerable devices[11] (Figure 5). Laser and radiofrequency devices represent the two available options for an antegrade approach[24].

Regarding fabric strength modification, a significant mechanical strength loss was observed following both MISF and LISF. In fact, the hole creates a zone where there is a lack of fabric material, which corresponds to (1) the material degraded with the fenestration and (2) the cutting balloon enlargement. In fact, following fenestration completion, the extension force applied to the sample is spread on a smaller sample cross section. Moreover, the hole creates a local stress concentration due to material rupture or degradation.

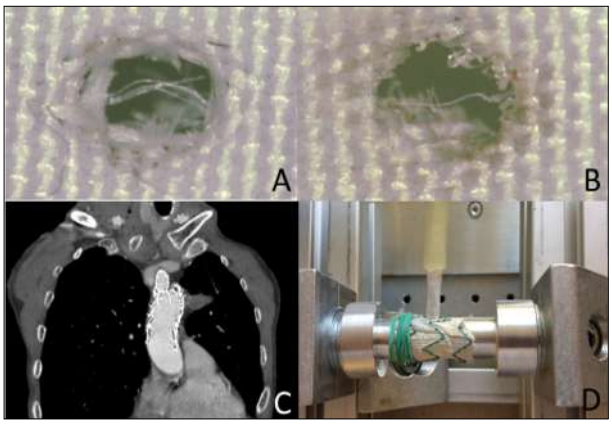

Figure 5

A: Microscopic view of a MISF using an 18G needle (*100)
B: Micoscopic viewLISF using an 0.9mm laser probe (*100)
C: MISF on the innominate trunk for endovascular aortic arch aneurysm repair
D: Cycling testing of a LISF

Valiant monofilament fabric is characterized by a larger strength loss when compared to multifilament fabrics (54% *vs.* 48%). Valiant material is very tight (Ig=236%) and monofilament yarns are non-deformable compared with multifilament. Only limited rearrangement can occur in the textile construction following ISF and more yarns are ruptured consequently. Similar tests were implemented by authors following radiofrequency fenestration [23]. Sample analysis revealed that multifilament fabric provided the best strength before and after fenestration, even after ballooning.

Needle penetration tends to separate the yarns in the textile. The textile construction is thus locally "rearranged" and characterized by a certain elastic recoil once the needle is removed, thereby reducing the diameter of the hole. This elastic recoil tends to press the hole edge against the branch, which increases the flood tightness in that zone. The phenomenon seems to be particularly observable with densest textile for which leakage is reduced compared to the other textile used [21]. The material being denser, the elastic recoil is consequently more important. The absence of elastic recoil regarding expanded polytetrafluoroethylene (ePTFE) membrane explains why major leakage was highlighted following both LISF and MISF. Therefore, our data did not support the use of this material in ISF clinical practice.

The elastic recoil also influences the behavior of the branched device under cyclic stress. Cycling results point out that the hole's surface area increases in a substantial way when the material is denser and when the laser fenestration technique is used. When more yarns are involved in the whole zone, the elastic recoil of the edge tends to generate more friction locally, which leads to more yarn degradation and hole's enlargement. Conversely, regarding the laser technique, the edge being burned and melted, the elastic recoil effect is locally annealed, yarns are broken and rupture can propagate easily. These results are in contradiction with other work published in literature. Ruthrauff *et al.* suggested that the fabric material was not damaged beyond the fenestration at 40 million cycles. However, they used radiofrequency puncture [25] After 170 000 cycles following LISF, we observed an increase in surface area with all textile fabric. Long term effects of LISF on the textile structure may be significant. Furthermore, cyclic test fatigue was performed with a unique longitudinal movement. Longer cycles test in different axes are needed to evaluate ISF long term behavior. To conclude, ISF creates significant textile damages with all available endograft textiles, whatever the technique used. LISF seemed to expose to a higher risk of mechanical resistance loss and leakage at the stent-fenestration interface. Multifilament polyethylene terephthalate (PET) textile fabric seemed more adapted to ISF techniques.

Conclusion

The performance of the fenestrations can be tuned by playing on the design of the fenestration. In term of mechanical performance, custom made fenestration remain the "gold standard". However, both PMSG and ISF techniques provided interesting alternative. Both could be improved with the standardization of the fenestration creation protocol.

References

1. Pini R, Giordano J, Ferri M, Palmieri B, Solcia M, Michelagnoli S, *et al.* The Italian Multicentre Registry of Fenestrated Anaconda™ Endografts for Complex Abdominal Aortic Aneurysms Repair. *Eur J Vasc Endovasc Surg* 2020; 60: 181-91.

2. Oderich GS, Ribeiro M, Hofer J, Wigham J, Cha S, Chini J, *et al.* Prospective, nonrandomized study to evaluate endovascular repair of pararenal and thoracoabdominal aortic aneurysms using fenestrated-branched endografts based on supraceliac sealing zones. *J Vasc Surg* 2017; 65: 1249-59.

3. Wanhainen A, Verzini F, Van Herzeele I, Allaire E, Bown M, Cohnert T, *et al.* Editor's Choice - European Society for Vascular Surgery (ESVS) 2019 Clinical Practice Guidelines on the Management of Abdominal Aorto-iliac Artery Aneurysms. *Eur J Vasc Endovasc Surg* 2019; 57: 8-93.

4. Hartley D, Anderson J, Lawrence-Brown M. Fenestrated Stent Grafts [Internet]. WO/2005/034808, 2005

5. Canonge J, Jayet J. Re « Re "Comprehensive Review of Physician Modified Aortic Stent Grafts: Technical and Clinical Outcomes": The Need for Uniform Reporting Standards of Physician Modified Studies ». *Eur J Vasc Endovasc Surg* 2021; in press.

6. Glorion M, Coscas R, McWilliams RG, Javerliat I, Goëau-Brissonniere O, Coggia M. A Comprehensive Review of *In Situ* Fenestration of Aortic Endografts. *Eur J Vasc Endovasc Surg* 2016; 52: 787-800.

7. Canonge J, Jayet J, Heim F, Chakfé N, Coggia M, Coscas R, *et al.* Comprehensive Review of Physician Modified Aortic Stent Grafts: Technical and Clinical Outcomes. *Eur J Vasc Endovasc Surg* 2021; 61: 560-9.

8. McWilliams RG, Murphy M, Hartley D, Lawrence-Brown MMD, Harris PL. *In situ* stent-graft fenestration to preserve the left subclavian artery. *J Endovasc Ther* 2004; 11: 170-4.

9. Qin J, Zhao Z, Wang R, Ye K, Li W, Liu X, *et al. In Situ* Laser Fenestration Is a Feasible Method for Revascularization of Aortic Arch During Thoracic Endovascular Aortic Repair. *J Am Heart Assoc* 2017; 6: e004542.

10. Le Houérou T, Fabre D, Alonso CG, Brenot P, Bourkaib R, Angel C, *et al. In Situ* Antegrade Laser Fenestrations During Endovascular Aortic Repair. *Eur J Vasc Endovasc Surg* 2018; 56: 356-62.

11. Li DL, Zeng QL, Xiang YL, Qiu CY, Li ZJ, He YY, *et al.* Experimental Analysis of the Quality of Needle-Assisted Fenestration in Aortic Stent-Grafts and the Differences Between Gradual and Rapid Balloon Dilation. *J Endovasc Ther* 2021; 28: 44-52.

12. Coscas R, Glorion M, Javerliat I, Goëau-Brissonniere O, Coggia M. *In Situ* Fenestration Through the Contralateral Iliac Artery to Convert an Aortouni-iliac Into a Bifurcated Endograft. *J Endovasc Ther* 2015; 22: 421-5.

13. Leger T, Tacher V, Majewski M, Touma J, Desgranges P, Kobeiter H. Image Fusion Guidance for *In Situ* Laser Fenestration of Aortic Stent graft for Endovascular Repair of Complex Aortic Aneurysm: Feasibility, Efficacy and Overall Functional Success. *Cardiovasc Intervent Radiol* 2019; 42: 1371-9.

14. Piazza R, Condino S, Alberti A, Berchiolli RN, Coppi G, Gesi M, *et al.* Design of a sensorized guiding catheter for *in situ* laser fenestration of endovascular stent. *Comput Assist Surg* 2017; 22: 27-38.

15. Jain AK, Oderich GS, Tenorio ER, Karkkainen JM, Mendes BC, Macedo TA, *et al.* VESS10. Natural History of Target Vessel Endoleaks After Fenestrated-Branched Endovascular Aortic Repair. *J Vasc Surg* 2018; 67: e53-4.

16. Kärkkäinen JM, Tenorio ER, Jain A, Mendes BC, Macedo TA, Pather K, *et al.* Outcomes of target vessel endoleaks after fenestrated-branched endovascular aortic repair. *J Vasc Surg* 2020; 72: 445-55.

17. Dossabhoy SS, Simons JP, Diamond KR, Flahive JM, Aiello FA, Arous EJ, *et al.* Reinterventions after fenestrated or branched endovascular aortic aneurysm repair. *J Vasc Surg* 2018; 68: 669-81.

18. Torsello GF, Herten M, Frank A, Müller M, Jung S, Torsello GB, *et al.* Performance of BeGraft and BeGraft+ Stent-Grafts as Bridging Devices for Fenestrated Endovascular Aneurysm Repair: An In Vitro Study. *J Endovasc Ther* 2019; 26: 787-94.

19. Torsello GF, Herten M, Müller M, Frank A, Torsello GB, Austermann M. Comparison of the Biomechanical Properties of the Advanta V12/iCast and Viabahn Stent-Grafts as Bridging Devices in Fenestrated Endografts: An In Vitro Study. *J Endovasc Ther* 2020; 27: 258-65.

20. Farivar BS, Brier C, Kuramochi Y, Eagleton MJ. Impact of bridging stent design and configuration on branch vessel durability after fenestrated endovascular repair of complex aortic aneurysms. *J Vasc Surg* 2021; 73: 819-25.

21. Jayet J, Heim F, Coggia M, Chakfe N, Coscas R. An Experimental Study of Laser *in situ* Fenestration of Current Aortic Endografts. *Eur J Vasc Endovasc Surg* 2018; 56: 68-77.

22. Penzkofer T, Na HS, Isfort P, Wilkmann C, Osterhues S, Besting A, *et al.* Electromagnetically Navigated *In Situ* Fenestration of Aortic Stent Grafts: Pilot Animal Study of a Novel Fenestrated EVAR Approach. *Cardiovasc Intervent Radiol* 2018; 41: 170-6.

23. Eadie LA, Soulez G, King MW, Tse LW. Graft durability and fatigue after *in situ* fenestration of endovascular stent grafts using radiofrequency puncture and balloon dilatation. *Eur J Vasc Endovasc Surg* 2014; 47: 501-8.

24. Evans E, Veeraswamy R, Zeigler S, Wooster M. Laser *in situ* Fenestration in Thoracic Endovascular Aortic Repair: A Single-Center Analysis. *Ann Vasc Surg* 2021, in press.

25. Ruthrauff AA, King MW, Soulez G, Tan KT, Crawford SA, Roche-Nagle G, *et al.* Effects of Pulsatile Fatigue on *In Situ* Antegrade Fenestrated Polyester Stent Grafts Deployed in a Patient-Specific Phantom Model of Juxtarenal Aortic Aneurysm. *J Vasc Interv Radiol* 2015; 26: 1551-8.

Infection

- ESVS 2019 clinical practice guidelines on the management of Vascular Graft and Stent Graft infections with EANM 211
- Vascular biomaterials: the (experimental) truth about infectability? 214
- All you need to know about biofilm 235
- Aortic Endograft Infections 245
- Cryopreserved allografts in vascular infection 258
- Investigation of Decellularized Porcine Biograft 267
- Versatility of Pericardial Patches in Vascular Surgery 276

European Society for Vascular Surgery (ESVS) 2019 clinical practice guidelines on the management of Vascular Graft and Stent Graft infections with endorsement of the European Association of Nuclear Medicine (EANM)

23

Nabil CHAKFÉ

The European Society for Vascular Surgery (ESVS) has developed clinical practice guidelines for the care of patients with vascular graft/endograft infection (VGEI). This was the first guidelines driven by scientific societies on (VGEI).

These guidelines can be downloaded at: https://pubmed.ncbi.nlm.nih.gov/32035742/

Introduction

Guidelines driven by scientific societies on vascular graft/endograft infection (VGEI) have not been published. The European Society for Vascular Surgery (ESVS) has developed clinical practice guidelines for the care of patients with VGEI. The aim of this document is to assist physicians involved in the diagnosis and treatment of patients with VGEI in selecting the best management strategy in different scenarios. The potential users of this guideline include angiologists, vascular, cardiovascular and general surgeons, infectiologists and radiologists, and the target population comprises patients with VGEI in supra-aortic trunks, thoracic and/or abdominal aorta, and peripheral arteries.

Guidelines have the purpose of promoting a standard of care according to specialists in the field, in this case represented by members of the ESVS. However, under no circumstance should these guidelines be seen as the legal standard of care in all patients. As the word guidelines states in itself, the document is a guiding principle, but the care given to a single patient is always dependent on the individual (symptom variability, comorbidities, age, etc.) and treatment setting (techniques available, local expertise).

The guidelines

These guidelines can be downloaded at: https://pubmed.ncbi.nlm.nih.gov/32035742/

Authorship

The members of this guidelines Writing Committee (WC) were selected by the ESVS, the European Association of Nuclear Medicine (EANM) and the Groupe de Recherche sur les Infections de Prothèses, to represent physicians involved in the management of patients with VGEI. They include vascular surgeons, radiologists, and infectious disease specialists. WC members have provided disclosure statements of all relationships that might be perceived as real or potential sources of conflicts of interest, which are kept on file at the ESVS headquarters. ESVS reviewers nor individual WC members received any financial support from third parties in direct or indirect relation to this guideline and all WC members and reviewers signed declaration of interest.
Experts from the WC, the ESVS Guidelines Committee, and reviewers who contributed to achieve the final document are given below:

Writing Committee

Nabil CHAKFÉ [1,A,C], Holger DIENER [2,A], Anne LEJAY [1,A,C], Ojan ASSADIAN [3,A], Xavier BERARD [4,A], Jocelyne CAILLON [5,C], Inge FOURNEAU [6,A], Andor WJM. GLAUDEMANS [7,B], Igor KONCAR [8,A], Jes LINDHOLT [9,A], Germano MELISSANO [10,A], Ben SALEEM [11,A], Eric SENNEVILLE [12,C], Riemer HJA. SLART [7,B], Zoltan SZEBERIN [13,A], Omke TEEBKEN [14,A], Maarit VENERMO [15,A], Frank VERMASSEN [16,A], Thomas R. WYSS [17,A].

Guidelines Committee

Frederico BASTOS GONCALVES [18,A], Gert de BORST [19,A], Stavros K KAKKOS [20,A], Philippe KOLH [21,A], Riikka TULAMO [15,A], Melina VEGA de CENIGA [22,A], Anders WANHAINEN [23,A].

External reviewers

Regula S. von ALLMEN [24,A], Jos C van den BERG [25,A], Sebastien E DEBUS [26,A], Mark JW KOELEMAY [27,A], Jose P. LINARES-PALOMINO [28,A], Jean-Baptiste RICCO [29,A], Gregory LL. MONETA [30,A].

References

1. Department of Vascular Surgery and Kidney Transplantation, University of Strasbourg, University Hospital of Strasbourg, Strasbourg, France.
2. Department of Vascular Medicine, University Heart and Vascular Center, Hamburg, Germany.
3. Department for Hospital Epidemiology and Infection Control, Medical University of Vienna, Vienna General Hospital, Vienna, Austria.
4. Department of Vascular Surgery, University of Bordeaux, University Hospital of Bordeaux, Bordeaux, France.
5. Department of Bacteriology, University Hospital of Nantes, Nantes, France.
6. Department of Vascular Surgery, University Hospitals Leuven, Leuven, Belgium.
7. Departments of Nuclear Medicine and Molecular Imaging and Radiology, University of Groningen, Groningen, Netherlands
8. Clinic for Vascular and Endovascular Surgery, Belgrade, Serbia.
9. Department of Cardiovascular and Thoracic Surgery, Odense University Hospital, Odense, Denmark.
10. Division of Vascular Surgery, 'Vita Salute' University, Scientific Institute H. San Raffaele, Milan, Italy.

11. Department of Surgery, Division of Vascular Surgery, University Medical Centre Groningen, University of Groningen, Groningen, The Netherlands.
12. Department of Infectious Diseases, Gustave Dron Hospital, University of Lille, Tourcoing, France.
13. Department of Vascular Surgery, Semmelweis University, Budapest, Hungary.
14. Department of Vascular Surgery, Klinikum Peine, Peine, Germany.
15. Department of Vascular Surgery, University of Helsinki, University Hospital of Helsinki, Helsinki, Finland.
16. Department of Thoracic and Vascular Surgery, Ghent University Hospital, Ghent, Belgium.
17. Department of Cardiovascular Surgery, Inselspital, Bern University Hospital, University of Bern, Bern, Switzerland.
18. University Hopistal of Lisboa, NOVA Medical School, Lisbon, Portugal.
19. Department of Vascular Surgery, University Medical Center Utrecht, The Netherlands.
20. University of Patras Medical School, Patras, Greece.
21. Department of Biomedical and Preclinical and Sciences, University of Liège, Liège, Belgium.
22. Hospital de Galdakao-Usansolo, Bizkaia, Spain.
23. Department of Surgical Sciences, Section of Vascular Surgery, Uppsala University, Uppsala, Sweden.
24. Clinic for Vascular Surgery, Kantonsspital St Gallen, St. Gallen, Switzerland.
25. University Hospital of Bern, Bern, Switzerland.
26. Department for Vascular Medicine, Vascular Surgery, Angiology and Endovascular Interventions, University Heart and Vascular Center, Hamburg-Eppendorf, Germany.
27. Department of Surgery, Amsterdam Cardiovascular Sciences, University of Amsterdam, Amsterdam, The Netherlands.
28. Department of Vascular Surgery, University Hospital Virgen de las Nieves, Granada University, Granada, Spain.
29. Department of Vascular Surgery, University Hospital of Poitiers, Poitiers, France.
30. Division of Vascular Surgery, Knight Cardiovascular Institute, Oregon Health & Science University, Portland, USA.

A: European Society for Vascular Surgery
B: European Association of Nuclear Medicine
C: Groupe de Recherche sur les Infections de Prothèses

Vascular biomaterials: the (experimental) truth about infectability?

24

Mathilde PUGES, Fatima M'ZALI, Sabine PEREYRE, Cécile BEBEAR, Charles CAZANAVE, Xavier BERARD

Many experimental studies have been conducted so far to evaluate vascular grafts infectability and to elaborate strategies to prevent or to treat their occurrence. We conducted a systematic literature research to collect and summarize key features of infectability assessment technics in vascular grafts and endografts infections (VGEIs) experimental models.

A systematic literature search was conducted using Medline and Cochrane databases, with no limit on the date of publication, until August 10, 2021. *Ex vivo*, *in vitro*, *in vivo* animal studies on VGEIs, published in English or French, were selected. Cross references retrieved from selected articles on Pubmed database were also included in the search. We collected data on the techniques and the protocols performed for vascular graft infectability assessment.

A total of 243 studies were included in the review after reading the full-length article, 55 *in vitro* studies, 169 animal studies, 17 combining the two models and 2 *ex vivo* studies. Many experimental techniques were performed, with a lot of protocol discrepancies. The main conducted experiments were bacterial culture, with (n=82 studies) or without sonication (n=120), histopathology (n=69), scanning electron microscopy (n=36) and graft diffusion test (n=28). These technics were used to answer different research questions corresponding to different graft infection steps, such as microbial adhesion and/or viability, biofilm biomass or organization, human cell reaction or antimicrobial activity.

The techniques used in VGEIs experimental studies allowed the investigation of the different steps of vascular grafts infectability. Many tools are available but should be precociously selected according to the research issue.

Introduction

Vascular graft and endograft infections (VGEIs) are still associated with high morbidity, mortality and relapse rates[1]. The issue of vascular biomaterials' infectability is of a particular importance to improve VGEIs outcome, however, even the word "infectability" is not clearly defined in the literature. The first occurrence of this word appears in 1975 in an experimental study, defined as "that the susceptibility of a prosthetic graft to infection"[2], however no consensual definition is currently available in the literature. This first definition gives rise to multiple notions of what susceptibility to infection can be. Indeed, microbial colonization of a biomaterial surface implies several crucial steps which involve different pathophysiological mechanisms. Infectability assessment should be considered through these different mechanisms. Two recent well-conducted reviews have been published on pre-clinical models evaluating vascular graft coating and silver grafts[3,4], but no review has been conducted so far on the analysis

performed in experimental models to assess vascular grafts infectability. We conducted this review to collect and summarize key features of infectability assessment technics in VGEIs experimental models. The second aim was to classify these technics according to the different research issues.

Material and methods

The study was conducted in accordance with the PRISMA (Preferred reporting items for systematic reviews and meta-analysis) guidelines [5] and the PICO strategy [patient population (P), intervention (I), comparison (C), and outcomes (O)] which was used to structure and respond to the research question. PICO criteria were: "In *in vitro* and *in vivo* models of VGEIs (P), which experimental techniques (I) are the most accurate (C) to investigate the issues on vascular graft infectability (O)"?

Search strategy and information sources

A duplicate comprehensive literature hand search was conducted by M.P. and C.C using Medline and Cochrane databases, with no limit on the date of publications. Disagreements between M.P and C.C were resolved by consensus. If consensus was not achievable, a third opinion was taken from X.B. We updated the research on August 10, 2021. The search terms for Medline and the Cochrane Database search, were as follows: "vascular graft infection", combined, by the mean of the Boolean operator "AND", with "animal study", "animal model", "*in vitro* study", or "*in vitro* model" We also used the MeSH terms "blood vessel prosthesis" AND "infections" AND "models, animal", and "blood vessel prosthesis" AND "infections" AND "*in vitro* techniques". For each included article, the reference list and the first 20 related articles on Pubmed were screened to retrieve potential relevant articles.

Eligibility criteria and study selection

Studies were selected according to the following criteria. Only *in vitro* and *in vivo* animal studies on VGEIs, published in English or French, were selected. Clinical studies on human beings and experimental studies on other device infections were excluded from analysis. Studies were first selected on title and abstract basis, then on full text. Duplicates were discarded.

Data collection process

Data were extracted by M.P. and C.C. From each study, we collected the source (main author, journal and year of publication) and the details the analysis performed for infection assessment.

Results of the comprehensive review

A total of 243 articles were included in the comprehensive review, 55 *in vitro* studies, 169 animal studies, 17 which combined both models and 2 *ex vivo* studies (Flow Chart in Figure 1). We successively detailed the diverse analysis performed to study infectability and their purposes, which are summarized in Supplemental Table 1 and illustrated in Figure 2.

In animal and *ex vivo* studies, many authors described the macroscopic signs of infection, sometimes with a precise scale [6], particularly anastomoses or graft rupture, abscess, gross purulence, graft patency and incorporation [7]. They also registered the onset of death due to infection [8]. In some studies, the clinical evolution, sepsis but also graft rupture, thrombosis and death, were the only criterion chosen by the authors to evaluate graft infectivity [9].
However, in the great majority of studies, many other analyses were performed.

Supplemental Table 1: Experimental analysis for vascular graft infectability assessment.

Experimental design	Analysis *in vitro*	Reference
Microbial culture		
In vitro and *in vivo*	Bacterial count after sonication	(1–84)
In vitro and *in vivo*	Bacterial count without sonication	(14,20,28,65–68,82,85–197)
In vitro	Bacterial count inside/outside the graft	(197,198)
In vitro and *in vivo*	Kill kinetic studies	(2,7,11,12,34,199–201)
In vitro and *in vivo*	Graft diffusion test	(22,63,86,99,100,102,109,141,148, 156,176,184,196,202–216)
Viability assessment		
In vitro	ATP assay	(4)
In vitro	Biofilm bacterial metabolism assays	(1,76,202)
Evaluation of microbial biomass with no viability assessment		
In vitro and *in vivo*	Optical density	(6,78,106,202,203,217)
In vitro	Autoradiography of radiolabelled bacteria	(8,60,147,166,218–221)
In vivo	Specific bacterial PCR	(106,213)
Antimicrobial activity in biofilm		
In vitro	MBIC and MBEC	(7,14,58,199,222–224)
Biofilm staining		
In vitro	Biofilm formation by crystal violet	(4,76,78)
In vitro	Energy-dispersive x-ray analysis	(13)
Microscopy		
In vivo and *ex vivo*	Histopathology	(24,27,32,42,46,49,51,63,64,66,67,70,71,75,81,85, 90,106,107,110,112,113,115–122,125–128,130,133–135, 139–141,145,149,150,154–159,161,163,168, 169, 173,174,183,187,194,208,221,225–233)
In vitro and *in vivo* and *ex vivo*	SEM: biofilm structure, bacterial adhesion or sonication efficacy	(4,6,7,9,13–16,18,26,29,67,75,76,85,90, 107,110,111, 135,141,156,160,164,165,179, 187,188,197,204,218,219,225,234–236)
In vitro and *in vivo* and *ex vivo*	TEM: bacteria, biofilm	(204,226,237)
In vitro and *in vivo*	Confocal microscopy	(21,58,78,235–239)
In vivo	FISH	(237)
Imaging		
In vivo	Non-invasive Biophotonic Imaging	(62)
In vivo	Imaging technics: MRI, angiogram	(175)
In vivo	Nuclear medicine: PET, radiolabelled leukocyte scintigraphy,	(178,237)
Inflammation analysis		
In vitro	Human cells activity assessment	(60,240)
In vivo	Systemic and/or local biomarkers	(25,40,47,60,238,242,243)

ATP: adenosine triphosphate, PCR: polymerase chain reaction, MBIC: minimum biofilm inhibitory concentration, MBEC: minimal biofilm eradication concentration, SEM: scanning electron microscopy, TEM : transmission electron microscopy, FISH: Fluorescence in situ hybridization, MRI : magnetic resonance imaging, PET: positron emission tomography.

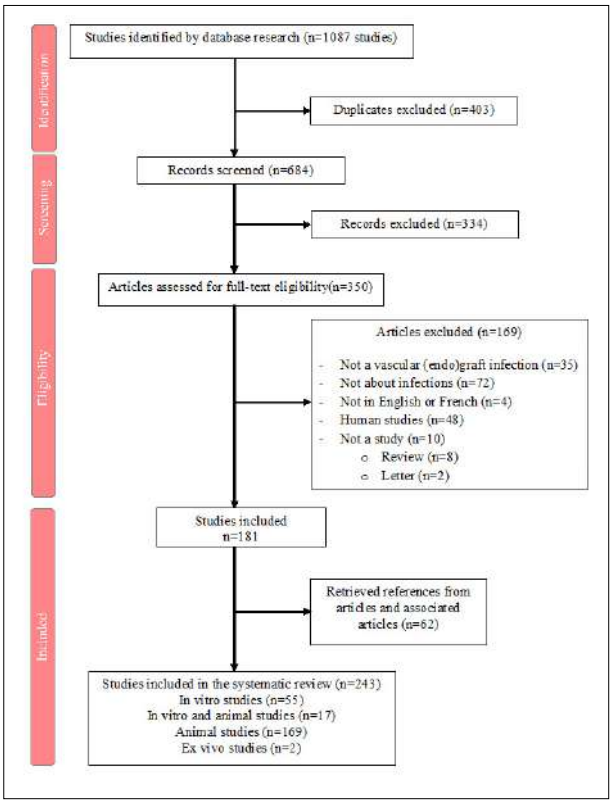
Identification
Screening
Eligibility
Included
Studies identified by database research (n=1087 studies)
Duplicates excluded (n=403)
Records screened (n=684)
Records excluded (n=334)
Articles assessed for full-text eligibility(n=350)
Articles excluded (n=169)
- Not a vascular (endo)graft infection (n=35)
- Not about infections (n=72)
- Not in English or French (n=4)
- Human studies (n=48)
- Not a study (n=10)
o Review (n=8)
o Letter (n=2)
Studies included n=181
Retrieved references from articles and associated articles (n=62)
Studies included in the systematic review (n=243)
In vitro studies (n=55)
In vitro and animal studies (n=17)
Animal studies (n=169)
Ex vivo studies (n=2)

Figure 1: Flow Chart according to PRISMA guidelines.

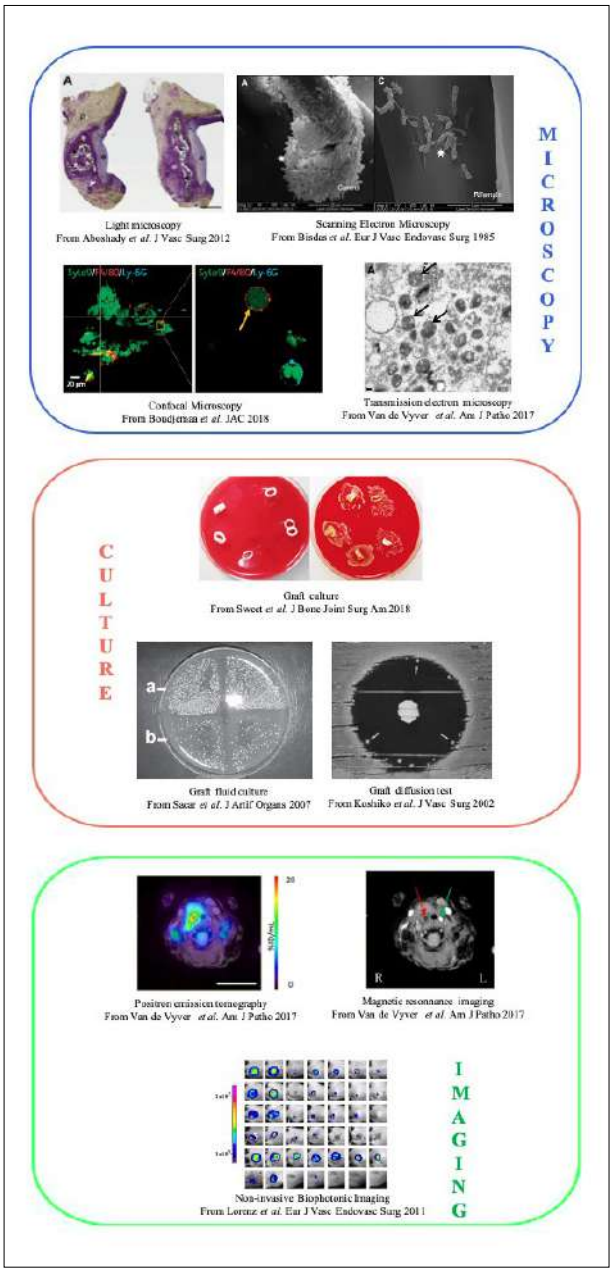
MICROSCOPY
Light microscopy
From Abushady et al. J Vasc Surg 2012
Scanning Electron Microscopy
From Bisdas et al. Eur J Vasc Endovasc Surg 1985
Confocal Microscopy
From Bondjeman et al. JAC 2018
Transmission electron microscopy
From Van de Vyver et al. Am J Pathol 2017
CULTURE
Graft culture
From Sweet et al. J Bone Joint Surg Am 2018
Graft fluid culture
From Sasar et al. J Artif Organs 2007
Graft diffusion test
From Koshiko et al. J Vasc Surg 2002
Positron emission tomography
From Van de Vyver et al. Am J Pathol 2017
Magnetic resonance imaging
From Van de Vyver et al. Am J Pathol 2017
IMAGING
Non-invasive Biophotonic Imaging
From Lorenz et al. Eur J Vasc Endovasc Surg 2011

Figure 2: Illustrations of selected experimental techniques for infectability assessment.

Microbial culture

The microbial count in colony forming units (CFU)/mL is often considered as the gold standard for the quantification of bacterial adherence on vascular graft material and is the most used analysis, both in *in vitro* and *in vivo* studies. The other tests are more confidential. Several types of microbial counts have been described in the literature and are detailed in the following paragraphs.

Microbial count on infected grafts

In most studies, grafts and perigraft tissues were processed by different technics before plating, in order to enhance bacterial culture sensitivity. Grafts were sometimes sonicated before culture (n=82 studies), sometimes associated with vortexing [10], but sonication process varied a lot among studies. Its length varied between 1 min and 20 min, but most often 5 min [11]. Ultrasound frequency was rarely specified and varied between 20 kHz and 60 KHz. Sonication efficacy was assessed in several studies either by scanning electron microscopy (SEM) [12] or optical microscopy [13]. However, most studies did not used sonication (n=120).

Sometimes, grafts were only vigorously agitated[14] or vortexed 30s to several minutes, until 1h of vortex[15]. Other technics were used, such as the homogenisation with a dispersing instrument[16], ultrasonic disruption[17], bead-beaters with glass beads[18], hand-crushing with a sterile mortar[19], tissue-grinding associated with sonication[20], or trypsin digestion of the graft and perigraft tissues[21].

However, in several studies, grafts were not processed before culture but only placed in broth medium before plating on agar[22]. Sometimes grafts were only rolled on agar and removed before culture[23], or only imprinted on agar before incubation[24].

Despite protocol discrepancies, microorganisms recovery was better with sonication compared to vortex alone[17] or ultrasonic disruption[17]. This superiority in bacterial recovery has been assessed both in *in vitro*[17,25] and animal models[20,26], especially for *Staphylococcus epidermidis*[17,20,25,26], but also *Staphylococcus aureus, Escherichia coli, Enterococcus faecalis* and *Klebsiella pneumoniae*[17].

Determination of bacterial localisation by culture (n=5 studies)

Some authors tried to localise bacteria on grafts, by comparing cultures of different graft sites. In animal models, blood cultures were frequently performed, sometimes combined with culture of organs harvested after euthanasia to better localise secondary infectious sites.

Kill kinetic studies (n=8 studies)

By repeating bacterial count in the supernatant at several times of culture, this analysis was meant to study the impact and the efficacy of several antibiotic molecules, and grafts infectivity or bactericidy of antimicrobial grafts[27]. A bactericidal effect was defined as a ≥ 3 $\log^{10}$ reduction in CFU compared with the initial inoculum[28].

Grafts diffusion test (n=28 studies)

The disk diffusion test has been adapted for determining grafts antimicrobial effects. Graft segments were placed on agar after bacterial plating, and after incubation, the inhibition zone was measured as the radius of the clear zone of inhibition from the outer edge of the device. This measure was sometimes repeated at several times in order to estimate the grafts bactericidy evolution over time. Rarely, graft digest was placed on thin paper disks placed on agar plates previsouly inoculated with bacteria. Pieces of grafts could also be embedded into agar medium containing bacteria before the inhibition zone measure.

Viability assessments

Adenosine triphosphate assay (n=2 studies)

The mitochondrial adenosine triphosphate (ATP) concentration, directly proportional to the amount of ATP in bacteria, was measured to quantify the number of viable bacteria. This test has also been used in this study to compare several antimicrobial molecules *in vitro*.

Biofilm bacterial metabolism assays (n=4 studies)

This colorimetric assay is based on the reduction of a yellow tetrazolium salt to purple formazan crystals by the mitochondrial dehydrogenase of metabolically active cells. This semi-quantitative test, also called MTT or XTT, has notably been used *in vitro* to evaluate micro-organisms metabolic activity in vascular grafts biofilm.

Evaluation of microbial biomass with no viability assessment

Supernatant optical density (n=6 studies)

The bacterial inoculum could as well be estimated by the medium optical density measure of the supernatant, but with no information on the bacterial viability. This technic was therefore often associated with a bacterial count.

Bacterial radiolabelling (n=8 studies)

Many studies have used various radionucleides to stain bacteria in order to quantify the bacterial biomass on the graft surface. *In vitro*, radionucleides stained either cytoplasm, such as Indium-111-oxine-labeled *S. aureus*[29], or bacterial desoxy ribonucleic acid (DNA), such as 35S-methionine[30] and methyl-3H-thymidine[31]. This technic has also been used to study bacterial adhesion on vascular grafts and to localize where bacteria adhered in animal models.

Real-time quantitative polymerase chain reaction (n=2 studies)

Keeling *et al.* evaluated a real-time quantitative polymerase chain reaction (RT-PCR) to detect genes associated with the expression of methicillin resistance (*mecA* and *femA*) in a rat model. They compared the PCR results of bacterial cultures of known concentrations to PCR results of graft and blood samples, in order to estimate the bacterial inoculum[32].

Antimicrobial activity in biofilm

Minimal biofilm inhibitory concentrations and minimum biofilm eliminating concentrations determination (n=7 studies)

Minimal *biofilm* inhibitory concentrations (MBIC) and minimum biofilm eliminating concentrations (MBEC) were often further compared to minimum inhibitory concentration (MIC). Before the concept of MBIC and MBEC, some authors determined both MIC and minimal bactericidal concentration (MBC) by the tube microdilution method or by agar dilution method. The impact on MIC and MBC of antimicrobial molecules has also been studied.

Biofilm staining

Crystal violet assay (n=3 studies)

Crystal violet assay (CV) is a basic dye that binds negatively charged molecules and thus stains both bacteria and the surrounding biofilm matrix[33]. This technic was especially used in *in vitro* studies, but also *in vivo* studies to characterize their bacterial strain before the onset of infection in animal models. Only one study reported that the measurement of CV via spectrophotometry was not suitable for vascular graft surfaces because of a high unspecific background staining[34]. However, two other studies have been published since this first observation, to evaluate the biofilm formation in contact with a graft coating agent. Microplates well's walls were covered either with gelatin, collagen or an antibiotic-containing fibrin gel before bacterial inoculation, culture then CV assay.

Energy-dispersive x-ray analysis (n=1 study)

Energy-dispersive x-ray analysis (EDX) has been used to analyse the production of mucin on the graft surface. Polysaccharide matrix was stained by the cationic stain ruthenium red and glycoproteins were stained with alcian blue[35].

Microscopy

Light microscopy and histopathology (n=69 studies)

In animal models, histopathology was frequently used to assess signs of infection after hematoxylin and eosin and/or Gram staining. In some studies, graft infection was assessed only on histological analysis. Some authors also used histology to study grafts ruptures due to infection, graft anastomosis and perigraft tissue inflammatory reaction and graft endothelialisation. Immunohistochemistry was performed in several studies, either to stain leukocytes or endothelial cells. Light microscopy has also been used to assess sonication's efficacy.

Scanning electron microscopy (n=36 studies)

Scanning electron microscopy (SEM) has especially been used in order to better understand VGEI physiopathology, notably biofilm formation and micro-organisms adhesion and organisation on the graft surface. Rarely, SEM results were analysed to estimate the approximate number of adhesive bacterial microcolonies on graft segments. SEM has also been used to observe biofilm formation kinetics on the graft surface by serial acquisitions, graft endothelialisation and susceptibility to infection. Some studies tried to assess the sonication efficacy on dislodging bacteria by SEM, or the efficacy of several antimicrobial treatments or antiseptics molecules on infected vascular grafts. Only one *ex vivo* study used SEM to analysed explanted infected grafts from patients operated for VGEI (36).

Transmission electron microscopy (n=3 studies)

Studies using transmission electron microscopy (TEM) are much less frequent than SEM. Webb *et al.* used TEM after ruthenium red mucopolysaccharides staining of *in vitro* infected grafts[37]. *In vivo*, Van de Vyver *et al.* used marked anti-lectin antibodies to visualise the extracellular matrix[38].

Confocal microscopy (n=8 studies)

Confocal microscopy has been firstly applied by Osada *et al.* in 1999 to study and compare bacterial adhesion[39]. *In vitro*, confocal microscopy has been used to assess the thickness, the density and the formation kinetics of biofilm on various grafts, with different dyes. In animal models, confocal microscopy has been applied to localize bacteria, immune cells and antibiotics with specific antibodies marked with fluorochromes.

Fluorescence *in situ* hybridization (n=1 study)

Fluorescence *in situ* hybridization (FISH) has been used to localize bacteria on vascular grafts, both on *in vitro* and *in vivo* models, with fluorescein isothiocyanate (FITC)-labeled probe complementary to the 16S ribosomal ribonucleic acid (rRNA) in most microorganisms, combined with a *S. aureus* specific probe and 4′,6-diamidino-2-phenylindole (DAPI) for nucleic acid counterstaining[38].

Imaging

In vivo bioluminescence imaging (n=1 study)

This non-invasive imaging technic was evaluated only once in VGEIs. The authors inoculated a bioluminescent *S. aureus* strain, genetically engineered in order to express a modified Photorhabdus luminescence lux operon, on vascular grafts subcutaneously implanted in mice backs. The real-time bioluminescence was correlated to the total number of bacteria to estimate the bacterial burden [40].

Magnetic resonance imaging (n=2 studies)

Magnetic resonance imaging (MRI) has been evaluated in one murine study to assess changes in the blood flow velocity after the infection of a carotid catheter [38]. Peter *et al.* also compared nuclear magnetic resonance to angiography for the diagnosis of VGEIs in a canine model [41].

Lymphography (n=1 study)

White *et al.* used lymphography in a dog model of VGEI and demonstrated that there was a periaortic pooling of lymph in the immediate postoperative period [42].

Nuclear medicine imaging (n=2 studies)

^{18}F-Fluorodeoxyglucose-Positron emission tomography (^{18}F FDG-PET) has been applied in one murine study to analyse FDG uptake after infection [38]. Another study evaluated radiolabelled leucocyte scintigraphy performance in the diagnostic of acute VGEI diagnosis in dogs [43].

Inflammation analysis

Systemic and local biomarkers (n=7 studies)

Several studies associated graft analysis and plasmatic biomarkers and many pro-inflammatory cytokines, such as interleukins, TNF-alpha or IFN-gamma. Some inflammatory biomarkers have also been quantified in the perigraft fluid.

Human cells activity (n=2 studies)

The impact of graft silver-coating on neutrophils functions has been analysed by fluorometric analysis. Human neutrophils were incubated with two grafts, coated and uncoated, then with *Escherichia coli* [44]. The effect of an infected perigraft fluid on fibroblasts proliferative activity has also been evaluated by the incorporation of [3H]thymidine into fibroblasts deoxyribonucleic acid [21].

Discussion

We conducted a comprehensive review on 243 studies evaluating infectability assessment analysis in VGEIs experimental models. Many interesting technics have been used so far to answer various research questions on vascular grafts infectability, and future researchers should select the analysis to perform according to their hypotheses. We summed up all the analysis performed for infectability assessment in experimental models of VGEIs according to the research issue in Figure 3.

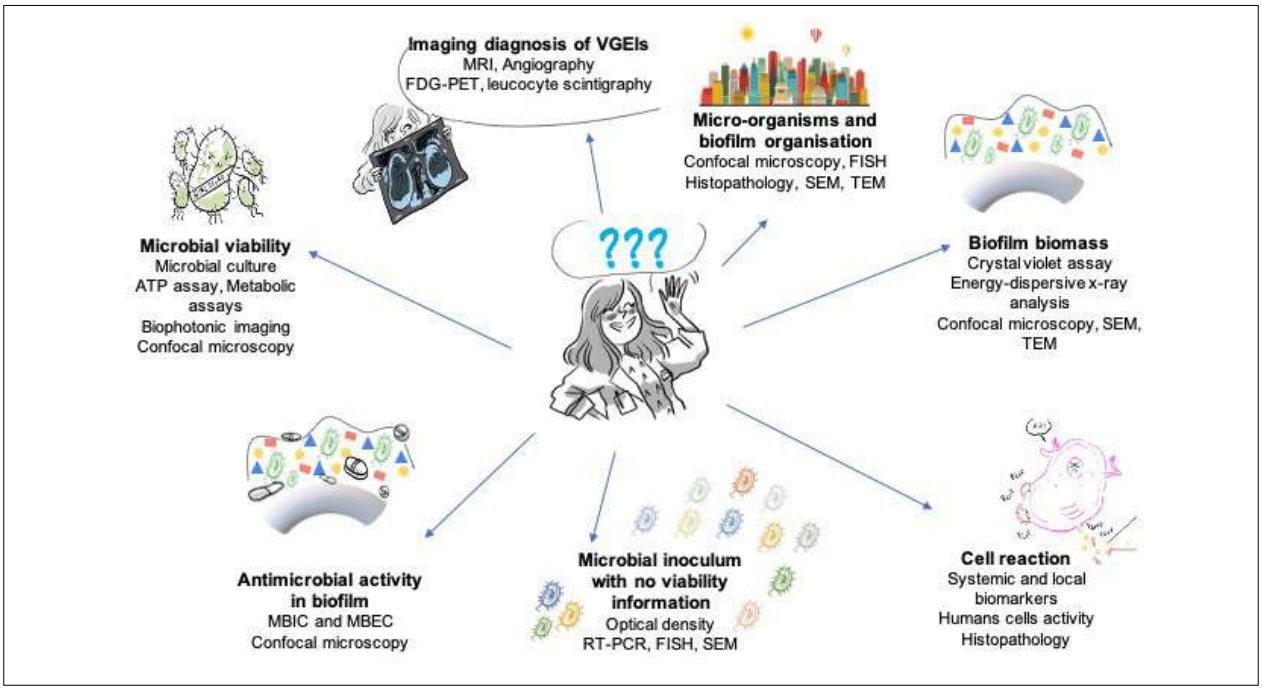

Figure 3: Experimental analysis relevant to answer selective research questions.
ATP: Adenosine tri-phosphate, MBIC: Minimal biofilm inhibitory concentration, MBEC: Minimum biofilm eliminating concentration, RT-PCR: Magnetic resonance imaging, FDG-PET: Fluorodesoxyglucose-position emission tomography, FISH: Fluorescence *in situ* hybridization.

In the following paragraphs, we we will focus on three main points of interest: the necessity of protocol standardisation and particularly the importance of sonication before microbial culture, the need for techniques which take into account adhesion and biofilm formation and finally the potential contribution of new non-invasive techniques.

However, infectability assessment technics need standardisation to be relevant and applicable to clinical practice. Indeed, experimental protocols varied a lot among studies, especially for microbial culture. For instance, in most studies, which appeared to be the earliest ones, infected vascular grafts were not sonicated. Sonication better efficacy for microbial recovery has been assessed in several *in vitro* and *in vivo* studies on vascular graft infections [17,20,25,26]. Its clinical impact on VGEIs microbiological diagnosis has been demonstrated in bone and joint infections (BJI) [45] and remains probable in VGEIs [46]. It should therefore be used in experimental studies before any graft's bacterial count. However, sonication protocol needs standardization, and we propose a protocol based on the most employed protocols in the previously published studies which might offer the best microbial recovery along with the maximal viability. Grafts should be vortexed for 30 seconds, sonicated for five minutes at a ultrasonic frequency comprised between 35 and 50 kHz, and vortexed for another 30 seconds before sonicate fluid plating[11,45,46].

Furthermore, some issues remain under-explored in VGEIs field, especially microbial adhesion and biofilm. In the vast majority of the studies, grafts infectivity experiments did not include any analysis of biofilm. Investigations on antimicrobial therapy in experimental models of VGEIs are rare, particularly regarding their activity in presence of VGEIs biofilm. More importantly no particular attention was given to antimicrobials ability to penetrate biofilm and to differentiate antimicrobials activity in presence of an established biofilm. Bacterial adherence and biofilm formation on grafts are certainly key steps to understand the onset of VGEIs and infection relapses. Some very interesting studies have been recently

published recently using confocal microscopy to analyse bacterial biofilm formation on different grafts[11]. Confocal microscopy has also allowed the recent assessment that biofilm structures were correlated to antibiotics activity, and that *S. aureus* was able to survive inside macrophages. In the same study, the authors also found that neither daptomycin nor vancomycin were able to penetrate macrophages[47]. These recent findings have allowed a great progress in the understanding of VGEI and have opened up a whole new area for VGEIs research, where VGEIs physiopathology needs to be reinterpreted through the lens of biofilm and immune cells. Indeed, this intracellular bacterial persistence has already been described in BJI. *S. aureus* and *S. epidermidis* can persist in the acidic phagolysomes of osteoblasts and fibroblasts, partly as small-colony variants, and that might contribute to chronic BJI relapses[48]. They further identified antibiotics with intracellular activities which should be preferred in BJI therapy in order to eradicate this lysosomal reservoir of bacteria[48]. In any case, research on biofilm formation, biofilm characteristics and the best antimicrobials active in biofilm is far more advanced in BJI field. However, findings on BJI biofilm cannot be directly extrapolated to VGEIs due to many differences between these two types of infections, including cell environment, blood flow and high shear stress applied on vascular grafts. Even microorganisms are different and polymicrobial infections are more frequent in VGEIs, especially in aortic position.

New technics which allow *in vivo* imaging, such as bioluminescence and fluorescent imaging technologies appear particularly of interest, are mentioned as a research priorities the recently published European consensus (1) and should be promoted. These techniques offer the opportunity to observe the *in vivo* course of biomaterial-associated infections in small animals, without the need to sacrifice animals at different time points after the onset of infection[49], and could be useful for the *in vivo* evaluation of antimicrobial treatments and/or antimicrobial graft coatings effects on bacterial biofilm[49]. To our knowledge, only Lorenz *et al.* studied bioluminescent imaging in VGEIs[40]. This approach has also been evaluated in animal models of BJI[50], and vascular catheters[51]. Other promising non-invasive technics have been evaluated in VGEIs, such as MRI and PET-CT[38], or in vascular catheter infections with FDG-MicroPET[52]. At last, alternative technologies to avoid animal testing, such as *ex vivo* flow models, which have already been experimented on VGEIs field, but also computed simulation will hopefully increase in the coming years[53].

Hopefully this review will support the need for protocol standardization in order to help experimental studies' comparability, but also the importance of selecting accurate techniques to get closer to the truth about vascular biomaterials infectability.

Conclusion

The truth about biomaterials infectability is plural, depending on the time of infection which is intended to be investigated. Many infectability analysis tools are available but should be precociously selected according to the research issue. Moreover, experimental protocols need standardisation to allow studies' results comparison.

Authors participation

MP: literature hand search, articles analysis, manuscript redaction
CC: literature hand search, articles analysis, manuscript proof-reading
SP: manuscript proof-reading
CB: manuscript proof-reading
FM: manuscript proof-reading, english editing
XB: study design, manuscript redaction and proof-reading

References

1. Chakfé N, Diener H, Lejay A, Assadian O, Berard X, Caillon J, *et al.* Editor's Choice - European Society for Vascular Surgery (ESVS) 2020 Clinical Practice Guidelines on the Management of Vascular Graft and Endograft Infections. *Eur J Vasc Endovasc Surg* 2020; 59: 339-84.

2. Malone JM, Moore WS, Campagna G, Bean B. Bacteremic infectability of vascular grafts: the influence of pseudointimal integrity and duration of graft function. *Surgery* 1975; 78: 211-6.

3. Mufty H, Van Den Eynde J, Meuris B, Metsemakers WJ, Van Wijngaerden E, Vandendriessche T, *et al.* Pre-clinical *in vivo* Models of Vascular Graft Coating in the Prevention of Vascular Graft Infection: A Systematic Review. *Eur J Vasc Endovasc Surg* 2021; 62: 99-118.

4. Mufty H, Van den Eynde J, Steenackers HP, Metsemakers W-J, Meuris B, Fourneau I. A systematic review of preclinical data regarding commercial silver-coated vascular grafts. *J Vasc Surg* 2021; 74: 1386-93.

5. Moher D, Shamseer L, Clarke M, Ghersi D, Liberati A, Petticrew M, *et al.* Preferred reporting items for systematic review and meta-analysis protocols (PRISMA-P) 2015 statement. *Syst Rev* 1 2015; 4: 1.

6. Roon AJ, Malone JM, Moore WS, Bean B, Campagna G. Bacteremic infectability: a function of vascular graft material and design. *J Surg Res* 1977; 22: 489-98.

7. Geary KJ, Tomkiewicz ZM, Harrison HN, Fiore WM, Geary JE, Green RM, *et al.* Differential effects of a gram-negative and a gram-positive infection on autogenous and prosthetic grafts. *J Vasc Surg* 1990; 11: 339-45; discussion 346-347.

8. Sakaguchi H, Marui A, Hirose K, Nomura T, Arai Y, Bir SC, *et al.* Less-invasive and highly effective method for preventing methicillin-resistant Staphylococcus aureus graft infection by local sustained release of vancomycin. *J Thorac Cardiovasc Surg* 2008; 135: 25-31.

9. Shah PM, Ito K, Clauss RH, Babu SC, Reynolds BM, Stahl WM. Expanded microporous polytetrafluoroethylene (PTFE) grafts in contaminated wounds: experimental and clinical study. *J Trauma* 1983; 23: 1030-3.

10. Kirkton RD, Prichard HL, Santiago-Maysonet M, Niklason LE, Lawson JH, Dahl SLM. Susceptibility of ePTFE vascular grafts and bioengineered human acellular vessels to infection. *J Surg Res* 2018; 221: 143-51.

11. Revest M, Jacqueline C, Boudjemaa R, Caillon J, Le Mabecque V, Breteche A, *et al.* New *in vitro* and *in vivo* models to evaluate antibiotic efficacy in Staphylococcus aureus prosthetic vascular graft infection. *J Antimicrob Chemother* 2016; 71: 1291-9.

12. Schmitt DD, Bandyk DF, Pequet AJ, Towne JB. Bacterial adherence to vascular prostheses. A determinant of graft infectivity. *J Vasc Surg* 1986; 3: 732-40.

13. Balaban N, Giacometti A, Cirioni O, Gov Y, Ghiselli R, Mocchegiani F, *et al.* Use of the quorum-sensing inhibitor RNAIII-inhibiting peptide to prevent biofilm formation *in vivo* by drug-resistant Staphylococcus epidermidis. *J Infect Dis* 2003; 187: 625-30.

14. Benvenisty AI, Tannenbaum G, Ahlborn TN, Fox CL, Modak S, Sampath L, *et al.* Control of prosthetic bacterial infection: evaluation of an easily incorporated, tightly bound, silver antibiotic PTFE graft. *J Surg Res* 1988 ;44: 1-7.

15. Staneviciute E, Na'amnih W, Kavaliauskas P, Prakapaite R, Ridziauskas M, Kevlicius L, *et al.* New in vitro model evaluating antiseptics' efficacy in biofilm-associated Staphylococcus aureus prosthetic vascular graft infection. *J Med Microbiol* 2019; 68: 432-9.

16. Muhl E, Gatermann S, Iven H, Dendorfer A, Bruch HP. Local application of vancomycin for prophylaxis of graft infection: release of vancomycin from antibiotic-bonded Dacron grafts, toxicity in endothelial cell culture, and efficacy against graft infection in an animal model. *Ann Vasc Surg* 1996; 10: 244-53.

17. Padberg FT, Smith SM, Eng RH. Optimal method for culturing vascular prosthetic grafts. *J Surg Res* 1992; 53: 384-90.

18. Javerliat I, Goëau-Brissonnière O, Sivadon-Tardy V, Coggia M, Gaillard J-L. Prevention of Staphylococcus aureus graft infection by a new gelatin-sealed vascular graft prebonded with antibiotics. *J Vasc Surg* 2007; 46: 1026-31.

19. Coggia M, Goëau-Brissonnière O, Leflon V, Nicolas MH, Pechère JC. Experimental treatment of vascular graft infection due to Staphylococcus epidermidis by *in situ* replacement with a rifampin-bonded polyester graft. *Ann Vasc Surg* 2001; 15: 421-9.

20. Bergamini TM, Bandyk DF, Govostis D, Vetsch R, Towne JB. Identification of Staphylococcus epidermidis vascular graft infections: a comparison of culture techniques. *J Vasc Surg* 1989; 9: 665-70.

21. Henke PK, Bergamini TM, Watson AL, Brittian KR, Powell DW, Peyton JC. Bacterial products primarily mediate fibroblast inhibition in biomaterial infection. *J Surg Res* 1998; 74: 17-22.

22. Lachapelle K, Graham AM, Symes JF. Antibacterial activity, antibiotic retention, and infection resistance of a rifampin-impregnated gelatin-sealed Dacron graft. *J Vasc Surg* 1994; 19: 675-82.

23. Fletcher JP, Dryden M, Munro R, Xu JH, Hehir MD. Establishment of a vascular graft infection model in the sheep carotid artery. *Aust N Z J Surg* 1990; 60: 801-3.

24. Richardson RL, Pate JW, Wolf RY, Ledes C, Hopson WB. The outcome of antibiotic-soaked arterial grafts in guinea pig wounds contaminated with E. coli or S. aureus. *J Thorac Cardiovasc Surg* 1970; 59: 635-7.

25. Wengrovitz M, Spangler S, Martin LF. Sonication provides maximal recovery of staphylococcus epidermidis from slime-coated vascular prosthetics. *Am Surg* 1991; 57: 161-4.

26. Tollefson DF, Bandyk DF, Kaebnick HW, Seabrook GR, Towne JB. Surface biofilm disruption. Enhanced recovery of microorganisms from vascular prostheses. *Arch Surg* 1987; 122: 38-43.

27. Berard X, Puges M, Pinaquy J-B, Cazanave C, Stecken L, Bordenave L, *et al.* In vitro Evidence of Improved Antimicrobial Efficacy of Silver and Triclosan Containing Vascular Grafts Compared with Rifampicin Soaked Grafts. *Eur J Vasc Endovasc Surg* 2019; 57: 424-32.

28. Giacometti A, Cirioni O, Ghiselli R, Goffi L, Mocchegiani F, Riva A, *et al.* Efficacy of polycationic peptides in preventing vascular graft infection due to Staphylococcus epidermidis. *J Antimicrob Chemother* 2000; 46: 751-6.

29. Rosenman JE, Pearce WH, Kempczinski RF. Bacterial adherence to vascular grafts after in vitro bacteremia. *J Surg Res.* 1985;38(6):648-55.

30. Zdanowski Z, Ribbe E, Schalén C. Influence of some plasma proteins on in vitro bacterial adherence to PTFE and Dacron vascular prostheses. *APMIS* 1993; 101: 926-32.

31. Malangoni MA, Livingston DH, Peyton JC. The effect of protein binding on the adherence of staphylococci to prosthetic vascular grafts. *J Surg Res* 1993; 54: 168-72.

32. Keeling WB, Myers AR, Stone PA, Heller L, Widen R, Back MR, *et al.* Regional antibiotic delivery for the treatment of experimental prosthetic graft infections. *J Surg Res* 2009; 157: 223-6.

33. Stepanović S, Vuković D, Dakić I, Savić B, Švabić-Vlahović M. A modified microtiter-plate test for quantification of staphylococcal biofilm formation. *J Microbiol Methods* 2000; 40: 175-9.

34. Herten M, Bisdas T, Knaack D, Becker K, Osada N, Torsello GB, *et al.* Rapid in Vitro Quantification of S. aureus Biofilms on Vascular Graft Surfaces. *Front Microbiol* 2017; 8: 2333.

35. Schmitt DD, Bandyk DF, Pequet AJ, Malangoni MA, Towne JB. Mucin production by Staphylococcus epidermidis. A virulence factor promoting adherence to vascular grafts. *Arch Surg* 1986; 121: 89-95.

36. Chakfe N, Guidoin R, Marois M, Roy PE, Douville Y, Roy P, *et al.* A pathological study of arterial prostheses surgically excised after overt clinical infection. *J Biomater Appl* 1991; 5: 227-46.

37. Webb LX, Myers RT, Cordell AR, Hobgood CD, Costerton JW, Gristina AG. Inhibition of bacterial adhesion by antibacterial surface pretreatment of vascular prostheses. *J Vasc Surg* 1986; 4: 16-21.

38. Van de Vyver H, Bovenkamp PR, Hoerr V, Schwegmann K, Tuchscherr L, Niemann S, *et al.* A Novel Mouse Model of Staphylococcus aureus Vascular Graft Infection: Noninvasive Imaging of Biofilm Development *in Vivo*. *Am J Pathol* 2017; 187: 268-79.

39. Osada T, Yamamura K, Fujimoto K, Mizuno K, Sakurai T, Ohta M, *et al.* Prophylaxis of local vascular graft infection with levofloxacin incorporated into albumin-sealed dacron graft (LVFX-ALB Graft). *Microbiol Immunol* 1999; 43: 317-21.

40. Lorenz U, Schäfer T, Ohlsen K, Tiurbe GC, Bühler C, Germer C-T, *et al. In vivo* detection of Staphylococcus aureus in biofilm on vascular prostheses using non-invasive biophotonic imaging. *Eur J Vasc Endovasc Surg* 2011; 41: 68-75.

41. Peter AO, Spangler S, Martin LF. Evaluation of three techniques for documenting Staphylococcus epidermidis vascular prosthetic graft infections. *Am Surg* 1991; 57: 80-5.

42. White JV, Benvenisty AI, Reemtsma K, Voorhees AB, Fox CL, Modak S, *et al.* Simple methods for direct antibiotic protection of synthetic vascular grafts. *J Vasc Surg* 1984; 1: 372-80.

43. Dries D, Alazraki N, Lawrence P, Murphy K, Kercher J, Datz F, *et al.* Detection of acute synthetic vascular graft infection with 111In-labeled leukocyte scanning: an animal study. *AJR Am J Roentgenol* 1985; 145: 1053-6.

44. Tautenhahn J, Meyer F, Buerger T, Schmidt U, Lippert H, Koenig W, *et al.* Interactions of neutrophils with silver-coated vascular polyester grafts. Langenbecks *Arch Surg* 2010; 395: 143-9.

45. Trampuz A, Piper KE, Jacobson MJ, Hanssen AD, Unni KK, Osmon DR, *et al.* Sonication of removed hip and knee prostheses for diagnosis of infection. *N Engl J Med* 2007; 357: 654-63.

46. Puges M, Pereyre S, Bérard X, Accoceberry I, Le Roy C, Stecken L, *et al.* Comparison of Genus Specific PCR and Culture with or without Sonication for Microbiological Diagnosis of Vascular Graft Infection. *Eur J Vasc Endovasc Surg* 2018; 56: 562-71.

47. Boudjemaa R, Steenkeste K, Jacqueline C, Briandet R, Caillon J, Boutoille D, *et al.* Live intramacrophagic Staphylococcus aureus as a potential cause of antibiotic therapy failure: observations in an *in vivo* mouse model of prosthetic vascular material infections. *J Antimicrob Chemother* 2018; 73: 2418-21.

48. Valour F, Trouillet-Assant S, Riffard N, Tasse J, Flammier S, Rasigade J-P, *et al.* Antimicrobial Activity against Intraosteoblastic Staphylococcus aureus. *Antimicrob Agents Chemother* 2015; 59: 2029-36.

49. Sjollema J, Sharma PK, Dijkstra RJB, van Dam GM, van der Mei HC, Engelsman AF, *et al.* The potential for bio-optical imaging of biomaterial-associated infection *in vivo*. *Biomaterials* 2010; 31: 1984-95.

50. Li D, Gromov K, Søballe K, Puzas JE, O'Keefe RJ, Awad H, *et al.* Quantitative mouse model of implant-associated osteomyelitis and the kinetics of microbial growth, osteolysis, and humoral immunity. *J Orthop Res* 2008; 26: 96-105.

51. Chauhan A, Lebeaux D, Ghigo J-M, Beloin C. Full and Broad-Spectrum *In Vivo* Eradication of Catheter-Associated Biofilms Using Gentamicin-EDTA Antibiotic Lock Therapy. *Antimicrob Agents Chemother* 2012; 56: 6310-8.

52. Garrido V, Collantes M, Barberán M, Peñuelas I, Arbizu J, Amorena B, *et al. In Vivo* Monitoring of Staphylococcus aureus Biofilm Infections and Antimicrobial Therapy by [18 F]Fluoro-Deoxyglucose–MicroPET in a Mouse Model. *Antimicrob Agents Chemother* 2014; 58: 6660-7.

53. Coscas R, Senemaud J. Experimenters or Amateurs? *Eur J Vasc Endovasc Surg* 2020; 60: 253.

Supplemental Table 1 / References

1. Tammer I, Reuner J, Hartig R, Geginat G. Induction of Candida albicans biofilm formation on silver-coated vascular grafts. *J Antimicrob Chemother* 2014;69(5):1282-5.

2. Garrison JR, Henke PK, Smith KR, Brittian KR, Lam TM, Peyton JC, *et al.* In vitro and in vivo effects of rifampin on Staphylococcus epidermidis graft infections. *ASAIO J* 1997;43(1):8-12.

3. Farooq M, Freischlag J, Kelly H, Seabrook G, Cambria R, Towne J. Gelatin-sealed polyester resists Staphylococcus epidermidis biofilm infection. *J Surg Res* 1999;87(1):57-61.

4. Herten M, Bisdas T, Knaack D, Becker K, Osada N, Torsello GB, *et al.* Rapid in Vitro Quantification of S. aureus Biofilms on Vascular Graft Surfaces. *Front Microbiol* 2017;8:2333.

5. Woźniak W, Kozińska A, Ciostek P, Sitkiewicz I. Susceptibility of Vascular Implants to Colonization in vitro by Staphylococcus aureus, Staphylococcus epidermidis, Enterococcus faecalis and Pseudomonas aeruginosa. *Pol J Microbiol* 2017;66(1):125-9.

6. Bisdas T, Beckmann E, Marsch G, Burgwitz K, Wilhelmi M, Kuehn C, *et al.* Prevention of vascular graft infections with antibiotic graft impregnation prior to implantation: in vitro comparison between daptomycin, rifampin and nebacetin. *Eur J Vasc Endovasc Surg* 2012;43(4):448-56.

7. Idelevich EA, Knaack D, Nugroho NT, Peters G, Bisdas T, Molinaro S, *et al.* Comparative in vitro activity of bacteriophage endolysin HY-133 against Staphylococcus aureus attached to vascular graft surface. *Med Microbiol Immunol* 2020;209(1):51-7.

8. Malangoni MA, Livingston DH, Peyton JC. The effect of protein binding on the adherence of staphylococci to prosthetic vascular grafts. *J Surg Res* 1993;54(2):168-72.

9. Schmitt DD, Bandyk DF, Pequet AJ, Towne JB. Bacterial adherence to vascular prostheses. A determinant of graft infectivity. *J Vasc Surg* 1986;3(5):732-40.

10. Phaneuf MD, Ozaki CK, Bide MJ, Quist WC, Alessi JM, Tannenbaum GA, *et al.* Application of the quinolone antibiotic ciprofloxacin to Dacron utilizing textile dyeing technology. *J Biomed Mater Res* 1993;27(2):233-7.

11. Berard X, Stecken L, Pinaquy J-B, Cazanave C, Puges M, Pereyre S, *et al.* Comparison of the Antimicrobial Properties of Silver Impregnated Vascular Grafts with and without Triclosan. *Eur J Vasc Endovasc Surg* 2016;51(2):285-92.

12. Berard X, Puges M, Pinaquy J-B, Cazanave C, Stecken L, Bordenave L, *et al.* In vitro Evidence of Improved Antimicrobial Efficacy of Silver and Triclosan Containing Vascular Grafts Compared with Rifampicin Soaked Grafts. *Eur J Vasc Endovasc Surg* 2019;57(3):424-32.

13. Schmitt DD, Bandyk DF, Pequet AJ, Malangoni MA, Towne JB. Mucin production by Staphylococcus epidermidis. A virulence factor promoting adherence to vascular grafts. *Arch Surg* 1986;121(1):89-95.

14. Edmiston CE, Goheen MP, Seabrook GR, Johnson CP, Lewis BD, Brown KR, *et al.* Impact of selective antimicrobial agents on staphylococcal adherence to biomedical devices. *Am J Surg* 2006;192(3):344-54.

15. Steffen V, Marsch G, Burgwitz K, Kuehn C, Teebken OE. Resistance to infection of long-term cryopreserved human aortic valve allografts. *J Thorac Cardiovasc Surg* 2016;151(5):1251-9.

16. Camiade C, Goldschmidt P, Koskas F, Ricco JB, Jarraya M, Gerota J, *et al.* Optimization of the resistance of arterial allografts to infection: comparative study with synthetic prostheses. *Ann Vasc Surg* 2001;15(2):186-96.

17. Kuehn C, Graf K, Mashaqi B, Pichlmaier M, Heuer W, Hilfiker A, *et al.* Prevention of early vascular graft infection using regional antibiotic release. *J Surg Res* 2010;164(1):e185-191.

18. Heafner TA, Lewis C, Baluh G, Clemens M, Propper B, Arthurs ZM. Initial Inoculation Concentration Does Not Affect Final Bacterial Colonization of In vitro Vascular Conduits. *Surg Infect (Larchmt)* 2018;19(3):352-7.

19. Siverhus DJ, Schmitt DD, Edmiston CE, Bandyk DF, Seabrook GR, Goheen MP, *et al.* Adherence of mucin and non-mucin-producing staphylococci to preclotted and albumin-coated velour knitted vascular grafts. *Surgery* 1990;107(6):613-9.

20. Padberg FT, Smith SM, Eng RH. Optimal method for culturing vascular prosthetic grafts. *J Surg Res*1992;53(4):384-90.

21. Ditkowski B, Veloso TR, Bezulska-Ditkowska M, Lubig A, Jockenhoevel S, Mela P, *et al.* An In Vitro Model of a Parallel-Plate Perfusion System to Study Bacterial Adherence to Graft Tissues. *J Vis Exp* 2019;(143).

22. Darouiche RO, Mansouri MD. In vitro activity and in vivo efficacy of antimicrobial-coated vascular grafts. *Ann Vasc Surg* 2004;18(4):497-501.

23. Shimabukuro K, Hirose H, Mori Y, Takagi H, Iwata H, Kawamura Y. Local treatment of Dacron patch graft infected with biofilm-producing Staphylococcus epidermidis using antibiotic-releasing porous apatite ceramic: an experimental study in the rabbit. *J Vasc Surg* 2004;39(6):1361.

24. Ozaki CK, Phaneuf MD, Bide MJ, Quist WC, Alessi JM, LoGerfo FW. In vivo testing of an infection-resistant vascular graft material. *J Surg Res* 1993;55(5):543-7.

25. Lozano FS, Cascajo C, García-Sánchez E, Barros MB, García-Criado FJ, Parreño F, *et al.* Bacterial translocation as a source of Dacron-graft contamination in experimental aortic operation: the importance of controlling SIRS. *Surgery* 2006;140(1):83-92.

26. Fischer PE, Schroeppel TJ, Fabian TC, deRijk WG, Edwards NM, Magnotti LJ, *et al.* Antibiotic-coated ePTFE decreases graft colonization and neointimal hyperplasia. *J Surg Res* 2009;156(2):199-204.

27. Shell DH, Croce MA, Cagiannos C, Jernigan TW, Edwards N, Fabian TC. Comparison of small-intestinal submucosa and expanded polytetrafluoroethylene as a vascular conduit in the presence of gram-positive contamination. *Ann Surg* 2005;241(6):995-1001; discussion 1001-1004.

28. Sacar M, Onem G, Baltalarli A, Sacar S, Turgut H, Goksin I, *et al.* Neuraminidase produces a decrease of adherence of slime-forming Staphylococcus aureus to gelatin-impregnated polyester fiber graft fabric: an experimental study. *J Artif Organs* 2007;10(3):177-80.

29. Evers BM, Giammara BL, Jubenville D, Malangoni MA. Glycocalyx Enhances Prosthetic Vascular Graft Infection. MRS Online Proceedings Library Archive. ed 1987;110. Avaialable on: https://www.cambridge.org/core/journals/mrs-online-proceedings-library-archive/article/glycocalyx-enhances-prosthetic-vascular-graft-infection/A8020845B941240E4929D805FD9338B7

30. Dell'Acqua G, Giacometti A, Cirioni O, Ghiselli R, Saba V, Scalise G, *et al.* Suppression of drug-resistant Staphylococcal Infections by the quorum-sensing inhibitor RNAIII-inhibiting peptide. *J Infect Dis* 2004;190(2):318-20.

31. Yasim A, Gul M, Atahan E, Ciragil P, Aral M, Ergun Y. Efficacy of vancomycin, teicoplanin and fusidic acid as prophylactic agents in prevention of vascular graft infection: an experimental study in rat. *Eur J Vasc Endovasc Surg* 2006;31(3):274-9.

32. Mese B, Bozoglan O, Elveren S, Eroglu E, Gul M, Celik A, *et al.* Efficacy of linezolid, teicoplanin, and vancomycin in prevention of an experimental polytetrafluoroethylene graft infection model caused by methicillin-resistant Staphylococcus aureus. *Med Sci Monit* 2015;21:909-14.

33. Cirioni O, Giacometti A, Ghiselli R, Kamysz W, Silvestri C, Orlando F, *et al.* The lipopeptides Pal-Lys-Lys-NH(2) and Pal-Lys-Lys soaking alone and in combination with intraperitoneal vancomycin prevent vascular graft biofilm in a subcutaneous rat pouch model of staphylococcal infection. *Peptides* 2007;28(6):1299-303.

34. Giacometti A, Ghiselli R, Cirioni O, Mocchegiani F, Orlando F, Del Prete MS, *et al.* Prophylactic efficacy of linezolid alone or combined with levofloxacin and vancomycin in a rat subcutaneous pouch model of graft infection caused by Staphylococcus epidermidis with intermediate resistance to glycopeptides. *J Antimicrob Chemother* 2003;52(4):724-6.

35. Cirioni O, Giacometti A, Ghiselli R, Dell'Acqua G, Gov Y, Kamysz W, *et al.* Prophylactic efficacy of topical temporin A and RNAIII-inhibiting peptide in a subcutaneous rat Pouch model of graft infection attributable to staphylococci with intermediate resistance to glycopeptides. *Circulation* 2003;108(6):767-71.

36. Ghiselli R, Giacometti A, Cirioni O, Mocchegiani F, Orlando F, Kamysz W, *et al.* Temporin A as a prophylactic agent against methicillin sodium-susceptible and methicillin sodium-resistant Staphylococcus epidermidis vascular graft infection. *J Vasc Surg* 2002;36(5):1027-30.

37. Cirioni O, Mocchegiani F, Ghiselli R, Silvestri C, Gabrielli E, Marchionni E, *et al.* Daptomycin and rifampin alone and in combination prevent vascular graft biofilm formation and emergence of antibiotic resistance in a subcutaneous rat pouch model of staphylococcal infection. *Eur J Vasc Endovasc Surg* 2010;40(6):817-22.

38. Giacometti A, Cirioni O, Ghiselli R, Goffi L, Mocchegiani F, Riva A, *et al.* Polycationic peptides as prophylactic agents against methicillin-susceptible or methicillin-resistant Staphylococcus epidermidis vascular graft infection. *Antimicrob Agents Chemother* 2000;44(12):3306-9.

39. Ghiselli R, Giacometti A, Goffi L, Cirioni O, Boccoli G, Mocchegiani F, *et al.* Efficacy of rifampin-levofloxacin as a prophylactic agent in preventing Staphylococcus epidermidis graft infection. *Eur J Vasc Endovasc Surg* 2000;20(6):508-11.

40. Bergamini TM, Peyton JC, Cheadle WG. Prophylactic antibiotics prevent bacterial biofilm graft infection. *J Surg Res* 1992; 52(2):101-5.

41. Arya R, Ravikumar R, Santhosh RS, Princy SA. SarA based novel therapeutic candidate against Staphylococcus aureus associated with vascular graft infections. *Front Microbiol* 2015;6:416.

42. Atahan E, Gul M, Ergun Y, Eroglu E. Vascular graft infection by Staphylococcus aureus: efficacy of cefazolin, teicoplanin and vancomycin prophylaxis protocols in a rat model. *Eur J Vasc Endovasc Surg* 2007;34(2):182-7.

43. Fujimoto K, Yamamura K, Osada T, Hayashi T, Nabeshima T, Matsushita M, *et al.* Subcutaneous tissue distribution of vancomycin from a fibrin glue/Dacron graft carrier. *J Biomed Mater Res* 1997;36(4):564-7.

44. Fujimoto K, Yamamura K, Hayashi T, Osada T, Sakurai T. Effect of levofloxacin-albumin Dacron graft on graft infection. *Jpn J Pharmacol* 1995;69(4):443-5.

45. Yamamura K, Sakurai T, Yano K, Osada T, Nabeshima T. Prevention of vascular graft infection by sisomicin incorporated into fibrin glue. *Microbiol Immunol* 1995;39(11):895-6.

46. Kirkton RD, Prichard HL, Santiago-Maysonet M, Niklason LE, Lawson JH, Dahl SLM. Susceptibility of ePTFE vascular grafts and bioengineered human acellular vessels to infection. *J Surg Res* 2018;221:143-51.

47. Ozturk B, Kurtoglu T, Durmaz S, Kozaci LD, Abacigil F, Ertugrul B, *et al.* The effects of ozone on bacterial growth and thiol-disulphide homeostasis in vascular graft infection caused by MRSA in rats. *Acta Cir Bras* 2017;32(3):219-28.

48. Morishima M, Marui A, Yanagi S, Nomura T, Nakajima N, Hyon S-H, *et al.* Sustained release of vancomycin from a new biodegradable glue to prevent methicillin-resistant Staphylococcus aureus graft infection. *Interact Cardiovasc Thorac Surg* 2010;11(1):52-5.

49. Sato S, Nitta Y, Saiki Y, Kawamoto S, Iguchi A, Kaku M, *et al.* Enhanced perigraft angiogenesis prevents prosthetic graft infection. *Ann Thorac Surg* 2008;86(4):1278-84.

50. Ghiselli R, Giacometti A, Goffi L, Cirioni O, Mocchegiani F, Orlando F, *et al.* Prophylaxis against Staphylococcus aureus vascular graft infection with mupirocin-soaked, collagen-sealed dacron. *J Surg Res* 2001;99(2):316-20.

51. Bozoglan O, Mese B, Eroglu E, Elveren S, Gul M, Celik A, *et al.* Which prosthesis is more resistant to vascular graft infection: polytetrafluoroethylene or Omniflow II biosynthetic grafts? *Surg Today* 2016;46(3):363-70.

52. Ghiselli R, Giacometti A, Cirioni O, Dell'Acqua G, Mocchegiani F, Orlando F, *et al.* RNAIII-inhibiting peptide and/or nisin inhibit experimental vascular graft infection with methicillin-susceptible and methicillin-resistant Staphylococcus epidermidis. *Eur J Vasc Endovasc Surg* 2004;27(6):603-7.

53. Giacometti A, Cirioni O, Ghiselli R, Goffi L, Mocchegiani F, Riva A, *et al.* Efficacy of polycationic peptides in preventing vascular graft infection due to Staphylococcus epidermidis. *J Antimicrob Chemother* 2000;46(5):751-6.

54. Cirioni O, Mocchegiani F, Cacciatore I, Vecchiet J, Silvestri C, Baldassarre L, *et al.* Quorum sensing inhibitor FS3-coated vascular graft enhances daptomycin efficacy in a rat model of staphylococcal infection. *Peptides* 2013;40:77-81.

55. Simonetti O, Cirioni O, Mocchegiani F, Cacciatore I, Silvestri C, Baldassarre L, *et al.* The efficacy of the quorum sensing inhibitor FS8 and tigecycline in preventing prosthesis biofilm in an animal model of staphylococcal infection. *Int J Mol Sci* 2013;14(8):16321-32.

56. Ghiselli R, Giacometti A, Cirioni O, Mocchegiani F, Orlando F, Del Prete M, *et al.* Quinupristin/dalfopristin bonding in combination with intraperitoneal antibiotics prevent infection of knitted polyester graft material in a subcutaneous rat pouch model infected with resistant Staphylococcus epidermidis. *Eur J Vasc Endovasc Surg* 2002;24(3):230-4.

57. Turgut H, Sacar S, Kaleli I, Sacar M, Goksin I, Toprak S, *et al.* Systemic and local antibiotic prophylaxis in the prevention of Staphylococcus epidermidis graft infection. *BMC Infect Dis* 2005;5:91.

58. Revest M, Jacqueline C, Boudjemaa R, Caillon J, Le Mabecque V, Breteche A, *et al.* New in vitro and in vivo models to evaluate antibiotic efficacy in Staphylococcus aureus prosthetic vascular graft infection. *J Antimicrob Chemother* 2016;71(5):1291-9.

59. Jean-Baptiste E, Blanchemain N, Neut C, Chai F, Maton M, Martel B, *et al.* Evaluation of the anti-infectious properties of polyester vascular prostheses functionalised with cyclodextrin. *J Infect* 2014;68(2):116-24.

60. Henke PK, Bergamini TM, Watson AL, Brittian KR, Powell DW, Peyton JC. Bacterial products primarily mediate fibroblast inhibition in biomaterial infection. *J Surg Res* 1998;74(1):17-22.

61. Mora EM, Cardona MA, Simmons RL. Enteric bacteria and ingested inert particles translocate to intraperitoneal prosthetic materials. *Arch Surg* 1991;126(2):157-63.

62. Lorenz U, Schäfer T, Ohlsen K, Tiurbe GC, Bühler C, Germer C-T, *et al.* In vivo detection of Staphylococcus aureus in biofilm on vascular prostheses using non-invasive biophotonic imaging. *Eur J Vasc Endovasc Surg* 2011;41(1):68-75.

63. Gahtan V, Esses GE, Bandyk DF, Nelson RT, Dupont E, Mills JL. Antistaphylococcal activity of rifampin-bonded gelatin-impregnated Dacron grafts. *J Surg Res* 1995;58(1):105-10.

64. Bandyk DF, Kinney EV, Riefsnyder TI, Kelly H, Towne JB. Treatment of bacteria-biofilm graft infection by in situ replacement in normal and immune-deficient states. *J Vasc Surg* 1993;18(3):398-405; discussion 405-406.

65. Bergamini TM, Bandyk DF, Govostis D, Vetsch R, Towne JB. Identification of Staphylococcus epidermidis vascular graft infections: a comparison of culture techniques. *J Vasc Surg* 1989;9(5):665-70.

66. Vetsch R, Bandyk DF, Schmitt DD, Bergamini TM, Storey JD, Towne JB. Anastomotic tensile strength following in situ replacement of an infected abdominal aortic graft. *Arch Surg* 1989;124(4):425-8.

67. Tollefson DF, Bandyk DF, Kaebnick HW, Seabrook GR, Towne JB. Surface biofilm disruption. Enhanced recovery of microorganisms from vascular prostheses. *Arch Surg* 1987;122(1):38-43.

68. Coggia M, Goëau-Brissonnière O, Leflon V, Nicolas MH, Pechère JC. Experimental treatment of vascular graft infection due to Staphylococcus epidermidis by in situ replacement with a rifampin-bonded polyester graft. *Ann Vasc Surg* 2001;15(4):421-9.

69. Schmacht D, Armstrong P, Johnson B, Pierre K, Back M, Honeyman A, *et al.* Graft infectivity of rifampin and silver-bonded polyester grafts to MRSA contamination. *Vasc Endovascular Surg* 2005;39(5):411-20.

70. Schneider F, O'Connor S, Becquemin JP. Efficacy of collagen silver-coated polyester and rifampin-soaked vascular grafts to resist infection from MRSA and Escherichia coli in a dog model. *Ann Vasc Surg* 2008;22(6):815-21.

71. Bergamini TM, Bandyk DF, Govostis D, Kaebnick HW, Towne JB. Infection of vascular prostheses caused by bacterial biofilms. *J Vasc Surg* 1988;7(1):21-30.

72. Giacometti A, Cirioni O, Ghiselli R, Orlando F, D'Amato G, Kamysz W, *et al.* Temporin A soaking in combination with intraperitoneal linezolid prevents vascular graft infection in a subcutaneous rat pouch model of infection with Staphylococcus epidermidis with intermediate resistance to glycopeptides. *Antimicrob Agents Chemother* 2004;48(8):3162-4.

73. Atahan E, Katrancioglu N, Oztop Y, Tuncer E, Ozer H, Manduz S, *et al.* Vascular graft infection by Staphylococcus aureus: efficacy of linezolid, teicoplanin and vancomycin systemic prophylaxis protocols in a rat model. *Cardiovasc J Afr* 2009;20(2):122-5.

74. Yolgosteren A, Kumtepe G, Payaslioglu M, Ozakin C. In-vivo evaluation of the effect of cyanoacrylate on prosthetic vascular graft infection-does cyanoacrylate increase the severity of infection? *Vasa* 2020;49(4):281-4.

75. Salmoukas C, Ruemke S, Rubalskii E, Burgwitz K, Haverich A, Kuehn C. Vascular Graft Pre-Treatment with Daptomycin Prior to Implantation Prevents Graft Infection with Staphylococcus aureus in an In Vivo Model. *Surg Infect (Larchmt)* 2020;21(2):161-8.

76. Doan VN, Truong TT, Tran HLB. Development of local vancomycin delivery system from fibrin gel to prevent Staphylococcus aureus biofilms graft infection. *J Biosci* 2020;45:124.

77. Nurkay Katrancioglu. Is sustained release of vancomycin from fibrin glue effective to prevent methicillin-resistant Staphylococcus aureus graft infection? Afr J Microbiol Res. 30 janv 2012;6(4). Available on http://www.academicjournals.org/AJMR/abstracts/abstracts/abstract%202012 /30Jan/Katrancioglu%20et%20al.htm

78. Schweizer TA, Shambat SM, Haunreiter VD, Mestres CA, Weber A, Maisano F, *et al.* Polyester Vascular Graft Material and Risk for Intracavitary Thoracic Vascular Graft Infection1. *Emerg Infect Dis* 2020;26(10):2448-52.

79. Obermeier A, Matl FD, Schwabe J, Zimmermann A, Kühn KD, Lakemeier S, *et al.* Novel fatty acid gentamicin salts as slow-release drug carrier systems for anti-infective protection of vascular biomaterials. *J Mater Sci: Mater Med* 2012;23(7):1675-83.

80. Sacar M, Goksin I, Baltalarli A, Turgut H, Sacar S, Onem G, *et al.* The Prophylactic Efficacy of Rifampicin-Soaked Graft in Combination with Systemic Vancomycin in the Prevention of Prosthetic Vascular Graft Infection: An Experimental Study. *J Surg Res* 2005;129(2):329-34.

81. Giacometti A, Cirioni O, Ghiselli R, Goffi L, Viticchi C, Mocchegiani F, *et al.* Mupirocin prophylaxis against methicillin-susceptible, methicillin-resistant, or vancomycin-intermediate Staphylococcus epidermidis vascular-graft infection. *Antimicrob Agents Chemother* 2000;44(10):2842-4.

82. Wengrovitz M, Spangler S, Martin LF. Sonication provides maximal recovery of staphylococcus epidermidis from slime-coated vascular prosthetics. *Am Surg* 1991;57(3):161-4.

83. Balaban N, Cirioni O, Giacometti A, Ghiselli R, Braunstein JB, Silvestri C, *et al.* Treatment of Staphylococcus aureus Biofilm Infection by the Quorum-Sensing Inhibitor RIP. *Antimicrob Agents Chemother* 2007;51(6):2226-9.

84. Domenico P, Gurzenda E, Giacometti A, Cirioni O, Ghiselli R, Orlando F, *et al.* BisEDT and RIP act in synergy to prevent graft infections by resistant staphylococci. *Peptides* 2004;25(12):2047-53.

85. Clark RE, Margraf HW. Antibacterial vascular grafts with improved thromboresistance. *Arch Surg* 1974;109(2):159-62.

86. Hardman S, Cope A, Swann A, Bell PRF, Naylor AR, Hayes PD. An in vitro model to compare the antimicrobial activity of silver-coated versus rifampicin-soaked vascular grafts. *Ann Vasc Surg* 2004;18(3):308-13.

87. Ueberrueck T, Zippel R, Tautenhahn J, Gastinger I, Lippert H, Wahlers T. Vascular graft infections: in vitro and in vivo investigations of a new vascular graft with long-term protection. *J Biomed Mater Res Part B Appl Biomater* 2005;74(1):601-7.

88. Demirag MK, Esen S, Zivalioglu M, Leblebicioglu H, Keceligil HT. The effect of aspirin on adherence of slime-producing, coagulase-negative staphylococci to vascular grafts. *Ann Vasc Surg* 2007;21(4):464-7.

89. Fujita M, Kinoshita M, Ishihara M, Kanatani Y, Morimoto Y, Simizu M, *et al.* Inhibition of vascular prosthetic graft infection using a photocrosslinkable chitosan hydrogel. *J Surg Res* 2004;121(1):135-40.

90. Staneviciute E, Na'amnih W, Kavaliauskas P, Prakapaite R, Ridziauskas M, Kevlicius L, *et al.* New in vitro model evaluating antiseptics' efficacy in biofilm-associated Staphylococcus aureus prosthetic vascular graft infection. *J Med Microbiol* 2019;68(3):432-9.

91. Goëau-Brissonnière O, Péchère JC, Guidoin R, Noël HP. [Experimental staphylococcal colonization of a Dacron arterial prosthesis (author's transl)]. *J Chir (Paris)* 1980;117(6-7):397-401.

92. Goëau-Brissonière O, Pechère JC, Guidoin R, Noël HP, Couture J. Experimental colonization of vascular grafts with Staphylococcus aureus. *Can J Surg* 1983;26(6):540-5.

93. Sardelic F, Ao PY, Taylor DA, Fletcher JP. Prophylaxis against Staphylococcus epidermidis vascular graft infection with rifampicin-soaked, gelatin-sealed Dacron. *Cardiovasc Surg* 1996;4(3):389-92.

94. Sardelic F, Peng YA, Fletcher JP. Development of a Staphylococcus epidermidis vascular graft infection model in sheep. *Aust N Z J Surg* 1995;65(7):503-6.

95. Sardelic F, Ao PY, Fletcher JP. Rifampicin impregnated Dacron grafts: no development of rifampicin resistance in an animal model. *Eur J Vasc Endovasc Surg* 1995;9(3):314-8.

96. Fletcher JP, Dryden M, Munro R, Xu JH, Hehir MD. Establishment of a vascular graft infection model in the sheep carotid artery. *Aust N Z J Surg* 1990;60(10):801-3.

97. Vicaretti M, Hawthorne WJ, Ao PY, Fletcher JP. An increased concentration of rifampicin bonded to gelatin-sealed Dacron reduces the incidence of subsequent graft infections following a staphylococcal challenge. *Cardiovasc Surg* 1998;6(3):268-73.

98. D'Addato M, Curti T, Freyrie A, Agus GB, Bertini D, Biasi G. Prevention of early graft infection with rifampicin-bonded Gelseal grafts: a multicentre experimental study. *Cardiovasc Surg* 1994;2(2):254-8.

99. Avramovic JR, Fletcher JP. Rifampicin impregnation of a protein-sealed Dacron graft: an infection-resistant prosthetic vascular graft. *Aust N Z J Surg* 1991;61(6):436-40.

100. Avramovic J, Fletcher JP. Prevention of prosthetic vascular graft infection by rifampicin impregnation of a protein-sealed Dacron graft in combination with parenteral cephalosporin. *J Cardiovasc Surg (Torino)* 1992;33(1):70-4.

101. Vicaretti M, Hawthorne W, Ao PY, Fletcher JP. Does in situ replacement of a staphylococcal infected vascular graft with a rifampicin impregnated gelatin sealed Dacron graft reduce the incidence of subsequent infection? International Angiology: A Journal of the International Union of Angiology. 1999;18(3):225-32.

102. Okahara K, Kambayashi J, Shibuya T, Kawasaki T, Sakon M, Dohi Y, *et al.* An infection-resistant PTFE vascular graft; spiral coiling of the graft with ofloxacin-bonded PTFE thread. *Eur J Vasc Endovasc Surg* 1995;9(4):408-14.

103. Huh J, Chen JC, Furman GM, Malki C, King B, Kafie F, *et al.* Local treatment of prosthetic vascular graft infection with multivesicular liposome-encapsulated amikacin. *J Surg Res* 1998;74(1):54-8.

104. Chen JC, Wilson SE. Rabbit model for the study of aortic graft infection. *J Invest Surg* 1997;10(5):305-9.

105. Murase K, Hirose H, Mori Y, Takagi H, Iwata H, Sago T, *et al.* Graft-preserving treatment for vascular graft infected with Staphylococcus aureus with antibiotic-releasing porous apatite ceramic in the rabbit. *J Vasc Surg* 2003;38(2):368-73.

106. Simon TE, Johnson RJ, Naig AL, Brockmeyer JR, Prasad BM, White PW. Permacol interposition graft as an alternative to vein in contaminated wounds using a rabbit model. *Ann Vasc Surg* 2015;29(6):1307-14.

107. Buckels JA, Nordestgaard AG, Wilson SE. Microporous vascular grafts do not require neointima for resistance to bacteremic infection. *J Vasc Surg* 1987;5(1):198-202.

108. Sago T, Mori Y, Takagi H, Iwata H, Murase K, Kawamura Y, *et al.* Local treatment of Dacron patch graft contaminated with Staphylococcus aureus with antibiotic-releasing porous apatite ceramic: an experimental study in the rabbit. *J Vasc Surg* 2003;37(1):169-74.

109. Lachapelle K, Graham AM, Symes JF. Antibacterial activity, antibiotic retention, and infection resistance of a rifampin-impregnated gelatin-sealed Dacron graft. *J Vasc Surg* 1994;19(4):675-82.

110. Ricci MA, Mehran RJ, Petsikas D, Mohamed F, Guidoin R, Marois Y, *et al.* Species differences in the infectability of vascular grafts. *J Invest Surg* 1991;4(1):45-52.

111. Mehran RJ, Ricci MA, Graham AM, Carter K, Symes JF. Porcine model for vascular graft studies. *J Invest Surg* 1991;4(1):37-44.

112. Muhl E, Gatermann S, Iven H, Dendorfer A, Bruch HP. Local application of vancomycin for prophylaxis of graft infection: release of vancomycin from antibiotic-bonded Dacron grafts, toxicity in endothelial cell culture, and efficacy against graft infection in an animal model. *Ann Vasc Surg* 1996;10(3):244-53.

113. Gao H, Sandermann J, Prag J, Lund L, Lindholt JS. Prevention of primary vascular graft infection with silver-coated polyester graft in a porcine model. *Eur J Vasc Endovasc Surg* 2010;39(4):472-7.

114. Gao H, Sandermann J, Prag J, Lund L, Lindholt JS. Rifampicin-soaked silver polyester versus expanded polytetrafluoro-ethylene grafts for in situ replacement of infected grafts in a porcine randomised controlled trial. *Eur J Vasc Endovasc Surg* 2012;43(5):582-7.

115. Stull MC, Clemens MS, Heafner TA, Watson JDB, Arthurs ZM, Propper BW. Prosthetic Graft Patency in the Setting of a Polymicrobial Infection in Swine (Sus scrofa). *Ann Vasc Surg* 2016;36:265-72.

116. Thibodeaux LC, James KV, Lohr JM, Welling RE, Roberts WH. Infection of endovascular stents in a swine model. *Am J Surg* 1996;172(2):151-4.

117. Paget DS, Bukhari RH, Zayyat EJ, Lohr JM, Roberts WH, Welling RE. Infectibility of endovascular stents following antibiotic prophylaxis or after arterial wall incorporation. *Am J Surg* 1999;178(3):219-24.

118. Hearn AT, James KV, Lohr JM, Thibodeaux LC, Roberts WH, Welling RE. Endovascular stent infection with delayed bacterial challenge. *Am J Surg* 1997;174(2):157-9.

119. Rowe NM, Impellizzeri P, Vaynblat M, Lawson NM, Kim YD, Sierra M, *et al.* Studies in thoracic aortic graft infections: the development of a porcine model and a comparison of collagen-impregnated dacron grafts and cryopreserved allografts. *J Thorac Cardiovasc Surg* 1999;118(5):857-65.

120. Hernandez-Richter T, Schardey HM, Löhlein F, Heiss MM, Redondo-Müller M, Hammer C, *et al.* The prevention and treatment of vascular graft infection with a Triclosan (Irgasan)-bonded Dacron graft: an experimental study in the pig. *Eur J Vasc Endovasc Surg* 2000;20(5):413-8.

121. Mehran RJ, Graham AM, Ricci MA, Symes JF. Evaluation of muscle flaps in the treatment of infected aortic grafts. *J Vasc Surg* 1992;15(3):487-94.

122. Clemens MS, Stull MC, Hata KW, Heafner TA, Watson JDB, Arthurs ZM, *et al.* Antimicrobial-bonded graft patency in the setting of a polymicrobial infection in swine (Sus scrofa). *J Vasc Surg* 2017;66(4):1210-6.

123. Richardson RL, Pate JW, Wolf RY, Ledes C, Hopson WB. The outcome of antibiotic-soaked arterial grafts in guinea pig wounds contaminated with E. coli or S. aureus. *J Thorac Cardiovasc Surg* 1970;59(5):635-7.

124. Stenger M, Behr-Rasmussen C, Klein K, Grønnemose RB, Andersen TE, Klitgaard JK, *et al.* Systemic thioridazine in combination with dicloxacillin against early aortic graft infections caused by Staphylococcus aureus in a porcine model: In vivo results do not reproduce the in vitro synergistic activity. PLoS ONE. 2017;12(3):e0173362.

125. Jernigan TW, Croce MA, Cagiannos C, Shell DH, Handorf CR, Fabian TC. Small intestinal submucosa for vascular reconstruction in the presence of gastrointestinal contamination. *Ann Surg* 2004;239(5):733-8; discussion 738-740.

126. Kron IL, Georgitis JW, Holmes P, Britton RC. Propagation of sepsis in vascular grafts. *Arch Surg* 1980;115(7):878-9.

127. Aboshady I, Raad I, Shah AS, Vela D, Dvorak T, Safi HJ, *et al.* A pilot study of a triple antimicrobial-bonded Dacron graft for the prevention of aortic graft infection. *J Vasc Surg* 2012;56(3):794-801.

128. Aboshady I, Raad I, Vela D, Hassan M, Aboshady Y, Safi HJ, *et al.* Prevention of perioperative vascular prosthetic infection with a novel triple antimicrobial-bonded arterial graft. *J Vasc Surg* 2016;64(6):1805-14.

129. Haverich A, Hirt S, Karck M, Siclari F, Wahlig H. Prevention of graft infection by bonding of gentamycin to Dacron prostheses. *J Vasc Surg* 1992;15(1):187-93.

130. Johnson JJ, Alex Jacocks M, Gauthier SC, Irwin DA, Wolf RF, Garwe T, *et al.* Establishing a swine model to compare vascular prostheses in a contaminated field. *J Surg Res*2013;181(2):355-8.

131. Chilukuri DM, Shah JC. Local delivery of vancomycin for the prophylaxis of prosthetic device-related infections. Pharm Res. 2005;22(4):563-72.

132. Sweet FA, Forsthoefel CW, Sweet AR, Dahlberg RK. Local Versus Systemic Antibiotics for Surgical Infection Prophylaxis in a Rat Model. *J Bone Joint Surg Am* 2018;100(18):e120.

133. Fujishiro K, Nishikimi N, Watanabe N, Sakurai T, Komori K, Ohta M. The retroperitoneum protects prosthetic graft material from intraperitoneal contamination: an experimental study. *Eur J Vasc Endovasc Surg* 2006;31(3):280-3.

134. Aksoy M, Turnadere E, Ayalp K, Kayabali M, Ertugrul B, Bilgic L. Cyanoacrylate for wound closure in prosthetic vascular graft surgery to prevent infections through contamination. *Surg Today* 2006;36(1):52-6.

135. Anderson CA, Sawyer MA, Cordts PA, Cordts PR, Demaioribus CA, Nauschuetz KN. Seromuscular enteric pedicles and prosthetic aortic graft complications in a porcine abdominal trauma model. An experimental study. Digestive *Surgery* 2000;17(2):126-31.

136. Canbeyli İD, Kabalcı M, Çırpar M, Tiryaki M, Oktaş B. Mesenchymal stem cells have significant anti-infective effect on methicillin-resistant Staphylococcus epidermidis vascular graft infections. Eklem Hastalik Cerrahisi. 2019;30(3):201-11.

137. Artini M, Scoarughi GL, Papa R, Cellini A, Avanzolini C, Mileto E, *et al.* Comparison of anti-bacterial prophylactic properties of two different vascular grafts: action of anti-bacterial graft coating and systemic antibiotic treatment. Int J Immunopathol Pharmacol. 2010;23(1):383-6.

138. Sakaguchi H, Marui A, Hirose K, Nomura T, Arai Y, Bir SC, *et al.* Less-invasive and highly effective method for preventing methicillin-resistant Staphylococcus aureus graft infection by local sustained release of vancomycin. *J Thorac Cardiovasc Surg* 2008;135(1):25-31.

139. Hirose K, Marui A, Arai Y, Nomura T, Inoue S, Kaneda K, *et al.* Sustained-release vancomycin sheet may help to prevent prosthetic graft methicillin-resistant Staphylococcus aureus infection. *J Vasc Surg* 2006;44(2):377-82.

140. Hernández-Richter T, Schardey HM, Wittmann F, Mayr S, Schmitt-Sody M, Blasenbreu S, *et al.* Rifampin and Triclosan but not silver is effective in preventing bacterial infection of vascular dacron graft material. *Eur J Vasc Endovasc Surg* 2003;26(5):550-7.

141. Greco RS, Harvey RA. The biochemical bonding of cefoxitin to a microporous polytetrafluoroethylene surface. *J Surg Res* 1984;36(3):237-43.

142. Javerliat I, Goëau-Brissonnière O, Sivadon-Tardy V, Coggia M, Gaillard J-L. Prevention of Staphylococcus aureus graft infection by a new gelatin-sealed vascular graft prebonded with antibiotics. *J Vasc Surg* 2007;46(5):1026-31.

143. Colburn MD, Moore WS, Chvapil M, Gelabert HA, Quiñones-Baldrich WJ. Use of an antibiotic-bonded graft for in situ reconstruction after prosthetic graft infections. *J Vasc Surg* oct 1992;16(4):651-8; discussion 658-660.

144. Parsons RE, Sanchez LA, Marin ML, Holbrook KA, Faries PL, Suggs WD, *et al.* Comparison of endovascular and conventional vascular prostheses in an experimental infection model. *J Vasc Surg* 1996;24(6):920-5; discussion 925-926.

145. White JV, Freda J, Kozar R, Serfass D, Cundy K, Comerota AJ, *et al.* Does bacteremia pose a direct threat to synthetic vascular grafts? *Surgery* 1987;102(2):402-8.

146. Rubin JR, Malone JM, Goldstone J. The role of the lymphatic system in acute arterial prosthetic graft infections. *J Vasc Surg* 1985;2(1):92-8.

147. Keller JD, Falk J, Bjornson HS, Silberstein EB, Kempczinski RF. Bacterial infectibility of chronically implanted endothelial cell-seeded expanded polytetrafluoroethylene vascular grafts. *J Vasc Surg* 1988;7(4):524-30.

148. Sobinsky KR, Flanigan DP. Antibiotic binding to polytetrafluoroethylene via glucosaminoglycan-keratin luminal coating. *Surgery* 1986;100(4):629-34.

149. Knosalla C, Goëau-Brissonnière O, Leflon V, Bruneval P, Eugène M, Pechère JC, *et al.* Treatment of vascular graft infection by in situ replacement with cryopreserved aortic allografts: an experimental study. *J Vasc Surg* 1998;27(4):689-98.

150. Dacey LJ, Miett TO, Huntsman WT, Colen LB, Schned AR, McDaniel MD. Efficacy of muscle flaps in the treatment of prosthetic vascular graft infections. *J Surg Res* 1988;44(5):566-72.

151. Birinyi LK, Douville EC, Lewis SA, Bjornson HS, Kempczinski RF. Increased resistance to bacteremic graft infection after endothelial cell seeding. *J Vasc Surg* 1987;5(1):193-7.

152. Greco RS, Trooskin SZ, Donetz AP, Harvey RA. The application of antibiotic bonding to the treatment of established vascular prosthetic infection. *Arch Surg* 1985;120(1):71-5.

153. Ney AL, Granja JA, Schuster PA, Tsukayama DT, Jacobs DM, Bubrick MP. The use of biodegradable amikacin microspheres to prevent vascular graft infection. *J Surg Res* 1994;57(6):698-705.

154. McDaniel MD, Schned AR, Beck JR. Efficacy of silver sulfadiazine in the treatment of prosthetic arterial bypass graft infection. Surg Gynecol Obstet. 1986;162(2):169-73.

155. Litzler PY, Thomas P, Danielou E, Lucq J, Jacques B, Frebourg N, *et al.* Bacterial resistance of refrigerated and cryopreserved aortic allografts in an experimental virulent infection model. *J Vasc Surg* 1999;29(6):1090-6.

156. Moore WS, Chvapil M, Seiffert G, Keown K. Development of an infection-resistant vascular prosthesis. *Arch Surg* 1981;116(11):1403-7.

157. Moore WS, Malone JM, Keown K. Prosthetic arterial graft material. Influence on neointimal healing and bacteremic infectibility. *Arch Surg* 1980;115(11):1379-83.

158. Roon AJ, Malone JM, Moore WS, Bean B, Campagna G. Bacteremic infectability: a function of vascular graft material and design. *J Surg Res* 1977;22(5):489-98.

159. Malone JM, Moore WS, Campagna G, Bean B. Bacteremic infectability of vascular grafts: the influence of pseudointimal integrity and duration of graft function. *Surgery* 1975;78(2):211-6.

160. Benvenisty AI, Tannenbaum G, Ahlborn TN, Fox CL, Modak S, Sampath L, *et al.* Control of prosthetic bacterial infection: evaluation of an easily incorporated, tightly bound, silver antibiotic PTFE graft. *J Surg Res* 1988;44(1):1-7.

161. Shue WB, Worosilo SC, Donetz AP, Trooskin SZ, Harvey RA, Greco RS. Prevention of vascular prosthetic infection with an antibiotic-bonded Dacron graft. *J Vasc Surg* 1988;8(5):600-5.

162. Bennion RS, Williams RA, Wilson SE. Comparison of infectibility of vascular prosthetic materials by quantitation of median infective dose. *Surgery* 1984;95(1):22-6.

163. Wilson SE, Hermosillo CX, Parsa F, Gordon HE. Experimental infection of dacron and bovine grafts. *J Surg Res* 1975;18(3):221-7.

164. Leport C, Goeau-Brissonniere O, Lebrault C, Pechere JC. Les infections experimentales de protheses vasculaires : Role du materiau dans la sensibilite a la colonisation et prophylaxie de l'infection tardive. Médecine et Maladies Infectieuses. 1989;19(11, Part 2):645-51.

165. Goëau-Brissonnière O, Leport C, Guidoin R, Lebrault C, Péchère JC, Bacourt F. Experimental colonization of an expanded polytetrafluoroethylene vascular graft with Staphylococcus aureus: a quantitative and morphologic study. *J Vasc Surg* 1987;5(5):743-8.

166. Rosenman JE, Pearce WH, Kempczinski RF. Bacterial adherence to vascular grafts after in vitro bacteremia. *J Surg Res* 1985;38(6):648-55.

167. Koskas F, Goëau-Brissonnière O, Nicolas MH, Bacourt F, Kieffer E. Arteries from human beings are less infectible by Staphylococcus aureus than polytetrafluoroethylene in an aortic dog model. *J Vasc Surg* 1996;23(3):472-6.

168. Badylak SF, Coffey AC, Lantz GC, Tacker WA, Geddes LA. Comparison of the resistance to infection of intestinal submucosa arterial autografts versus polytetrafluoroethylene arterial prostheses in a dog model. *J Vasc Surg* 1994;19(3):465-72.

169. Geary KJ, Tomkiewicz ZM, Harrison HN, Fiore WM, Geary JE, Green RM, *et al.* Differential effects of a gram-negative and a gram-positive infection on autogenous and prosthetic grafts. *J Vasc Surg* 1990;11(2):339-45; discussion 346-347.

170. Shah PM, Ito K, Clauss RH, Babu SC, Reynolds BM, Stahl WM. Expanded microporous polytetrafluoroethylene (PTFE) grafts in contaminated wounds: experimental and clinical study. J Trauma. 1983;23(12):1030-3.

171. Goëau-Brissonnière OA, Fabre D, Leflon-Guibout V, Di Centa I, Nicolas-Chanoine M-H, Coggia M. Comparison of the resistance to infection of rifampin-bonded gelatin-sealed and silver/collagen-coated polyester prostheses. *J Vasc Surg* 2002;35(6):1260-3.

172. Lehnhardt FJ, Torsello G, Claeys LG, Pfeiffer M, Wachol-Drewek Z, Grundmann RT, *et al.* Systemic and local antibiotic prophylaxis in the prevention of prosthetic vascular graft infection: an experimental study. *Eur J Vasc Endovasc Surg* 2002;23(2):127-33.

173. Martin LF, Harris JM, Fehr DM, Peter AO, Appelbaum PC, Spangler SK, *et al.* Vascular prosthetic infection with Staphylococcus epidermidis: experimental study of pathogenesis and therapy. *J Vasc Surg* 1989;9(3):464-71.

174. Weiss JP, Lorenzo FV, Campbell CD, Myerowitz RL, Webster MW. The behavior of infected arterial prostheses of expanded polytetrafluoroethylene (Gore-Tex). *J Thorac Cardiovasc Surg* 1977;73(4):630-6.

175. Peter AO, Spangler S, Martin LF. Evaluation of three techniques for documenting Staphylococcus epidermidis vascular prosthetic graft infections. *Am Surg* 1991;57(2):80-5.

176. Shah PM, Modak S, Fox CL, Babu SC, Sampath L, Clauss RH, *et al.* PTFE graft treated with silver norfloxacin (AgNF): drug retention and resistance to bacterial challenge. *J Surg Res* 1987;42(3):298-303.

177. Alfonsi P, Coggia M, Leflon-Guibout V, Sessler DI, Goëau-Brissonnière O, Chauvin M. Mild hypothermia does not increase bacterial proliferation on implanted vascular grafts. *Am J Surg* 2002;184(1):37-40.

178. Dries DJ, Alazraki N, Lawrence PF, Murphy KM, Kercher J, Datz FL, *et al.* Detection of acute synthetic vascular graft infection with 111In-labeled leukocyte scanning: an animal study. AJR Am J Roentgenol. 1985;145(5):1053-6.

179. Leport C, Goëau-Brissonnière O, Lebrault C, Vildé JL, Pechére JC. Mechanisms of ceftriaxone prophylaxis against late bacteremic vascular graft infection caused by Staphylococcus aureus in a dog model. *Ann Vasc Surg* 1991;5(6):500-5.

180. Bricker DL, Beall AC, DeBakey ME. The differential response to infection of autogenous vein versus dacron arterial prosthesis. Chest. 1970;58(6):566-70.

181. Wakefield TW, Schaberg DR, Pierson CL, Bouffard JA, Petry NA, Nolan KD, *et al.* Treatment of established prosthetic vascular graft infection with antibiotics preferentially concentrated in leukocytes. *Surgery* 1987;102(1):8-14.

182. Ney AL, Kelly PH, Tsukayama DT, Bubrick MP. Fibrin glue-antibiotic suspension in the prevention of prosthetic graft infection. J Trauma. 1990;30(8):1000-5; discussion 1005-1006.

183. Shenk JS, Ney AL, Tsukayama DT, Olson ME, Bubrick MP. Tobramycin-adhesive in preventing and treating PTFE vascular graft infections. *J Surg Res* 1989;47(6):487-92.

184. McDougal EG, Burnham SJ, Johnson G. Rifampin protection against experimental graft sepsis. *J Vasc Surg* 1986;4(1):5-7.

185. Rutledge R, Baker VV, Sherertz R, Johnson G. Rifampin and cefazolin as prophylactic agents. A comparison in an animal model of vascular graft infection. *Arch Surg* 1982;117(9):1164-5.

186. Goëau-Brissonnière O, Mercier F, Nicolas MH, Bacourt F, Coggia M, Lebrault C, *et al.* Treatment of vascular graft infection by in situ replacement with a rifampin-bonded gelatin-sealed Dacron graft. *J Vasc Surg* 1994;19(4):739-41.

187. Greco RS, Harvey RA, Smilow PC, Tesoriero JV. Prevention of vascular prosthetic infection by a benzalkonium-oxacillin bonded polytetrafluoroethylene graft. Surg Gynecol Obstet. 1982;155(1):28-32.

188. Kirksey L, Brener BJ, Hertz S, Parsonnet V. Prophylactic antibiotics prior to bacteremia decrease endovascular graft infection in dogs. *Vasc Endovascular Surg* 2002;36(3):171-8.

189. Gao H, Lund L, Prag J, Sandermann J, Lindholt JS. Laparoscopic diagnosis and treatment of aortic vascular prosthetic graft infections in a porcine model. *Eur J Vasc Endovasc Surg* 2008;35(1):41-5.

190. Cruz NI, Canario QM. Muscle flaps in the management of vascular grafts in contaminated wounds: an experimental study in dogs. Plast Reconstr Surg. 1988;82(3):480-5.

191. Nakamoto DA, Rosenfield ML, Haaga JR, Merritt K, Sachs PB, Hutton MC, *et al.* Young Investigator Award. In vivo treatment of infected prosthetic graft material with urokinase: an animal model. *J Vasc Interv Radiol* 1994;5(4):549-52.

192. Stanevičiūtė E, Builytė IU, Ridziauskas M, Besusparis J, Kirkliauskienė A, Zabulis V, *et al.* Efficacy of Antiseptic Solutions in Treatment of Staphylococcus Aureus Infected Surgical Wounds with Patches of Vascular Graft: An Experimental Study in Rats. Medicina (Kaunas). 2019;55(4):E106.

193. Onem G, Sacar M, Sacar S, Sakarya S, Turgut H, Ozcan AV, *et al.* Neuraminidase decreases in vitro adherence of slime-forming coagulase-negative staphylococci to biosynthetic ovine collagen vascular graft. Adv Ther. 2006;23(2):256-62.

194. Hernández-Richter T, Schardey HM, Heiss MM, Löhlein F, Schildberg FW. [Experimental study of antiseptic (tauroline, taurolidine) and antibiotic (sulmycin implant) drugs in vascular prosthesis infections in a standardized infection model]. Zentralbl Chir. 2001;126(5):407-12.

195. Ditkowski B, Leeten K, Jashari R, Jones E, Heying R. Staphylococcus aureus adheres avidly to decellularised cardiac homograft tissue in vitro in the fibrinogen-dependent manner. Cardiol Young. 2020;30(12):1783-7.

196. Karck M, Forgione L, Haverich A. The efficacy of controlled antibiotic release for prevention of polyethyleneterephthalate-(Dacron-) related infection in cardiovascular *Surgery* Clin Mater. 1993;13(1-4):149-54.

197. Baker WH, Cram AE, O'Connor JE. An evaluation of combined routes of antibiotic administration in vascular reconstructive *Surgery* A study of local plus parenteral administration of cephaloridine in dogs. *J Thorac Cardiovasc Surg* 1973;66(1):131-2.

198. Sasaki Y. The in vitro research of bacterial invasion of prosthetic vascular grafts: comparison of elastomer-sealed and gelatin-coated Dacron vascular grafts. Surgery Today. 2014;44(8):1542-7.

199. Narasimhan S, Aslam S, Lin PH, Bechara CF, Mansouri MD, Darouiche RO. Bacterial translocation across ePTFE vascular graft surfaces. *J Infect* 2010;60(6):486-90.

200. Bergamini TM, McCurry TM, Bernard JD, Hoeg KL, Corpus RA, James BE, *et al.* Antibiotic efficacy against Staphylococcus epidermidis adherent to vascular grafts. *J Surg Res* 1996;60(1):3-6.

201. Saito A, Motomura N, Kakimi K, Narui K, Noguchi N, Sasatsu M, *et al.* Vascular allografts are resistant to methicillin-resistant Staphylococcus aureus through indoleamine 2,3-dioxygenase in a murine model. *J Thorac Cardiovasc Surg* 2008;136(1):159-67.

202. Ricco J-B, Assadian A, Schneider F, Assadian O. In vitro evaluation of the antimicrobial efficacy of a new silver-triclosan vs a silver collagen-coated polyester vascular graft against methicillin-resistant Staphylococcus aureus. *J Vasc Surg* 2012;55(3):823-9.

203. Osińska-Jaroszuk M, Ginalska G, Belcarz A, Uryniak A. Vascular prostheses with covalently bound gentamicin and amikacin reveal superior antibacterial properties than silver-impregnated ones--an in vitro study. *Eur J Vasc Endovasc Surg* 2009;38(6):697-706.

204. Henry R, Harvey RA, Greco RS. Antibiotic bonding to vascular prostheses. *J Thorac Cardiovasc Surg* 1981;82(2):272-7.

205. Webb LX, Myers RT, Cordell AR, Hobgood CD, Costerton JW, Gristina AG. Inhibition of bacterial adhesion by antibacterial surface pretreatment of vascular prostheses. *J Vasc Surg* 1986;4(1):16-21.

206. Harvey RA, Greco RS. The noncovalent bonding of antibiotics to a polytetrafluoroethylene-benzalkonium graft. *Ann Surg* 1981;194(5):642-7.

207. Kacem I, Laurent T, Blanchemain N, Neut C, Chai F, Haulon S, *et al.* Dyeing and antibacterial activation with methylene blue of a cyclodextrin modified polyester vascular graft. J Biomed Mater Res A. 2014;102(9):2942-51.

208. Leblebicioglu H, Sencan I, Gunaydin M, Esen S, Eroglu C, Sunbul M. Elution of vancomycin and tobramycin bonded to vascular grafts. J Chemother. 1999;11(1):46-9.

209. Koshiko S, Sasajima T, Muraki S, Azuma N, Yamazaki K, Chiba K, *et al.* Limitations in the use of rifampicin-gelatin grafts against virulent organisms. *J Vasc Surg* 2002;35(4):779-85.

210. White JV, Benvenisty AI, Reemtsma K, Voorhees AB, Fox CL, Modak S, *et al.* Simple methods for direct antibiotic protection of synthetic vascular grafts. *J Vasc Surg* 1984;1(2):372-80.

211. Jean-Baptiste E, Blanchemain N, Martel B, Neut C, Hildebrand HF, Haulon S. Safety, healing, and efficacy of vascular prostheses coated with hydroxypropyl-ß-cyclodextrin polymer: experimental in vitro and animal studies. *Eur J Vasc Endovasc Surg* 2012;43(2):188-97.

212. Chervu A, Moore WS, Chvapil M, Henderson T. Efficacy and duration of antistaphylococcal activity comparing three antibiotics bonded to Dacron vascular grafts with a collagen release system. *J Vasc Surg* 1991;13(6):897-901.

213. Fischer PE, Fabian TC, deRijk WG, Edwards NM, DeCuypere M, Landis RM, *et al.* Prosthetic vascular conduit in contaminated fields: a new technology to decrease ePTFE infections. *Am Surg* 2008;74(6):524-8; discussion 528-529.

214. Keeling WB, Myers AR, Stone PA, Heller L, Widen R, Back MR, *et al.* Regional antibiotic delivery for the treatment of experimental prosthetic graft infections. *J Surg Res* 2009;157(2):223-6.

215. Kinney EV, Bandyk DF, Seabrook GA, Kelly HM, Towne JB. Antibiotic-bonded PTFE vascular grafts: the effect of silver antibiotic on bioactivity following implantation. *J Surg Res* 1991;50(5):430-5.

216. Powell TW, Burnham SJ, Johnson G. A passive system using rifampin to create an infection-resistant vascular prosthesis. *Surgery* 1983;94(5):765-9.

217. Freyrie A, Curti T, Rodio M, Masetti L, Bignozzi L, Sanguinetti V, *et al.* Interaction between vascular prostheses and rifampicin in the prevention of the grafts infection. An experimental study. Int Angiol. 1992;11(2):113-6.

218. Ginalska G, Kowalczuk D, Osińska M. Amikacin-loaded vascular prosthesis as an effective drug carrier. Int J Pharm. 2007;339(1-2):39-46.

219. Zdanowski Z, Ribbe E, Schalén C. Influence of some plasma proteins on in vitro bacterial adherence to PTFE and Dacron vascular prostheses. APMIS. 1993;101(12):926-32.

220. Harris JM, Martin LF. An in vitro study of the properties influencing Staphylococcus epidermidis adhesion to prosthetic vascular graft materials. *Ann Surg* 1987;206(5):612-20.

221. Sugarman B. In vitro adherence of bacteria to prosthetic vascular grafts. Infection. 1982;10(1):9-14.

222. Rosenman JE, Kempczinski RF, Berlatzky Y, Pearce WH, Ramalanjaona GR, Bjornson HS. Bacterial adherence to endothelial-seeded polytetrafluoroethylene grafts. *Surgery* 1985;98(4):816-23.

223. Thaller MC, Selan L, Fiorani P, Passariello C, Rizzo L, Speziale F. A comparative in vitro evaluation of different therapeutic protocols for vascular graft infections. *Eur J Vasc Endovasc Surg* 1997;14 Suppl A:35-7.

224. Blanchemain N, Laurent T, Chai F, Neut C, Haulon S, Krump-konvalinkova V, *et al.* Polyester vascular prostheses coated with a cyclodextrin polymer and activated with antibiotics: cytotoxicity and microbiological evaluation. Acta Biomater. 2008;4(6):1725-33.

225. Hernández-Richter T, Schardey HM, Löhlein F, Fleischer CT, Walli AK, Boos KS, *et al.* Binding kinetics of triclosan (Irgasan) to alloplastic vascular grafts: an in vitro study. *Ann Vasc Surg* 2000;14(4):370-5.

226. Chakfe N, Guidoin R, Marois M, Roy PE, Douville Y, Roy P, *et al.* A pathological study of arterial prostheses surgically excised after overt clinical infection. J Biomater Appl. 1991;5(3):227-46.

227. Freytag CC, Tautenhahn J, König W, Lippert H, Bürger T. Ultrastructural analysis of an infected collagen-coated vascular graft. *Vasa* 2003;32(1):31-5.

228. Harrison JH. Influence of infection on homografts and synthetic (teflon) grafts; a comparative study in experimental animals. AMA *Arch Surg* 1958;76(1):67-73.

229. Stone KS, Walshaw R, Sugiyama GT, Dean RE, Dunstan RW. Polytetrafluoroethylene versus autogenous vein grafts for vascular reconstruction in contaminated wounds. *Am J Surg* 1984;147(5):692-5.

230. Bradham RR, Cordle F, McIVER FA. Effect of bacteria on vascular prostheses. *Ann Surg* 1961;154(6)Suppl:187-91.

231. Knott LH, Crawford FA, Grogan JB. Comparison of autogenous vein, dacron and Gore-Tex in infected wounds. *J Surg Res* 1978;24(4):288-93.

232. Cavallaro A, Sciacca V, Cisternino S, di Marzo L, Mingoli A, Farina C, *et al.* Bacteremic Infectability of Vascular Grafts: An Experimental Study. Vascular *Surgery* 1991;25(2):89-99.

233. Balaban N, Gov Y, Giacometti A, Cirioni O, Ghiselli R, Mocchegiani F, *et al.* A Chimeric Peptide Composed of a Dermaseptin Derivative and an RNA III-Inhibiting Peptide Prevents Graft-Associated Infections by Antibiotic-Resistant Staphylococci. *Antimicrob Agents Chemother* 2004;48(7):2544-50.

234. Balaban N, Giacometti A, Cirioni O, Gov Y, Ghiselli R, Mocchegiani F, *et al.* Use of the quorum-sensing inhibitor RNAIII-inhibiting peptide to prevent biofilm formation in vivo by drug-resistant Staphylococcus epidermidis. *J Infect Dis* 2003;187(4):625-30.

235. Ginalska G, Osinska M, Uryniak A, Urbanik-Sypniewska T, Belcarz A, Rzeski W, *et al.* Antibacterial activity of gentamicin-bonded gelatin-sealed polyethylene terephthalate vascular prostheses. *Eur J Vasc Endovasc Surg* 2005;29(4):419-24.

236. Wang Y, He C, Feng Y, Yang Y, Wei Z, Zhao W, *et al.* A chitosan modified asymmetric small-diameter vascular graft with anti-thrombotic and anti-bacterial functions for vascular tissue engineering. J Mater Chem B. 2020;8(3):568-77.

237. Strathmann M, Wingender J. Use of an oxonol dye in combination with confocal laser scanning microscopy to monitor damage to Staphylococcus aureus cells during colonisation of silver-coated vascular grafts. Int J Antimicrob Agents. 2004;24(3):234-40.

238. Van de Vyver H, Bovenkamp PR, Hoerr V, Schwegmann K, Tuchscherr L, Niemann S, *et al.* A Novel Mouse Model of Staphylococcus aureus Vascular Graft Infection: Noninvasive Imaging of Biofilm Development in Vivo. Am J Pathol. 2017;187(2):268-79.

239. Boudjemaa R, Steenkeste K, Jacqueline C, Briandet R, Caillon J, Boutoille D, *et al.* Live intramacrophagic Staphylococcus aureus as a potential cause of antibiotic therapy failure: observations in an in vivo mouse model of prosthetic vascular material infections. *J Antimicrob Chemother* 2018;73(9):2418-21.

240. Osada T, Yamamura K, Fujimoto K, Mizuno K, Sakurai T, Ohta M, *et al.* Prophylaxis of local vascular graft infection with levofloxacin incorporated into albumin-sealed dacron graft (LVFX-ALB Graft). *Microbiol Immunol* 1999;43(4):317-21.

241. Tautenhahn J, Meyer F, Buerger T, Schmidt U, Lippert H, Koenig W, *et al.* Interactions of neutrophils with silver-coated vascular polyester grafts. Langenbecks *Arch Surg* 2010;395(2):143-9.

242. Langerhuus SN, Tønnesen EK, Jensen KH, Damgaard BM, Heegaard PMH, Halekoh U, *et al.* Brief report: biomarkers of aortic vascular prosthetic graft infection in a porcine model with Staphylococcus aureus. *Eur J Clin Microbiol Infect Dis* 2010;29(11):1453-6.

243. Gul M, Yasim A, Aral M. The levels of cytokines in rats following the use of prophylactic agents in vascular graft infection. Bratisl Lek Listy. 2010;111(6):316-20.

All you need to know about biofilm

25

Paweł TULINSKI, Régis VILLET

Biofilms are complex, multispecies bacteria communities attached to the biotic and abiotic surfaces. However, in the medical setting, biofilms cause a serious problem of nosocomial infection, especially linked to medical devices. Biofilm-related infections are difficult to treat due to the complexity and antibiotic resistance. It has been recognized that it is necessary to design new strategies to prevent biofilm formation on the surface of medical devices as well as develop new effective strategies for biofilm eradication. Thus, novel screening technologies are necessary to bring anti-biofilm solutions to patients. In this review, apart from the general overview of biofilm infection, we would like to emphasize the need to develop novel and suitable biofilm technologies to study it. Particularly, we would like to underline the need for new biofilm models that will mimic human pathology as a preclinical screening platform.

Introduction

Microorganisms, such as bacteria, exhibit two modes of living: planktonic and biofilm. The biofilm is structured communities, mainly polymicrobial, that are embedded in a self-produced extracellular matrix. The formation of biofilm is initiated by planktonic bacteria that started to create aggregates on the surface until the formation of the mature complex structure called a biofilm [1]. Notably, the bacterial cells in the biofilm display contrasting characteristics and behaviour to the planktonic cells, *e.g.* differences in global gene expression and more tolerant to the antibiotics. Biofilm formation represents a significant cause of concern imposing a huge burden on the public healthcare system throughout the world. Most of the bacteria (over 80%) live as a biofilm [1,2]. The presence of the biofilm results in an intimidating challenge for the medical care sector. According to the National Institutes of Health (NIH, USA), more than 80% of infections including chronic infectious diseases are associated with the presence of a biofilm [3]. Biofilm microbial infections can be classified into two main types:

(i) Intrinsic to host tissues (opportunistic infections including cystic fibrosis, osteomyelitis, urethritis, nonhealing wounds, native valve infectious endocarditis, and periodontitis),

(ii) associated with indwelling medical devices (such as intravascular and urinary catheters, pacemakers, heart valves, endotracheal tubes and orthopaedic implants).

Medical devices that are implanted in nearly all districts of the body trigger a local immune-compromised environment in the host and provide a fertile environment for biofilm production promoting medical device-associated infection. Medical device-associated infection management involves lengthy and costly treatments (*i.e.*, long-term hospitalization, multiple risky surgeries, prolonged antibiotic therapy and secondary complications). Despite advances in biomaterials and surgical techniques, the cardiac and orthopaedic device associated infections remain an unmet clinical complication [4]. It is estimated that up to 70% of nosocomial infections are associated with biomaterials or implants [3]. Remarkably, biofilm-related infection, only in the USA, affects more than 17 million people with more than half a million deaths, with an annual cost of $94 billion [5].

Biofilm formation

Biofilm formation, on any surface, mainly involves three steps. The first step involves the attachment of cells to a surface (primarily mediated by sedimentation, Brownian motions, and hydrodynamic forces), while adhesion to the substrate is governed by Lifshitz – Van der Waals, acid-base, hydrophobic, and electrostatic interactions [6] followed by the assembly of cells to form micro-colonies and finally evolve into a biofilm with a so-called "mature" structured matrix. After the full development of the biofilm, its detachment is the result of both passive and active mechanical processes [7]. Detachment implies shear stress (abrasion, erosion, and sloughing) and the impact of immune attack from the host (grazing). Moreover, dispersion requires the sensing and processing of a particular signal (QS, c-di-GMP, small regulatory RNAs, cis-2-decenoic acid, guanosine tetraphosphate and guanosine pentaphosphate ((p)ppGpp)) [8]. In the case of abiotic surfaces, like implants and medical devices, the initial bacterial adherence takes place within the formed conditioning film, which may be used by the attached bacteria as a source of nutrients. Specifically, conditioning films are thin biopolymeric coatings formed at the interface of a material surface and the aqueous medium provided by body fluids and secretions [8]. The presence of conditioning films consequently modifies the physicochemical properties of the surface influencing bacterial adherence. Other factors including roughness, porosity, pore topology, charge and hydrophobicity/hydrophilicity of the surface also influence bacterial adherence. Bacterial interactions with surfaces allow them not only to sense the surface but also to become progressively adapted to it. The mechanical cues experience during surface sensing causes molecular alteration at the biochemical level (mechanotransduction), which gradually increase the attachment of the loosely adhered cells [8]. Once a strong bacteria-to-surface adhesion has been achieved, attaches bacteria grow leading to the activation of specific inter-cellular communication, the secretion of extracellular polymeric substance (EPS) matrix, and the establishment of "microcolonies". At this point, multiple layers from microcolonies will form complex structural features refereed as "macrocolonies" called mature biofilm.

Biofilm features

EPS matrix (50%-90% of the biofilm) which is mainly composed of water (97%) and biomolecules including polysaccharides (exopolysaccharides, lipo-associated and wall-associated teichoic acids, and cellulose) proteins, nucleic acids, lipids and ions [1,8]. Also, extracellular proteinaceous bacterial structures such as pili and flagella, together with extracellular DNA (eDNA) and curli, serve as structural elements that contribute to stabilize and strengthen the EPS matrix. The effective communication between bacterial cells at this stage is a key factor for the transition from a fairly simple aggregated state into the initial bacterial arrangement, which will further develop into a complex and well-structured community style of living. For this purpose, a cell-to-cell communication mechanism knows as quorum sensing (QS) is utilized by bacteria to collectively adapt through the activation/repression of target genes. Some of the biofilm-associated collective behaviour influenced by QS include the spread of beneficial mutations such as the regulation of EPS matrix production, modulation of nutrient utilization, expression of virulence factor, synthesis of biosurfactants, and regulation of antimicrobial resistance[9]. The EPS matrix protects against various stress conditions and makes them resistant to the innate immune system [10]. Therefore, the concentration of antimicrobials required to inhibit biofilms is between 10 and 10,000 times greater than the corresponding concentration required to eliminate bacterial cells in planktonic form resulting in a high rate of treatment failure [1,11].

The formation of bacterial biofilms is one of the main causes of bacterial resistance. Several mechanisms are responsible for increasing the antibiotic tolerance of the biofilm, including

(i) reduced diffusion or sequestration of antimicrobials through the extracellular matrix of the biofilm[12-15],

(ii) the presence of slow growth and even dormant cells (persistent), and highly refractory to antibiotics targeting bacterial metabolism[14,16],

(iii) activation of efflux pumps[9]

(iv) exchange of mobile genetic elements encoding a resistance determinant[17].

Biofilm infections require the administration of a high dose of antibiotics[18]. Even when applied topically, antibiotics rarely reach bacteria found in mature biofilms at therapeutic concentrations and it has been shown that certain antibiotics are even able to induce biofilm formation as an adaptive strategy [18-20]. Within a biofilm, bacteria will combine a set of strategies that will allow them to greatly reduce their susceptibility to treatments, *e.g.* mechanical protection into the EPS matrix, slowing down of metabolism, degradation of antibiotics in the EPS matrix, activation of efflux pumps, transfer of resistance genes)[1]. Bacteria will not only become resistant but may also be able to spread throughout the body[21]. Furthermore, the dispersed cells have the advantage of having gone through a change in phenotype during biofilm development as well as further genetic modifications after the stress conditions generated by biofilm gradients[22]. These modifications that once permitted them to express a more virulent and resistant phenotype are partially maintained[23]. Moreover, biofilm is a source of the persister cells. Persisters are bacteria cells that can survive, through growth arrest, during exposure to antibiotic treatment at a concentration that should be lethal[24]. This subpopulation exhibiting a transient reversible phenotype allowing

(i) to survive significant antibiotic exposure without MIC change and

(ii) to regrow after antibiotic exposure and recurrence of chronic infections

Biofilm will depend on the type of microbes forming them, interactions with host immune effectors, and the physicochemical and mechanical properties of the microenvironment. At different depths in biofilm, the pH, oxygen content and metabolism are different[1]. This reflects the level of complexity for the study of biofilms and the development of specific strategies to develop suitable and effective antimicrobials solutions for their prevention or eradication.

Infection on medical devices

Implantable medical devices are an integral part of medical practice. In 2014, the global market of implantable biomaterial was valued at $79.1 billion (including $40 billion for cardiovascular devices) and should reach almost $133 billion in 2022 (including $60 billion for cardiovascular devices)[25]. Nonetheless, implantation of the foreign bodies to humans is creating favourable conditions for bacteria attachment and propagation leading to develop infection and treatment complications. It is estimated that biofilm affects 2% of knee prostheses, 4% of mechanical heart valves, pacemakers and defibrillators, 10% of ventricular devices and 40% of ventricular assist devices.[11] The implantable medical devices such as cardiac pacemakers, artificial heart valves, centre venous catheters, various catheters, prostheses or even contact lenses carry the risk of the development of biofilm-related infections.[26] Consequently, medical device infection may have a negative impact on the quality of life, increase the healthcare cost and cause life-threatening conditions. The microorganism can contaminate medical devices in various ways. First of all, pathogens can be transferred from the external environment or relocation from the surrounding tissues such as skin during the surgery to the surface of the device. Subsequently,

implanted material can be colonized by bacteria naturally occurring in the human body as a part of the natural flora for example by bacteria from the respiratory, urinary or gastrointestinal tract [3]. Regardless of whether the bacteria that might cause infection are present inside or outside the body, medical device-related infections always begin with the colonization of bacteria on the surface of the device leading to the formation of biofilms. The common use of medical devices and association with medical device-associated biofilm infections continue to pose a serious threat to human health. The biofilm infection associated with medical devices has become a significant source of nosocomial infections[26]. Nowadays, biofilm formation is recognized as one of the most important virulence factors in medical device-associated infections. The diagnosis of biofilm infection is also very challenging. Currently, there are no standardized procedures to detect biofilm and validate antibiotic therapy in clinics [11]. The latest guidelines to assist healthcare professionals in the diagnosis of biofilm infection were published in 2014 by the European Society for Clinical Microbiology and Infectious Disease [27]. Nonetheless, this recommendation only suggests some detection methods to identify the bacteria causing biofilm infection such as PCR. Typically, the conventional clinical diagnostic approach on microorganisms is based on the agar plating methodology to identify the specific bacteria species. To perform correct bacteria identification, many clinical samples follow the sonication procedure to disrupt bacteria aggregates. Subsequently, to choose a suitable antibiotic treatment, the determination of the minimum inhibitory concentration (MIC) is performed on the planktonic, free-living and pure culture of bacteria[11, 27]. Independently, in the research setting, there are various methods to study biofilm. However, there are no established and standardized protocols applied to clinics [11]. However, it has been stressed that naturally biofilms are found to be multispecies. Notably, the natural occurring biofilm will differ from the monospecies biofilm investigated in the laboratory setting.

Strategies for the biofilm control

There are two main strategies to control biofilm infection. The first approach is to destroy mature biofilm. The second strategy is to prevent biofilm formation on the surfaces by the inhibit the attachment of bacteria or disrupt biofilm formation on the initial steps.

Biofilm eradication

In clinical practice, it is difficult to diagnose and treat biofilm infection effectively. Bacterial biofilms are involved in most device-associated infections and remain a real challenge for modern medicine (28). Some other reasons also contribute to the stubbornness of mature biofilms like the presence of the β-lactam antibacterial agent, the activation of the bacterial efflux pumps the deepest part of biofilm and the most responsible for the chronicity of the infection. To date, the different strategies against mature biofilm mainly include the destruction of the EPS matrix to improve drug permeability and kill the embedded bacteria, the quorum quenching and the control of the intercellular interaction pathways to induce the dispersion of biofilms [29]. Moreover, the presence of persister cells in biofilm brings additional challenges to eradicate biofilm [23,24].

In a bacterial biofilm, the EPS matrix acts as a barrier to protect bacteria from antibacterial agents, and then a first approach consists of using strategies to destroy the matrix to facilitate access to antimicrobial drugs. The use of related enzymes (*e.g.* alginase, deoxyribonuclease I, dispersin B and lysostaphin) can destroy or eliminate EPS and improves the bactericidal effect of antibacterial agents. More recently, several innovative approaches using nanomaterials have been explored. We can categorize the nanomaterials in biofilm treatment into three groups: including nanomaterials with intrinsic biofilm-eradication properties, nanomaterials as delivery vehicles for biofilm-eradication agents, and responsive nanomaterials [28]. Below, we highlighted, in our point of view, the most promising strategies for biofilm eradication.

Nanoparticles

A key type of nanoparticle (NP) with intrinsic anti-biofilm activities is metallic nanoparticles. Some researches showed anti-biofilm activity of gold nanoparticles (AuNPs) [30]. Nanocarriers with their intrinsic high surface-area-to-volume radio and rich surface chemistry can be designed to have a controllable therapeutic dose, improve the stability of their "cargo", or temporal and spatial cargo release [28]. Nanocarriers can be made from various organic and inorganic materials, and some even have intrinsic antimicrobial or antibiofilm properties. A straightforward design involves using antibiotics in nanocarriers [28]. Other nanocarriers systems (*e.g.* chitosan, AuNPs, poly lactic co-glycolic acid, PLGA, or silicas) have also been developed to deliver non-drug agents, such as enzymes like DNAse I, or essential oils. Another group of nanocarriers are based on the delivery of nitric oxide (NO) as a reactive free radical. Magnetic field, light, or the pH of the micro-environment have been exploited to activate a nanomaterial or transform it into a more active species to destroy bacterial biofilm [28]. Some non-specific biofilm disruption mechanisms such as heat and physical force allow for a wide range of bacterial biofilms to be targeted. Under the force of a magnetic field, magnetic-iron oxide nanoparticles (IONs) create artificial channels in biofilms, which achieved antibiotic penetration and bacterial killing. IONs can be conjugated with metal ions (*e.g.* zinc or silver), or amine, carboxylate and isocyanate. In an acidic environment, certain nanomaterials can catalyze the production of oxidative species. As a result, stimuli such as local pH and/or H_2O_2 can be exploited to assist in the treatment of biofilms. IONs nanoparticles with peroxide-like activity catalyse H_2O_2 into free radicals through the Fenton reaction. pH-activated nanomaterials containing farnesol, a hydrophobic bactericidal agent can release the farnesol *in situ* and then disrupt the biofilm. Another strategy is photodynamic treatment or photothermal ablation, which is based on light-induced transformation or degradation of nanomaterials, or the generation of heat. Laser-induced vapour nanobubbles (VNB) can increase the diffusion and efficiency of drugs within the bacterial biofilm. AuNPs can deeply penetrate the biofilm because of their small size (70nm). When AuNPs absorb a high-intensity laser pulse, the temperature of the AuNPs will rise rapidly and water vapour nanobubbles will rapidly appear around them and then implode and then create gaps within the biofilm, thus facilitating antibiotic penetration and transport. Moreover, VNB can be combined with nanocarriers containing antibiotics. Mechanical force induced by VNB trigger antibiotic release from nanocarriers close to sessile bacteria. Recently, graphitic carbon nitride (g-C3N4) has been shown as an efficient photocatalyst and photodegrading agent, which generated reactive oxygen species (ROS). Another approach for bacterial biofilm treatment using chitosan nanoparticles functionalized with Rose Bengal, a photosensitizer agent, to enhance photodynamic therapy. The combination therapy concept has attracted significant interest to increase treatment efficacy like a combination of environment pH and near-infrared light (NIR). Zwitterionic AuNPs turned into a negative charge in acidic pH (ca. 5.5) in the bacterial biofilm and then form aggregates. NIR irradiation then allowed the aggregates to convert and concentrate the photon energy into heat, causing local disruption of the biofilm. [28, 30]

Signalling

Bacteria control important developmental processes by sensing and responding to environmental signals. Two widely conserved and important strategies that bacteria employ to sense changes in population density and local environmental conditions are quorum sensing (QS) and cyclic di-GMP (c-di-GMP) signalling, respectively [30]. c-di-GMP mentioned above can regulate various EPS-producing exoenzymes, polysaccharides and adhesins, and also functions as key dispersal signals. QS enables bacteria to restrict the expression of specific genes when the population has a high cell density, resulting in more beneficial phenotypes. QS requires the binding of a signalling molecule to its corresponding transcriptional regulator, which activates the downstream transcription of selected targets, and then the production of many virulent determinants in pathogenic bacteria which requires cell-cell communication. Hence, quorum quenching, the process that prevents QS by disrupting signalling, can be achieved by [30]

(i) inhibiting the synthesis of signalling molecules,

(ii) mimicking signalling molecules and binding to their receptors,

(iii) degrading signalling molecules, and

(iv) modifying signalling molecules.

Antimicrobial peptides

Antimicrobial peptides (AMPs) represent one of the main approaches to treat biofilms independent of the presence of microbial activity. One advantage of AMPs is that they are widely conserved and therefore attractive as broad-acting antimicrobial agents that may be useful against both bacterial and fungal biofilms. Although some peptides can have potent antibacterial properties, peptides have poor *in vivo* stability, time-consuming synthesis and high cost. Considering these factors, researchers have been working on developing peptides mimics [31].

Bacteriophages

Phage-based therapies have become interesting alternatives for biofilm removal. These alternatives include the application of simple lytic phages, phage cocktails, a phage derived enzymes, genetically manipulated phages, and their use in combination with traditional antibiotics. The diversity of possible treatments is wide, allowing the design of the appropriate treatment for each case, and favouring personalized medicine. However, further research is still needed to improve efficacy and safety protocols, taking into account the particularities of each biofilm. In addition, more knowledge about phages is needed to increase social acceptance of phage-based treatments to improve their regulation and promote their use in the health and industrial areas [32].

Even new therapeutic solutions for biofilm treatment may not fully reduce the biofilm infection complication cost. Subsequently, the biofilm prevention approach seems to be more beneficial for a patient and health care system by limiting the development of the infection, replacement of the infected device, re-administration to the hospital and additional treatment.

Biofilm prevention

Prevention of biofilm formation on medical devices is more cost-effective than the treatment of the infected implant and improves patient quality of life [3].

Antimicrobial-resistant infections are currently increasing in alarming haste. It is predicted that by 2050, antibiotics therapy failure can claim up to 10 million lives each year. The development of new ways to inhibit bacterial colonization and biofilm formation, especially on medical devices, is an alternative for antibiotic therapy [33].

Many approaches that can prevent biofilm formation on medical materials are in development [3]. We can classify them into two main groups [34,35]:

- Passive/physical – inhibition of the bacteria attachment to the surface or contact killing,

- Active/chemical – realise molecule that will kill bacteria cells by contact with the surface to prevent bacterial adhesion and biofilm development.

The passive approach aims to prevent initial bacteria cell attachment to the material. This approach is aiming for surface modification of biomaterial achieved by imprinting nanostructure and changing the physical properties of the surface itself. The target of the surface modification is to alter the physicochemical properties and/or topological features of the surface to limit the interaction of bacteria with the surface. The effectiveness of this approach will depend on the type of bacteria, the substrate, and the environmental conditions. To achieved antifouling properties, the surfaces of biomaterial can be covered with various types of polymers such as hydrophilic polymers, zwitterionic polymers, hydrophobic polymers, or by engineering surface. Using different technologies such as nanoimprinting lithography, matrix-assisted pulsed laser evaporation or plasma etching, material engineers can modify biomaterial properties such as surface areas roughness, topography, energy, hydrophilicity, etc., to reduce the probability of the bacteria attachment [3,33,35]. Similar approaches have been deployed in other areas such as food, engineering, marine industry etc..., where biofilm prevention is also challenging [36]. Remarkably, these solutions have been inspired by nature itself. It is well-known that various organisms like plants, insects or animals developed bactericidal surfaces. When a specific microorganism is in direct contact with them, it is killed. The bactericidal effects of natural-occurring surfaces are due to the presence of diverse nanostructures that can penetrate through the bacterial cell wall/membrane upon contact or even break the bacteria cell wall/membrane, in the manner to kill the bacteria [33].

The active approach intends to kill bacteria cells by direct contact with the surface, inhibit bacteria growth or interrupt the metabolic pathways correlated *e.g.* with biofilm formation. This strategy involves the use of thin coatings with incorporated antimicrobial agents [35,37.] Please note that most of the active ingredients are used also in biofilm eradication strategies and they were discussed in detail above. To summarize, please find below the list of the active antimicrobial agents that are used in biofilm prevention strategy [34]:

- Polycationic biocides: their activity relying on the electrostatic binding between the positively charged molecules of the biocide and the intrinsically negatively charged cell wall of bacteria, which results in the damage of the latter and subsequently cells death.

- Antimicrobial peptides: small peptides with bactericidal properties, with the permeabilization of the cellular membrane as the main mechanism of action.

- Antimicrobial enzyme: mainly targeting extracellular matrix

- Antibiotics

- Antiseptic agents

- Organic substrates

- Metals

The active antibiofilm surfaces rely on the immobilization of the active molecule on the surface with or without the drug-releasing mechanism.

Moreover, to achieve better antibiofilm coating, we can combine those two strategies. For example, a new surface coating can be designed with dual functionality: prevent the bacterial adhesion together with the release of the bacterial–killing agent. In the literature, there are some examples of this strategy [34].

Currently, there are only four types of coating of medical devices that have clinical results: Using metal – silver and iodine coating, using antibiotics: gentamicin and using polymers: Hyaluronic acid and Poly-lactic acid [33]. Nevertheless, many other antifouling and antimicrobial biomaterial-based surface treatments are in development [37]. Another crucial aspect of the antibiofilm coating solution is safety and toxicity. For example, the usage of silver-based medical devices has been discussed due to the potential toxicity. It is well known, that intake of the silver leads to accumulation of silver in the body. However, all

clinical data demonstrated the clinical safety and efficacy of the silver-coated implants [38]. Notably, the use of antibiotic coated surfaces has a significant concern due to the emergence of multi-drug resistant strains of infectious diseases. The novel surface modification strategies need further authorization to ensure results from laboratory investigation are translated to clinics. Moreover, newly developed materials also have to demonstrate the physiological relevance and lack of toxicity. For example, in the case of the cardiovascular implant, the surface modification should prevent bacterial adhesion, platelet adhesion and reduction of the smooth muscle cells propagation, but promote endothelial cell growth. The novel research on antibiofilm strategies are important and the effect of the biofilm prevention activities need to prove and apply to clinics. It seems that most of the biofilm preventing strategies do not cause the developing resistance mechanism in bacteria similar to the antibiotic resistance. However, the researcher should not forget the necessity to monitor whenever bacteria can adapt to the new surfaces and increase the change for attachment and biofilm formation.

Conclusion

Biofilms are present on earth since the beginning of life (3.4 billion years) [39]. Nonetheless, our understanding of the nature of the biofilm is a relatively novel branch of microbiology. Based on the Pubmed database (pubmed.ncbi.nlm.nih.gov), the first biofilm paper was published in 1975, but in clinical microbiology, the term biofilm is relatively has been introduced ten years later in 1985. Although the first bacteria biofilm was already described in 1677 by Antony Leeuwenhoek [8]. Biofilm research received a great interest in the 2000s, until now there have been over 65000 manuscripts investigating biofilm. However, only less than 10% of the published papers describing the antibiofilm investigation. Consequently, now there are only 145 register clinical trials with the term ‘biofilm” recorded as a condition or disease (www.clinicalTrials.gov).

Moreover, biofilm infections are not only limited to medical devices, but also to opportunistic infections that can develop in organs or tissues such as periodontitis or nonhealing wounds. Furthermore, biofilms are formed in other places where can cause problems such as the food industry, drinkable water supplies, marine industry, etc. Biofilms, however, also have beneficial roles in the environment that can be applied to the industry for example in plant protection, bioremediation, wastewater treatment, etc.
Our current knowledge on biofilm formation, maturation, composition, structure and ways to prevent and destroy biofilm is relatively new. The boost of the biofilm research came together with the development of various models. In the past decade, there have been published some excellent reviews summarizing technologies and models to investigate biofilms, highlighting the advantages and disadvantages of every model available today [8,40,41]. There are a lot of questions and problems related to the biofilm investigation technological. In our point of view, a biofilm investigation is a multidisciplinary mission. We believe that the success of developing novel biofilm control strategies needs collaboration between researchers, engineers, medical doctors and as well as financial executives to achieve a better future for the patients.

The more we would like to investigate new biofilm control strategies related to medicine, the more obvious is the need of developing more advanced models that more closely mimic the *in vivo* pathology. New models need to diminish the gap between *in vitro* and *in vivo* settings, together with bringing us closer to models that can be used as a pre-clinical screening platform. We believe that developing one standard model to investigate biofilm formation, mature and it is destruction/prevention is impractical. When validating new biomaterials/drugs or working with the specific pathology, many biological characteristics such as temperature, cell diversity, immune response, shear condition, volume, etc. need to be incorporated in the model design. The recent progress in microfluidics technology and the development of organ-on-chip strategy [42] should open new possibilities to design pathology-customized platforms to

validate novel biofilm control strategies with translatability to the clinics. Together with other advances in technological improvement over the last few decades such as the multi-OMIC approach and advance microscopy, we might be able to verify how close we can mimic the *in vivo* environment and validate its relevance for pre-clinical evaluation. Here, we would like to propose that new technologies integrating 3D bioprinting, immune response and high-throughput screening capabilities should be developed with a common name: a biofilm-on-chip.

References

1. Flemming HC, Wingender J, Szewzyk U, Steinberg P, Rice SA, Kjelleberg S. Biofilms: an emergent form of bacterial life. *Nat Rev Microbiol* 2016; 14: 563-75.

2. Rumbaugh KP, Sauer K. Biofilm dispersion. *Nat Rev Microbiol* 2020; 18: 571-86.

3. Khatoon Z, McTiernan CD, Suuronen EJ, Mah TF, Alarcon EI. Bacterial biofilm formation on implantable devices and approaches to its treatment and prevention. *Heliyon* 2018; 4: e01067.

4. Olmos D, González-Benito J. Polymeric Materials with Antibacterial Activity: A Review. *Polymers (Basel)* 2021; 13; 613.

5. Wolcott RD, Rhoads DD, Bennett ME, Wolcott BM, Gogokhia L, Costerton JW, *et al.* Chronic wounds and the medical biofilm paradigm. *J Wound Care* 2010; 19: 45-53.

6. Carniello V, Peterson BW, van der Mei HC, Busscher HJ. Physico-chemistry from initial bacterial adhesion to surface-programmed biofilm growth. *Adv Colloid Interface Sci* 2018; 261: 1-14.

7. Boles BR, Horswill AR. Agr-mediated dispersal of Staphylococcus aureus biofilms. *PLoS Pathog* 2008; 4: e1000052.

8. Guzmán-Soto I, McTiernan C, Gonzalez-Gomez M, Ross A, Gupta K, Suuronen EJ, *et al.* Mimicking biofilm formation and development: Recent progress in *in vitro* and *in vivo* biofilm models. *iScience* 2021; 24: 102443.

9. Hall CW, Mah TF. Molecular mechanisms of biofilm-based antibiotic resistance and tolerance in pathogenic bacteria. *FEMS Microbiol Rev* 2017; 41: 276-301.

10. Scherr TD, Heim CE, Morrison JM, Kielian T. Hiding in Plain Sight: Interplay between Staphylococcal Biofilms and Host Immunity. *Front Immunol* 2014; 5: 37.

11. Silva NBS, Marquea LA, Röder DDB. Diagnosis of biofilm infections: current methods used, challenges and perspectives for the future. *J Appl Microbiol* 2021 in presss.

12. Davies D. Understanding biofilm resistance to antibacterial agents. *Nat Rev Drug Discov* 2003; 2: 114-22.

13. Hall-Stoodley L, Stoodley P. Evolving concepts in biofilm infections. *Cell Microbiol* 2009; 11: 1034-43.

14. Lewis K. Persister cells, dormancy and infectious disease. *Nat Rev Microbiol* 2007; 5: 48-56.

15. McDougald D, Rice SA, Barraud N, Steinberg PD, Kjelleberg S. Should we stay or should we go: mechanisms and ecological consequences for biofilm dispersal. *Nat Rev Microbiol* 2011; 10: 39-50.

16. Miyaue S, Suzuki E, Komiyama Y, Kondo Y, Morikawa M, Maeda S. Bacterial Memory of Persisters: Bacterial Persister Cells Can Retain Their Phenotype for Days or Weeks After Withdrawal From Colony-Biofilm Culture. *Front Microbiol* 2018; 9: 1396.

17. Madsen JS, Burmolle M, Hansen LH, Sorensen SJ. The interconnection between biofilm formation and horizontal gene transfer. *FEMS Immunol Med Microbiol* 2012; 65: 183-95.

18. Lebeaux D, Ghigo JM, Beloin C. Biofilm-related infections: bridging the gap between clinical management and fundamental aspects of recalcitrance toward antibiotics. *Microbiol Mol Biol Rev* 2014; 78: 510-43.

19. Hoffman LR, D'Argenio DA, MacCoss MJ, Zhang Z, Jones RA, Miller SI. Aminoglycoside antibiotics induce bacterial biofilm formation. *Nature* 2005; 436: 1171-5.

20. Kaplan JB. Antibiotic-induced biofilm formation. *Int J Artif Organs* 2011; 34: 737-51.

21. Levin-Reisman I, Ronin I, Gefen O, Braniss I, Shoresh N, Balaban NQ. Antibiotic tolerance facilitates the evolution of resistance. *Science* 2017; 355: 826-30.

22. Hogan DA, Kolter R. Pseudomonas-Candida interactions: an ecological role for virulence factors. *Science* 2002; 296: 2229-32.

23. Yan J, Bassler BL. Surviving as a Community: Antibiotic Tolerance and Persistence in Bacterial Biofilms. *Cell Host Microbe* 2019; 26: 15-21.

24. Balaban NQ, Helaine S, Lewis K, Ackermann M, Aldridge B, Andersson DI, *et al.* Definitions and guidelines for research on antibiotic persistence. *Nat Rev Microbiol* 2019; 17: 441-8.

25. Taylor O. Global Markets For Implantable Biomaterials [market report on the Internet]. 2015. https://www.bccresearch.com/market-research/advanced-materials/implantable-biomaterials-markets-report.html

26. Li X, Sun L, Zhang P, Wang Y. Novel Approaches to Combat Medical Device-Associated BioFilms. *Coatings* 2021; 11: 294.

27. Hoiby N, Bjarnsholt T, Moser C, Bassi GL, Coenye T, Donelli G, *et al.* ESCMID guideline for the diagnosis and treatment of biofilm infections 2014. Clin Microbiol Infect 2015; 21 Suppl 1: S1-25.

28. Tran HM, Tran H, Booth MA, Fox KE, Nguyen TH, Tran N, *et al.* Nanomaterials for Treating Bacterial Biofilms on Implantable Medical Devices. *Nanomaterials (Basel)* 2020; 10: 2253.

29. Jiang Y, Geng M, Bai L. Targeting Biofilms Therapy: Current Research Strategies and Development Hurdles. *Microorganisms* 2020; 8: 1222.

30. Makabenta JMV, Nabawy A, Li CH, Schmidt-Malan S, Patel R, Rotello VM. Nanomaterial-based therapeutics for antibiotic-resistant bacterial infections. *Nat Rev Microbiol* 2021; 19: 23-36.

31. Yasir M, Willcox MDP, Dutta D. Action of Antimicrobial Peptides against Bacterial Biofilms. *Materials (Basel)* 2018; 11: 2468.

32. Tian F, Li J, Nazir A, Tong Y. Bacteriophage - A Promising Alternative Measure for Bacterial Biofilm Control. *Infect Drug Resist* 2021; 14: 205-17.

33. Tripathy A, Sen P, Su B, Briscoe WH. Natural and bioinspired nanostructured bactericidal surfaces. *Adv Colloid Interface Sci* 2017; 248: 85-104.

34. Balaure PC, Grumezescu AM. Recent Advances in Surface Nanoengineering for Biofilm Prevention and Control. Part II: Active, Combined Active and Passive, and Smart Bacteria-Responsive Antibiofilm Nanocoatings. *Nanomaterials (Basel, Switzerland).* 2020;10(8):1527.

35. Balaure PC, Grumezescu AM. Recent Advances in Surface Nanoengineering for Biofilm Prevention and Control. Part I: Molecular Basis of Biofilm Recalcitrance. Passive Anti-Biofouling Nanocoatings. *Nanomaterials (Basel)* 2020; 10: 1230.

36. Muhammad MH, Idris AL, Fan X, Guo Y, Yu Y, Jin X, *et al.* Beyond Risk: Bacterial Biofilms and Their Regulating Approaches. *Front Microbiol* 2020; 11: 928.

37. Scialla S, Martuscelli G, Nappi F, Singh SSA, Iervolino A, Larobina D, *et al.* Trends in Managing Cardiac and Orthopaedic Device-Associated Infections by Using Therapeutic Biomaterials. *Polymers* 2021; 13: 1556.

38. Savvidou OD, Kaspiris A, Trikoupis I, Kakouratos G, Goumenos S, Melissaridou D, *et al.* Efficacy of antimicrobial coated orthopaedic implants on the prevention of periprosthetic infections: a systematic review and meta-analysis. *J Bone Jt Infect* 2020; 5: 212-22.

39. Hall-Stoodley L, Costerton JW, Stoodley P. Bacterial biofilms: from the natural environment to infectious diseases. *Nat Rev Microbiol* 2004; 2: 95-108.

40. Azeredo J, Azevedo NF, Briandet R, Cerca N, Coenye T, Costa AR, *et al.* Critical review on biofilm methods. *Crit Rev Microbiol* 2017; 43: 313-51.

41. Lebeaux D, Chauhan A, Rendueles O, Beloin C. From *in vitro* to *in vivo* Models of Bacterial Biofilm-Related Infections. *Pathogens* 2013; 2: 288-356.

42. Chen X, Zhang YS, Zhang X, Liu C. Organ-on-a-chip platforms for accelerating the evaluation of nanomedicine. *Bioact Mater* 2021; 6: 1012-27.

Aortic Endograft Infections

26

Diletta LOSCHI, Annarita SANTORO, Enrico RINALDI, Andrea KAHLBERG, Roberto CHIESA, Germano MELISSANO

Endograft (EG) infection is un uncommon but potentially life-threatening complication of both endovascular repair of both thoracic and abdominal aneurysm. It is a serious pathology associated with increased in-hospital mortality (with even higher rates in case of associated aorto-esophageal (AEF) /bronchial (ABF) /enteric fistula), long-term mortality and comorbidity. A list of criteria concerning clinical, surgical, radiological, and laboratory findings has been proposed by *Management of Aortic Graft Infection Collaboration (MAGIC)* (Table 1), with vascular graft or endograft infection (VGEI) suspicion in the presence of one major or two minor criteria and diagnosis when in the presence of at least a single major criterion and any other criterion.

Diagnosis is complex, requiring a multidisciplinary evaluation using a combination of microbiology tests for micro-organism detecting and diagnostic imaging (traditional methods and nuclear methods). No specific intervention has received strong recommendation with high level of evidence as a protective measure.

Treatment should be carefully chosen and planned, because, although in theory it is quite clear that vascular graft excision would be the best option for definitive treatment, in practice only a small percentage of patients are actually suitable for this major surgery with an acceptable risk. Conservative treatment should be considered for patients unfit-for-surgery, but not recommended in patients with AEF/ABF who have a 100% death rate at 1 year, except in a palliative setting.
The treatment of choice in fit-for-surgery patients is total endograft explantation with arterial reconstruction with new infection-resistant prosthetic grafts or biologic tissue (homograft/ pericardium), perigraft tissue debridement and fistula repair.

In case of acute bleeding, an emergency endovascular intervention to restore hemodynamic stability may be performed as a bridge to open surgery to obtain hemodynamic stabilization. In this chapter we will review management, preventive strategies and treatment modalities for endograft infections.

Introduction

The management of vascular graft and endograft infection (VGEI) is highly complex and clinical approaches and outcomes vary widely. Aortic endograft (EG) infection is a serious and often fatal pathology despite of all the recent surgical and medical advances. When it does occur, detection and definitive therapy are often delayed, with potentially catastrophic consequences and increased in-hospital and long term mortality.[1] If not recognized or treated promptly, implant failure will occur as a result of sepsis, vessel disruption and hemorrhage, or thrombosis with end-organ ischemia[2].

Advancements in EG design and technology along with improvements in operators' experience has led to an increase of both thoracic endovascular aortic repair (TEVAR) and endovascular abdominal aortic repair (EVAR) which are considered as a safe and less invasive alternative to aortic open repair and in most cases the treatment of choice in many centres for aortic aneurysm, dissection, traumatic injury, aortic coarctation and other related conditions. The number of endovascular aortic repair has consistently increased over the last decades. Although initially used only in significantly compromised patients for whom open surgical repair would carry prohibitively high risk, it has been extended to patients with fewer comorbidities. It is not surprising that with its expanding use the device-related complications rate (endoleaks, EG migration, limb kinking and/or stenosis and infection with oesophageal/bronchial and enteric fistula) has increased accordingly.

The growing number of EVAR/TEVAR also brings a growing number of aorto-enteric fistula (AEF) or aortobronchial fistula (ABF); the proposed mechanism of fistula formation in case of endovascular repair include persistent endoleak with growth of the aneurysmal sac, erosion of the EG through the aorta, endotension and infection at the time of EG placement [3-4]. Besides this, as published in the MAEFISTO Study [5] in an evaluation of 3932 patients from 8 Italian centres from 1997 to 2013 who underwent EVAR, treatment in an urgent/emergent setting and anastomotic pseudoaneurysm as indication for EVAR were significantly associated with AEF development. In urgent/emergency surgery, the presence of a hematoma compressing surrounding structures or the overall increase in local inflammation may contribute to the genesis of AEF [5].

Epidemiology

Thoracic/thoraco-abdominal endograft infections

Thoracic EG infections range from 1.53% to 4.77% [6-7] and are still associated with a considerable mortality rate that exceeds 70% in the largest published series [8-10]. AEF and ABF are common presentations of thoracic EG infection that carry a worse prognosis. As results from a multicenter study by the San Raffaele group [8] on 1113 patients who underwent TEVAR between 1998 and 2008, AEF or ABF occurred in 1.7%, with increased incidence in anastomotic pseudoaneurysm, significantly associated with AEF/ABF development (16% *vs.* 2%; P Z 0.009), with an increased risk in emergently performed procedures (37% *vs.* 13%; P Z 0.008).

Abdominal endograft infections

EG infection has been reported to occur in 0.4–3.0% of cases after EVAR of the abdominal aorta [11-13]. Mortality rates ranges from 25% to 50% and are usually secondary to septic shock or hemorrage [12-14].
The MAEFISTO study showed that the incidence of AEF following EVAR was 0.46% (15/3262) in case of EVAR performed for atherosclerotic aneurysmal disease, and 3.9% (7/179) in case of EVAR performed for post-surgical pseudoaneurysm.
Both anastomotic pseudoaneurysm as the indication to EVAR and urgent / emergent EVAR were significantly associated with AEF development (34% *vs.* 5%, $p < 0.0001$; and 22% *vs.* 8%, $p = 0.01$).

Classification

As far as both open surgery grafts and endovascular EG are concerned, the *Management of Aortic Graft Infection Collaboration (MAGIC)*, has developed a list of major and minor criteria regarding clinical, surgical, radiological, and laboratory findings [15] (Table 1). If infection is suspected, a complete evaluation of the patient's clinical status, signs of infection, and comorbidities according to the MAGIC criteria can be done (recommendation Class of Evidence I, Level C from the latest ESVS Guidelines) [15-17]: VGEI is suspected in the presence of one major or two minor criteria of the three different categories and diagnosed when there is at least a single major criterion and another criterion from other categories [15]. A second classification, based on time of appearance, divided Aortic VGEI into early (< 4 months) or late (> 4 months) onset, despite its clinical relevance still remains a subject of debate [17].

Table 1: Management of Aortic Graft Infection Collaboration classification

	Clinical/Surgical	Radiology	Laboratory
Major Criteria	- Perigraft/aneurysm sac pus (confirmed by microscopy) - Open wound with exposed graft or communicating sinus - Aorto-enteric/aorto-bronchial fistula detection - Graft insertion in an infected site (fistula, mycotic aneurysm or infected pseudo-aneurysm)	- Perigraft fluid more than 3 months after intervention (detected with CTA) - Perigraft gas more than 7 weeks after intervention (detected with CTA) - Increase in perigraft gas volume detection on serial imaging	- Organisms recovered from an explanted graft - Organisms recovered from an intraoperative specimen - Organisms recovered from a percutaneous aspirate of perigraft fluid
Minor Criteria	- Localised clinical features of graft infection (erythema, warmth, swelling, purulent discharge, pain) - Fever more than 38C with graft infection as most likely cause	- Other: suspicious perigraft gas/ fluid soft tissue inflammation, aneurysm expansion, pseudo-aneurysm formation: focal bowel wall thickening, discitis/osteomyelitis, suspicious metabolic activity on FDGPET/CT, radiolabelled leukocyte uptake	- Blood culture(s) positive with no apparent source, exception made for graft infection - Abnormally elevated inflammatory markers with graft infection as most likely cause (erythrocyte sedimentation rate, C reactive protein, white cell count)

Pathogenesis

Several factors may contribute to the pathogenesis of VGEI [18]. Experimental data showed that EG present lower bacterial resistance and greater bacterial adherence, two main factor that show a strong correlation with the length of EG [19-20].

Several causative mechanisms have been recognized: hematogenous seeding, local bacterial translocation and iatrogenous contamination [21]; procedures with multiple catheter manipulations inside an EG have been found responsible for infection as well [21-22]. As previously mentioned, urgent/emergency procedures are associated with a significantly higher percentage of EG infection [8].

Presence of AEF or ABF can contribute to the development of late VGEI. With a rate reaching 5% of treated patients in the largest case series [1], fistulization into the esophagus or the trachea/bronchus is defined as a potential late complication after both open thoracic aortic replacement and TEVAR [23]. Ischemic insult to the bronchial or esophageal wall (as the stent graft may interfere with esophageal and bronchial feeding arteries) [24], progressive mechanical erosion by noncompliant structures (*e.g.* excluded thrombosed aneurysms) (Figure 1) or the endograft itself which acts as a stiff foreign body [25], may play an important role in the pathogenesis. Excessive EG oversizing has been found to impact in long-term deterioration of the arterial wall, EG migration, and aortic aneurysm enlargement, and should be considered as a possible mechanism of fistulization [26].

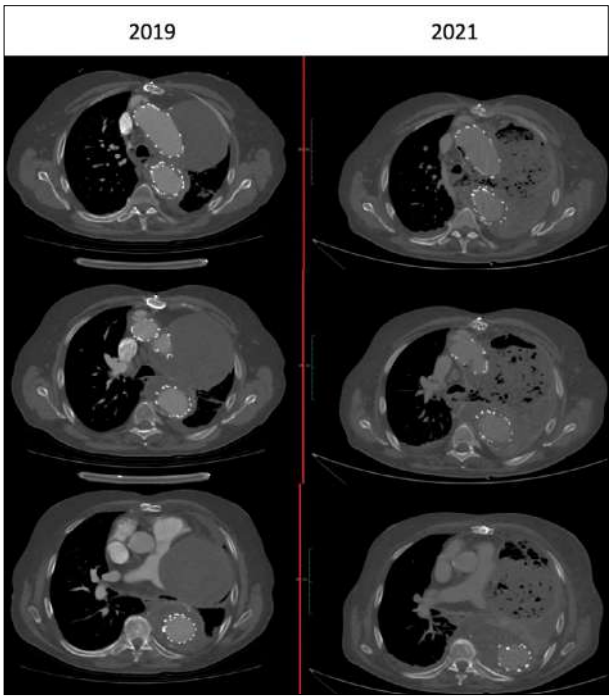

Figure 1: Endograft infection after total endovascular aortic arch replacement (Ishimaru zone 0) + supraortic trunk debranching.

2019: One-month follow up CTA

2021: Aneurysm sac infection with perigraft air

Clinical presentation

Endograft infection may have three different modes of clinical presentation: non specific signs of low grade sepsis, severe systemic sepsis and signs of aorto-enteric fistula [27]. Patients with sepsis as the predominant feature have similar symptoms to those with infection of a surgically implanted aortic graft; symptoms of low-grade sepsis include general malaise, weight-loss and lethargy; signs of systemic sepsis include fever and a systemic inflammatory response; Aorto-enteric fistula, which may or may not be associated with signs of sepsis. In the series published by Ducasse *et al.* [28] 40% of patients presented with gastrointestinal hemorrhage, the remaining 60% with signs of systemic sepsis.

Post-implantation syndrome, a clinical entity characterized by temporary fever associated with elevated leukocytes and CRP may follow endograft implantation and it should be clearly distinguished from infection [29].

Thoracic/thoraco-abdominal endograft infections

Thoracic back pain is a common presenting symptom, caused by inflammation of the aorta/surrounding structures. In the Italian multicentre national survey[4], nearly 90% of patients presented with hematemesis/hemoptysis and approximately half had signs of shock.

Abdominal endograft infections

Abdominal and back pain are common presenting symptoms and are related to inflammation of the aorta and its surrounding structures. Pseudoaneurysm or aortic rupture are prominent features in almost 10% of cases[27] and this possibility should be considered in any patient presenting with cardiovascular instability. Diabetic ketoacidosis, septic thromboembolism, and graft limb thrombosis are less common presentation.

Diagnosis

Microbiology and Sampling technique

Micro-organism identification is crucial in the process of patient's best treatment selection. (MAGIC major criteria)[15]. Gram positive bacteria are responsible pathogens in up to 58% of VGEI (Enterococci, Staphylococcus aureus, and coagulase negative staphylococci); Gram negative bacteria account for 34% and anaerobes 8%[30]. Microbiological sample has a crucial relevance since it may support determining the diagnosis of VGEI. Ideally samples should be harvested before the start of antimicrobial therapy or during pharmacological washout, however the most important feature affecting the test accuracy/relevance is adequate quantity and the absence of surrounding structures contamination[31]. Specimens obtained directly from the suspected infection site (surgically explanted prosthetic materials, intra-operatively obtained tissue and graft biopsies from the infected area, and/or at least three samples from perigraft fluid collection) provide the most meaningful results (direct samples should be collected in sterile containers)[32]. Indirect specimens (blood cultures, obtained from a superficial wound, a draining sinus, or otherwise close anatomical structures) might also be meaningful, especially when direct specimens collection is not possible; however, the results should be considered with caution.

Imaging (Conventional *vs.* Nuclear methods)

Conventional diagnostic methods

Ultrasound (US) is a widely used, non-invasive and low cost imaging modality to identify findings associated with VGEI as the presence of pseudoaneurysm, sustained presence of gas (still detected >7 weeks) and purely anechoic fluid collections (still detected>3 months after surgery)[33]. Its sensitivity for the diagnosis of VGEI is considered low and additional investigations are needed to confirm diagnosis. Computed tomography angiography (CTA) has been considered the gold standard for the VGEI diagnosis for a long time, detecting some peculiar features: perigraft air, ectopic gas, tissue infiltration, intrasac collections, fluid accumulation and soft-tissue attenuation, pseudoaneurysm, discontinuity of the aneurysmal wall or focal bowel thickening and direct contrast enhancement in the bowel in the arterial phase[18]. Although better than US, CTA sensitivity/specificity is variable[33]. As reported in a recent meta-analysis of patients with suspected VGEI, the pooled sensitivity of CTA in diagnosing VGEI was 0.67 (95% confidence interval [CI] 0.57 e 0.75) and the pooled specificity was 0.63 (95% CI 0.48 e 0.76). This meta-analysis showed that an isolated CTA may not provide enough evidence to establish the diagnosis of VGEI[34] and a second imaging modality such as 18F-FDG-PET/CT or WBCS combined with SPECT/CT might be considered.

One more recent meta-analysis reporting a series of patients with suspected aortic VGEI showed that Magnetic Resonance Angiography (MRA) sensitivity was 0.68 (95% CI 0.50 e 0.86), specificity 0.97 (95% CI 0.91 e 1.00) [35]. However, MRA is not used as the diagnostic modality of choice when suspecting VGEI owing to logistics and long acquisition times often resulting in motion artefacts.

18F-FDG PET/CT and Labelled Leucocytes

The underlying principle in 18F-fluoro-D-deoxyglucose positron emission tomography (18F-FDG-PET) is the uptake of radioactive labelled glucose in cells/tissue with enhanced glucose metabolism (inflammatory cells and micro-organisms as bacteria or fungi). With this diagnostic exam a differentiation between sterile periprosthetic collection and infected graft material could be made, but it should be combined with low dose CT for anatomical correlation. Nowadays, when performed in hybrid mode with FDG-PET/CT, provides accurate anatomical information about the site of infection [36]. The EANM and Society of Nuclear Medicine and Molecular Imaging published procedural guidelines on how to perform and interpret a 18F-FDG-PET scan [37]. There are different ways to analyse 18F-FDG-PET/CT results, but the most used is the calculated maximum standardised uptake value (SUVmax), with a SUVmax > 8 in the perigraft area as cut off value for distinguishing infected grafts from non-infected ones [37].

White blood cell scintigraphy (WBCS) detects infected sites considering the increase of accumulation of radiolabelled white blood cells (WBC) over time. Recently, procedural guidelines for the labelling of the WBC, the correct acquisition technique and interpretation mode for WBCS were published [38]. The presence of pathological accumulation of labelled WBC at the site of infection is crucial and could reinforce VGEI diagnosis. Two sets of images are required (2 and 4, 20 and 24 hours after injection) and an increase in size intensity over time is considered positive for infection. When positive, SPECT/CT in the hybrid mode is necessary for exact localisation of the infection (soft tissue only, graft, or extension) [38]. The exam is time consuming and labour intensive, as it needs to be performed at two different time points and in a specifically equipped laboratory. Besides this, its diagnostic accuracy depends on the region of the body investigated, as it shows less accuracy in the central parts of the body than in peripheral as the tracer is eliminated via the intestinal tract and taken up in the bone marrow.

Strategy to prevent aortic endograft infections

No difference of susceptibility to infection between different alloys currently used for EG has been demonstrated [39]. Prophylactic therapy refers to the administration of antibiotics before the occurrence of bacterial contamination, prior to surgery and at regular intervals during the procedure to maintain serum and tissue levels above the minimal bactericidal concentration [1]. Bactericidal are preferable to bacteriostatic after vascular interventions. All general principles regarding hygiene standards should minimize vascular infections: among them, respect a strict antiseptic protocol is the most relevant.

Despite all the existing evidences, in the latest guidelines [16] no specific intervention has received a strong recommendation with high level of evidence as a protective measure.

Management of infected aortic endograft

Conservative treatment

Antimicrobial therapy is the key principle of conservative treatment [16]. It is empirical and broad spectrum only in an acute phase when it is indicated to control sepsis, in a second phase the choice is based on antibiogram and percutaneous drainage results (US/CT guided). Conservative management is offered to patients unfit-for-surgery; alternatives include percutaneous drainage followed by irrigation with saline or antiseptic solution and extraction of infectious material from the cavity [7,43]. No consensus in the literature regarding the optimal antimicrobial therapy or administration period has been described. In usual clinical practice, for the initial 4-6 weeks it is given intravenously at the maximal tolerated dosage and then followed by an oral regimen once the acute phase has subsided. Although many authors indicate a mean duration of therapy of at least 6 months for VGEI, when the infection cannot be totally eradicated (excessive risk from the procedure prevents surgery) the patient is treated with intravenous antibiotics for 6 weeks and then continue with an oral regimen indefinitely [40-41]. Conservative treatment of patients with AEF or ABF is not recommended, except in a palliative setting, since it is associated with a 100% death rate at 1 year in a recent review [43].

Thoracic-thoracoabdominal infected aortic endograft

EG infection radical treatment consists in total EG explantation with arterial reconstruction, debridement, and fistula repair if present [44]. Due to the usually poor health condition of these patients and the extreme invasive procedure, it is burdened with high mortality rates [44]. Although in theory it is quite clear that vascular graft excision would be the best option for durable and definitive treatment (Figure 2), in practice only a small percentage of patients can be considered fit for this major surgery with an acceptable operative risk. Besides this, in some selected cases, as for example in the presence of supraortic-trunk stents, whose removal would require extra corporeal circulation, total EG explantation could be counterproductive and even dangerous. In these selected cases 1-2 stents could be left in place, in order to reduce the procedure invasiveness.

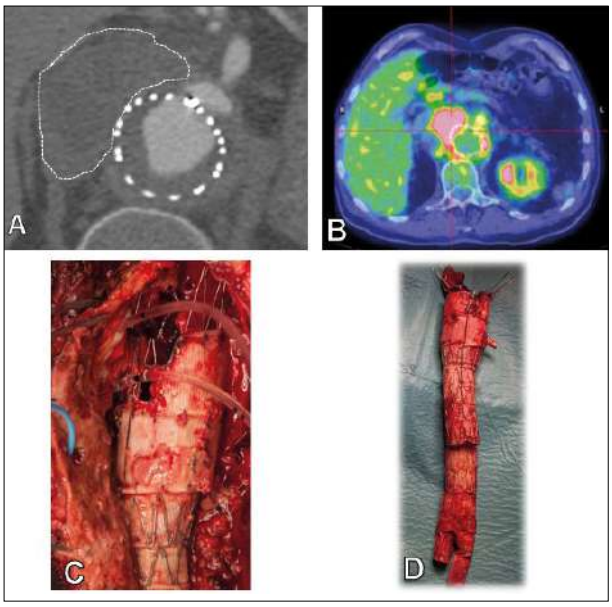

Figure 2 A: A post-operative CTA in a 70-years-old who underwent F-EVAR for extent IV TAAA

Figure 2 B: PET-CT showing perigraft fluid collection in a patient with fever

Figure 2 C: Fluid perigraft collection

Figure 2 D: Total endograft excision

In case of acute bleeding, an emergent endovascular intervention may be performed as a bridge to control the hemorrhage and obtain hemodynamic stabilization (Figure 3A, 3B)[1,45]. After that, the definitive treatment consisting in surgical replacement of the aortic infected graft, mainly using *in situ* repair with new infection-resistant prosthetic grafts, is the best choice to decrease risks of prolonged sepsis or reinfection (Figure 4).

Open surgery repair technique

A standard thoracoabdominal surgical repair is performed (general anesthesia, thoracophrenolaparotomy in the V–VII intercostal space, cerebrospinal fluid drainage, motor/somatosensory-evoked potential, left-heart bypass, 4°C Custodiol solution for kidney perfusion in case of thoracoabdominal aortic involvement) (Figure 5A). In case of associated fistula (AEF of ABF), it could be useful to prepare a pedicled intercostal muscle or omental flap to cover and reinforce the esophageal or bronchial lesion after repair. Once the infected aorta is isolated between clamps, the infected segment is transected and separated from the esophagus. The infected endograft is completely excised when possible (Figure 5B) and

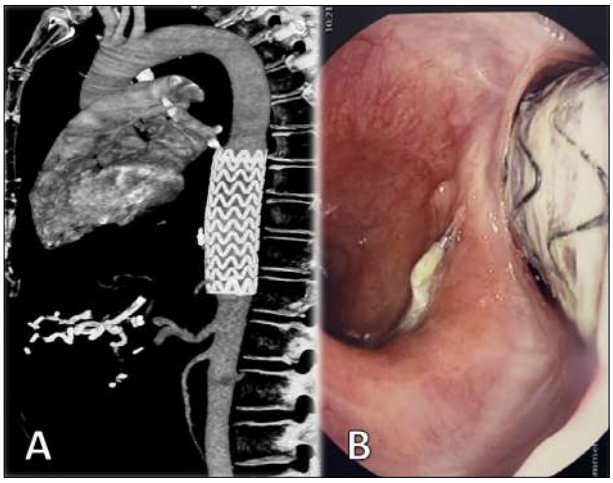

Figure 3A: CTA in a 52-years-old patient who underwent emergent TEVAR due to hematemesis in aorto-esophageal fistula after "sleeve gastrectomy" procedure – Angio TC showed excessive oversizing

Figure 3B: Esophagogastroduodenoscopy showing esophageal lesion and protruding endograft.

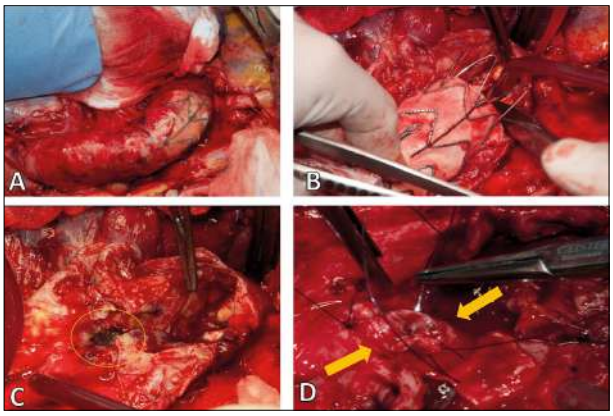

Figure 5A: Thoraco-abdominal aortic exposure in a patient who underwent thoracic aorta open replacement and TEVAR due to distal anastomotic pseudoaneurysm. Distal tract of infected thoracic prosthetic graft and aorto-esophageal fistula is showed

Figure 5B: Total infected thoracic endograft excision (extended from distal thoracic descending aorta to suprarenal abdominal aorta)

Figure 5C: Identification of Aorto-esophageal fistula. Methylene blue administration through a naso-esophageal tube during the procedure allowed AEF identification

Figure 5D: Esophageal raffia and double-layer suture

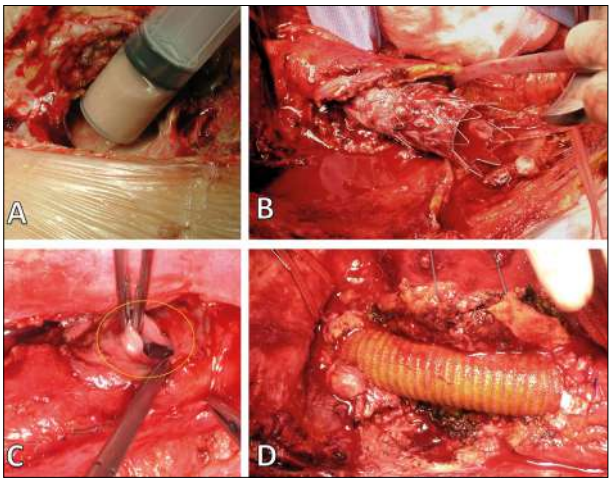

Figure 4A: Aorto-esophageal fistula after TEVAR complicated by abscess

Figure 4B: Compete removal of the infected graft

Figure 4C: Esophageal lesion

Figure 4D: Aortic reconstruction with silver triclosan prosthesis

sent for microbial cultures, perigraft tissues extensively debrided and the left pleural cavity is repeatedly washed with antiseptic solutions. Some authors [1,8] have described the use of *in situ* revascularization with a silver and triclosan, knitted, collagen-coated, polyester prosthesis *(InterGard Synergy; Maquet, La Ciotat, France)* (Figure 6).

In case of AEF, the lesion should be promptly identified (Figure 5C); Administration of methylene blue through a naso-esophageal tube could be useful.

Primary esophageal repair may be accomplished in case of limited lesions by means of double-layer separated stitches of the esophageal wall using absorbable sutures (Figure 5D). In this case it is usually reinforced with coverage by a previously prepared pedicled intercostal muscle flap/ omentum (Figure 7A) pulled up in the thorax. More extensive esophageal lesions may need partial or total resection of the esophagus (Figure 7B), with cervical closure that may be performed during the first operation (with nutritional jejunostomy) or in a staged reconstruction.

Cryopreserved aortic homografts use for *in situ* aortic revascularization has been proposed for thoracic aortic graft or EG infection, AEF, and ABF [1,42], but their resistance to infection is still matter of debate.

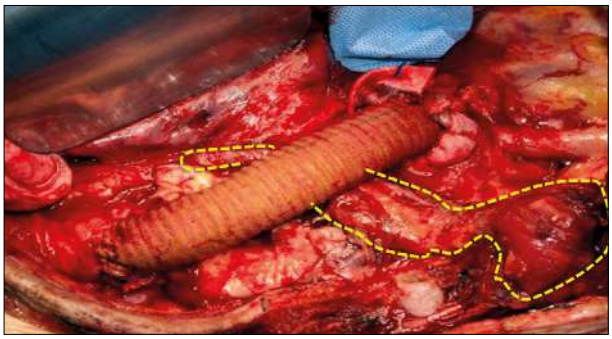

Figure 6: Aortic reconstruction with silver triclosan prosthesis and intercostal muscle flap was mobilized on the anterior intercostal artery, tagged around the fistula

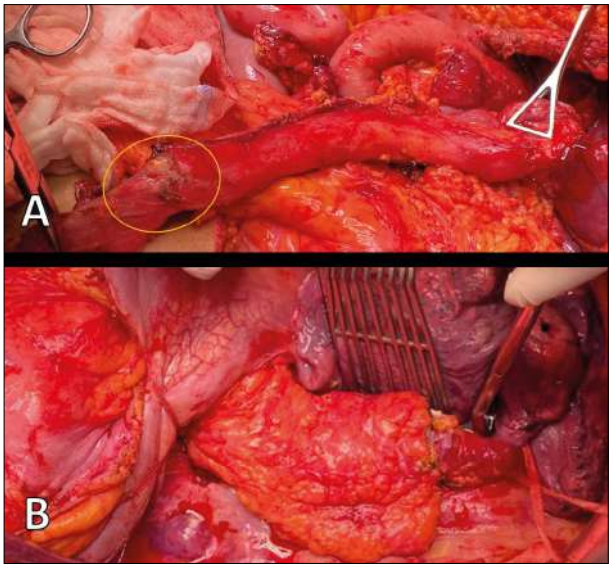

Figure 7: Primary esophageal repair:
A) reinforcement with coverage by omentum
B) partial/total resection of the esophagus

Endovascular treatment, hybrid strategies, and bridging modalities

Patients who received a combined treatment consisting of TEVAR associated with ABF/AEF repair, compared to patients who underwent TEVAR alone showed a trend of reduced mortality (mortality: 53% v 30%, respectively).

In active bleeding patients from an AEF/ABF, an endovascular approach can be used as an emergency strategy to restore hemodynamic stability [42], but it has considerable limitations, mainly related to the impossibility to eliminate the primary infected graft.

A multicentre study analysing 25 cases of AEF and ABF treated with TEVAR, reported a 30-day mortality rate of 28%, with overall mortality of 44% at 23-months follow-up and reintervention rate of 28% (mortality of 60%)[8].

As reported in an international multicentre registry (European Registry of Endovascular Aortic Repair Complications) in 2014-15, survival with a radical surgical approach was statistically significantly better when compared with any other treatment strategy in case of AEF and ABF after TEVAR alone[45].

Abdominal infected aortic endograft

When an AEF with stent-graft involvement is detected, its treatment is also ideally represented by total graft excision with arterial reconstruction, and associated bowel repair. As previously mentioned for thoracic repair, some circumstances in the abdominal tract could prevent total endograft excision (*e.g.* suprarenal stents); in this case total EG explantation could drive to adjuntive peri-operative risks (*e.g.* renal arteries damage) or need more proximal extension treatment.

Some factors, such as the procedure technical difficulties (often requiring a suprarenal or supraceliac aortic clamping)[5], the associated anemia and septic state at presentation and usually poor pre-existing conditions could affect these patients outcome. For all above reasons is not surprising that mortality after surgery for post-EVAR AEF is reported to be extremely high, ranging between 50% and 100%, independently from the adopted revascularization technique[14].

In situ reconstruction

In case of AEF repair, if possible, complete removal of all infected EG components is a good option, although partial extraction may be contemplated in frail patients, followed by *in situ* aortic reconstruction with graft covering with omentum or any other autogenous tissue. This technique has the advantage to obtain immediate limbs revascularization, to avoid groin and axillary incisions, exclude the risk of ascending aortic thrombosis and decrease long-term graft occlusion and amputation rate[28]. An alternative could be represented by cryopreserved allografts or venous grafts (so called “femoropopliteal neoaortoiliac systems”). In the recently published experience of the Vascular Low-Frequency Disease Consortium[46], among 206 abdominal or thoracic EG infections, 54 patients received cryopreserved allografts and 21 patients received neoaortoiliac systems, showing the limit of a longer operative time (> 500 minutes), but the advantage of better 5-year survival when compared to prosthetic replacements.

Extra-anatomical bypass

Infrarenal aortic ligation, extensive debridement, and extra-anatomical bypass represent another commonly used surgical technique to repair AEF in high grade contamination with associated purulent fluid collection or severe retroperitonitis[13,48]. It allows to perform revascularization before aortic EG explantation, even in two staged procedures in case of non-emergency setting, in order to reduce overall surgical stress. However, high risks of aortic stump disruptions (20%), graft occlusion resulting in amputation (29%), and reinfection (20%) should be considered[18].

Conclusions

Advancements in technology and improvement in operators' experience has led, in the last decades, to a growing number of TEVAR and EVAR performed, with a growing number of endovascular-related complications, among these EG infection without or with oesophageal/bronchial and enteric fistula.
Diagnosis may be challenging in the less defined clinical presentations, with different diagnostic methods that must be taken into account in order to ensure an early and accurate diagnosis.
Despite all the evidences, in the latest guidelines no specific intervention has received a strong recommendation with high level of evidence as a protective measure.
If the patient's risk profile contraindicates open surgery, he can be conservatively treated with intravenous antibiotics for 6 weeks and then continue with an oral regimen indefinitely. When a concomitant ABF or AEF is documented (that carries 100% death rate at 1 year), only truly inoperable patients are rejected to palliative cures.
Radical treatment for EG infections consists in total EG explantation with arterial reconstruction, débridement, and repair of the fistula if present; several technical variations have been proposed with procedure improvement throughout the years. Nevertheless, some factor heavily affect the outcome in these patients (*e.g.* procedure technical difficulties, associated anemia and septic state at presentation and usually poor pre-existing general conditions).
As a bridging modality in patients presenting active bleeding from an AEF or ABF, a primary endovascular approach can be used as an alternative strategy to stop bleeding and restore hemodynamic stability.

References

1. Kahlberg A, Melissano G, Mascia D, Loschi D, Grandi A, Chiesa R. How to best treat infectious complications of open and endovascular thoracic aortic repairs. *Semin Vasc Surg* 2017; 30: 95-102.
2. Bandyk DF. Vascular graft infections: epidemiology, microbiology, pathogenesis, and prevention. Bernhard VM, Towne JB. Complications in Vascular Surgery. *Quality Medical: St Louis* 1991:223
3. Saratzis N, Saratzis A, Melas N, Ktenidis K, Kiskinis D. Aortoduodenal fistulas after endovascular stent-graft repair of abdominal aortic aneurysms: single-center experience and review of the literature. *J Endovasc Ther* 2008; 15: 441-8.
4. Chiesa R, Melissano G, Marone EM, Kahlberg A, Marrocco-Trischitta MM, Tshomba Y. Endovascular treatment of aortoesophageal and aortobronchial fistulae. *J Vasc Surg* 2010; 51: 1185-202.
5. Kahlberg A, Rinaldi E, Piffaretti G, Speziale F, Trimarchi S, Bonardelli S, *et al.* Italy Results from the Multicenter Study on Aortoenteric Fistulization After Stent Grafting of the Abdominal Aorta (MAEFISTO). *J Vasc Surg* 2016; 64: 313-20.
6. Moulakakis KG, Mylonas SN, Antonopoulos CN, Kakisis JD, Sfyroeras GS, Mantas G, *et al.* Comparison of treatment strategies for thoracic endograft infection. *J Vasc Surg* 2014; 60: 1061-71.
7. Chiesa R, Tshomba Y, Kahlberg A, Marone EM, Civilini E, Coppi G, *et al.* Management of thoracic endograft infection. *J Cardiovasc Surg* (Torino) 2010; 51: 15-31.
8. Chiesa R, Melissano G, Marone EM, Marrocco-Trischitta MM, Kahlberg A. Aorto-oesophageal and aortobronchial fistulae following thoracic endovascular aortic repair: a national survey. *Eur J Vasc Endovasc Surg* 2010; 39: 273-9.
9. Lyons OT, Patel AS, Saha P, Clough RE, Price N, Taylor PR. A 14-year experience with aortic endograft infection: management and results. *Eur J Vasc Endovasc Surg* 2013; 46: 306-13.
10. LeMaire SA, Green SY, Kim JH, Sameri A, Parenti JL, Lin PH, *et al.* Thoracic or thoracoabdominal approaches to endovascular device removal and open aortic repair. *Ann Thorac Surg* 2012; 93: 726-32.
11. Daye D, Walker TG. Complications of endovascular aneurysm repair of the thoracic and abdominal aorta: evaluation and management Cardiovasc Diagn Ther 2018; 8: S138-S156.
12. Chaikof EL, Blankensteijn JD, Harris PL, White GH, Zarins CK, Bernhard VM, *et al.* Reporting standards for endovascular aortic aneurysm repair. *J Vasc Surg* 2002; 35: 1048-60.
13. Murphy EH, Szeto WY, Herdrich BJ, Jackson BM, Wang GJ, Bavaria JE, *et al.* The management of endograft infections following endovascular thoracic and abdominal aneurysm repair. *J Vasc Surg* 2013; 58: 1179-85.
14. Capoccia L, Speziale F, Menna D, Esposito A, Sirignano P, Rizzo AR, *et al.* Preliminary Results from a National Enquiry of Infection in Abdominal Aortic Endovascular Repair (Registry of Infection in EVAR--R.I.EVAR). *Ann Vasc Surg* 2016; 30: 198-204.

15. Lyons OT, Baguneid M, Barwick TD, Bell RE, Foster N, Homer-Vanniasinkam S, *et al.* Diagnosis of aortic graft infection: a case definition by the management of aortic graft infection collaboration (MAGIC). *Eur J Vasc Endovasc Surg* 2016; 52: 758-63.

16. Chakfé N, Diener H, Lejay A, Assadian O, Berard X, Caillon J, *et al.* European Society for Vascular Surgery (ESVS) 2020 Clinical Practice Guidelines on the Management of Vascular Graft and Endograft Infection. *Eur J Vasc Endovasc Surg* 2020: 59: 339-84.

17. BackMR. Local complications: graft infection. In: CronenwettJL, Johnston KW, editors. *Rutherford's vascular surgery* 2014. pp. 654-62.

18. Setacci C, Chisci E, Setacci F, Ercolini L, de Donato G, Troisi N *et al.* How To Diagnose and Manage Infected Endografts after Endovascular Aneurysm Repair. *Aorta (Stamford)* 2014; 2: 255-64.

19. Thibodeaux LC, James KV, Lohr JM, Welling RE, Roberts WH. Infection of endovascular stents in a swine model. *Am J Surg* 1996; 172: 151-4.

20. Hearn AT, James KV, Lohr JM, Thibodeaux LC, Roberts WH, Welling RE. Endovascular stent infection with delayed bacterial challenge. *Am J Surg* 1997; 174: 157-9.

21. Setacci C, De Donato G, Setacci F, Chisci E, Perulli A, Galzerano G, *et al.* Management of abdominal endograft infection. *J Cardiovasc Surg* (Torino) 2010; 51: 33-41.

22. Capoccia L, Mestres G, Riambau V. Current technology for the treatment of infection following abdominal aortic aneurysm fixation by endovascular repair (EVAR). *J Cardiovasc Surg (Torino)* 2014; 55: 381-9.

23. Dietrich EB. Endovascular intervention suite design In: White RA, Fogarty TJ. Peripheral Endovascular Interventions. *St. Louis: Mosby* 1996, pp. 129–139.

24. Eggebrecht H, Baumgart D, Radecke K, von Birgelen C, Treichel U, Herold U, *et al.* Aortoesophageal fistula secondary to stent-graft repair of the thoracic aorta. *J Endovasc Ther* 2004;11:161-7.

25. Hance KA, Hsu J, Eskew T, Hermreck AS. Secondary aortoesophageal fistula after endoluminal exclusion because of thoracic aortic transection. *J Vasc Surg* 2003; 37: 886-8.

26. VonFricken K, Karamanoukian HL, Ricci M, Taheri A, Bergsland J, Salerno TA. Aortobronchial fistula after endovascular stent graft repair of the thoracic aorta. *Ann Thorac Surg* 2000; 70: 1407-9.

27. Hobbs SD, Kumar S, Gilling-Smith GL. Epidemiology and diagnosis of endograft infection. *J Cardiovasc Surg (Torino)* 2010; 51: 5-14.

28. Ducasse E, Calisti A, Speziale F, Rizzo I, Misuraca M, Fiorani P. Aortoiliac stent graft infection: current problems and management. *Ann Vasc Surg* 2004; 18: 521-6.

29. Corfield L, Chan J, Chance T, Wilson N. Early pyrexia after endovascular aneurysm repair: are cultures needed? *Ann R Coll Surg Engl* 2011; 93: 111-3.

30. Batt M, Feugier P, Camou F, Coffy A, Senneville E, Caillon J, *et al.* A meta-analysis of outcomes after *in situ* reconstructions for aortic graft infection. *Angiology* 2018; 69: 370-9.

31. Baron EJ, Miller JM, Weinstein MP, Richter SS, Gilligan PH, Thomson Jr RB, *et al.* A guide to utilization of the microbiology laboratory for diagnosis of infectious diseases: 2013 Recom-mendations by the Infectious Diseases Society of America (IDSA) and the American Society for Microbiology (ASM). *Clin Infect Dis* 2013; 57: 22-121.

32. Osmon DR, Berbari EF, Berendt AR, Lew D, Zimmerli W, Steckelberg JM, *et al.* Diagnosis and management of prosthetic joint infection: clinical practice guidelines by the infectious diseases society of America. *Clin Infect Dis* 2013; 56: 1-25.

33. Bruggink JLM, Slart RHJA, Pol JA, Reijnen MMPJ, Zeebregts CJ. Current role of imaging in diagnosing aortic graft infections. *Semin Vasc Surg* 2011; 24: 182-90.

34. Reinders Folmer EI, Von Meijenfeldt GCI, Van der Laan MJ, Glaudemans AWJM, Slart RHJA, Saleem BR, *et al.* Diagnosis imaging in vascular graft infection: a systematic review and meta-analysis. *Eur J Vasc Endovasc Surg* 2018; 56: 719-29.

35. Shahidi S, Eskil A, Lundof E, Klaerke A, Jensen BS. Detection of abdominal aortic graft infection: comparison of magnetic reso-nance imaging and indium-labeled white blood cell scanning. *Ann Vasc Surg* 2007; 21: 586-92.

36. Keidar Z, Engel A, Hoffman A, Israel O, Nitecki S. Prosthetic vascular graft infection: the role of 18F-FDG PET/CT. *J Nucl Med* 2007; 48: 1230-6.

37. Jamar F, Buscombe J, Chiti A, Christian PE, Delbeke D, Donohoe LJ, *et al.* EANM/SNMMI Guideline for 18F-FDG use in inflammation and infection. *J Nucl Med* 2013; 54: 647-58.

38. Signore A, Jamar F, Israel O, Buscombe J, Martin-Comin J, Lazzeri E. Clinical indications, image acquisition and data interpretation for white blood cells and anti-granulocyte mono-clonal antibody scintigraphy: an EANM procedural guideline. *Eur J Nucl Med Mol Imaging* 2018; 45: 1816-31.

39. Haefner TA, Lewis C, Baluh G, Clemens M, Propper B, Arthurs ZM. Initial Inoculation Concentration Does Not Affect Final Bacterial Colonization of *In vitro* Vascular Conduits. *Surg Infect* 2018; 19: 352-7.

40. Spiliotopoulos K, Preventza O, Green SY, Price MD, Amarasekara HS, Davis BM, *et al.* Open descending thoracic or thoracoabdominal aortic approaches for complications of endo-vascular aortic procedures: 19-year experience. *J Thorac Cardiovasc Surg* 2018; 155: 10-8.

41. Revest M, Camou F, Senneville, Caillon J, Laurent F, Calvet B, *et al.* Medical treatment of prosthetic vascular graft infections: review of the literature and proposals of a working group. *Int J Antimicrobial Agents* 2015; 46; 254-65.

42. Kahlberg A, Grandi A, Loschi D, Vermassen F, Moreels N, Chakfe N, *et al.* Infection of descending thoracic aortic graft and endograft: a systematic review. *J Vasc Surg* 2019; 69: 1941-51.

43. Moulakakis KG, Sfyroeras GS, Mylonas SN, Mantas G, Papapetrou A, Antonopoulos CN, *et al.* Outcome after preservation of infected abdominal aortic endografts. *J Endovasc Ther* 2014; 21: 448-55

44. Girdauskas E, Falk V, Kuntze T, Borger MA, Schmidt A, Scheinert D, *et al.* Secondary surgical procedures after endovascular stent grafting of the thoracic aorta: successful approaches to a challenging clinical problem. *J Thorac Cardiovasc Surg* 2008; 136: 1289-94.

45. Czerny M , Reser D, Eggebrecht H, Janata K , Sodeck G, Etz C, *et al.* Aorto-bronchial and aorto-pulmonary fistulation after thoracic endovascular aortic repair: an analysis from the European Registry of Endovascular Aortic Repair Complications. Multicenter Study. *Eur J Cardiothorac Surg* 2015; 48: 252-7.

46. Fatima J, Duncan AA, de Grandis E, Oderich GS, Kalra M, Gloviczki P, *et al.* Treatment strategies and outcomes in patients with infected aortic endografts. *J Vasc Surg* 2013; 58: 371-9.

47. Smeds MR, Duncan AA, Harlander-Locke MP, Lawrence PF, Lyden S, Fatima J, *et al.* Vascular Low-Frequency Disease Consortium. Treatment and outcomes of aortic endograft infection. *J Vasc Surg* 2016; 63: 332-40.

48. Laser A, Baker N, Rectenwald J, Eliason JL, Criado-Pallares E, Upchurch GR Jr. Graft infection after endovascular abdominal aortic aneurysm repair. *J Vasc Surg* 2011; 54: 58-63.

Cryopreserved allografts in vascular infection

27

David GARBAISZ, Zoltan SZEBERIN

The aim of this study was to review the literature of the last 5 years showing allograft use in vascular septic conditions, which helps to provide insight into the current results of vascular allografts.

Data were collected between 1st January, 2016 and 30th June, 2021. A systematic search was conducted for publications of cryopreserved allograft usage for vascular infection in Medline and Pubmed databases. The results of the publications were reviewed based on the following key endpoints: study design, patient's characteristics, mortality rate, graft related complication and reintervention rate, graft patency, limb salvage, graft reinfection rate and survival rate.

After a systematic search, 13 publications were included. The articles were divided into two groups: aortic and peripheral. The aortic group included nine studies covering the data of 511 patients. Early mortality rate (< 30 days) was between 2.8% and 42.8%. Allograft related reintervention rates ranged between 5.9% and 29% (early and late). The rate of reinfection was below 10 %. Four studies were included into the peripheral group covering the data of 252 patients. Early mortality rate (< 30 days) was between 2.0% and 38%. Allograft related reintervention rates ranged between 4.0% and 55% (early and late). Reinfection rate is around 4%, but only poor quality data are available.

Vascular infections remain a challenging problem, however, cryopreserved allografts show low reinfection rate and reasonable durability; thus, allografts may be an acceptable option for reconstruction.

Introduction

Vascular prosthetic graft infection (VGI) or vascular surgery in an infected field are one of the most difficult situations for vascular surgeons. Incidence of VGI after open vascular surgery is up to 2%.[1, 2] Septic vascular complications occur with high morbidity and mortality. Moreover, the difficult situation often aggravated by the poor general condition of patients and a number of comorbidities. There is no consensus of the ideal surgical treatment, total or partial excision of the infected prosthesis, broad debridement, drainage and in-situ or extra anatomical reconstruction are all accepted. *In situ* reconstruction may involve additional hazards, as there is a risk of recurrence of the infection, however, in many centers this is the generally accepted treatment method.

Aortic infection is one of the most dreadful conditions in septic vascular surgery, posing a significant challenge for vascular surgeons. There are two major appearances of aortic infection: native abdominal aortic infected aneurysms (incidence: 0.7-2.6%)[3] and abdominal aortic VGI and endovascular device infections (incidence: 0.2-3.0%; 0.1-1.2%, respectively)[4]. The mortality of infected (mycotic) aneurysms is increased.[5] Aortic graft infections result in remarkably high morbidity and mortality rates of 10-50%.[6] Aortic infection – either prosthetic graft or mycotic aneurysm – can be treated by the excision of the infected aneurysm or prosthetic graft following extra-anatomic bypass reconstruction or *in situ* reconstruction with different graft materials.

The other significant difficulty for the vascular surgeon is to perform peripheral arterial reconstruction in the setting of an infected field or VGI. Surgical therapy consists of excision of all infected tissues, drainage and restoration of vascular continuity either with extra-anatomic bypass or in-situ reconstruction. Peripheral VGI has been reported in up to 2.5% in femoro-femoral prosthetic bypasses [7] and in up to 2.8% in femoro-popliteal prosthetic bypasses [8, 9].

In septic vascular surgery, there is no consensus on the type of the ideal graft material. Several types of vascular grafts are considered for *in situ* reconstruction; however, the best choice is the autologous vascular graft (autograft). Due to lack or inadequacy of the autograft, silver or antibiotic-bonded prosthetic graft, xenologous graft (xenograft) and fresh or cryopreserved allogen graft (allograft, homograft) may be considered for vascular reconstruction.

Allograft means a biological vascular graft, which was explanted during multiple organ donation from humans, and its use can be recommended during graft replacement in the presence of VGI either in the case of aortic or peripheral VGI or operation in an infected field. The use of allograft has decades of experience. The first human aortic allograft implantation was performed by Gross. [10] De Bakey *et al.* [11] used aortic allograft for the first time in occlusive aortic disease.

Our aim was to review the literature of the last 5 years showing cryopreserved allograft use in vascular septic conditions, which helps to provide insight into the current results of cryopreserved vascular allografts. Our study may help to build a unified consensus on the use of graft material in septic vascular surgery that is currently lacking.

Methods

Data were collected using manuscripts published between 1st January, 2016 and 30th June, 2021. A systematic search was conducted for publications of interest in Medline and Pubmed databases. The Preferred Reporting Items for Systematic Reviews and Meta-Analyses (PRISMA) guidelines were used to perform our review.

During the database search, the Medical Subject Headings (MESH) terms were used. We performed the search in the database using the following keywords: "vascular" [All Fields], "allograft" [All Fields], "homograft" [All Fields] "cryopreserved" [All Fields], and "infection" [All Fields], with search filters: 5 years, full text, English.

Our inclusion criterias were: full text, English language, original article and abstract available. Publications were investigated focusing on the use of cryopreserved aortic, arterial and venous allografts for reconstruction after aortic or peripheral lower extremity native or secondary VGI. Articles that present multiple graft materials which are analyzed together, were excluded. The exclusion criterias included articles available only with an abstract, other language, review article, conference abstract, research letter and case report.

The included publications were investigated according to the following study endpoints: study design, patient's characteristics, mortality rate, graft related complication and reintervention rate, graft patency, limb salvage, graft reinfection rate and survival rate.
Article search, selection and data extraction were undertaken by two investigators.

Results and Discussion

Data Collection

The database search-with keywords detailed above and filter settings-identified 48 potentially eligible publications. Following review of the titles and abstracts, 19 were eligible for our study requirements. After further review of the articles, 6 more publications were excluded for the following reasons: review articles, case reports and research letter. The remaining 13 articles were included in our review. Reviewed articles were divided into two groups according to the topic of the publications: aortic and peripheral. Two articles were suitable to be included into both groups, in both cases we decided based on the structure of the studies.

The small number of manuscripts found during the search show that usage of cryopreserved allograft during vascular infections is a less studied subject of vascular surgery. This may be due to the fact that to date, there is no consensus on graft material during vascular infection, previous variable results of allograft implantation are still debated, and the few homograft banks are still difficult to access worldwide.

Aortic

Nine studies were included into the aortic group about cryopreserved allograft implantation for infected abdominal aortic aneurysm repair and/or surgery of abdominal aortic prosthetic graft and endovascular device infections (Table 1). The majority of the studies were single center studies, which are based on prospectively collected and retrospectively analyzed data. The investigated period ranges from 1997 to 2018. Reviewed articles include 511 patients. Most of the studies are low patient volume investigations, however, three of them report higher volume: 71 [12], 96 [13] and 200 [6] patients.

As in the case of cardiovascular disease in general, the vast majority of patients are males, and their mean age ranges from 64.2 to 71 years.

Early mortality rate (< 30 days) is between 2.8% and 42.8%. Four studies reported mortality rates below 10 percent [12,14-16], two papers reported between 10 and 25 percent [17, 18] and one study reports death rates above 40 percent [19]. Mortality data from the latter study are extremely high, but similarly high data can be found in the literature. Coselli *et al.* [20] performed polyethylene terephthalate (PET) prosthesis and cryopreserved allograft implantation in thoracic aortic infection and also reported similarly high mortality (42%). It is important to note that both studies report homograft results used in thoracic aortic infection, and the mortality rate of thoracic aortic infection is very high, up to 75 percent. [9] Late mortality data were approximately similar to early mortality data, they range between 2.8% and 42%.

Publications which reported allograft related reintervention rates range between 5.9% and 29% (early and late). Ben Ahmed *et al.* [12] reported 3% early lethal allograft rupture rate, and they did not observe any dilation or aneurysm of the allografts. Similarly in the investigation of Bossi M *et al.* [17], no rupture, degenerated aneurysm or re-infection occurred. Weiss *et al.* [15] found relatively high graft related complication rates in 12% of patients (early) and 29% of patients (late), including graft stenosis (16%), occlusion (13%) and pseudoaneurysm formation (10%). The appearance of graft-related complications is thought to be alarming according to their conclusions, however, they consider the type of conservation procedure to be important. Couture *et al.* [6] reported allograft related complications in 7.5% (early) and 12.5% (late), and they concluded that midterm allograft related complications are common but associated with low mortality and amputation rates. According to most of the studies, graft collection, conservation and preoperative handling techniques have a great importance in avoiding allograft-related complications. Most of the studies concluded that graft-related complications occur less in the case of cryopreserved allograft implantation than in the case of fresh allograft usage. Cryopreserved allograft

seems to have better collagen preservation and mechanical stability [21, 22], in addition cryopreservation does not affect the viscoelasticity of muscular arteries and the wall structure of elastic arteries [23].

The reviewed publications reported approximately similar survival rates, generally 1- and 3-year data were provided. 1-year survival rate ranges from 70% to 80% and 3-year survival rate ranges from 60% to 70%. Few articles reported 5-year survival rate ranges, they ranged between 54% and 66%.

VGI is a dreaded and significant complication in septic vascular surgery. *In situ* replacement of infected vascular prostheses with antibiotic-soaked PET grafts has an 11% reinfection rate, compared with less than 4% reinfection after allograft implantation. [13] However, the best reinfection rate results can be achieved with autologous graft replacement.

The rate of reinfection, reported by all articles analyzed in this paper was below 10 %. Several articles reported that there was no reinfection among the series they investigated. [16-19] One article reported a higher reinfection rate of 8.5%. [6]

To minimize graft reinfection following allograft implantation during infection, the publications recommended a multimodal surgical approach: complete original graft removal, aggressive peri-prosthetic debridement of contaminated tissues, coverage of the implanted allograft with a pediculated omentum flap (abdominal cases), close follow-up and prolonged multiple anti-microbial therapy.

Publications agree that allograft implantation is a valuable choice in aortic infection and an option with acceptable, relatively low morbidity and mortality outcomes. Just one article reported frequent graft-related complications and suggests that special attention should be paid to this fact. [15] In general, low incidence of graft degeneration and graft-related complications following cryopreserved allograft implantation has been reported. Several studies mentioned the importance of homograft conservation, graft handling and surgical technique to achieve better surgical outcomes.

The small number of homograft banks and the difficult availability of allografts are mentioned as a common problem.

Table 1: Summary of publication data – aortic (NA: not available)

Authors	Study design	Study period	No of patients	Male	Mean age	Early mortality (<30 days)	Rate of reoperation	Late mortality (>30 days)	Graft patency	Graft re-infection rate	Postoperative complications	Allograft related complications / reintervention	Survival
Masabni [14]	single center retrospective	August 2007 – August 2017	17	12 (71%)	68.3	5.9%	17.6%	NA	NA	5.9%	NA	5.9% (early) 23.4% (late)	1 month, 6 months, 1 year, and 3 years, estimated survival was 94%, 82%, 75%, and 64%

Ben Ahmed [12]	double-center retrospective	Jan. 2000 - July 2016	71	91.5%	65.2	2.8%	15.5%	2.8%	Primary patency rates at 1 year, 3 years, and 5 years were 100%, 93.5%, and 93.5% Assisted primary patency rates at 1 year, 3 years, and 5 years were 100%, 96%, and 96%	4.2%	50.7% (early)	5.6% (early) 12.7% (late)	Survival rates at 1 year, 3 years, and 5 years were75%, 64%, and 54%
Bossi M [17]	single center prospectively collected retrospectively analyzed	Jan. 2010 - March 2016	21	19 (90%)	71 ± 12	14%	NA	22%	Estimated survival was 64% at 3 years	0.0%	NA	NA	Estimated survival was 64% at 3 years
Weiss [15]	single center, retrospective	2000-2015	33	91%	67	6%	NA	42%	NA	6%	NA	12% (early) 29% (late)	The estimated survival at 1, 3, and 5 years was 88%, 81%, and 66%
Arasu [18]	single center, retrospective	2010-2018	13	NA	NA	23%	NA	8%	overall primary graft patency: 89%	0.0%	8 (62%)	NA	early 77%, late 69%
Heo [16]	single center retrospective review of prospectively collected data	May 2006 - July 2015	25	80% (n=20)	70.2	8%	NA	20%	NA	0.0%	24% (early)	12%	Patient survival was 74% and event-free survival was 58% at 3 years
Couture [6]	single center prospectively collected and retrospectively reviewed	Jan. 2009 - Dec. 2017	35	n=31	65.6	42.8%	31.5%	22.5%	NA	0.0%	NA	11.4%	The 1-and 2-year survival rates were 49.3% and 42.5%
Minga Lowampa [13]	single center retrospective analysis of prospectively collected data	July 2000 - July 2015	96 (3 groups)	NA	NA	9%	NA	NA	NA	NA	NA	29%, 44%	5-year: 44%, 90%
Couture *et al.* [6]	single center retrospective	Jan. 1997 – Dec. 2013	200	184 (92%)	64.2	11%	29.5%	26.5%	The one, three, and five year primary patency rates were, respectively, 92%, 84%, and 80%	8.5%	NA	7.5% (early) 12.5% (late)	1, 3, and 5 year survival rates were, respectively, 76%, 66%, and 56%

Peripheral

Four studies were included in the peripheral group on the topic of cryopreserved allograft implantation during surgery of VGI or operation on an infected field (Table 2).

One of the analyzed papers is a single center study, which is based on prospectively collected and retrospectively analyzed data and three studies are single center retrospective investigations. The investigated period ranges from 1992 to 2018. Reviewed articles included 252 patients. Most of the studies were low patient volume investigations, however, one paper reports higher volume of 118 [24] patients.
As in the case of cardiovascular disease in general, the vast majority of patients are males, and their mean age ranges from 61 to 69 years.

Lejay *et al.* [25] investigated cryopreserved arterial allograft for arterial reconstruction in patients with prosthetic infection. They divided patients into two groups. In Group 1, surgery was performed at the aorto-iliac level (47%), in Group 2, operation was performed at peripheral level (53%). Based on their study, they underline that the results are not as favourable as it was postulated. Five-year allograft related reintervention rate was 55% in Group 1 and 33% in Group 2. They highlighted that data regarding allograft related re-intervention are conflicting, which can be attributed to the technical differences in cryopreserved arterial allograft management. Homograft conservation, graft handling, and surgical technique may affect long-term outcomes. Similarly, conflicting results have been reported for allograft reinfection. They emphasized that early multidisciplinary team engagement in the diagnosis and management process of graft infection has a great importance.

Furlough *et al.* [26] studied peripheral artery reconstructions using cryopreserved arterial allografts in infected cases. They highlighted that one of the main advantages of allograft implantation is the low reinfection rate. The rate of reinfection in their study was 3.5%, as opposed to prosthetic grafts, which have a reinfection rate of 10% based on literature data. [27, 28] To prevent graft reinfection, they performed additional procedures, such as selective muscle flap coverage and vacuum-assisted wound drainage systems. Similarly convincing low amputation rate has been reported, with a total of one graft-related amputation mentioned in their paper. The process of allograft conservation and handling has a great importance, which can determine graft-related complications. They described two major allograft related complications, such as graft thrombosis and graft degeneration. For both complications, two patients were reported in their results. In summary, their results are very favorable, but it should be noted that their conclusions are based on small sample size.

Mestres *et al.* [24] reported a 20-year experience of cryopreserved arterial allografts for vascular infections. In their publication, the reported 30-day mortality rate was 38% for infected patients, which is higher than in other reports in the literature. [28,29] This result is explained by the fact, that half of the operations were done on an urgent/emergent basis, and a significant proportion of patients had additional comorbidities, which required concomitant non-vascular procedures as well. In their conclusions, they emphasized two major difficulties. First, vascular allografts were very difficult to obtain, and second, there is no gold standard in the treatment of vascular infection. In many vascular centers, allograft is not available in urgencies/emergencies. The authors concluded that allografts have remarkably good results in a multimorbid population.

Heinola *et al.* [30] investigated cryopreserved venous allografts in supra-inguinal reconstructions. In their study, only venous allografts were examined, as their previous experience showed more complications in arterial allografts. Acute graft thrombosis and atherosclerotic degeneration were more common in arterial allografts. The cryopreservation method used by the research group did not preserve endothelial function, thus preventing immunological reactions which could cause vascular occlusion. It is important to highlight that they also emphasize low graft reinfection rate, which is 4% in their results. They concluded, that cryopreserved venous allografts appear to be an infection resistant and reasonably safe reconstruction material.

Table 2: Summary of publication data – peripheral (NA: not available)

Authors	Study design	Study period	No of patients/procedures	Male	Mean age	Early mortality (<30 days)	Late mortality (>30 days)	Graft patency	Limb salvage	Graft reinfection rate	Postoperative complications	Allograft related complications/reintervention	Survival
Lejay [25]	single center retrospective analysis of prospectively collected data	Jan. 2005 - Dec. 2014	Group 1 (aortoiliac): 25 patients	Group 1: 20 men (80%)	Group 1: 65 years	Group 1: 8%	Group 1: 15 patients	Group 1: Primary patency was 96% at 12 and 24 months and 89% at 60 months	Group 1: 100% at 12, 24, and 60 months	unclear data	Group 1: 24%	Allograft related re-intervention was 22%, 40%, and 55% at 12, 24, and 60 months	Group 1: Survival was 80%, 68%, and 40% at 12, 24, and 60 months
			Group 2 (peripheral): 28 patients	Group 2: 20 men (71%)	Group 2: 68 years	Group 2: 0.0%	Group 2: 8 patients	Group 2: Primary patency rate was 96%, 86%, and 59% at 12, 24, and 60 months	Group 2: 100%, 93%, and 89% at 12, 24, and 60 months		Group 2: 14%	Group 2: At 12, 24, and 60 months, the allograft related re-intervention rate was 11%, 25%, and 33%	Group 2: 100%, 93%, and 68% at 12, 24, and 60 months
Furlough [26]	single center retrospective	Jan. 2002 - July 2017	57 reconstructions	35 men	61	9%	NA	NA	NA	3.5%	NA	14% (early) 15.8% (late)	
Mestres [24]	single center, retrospective	Oct. 1992 - May 2014	118	87%	64	38%	NA	NA	NA	NA	NA	15% (early) 21% (late)	5.9 years
Heinola [30]	single center, retrospective	Feb. 2012 - March 2018	24	65%	69	9%	9%	NA	100%	4%	43%	4%	74%

Conclusion

In conclusion, VGI remains a significant and challenging problem in vascular surgery. There is still no consensus in septic vascular surgery on treatment options, especially on the graft material used for reconstruction. Cryopreserved allograft may be an acceptable choice for either aortic or peripheral arterial reconstruction, although the results remain controversial. Based on the results of the publications, the main conclusions are that cryopreserved allografts show low reinfection rate and reasonable durability. The results of graft patency, especially at the peripheral level, remain controversial.

Several articles highlighted the importance of conservation and handling techniques of cryopreserved allografts, which could determine the incidence of graft-related complications. The development and standardization of cryopreservation methods is an important task in the future.

Research and publications in recent years have helped bring us closer to a consensus, but there are still many unanswered questions.

One of the main difficulties –which is mentioned in most papers -is the lack of easily accessible homograft banks and thus the poor availability of allografts. As a result, few research is being done on cryopreserved allografts, and good quality publications are rare. In addition, most of the studies are based on low volume investigations, making it difficult to draw solid conclusions.

The other obstacle is that most of the studies are single center studies. It would be important to conduct multi-center studies, emphasizing the establishment of international collaboration in this field of vascular surgery.

References

1. Debus ES, Diener H. Reconstructions Following Graft Infection: An Unsolved Challenge. *Eur J Vasc Endovasc Surg* 2017; 53: 151-2.

2. Lorentzen JE, Nielsen OM, Arendrup H, Kimose HH, Bille S, Andersen J, *et al.* Vascular graft infection: an analysis of sixty-two graft infections in 2411 consecutively implanted synthetic vascular grafts. *Surgery* 1985; 98: 81-6.

3. Kahlberg A, Melissano G, Tshomba Y, Leopardi M, Chiesa R. Strategies to treat thoracic aortitis and infected aortic grafts. *J Cardiovasc Surg (Torino)* 2015; 56: 269-80.

4. Cronenwett JL, Johnson KW. Rutherford's Vascular Surgery: Elsevier; 2014.

5. Oderich GS, Panneton JM, Bower TC, Cherry KJ, Jr., Rowland CM, Noel AA, *et al.* Infected aortic aneurysms: aggressive presentation, complicated early outcome, but durable results. *J Vasc Surg* 2001; 34: 900-8.

6. Couture T, Gaudric J, Du Montcel ST, Jayet J, Verscheure D, Davaine JM, *et al.* Short and Mid Term Outcomes of Cryopreserved Abdominal Aortic Allografts Used as a Substitute for Infected Prosthetic Grafts in 200 Patients. *Eur J Vasc Endovasc Surg* 2021; 62: 89-97.

7. Eiberg JP, Røder O, Stahl-Madsen M, Eldrup N, Qvarfordt P, Laursen A, *et al.* Fluoropolymer-coated dacron *versus* PTFE grafts for femorofemoral crossover bypass: randomised trial. *Eur J Vasc Endovasc Surg* 2006; 32: 431-8.

8. Exton RJ, Galland RB. Major groin complications following the use of synthetic grafts. *Eur J Vasc Endovasc Surg* 2007; 34: 188-90.

9. Chakfé N, Diener H, Lejay A, Assadian O, Berard X, Caillon J, *et al.* Editor's Choice - European Society for Vascular Surgery (ESVS) 2020 Clinical Practice Guidelines on the Management of Vascular Graft and Endograft Infections. *Eur J Vasc Endovasc Surg* 2020; 59: 339-84.

10. Gross RE. Treatment of certain aortic coarctations by homologous grafts; a report of nineteen cases. *Ann Surg* 1951; 134: 753-68.

11. Debakey ME, Creech O, Cooley DA. Occlusive disease of the aorta and its treatment by resection and homograft replacement. *Ann Surg* 1954; 140: 290-310.

12. Ben Ahmed S, Louvancourt A, Daniel G, Combe P, Duprey A, Albertini JN, *et al.* Cryopreserved arterial allografts for *in situ* reconstruction of abdominal aortic native or secondary graft infection. *J Vasc Surg* 2018; 67: 468-77.

13. Minga Lowampa E, Holemans C, Stiennon L, Van Damme H, Defraigne JO. Late Fate of Cryopreserved Arterial Allografts. *Eur J Vasc Endovasc Surg* 2016; 52: 696-702.

14. Masabni K, Weaver MR, Kandagatla P, Shepard AD, Huang J, Al Adas Z, *et al.* Cryopreserved Allograft in the Management of Native and Prosthetic Aortic Infections. *Ann Vasc Surg* 2019; 56: 1-10.

15. Weiss S, Bachofen B, Widmer MK, Makaloski V, Schmidli J, Wyss TR. Long-term results of cryopreserved allografts in aortoiliac graft infections. *J Vasc Surg* 2021; 74: 268-75.

16. Heo SH, Kim YW, Woo SY, Park YJ, Kim DK, Chung DR. Recent Results of *In Situ* Abdominal Aortic Reconstruction with Cryopreserved Arterial Allograft. *Eur J Vasc Endovasc Surg* 2017; 53:158-67.

17. Bossi M, Tozzi M, Franchin M, Ferraro S, Rivolta N, Ferrario M, *et al.* Cryopreserved Human Allografts for the Reconstruction of Aortic and Peripheral Prosthetic Graft Infection. *Ann Vasc Dis* 2017; 10: 391-7.

18. Arasu R, Campbell I, Cartmill A, Cohen T, Hansen P, Muller J, *et al.* Management of primary mycotic aneurysms and prosthetic graft infections: an 8-year experience with in-situ cryopreserved allograft reconstruction. *ANZ J Surg* 2020; 90: 1716-20.

19. Couture T, Gaudric J, Davaine JM, Jayet J, Chiche L, Jarraya M, *et al.* Results of cryopreserved arterial allograft replacement for thoracic and thoracoabdominal aortic infections. *J Vasc Surg* 2021; 73: 626-34.

20. Coselli JS, Köksoy C, LeMaire SA. Management of thoracic aortic graft infections. *Ann Thorac Surg* 1999; 67: 1990-3; discussion 7-8.

21. Gournier JP, Adham M, Favre JP, Raba M, Bancel B, Lepetit JC, *et al.* Cryopreserved arterial homografts: preliminary study. *Ann Vasc Surg* 1993; 7: 503-11.

22. Vogt PR. Arterial allografts in treating aortic graft infections: something old, something new. *Semin Vasc Surg* 2011; 24: 227-33.

23. Rosset E, Friggi A, Novakovitch G, Rolland PH, Rieu R, Pellissier JF, *et al.* Effects of cryopreservation on the viscoelastic properties of human arteries. *Ann Vasc Surg* 1996; 10: 262-72.

24. Mestres CA, Quintana E, Kopjar T, Ambrosioni J, Almela M, Fuster D, *et al.* Twenty-year experience with cryopreserved arterial allografts for vascular infections. *Eur J Cardiothorac Surg* 2019; 55: 358-65.

25. Lejay A, Delay C, Girsowicz E, Chenesseau B, Bonnin E, Ghariani MZ, *et al.* Cryopreserved Cadaveric Arterial Allograft for Arterial Reconstruction in Patients with Prosthetic Infection. *Eur J Vasc Endovasc Surg* 2017; 54: 636-44.

26. Furlough CL, Jain AK, Ho KJ, Rodriguez HE, Tomita TM, Eskandari MK. Peripheral artery reconstructions using cryopreserved arterial allografts in infected fields. *J Vasc Surg* 2019; 70: 562-8.

27. Brown KE, Heyer K, Rodriguez H, Eskandari MK, Pearce WH, Morasch MD. Arterial reconstruction with cryopreserved human allografts in the setting of infection: A single-center experience with midterm follow-up. *J Vasc Surg* 2009; 49: 660-6.

28. Vogt PR, Brunner-La Rocca HP, Carrel T, von Segesser LK, Ruef C, Debatin J, *et al.* Cryopreserved arterial allografts in the treatment of major vascular infection: a comparison with conventional surgical techniques. *J Thorac Cardiovasc Surg* 1998; 116: 965-72.

29. Kieffer E, Gomes D, Chiche L, Fléron MH, Koskas F, Bahnini A. Allograft replacement for infrarenal aortic graft infection: early and late results in 179 patients. *J Vasc Surg* 2004; 39: 1009-17.

31. Heinola I, Kantonen I, Mattila I, Albäck A, Venermo M. Cryopreserved Venous Allografts in Supra-inguinal Reconstructions: A Single Centre Experience. *Eur J Vasc Endovasc Surg* 2019; 58: 912-9.

Investigation of Decellularized Porcine Biograft

28

Gábor FAZEKAS, Gábor MENYHEI, Gábor JANCSÓ

Conventional bypass surgery plays an important role among other options in treating symptomatic atherosclerotic disease of the lower extremities. Graft infection is a dreadful complication following prosthetic vascular graft utilization. Successfull treatment of septic vascular graft can be only achieved by graft replacement in the most of the cases. Among other options, a biological vascular graft could serve as an alternative choice. To reduce immunogenicity, decellularization of the tissue is necessary. Our aim was to determine an efficient decellularization method and to evaluate the decellularized porcine-biografts' adaptability.

Cell removal effectiveness and extracellular matrix structure preservation of the decellularization protocol was analyzed by histological stainings. Pressure tests were performed to determine mechanical properties of the treated grafts. Decellularized vascular grafts were interpositioned in the infrarenal part of porcines' aorta. After a 6 month follow-up period, implanted samples were removed and evaluated using light- and electron-microscopy.

Histological results showed complete removal of cells and preserved connective tissue fiber-structure following decellularization. Pressure tests demonstrated similar biomechanical compliance to fresh vessels. In nine out of ten cases, porcines survived the follow-up period. Graft rejection, intimal hyperplasia, reocclusion and/or aneurysm formation were not observed. Presence of host-cells and neo-endothelization in the implanted aortic segment were microscopically confirmed.

This decellularization protocol enables a cost-effective preparation of biological grafts featuring reduced immunogenicity. The implanted grafts did not degenerate during the 6-month follow-up period, the lack of graft rejection suggests acceptable immunological tolerance, while recipient cells migrate into, proliferate and differentiate, thus creating the possibility for further use as an optional vascular graft.

Introduction

One of the most dreadful complications of prosthetic bypass surgery is graft infection. The treatment of septic graft is professionally considered among the most difficult challenges in vascular surgery, including a high morbidity and mortality rate. In milder cases, only superficial wound infection occurs. However, deep spreading of the inflammation, including the area of the reconstruction, or development of generalized sepsis is a challenging complication for the specialists. These infections can develop also in the postoperative period (early infections) and much later (late infections), too.

There are different methods to treat graft infection, ranging from drainage to complete graft removal, however, in most cases, survival of the limb and/or the patient can be assured only with successful graft replacement. To effectively achieve this, impregnated (antibiotics, silver) prosthetic grafts or biological grafts (which is more advantageous to eliminate infections) be used. However, expensive impregnated grafts are subject to frequent occurrences of reinfection, and in several countries they are no longer

approved for human implantation. The use of autologous grafts, which currently proves to be the best solution, significantly increases the operative risk and their availability is restricted. The application of cadaver, cryopreserved homologous grafts is a favorable option, nevertheless, these grafts are considerably expensive, their storage requires special infrastructure and the availability is, at present, limited. The third group of biological grafts are xenografts, originating from another species.

The goal of our investigation was the development of a biological vascular graft, which combines the favorable properties of the different types of grafts, thus could be an alternative choice for graft replacement in the septic vascular surgical field. Advantages of these grafts include adequate biomechanical properties, high resistance against infections and unlimited availability.[1-3] However, the most distinct disadvantage of biograft is the triggering of the immune response.[1-4] To reduce immunogenicity, decellularization of the graft is necessary.[1-5] Decellularization removes all cellular components from the tissue, preserving the original structure of the connective tissue scaffold.[1,4] Following implantation, hosts cells migrate into, proliferate and differetiste in the implanted graft's scaffold, and, consequently, the "harmful" immune response will not develop against the new tissue.[1,2,5]

Materials and methods

Series – Examination of decellularized porcine aortic segments

Decellularization:

Infrarenal aortic segments were freshly excised from porcines. Following separation of the adhesive tissue, a macroscopic examination was performed to exclude any pathology, and aortic segments (2cm in length and diameter about 8mm) were next washed in sterile phosphate buffered saline (PBS) to remove residual traces of blood. Aortic segments were decellularized through continuous shaking in 1% sodium-duodecyl-sulfate (SDS; Sigma-Aldrich Chemie Gmbh, Steinheim, Germany), and 0.05% sodium-azide (NaN3; Alfa Aesar Gmbh & Co, Karlsruhe, Germany), in phosphate buffered saline (PBS; Sigma-Aldrich Chemie Gmbh, Steinheim, Germany), at room temperature, for 48 hours. The solution was exchanged every 6 hours. At the end of the decellularization protocol, the aortic segments were washed using PBS for 12 hours to effectively remove residual detergents and cell debris.[6,7]

Light microscopy evaluation:

Prepared segments of aortic wall were fixed for 24 hours in 10% neutral buffered formalin, in support of routine histological examination. Cross-sectional and longitudinal tissue blocks were embedded using paraffin, and 2-4 micrometer thick sections were sliced. Sections were stained applying 3 different methods, using protocols recommended by the manufacturers. Hematoxylin-Eosin (HE) staining demonstrated the cell-removal effectiveness of the decellularization protocol. Orcein and Masson-Trichrome (MT) histochemistry stains illustrated the structure of the connective tissue fibers, and the preservation of elastic and collagen fibers (both from Bio-Optica, Milano, Italy). Histological sections were analyzed using Pannoramic Viewer software (3DHistec Ltd.) and 100x magnification. Absence or presence of cell nuclei and preservation of extracellular matrix (ECM) compared with native samples were evaluated by two independent pathologists.

Transmission electron microscopy evaluation:

Samples of vessels were prepared for transmission electron microscopy (TEM) examination by fixation in 2% formaldehyde and 2.5% glutaraldehyde containing solution, for 12 hours, maintained to 4°C. Following fixation, 50-60nm thick sections were cut, and an examination was performed using a JEOL

JEM-1200EX II transmission electron microscop, at 80kV. Efficacy of treatment, based on lack or presence of cells, and, the occurrent changes in the ECM structure, were analyzed after decellularization and accomplished by two independent observers.

Mechanical Tests:

Pressure Test: Pressure tests were performed using sections of vessels 3-4 cm in length, excised from the infrarenal part of the aorta. The distal end of the vessels were closed with a continous suture by using 6/0 Prolene. Side branches were ligated with 2/0 Polypropylene thread, if present. After cannulation of the proximal end of the aorta with an ordinary vessel cannula, this proximal end was fixed and ligated to the cannula by using 2/0 Polypropylene thread. The samples were next flushed with 37 °C PBS to remove residual air. Subsequently, the vessels were slowly inflated to 225 mmHg with 37 °C PBS, using an inflation device (Cook Medical, Alabama, USA), maintaining this pressure five times for one minute. Photo documentation was performed to demonstrate adequate mechanical stability in cases of each treated and native aortic samples.

Suture Retention Test: Suture retention tests were performed using the same methodology and inflation device as mentioned above. After creating an anastomosis between the 3-4 cm long native and treated vessel segments, the distal ends were closed with a continous suture. 6/0 Prolene thread was utilized for each suture and 2/0 Polypropylene thread for ligations and fixations. Following cannulation and fixation of the proximal end, deaerated samples were slowly inflated to 225 mmHg with 37 °C PBS, maintaining this pressure five times for one minute. Photo documentation was performed to illustrate adequate suture retention strength.

Series – Follow-up and examination of decellularized porcine biografts following implantation

Surgical Preparation

Yorkshire pigs of either sex, between 22 and 25 kg of weight, declared free of clinically evident diseases, were entered into this study. Fifteen (n=15) Yorkshire pigs were randomly selected to perform this animal study. Infrarenal aortic segments, measuring 2cm long, were removed from five (n=5) pigs. These samples were decellularized, and then stored in penicillin-streptomycin containing Earle's Medium 199, maintained to 4°C, until implantation. The rest of the porcines (n=10) have undergone vessel implantation. Within the confines of a sterile operating room, pigs were premedicated using an intramuscular injection of 15 mg/kg ketamine hydrochloride (Vetalar, Fort Dodge) and 3 mg/kg xylazine hydrochloride (Sigma-Aldrich), then anesthetized using continous intravenous administration of 3 mg/kg ketamine hydrochloride (Vetalar, Fort Dodge) and 1-2 mg/kg xylazine hydrochloride (Sigma-Aldrich) per hour. An intratracheal intubation was performed, and the pigs were mechanically ventilated (Harvard) with oxygen (1l/min) and N2O (3l/min) supplemented room air. A catheter was placed in the right external jugular vein in support of effective drug administration and fluid infusions. Slow, intravenous infusion of normal saline maintained hydration throughout the surgery and additional anesthetics were administered, as required.

Following procedural scrubbing and isolation, a total median laparotomy was performed. The intestines were retained, the retroperitoneal plane was opened, and the infrarenal part of the abdominal aorta was dissected. 2500 IU of Na-heparine intravenous administration was performed to prevent clot formation. DeBakey clamps were used for aortic exclusion. Following clamping of the aorta, a segment, measuring 2cm long, was removed, and a corresponding segment of decellularized biological aortic graft, including the appropriate diameter and length, was interposed (end-to-end anastomosis with continous suture by 5/0 Prolene). After tubing, the abdominal wall was closed by the use of a loop, and at the final phase

of the procedure, a continous skin suture was performed. Antibiotical prophylaxis was achieved by 0,5mg Cefazoline intravenously.

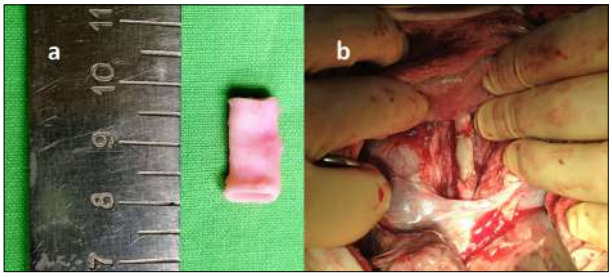

Figure 1: Decellularized aortic graft before **(a)** and after **(b)** implantation.

After the surgery femoral pulses were controlled, and all operated animals were placed under strict observation over the ensuing days. On postoperative day three, surviving porcines were transported to their original millieu for the next six months. Following this period, they were transported back to the laboratory, and resection of the infrarenal part of abdominal aorta was performed under sterile, surgical conditions. Explanted segments of aorta, including the original aortic wall, implanted vessel and the anastomotic region, were evaluated by light and transmission electron microscopy. (Figure 1)

Light microscopy evaluation:

Implanted and surrounding native segments of the aortic wall were fixed for the next 24 hours, in 10% neutral buffered formalin, for routine histological examination. Cross-sectional and longitudinal tissue blocks were embedded into paraffin, and 2-4micrometer thick sections were cut. Sections were stained applying four different methods, using protocols recommended by the manufacturers. Routine HE staining confirmed the presence of novel cells and the remodelling of the endothelial layer in the implanted graft. Histochemistry, using orcein staining for visualization of elastin, including Masson-trichrome staining the collagen, were performed. Re-colonization of myofibroblasts and smooth muscle cells were substantiated by smooth cell actin immunostaining in the implanted grafts, using the smooth muscle actin (SMA) specific mouse monoclonal antibody (clone: 1A4, Histopathology, Ltd., Pécs, Hungary), and the HISTOLS® micro-polymer-based peroxidase detection system (Histopathology, Ltd., Pécs, Hungary). Nonsmooth muscle-derived cells and tissue elements, located in the samples, served as negative controls for the specificity of the antibody. Similar to all the above procedures, Pannoramic Viewer software and 100x magnification were implemented towards effectively evaluating the presence of reendothelialization, recolonization of novel cells and structure of ECM in the sections of the implanted segments, confirmed by two independent pathologists.

Transmission electron microscopy evaluation:

Samples of vessels were prepared for TEM examination using the identical method described above, to substantiate the reappearence of cells in the implant scaffold, confirmed by two independent observers.

Results

Series – Examination of decellularized porcine aortic segments

Light microscopy evaluation:

The effectiveness of the decellularization method was based on the histological findings, which proved consistently uniform throughout all investigated samples. The native aortic wall was stained for control. HE staining proved complete removal of cells. Orcein and MT staining showed only two layers (tunica

media and adventitia) and decreased wall-thickness in the treated samples, compared with the native tissue. There was only a minimal change in the fibers' structure, however, the destruction was not significantly notable. (Figure 2)

Transmission electron microscopy evaluation:

The lack of cellular elements and the connective tissue fibers' retained microstructure were noticeable. (Figure 3)

Mechanical Tests:

In order to assess the effects of decellularization on mechanical stability, pressure and suture retention tests were performed. During the five cycle of inflation there was no rupture of aortic wall or sign of leakage in any cases of the decellularized samples. Moreover, sutures adequately withstood the intraluminal pressure, without any sign of leakage in the suture line. (Figure 4)

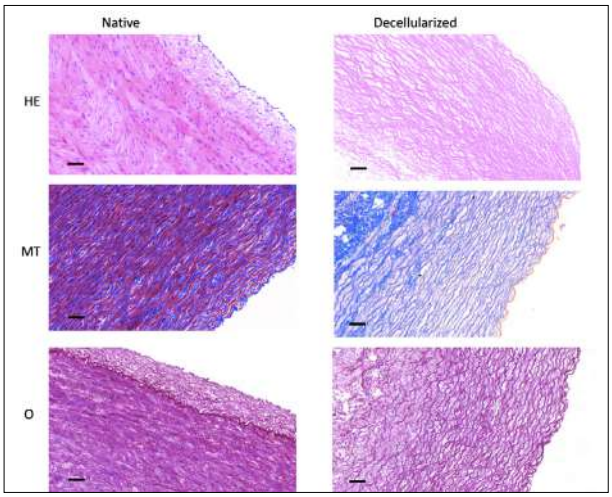

Figure 2: Hematoxylin-eosin (HE), Masson-trichrome (MT) and Orcein (O) staining of native and decellularized porcine aorta. (Bars=50μm).

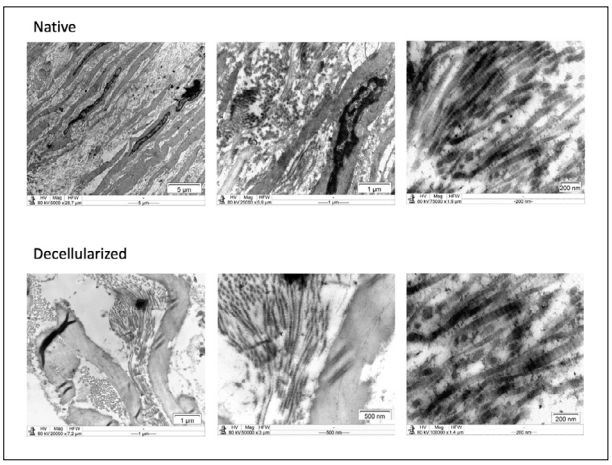

Figure 3: Transmission electron microscopy of native and decellularized aorta. Sections of native aorta show normal cells and cell nuclei, just as regular structure of the extra-cellular matrix. Treated sections demonstrate the lack of cells and cell nuclei among preserved structure of collagen fibers.

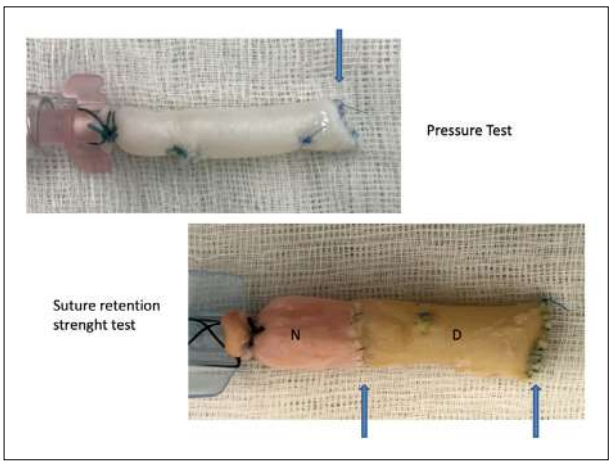

Figure 4: Mechanical tests: Decellularized graft and sample with anastomosis between treated (D) and native (N) aortic segment are inflated with 225Hgmm. There is no sign of vessel rupture or leakage at the suture lines. (blue arrows indicate the suture lines).

Series - Examination of implanted grafts

Decellularized porcine aortic grafts were surgically easy to handle. Suture strength was adequate, and there was no significant bleeding during and following the operation. Nine out of ten porcines, between 108 and 123 kg of weight, survived for 6 months following aortic tubing with grafts decellularized by protocol 2. One porcine succumbed on the second postoperative day in ileus. The autopsy did not reveal any evidence of a potential surgical mistake. No other complication was observed during the follow-up period in the surviving porcines. We did not observe weight loss, or any signs of discomfort or pain in the remaining 9 animals. During the second operation, well-incorporated, and suitably pulsating grafts were perceptible without any pathological transformation or perigraft reaction. Signs of graft versus host reaction, intraluminal clot formation or aneurysmatic degeneration were not observed in any of these cases. The implanted grafts demonstrated a proportional increase in diameter and length (Figure 5).

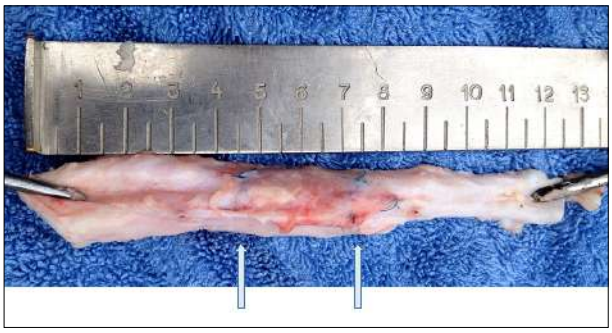

Figure 5: Explanted infrarenal segment of aorta containing the implanted biograft (white arrows indicate the suture lines)

Light microscopy evaluation:

Cross-sectional and longitudinal tissue sections were examined, and the latter contained the suture line with a continous transition between the native aorta and the implanted segment. The HE staining showed a large population of fibroblast-like and smooth muscle cells within the implant, including a continous, regular, single cell-line endothelial layer covering the entire luminal surface. SMA staining proved the presence of novel smooth muscle cells within the graft. MT and Orcein staining confirmed the preserved structure of collagen and elastic fibers in all layers. (Figure 6)

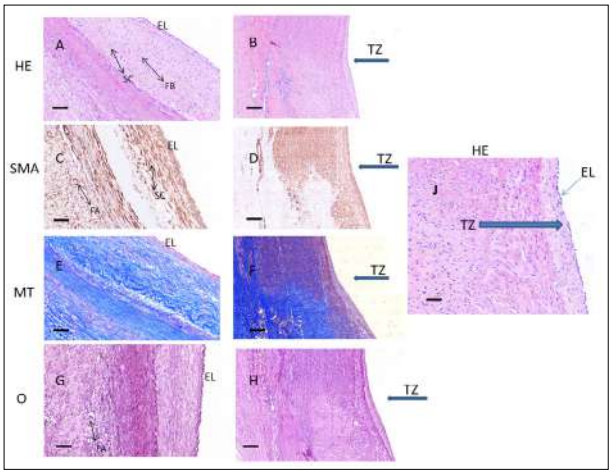

Figure 6: Cross-sectional (A,C,E,G) and longitudinal (B,D,F,H,J) sections of the explanted aorta biograft. Longitudinal sections contain the level of anastomosis.
Staining methods: Hematoxylin-eosin-HE (A,B,J), Smooth Cell Actin-SMA (C,D), Masson-trichrome-MT (E,F), Orcein-O (G,H)
All of the samples (especially HE) shows regular, single-layer endothelium (EL), demonstrated more graphically on picture J. Arrows indicate the transition zone (TZ) with continous endothelial layer. Novel fibroblasts (FB) and smooth muscle cells (SC) are present on HE-stained sections. Groups of smooth cells (SC) appear on actin-stained sections. Ordinate collagen and elastic fibers can be visualized by MT and Orcein staining. Feeding arterioles (FA), vasa vasorum are visible in the external layer of implanted grafts.
Bars (A,C,E,G): 100µm
Bars (B,D,F,H): 200µm
Bar (J): 50 µm

Transmission electron microscopy evaluation:

TEM demonstrated the reappearance of native arterial wall cells (fibroblasts, myofibroblasts, smooth muscle cells) among regular connective tissue fibers within the biograft. (Figure 7)

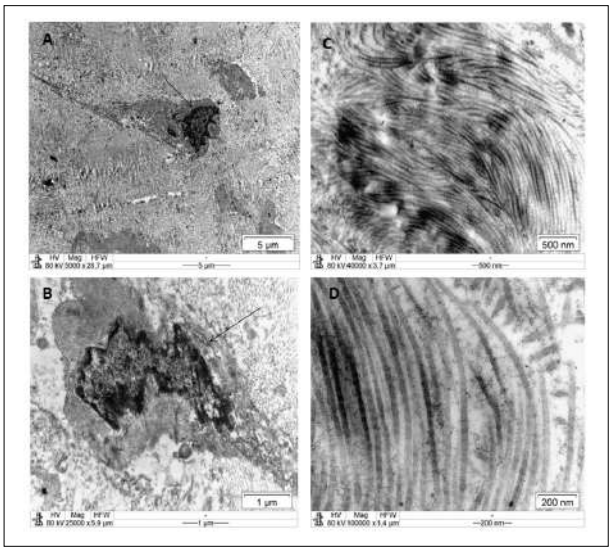

Figure 7: Transmission electron microscopy of tunica media of the implanted biograft.

A and **B** pictures show a newly appeared, normal cell in the implants scaffold (arrows indicate) in different magnification, while picture **C** and **D** show regular structure collagen fibers.

Discussion

Presently, the use of autologous vascular grafts is the best solution towards effectively replacing septic vascular prostheses, and serve in providing excellent patency and a low reinfection rate. The removal of veins prolongs the procedural time and increases the perioperative morbidity, thus, this method is not ideally suitable to all, particularly to high risk patients.[3] In these cases, silver or antibiotic impregnated grafts are generally applied, resulting in a variable success-rate with regards to the potentiality of reinfection.[8-10] Application of homografts is a well-known, recommended option, generally associated with good results and high resistance against infection, however, there is the potential risk of graft degeneration, in addition, the availability is limited.[3,11] In consideration of vessel allo-and xenotransplantation, decellularization of the donor tissue may prevent or decrease graft versus host reaction, and subsequent graft degeneration.

Varying methods are known for decellularization, with a disparate success rate in cell elimination. The most effective decellularization protocols include combinations of physical, chemical, and enzymatic treatments. It is well-known in scientific and medical research circles, that potential and varying combinations of decellularization methodologies are not perfectly successful in the removal of all cellular components, however, diminishing this content as much as possible without significant damage in the scaffold may result in a higher succes rate following implantation.[7]

In our investigation, we have used a combined (physical and chemical treatment) decellularization protocol. This method was effective in cell removal, while preserved the connective tissue fiber-structure, confirmed by histological stainings and transmission electronmicroscopy. Mechanical tests, using 225 mmHg intraluminal pressure (which is nearly two times higher, than physiological systolic pressure), showed adequate mechanical stability and suture retention strength, without rupture or leakage.

Use of homograft was published first in the 1950's, with positive early, but less favorable late outcome, due to their degeneration.[12-4] Applying xenografts showed promising initial results during the 80's, however, frequent, late aneurysm formations generally supplanted it from additional utilization.[15,16] Alloplastic grafts appeared in the meantime, and became more and more popular due to their unlimited availability and easy handling. Nevertheless, autologous grafts remained the gold standard in cardiovascular surgery, in terms of primary reconstruction, such as redo surgery, particularly with respect to infected areas.

Due to the above mentioned complications and subsequent unfavorable long-term results, the use of biological grafts was limited from the initial attempts for a long time. Primary complications were: restenosis due to intimal hyperplasia, aneurysm formation caused by degeneration, and graft thrombosis. Autologous vein graft is not available in an estimated 20-40% of the cases.[11,17] The use of synthetic grafts for distal bypasses demonstrates low patency rate, and, in addition, the application of impregnated alloplastic grafts in septic surgery offers a variable outcome in terms of the risk of reinfection.[8-10] Due to this reasoning, and, in addition to the continous progress in vascular surgery, the increasing number of cases resulting in higher complication rate, focused again the attention to the development of biological vascular grafts.

The advantages of xenogenic materials, compared with alloplastic materials, include superior handling, high resistance to infection and reinfection, minimal bleeding tendency at the suture line.[3] These benefits, however, at this time, are only based on experience, not on clinical evidence.[3] Several publications described successful application of pericardial xenografts used in treating infected areas, however, experiences with usage of these grafts in replacement of the infrarenal aorta are limited.[18] McMillan *et al.* reported a high success rate without reinfection (50 from 51 cases in a 2.1 years mean follow-up period), following septic PTFE graft removal, replaced with a bovine pericardial patch in the inguinal region.[19] Some authors preferred the use of a pericardial tube-graft to replace an infected aortic graft. Czerny *et al.* published effective treatment of infected aortic prosthesis by removal and reconstruction with a self-made xenopericardial tube graft. Freedom from reinfection proved 100% within a 24 months follow-up period.[20] Dulbecco *et al.* made a successful reconstruction with a bovine pericardial tubular aorto-bifemoral graft in case of an aortic graft infection.[21] Lutz *et al.* used a hand-sewn bovine pericardial xenoprosthesis for in situ graft replacement of infected descending or infrarenal aortic graft. Technical success and primary patency rates were 100%, and complete initial healing could be achieved in 76.9%. During the mean follow-up of 9 months, recurrent infection developed in 2 out of 12 cases, however, the mortality rate was considerably high (41.7%).[18]

In our investigation, cell free vascular biografts were applied for aortic implantation, which demonstrated excellent mid-term results. Decellularized grafts were surgically easy to handle, proved to be mechanically adequate, and there was no significant bleeding at the suture line. During the second surgeries, well-incorporated, well-pulsating grafts were found. In addition, graft thrombosis did not develop, and there was no sign of infection, graft deterioration or intimal hyperplasia after removal. Complication developed only in one case, one pig succumbed in postoperative ileus. Histological findings demonstrated the reappearence of cells in the implanted scaffold, a regular, single-layer endothelium without neointima formation in the suture line, moreover, the presence of inflammatory cells were not observed.

The late outcome would be probably the same considering the human application of porcine arterial xenografts, such as, in the described earlier attempts, include aneurysmatic degeneration and graft thrombosis. However, the aim of the utilization is to abolish the septic focus, to ensure limb salvage and to improve survivability rates of patients, when there is no other option. Following successful eradication of the potential infection and complete healing, in the event of any complication, the xenograft may electively be replaced with an additional graft.

In summary, knowing the late complications of its utilization, however, high resistance to infection and reinfection, usage of decellularized xenografts may offer an ”ultimum refugium” in support of graft replacement, in the treatment of patients suffering from septic vascular graft, if autologous graft or eligible homograft is not available.

Further investigations, clinical data and close follow-up are necessary to support applicability of our findings in human patients.

Acknowledgement

This study was supported by the Hungarian Science Research Fund OTKA-K108596.

References

1. Fitzpatrick JC, Clark PM, Capaldi FM. Effect of decellularization protocol on the mechanical behavior of porcine descending aorta. *Int J Biomater* 2010; 2010: 620503.

2. Xiong Y, Chan WY, Chua AW, Feng J, Gopal P, Ong YS, *et al.* Decellularized porcine saphenous artery for small-diameter tissue-engineered conduit graft. *Artif Organs* 2013; 37: 74-87.

3. Töpel I, Uhl C, Ayx I, Steinbauer M. Xenografts in septic vascular surgery. *Gefasschirurgie* 2016; 21: 55-8.

4. Gilbert TW, Sellaro TL, Badylak SF. Decellularization of tissues and organs. Biomaterials 2006; 27: 3675-83.

5. Conklin BS, Richter ER, Kreutziger KL, Zhong DS, Chen C. Development and evaluation of a novel decellularized vascular xenograft. *Med Eng Phys* 2002; 24: 173-83.

6. Weymann A, Radovits T, Schmack B, Korkmaz S, Li S, Chaimow N, *et al.* Total aortic arch replacement: superior ventriculo-arterial coupling with decellularized allografts compared with conventional prostheses. *PLoS One* 2014; 9: e103588.

7. Weymann A, Schmack B, Okada T, Soós P, Istók R, Radovits T, *et al.* Reendothelialization of human heart valve neoscaffolds using umbilical cord-derived endothelial cells. *Circ J* 2013; 77: 207-16.

8. Young RM, Cherry KJ, Davis PM, Gloviczki P, Bower TC, Panneton JM, *et al.* The results of in situ prosthetic replacement for infected aortic grafts. *Am J Surg* 1999; 178: 136-40.

9. Bandyk DF, Novotney ML, Johnson BL, Back MR, Roth SR. Use of rifampin soaked gelatin-sealed polyester grafts for in situ treatment of primary aortic and vascular prosthetic infections. *J Surg Res* 2001; 95: 44-9.

10. Bandyk DF, Novotney ML, Back MR, Johnson BL, Schmacht DC. Expanded application of in situ replacement for prosthetic graft infection. *J Vasc Surg* 2001; 34: 411-9.

11. Nagy Z, Oláh Z, Kókai J, Molnár AB, Laczkó Á, Szabó GV, *et al.* Role of the homograft bypass in extremity inferior's reconstructions. *Magy Seb* 2017; 70: 5-12.

12. Barner HB, DeWeese JA, Dale WA, Mahoney EB. Aneurysmal degeneration of femoropopliteal arterial homografts. *JAMA* 1966; 196: 631-4.

13. Knox WG, Miller RE. Long-term appraisal of aortic and arterial homografts implanted in years 1954-1957. *Ann Surg* 1970; 172: 1076-8.

14. Szilagyi DE, Rodriguez FJ, Smith RF, Elliott JP. Late fate of arterial allografts. Observation 6 to 15 years after implantation. *Arch Surg* 1970; 101: 721-33.

15. Nemes A, Acsády G, Fraefel W, Lichti H, Monos E, Oertli R, *et al.* Application of a vascular graft material (Solcograft-P) in experimental surgery. *Biomaterials* 1985; 6: 303-11.

16. Schröder A, Imig H, Peiper U, Neidel J, Petereit A. Results of a bovine collagen vascular graft (Solcograft-P) in infra-inguinal positions. Eur J Vasc Surg 1988; 2: 315-21.

17. Salacinski HJ, Goldner S, Giudiceandrea A, Hamilton G, Seifalian AM, Edwards A, *et al.* The mechanical behavior of vascular grafts: a review. *J Biomater Appl* 2001; 15: 241-78.

18. Lutz B, Reeps C, Biro G, Knappich C, Zimmermann A, Eckstein HH. Bovine Pericardium as New Technical Option for In Situ Reconstruction of Aortic Graft Infection. *Ann Vasc Surg* 2016; 41: 118-26.

19. McMillan WD, Leville CD, Hile CN. Bovine pericardial patch repair in infected fields. *J Vasc Surg* 2012; 55: 1712-5.

20. Czerny M, von Allmen R, Opfermann P, Sodeck G, Dick F, Stellmes A, *et al.* Self-made pericardial tube graft: a new surgical concept for treatment of graft infections after thoracic and abdominal aortic procedures. Ann Thorac Surg 2011; 92: 1657-62.

21. Dulbecco E, Camporrotondo M, Blanco G, Haberman D. In situ reconstruction with bovine pericardial tubular graft for aortic graft infection. *Rev Bras Cir Cardiovasc* 2010; 25: 249-52.

Versatility of Pericardial Patches in Vascular Surgery

29

John LANGFORD, Jianbiao XU, Hualong BAI, Alan DARDIK

Bovine pericardium is a decellularized xenograft that has been used for a wide variety of surgical applications since the 1970s. One of the most prevalent uses is as a vascular patch to close arteriotomies in medium sized vessels such as after carotid or femoral endarterectomy. The last decade has advanced our understanding of how this material heals after implantation; in addition, there have been advances in manipulation of the patch to create next generation implantable devices. The most recent data shows that pericardial patches may be superior to other materials used as patches for carotid endarterectomy; in addition, there has been successful use of bovine pericardium in infected fields in a multitude of surgical settings.

Introduction

Bovine pericardium is a decellularized xenograft that was first used as a heart valve replacement material in 1971, with initial interest in this material focused on its near normal valve function, long-term clinical success and lack of need for anticoagulation[1]. Since then, pericardium has been used for multiple surgical indications including repair of cardiac defects[2], sealing of lung suture lines[3], dural patches[4], hernia repairs[5] and vessel reconstruction[6]. Among vascular surgeons, pericardium is commonly used after arteriotomy as a patch to reduce the occurrence of restenosis. These patches remain popular due to their off-the-shelf availability, easily surgical handling and ability for immediate use of completion ultrasound[7].

Pericardium is decellularized with detergents and enzymes that remove the cellular components[8]. After decellularization, the remaining tissue consists of the extracellular matrix that is primarily collagen; these matrix proteins are conserved to a high degree across species and therefore not generally immunoreactive. In many protocols, the matrix proteins are frequently crosslinked using glutaraldehyde that increases the tissue strength, inhibits biodegradation and sterilizes the tissue[9]. Although glutaraldehyde strengthens the patch, all residual traces need to be removed since glutaraldehyde can lead to calcification *in vivo*[10]. Multiple protocols are used to limit calcification, but no method is perfect[10-12]. Despite this potential issue with long-term calcification, the decellularized pericardium incorporates into host tissue[13-16].

Pericardial Healing in Vascular Repair

Pericardium is anisotropic, with different structures of the serous (parietal) and fibrous (mediastinal) surfaces; the serous surface consists of endothelium and basement membrane whereas the fibrous surface is connective tissue (Figure 1). After decellularization, the extracellular matrix of pericardium retains differences in the composition of the serous side compared to the fibrous side; the serous side is mainly composed of laminin and collagen IV, while the fibrous side is mainly composed of collagen I[17].

In *in vitro* studies, laminin is important for early (<6 hours) cell migration and collagen IV is important for later (6-24 hours) cell migration [17], suggesting that the orientation of the implanted pericardial patch may have importance in host integration and the importance of implanting pericardial patches in the appropriate orientation with the serous side oriented to the vessel lumen.

Patch healing has been most commonly described in the vascular system, in both arterial and venous repairs [13, 14, 16]. In a pericardial patch that was used to close a rat aortic arteriotomy, there were increasing numbers of infiltrating cells over time [13]. These cells were both macrophages (CD68+) and endothelial progenitor cells (CD34+/VEGFR2+), with endothelial progenitor cells on the patch surface as early as day 7 (Figure 2); these endothelial progenitor cells were arterial progenitor cells that expressed the arterial determinant Ephrin-B2.

In a similar venous model in which pericardial patches were used to close a venotomy in the inferior vena cava, there was similar host cell infiltration into the patch as well as onto the luminal surface; however, in the venous environment the endothelial progenitor cells were venous progenitor cells that expressed the venous determinant Eph-B4 [14]. Interestingly, when patches were placed in the inferior vena cava and an aortocaval arteriovenous fistula was performed distal to the patch, exposing the patch to both arterial and venous blood flow, both venous and arterial progenitor cells were observed in the patch (Figure 2) [15].

These data show that bovine pericardial patches allow for adaptive healing depending on the environment into which they are placed. Patches that are placed into an arterial environment show accumulation of arterial progenitor cells [13], and patches that are placed into a venous environment show accumulation of venous progenitor cells[14]; patches placed into a fistula environment show accumulation of both arterial and venous progenitor cells [15]. The ability of pericardial patches to act as a scaffold supporting differential healing depending on the host environment is similar to native tissue

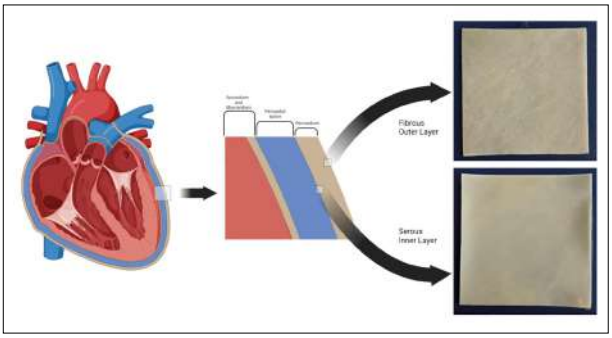

Figure 1: The left side of the figure shows a diagram of the heart with surrounding pericardium. The middle panel is a magnified view of the pericardium and heart wall. The right shows the different surfaces of the decellularized pericardium. The top panel shows the fibrous layer which is the external part of the pericardium. The bottom panel shows the serous portion of the pericardium which is normally in contact with the heart.

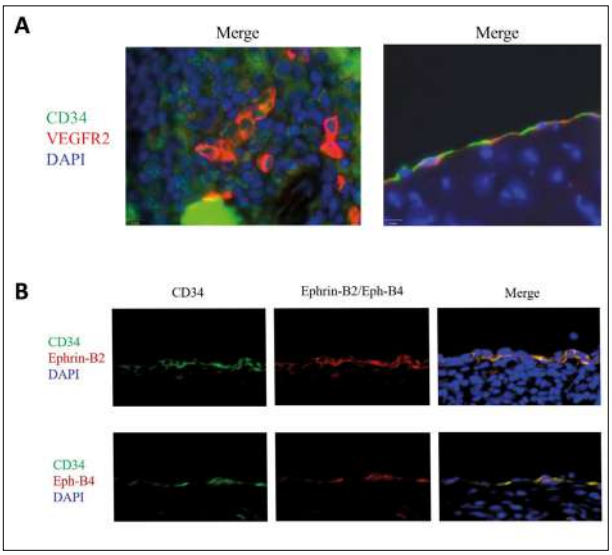

Figure 2: Host cell infiltration into a pericardial patch.

A: Left panel, infiltrating cells within a bovine pericardial patch examined with immunofluorescence, day 7 after implantation in the rat aortic patch model; green, CD34; red, VEGFR2; blue, DAPI; merged panel is shown; data from Bai, *et al.* (2016) [31]. Right Panel, luminal surface of a bovine pericardial patch examined with immunofluorescence, day 7. Green, CD34; red, VEGFR2, blue DAPI; merged panel is shown; data from Li, *et al.* (2012) [13].

B: Luminal surface of a bovine pericardial patch in the rat inferior vena cava and exposed to an arteriovenous fistula, examined with immunofluorescence, day 7. Top panels, Green, CD34; red, Ephrin-B2, blue DAPI; Bottom panels, Green, CD34; red, Eph-B4, blue DAPI.

patches [18]. The ability to support successful integration into host vessels has likely been a factor to its common clinical use; bovine pericardium was be used in 51,480 of 70,987 (73%) patch angioplasties after carotid endarterectomy (CEA) from 2003 to 2017, making it the most commonly used material in recent years [19].

Pericardial Patches in Carotid Endarterectomy

Patch angioplasty is used after CEA to lower the risk of both immediate stroke and late restenosis compared with primary closure; however, risks that are associated with patch angioplasty include pseudoaneurysm formation, thrombosis, and infection. Biasi *et al.* reported one of the first uses of pericardial patches to close the carotid artery after CEA [20]. Since the optimal patch material is not established for vessel closure, multiple materials have been used, including polyethylene terephthalate (PET), expanded polytetrafluorethylene (ePTFE) and autologous vein (Table 1).

Table 1. Summary of studies comparing pericardium to other materials as a patch for carotid endarterectomy.

Study	Materials compared	Type of Study	Number of patients	Outcomes evaluated	Major Findings	Significant?
Marien *et al.* [21]	Dacron *vs.* Pericardium	Prospective	92	Suture line bleeding at 3 and 4 minutes, hematoma, TIA, stroke, death	Reduced suture line bleeding in pericardium *vs.* Dacron at 3 minutes (14% *vs.* 55%) and 4 minutes (4% *vs.* 30%). Reduced bleeding in pericardium *vs.* Dacron (6.25 ± 0.55g *vs.* 16.34 ± 1.85g)	Yes (P<0.001) Yes (P<0.001)
Ho *et al.* [22]	Dacron *vs.* Pericardium	Retrospective	1331	Infection, hematoma, pseudoaneurysm formation, 30-day stroke, 30-day mortality, 5-year mortality, 5-year restenosis	Increased 5-year survival in pericardium *vs.* Dacron (77.9% ± 3.6% *vs.* 60.8% ± 2.1%)	Yes (P=0.03)
Stone *et al.* [23]	PTFE *vs.* Pericardium	Prospective Randomized Trial	200	Hemostasis time, TIA, stroke, thrombosis, Infection, hematoma	Quicker hemostasis in pericardium *vs.* PTFE (3.09 minutes *vs.* 4.90 minutes) No difference in reexploration for hematoma, TIA, stroke or infection	Yes (P=0.027) No

Kim *et al.* [24]	Autogenous Vein *vs.* Pericardium	Retrospective	456	Total operating time, 30-day post-operative complications, restenosis, aneurysmal dilation	Shorter operative time in pericardium *vs.* autogenous vein (175.8 ± 35.1 *vs.* 195.4 ± 43.8) Less aneurysmal dilation in pericardium *vs.* autogenous vein (0% *vs.* 2.0%)	Yes (P<0.01) Yes (P<0.05)
Edenfield *et al.* [19]	Pericardium, Dacron, Vein, PTFE and primary closure	Retrospective Database Review	70,987	Neurologic events (Stroke or TIA), return to OR, restenosis	Pericardium was associated with the lowest rate of return to the operating room: 1.8% Pericardium had the lowest rate of neurological events: 1.5% Pericardium had the lowest rate of >80% restenosis at 1 year: 1.3%	Yes (P<0.01) Yes (P<0.01) Yes (P<0.01)
Lazarides *et al.* [25]	Pericardium, EvE, Vein, PTFE, Dacron, Polyurethane	Meta-analysis	4,440	30-day combined stroke and death rate, late restenosis	Pericardium with lower rates of 30-day stroke/ death than Dacron, Polyurethane, primary closure and vein patch Pericardium with lower rates of restenosis than Dacron, polyurethane, primary closure and vein patch	No No
Texakalidis *et al.* [48]	Pericardium *vs.* Synthetics	Meta-Analysis	290	30-day stroke, TIA, hematoma, death	Pericardium and synthetics had similar rates of: 30-day stroke (RR, 1.44; 95% CI, 0.19-10.79) TIA (RR, 1.05; 95% CI, 0.11-10.27) Neck hematoma (RR, 4.01; 95% CI, 0.46-34.85) Death (RR, 4.01; 95% CI 0.46-34.85)	 No No No No
Orrapin *et al.* [49]	Pericardium, Autologous vein, PTFE, Dacron, polyurethane, polyester	Meta-Analysis	2,2278	Postoperative and long-term stroke, transient ischemic attack, death, artery narrowing or blockage, artery rupture, cranial nerve palsy, wound infection, bleeding, reoperation, pseudoaneurysm	Pericardium has a reductio in long-term ipsilateral stroke (OR4.17, 95% CI 0.46 to 38.02)	No

TIA Transient Ischemic Attack; PTFE polytetrafluroethylene; EvE Eversion Endarterectomy

Pericardial patches have been reported to have reduced suture line bleeding and improved long-term survival compared with PET patches [21, 22]. Marien *et al.* reported a prospective comparison of 51 bovine pericardial patches and 44 PET patches after CEA; pericardial patches were associated with less subjective bleeding at both 3 and 4 minutes, as well as less objectively measured blood loss [21]. Ho *et al.* reported their experience with 1331 patients treated with CEA; although there was no significant difference among different patch materials in either short-term outcomes such as infection, hematoma, or pseudoaneurysms, or in 5-year rates of restenosis, 5-year survival was significantly improved in patients treated with pericardial patches compared with patients treated with Dacron patches (78% *vs.* 61%) [22].

Pericardium may be more resistant to infection compared with other patches. Stone *et al.* prospectively evaluated 200 patients treated with CEA and patch closure and showed little difference among pericardial or ePTFE patches other than quicker hemostasis with pericardial patches; however, pericardial patches had reduced infections compared to ePTFE (0% *vs.* 3%) [23]. Similarly, long-term (10-year) outcomes after pericardial patches showed less aneurysmal dilation in pericardial patches compared to autologous vein (0% *vs.* 2%) [24].

Two studies with large numbers of patients have shown that pericardial patches may have improved outcomes compared with other materials [19, 25]. An analysis of 70,987 patients treated with CEA in the Vascular Quality Initiative database (2003 to 2017) showed that pericardium was the most commonly used material (72.5%) and was associated with significantly lower rates of returning to the operating room and fewer neurological events as well as 1-year rates of restenosis [19]. A network meta-analysis of 23 randomized trials showed that pericardial patch closure was associated with the highest probability of being the best method of closure of any patch material, with respect to the one month combined stroke/death rate [25].

These studies suggest that direct comparison of pericardial patches to other materials appears to show that pericardium is either equivalent or slightly better than other materials in multiple outcomes, most notably less suture line bleeding and lower rates of restenosis. However, most of these studies are retrospective and suggest the need for more prospective data.

Pericardial Patches and Infections

With any implanted prosthetic material one of the most feared complications is infection as there are few good solutions [26]; the biofilm that develops around the prosthetic is typically resistant to antibiotics [27] and requires removal, a particular problem in vessels and for which the patch closure was originally performed. In prosthetic patch repair after CEA there is an estimated infection risk of 0.5%-1% [28], and patch infections may lead to pseudoaneurysm formation that can blowout or cause stroke or death [29, 30]. Although rare, these complications confer significant morbidity, and optimally should be prevented.

A common practice in vascular surgery is to soak materials in saline containing antibiotics immediately prior to surgical implantation. Treating pericardial patches with antibiotics does

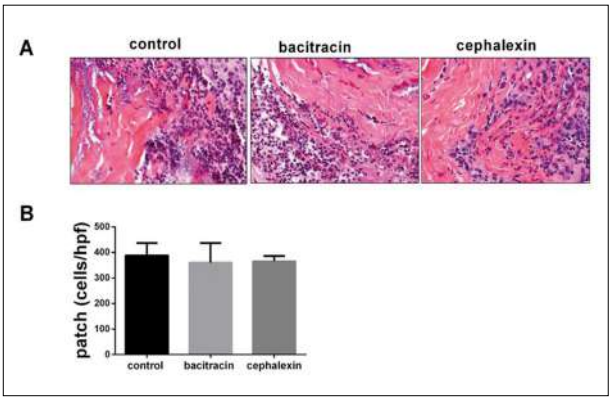

Figure 3: Cellular infiltration into bovine pericardial patches, day 30. Rat aortic patch model, pretreatment with control or antibiotics.

A: H&E showing cellular infiltration into pericardial patch.

B: Bar graph showing number of cells in patches; Data from Bai, *et al.* (2016) [31].

not appear to alter patch healing; patches that were pre-treated with bacitracin or cephalexin showed no significant difference in patch healing at days 7 and 30 (Figure 3)[31]. This important data supports that common practice of pretreating patches with antibiotics to minimize the risk of infection.

Since infection of implanted prosthetics is associated with devastating complications, reoperation with explantation remains the most commonly used treatment. In the setting of an infected field, it is imperative to use materials that have a low likelihood of becoming reinfected. Autogenous grafts and allografts have the lowest rates of reinfection[32], leading to the use of autologous tissue as the preferred treatment material[33]. However, autologous grafts need to be harvested, leading to increased operative time and multiple surgical sites in these ill patients. As such, pericardium has been used as a readily available alternative, since pericardial patches appear to have low rates of reinfection[22, 34]. One single center retrospective review of 256 bovine pericardial patch closures over a 12-year period reported no patch infections[34]. Another retrospective study with 9-year follow-up reported an infection rate of 0.6% (3/457) in pericardial patches[22].

The low infection rates associated with pericardium has led surgeons to use them in infected fields in a variety of scenarios including as simple patches or more recently as tube grafts (Table 2). Pericardial patches were used to close arteriotomies in 48 patients undergoing removal of infected ePTFE grafts, bypasses and patches; after 2 years of follow-up none of these patches had evidence of recurrent infection[35]. A small series of 5 transplant recipients that developed infectious vascular complications were repaired with a pericardial patch or a tube interposition graft; after 16 months none of these patients had any complications or signs of infection[6]. A recent retrospective analysis of 21 patients who were treated with prefabricated pericardial grafts for aortic reconstruction in the setting of infection showed 89% 2-year freedom from reinfection[36]. These encouraging data support the use of pericardium in infected fields, at least when no other options are available.

Table 2. Summary of studies reporting infection rates with bovine pericardium

Study	Type of Study	Type of Surgery	Type of Infection	Number of Procedures	Follow-up time	Major Findings
Ho ***et al.***[22]	Retrospective Review	Carotid Endarterectomy	Infection after primary surgery	457	0-182 months (mean 46.1 months)	3 (0.6%) patients developed postoperative infection
Stone ***et al.***[23]	Prospective Randomized Trial	Carotid Endarterectomy	Infection after primary surgery	98	0-44 months (mean 15 months)	No patients developed patch infection
Papakostas ***et al.***[34]	Retrospective Review	Carotid Endarterectomy	Infection after primary surgery	256	12-144 months	No patients developed patch infection
McMilan ***et al.***[35]	Retrospective Review	Removal of infected PTFE grafts and placement pericardial patches	Replacement of graft in infected field	51	3-48 months (mean 2.1 years)	1 patient required patch replacement for recurrent infection. No patches ruptured.
Garcia Aroz ***et al.***[6]	Retrospective Review	Patch or interposition graft for infected fields of transplant recipients	Replacement of graft in infected field	5	6-31 months (median 16 months)	No patients developed patch infection

Burghuber *et al.* [36]	Retrospective Review	Aortic graft placement or aorto-iliac reconstruction	Replacement of graft in infected field (62%) Graft used in patient with systemic infection (38%)	21	2.1-56.1 months (median 21.6 months)	2-year freedom from infection rate of 89%
Alslaim *et al.* [50]	Case Study	Inferior Vena Cava Reconstruction	Complicated xanthogranulomatous pyelonephritis and grossly infected field	1	6 months	Graft remained patent and uninfected
Lutz *et al.* [51]	Retrospective Review	Aortic Reconstruction	Aortic Graft infections and mycotic aneurysm	13	1-27 months (median 9 months)	Complete infection control was 75%. 2 patients with recurrent retroperitoneal infection and rupture of graft.

PTFE polytetrafluroethylene

Pericardium and Nanoparticles

Pericardial patches are mostly collagen and therefore can be modified prior to implantation. Gold nanoparticles have been bound to decellularized vascular tissue to create composite prosthetic patches that were successfully incorporated into host arteries [37, 38]. More recently, nanoparticles containing therapeutics were covalently bound to commercially available pericardial patches and these patches had reduced neointimal hyperplasia and pseudoaneurysm formation [39, 40].

Nanoparticles are ~100 nm spherical structures comprised of either natural or synthetic polymers [41]. These spheres allow delivery of both hydrophilic or hydrophobic drugs in a controlled fashion. Poly (lactic-co-glycolic acid) (PLGA) is a biodegradable polymer that is currently approved for use in human patients [42]. PLGA nanoparticles were covalently bonded to a pericardial patch by linking the amine groups of the collagen to the carboxyl groups of the nanoparticles; this process allowed for nanoparticles to not only be bound to the surface of the patch but also within the patch fibers, increasing the size of the reservoir for drug delivery and allowing sustained release of drug for 21 days (Figure 4) [39].

The prolonged release of drugs from nanoparticles bonded to patches allows the opportunity to use patches as a localized drug delivery system. One use has been to treat neointimal hyperplasia that leads to restenosis due to smooth muscle

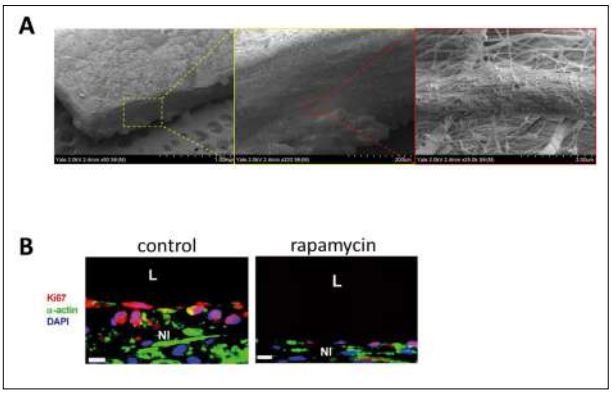

Figure 4: Bonding of nanoparticles to a bovine pericardial patch,

A: Examined in cross section with scanning electron microscopy. Panels are 50x, 220x, 25000x magnification. Data from Bai, *et al.* (2017) [39].

B: Bonding of nanoparticles containing rapamycin to bovine pericardial patches showed decreased smooth muscle cell proliferation and reduced neointimal thickness. Green, alpha actin; red, Ki67, blue DAPI; merged panel is shown. L, Lumen; NI, neointima. Data from Bai, *et al.* (2017) [39].

cell proliferation and migration; nanoparticles can deliver rapamycin, an inhibitor of proliferation that diminishes neointimal hyperplasia and restenosis [43, 44]. In a rat venous patch angioplasty model, rapamycin-eluting nanoparticles showed decreased smooth muscle cell prolilferation and neointimal thickening on the patch, with preservation of luminal endothelium (Figure 4) [39].

Another application of local drug release using nanoparticles bonded to the patch is for the treat of pseudoaneurysm formation, a long-term complication of prosthetics [45]. In a rat model of aortic patch angioplasty, nanoparticles that released TGF-β1 were able to significantly decrease the rate of pseudoaneurysm formation (7%) compared to control patches (88%); conversely, nanoparticles releasing a TGF-β1 receptor inhibitor showed increase pseudoaneurysm formation (40). This data shows the feasibility of using patches as a surgically implantable drug delivery system.

Although nanoparticles bonded to patches can be used for local drug delivery, they could potentially be used to deliver drugs to more distal sites. Patches implanted into the IVC of rats showed some shedding of nanoparticles that were found in the liver, spleen and kidneys [39]. Although originally considered an off-target effect, these distal locations could be harnessed as targeted delivery sites, for example for hepatic drug delivery. Figure 5 shows drug delivery from a pericardium patch that was implanted in the IVC to the liver and other end organs over time. It appears possible that a nanoparticle-patch can be implanted to deliver a variety of sustained therapeutics.

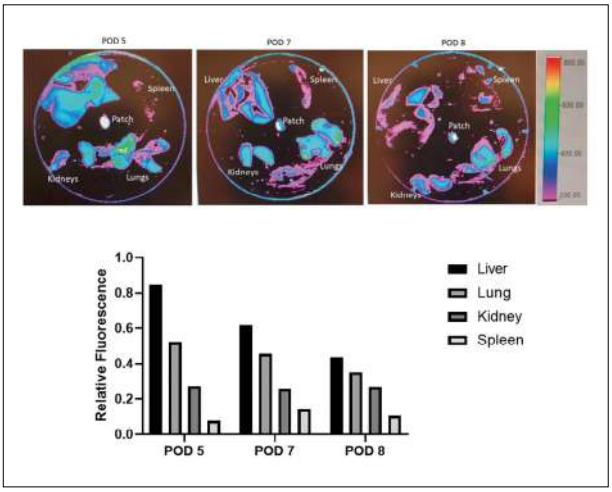

Figure 5: Drug delivery to the liver and other organs from a patch implanted in the inferior vena cava. Upper panel, IVIS imaging showing rhodamine nanoparticle distribution in several organs, explanted on days 5, 7 and 8. There appears to be a declining signal in end organs over time. Lower panel, bar graph showing relative fluorescence of organs over time.

Ethical Concerns with Xenografts

Respect of patient autonomy is a fundamental principle of ethical medical care. For truly informed decision-making, patients must be aware of available treatment options, and many factors, such as personal or religious beliefs, affect the decision to pursue particular treatment options in preference to others. Implantation of xenografts my present issues for patients that may be opposed to the use of materials from animals or specific animal species [46]; the use of bovine pericardial patches may present issues for patients requiring vascular surgery [47]. Inclusion of discussion of the different materials available for patch closure, such as performed during carotid endarterectomy, as part of the informed consent process is important and can be discussed routinely; disclosing the intended use of animal-derived tissue allows patients to participate in their care and choose other options in accordance with their values and beliefs, beyond a simple risk/benefit analysis. As the choices of biomaterials continues to expand, it is critical that patients continue to be educated about treatment options to make the best possible informed decision for their care.

Conclusion

Pericardial patches are currently used for patch angioplasty with similar or potentially superior results compared with other materials. Pericardial patches also appear to have reasonable use in vessel reconstruction in infected fields. Interestingly, pericardium can covalently bind nanoparticles to create a next generation drug delivery system. With continued research these advances may be able to create personalized therapeutics for a variety of applications.

References

1. Ionescu MI, Tandon AP, Mary DA, Abid A. Heart valve replacement with the Ionescu-Shiley pericardial xenograft. *J Thorac Cardiovasc Surg* 1977; 73:31-42.
2. Neethling WML, Strange G, Firth L, Smit FE. Evaluation of a tissue-engineered bovine pericardial patch in paediatric patients with congenital cardiac anomalies: initial experience with the ADAPT-treated CardioCel(R) patch. *Interact Cardiovasc Thorac Surg* 2013; 17: 698-702.
3. Rathinam S, Naidu BV, Nanjaiah P, Loubani M, Kalkat MS, Rajesh PB. BioGlue and Peri-strips in lung volume reduction surgery: pilot randomised controlled trial. *J Cardiothorac Surg* 2009; 4: 37.
4. Filippi R, Schwarz M, Voth D, Reisch R, Grunert P, Perneczky A. Bovine pericardium for duraplasty: clinical results in 32 patients. *Neurosurg Rev* 2001; 24: 103-7.
5. Limpert JN, Desai AR, Kumpf AL, Fallucco MA, Aridge DL. Repair of abdominal wall defects with bovine pericardium. *Am J Surg* 2009; 198: e60-5.
6. Garcia Aroz S, Spaggiari M, Jeon H, Oberholzer J, Benedetti E, Tzvetanov I. The use of bovine pericardial patch for vascular reconstruction in infected fields for transplant recipients. *J Vasc Surg Cases Innov Techn* 2017; 3: 47-9.
7. Muto A, Nishibe T, Dardik H, Dardik A. Patches for carotid artery endarterectomy: current materials and prospects. *J Vasc Surg* 2009; 50: 206-13.
8. Li X, Guo Y, Ziegler KR, Model LS, Eghbalieh SD, Brenes RA, *et al.* Current usage and future directions for the bovine pericardial patch. *Ann Vasc Surg* 2011; 25: 561-8.
9. Courtman DW, Pereira CA, Kashef V, McComb D, Lee JM, Wilson GJ. Development of a pericardial acellular matrix biomaterial: biochemical and mechanical effects of cell extraction. *J Biomed Mater Res* 1994; 28: 655-66.
10. Rao KP, Shanthi C. Reduction of calcification by various treatments in cardiac valves. *J Biomater Appl* 1999; 13: 238-68.
11. Neethling WM, Hodge AJ, Clode P, Glancy R. A multi-step approach in anti-calcification of glutaraldehyde-preserved bovine pericardium. *J Cardiovasc Surg (Torino)* 2006; 47: 711-8.
12. Salameh A, Greimann W, Vondrys D, Kostelka M. Calcification or Not. This Is the Question. A 1-Year Study of Bovine Pericardial Vascular Patches (CardioCel) in Minipigs. *Semin Thorac Cardiovasc Surg* 2018; 30: 54-9.
13. Li X, Jadlowiec C, Guo Y, Protack CD, Ziegler KR, Lv W, *et al.* Pericardial patch angioplasty heals via an Ephrin-B2 and CD34 positive cell mediated mechanism. *PLoS One* 2012; 7: e38844.
14. Bai H, Wang M, Foster TR, Hu H, He H, Hashimoto T, *et al.* Pericardial patch venoplasty heals via attraction of venous progenitor cells. *Physiol Rep* 2016; 4: e12841.
15. Protack CD, Foster TR, Hashimoto T, Yamamoto K, Lee MY, Kraehling JR, *et al.* Eph-B4 regulates adaptive venous remodeling to improve arteriovenous fistula patency. *Sci Rep* 2017; 7: 15386.
16. Del Campo C, Konok GP. Use of a pericardial xenograft patch in repair of resected retrohepatic vena cava. *Can J Surg* 1994; 37: 59-61.
17. Xing Q, Parvizi M, Lopera Higuita M, Griffiths LG. Basement membrane proteins modulate cell migration on bovine pericardium extracellular matrix scaffold. *Sci Rep* 2021; 11: 4607.
18. Bai H, Guo J, Liu S, Guo X, Hu H, Wang T, *et al.* Autologous tissue patches acquire vascular identity depending on the environment. *Vasc Investig Ther* 2018; 1: 14-23.
19. Edenfield L, Blazick E, Eldrup-Jorgensen J, Healey C, Bloch P, Hawkins R, *et al.* Outcomes of carotid endarterectomy in the Vascular Quality Initiative based on patch type. *J Vasc Surg* 2020; 71: 1260-7.
20. Biasi GM, Mingazzini P, Baronio L, Sampaolo A. Processed bovine pericardium as patch angioplasty for carotid endarterectomy: a preliminary report. *Cardiovasc Surg* 1996; 4: 591-5.
21. Marien BJ, Raffetto JD, Seidman CS, LaMorte WW, Menzoian JO. Bovine pericardium *vs.* dacron for patch angioplasty after carotid endarterectomy: a prospective randomized study. *Arch Surg* 2002; 137: 785-8.
22. Ho KJ, Nguyen LL, Menard MT. Intermediate-term outcome of carotid endarterectomy with bovine pericardial patch closure compared with Dacron patch and primary closure. *J Vasc Surg* 2012; 55: 708-14.

23. Stone PA, AbuRahma AF, Mousa AY, Phang D, Hass SM, Modak A, *et al.* Prospective randomized trial of ACUSEAL versus Vascu-Guard patching in carotid endarterectomy. *Ann Vasc Surg* 2014; 28: 1530-8.

24. Kim JH, Cho YP, Kwon TW, Kim H, Kim GE. Ten-year comparative analysis of bovine pericardium and autogenous vein for patch angioplasty in patients undergoing carotid endarterectomy. *Ann Vasc Surg* 2012; 26: 353-8.

25. Lazarides MK, Christaina E, Argyriou C, Georgakarakos E, Tripsianis G, Georgiadis GS. Network Meta-Analysis of Carotid Endarterectomy Closure Techniques. *Eur J Vasc Endovasc Surg* 2021; 61: 181-90.

26. Fatima J, Federico VP, Scali ST, Feezor RJ, Berceli SA, Giles KA, *et al.* Management of patch infections after carotid endarterectomy and utility of femoral vein interposition bypass graft. *J Vasc Surg* 2019; 69: 1815-23.

27. Edmiston CE, McBain AJ, Roberts C, Leaper D. Clinical and microbiological aspects of biofilm-associated surgical site infections. *Adv Exp Med Biol* 2015; 830: 47-67.

28. Naylor R. Management of prosthetic patch infection after CEA. *J Cardiovasc Surg (Torino)* 2016; 57: 137-44.

29. Branch CL, Davis CH. False aneurysm complicating carotid endarterectomy. *Neurosurgery* 1986; 19: 421-5.

30. Naughton PA, Garcia-Toca M, Rodriguez HE, Pearce WH, Eskandari MK, Morasch MD. Carotid artery reconstruction for infected carotid patches. *Eur J Vasc Endovasc Surg* 2010; 40: 492-8.

31. Bai H, Kuwahara G, Wang M, Brownson KE, Foster TR, Yamamoto K, *et al.* Pretreatment of pericardial patches with antibiotics does not alter patch healing *in vivo*. *J Vasc Surg* 2016; 63: 1063-73.

32. O'Connor S, Andrew P, Batt M, Becquemin JP. A systematic review and meta-analysis of treatments for aortic graft infection. *J Vasc Surg* 2006; 44: 38-45.

33. Seeger JM. Management of patients with prosthetic vascular graft infection. *Am Surg* 2000; 66: 166-77.

34. Papakostas JC, Avgos S, Arnaoutoglou E, Nassis C, Peroulis M, Bali C, *et al.* Use of the vascu-guard bovine pericardium patch for arteriotomy closure in carotid endarterectomy. Early and long-term results. *Ann Vasc Surg* 2014; 28: 1213-8.

35. McMillan WD, Leville CD, Hile CN. Bovine pericardial patch repair in infected fields. *J Vasc Surg* 2012; 55: 1712-5.

36. Burghuber CK, Konzett S, Eilenberg W, Nanobachvili J, Funovics M, Hofmann W, *et al.* Novel Prefabricated Bovine Pericardial Grafts as Alternate Conduit for Septic Aorto-Iliac Reconstruction. *J Vasc Surg* 2021; 73: 2123-31.

37. Ostdiek AM, Ivey JR, Hansen SA, Gopaldas R, Grant SA. Feasibility of a nanomaterial-tissue patch for vascular and cardiac reconstruction. *J Biomed Mater Res B Appl Biomater* 2016; 104: 449-57.

38. Ostdiek AM, Ivey JR, Grant DA, Gopaldas J, Grant SA. An in vivo study of a gold nanocomposite biomaterial for vascular repair. *Biomaterials* 2015; 65: 175-83.

39. Bai H, Lee JS, Chen E, Wang M, Xing Y, Fahmy TM, *et al.* Covalent modification of pericardial patches for sustained rapamycin delivery inhibits venous neointimal hyperplasia. *Sci Rep* 2017; 7: 40142.

40. Bai H, Lee JS, Hu H, Wang T, Isaji T, Liu S, *et al.* Transforming Growth Factor-beta1 Inhibits Pseudoaneurysm Formation After Aortic Patch Angioplasty. *Arterioscler Thromb Vasc Biol* 2018; 38: 195-205.

41. Danhier F, Ansorena E, Silva JM, Coco R, Le Breton A, Preat V. PLGA-based nanoparticles: an overview of biomedical applications. *J Control Release* 2012; 161: 505-22.

42. Sadat Tabatabaei Mirakabad F, Nejati-Koshki K, Akbarzadeh A, Yamchi MR, Milani M, Zarghami N, *et al.* PLGA-based nanoparticles as cancer drug delivery systems. *Asian Pac J Cancer Prev* 2014; 15: 517-35.

43. Roqué M, Reis ED, Cordon-Cardo C, Taubman MB, Fallon JT, Fuster V, *et al.* Effect of p27 Deficiency and Rapamycin on Intimal Hyperplasia: *In Vivo* and *In Vitro* Studies Using a p27 Knockout Mouse Model. *Lab Invest* 2001; 81: 895-903.

44. Morice MC, Serruys PW, Sousa JE, Fajadet J, Ban Hayashi E, Perin M, *et al.* A randomized comparison of a sirolimus-eluting stent with a standard stent for coronary revascularization. *N Engl J Med* 2002; 346: 1773-80.

45. Defillo A, Zelensky A, Pulivarthi S, Lowary JL, Nussbaum ES, Lassig JP, *et al.* Non-infected carotid artery pseudoaneurysm 29 years after endarterectomy, endovascular management with covered stent. *J Neurosurg Sci* 2012; 56: 145-9.

46. Rodger D, Blackshaw BP. Using animal-derived constituents in anaesthesia and surgery: the case for disclosing to patients. *BMC Med Ethics* 2019; 20: 14.

47. Hodge S, Greaves N, Murray D. The Use of Bovine Pericardial Patches in Vascular Surgery: Where do we Draw the Line in Obtaining Informed Consent? *Ann Vasc Surg* 2021; ahead of print.

48. Texakalidis P, Giannopoulos S, Charisis N, Giannopoulos S, Karasavvidis T, Koullias G, *et al.* A meta-analysis of randomized trials comparing bovine pericardium and other patch materials for carotid endarterectomy. *J Vasc Surg* 2018; 68: 1241-56.

49. Orrapin S, Benyakorn T, Howard DP, Siribumrungwong B, Rerkasem K. Patches of different types for carotid patch angioplasty. *Cochrane Database Syst Rev* 2021; 2: CD000071.

50. Alslaim H, Chung J, Kruse E, Shukla M, Agarwal G. Iatrogenic Inferior Vena Cava Resection Requiring Reconstruction. *Vasc Endovascular Surg* 2021: ahead of print.

51. Lutz B, Reeps C, Biro G, Knappich C, Zimmermann A, Eckstein HH. Bovine Pericardium as New Technical Option for *In Situ* Reconstruction of Aortic Graft Infection. *Ann Vasc Surg* 2017; 41: 118-26.

Compliance

- A systematic review of stent-graft materials "PTFE *vs.* Polyester" in endovascular repair of abdominal aortic aneurysms 287
- Compliance mismatch and flow pattern in endovascular aortic repairs 296
- Modifications in aortic stiffness after endovascular or open aortic repair: a systematic review and meta-analysis 305

A systematic review of stent-graft materials "PTFE *vs.* Polyester" in endovascular repair of abdominal aortic aneurysms

30

Yogesh ACHARYA, Niamh HYNES, Sherif SULTAN

To compare the available contemporary stent-graft materials, polytetrafluoroethylene (PTFE) versus polyethylene terephthalate (PET), in endovascular aneurysm repair (EVAR) of abdominal aortic aneurysm (AAA).

This systematic review and meta-analysis was performed according to the Preferred Reporting Items for Systematic Reviews and Meta-Analyses (PRISMA) guidelines. Relevant studies were searched using the MEDLINE Ovid, Embase Ovid, CINAHL, and Cochrane Central Register of Controlled Trials (CENTRAL) (Cochrane Library; latest issue) in the Cochrane Library. Only the randomised controlled trials (RCTs) or controlled clinical trials (CCTs) with pre-specified outcomes were included.

None of the search results met the inclusion criteria and we did not find any RCT or CCT to support post-procedural outcomes following EVAR with specific stent-graft materials.

There is a lack of evidence to support implications of specific stent-graft materials, *i.e.* PTFE *vs.* PET, in post-procedural outcomes following endovascular repair of AAA, which necessitates future studies to compare the available stent-graft materials regarding procedural and clinical outcomes.

Introduction

Judicious use of endovascular aneurysm repair (EVAR) has revolutionised therapeutic tactics in the management of aortic pathology.[1] Polytetrafluoroethylene (PTFE) and polyethylene terephthalate (PET) are the two most common stent-graft materials; however, there is no systematic review and meta-analysis in the Cochrane Library or elsewhere in the literature, which we could identify, that compares and discusses PTFE and PET stent-graft materials explicitly in abdominal aortic aneurysm (AAA) repair.[2-4] Two subsequent previous reviews in 2015 for stent-graft types for endovascular repair, Duffy JM *et al.*[2] for AAA, and Rolph R *et al.*[3] for thoracic aortic aneurysm, could not find randomised studies to appraise the available evidence. The only systematic review in Cochrane Library to date is the one that explicitly addresses stent-graft materials in peripheral arteries, whereas similar studies in AAA repair is lacking.[4] As there is no primary evidence and systematic review to support the preference of PTFE based endograft over PET-based endografts or vice versa, we lack consensus regarding the choice of stent-graft materials during EVAR. This lack of definitive data on different stent-graft materials and their configuration in

AAA repair necessitates a comprehensive systematic review to elucidate the post-procedural outcome of EVAR in terms of endograft for different outcomes like graft failure cardiovascular events, and short- and long-term complications with related morbidity and mortality.

We conducted a comprehensive systematic review of endovascular repair of AAA to identify and analyse the currently available evidence. The primary aim was to compare the available contemporary stent-graft materials, PTFE versus PET, on aneurysm related mortality and cardiovascular outcomes. Secondary aims include graft specific complications and reintervention rate. Subgroup analysis will be done to compare graft configuration on clinical outcomes. The systematic review will be followed by meta-analysis, as applicable.

Methods

This systematic review was undertaken based on the proposal for systematic review in accordance with the PRISMA guidelines [5] and recommendations described in the Cochrane Handbook for Systematic Reviews of Interventions. [6]

Types of studies:

The methodological approaches undertaken in this review were agreed on a priori. Only the randomised controlled trials (RCTs) and controlled clinical trials (CCTs) were considered to determine the effectiveness of an intervention.

Types of participants:

We included all the patients who underwent endovascular elective repair of AAA.

Types of interventions and comparator:

We compared the endovascular repair of AAA using PTFE-based endograft against PET-based endograft.

Types of outcome measures:

Primary outcomes:

1) aneurysm-related death (including rupture and death within 30-days of procedure), and

2) major adverse cardiovascular events (myocardial infarction, heart failure, arrhythmia, cardiovascular death).

Secondary outcomes:

1) endoleak,
2) aneurysm sac expansion,
3) reintervention,
4) graft infection,
5) thrombosis,
6) post-implantation syndrome, and
7) all-cause mortality.

Study eligibility criteria:

All RCTs and CCTs that assess the effects of stent-graft materials 'PTFE versus PET' while performing the elective endovascular repair of AAA were eligible for inclusion. Studies that failed to include at least one primary outcome, reported only one of the stent-graft materials, 'PTFE or PET', had three or fewer cases, and studies which did not make clear distinction between stent-graft materials were excluded.

Search strategy:

Electronic searches:

A comprehensive literature search of the MEDLINE Ovid, Embase Ovid, CINAHL, and Cochrane Central Register of Controlled Trials (CENTRAL) (Cochrane Library; latest issue) in the Cochrane Library was conducted (Appendix 1). The subject strategies of databases were modelled on the search strategy designed for MEDLINE Ovid.
We also searched the ongoing trials registers: US National Institutes of Health Ongoing Trials Register ClinicalTrials.gov; World Health Organization International Clinical Trials Registry Platform; and Stroke Trials Registry.

Searching other resources:

In an effort to identify further published, unpublished, and ongoing trials, we conducted the secondary searches: bibliographies of included studies and any relevant systematic reviews identified for further references to relevant trials and used the Web of Science cited reference search to forward track relevant references; contacted original authors for clarification and further data on trial reports that were unclear; and contacted experts, trialists, and organisations in the field to obtain additional information of any unpublished or ongoing clinical trials data and/or information.

Selection of studies:

Two review authors (YA and SS) performed an independent assessment of the titles and abstracts of all the identified studies, to be followed with the full texts assessment after the initial title/abstract screening. Any disagreement regarding the selection of the studies was resolved with consensus. A third author (NH) was consulted if the agreement could not be reached to resolve any disagreement.

Data extraction and management:

Two review authors (YA and SS) planned to extract data using a pre-designed data table based on the study objectives and outcomes. Any disagreement on data extraction was resolved with consensus or with the help of a third review author (NH).

Assessment of risk of bias in included studies:

The risk of bias was to be assessed by two review authors (YA and SS), and any disagreement was to be resolved with consensus or with the help of third reviewers (NH). Visual assessment of the funnel's symmetry was used where the symmetrical funnel plot indicated a low risk of bias. Furthermore, risk of bias (RoB) within the studies was to be independently assessed based on the given characteristics: randomisation sequence generation and allocation concealment (selection bias), blinding (performance and detection bias), completeness of outcome data (attrition bias), selective outcome reporting (reporting bias), and other possible sources of bias, as applicable. The reviewer's judgments about each risk of bias item were to be assessed and presented as an overall summary and percentages across all included studies. Furthermore, the Cochrane standard RoB tool was to be represented with the risk of bias graph and summary figure for reporting bias as low, high, or unclear risk.

Data synthesis:

- Measures of treatment:

We planned to perform the analyses based on intention-to-treat principles. Dichotomous outcomes were to be represented with risk ratios (RRs) with 95% confidence intervals (CIs). Continuous data were to be expressed with mean differences (MDs), standard deviations (SDs) and associated 95% CIs. Furthermore, survival analysis was planned to be used for time-to-event analysis to be expressed with hazard ratios (HRs) with 95% CIs. We planned to contact the individual study authors if there were any missing data.

- Assessment of heterogeneity:

Heterogeneity will be assessed by the visual inspection of forest plots added with results obtained through I^2 statistic, Tau^2 statistic, and Chi^2 test.[6] Any outcomes with substantial heterogeneity were to be explored using the subgroup analyses or re-analysis, excluding specific trial(s). A two-sided p-value of <0.05 was considered statistically significant.

- Sub-group analysis:

Sub-group analysis was to be carried out if there were considerable heterogeneity within the included studies to elucidate the possible reasons for this heterogeneity. Furthermore, subgroup analysis was planned to be performed on 1) proximal or distal fixation patterns with and without barbs, 2) the presence of exoskeleton, and 3) the main body configuration consisting of either ringed or Z-stents.

Sensitivity analysis:

We planned to perform the sensitivity analyses based on trial types, *i.e.*, RCT *vs.* CCT, and the risk of bias to see the impact of low bias on outcomes.

Results

The search generated 2178 references (PubMed: 1,494 results, Embase: 616, and CINAHL: 68). A total of 381 duplicates were identified and removed. The titles and abstracts of the remaining 1797 studies were then reviewed. Of the 1797 studies reviewed, we only carried forward 45 studies to full-text review and included or excluded studies based on study type and PICO (Figure 1). However, none of the studies met the inclusion criteria, and we did not find any RCT or CCT that compared stent-graft materials in endovascular repair of AAA.

We did not perform risk of bias analysis, investigate heterogeneity, and undertake sensitivity and subgroup analysis, as data synthesis was not conducted due to the lack of studies.

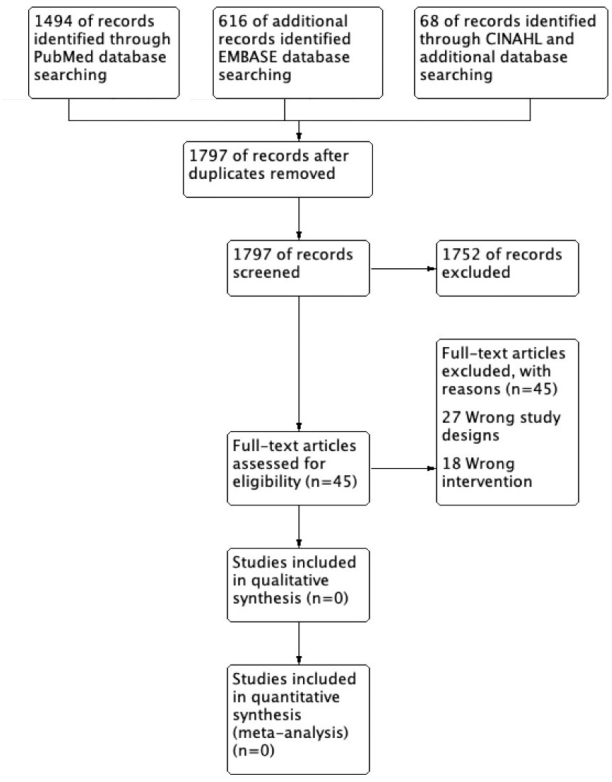
1494 of records identified through PubMed database searching
616 of additional records identified EMBASE database searching
68 of records identified through CINAHL and additional database searching
1797 of records after duplicates removed
1797 of records screened
1752 of records excluded
Full-text articles excluded, with reasons (n=45)
27 Wrong study designs
18 Wrong intervention
Full-text articles assessed for eligibility (n=45)
Studies included in qualitative synthesis (n=0)
Studies included in quantitative synthesis (meta-analysis) (n=0)

Figure 1: PRISMA study flow diagram.

Discussion

We did not find any RCT or CCT to support post-procedural outcomes following EVAR with specific stent-graft materials.
The ideal design of the thoracic and abdominal aortic stent-grafts is to emulate the native aorta. As such, the stent-graft polymers should be lightweight but strong and resilient and capable of withstanding the impact of normal pulsatile high flow arterial blood pressure. However, ePTFE and PET are synthetic polymers that are relatively stiff and rigid compared to the native aorta.[1, 7-11]

The efficacy of EVAR rests on the aortic sac segregation from systematic pressure and sac shrinkage. There was reduced early perioperative morbidity and mortality with EVAR compared to open surgical repair (OSR).[12] However, this advantage was not maintained at the long-term follow-up, and arguably, these implications could be attributed to the adverse impact of the stent-graft materials on the cardiovascular hemodynamics.[1, 7, 8, 12-19] Although not powered to demonstrate the difference in outcomes based on endografts, the EVAR I trial showed reduced major adverse clinical events (MACEs) with the PTFE based GORE Excluder graft.[20,21] However, there are no head-on-head randomised clinical trials to compare currently available endografts. Furthermore, direct comparisons are further complicated by the heterogeneity of individual manufacturers'' differences in endograft design and procedural deployment techniques.[22, 23]

Consequently, it is difficult to accurately predict the impact of the stent-graft materials on hemodynamic alteration.[24] However, there is increasing evidence that aortic implanted devices alter cardiac remodelling coupled with acute systolic hypertension, elevated pulse pressure, and reduced coronary perfusion.[8, 14-16] Furthermore, a continuous increase in the aortic wall stress could have deleterious cerebral, renal and mesenteric effects.[1, 7, 8, 14-16] Currently, pulse wave velocity (PWV) is used as a surrogate marker to demonstrate changes in stiffness following EVAR. PTFE endografts had been reported to offer significantly stronger resistance to dilatation than PET-based endografts initially, albeit this advantage is lost over time.[25] Similarly, there were lower complications, like type I/II/III endoleaks, migration, and kinking.26 However, there are no reports of obvious advantages in outcome during long-term follow-up. The only obvious advantage of the PTFE based endografts compared to PET could be the development of the post-implantation syndrome (PIS). PIS has been reported in up to two-thirds of the patients following EVAR,[27] resulting in acute liver and/or multiple-organ failure.[28-33] Ito *et al.*,[27] Voûte *et al.*,[34] and Sartipy[35] implicated PET-based endografts in the development of postoperative pyrexia, PIS, and longer hospital stay post-EVAR compared to the PTFE-based endografts.

Endografts with woven PET are associated with a more robust inflammatory response which results in endothelial damage. Ferreira *et al.*[36] suggested a possible interlink between PIS and increased cardiovascular mortality. Also, polyester implanted grafts result in an augmented inflammatory response, mainly due to IL-8 serum levels. IL-8 is a neutrophil chemoattractant that exerts different pro-tumoural functions and plays a vital role in tumour progression and metastasis. This may elucidate the probable malignant potential of PET-based endografts.[37, 38] However, there are no controlled studies at present to substantiate these findings.

Finally, we can conclude that we undertook this systematic review to investigate device-materials related adverse outcomes, *i.e.*, PTFE *vs.* PET; however, not surprisingly, we did not find any RCTs or CCTs which were structured or powered to answer these specific questions. Despite uncertainty in the specific role played by stent-graft materials, there are increasing evidence of adverse hemodynamic alteration post-EVAR, therefore, the best solution in the short-term could be to reduce the stented length of the aorta, whilein the longer term encourage continuous improvement in stent-graft materials and design.[39]

This lack of randomised study is a motivation for undertaking a RCT, which owing to the variation in specialisation across aortic centres may require us to utilise cluster-randomisation. However, the logistical difficulties of undertaking an RCT should not be underestimated. In order to recruit large numbers and obtain sufficient funding, international collaboration is required. Before this, the next logical step is to undertake patient-level meta-analysis to inform specific trial outcomes. Other means of collecting evidence, such as prospective registers, should also be encouraged.

Limitations

An important limitation of our review is that we only sought to include RCTs and excluded other clinical studies. Observation studies and non-randomized trials could have been an essential source of information given the non-availability of RCTs and/or CCTs. As we could not find any RCTs based on our study objectives, we could not reach a consensus regarding the implications of the specific stent-graft materials in the post procedural outcomes following EVAR. Of consideration is that stent-graft material alone is difficult to investigate because of confounding factors. The evidence regarding the possible post procedural outcomes implicated to the stent-graft materials could also be attributed to the device design, shape, and the presence of an exoskeleton versus an endoskeleton.

Conclusion

There is a lack of evidence to support implications of specific stent-graft materials, *i.e.* PTFE *vs.* PET, in post-procedural outcomes following endovascular repair of AAA. In the absence of robust evidence, the only way forward is to plan and perform an RCT or CCT to compare the available stent-graft materials regarding procedural and clinical outcomes.

References

1. Parodi JC, Palmaz JC, Barone HD. Transfemoral intraluminal graft implantation for abdominal aortic aneurysms. *Ann Vasc Surg* 1991; 5: 491-9.

2. Duffy JM, Rolph R, Waltham M. Stent graft types for endovascular repair of abdominal aortic aneurysms. *Cochrane Database Syst Rev* 2015; 2015: CD008447.

3. Rolph R, Duffy JM, Waltham M. Stent graft types for endovascular repair of thoracic aortic aneurysms. *Cochrane Database Syst Rev* 2015; 2015: CD008448.

4. Roll S, Müller-Nordhorn J, Keil T, Scholz H, Eidt D, Greiner W, *et al.* Dacron *vs.* PTFE as bypass materials in peripheral vascular surgery--systematic review and meta-analysis. *BMC Surg* 2008; 8: 22.

5. Liberati A, Altman DG, Tetzlaff J, Mulrow C, Gøtzsche PC, Ioannidis JPA *et al.* The PRISMA statement for reporting systematic reviews and meta-analyses of studies that evaluate health care interventions: explanation and elaboration. *Ann Intern Med* 2009; 151: W65-W94.

6. Higgins JPT, Thomas J, Chandler J, Cumpston M, Li T, Page MJ, *et al.* Cochrane Handbook for Systematic Reviews of Interventions version 6.0 (updated July 2019). *Cochrane* 2019. Available from www.training.cochrane.org/handbook.

7. Volodos' NL, Shekhanin VE, Karpovich IP, Troian VI, Gur'ev IuA. A self-fixing synthetic blood vessel endoprosthesis. *Vestn Khir Im I I Grek* 1986; 137: 123-5.

8. Sultan S, O'Donohoe M, Colgan MP, Moore D, Shanik G. Critical Ischemia: Transfemoral Endoluminal Aortic Management: A Minimally Invasive Option in Aortic Intervention. *Vascular Surgery* 1999; 33: 179-84.

9. Moulakakis KG, Kadoglou NPE, Antonopoulos CN, Mylonas SN, Kakisis J, Papadakis I, *et al.* Changes in Arterial Stiffness and N-terminal pro-brain natriuretic peptide Levels after Endovascular Repair of Descending Thoracic Aorta. *Ann Vasc Surg* 2017; 38: 220-26.

10. Kleinstreuer C, Li Z, Basciano CA, Seelecke S, Farber MA. Computational mechanics of nitinol stent grafts. *J Biomech* 2008; 41: 2370-8.

11. Roccabianca S, Figueroa CA, Tellides G, Humphrey JD. Quantification of regional differences in aortic stiffness in the aging human. *J Mechl Behav Biomed Mat* 2014; 29: 618-34.

12. Paravastu SC, Jayarajasingam R, Cottam R, Palfreyman SJ, Michaels JA, Thomas SM. Endovascular repair of abdominal aortic aneurysm. *Cochrane Database Syst Rev* 2014; 2014: CD004178.

13. Vlachopoulos C, Aznaouridis K, Stefanadis C. Prediction of cardiovascular events and all-cause mortality with arterial stiffness: A systematic review and meta-analysis. *J Am Coll Cardiol* 2010; 55: 1318-27.

14. Sweeney KJ, Evoy D, Sultan S, Coates C, Moore DJ, Shanik DG, *et al.* Endovascular Approach to Abdominal Aortic Aneurysms Limits the Postoperative Systemic Immune Response. *Eur J Vasc Endovasc Surg* 2002; 23: 303-8.

15. Hynes N, Kok N, Manning B, Mahendran B, Sultan S. Abdominal Aortic Aneurysm Repair in Octogenarians versus Younger Patients in a Tertiary Referral Center. *Vascular* 2005; 13: 275-85.

16. Hynes N, Sultan S. A Prospective Clinical, Economic, and Quality-of-Life Analysis Comparing Endovascular Aneurysm Repair (EVAR), Open Repair, and Best Medical Treatment in High-Risk Patients With Abdominal Aortic Aneurysms Suitable for EVAR: The Irish Patient Trial. *J Endovasc Ther* 2007; 14: 763-76.

17. Elhelali A, Kavanagh EP, Hynes NM, Tawfick WM, Sultan S. Long-Term Outcomes of Open Repair of Inflammatory and Atherosclerotic Abdominal Aortic Aneurysms. *J Surg* 2016; 12: 5-8.

18. Sultan S, Hynes N. Clinical Efficacy and Cost per Quality-Adjusted Life Years of Pararenal Endovascular Aortic Aneurysm Repair Compared With Open Surgical Repair. *J Endovasc Ther* 2011; 18: 181-96.

19. Nauta FJH, Kamman AV, Ibrahim EH, Agarwal PP, Yang B, Kim K, *et al.* Assessment of Cardio-vascular Remodelling following Endovascular aortic repair through imaging and computation: the CORE prospective observational cohort study protocol. *BMJ Open* 2016; 6: e012270.

20. United Kingdom EVAR Trial Investigators, Greenhalgh RM, Brown LC, Powell JT, Thompson SG, Epstein D, Sculpher MJ. Endovascular versus open repair of abdominal aortic aneurysm. *N Engl J Med* 2010; 362: 1863-71.

21. United Kingdom EVAR Trial Investigators, Greenhalgh RM, Brown LC, Powell JT, Thompson SG, Epstein D. Endovascular repair of aortic aneurysm in patients physically ineligible for open repair. *N Engl J Med* 2010; 362: 1872-80.

22. Malas MB, Freischlag JA. Interpretation of the results of OVER in the context of EVAR trial, DREAM, and the EUROSTAR registry. *Semin Vasc Surg* 2010; 23: 165-9.

23. Kim HO, Yim NY, Kim JK, Kang YJ, Lee BC. Endovascular Aneurysm Repair for Abdominal Aortic Aneurysm: A Comprehensive Review. *Korean J Radiol* 2019; 20: 1247-65.

24. Georgakarakos E, Argyriou C, Schoretsanitis N, Ioannou CV, Kontopodis N, Morgan R, *et al.* Geometrical factors influencing the hemodynamic behaviour of the AAA stent grafts: essentials for the clinician. *Cardiovasc Intervent Radiol* 2014; 37: 1420-9.

25. Stollwerck PL, Kozlowski B, Sandmann W, Grabitz K, Pfeiffer T. Long-term dilatation of polyester and expanded polytetrafluoroethylene tube grafts after open repair of infrarenal abdominal aortic aneurysms. *J Vasc Surg* 2011; 53: 1506-13.

26. Patel R, Powell JT, Sweeting MJ, Epstein DM, Barrett JK, Greenhalgh RM. The UK EndoVascular Aneurysm Repair (EVAR) randomised controlled trials: long-term follow-up and cost-effectiveness analysis. *Health Technol Assess* 2018; 22: 1-132.

27. Ito E, Toya N, Fukushima S, Nishie R, Akiba T, Ohki T. Polyester Grafts Are a Risk Factor for Postimplantation Syndrome after Abdominal Endovascular Aneurysm Repair: Retrospective Analysis for Polyester Graft, Excluder®, and Endologix Powerlink®/AFX®. *Ann Vasc Dis* 2018; 11: 520-4.

28. Arnaoutoglou E, Kouvelos G, Papa N, Kallinteri A, Milionis H, Koulouras V, *et al.* Prospective evaluation of post-implantation inflammatory response after EVAR for AAA: influence on patients' 30 day outcome. *Eur J Vasc Endovasc Surg* 2015; 49: 175-83.

29. Syk I, Brunkwall J, Ivancev K, Lindblad B, Montgomery A, Wellander E, Wisniewski J, *et al.* Postoperative fever, bowel ischaemia and cytokine response to abdominal aortic aneurysm repair--a comparison between endovascular and open surgery. *Eur J Vasc Endovasc Surg* 1998; 15: 398-405.

30. Arnaoutoglou E, Papas N, Milionis H, Kouvelos G, Koulouras V, Matsagkas MI. Post-implantation syndrome after endovascular repair of aortic aneurysms: need for postdischarge surveillance. *Interact Cardiovasc Thorac Surg* 2010; 11: 449-54.

31. Moulakakis KG, Alepaki M, Sfyroeras GS, Antonopoulos CN, Giannakopoulos TG, Kakisis J, *et al.* The impact of endograft type on inflammatory response after endovascular treatment of abdominal aortic aneurysm. *J Vasc Surg* 2013; 57: 668-77.

32. Ohara N, Miyata T, Oshiro H, Shigematsu H, Ohki T. Adverse outcome following transfemoral endovascular stent-graft repair of an abdominal aortic aneurysm in a patient with severe liver dysfunction: report of a case. *Surg Today* 2000; 30: 764-7.

33. Blum U, Voshage G, Lammer J, Beyersdorf F, Töllner D, Kretschmer G, *et al.* Endoluminal stent-grafts for infrarenal abdominal aortic aneurysms. *N Engl J Med* 1997; 336: 13-20.

34. Voûte MT, Bastos Gonçalves FM, van de Luijtgaarden KM, Klein Nulent CG, Hoeks SE, Stolker RJ, *et al.* Stent graft composition plays a material role in the postimplantation syndrome. *J Vasc Surg* 2012; 56: 1503-9.

35. Sartipy F, Lindström D, Gillgren P, Ternhag A. The Impact of Stent Graft Material on the Inflammatory Response After EVAR. *Vasc Endovascular Surg* 2015; 49: 79-83.

36. Ferreira RS, Oliveira-Pinto J, Ultee K, Vôute M, Oliveira NFG, Hoeks S, *et al.* Post Implant Syndrome Influences Long-term Cardiovascular Prognosis After EVAR. *Eur J Vasc Endovasc Surg* 2019; 58Supple3: e808.

37. Yuan A, Chen JJ, Yao PL, Yang PC. The role of interleukin-8 in cancer cells and microenvironment interaction. *Front Biosci* 2005; 10: 853-65.

38. Alfaro C, Sanmamed MF, Rodríguez-Ruiz ME, Teijeira Á, Oñate C, González Á, *et al.* Interleukin-8 in cancer pathogenesis, treatment and follow-up. *Cancer Treat Rev* 2017; 60: 24-31.

Appendix 1: Comprehensive search plan based on population, intervention, compartor and outcomes (PICO) with sample search terms employed in Medline Ovid.

Details	Search strategy for the following study: A systematic review of stent-graft materials 'PTFE vs Polyester' in endovascular repair of abdominal aortic aneurysms
Population	Participants with abdominal and/or thoracic aneurysm.
Intervention and Comparison	Endovascular aneurysm repair using PTFE-based endografts. Endovascular aneurysm repair using polyester-based endografts.
Outcomes	**Primary outcomes:** 1) aneurysm-related death (including rupture and death within 30-days of procedure), and 2) major adverse cardiovascular events (myocardial infarction, heart failure, arrhythmia, cardiovascular death). **Secondary outcomes**: 1) endoleak, 2) aneurysm sac expansion, 3) reintervention, 4) graft infection, 5) thrombosis, 6) post-implantation syndrome, and 7) all-cause mortality.
Search terms employed in Medline Ovid:	((MH "Aortic Aneurysm, Abdominal") OR (MH "Aortic Aneurysm+") OR (MH "Aorta, Thoracic") OR (MH "Aortic Rupture") OR (MH "Aneurysm, Dissecting+") OR TI ("aortic tear" OR "aortic dissection" OR "aortic aneurysm") OR AB ("aortic tear" OR "aortic dissection" OR "aortic aneurysm")) AND (TI ("endovascular aortic repair" OR "EVAR" OR "TEVAR" OR "thoracic endovascular aortic repair" OR "thoracoabdominal endovascular repair" OR "fenestrated endovascular aortic repair" OR "FEVAR" OR "branched endovascular aortic repair" or "BEVAR") OR AB ("endovascular aortic repair" OR "EVAR" OR "TEVAR" OR "thoracic endovascular aortic repair" OR "thoracoabdominal endovascular repair" OR "fenestrated endovascular aortic repair" OR "FEVAR" OR "branched endovascular aortic repair" or "BEVAR") OR (MH "Endovascular Procedures+")) AND (TI ("stent-graft material" OR " Polytetrafluoroethylene" OR "PTFE") OR AB ("stent-graft material" OR " Polytetrafluoroethylene" OR "PTFE")) AND (TI ("myocardial infarction" OR "MI" OR "heart failure" OR "stroke" OR "Cardiovascular mortality" OR "hypertension" OR "aortic related death" OR "non fatal myocardial infarction") OR AB ("myocardial infarction" OR "MI" OR "heart failure" OR "stroke" OR "Cardiovascular mortality" OR "hypertension" OR "aortic related death" OR "non fatal myocardial infarction") OR (MH "Myocardial Infarction+") OR(MH "Heart Failure+") OR(MH "Stroke+")) AND (TI ("graft infection" OR "graft migration" OR "endoleak" OR "stent fracture" OR "graft thrombosis" OR "pseudoaneurysm formation") OR AB ("graft infection" OR "graft migration" OR "endoleak" OR "stent fracture" OR "graft thrombosis" OR "pseudoaneurysm formation") OR (MH "Blood Vessel Prosthesis"))

Search terms employed in Medline Ovid:	((exp abdominal aortic aneurysm/ OR exp aortic aneurysm/ OR exp thoracic aorta aneurysm/ OR exp aortic rupture/ OR exp dissecting aneurysm/) OR ("aortic tear" OR "aortic dissection" OR "aortic aneurysm").ab. OR ("aortic tear" OR "aortic dissection" OR "aortic aneurysm").ti.) AND (("endovascular aortic repair" OR "EVAR" OR "TEVAR" OR "thoracic endovascular aortic repair" OR "thoracoabdominal endovascular repair" OR "fenestrated endovascular aortic repair" OR "FEVAR" OR "branched endovascular aortic repair" or "BEVAR").ab. OR ("endovascular aortic repair" OR "EVAR" OR "TEVAR" OR "thoracic endovascular aortic repair" OR "thoracoabdominal endovascular repair" OR "fenestrated endovascular aortic repair" OR "FEVAR" OR "branched endovascular aortic repair" OR "BEVAR").ti. OR (exp endovascular surgery/)) AND (("stent-graft material" OR " Polytetrafluoroethylene" OR "PTFE").ab. OR ("stent-graft material" OR " Polytetrafluoroethylene" OR "PTFE").ti.)) AND (("myocardial infarction" OR "MI" OR "heart failure" OR "stroke" OR "Cardiovascular mortality" OR "hypertension" OR "aortic related death" OR "non fatal myocardial infarction").ab. OR ("myocardial infarction" OR "MI" OR "heart failure" OR "stroke" OR "Cardiovascular mortality" OR "hypertension" OR "aortic related death" OR "non fatal myocardial infarction").ti. OR (exp heart infarction/ OR exp heart failure/ OR exp cerebrovascular accident/)) AND (("graft infection" OR "graft migration" OR "endoleak" OR "stent fracture" OR "graft thrombosis" OR "pseudoaneurysm formation").ab. OR ("graft infection" OR "graft migration" OR "endoleak" OR "stent fracture" OR "graft thrombosis" OR "pseudoaneurysm formation").ti. OR (exp blood vessel prosthesis/ OR exp blood vessel transplantation/ OR exp blood vessel graft/))
Databases, websites and registries	MEDLINE Ovid, Embase, CINAHL, and Cochrane Central Register of Controlled Trials (CENTRAL). Subject strategies of databases were modelled on the search strategy designed for MEDLINE Ovid. US National Institutes of Health Ongoing Trials Register ClinicalTrials.gov; World Health Organization International Clinical Trials Registry Platform; and Stroke Trials Registry.
Thesauri to be checked	MeSH for CENTRAL and Medline, and Emtree for Embase.
Records retrieved from each source	To be recorded on pre-designed template as per the priori.
Reference management software	Endnote X8.2 and Covidence

Compliance mismatch and flow pattern in endovascular aortic repairs

31

Anna RAMELLA, Elena REDAELLI, Francesco MIGLIAVACCA, Giulia LURAGHI

Endovascular Aortic Repair (EVAR) is a minimally invasive technique to treat thoracic aortic pathologies, as aneurysms and dissections. Despite its increasing use, many critical factors of EVAR are not well understood. In this respect, in vitro, and in silico studies have the great potential to increase our understanding of the procedure, perform further device and procedural optimization, and help in clinical training. This review paper provides an overview of previous in vitro and in silico studies on EVAR treatments, with a special emphasis on the compliance mismatch induced by the implanted device. The compliance mismatch phenomenon, which has an impact on the hemodynamics after EVAR, occurs at the interface device-arterial wall where a difference in compliance is observed due to the mechanical coupling.

Introduction

According to the World Health Organization, cardiovascular diseases are the main cause of death worldwide [1] and most of them are related to the aorta because of the degeneration of the arterial wall. The most common diseases involving the aorta are aneurysms and dissections: the former, by definition, is an enlargement of more than 50% of the normal diameter of the aorta; the latter occurs when a laceration of the intima layer forms a false lumen between the intima and the media, thus blood flows in both the true lumen and the false lumen.

Nowadays, aneurysms and dissections are largely treated by an endovascular procedure named endovascular aortic repair (EVAR) which consists of placing a self-expanding stent-graft composed of a metal stent with a layer of fabric into the diseased aorta to recreate the original lumen. In this way, the natural fluid dynamics is restored, and the aortic wall is no more abnormally stressed; the risk of rupture is intentionally reduced.

The procedure consists of inserting a crimped stent placed into a small delivery system through the femoral artery of the patient and delivering it to the aorta by means of fluoroscopy images. Once the correct position is reached, the catheter is withdrawn, and the stent-graft expands covering the diseased region and reconstructing the vessel. The success is achieved when the endograft is deployed accurately and the aneurysm or the dissection is excluded from the circulation [2,3]. Although the short-term success of this technique is very high, the main disadvantages appear in the long term [4]. Endoleaks are the most common complication, and they represent a persistent blood flow perfusing the aneurysmatic sac or the false lumen, thus indicating a failure [5]. In the case of aneurysms, endoleaks increase the risk of expansion and eventually rupture, so generally, a secondary reintervention is envisioned. Endograft migration is a common complication defined as a displacement of the device by more than 5 - 10 mm from its original position [6]. Some post-procedural systemic complications may occur such as end-organ ischemia, cerebrovascular events, and post-implantation syndrome that is an inflammatory immune-mediated response [6].

In dissection cases, due to the fragility of the dissected tissue, the interaction between the aortic wall and the stent-graft may cause additional tears to occur. Dissections can propagate proximally towards the heart or distally towards the iliac region [7]. Moreover, although it is not usually reported as common complication of EVAR, an important aspect to be considered is the compliance mismatch. The compliance mismatch, caused by the implanted device which alters the stiffness (or distensibility) of the vessel, may also alter the hemodynamic of the aorta eventually generating an inflammatory response [8].
The compliance mismatch after EVAR is usually correlated with the aortic pulse wave velocity (PWV) change, which is a direct measure for arterial stiffness [9]. Evidence suggests that the PWV increment after EVAR is associated with increased cardiovascular risk [10]. Increases in PWV are detected from baseline to 1 week [11] and also to 6 months [12] postoperatively. Moreover, the compliance mismatch depends on the specific implanted stent-graft [13].

In the light of the described complications, it appears evident that fluid dynamics and structural forces play an important role exacerbated by the different mechanical properties of the native vessel and the synthetic graft.

To gain insight into the problem, in vitro and in silico studies have the potential to help our understanding of the procedure. In this review, a non-exhaustive overview of the literature on EVAR in vitro and in silico evaluation is presented. In particular, we focus the attention on the compliance mismatch and PWV increase after the EVAR procedure.

Compliance mismatch and pulse wave velocity

Arterial compliance is the property of changing vessel diameter or cross-sectional area triggered by a change in blood pressure. The elastic nature of the aorta plays the role of 'second pump' during diastole thanks to its compliance by modulating the flow to the tissues and changing the pulsatility nature of the blood. As a result, this function guarantees proper blood perfusion to the tissues.

When a graft, a stent-graft, or a stent is implanted, the compliance mismatch refers to the difference in compliance at the interface device/arterial wall and it represents a new property of the device-to-arterial wall mechanical coupling.

The reduction in compliance induced by the presence of an endovascular device influences the hemodynamics and it can induce thickening of the tunica intima of vessel walls, with consequent partial or complete occlusion of the aorta. Moreover, as a consequence, the pulsatility nature of blood is modified from its natural behavior generating collateral systemic problems [14].

Jeong *et al.* [15] investigated that there is not a standardized method to calculate the compliance but it is often studied by its related effects (increased PWV or abnormal wall shear stress distribution [16]). By definition, compliance is the variation of volume over the variation of pressure. Different studies [17–19] consider some significant sections along the region of interest and calculate the compliance as reported in the following formula:

$$C = \frac{1}{A_s} \cdot \frac{\Delta A}{\Delta p} \qquad (1)$$

where ΔA and Δp are the difference between systole and diastole in cross-section and pressure respectively and A_S is the cross-sectional area during systole.

The choice of considering a few cross-sections and not the entire volume is justified by the mostly radial deformation of the vessel (with respect to the longitudinal deformation). The endoleak effect influences the results because the aortic wall at the device location still expands radially thanks to the external blood flow. For this reason, the more endoleaks are present, the less the compliance mismatch phenomenon is evident.

PWV has been used as a surrogate parameter [20] for arterial stiffness. A stiffer aorta has a reduced storage capability, causing higher PWV and increasing the amount of pulse wave reflection and cardiac afterload [21]. The PWV is defined as

$$PWV = \frac{\Delta d}{\Delta t} \qquad (2)$$

where Δd is the distance between the inlet section (ascending aorta) and the outlet section (descending aorta) and Δt is the difference in time between the two pressure systolic peaks measured at the inlet and outlet sections.

van Herwaarden *et al.* [14] used magnetic resonance angiography to measure the wall compliance difference between pre- and post- EVAR and also between different stent-grafts. The vessel diameter changes were measured directly from the images and the stiffness (indicated by the aortic stiffness and the elastic modulus) resulted higher after the stent-graft implantation in particular at the level of the aneurysm sac. Moreover, the stent-graft design impacted the stiffness of the aneurysm neck.

Despite the above-cited study in which clinical data from a real patient were directly analyzed, the compliance mismatch is, in general, assessed by means of ad hoc in vitro and in silico studies. They can be designed specifically to analyze individual or confined aspects of the aorta-device environment, which is not feasible with in vivo analyses.

Examples of experimental literature studies

The reduction in compliance induced by the presence of a vascular prosthesis or endovascular device influences the hemodynamics in terms of blood flow patterns and stresses in the aortic wall. The changes in fluid velocity and variations in wall shear stress are a direct consequence of the compliance mismatch phenomenon. This is confirmed by Morris *et al.*[17], who experimentally investigated the arterial wall/device compliance mismatch of four stent-graft devices within the supra- and infrarenal locations for the treatment of abdominal aortic aneurysms. The devices were tested within a patient-specific abdominal aortic aneurysm perfusion model. Their work confirmed that a decrease in compliance in the stented region leads to an increased PWV and increased pulsatile arterial energy loss.

De Beaufort *et al.* [22,23] tested 4 different stent-grafts in health porcine thoracic aortas aimed at investigating whether the stiffening effects of stent graft deployment are dependent on stent-graft type and length. They found out that the aortic stiffness increased significantly after stent-graft deployment with each of the four types of stent-graft, with the increase in aortic stiffness depending on the extent of stent-graft coverage.

Legerer *et al.*[24] performed experiments on a biventricular mock circulation loop to optimize the compliance of a textile graft prosthesis by changing the transverse device cross-section. In their study, device compliance and the PWV were considered as target goals in optimizing the device performance.
Table 1 presents a synthetic overview of the analyzed in vitro studies.

Table 1: Summary of the in vitro analyzed studies

Paper	Aorta	Devices	Boundary conditions
Morris *et al.* [17]	Patient-specific flexible aorta with aneurism.	4 commercial stent-grafts	Pulsatile flow
De Beaufort *et al.* [22,23]	Porcine thoracic healthy aortas	4 commercial stent-grafts	Pulsatile flow
Legerer *et al.* [24]	None	Commercial ascending aortic graft	Pulsatile flow

Examples of computational literature studies

Computational analyses have been demonstrated to add rich information in studying the endografts effects on the arterial wall and blood flow after the implantation procedure. Among them, the Finite Element Analysis (FEA), Computational Fluid-Dynamic (CFD), and the Fluid-Structure Interaction (FSI) methods are the mostly adopted. (Figure 1). In particular, FEA allows reproducing the clinical procedure and simulating the structural mechanics – in terms of stresses and strains and deployed configuration – of both the stent-graft and the vessel. CFD is a numerical technique to model the hemodynamics with the strong hypothesis that blood flows into a rigid or imposed moving vessel and device, thus neglecting blood induced wall motion and deformation. The most complete tool is the FSI analysis which couples the hemodynamics and the structural mechanics: correct material properties are assigned to each component to simulate the real physics of the problem. Indeed, the effects of both the fluid dynamics and the structural forces can be assessed: the FSI technique allows the study of arterial fluid mechanics by accounting for both the instantaneous fluid forces acting on the wall and the effects of the wall motion on the fluid dynamic field.

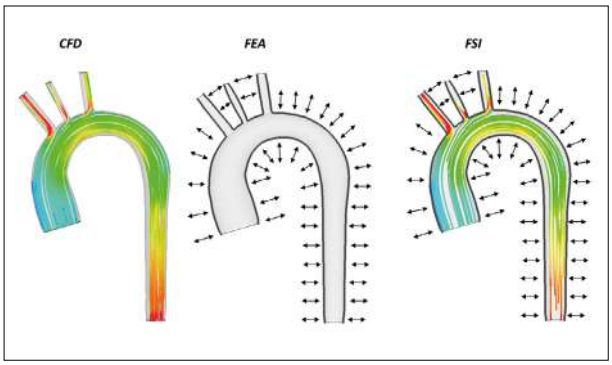

Figure 1: With a CFD simulation, flow velocities, streamlines and wall shear stresses can be computed but the aortic wall is fixed and cannot deform. A FEA simulation can provide displacements and stresses in the aortic wall, but the flow is absent. An FSI simulation can give a complete picture of the physics of the problem.

Most of the studies on EVAR in the numerical arena are investigated with purely CFD simulations. CFD analyses are used to evaluate the hemodynamics or to calculate the PWV.
The study by Vardoulis *et al.* [19] proposed a 1-dimensional CFD model to study the effect of a graft prosthesis implantation in the aortic arch comparing the results with a control case without the graft. The presence of the graft increases the PWV of the system; moreover, the PWV is more affected if the device is placed in a more distal position.

A different study [16] uses a CFD model to predict changes in blood flow at the graft-artery anastomosis induced by high, medium, and low compliance grafts. The graft compliance is taken into account by decreasing the graft diameter in the different computational models. The results show zones of recirculation at the anastomosis which are more evident in lower compliance (so, lower diameter) graft. In Morris *et al.* [25], the authors proposed a CFD study to assess the hemodynamics in two different

bifurcated stent-grafts with an idealized geometry. They evaluate the PWV and discover an increase in blood pressure with a consequent reduction in flow rate due to wave reflections phenomena at the device bifurcation level.
van Bakel *et al.*[26] proposed a quantification analysis of the hemodynamic impact of EVAR in patient-specific aortas using CFD and comparing the pre- and post-implantation cases. The presence of the device increases the maximum blood flow velocity, especially in the supraortic branches.
In the majority of the analyzed CFD studies[16,19,25], the numerical analysis is performed together with experimental studies to link the blood flow patterns (form simulations) with the compliance mismatch phenomenon (from experiments). This is the reason why a CFD simulation is not satisfactory for the study of the compliance mismatch phenomenon and an FSI model would be the best choice.
With FSI simulations the compliance parameter (eq. 1) can be directly calculated by quantifying not only the changes in pressure –which can be easily quantified also using CFD simulations –but even the vessel cross-section area variations.

A limited number of studies analyzing the compliance mismatch induced by the presence of a stent-graft by means of FSI simulations are present in the literature. The most relevant are here reported and they can be grouped into two classes: the former where the presence of the device is considered by changing the mechanical properties of the portion of the aortic wall interacting with the stent-graft; the latter where the device is present together with the aortic vessel. The reason for the former choice is to reduce the computational costs and the complexity of the simulation, with the drawback to miss important aspects like the interaction of the device with the arterial tissues.

The study by Tortoriello *et al.*[27] proposed an axial-symmetrical numerical perturbative approach to study a pulsatile flow in a vessel with elastic properties. The presence of the device is considered by varying the section of the vessel. The goal of their work was to highlight the influence of compliance mismatch, and possibly area variation in stented arteries. They observed altered hemodynamics at the prosthesis edges (proximal and distal) and verified that the main flow modifications in presence of compliance mismatch are probably associated with changes in the vessel section.

A similar approach is followed by Surovtsova *et al.*[28] who presented a numerical model of blood flow in a compliant vessel to study the mechanical effects caused by the local stiffening of an artery. The geometry consists of two elastic tubes with different Young modulus to simulate the presence of the device. The stiffening of the artery causes an increase in the blood wave speed. Moreover, a blood wave reflection is observed with a value of reflection which depends on the difference in Young modulus between the host vessel and the artificial implant.

Similarly, He *et al.*[29] simulated the presence of the device by altering the mechanical properties of an idealized artery. The vessel is simulated with a linear elastic material with an increased Young's Modulus in the stented region. The arterial compliance mismatch induces differences in the mechanical characteristics of the vessel wall at different locations. The arterial compliance mismatch could induce the differences of mechanical characteristics between different locations. Indeed, while the overall velocity distribution at different locations is not affected, higher velocity values are reached in the stiffer region.

A similar approach is observed in the study by Selvarasu *et al.*[30] where the stented region is mimicked by increasing the thickness of the idealized vessel, which consequently modifies the mechanical properties of the arterial wall. The difference in compliance due to the presence of the stent leads to changes in blood particles' residence time and recirculation zones at the proximal and distal ends of the device. The local hemodynamic alterations play a crucial role in creating a pathological condition in the arterial endothelium especially where a compliance discontinuity is present.
The limitations of these studies are the use of a straight vessel, not representative of a real aorta; furthermore, neither the graft prosthesis nor stent implantation is introduced in the models.

In the study proposed by Molony *et al.*[18], an FSI approach is followed introducing the stent-graft model. To limit the complexity of the simulation the authors modeled the device as a conduit with a Young's Modulus in between the one of the stent and the one of the graft; furthermore, the stent-conduit is assumed to be tied to the artery wall thus ignoring the possibility of endoleaks or local migration. When the device is present the arterial stiffness increases, and this leads to a reduction in the wall compliance. Table 2 presents a synthetic overview of the analyzed in silico studies.

Table 2: Summary of the in silico analyzed studies

Paper	Numerical analsys	Aorta model	Devices model	Boundary conditions
Vardoulis *et al.* [19]	CFD (1D)	1D aortic arch	Dacron graft	Inlet: unknown Outlet: WK circuits
Post *et al.* [16]	CFD	Straight vessel	Grafts with 3 different diameters	Inlet: pressure Outlet: pressure
Morris *et al.* [25]	CFD	None	Commercial stent-graft – simplified geometry	Inlet: velocity Outlet: pressure
van Bakel *et al.* [26]	CFD	Patient specific thoracic heathy aortas	Commercial stent-graft	Inlet: patient specific flow rate Outlet: WK circuits
Tortoriello *et al.* [27]	FSI - Axial-symmetrical numerical approach	Straight vessel Linear elastic	No device – different section in the vessel in the implantation region	unknown
Surovtsova *et al.* [28]	FSI (1D)	Straight vessel Linear elastic	No device – different E in the vessel in the implantation region	Inlet: velocity Outlet: unknown
He *et al.* [29]	FSI	Straight vessel Linear elastic	No device – different E in the vessel in the implantation region	Inlet: flow rate Outlet: pressure
Selvarasu *et al.* [30]	FSI	Straight vessel Linear elastic	No device – different wall thickness in the vessel in the implantation region	Inlet: velocity Outlet: pressure
Molony *et al.* [18]	FSI	Patient-specific abdominal aorta with aneurism Isotropic Hyperelastic	Simplified stent-graft geometry	Inlet: velocity Outlet: pressure

Future perspectives

In the in silico medicine arena which has become increasingly popular, the numerical studies on clinical procedure (*e.g.* endovascular aortic repair, transcatheter aortic valve implantation, endovascular thrombectomy procedure), can be divided into idealized [31,32] and patient-specific [33,34]. In general, in the numerical methodology development, technical aspects and specific clinical questions are assessable with an idealized approach. On the contrary, the patient-specific approach is more labor-intensive and time-consuming but gives a more realistic view of the clinical scenario.

From the present review, it is evident that the literature is lacking of relevant FSI studies of stent-grafts in the descending thoracic aorta without involving strong simplifications in the model. The completeness of the simulation is a crucial point since the compliance mismatch depends on the device and its materials. In this context, recently, our research group has started to develop a new numerical FSI tool to appraise the compliance mismatch phenomenon in that region considering the correct stent-graft materials. Two-way, strongly coupled, and boundary-fitted FSI simulations are carried out to simulate the hemodynamics for both the pre-and post-implantation conditions in an idealized aorta (figure 2A). Modelling the artery with a hyperelastic material is more realistic even if the computational costs increase. Of course, simulating the presence of some fibers families in the aortic wall makes the problem even more realistic with respect to a homogeneous hyperelastic material.

The device configuration has not been simplified, but both the stent and the graft components are modelled with the correct material properties. The stent material is a Nitinol shape memory alloy, while the graft is modelled with a linear elastic PET. In the simulation, contacts between the stent graft and the aorta are introduced. Blood is modelled as a Newtonian fluid and physiological velocity waveform is imposed as an inlet boundary condition; at the outlets, 3-elements Windkessel circuits are imposed to take into account the downstream resistances. The perspective of the developed FSI simulation is to carry out patient-specific cases (figure 2B). To the best of the authors' knowledge, this is the first work that assesses the aortic compliance mismatch after the EVAR procedure through FSI simulations assigning the correct materials and contacts to all the components (aortic wall, stent and graft).

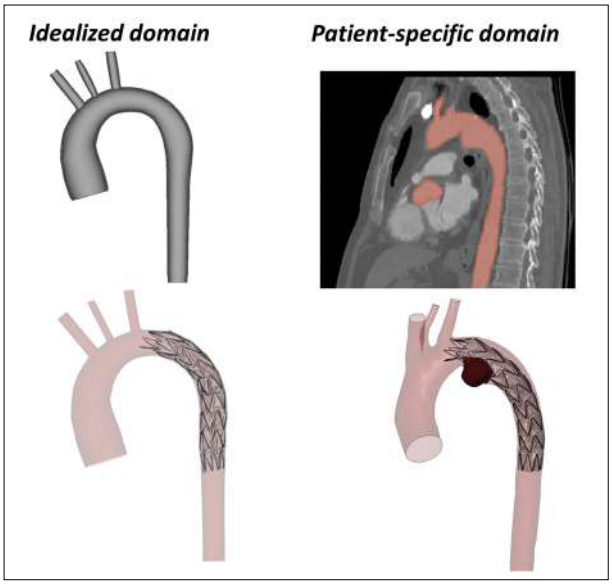

Figure 2: Idealized and patient-specific domains obtained from CAD geometry and CT images segmentation, respectively.

Discussion and conclusions

To assess the aortic compliance mismatch after the EVAR procedure FSI simulations are the mandatory choice. The adoption of FSI simulations – compared with CFD or FEA – is a crucial point to capture the complete physics of the system. Indeed, the completeness of a simulation is a key point since the compliance mismatch depends on the device, the aorta, and the respective materials: this is why FSI simulations are required. In addition, if the device is not properly modelled, local movements of the

device with respect to the aortic wall cannot be estimated without evaluating the risk of migration or immediate failure of the procedure.

Future works in modelling the EVAR procedures should be directed towards patient-specific aortas with the correct material parameters and boundary conditions – in terms of pressure and velocity. Also, modelling the presence of thrombi or calcifications in the pathological region would increase the completeness of the procedure prediction. Furthermore, different models of the devices can be virtually implanted and tested to compare the effects of different stent-graft designs on the compliance of the system. In fact, each device is characterized by a specific configuration and material which directly affect its compliance.

The whole implantation procedure can be reproduced in a virtual modality, to quantify the effects of compliance mismatch on the radial force exerted in the vessel wall, the device malapposition, and the hemodynamics in general.

Acknowledgements

This work has been supported from MIUR 302 FISR-FISR2019_03221 CECOMES.

References

1. https://www.who.int/news-room/fact-sheets/detail/the-top-10-causes-of-death.

2. Goodney P, Travis L, Lucas F, Fillinger M, Goodman D, Cronenwett J, *et al.* Survival after open versus endovascular thoracic aortic aneurysm repair in an observational study of the Medicare population. *Circulation* 2011; 124: 2661-9.

3. Gopaldas R, Huh J, Dao T, LeMaire S, Bakaeen F, Coselli J. Superior nationwide outcomes of endovascular versus open repair for isolated descending thoracic aortic aneurysm in 11,669 patients. *J Thorac Cardiovasc Surg* 2010; 140: 1001-10.

4. Gutsche J, Cheung A, McGarvey M, Moser W, Szeto W, Carpenter J, *et al.* Risk factors for perioperative stroke after thoracic endovascular aortic repair. *Ann Thorac Surg* 2007; 84: 1195-200.

5. Grabenwöger M, Alfonso F, Bachet J, Bonser R, Czerny M, Eggebrecht H, *et al.* Thoracic Endovascular Aortic Repair (TEVAR) for the treatment of aortic diseases: A position statement from the European Association for Cardio-Thoracic Surgery (EACTS) and the European Society of Cardiology (ESC), in collaboration with the European Assoc. *Eur Heart J* 2012; 33:1558-63.

6. Daye D, Walker TG. Complications of endovascular aneurysm repair of the thoracic and abdominal aorta: Evaluation and management. *Cardiovasc Diagn Ther* 2018; 8: S138-56.

7. Ma T, Liu F, Chen B, Jiang JH, Shi Y, Guo DQ, *et al.* Intraoperative Stent-Graft-Induced Aortic Intimal Intussusception During TEVAR for Type B Aortic Dissection. *J Endovasc Ther* 2021: in press

8. Murphy EH, Szeto WY, Herdrich BJ, Jackson BM, Wang GJ, Bavaria JE, *et al.* The management of endograft infections following endovascular thoracic and abdominal aneurysm repair. *J Vasc Surg* 2013; 58: 1179-85.

9. Hori D, Akiyoshi K, Yuri K, Nishi S, Nonaka T, Yamamoto T, *et al.* Effect of endoskeleton stent graft design on pulse wave velocity in patients undergoing endovascular repair of the aortic arch. *Gen Thorac Cardiovasc Surg* 2017; 65: 506-11.

10. Marketou M, Papadopoulos G, Kontopodis N, Patrianakos A, Nakou E, Maragkoudakis S, *et al.* Early Left Ventricular Global Longitudinal Strain Deterioration After Aortic Aneurysm Repair: Impact of Aortic Stiffness. *J Endovasc Ther* 2021; 28: 352-9.

11. Papadopoulos G, Kontopodis N, Marketou ME, Patrianakos A, Lioudaki S, Parthenakis FI, *et al.* Analysis of Echocardiographic Markers and Pulse Wave Velocities in a Patient Who Developed New Cardiac Symptoms after Implantation of an Aortic Endograft. *Ann Vasc Surg* 2019; 58: e11-381.

12. Moulakakis KG, Kadoglou NPE, Antonopoulos CN, Mylonas SN, Kakisis J, Papadakis I, *et al.* Changes in Arterial Stiffness and N-terminal pro-brain natriuretic peptide Levels after Endovascular Repair of Descending Thoracic Aorta. *Ann Vasc Surg* 2017; 38: 220-6.

13. van Noort K, Holewijn S, Schuurmann RCL, Boersen JT, Overeem SP, Jebbink EG, *et al.* Effect of abdominal aortic endoprostheses on arterial pulse wave velocity in an in vitro abdominal aortic flow model. *Physiol Meas* 2018; 39: 104001.

14. van Herwaarden JA, Muhs BE, Vincken KL, van Prehn J, Teutelink A, Bartels LW, *et al.* Aortic compliance following EVAR and the influence of different endografts: Determination using dynamic MRA. *J Endovasc Ther* 2006; 13: 406-14.

15. Jeong Y, Yao Y, Yim EKF. Current understanding of intimal hyperplasia and effect of compliance in synthetic small diameter vascular grafts. *Biomater Sci* 2020; 8: 4383-95.

16. Post A, Diaz-Rodriguez P, Balouch B, Paulsen S, Wu S, Miller J, *et al.* Elucidating the role of graft compliance mismatch on intimal hyperplasia using an ex vivo organ culture model. *Acta Biomater* 2019; 89: 84-94.

17. Morris L, Stefanov F, Hynes N, Diethrich EB, Sultan S. An Experimental Evaluation of Device/Arterial Wall Compliance Mismatch for Four Stent-Graft Devices and a Multi-layer Flow Modulator Device for the Treatment of Abdominal Aortic Aneurysms. *Eur J Vasc Endovasc Surg* 2016; 51: 44-55.

18. Molony DS, Callanan A, Kavanagh EG, Walsh MT, McGloughlin TM. Fluid-structure interaction of a patient-specific abdominal aortic aneurysm treated with an endovascular stent-graft. *Biomed Eng Online* 2009; 8: 24.

19. Vardoulis O, Coppens E, Martin B, Reymond P, Tozzi P, Stergiopulos N. Impact of aortic grafts on arterial pressure: a computational fluid dynamics study. *Eur J Vasc Endovasc Surg* 2011; 42: 704-10.

20. De Luca M, Iacono O, Valente V, Giardino F, Crisci G, Lettieri M, *et al.* Can pulse wave velocity (PWV) alone express arterial stiffness? A neglected tool for vascular function assessment. *J Basic Clin Physiol Pharmacol* 2021in press.

21. de Beaufort HWL, Nauta FJH, Conti M, Cellitti E, Trentin C, Faggiano E, *et al.* Extensibility and Distensibility of the Thoracic Aorta in Patients with Aneurysm. *Eur J Vasc Endovasc Surg* 2017; 53: 199-205.

22. de Beaufort HWL, Coda M, Conti M, van Bakel TMJ, Nauta FJH, Lanzarone E, *et al.* Changes in aortic pulse wave velocity of four thoracic aortic stent grafts in an ex vivo porcine model. *PLoS One* 2017; 12.

23. de Beaufort HWL, Conti M, Kamman A V., Nauta FJH, Lanzarone E, Moll FL, *et al.* Stent-Graft Deployment Increases Aortic Stiffness in an Ex Vivo Porcine Model. *Ann Vasc Surg* 2017; 43: 302-8.

24. Legerer C, Stevens M, Vazquez GM, Müller T, Ferrington L. An experimental evaluation of a concept to improve conventional aortic prostheses. *J Biomech* 2020; 112: 110010.

25. Morris L, Stefanov F, McGloughlin T. Stent graft performance in the treatment of abdominal aortic aneurysms: The influence of compliance and geometry. *J Biomech* 2013; 46: 383-95.

26. van Bakel TM, Romarowski RM, Morganti S, van Herwaarden JA, Moll FL, de Beaufort HW, *et al.* Blood Flow after Endovascular Repair in the Aortic Arch: A Computational Analysis. *Aorta (Stamford)* 2018; 6: 81-7.

27. Tortoriello A, Pedrizzetti G. Flow-tissue interaction with compliance mismatch in a model stented artery. *J Biomech* 2004; 37: 1-11.

28. Surovtsova I. Effects of compliance mismatch on blood flow in an artery with endovascular prosthesis. *J Biomech* 2005; 38: 2078-86.

29. He F, Hua L, Gao LJ. A computational model for biomechanical effects of arterial compliance mismatch. *Appl Bionics Biomech* 2015; 2015: 213236.

30. Selvarasu NKC, Tafti DK, Vlachos PP. Hydrodynamic effects of compliance mismatch in stented arteries. *J Biomech Eng* 2011; 133: 021008.

31. Kusner J, Luraghi G, Khodaee F, Rodriguez Matas JF, Migliavacca F, Edelman ER, *et al.* Understanding TAVR device expansion as it relates to morphology of the bicuspid aortic valve: A simulation study. *PLoS One* 2021; 16: e0251579.

32. Luraghi G, Rodriguez Matas JF, Dubini G, Berti F, Bridio S, Duffy S, *et al.* Applicability assessment of a stent-retriever thrombectomy finite-element model. *Interface Focus* 2021; 11: 20190123.

33. Luraghi G, Bridio S, Felix Rodriguez Matas J, Dubini G, Boodt N, Gijsen FJH, *et al.* The first virtual patient-specific thrombectomy procedure. *J Biomech* 2021; 126: 110622.

34. Luraghi G, Migliavacca F, García-González A, Chiastra C, Rossi A, Cao D, *et al.* On the Modeling of Patient-Specific Transcatheter Aortic Valve Replacement: A Fluid–Structure Interaction Approach. *Cardiovasc Eng Technol* 2019; 10: 437-55.

Modifications in aortic stiffness after endovascular or open aortic repair: a systematic review and meta-analysis

32

Daniele BISSACCO, Michele CONTI, Maurizio DOMANIN, Daniele BIANCHI, Luigia SCUDELLER, Sara ALLIEVI, Ferdinando AURICCHIO, Santi TRIMARCHI

Increased aortic stiffness (AoS) has been recognized as a risk factor in the development of cardiovascular disease. The aim of this systematic review and meta-analysis is to assess the impact of endovascular and open aortic repair on AoS.

Pubmed, Scopus and Web of Science databases were systematically examined for relevant studies evaluating consequences of endovascular and open aortic repair in AoS values.

PRISMA-P statement was used to perform the research process. Papers containing data regarding AoS before and after both thoracic (TEVAR) and abdominal (EVAR) endovascular repair, as well as open surgical repair (OSR), were screened and included for detailed evaluation. A fixed effects model was used to perform analysis. The Newcastle-Ottawa Scale was calculated for each included study. The quality of the evidence was determined according to the Grading of Recommendations, Assessment, Development, and Evaluations (GRADE) system.

The first article cluster was composed of 367 papers. After removal of duplicates and adoption of inclusion/exclusion criteria, 14 articles were finally selected, 13 of them were selected for meta-analysis. Overall, the included articles had low risk of bias. Ten studies analyzed EVAR and three analyzed TEVAR. Five of the selected papers were case-control studies, with OSR adopted in four of these as EVAR comparator. Several graft types were used in the endovascular group. AoS increased after TEVAR and EVAR, in terms of pulse wave velocity (PWV), even though several spatial levels and measurement modality were adopted. No differences were described after OSR, although no pooled data could be analyzed.

The present meta-analysis showed that AoS varies after endovascular aortic repair but not after open repair. In particular EVAR demonstrated a significant increase in AoS measurement (PWV), as well as TEVAR. Although the heterogeneity and low number of available studies limit the strength of the results, this review highlights the potential deleterious role of endoprosthesis on the cardiovascular system, although further studies are needed to achieve robust evidence. These findings should inspire the development of new endovascular devices, minimizing their impact on the native aortic wall properties.

Introduction

Arterial stiffness may be defined as the resistance offered by vascular walls to deformation powered by a propulsive force (such as the cardiac pump). Although it remains an intrinsic arterial wall characteristic, it can be modified by several factors including cardiac status, vessel compliance, and peripheral resistance.[1] Furthermore, along the same artery (most notably in the aorta) arterial stiffness may vary due to modifications in quantitative and qualitative wall structure, leading to different elastic properties for each tract (ascending, arch, descending, abdominal).[2] Vascular stiffness, and particularly the aortic stiffness (AoS), has also been established as a marker of increased risk of cardiovascular disease.[3,4] A large body of evidence has demonstrated deleterious effects of an increased AoS on coronary blood flow, myocardial perfusion and left ventricular (LV) performance, causing myocardial fibrosis, LV hypertrophy and myocardial disfunction.[5-7] Furthermore, cerebral, renal, and liver blood flow impairment has been demonstrated, due to reduction in peripheral artery perfusion.[1] In fact, according to the Windkessel effect,[8] an increased AoS produces a suboptimal aortic blood volume storage during cardiac systole, with less available blood flow, and therefore peripheral vascularization, during cardiac diastole and aortic recoil.[9]

In this scenario, avoiding aortic and peripheral vessel stiffening would be beneficial to prevent pathological mechanisms triggering cardiovascular complications.
Thoracic or abdominal endovascular aortic repair (TEVAR and EVAR, respectively) have been demonstrated as safe, valid, and durable therapeutic choice for aortic disease, despite a paucity of published data regarding aortic and cardiac modifications as consequence of endograft implantation.[10] In fact, available commercially endoprostheses (in the majority of cases composed of nitinol or other metal alloy stents) increase aortic rigidity and thus aortic stiffness, potentially increasing long-term cardiovascular morbidity and mortality rate, via the aforementioned mechanisms.[11,12] Such an increase of aortic stiffness is a particularly important concern for young patients undergoing TEVAR or EVAR who have long-life expectancy, and consequently it is crucial to predict and improve long-term cardiovascular outcomes caused by graft-related AoS.[13]
The aim of this systematic review and meta-analysis was to evaluate the impact of endovascular or non-endovascular therapy (TEVAR, EVAR and open surgical repair [OSR]) on AoS, describing patients' baseline characteristics, methods of AoS measurement, endografts used and postoperative outcomes, comparing preoperative with postoperative AoS.

Methods

Design

The Preferred Reporting Items for Systematic Reviews and Meta-Analysis Protocols (PRISMA-P) statement,[14] was used. The protocol employed here is available on the International Prospective Register of Systematic Reviews database (PROSPERO, registration number 212257).[15] Suggestions offered by Koelemay and Vermeulen were also considered.[16]

Literature sources and research strategy

Two Authors (D.B. and M.C.) independently and systematically performed the entire research process. In case of disputes or discrepancies between researchers, a third Author (S.T.) was consulted to give the final judgement and provide consensus. Research was performed on November 3, 2020; studies selection was performed between November 4 and November 14, 2020. The entire literature search strategy process is presented in detail as follows.

The research was conducted on PubMed, Scopus and Web of Science, using as time range “January 1, 2000 - October 31, 2020”. Only articles in the English language were included. Keywords were selected using medical subject headings (MeSH) for PubMed and MeSH/EMTREE for Scopus. The keywords "vascular stiffness", "arterial stiffness", "aortic stiffness", "pulse wave velocity", "PWV", “elastic modulus”, “pulsatility index” and “aortic compliance” were combined with "endovascular aortic repair", "EVAR" and "TEVAR" to obtain the first publications cluster (see Appendix, part 1). To find further relevant keywords, a further search on the first 10 results obtained in Pubmed using a non-specific query (see Appendix, part 2) was done. When possible, only [MeSH terms] modality was used during query composition, in order to avoid confusing and redundant results. The Boolean operators “AND” and “OR” were used to connect keywords with each other. Furthermore, the reference lists of screened studies were screened for further relevant publications. Finally, the “Article in press” section of vascular and thoracic journals were reviewed to detect articles not yet indexed in scientific database (the full list is included in the Appendix, part 3).

The Rayyan QCRI (Qatar Computing Research Institute, Doha, Qatar [available at https://rayyan.qcri.org/]) was used to manage and screen selected papers. For each selected article the following data were extracted into a dataset, using an Excel spreadsheet (Microsoft Corp, Redmond, WA):
1) First Author, year of publication, nationality of researchers, research time period; 2) baseline patients’ characteristics, including type of aortic disease; 3) graft characteristics and type of intervention; 4) level of measurement (brachial-ankle, carotid-brachial, carotid-femoral, carotid-radial, central-carotid, central-radial, other level) 5) AoS outcomes (see below).
Missing data were flagged as such during data analysis. To obtain data from articles’ image and graphics, a dedicated digital image processing and measurement software was used, if necessary (ImageJ, U.S. National Institutes of Health, Bethesda, MD).

Inclusion and exclusion criteria

Only original papers on AoS providing analysis on patients treated with TEVAR and/or EVAR were included. Other inclusion criteria to obtain eligible papers were: 1) analysis on > 3 patients; 2) both pre-and post-endovascular repair analysis; 3) using the same patient cohort in both pre-and post-endovascular repair analysis; 4) providing clear results on AoS; 5) postoperative AoS measurement was assessed within 365 days after intervention; and 6) adopting standardized and validated AoS measurements, regarding subject condition, device used and AoS indices calculated, according to Chirinos *et al.* and the European Network for Non-invasive Investigation of Large Arteries expert consensus.[1,17] Among the existing AoS indices, pulse wave velocity (PWV) and augmentation index at 75 bpm (AI@75) were preferentially investigated, as main outcomes adopted in literature.

Exclusion criteria were the following: 1) reviews (both systematic and non-systematic); 2) *in vitro/ex-vivo* studies; 3) animal studies; 4) in silico studies; 5) patients underwent hybrid or multiple aortic treatments; and 6) letters, comments and editorials on small scale and/or incomplete experiences. Endovascular repair in both elective and urgent settings were included, if aligned with other criteria, as well as studies analyzing patients who underwent OSR.

Quality assessment

The Newcastle-Ottawa Scale (NOS) was used to assess the methodological quality of each observational cohort study included in the analysis.[18] For case-controlled studies the original NOS was applied, and for cohort studies the modified NOS was applied. To estimate the risk of bias in randomized controlled trials (RCTs), the Cochrane Handbook for Systematic Reviews of Interventions was used.[19] The overall certainty of evidence across the studies was graded according to the guidelines of the Grading of

Recommendations Assessment, Development, and Evaluation (GRADE) Working Group as high, moderate low, and very low. Two Authors independently (D.B and M.C.) performed the entire methodological quality assessment for each selected study.

Objectives

Objectives were identified and described using the PICO framework methodology. [20]
The main objective of this systematic review and meta-analysis was to estimate the difference in pre and post AoS, in terms of PWV, in patients treated with endovascular or non-endovascular therapy (TEVAR, EVAR, and OSR) for aortic disease, for the most used levels of measurement: brachial-ankle (B-A), carotid-femoral (C-F), carotid-radial (C-R), carotid-brachial (C-B) and central-carotid (C-C).
Secondary objectives were to analyze the following PICOs:
- differences in pre and post AoS, in terms of AI@75, in patients treated with endovascular or non-endovascular therapy (TEVAR, EVAR and OSR) for aortic disease, for the most used levels of measurement (B-A, C-F, C-R, C-B, and C-C).
-differences in pre-and post-interventional AoS, in terms of PWV and AI@75, comparing three groups: TEVAR, EVAR and OSR, pooling all data, irrespective of measurement level.

Statistical analysis

Nominal variables were reported as number (percentage); continuous variables were reported as mean ± standard deviation (sd). In case the original report only included mean pre-surgery and mean post-surgery values, mean difference and its variance was back calculated according to standard Lou and Wan formulas. In cases where median and interquartile ranges only were reported, estimation of mean and standard deviation were performed with standard Lou and Wan formulas. In meta-analysis after assessing heterogeneity (I^2 statistics <60%), fixed effect meta-analysis was used to pool results. Network meta-analysis was performed to estimate the relative effect of EVAR or OSR *versus* no treatment, and standardized mean difference was used as a summary measure. For treatment-measurement level combinations where only one study was found, no meta-analysis was possible. In case of multiple postoperative AoS measurements, the one closest to the procedure was included. Stata computer software version 16.0 (Stata Corporation, College Station, TX) was used for statistical analysis. A two-sided *p value* <0.05 was considered statistically significant.

Results

A total of 367 records were identified through primary database searching (Figure 1). After deletion of duplicates, 96 articles were screened. Among those, 45 papers were excluded because they failed to match the article topic (aortic stiffness and endovascular therapy), while 33 articles were excluded due to application of inclusion/exclusion criteria. The most frequent cause for exclusion was in-vitro or ex-vivo studies,

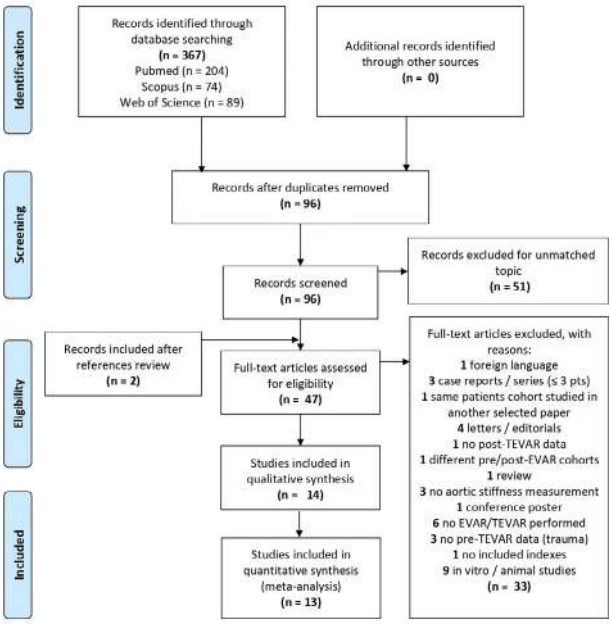
Identification
Screening
Eligibility
Included
Records identified through database searching (n = 367)
Pubmed (n = 204)
Scopus (n = 74)
Web of Science (n = 89)
Additional records identified through other sources (n = 0)
Records after duplicates removed (n = 96)
Records screened (n = 96)
Records excluded for unmatched topic (n = 51)
Records included after references review (n = 2)
Full-text articles assessed for eligibility (n = 47)
Full-text articles excluded, with reasons:
1 foreign language
3 case reports / series (≤ 3 pts)
1 same patients cohort studied in another selected paper
4 letters / editorials
1 no post-TEVAR data
1 different pre/post-EVAR cohorts
1 review
3 no aortic stiffness measurement
1 conference poster
6 no EVAR/TEVAR performed
3 no pre-TEVAR data (trauma)
1 no included indexes
9 in vitro / animal studies
(n = 33)
Studies included in qualitative synthesis (n = 14)
Studies included in quantitative synthesis (meta-analysis) (n = 13)

Figure 1: Preferred Reporting Items for Systematic Reviews and Meta-Analysis Protocols (PRISMA) flowchart for systematic literature review for studies on aortic stiffness and aortic interventions.

followed by articles on AoS but lacking graft implantation. Studies on vascular trauma were also excluded because they did not provide preoperative data on AoS, rendering it impossible to quantify the impact of endoprosthesis. Finally, 14 articles published from 2006 to 2020 were included in the qualitative analysis.[21-34] One study[23] was not included in the quantitative analysis due to use of "unconventional" level and unit of AoS measurement.

Quality of studies

All selected papers were prospective, observational cohort studies. Despite some limitations, all studies reach satisfactory quality, with low risk of bias (see Appendix, part 4). None of the selected papers reported a conflict of interest or funding. However, the quality of evidence in the meta-analysis was very low for all outcomes.

Study and patient characteristics

Table I describes study characteristics. All selected papers derived from single-center experiences, with more than half resulting from Greek (4 studies)[21,22,25,30] or Japanese (4 studies)[26,27,33,34] groups. Abdominal aorta was the most investigated aortic tract (10 studies).[21,23-25,28-33] As a consequence, EVAR was used in the majority of cases. On the contrary, TEVAR was adopted in 3 studies.[22,26,34] One paper had a mixed TEVAR / EVAR population.[27] Comparison between groups was performed 9 studies[21,24-26,28,29,31-33], with OSR as the most common comparator.[24,28,29,32] Two studies compared different graft types (ePTFE *versus* Polyester covered[25] or endoskeleton *versus* exoskeleton endoprosthesis[26]), and one[33] analyzed aneurysm sac behavior after EVAR (no change, shrinkage or enlargement) according to postoperative AoS values. Although all papers on abdominal aortic tract were focused on abdominal aortic aneurysm (AAA), studies on thoracic aorta had mixed cohort with type B aortic dissection (TBAD)[22,34], intramural hematoma (IMH) and/or aortic pseudoaneurysm.[22] The paper with mixed TEVAR / EVAR population also described results for patients affected by thoracoabdominal aortic aneurysm (TAAA).[27] Unfortunately, the small number and suboptimal specific results description made disease-related subgroup analysis impossible.

Table II describes patients' baseline characteristics in the selected studies. As noted, in the majority of cases patients were male, with hypertension and slightly overweight (body mass index > 25 kg/m^2). All studies but two[23,32] treated patients with acceptable mean systolic blood pressure (<140 mmHg), with only one study[24] having high mean diastolic blood pressure (>90 mmHg).

Operative treatment and endovascular graft types

Although detailed operative description was not present in the majority of the selected papers, all patients underwent conventional EVAR and TEVAR. No unconventional or "out of instruction-for-use" grafts were used (Table III). Among the selected papers, only one performed endovascular repair of the aortic arch.[26] Regarding the number of endografts deployed, only two papers[22,34] presented a comparative analysis between patients with one, two or three thoracic implanted endoprosthesis, finding no difference in terms of PWV. Unfortunately, few data exist about the correlation between the type of endograft implanted and variation in AoS. One study[23] described augmented EM and AoS in patients treated with the Gore® Excluder® stent-graft (W.L. Gore and Associates Inc., AZ, USA) when compared to Medtronic™ Talent™ stent-graft (Medtronic Vascular Inc., CA, USA). Similar results were obtained by Hori and collaborators[26] who found significant or tendency towards increased PWV after device implantation with Excluder, Medtronic™ Endurant™ (Medtronic Inc., MN, US) and Cook® Zenith® (Cook Medical, IN, USA), when compared to the Endologix® Powerlink® (Endologix Inc., CA, USA). As mentioned, endoprostheses formed by a rigid endoskeleton seem to have lower impact on AoS when compared to exoskeleton grafts. On the contrary, one study on TEVAR patients found no differences among different graft types.[34]

Level and methods for AoS measurement

AoS were measured at several levels and with numerous methods (Table IV and Figure 2).
The most used methods to assess AoS was PWV, which was employed in all but two [23,24] papers. Some studies also used AI@75. [24,29-31] One study analyzed AoS through elastic modulus (EM) and aortic compliance measurements, using dynamic MRA at 4 levels: 3 cm above the renal arteries, between the renal arteries, 1 cm below the renal arteries, and at the level of maximum aneurysm sac diameter. [23]
PWV and AI@75 were assessed mostly adopting B-A (5 studies) [26,30,31,33,34] and /or C-F (5 studies) measurement levels. [21,22,25,31,32] Ad hoc devices were adopted to calculate PWV and AI@75. Measurements were also performed from 7 to 365 days after the procedure, although in the majority of cases were evaluated within 180 days.

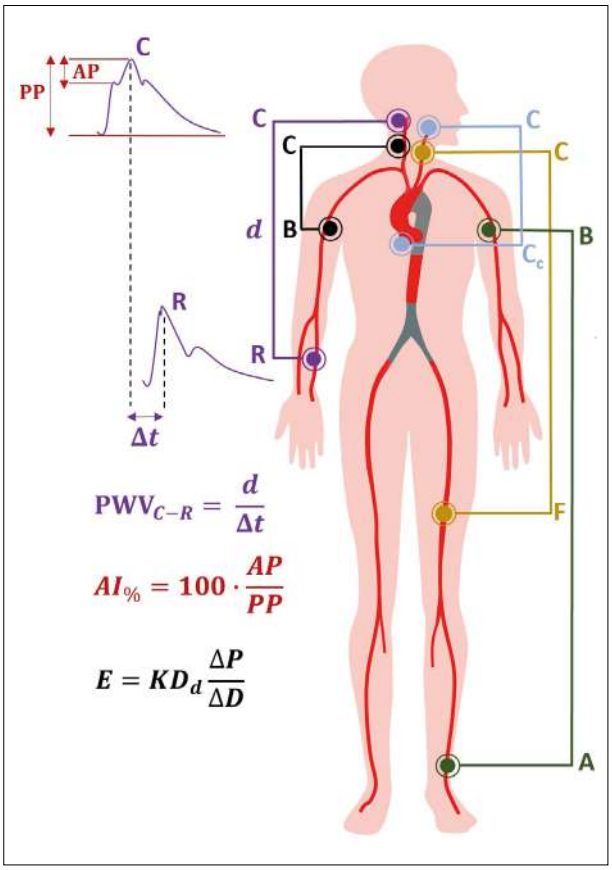

Figure 2: Schematic summary of levels and methods used to measure aortic stiffness (AoS), through pulse wave velocity (PWV), augmentation index (AI%) or elastic modulus (E). Sites of applanation tonometry measure for PWV computation are marked as follows: B= brachial, A=ankle, C= carotid, F=femoral, R=radial, Cc=central; d: C-R distance; Dt = time interval between C and R curves peaks; AP: Augmentation Pressure computed on C curve; PP: Pulse Pressure computed on C curve; E were computed according to [23], where K=133.3 is a constant that converts E from mmHg to N/m^2; DP is the variation in arterial blood pressure, and ΔD is the variation of aortic diameter at the location of interest.

Outcome results

Figure 3 summarizes meta-analysis results for PWV at each level of measurement, for EVAR (A), TEVAR (B) and OSR (C). As noted, PWV increased significantly after EVAR, particularly if measured as B-A (IC95% 0.07-1.32), C-F (IC95% 2.46-3.48) and C-C, although for the latter level of measurement only one study [28] was included in the analysis. Regarding TEVAR, PWV increased for both B-A (IC95% 0.81-2.48) and C-F levels of measurement, granting that for the latter only one study [22] was considered. Conversely, after OSR no differences were observed, for three levels of measurement (C-F, C-R, C-C) used separately in three different studies. [28,29,32] For AI@75, the 4 studies included in the analysis [24,29-31] reported data from different measurement levels, and results cannot be pooled together and analysed.

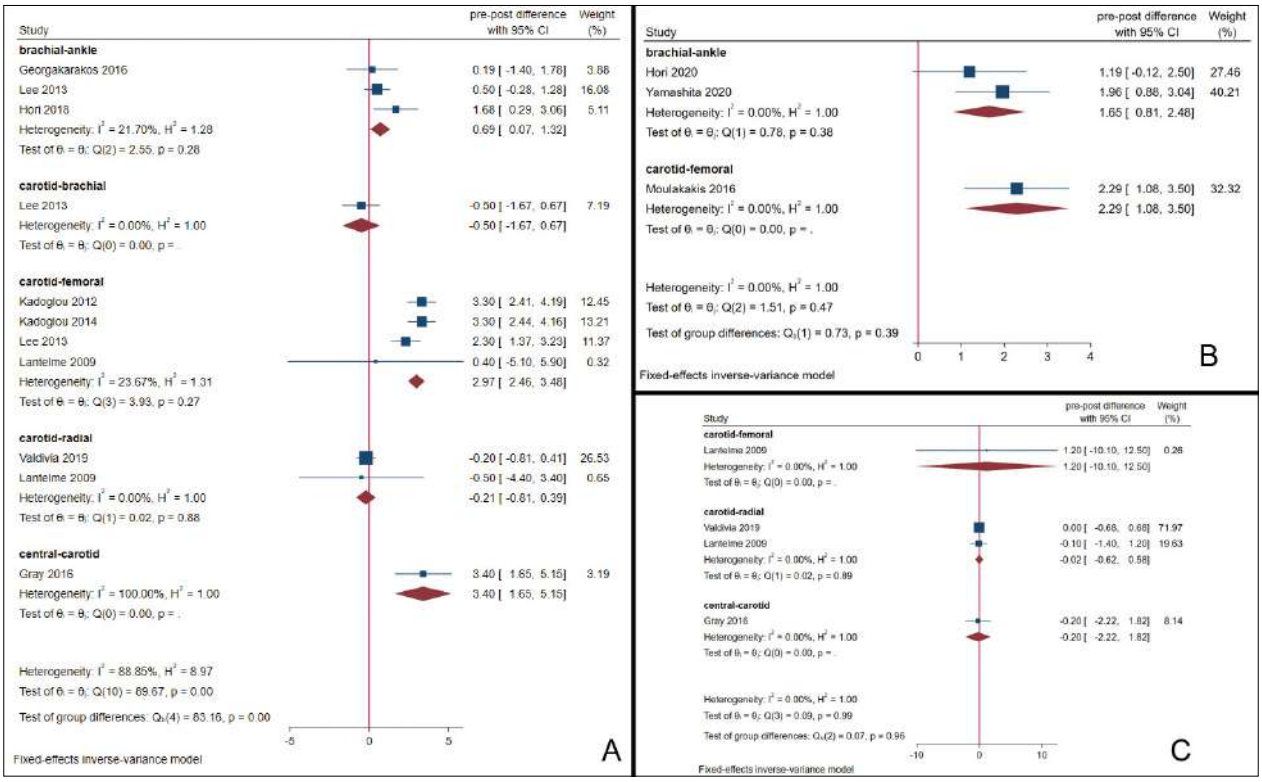

Figure 3: Forest plots of modification in pulse wave velocity after endovascular abdominal aortic repair (A), thoracic endovascular aortic repair (B) and open surgical repair (C) at different levels of measurement, based on data derived from selected studies. The solid squares denote the pre-post treatment difference and the weight of each study on pooled data, the horizontal lines represent the 95% confidence intervals (CIs), and the diamonds denote the pooled effect size.

Comparison in PWV modification after intervention was proposed for EVAR *versus* healthy controls in two studies [21,31] and EVAR *versus* OSR in three studies (see Appendix, Figure 1S). [28,29,32] Based on these analyses, PWV after EVAR was higher if compared with controls, although this was not statistically significant (IC95% –0.05-0.94) On the contrary, no differences were observed between EVAR and OSR (Figure 4). No studies investigated comparisons between AI@75 values in controls, EVAR, TEVAR *versus* OSR. These observations were consistent regardless of the level of measurement adopted in each study.

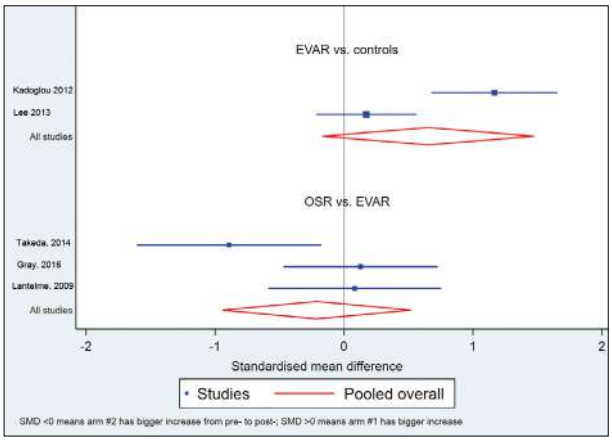

Figure 4: Forest plots of modifications in aortic stiffness (AoS) in comparative studies between Endovascular Abdominal Aortic Aneurysm Repair (EVAR) *versus* controls, and Open Surgical Repair (OSR) versus EVAR, regardless of the level of AoS measurement. Standard mean difference (SMD) < 0 indicates a bigger AoS increasing in controls (in the first plot) or EVAR (in the second plot), while a SMD > 0 indicates a bigger AoS increasing in EVAR (in the first plot) or OSR (in the second plot). The horizontal lines represent the 95% confidence intervals (CIs), and the diamonds denote the pooled effect size. For both comparisons p=ns.

Discussion

Arterial stiffness, and in particular AoS, is a well-known marker of central and peripheral cardiovascular disease, as well as independent predictor of cardiovascular complications.[1,35] The effects of arterial stiffening are mainly twofold: distally, a pathological cardiac wave transmission, with organ damage (particularly those at low resistance, such as brain and kidney) and proximally, an abnormal proximal cardiac wave reflection (with decreased coronary perfusion in diastole, impaired cardiac afterload and cardiac remodeling). While aging, genetic disease and lifestyle may contribute to increase AoS, aortic endografts may accelerate this process. De Beaufort and collaborators, in a mock model with 20 porcine thoracic aortas, found PWV value increased by a mean of 0.6 m/s or 8.9% from baseline after deployment of a 100-mm proximal stent graft ($p<0.001$), and by a mean of 1.4 m/s or 23.0% after distal extension of the stent graft ($p<0.001$).[36] These modifications may be more dangerous and deleterious in patients with a long-life expectancy, such as young and healthy ones, in whom pathological mechanisms of arterial stiffening may be reached gradually.

This systematic review and meta-analysis was conducted to analyze the impact of aortic intervention (both through graft and endograft use in thoracic and abdominal region) on aortic rigidity. Overall results indicate four main findings, regarding methods adopted and results achieved:

1) AoS in the literature is evaluated with several methods, parameters, and levels of measurement. This heterogeneity makes difficult direct comparison between published studies. Among levels of measurement, B-A and C-F are the most used for EVAR, while for TEVAR only B-A was analyzed for more than one study.

2) According to aortic region of interest for graft deployment, it seems to be less reasonable to evaluate AoS using C-C and C-R for both EVAR and TEVAR; similarly, C-B should not be used to evaluate AoS before and after EVAR. As recommended by a consensus statement17 and also supported by our findings, C-F may be the 'gold standard' for arterial stiffness measurement, due to the amount of published evidence using this method and because it requires little technical expertise.

3) PWV is the most commonly used measure to quantify AoS when compared with EM and AI@75.

4) Interestingly, AoS increase after TEVAR and EVAR is observed if measured with PWV, using C-F or B-A methods. Conversely, although poor results can be achieved for OSR, no modifications seem to occur.

These results are important also in terms of cardiac modifications during follow-up. TEVAR was associated with increased left ventricular mass and stroke work during follow-up.[37] Similarly, thoracic endografting resulted in an increased cardiac afterload and left ventricular hypertrophy in a canine model.[38] Graft deployment, as mentioned above, may lead to cardiovascular complications in patients without risk factors and concomitant traumatic aortic disease. In a group of 20 patients who experienced TEVAR for blunt traumatic aortic injury (BTAI), more than half (55%) developed hypertension during the follow-up period.[39] In particular, these patients were relatively young (age 41 ± 14 years) and none of the patients had reported previous cardiovascular events. Additionally, in BTAI patients PWV tends to be higher after TEVAR[40,41], although no preoperative evaluation can be provided, due to the urgency/emergency status of those who underwent TEVAR for BTAI. A careful balance of long-term *versus* short-term risks should be encouraged in these patients, particularly in cases of low grade BTAI (grade I or II) in which indications to TEVAR remain poorly defined.[41] The same reasoning should be observed to minimize long-term cardiovascular remodeling.

Regarding the type of endograft used, despite the lack of robust and pooled data, one study advocated that in AAA repair polyester covered stent-grafts showed greater PWV elevation when compared to ePTFE[25] and another study indicated that endoskeleton provides no significant PWV augmentation

if compared to exoskeleton stent grafts in arch and descending aorta repair [26] These pivotal results may be explained by the assumption that ePTFE and endoskeleton likely have a lower impact on aortic compliance, absorbing and transmitting the cardiac pulse wave similarly to the native aorta. Endoprosthesis manufacturing industries should be encouraged to improve graft characteristics in order to minimize the impact on the native aorta and make the treated aorta as much as possible equivalent to the normal one, in terms of mechanical and fluid dynamic properties. A similar statement may be used for OSR influence on AoS. While there are few data reported, with different AoS measures, polyester grafts used to open abdominal aortic repair seem to have no effect on pulse wave profile. This probably because of the lack of a nitinol skeleton, which may contribute to increased rigidity of the treated region.

Despite the notable results, this meta-analysis has some limitations due to the low number of selected studies, the wide range of methods used and the heterogeneity in aortic disease treated.
In particular, studies' heterogeneity did not permit any analysis of subgroups, *e.g.*, in terms of number of grafts deployed or pooled comparisons between graft types. In fact, different level of measurement and type of measurement (PWV, AI@75, etc.) lead to partial and suboptimal results. Moreover, no data regarding potential further AoS increase related to the number of grafts used are provided. Complexity of EVAR and TEVAR (*e.g.*, in cases of fenestrated or branched procedures) may also change AoS.
Finally, the limited number of studies permits robust results only in case of PWV measured using C-F and B-A for EVAR, making the remaining analysis poor in terms of significance. Despite this, our paper confirms and quantifies modifications after endovascular procedures.

Conclusion

AoS remains a well-known risk factor for cardiovascular disease, not only in terms of distal organ vasculature remodeling but also in terms of cardiac pump and pulse wave profile alterations. Endovascular aortic repair increases AoS, mainly after EVAR procedures, while OSR does not affect such aortic property.
However, no definitive conclusions can be made due to the wide range of AoS measurement modalities, through which the PWV measurement using C-F or B-A seems to be the most appropriate.
Further rigorous studies are needed to describe a valid protocol for level and unit of measure used to calculate AoS, analyzing long-term cardiovascular remodeling and complications, particularly in young patients.
Standardization of the metrics and measurement levels for the determination of AoS would improve the significance of comparative studies and enable meaningful suggestions for the management of this crucial parameter to improve patient outcomes and document best procedures for aortic repair.

Appendix

Supplementary data (Appendix) to this article can be found online.

Acknowledgments

Authors would like to thank Mr. Edward Kiegle for his revision of English grammar and syntax. Special thanks to Stefania Marconi, PhD for Figure 2.

References

1. Chirinos JA, Segers P, Hughes T, Townsend R. Large-Artery Stiffness in Health and Disease: JACC State-of-the-Art Review. *J Am Coll Cardiol* 2019; 74: 1237-63.

2. Jana S, Hu M, Shen M, Kassiri Z. Extracellular matrix, regional heterogeneity of the aorta, and aortic aneurysm. *Exp Mol Med* 2019; 51: 1-15.

3. Pierce GL. Mechanisms and Subclinical Consequences of Aortic Stiffness. *Hypertension* 2017; 70: 848-53.

4. Reference Values for Arterial Stiffness' Collaboration. Determinants of pulse wave velocity in healthy people and in the presence of cardiovascular risk factors: 'establishing normal and reference values'. *Eur Heart J* 2010; 31: 2338-50.

5. Palombo C, Kozakova M. Arterial stiffness, atherosclerosis and cardiovascular risk: Pathophysiologic mechanisms and emerging clinical indications. *Vascul Pharmacol* 2016; 77: 1-7.

6. Vlachopoulos C, Aznaouridis K, Stefanadis C. Prediction of cardiovascular events and all-cause mortality with arterial stiffness: a systematic review and meta-analysis. *J Am Coll Cardiol* 2010; 55: 1318-27.

7. Laurent S, Alivon M, Beaussier H, Boutouyrie P. Aortic stiffness as a tissue biomarker for predicting future cardiovascular events in asymptomatic hypertensive subjects. *Ann Med* 2012; 44 Suppl 1: S93-S97.

8. Mei CC, Zhang J, Jing HX. Fluid mechanics of Windkessel effect. *Med Biol Eng Comput* 2018; 56: 1357-66.

8. Belz GG. Elastic properties and Windkessel function of the human aorta. *Cardiovasc Drugs Ther* 1995; 9: 73-83.

9. Dobson G, Flewitt J, Tyberg JV, Moore R, Karamanoglu M. Endografting of the descending thoracic aorta increases ascending aortic input impedance and attenuates pressure transmission in dogs. *Eur J Vasc Endovasc Surg* 2006; 32: 129-35.

10. Georgakarakos E. Estimating the influence of aortic-stent grafts after endovascular aneurysm repair: Are we missing something? *Med Hypotheses* 2016; 97: 26-30.

11. Nauta FJH, de Beaufort HWL, Conti M, Marconi S, Kamman AV, Ferrara A, *et al.* Impact of thoracic endovascular aortic repair on radial strain in an ex vivo porcine model. *Eur J Cardiothorac Surg* 2017; 51: 783-9.

12. Nauta FJ, Conti M, Marconi S, Kamman AV, Alaimo G, Morganti S, *et al.* An experimental investigation of the impact of thoracic endovascular aortic repair on longitudinal strain. *Eur J Cardiothorac Surg* 2016; 50: 955-61.

13. Vallerio P, Maloberti A, D'Alessio I, Lista A, Varrenti M, Castelnuavo S, *et al.* Cardiovascular Remodeling after Endovascular Treatment for Thoracic Aortic Injury. *Ann Vasc Surg* 2019; 61: 134-41.

14. Page MJ, McKenzie JE, Bossuyt PM, Boutron I, Hoffmann TC, Mulrow CD, *et al.* The PRISMA 2020 statement: an updated guideline for reporting systematic reviews. *BMJ* 2021; 372: n71.

15. PROSPERO form on-line available at https://www.crd.york.ac.uk (visited on April 21,2021)

16. Koelemay MJ, Vermeulen H. Quick Guide to Systematic Reviews and Meta-analysis. *Eur J Vasc Endovasc Surg* 2016; 5: 309.

17. Laurent S, Cockcroft J, Van Bortel L, Boutouyrie P, Giannattasio C, Hayoz D, *et al.* Expert consensus document on arterial stiffness: methodological issues and clinical applications. *Eur Heart J* 2006; 27: 2588-605.

18. Stang A. Critical evaluation of the Newcastle-Ottawa scale for the assessment of the quality of nonrandomized studies in meta-analyses. *Eur J Epidemiol* 2010; 25: 603-5.

19. Cumpston M, Li T, Page MJ, Chandler J, Welch VA, Higgins JP, *et al.* Updated guidance for trusted systematic reviews: a new edition of the Cochrane Handbook for Systematic Reviews of Interventions. *Cochrane Database Syst Rev* 2019; 10: ED000142.

20. Schardt C, Adams MB, Owens T, Keitz S, Fontelo P. Utilization of the PICO framework to improve searching PubMed for clinical questions. *BMC Med Inform Decis Mak* 2007; 7: 16.

21. Kadoglou NP, Moulakakis KG, Papadakis I, Ikonomidis I, Alepaki M, Lekakis J, *et al.* Changes in aortic pulse wave velocity of patients undergoing endovascular repair of abdominal aortic aneurysms. *J Endovasc Ther* 2012; 19: 661-6.

22. Moulakakis KG, Kadoglou NPE, Antonopoulos CN, Mylonas SN, Kakisis J, Papadakis I, *et al.* Changes in Arterial Stiffness and N-terminal pro-brain natriuretic peptide Levels after Endovascular Repair of Descending Thoracic Aorta. *Ann Vasc Surg* 2017; 38: 220-6.

23. van Herwaarden JA, Muhs BE, Vincken KL, van Prehn J, Teutelink A, Bartels LW, *et al.* Aortic compliance following EVAR and the influence of different endografts: determination using dynamic MRA. *J Endovasc Ther* 2006; 13: 406-14.

24. Moloney MA, McHugh S, O' Donnell DH, Casey RG, Kavanagh EG, Grace PA, *et al.* Comparison of arterial stiffness and microcirculatory changes following abdominal aortic aneurysm grafting. *Ir J Med Sci* 2011; 180: 375-8.

25. Kadoglou NP, Moulakakis KG, Papadakis I, Ikonomidis I, Alepaki M, Spathis A, *et al.* Differential effects of stent-graft fabrics on arterial stiffness in patients undergoing endovascular aneurysm repair. *J Endovasc Ther* 2014; 21: 850-8.

26. Hori D, Yuri K, Kusadokoro S, Shimizu T, Kimura N, Yamaguchi A. Effect of endoprostheses on pulse wave velocity and its long-term outcomes after thoracic endovascular aortic repair. *Gen Thorac Cardiovasc Surg* 2020; 68: 1134-41.

27. Takeda Y, Sakata Y, Ohtani T, Tamaki S, Omori Y, Tsukamoto Y, *et al.* Endovascular aortic repair increases vascular stiffness and alters cardiac structure and function. *Circ J* 2014; 78: 322-8.

28. Gray C, Goodman P, Badger SA, O'Malley MK, O'Donohoe MK, McDonnell CO. Endovascular Aneurysm Repair Increases Aortic Arterial Stiffness When Compared to Open Repair of Abdominal Aortic Aneurysms. *Vasc Endovascular Surg* 2016; 50: 317-20.

29. Valdivia AR, Fuente MF, Santos AD, Murena MG, Lozano AR, Guaita JO, *et al.* Impact of the Aortic Graft on Arterial Stiffness and Inflammatory Biomarkers after Endovascular Aortic Repair or Open Surgical Repair in Abdominal Aortic Aneurysm Disease. *Ann Vasc Surg* 2019; 59: 84-90.

30. Georgakarakos E, Argyriou C, Georgiadis GS, Lazarides MK. Pulse Wave Analysis after Treatment of Abdominal Aortic Aneurysms with the Ovation Device. *Ann Vasc Surg* 2017; 40: 146-53.

31. Lee CW, Sung SH, Chen CK, Chen IM, Cheng HM, Yu WC, *et al.* Measures of carotid-femoral pulse wave velocity and augmentation index are not reliable in patients with abdominal aortic aneurysm. *J Hypertens* 2013; 31: 1853-60.

32. Lantelme P, Dzudie A, Milon H, Bricca G, Legedz L, Chevalier JM, *et al.* Effect of abdominal aortic grafts on aortic stiffness and central hemodynamics. *J Hypertens* 2009; 27: 1268-76.

33. Hori D, Nomura Y, Yamauchi T, Furuhata H, Matsumoto H, Kimura N, *et al.* Perioperative factors associated with aneurysm sac size changes after endovascular aneurysm repair. *Surg Today* 2019; 49: 130-6.

34. Yamashita Y, Oishi Y, Matsuyama S, Ushijima T, Fujita S, Kimura S, *et al.* Determinants of Changes in Arterial Stiffness after Thoracic Endovascular Aortic Repair. *Ann Vasc Surg* 2021; 70: 474-80.

35. Ben-Shlomo Y, Spears M, Boustred C, May M, Anderson SG, Benjamin EJ, *et al.* Aortic pulse wave velocity improves cardiovascular event prediction: an individual participant meta-analysis of prospective observational data from 17,635 subjects. *J Am Coll Cardiol* 2014; 63: 636-46.

36. de Beaufort HWL, Coda M, Conti M, van Bakel TMJ, Nauta FJH, Lanzarone E, *et al.* Changes in aortic pulse wave velocity of four thoracic aortic stent grafts in an ex vivo porcine model [published correction appears in PLoS One 2018;13: e0197453]. *PLoS One* 2017; 12: e0186080.

37. van Bakel TMJ, Arthurs CJ, Nauta FJH, Eagle KA, van Herwaarden JA, Moll FL, *et al.* Cardiac remodelling following thoracic endovascular aortic repair for descending aortic aneurysms. *Eur J Cardiothorac Surg* 2019; 55: 1061-70.

38. Yamashita Y, Oishi Y, Motomatsu Y, Hirayama K, Harada T, Ushijima T, *et al.* Thoracic endografting increases cardiac afterload and leads to left ventricular hypertrophy in dogs. *Eur J Cardiothorac Surg* 2019; 55: 618-25.

39. Vallerio P, Maloberti A, D'Alessio I, Lista A, Varrenti M, Castelnuovo S, *et al.* Cardiovascular Remodeling after Endovascular Treatment for Thoracic Aortic Injury. *Ann Vasc Surg* 2019; 61: 134-41.

40. Tzilalis VD, Kamvysis D, Panagou P, Kaskarelis I, Lazarides MK, Perdikides T, *et al.* Increased pulse wave velocity and arterial hypertension in young patients with thoracic aortic endografts. *Ann Vasc Surg* 2012; 26: 462-7.

41. D'Alessio I, Domanin M, Bissacco D, Rimoldi P, Palmieri B, Piffaretti G, *et al.* Thoracic endovascular aortic repair for traumatic aortic injuries: insight from literature and practical recommendations. *J Cardiovasc Surg (Torino)* 2020; 61: 681-96.

The Future

- Venous wall mechanical properties change after deep vein thrombosis: an experimental model 317
- Mechanics of small diameter arteries and dedicated vascular grafts: a short review 327
- Tissue Engineering Vascular Graft: current status and clinical application 338
- Xeltis: towards grafts from supramolecular materials 348
- Bioresorbable synthetic Heart Valves to induce *In Situ* tissue regeneration: recent advances and current challenges 359
- Tissue-Engineered Vascular Grafts: the promise of the Textile-Inspired approach 369
- Biohybrid Vascular Graft – Reduction of production time through the integration of textile reinforcement systems 378
- Relationship between hemodynamics and in-stent restenosis in femoral arteries 384
- Growth assessment of Engineered Vascular Grafts and Heart Valves 394

Venous wall mechanical properties change after deep vein thrombosis: an experimental model

33

Dragoslava P. VEKILOV, Adeline SCHWEIN, Louis MAGNUS, Nabil CHAKFÉ, Jean BISMUTH, K. Jane GRANDE-ALLEN

To avoid the serious complications associated with deep vein thrombosis (DVT), such as risk of pulmonary embolism, DVT patients are treated with anticoagulant, fibrinolytic, or endovascular therapies. These endovascular devices, however, are predominantly fabricated using materials designed for arterial conditions. The development of venous-specific devices is limited by a lack of information on the material properties of DVT-prone veins and on how DVT affects those properties.

We used a previously described porcine model of DVT using occlusion of the inferior vena cava (IVC) and iliac veins and injection of human recombinant thrombin. Pigs were euthanized at one-week time points, up to 5 weeks, and the suprahepatic IVC, infrarenal IVC, and iliac veins were excised. Following gross evaluation of the vein tissues and thrombus, uniaxial tensile testing was performed on longitudinal and circumferential sections of the DVT veins as well as healthy control tissues.

Fibrotic transformation of the thrombus, gradual incorporation into the venous wall, and eventual thrombus resolution were evident in the venous samples over time. Tensile testing on healthy control veins revealed location-specific differences in the thickness, stiffness, and failure strength. In the DVT model, thickness and longitudinal stiffness significantly increased over time. Differences in material properties between anatomical regions in the DVT model largely mirrored those seen in healthy tissue.

This data on the material behavior of veins under healthy *vs.* DVT conditions will inform the development of new endovascular devices that are tailored to specific regions of the major veins.

Introduction

Venous thromboembolism alters the mechanics, hemodynamics, and cell biology of the afflicted vein over the course of the disease, which presents as deep vein thrombosis (DVT) and/or pulmonary embolism (PE). In the US alone, there are as many as 600,000 cases of DVT each year, only 72% of which survive beyond 30 days.[1] Current treatment for central DVT, which occurs in the iliofemoral veins, brachiocephalic veins, inferior and superior vena cava, is often a multi-step process involving thrombolysis, balloon angioplasty, and stenting. The endovascular devices designed for these procedures, however, are often optimized for the treatment of arterial pathologies, despite the well-studied compositional, structural, and functional differences between arteries and veins.[2,3] While there is a clear need for venous-specific endovascular devices,[4] their development is constrained by a limited

understanding of venous mechanics. Because balloons, stents, and stent grafts used to treat DVT apply forces on the adjacent venous wall, the material properties of veins in healthy and diseased conditions are essential design criteria for these devices.

Over the past several decades, researchers have investigated venous mechanics and how they change in DVT, often employing small animal models to do so.[5] While these studies provide the only reported changes to material properties of the venous wall during DVT, their clinical application is limited due to disparities in size and complexity of the vascular systems. Thus, several groups have created large animal models of DVT in dogs, 6,7 baboons,[8–10] and pigs,[11–14] but their studies have predominantly focused on the biological response to thrombosis. One study assessed thrombus elasticity in a pig model using ultrasound elastography, but did not analyze the venous wall elasticity.[15]

In the present study, our aim was to (1) conduct mechanical analysis of the venous wall of a porcine model of central DVT and (2) characterize the material properties of healthy veins to serve as baseline values and to contribute to a general understanding of venous mechanics. Based on previous studies in rat models of thrombosis,[16–18] we hypothesized that the stiffness of the venous walls in this porcine model would increase over time.

Materials and Methods

Porcine Model of Occlusive Central Venous Deep Venous Thrombosis

The procedure for creating the porcine model of DVT has been previously described.[19] Experiments were done in accordance with the NIH Guide for the Care and Use of Laboratory Animals and approved by the Houston Methodist Hospital Institutional Animal Care and Use Committee. In short, 17 female domestic pigs (USDA class A, Oak Hill Genetics; Ewing, IL) and 7 female Yucatan pigs (USDA class A, S & S Farms; Ramona, CA) were anesthetized and subjected to a percutaneous balloon catheter procedure to occlude the infrarenal IVC and the iliac veins prior to injection of human recombinant thrombin (Figure 1A). After 2.5 hours, balloons were deflated, materials were removed, and the pigs recovered under veterinary care. Pigs were euthanized at one-week time points, up to five weeks. For healthy pigs, the IVC and iliac veins were harvested following euthanasia of pigs for non-cardiovascular studies.

Sample Preparation

At each DVT time point and in healthy pigs, the infrarenal IVC and the two iliac veins were harvested en bloc (Figure 1B,C). The anterior wall of the vein was marked with blue dye. The segment was then cut into 2 cm long segments for the infrarenal IVC 1 (IVC1), infrarenal IVC 2 (IVC2), right iliac (RI), and left iliac (LI) veins. The suprahepatic IVC (SH) was harvested separately for a non-thrombosed distal control. Tissue samples were stored in phosphate-buffered saline (PBS) at 4°C until testing, for a maximum of five days. Each segment was then cut along the lateral edge to open the vessel (Figure 1D).

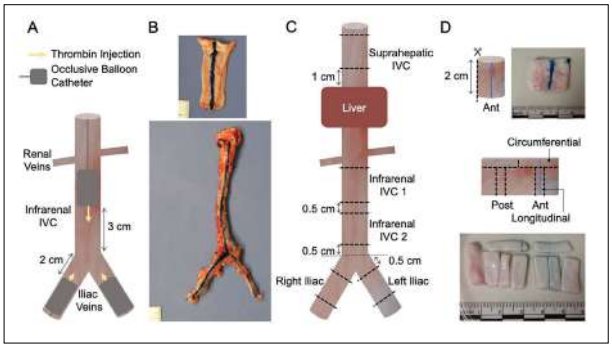

Figure 1: Porcine model of DVT and sample preparation.

(A) Occlusive balloon catheters were inserted in the infrarenal IVC and bilateral iliac veins prior to injection of human recombinant thrombin. Pigs were euthanized at one week timepoints, up to five weeks.

(B) The infrarenal IVC and iliac veins (bottom) and suprahepatic IVC (top) were harvested and the anterior face marked with a blue dye. Ruler marks are 1 mm.

(C) Sections were cut from multiple venous segments.

(D) Tissue sections were cut laterally, then longitudinal and circumferential strips were cut from the anterior and posterior walls for tensile testing.

Longitudinal and circumferential strips were cut from the anterior and posterior walls. In instances with interesting presentation of thrombus along the lateral wall, strips were taken from this region as well. If the tissue section was too small to acquire both longitudinal and circumferential strips, priority was given to longitudinal strips.

Thrombosis Progression Classification

Photographs of tissue sections acquired during sample preparation were reviewed to classify the level of thrombus present in each sample into one of four classifications: None, or no thrombus present; Unattached, or thrombus present but completely separable from the venous wall; Major Incorporation, or large continuous segment of fibrotic thrombus incorporated into and spanning the majority of the venous wall; and Minor Incorporation, or small pieces of fibrotic thrombus incorporated into the venous wall. To calculate the proportion of samples for each combination of factors, the number of samples per classification was divided by the total number of samples for each specific location and timepoint, excluding the healthy and SH samples.

Uniaxial Tensile Testing

To obtain accurate sample width and thickness dimensions, each sample was photographed in multiple orientations, along with a ruler, using a Leica MZ6 stereomicroscope (Wetzlar, Germany) prior to loading in the mechanical tester. The width and thicknesses were measured using ImageJ software (NIH; Bethesda, MD). Tissue strips were glued to balsa wood on both ends to prevent slippage from the grips during testing.

The tissue was then loaded into the EnduraTEC ELF 3220 (TA Instruments; Eden Prairie, MN) uniaxial tension tester, and the gauge length was measured as the length at which loading could be first detected. Tissues were preconditioned with 20 cycles of 3 mm displacement before being stretched to failure at a strain rate of 1 mm/second. The tissues were hydrated in a PBS bath, 37°C, for the duration of the test. Samples that failed prior to the stretch to failure step or that slipped from the tester grips were excluded.

The tissue widths and gauge lengths were used to convert raw load and displacement data to tension-strain curves, as previously described.[20] The maximum slope of the bilinear curve that spanned at least 4% strain was used to calculate the stiffness. The maximum tension achieved prior to failure was considered the failure strength.

Statistical Analysis

For all analyses (except thickness), samples were separated into longitudinal and circumferential groups, and analysis was performed on each orientation independently. Sample sizes for each group are reported in Table 1. The circumferential group had no samples for some animals at the 2 week timepoint, as well as for both iliac locations, so these samples were excluded from the circumferential analysis. Multifactorial analysis of variance (ANOVA) with post hoc Tukey's multiple comparisons test was performed using R Studio (R Studio; Boston, MA). Results were considered significant at $p<0.05$. Data are reported as mean ± standard deviation. Unless otherwise stated, the two-way ANOVA did not find significance for the interaction terms.

Table 1: Mechanical testing sample sizes

	Pigs	Longitudinal Samples						Circumferential Samples					
		SH	IVC1	IVC2	RI	LI	Total	SH	IVC1	IVC2	RI	LI	Total
H	10	18	19	19	9	14	**79**	16	7	7	2	-	**32**
1w	4	11	10	12	9	7	**49**	7	4	6	2	1	**20**
2w	2	4	6	5	5	6	**26**	4	-	-	-	-	**4**
3w	2	4	4	4	4	5	**21**	4	2	3	-	1	**10**
4w	3	6	7	6	4	4	**27**	6	2	2	2	-	**12**
5w	3	6	7	7	6	6	**32**	6	2	2	2	-	**12**
Total	**24**	**49**	**53**	**53**	**37**	**42**	**234**	**43**	**17**	**20**	**8**	**2**	**90**

SH = suprahepatic IVC; IVC1 = infrarenal IVC1; IVC2 = infrarenal IVC2; RI = right iliac vein; LI = left iliac vein; H = healthy; w = week

Results

Anterior *vs.* Posterior Differences

A three-way ANOVA showed no significant overall differences in longitudinal stiffness (p=0.1340) or thickness (p=0.1010) between anterior and posterior walls and did not show a difference at each location, except in one instance (data not shown). Therefore, the remaining analyses do not consider the wall side as a factor, and include the lateral wall sections of interest.

Presence of Thrombus

Thrombus was often visible in the segments after dissection (Figure 2). At 1 week, most samples had unattached thrombus (73%). Weeks 2 and 3 had the most samples with major incorporation of thrombus into the venous wall, 27% and 22% respectively. At weeks 4 and 5, more samples had minor incorporation (4 weeks: 11%; 5 weeks: 13%) compared to major incorporation (4 weeks: 7%; 5 weeks: 9%). LI had more samples with no thrombus present (50%), while RI had the most samples with major incorporation of thrombus (26%). The trends of IVC1 and IVC2 closely matched over time.

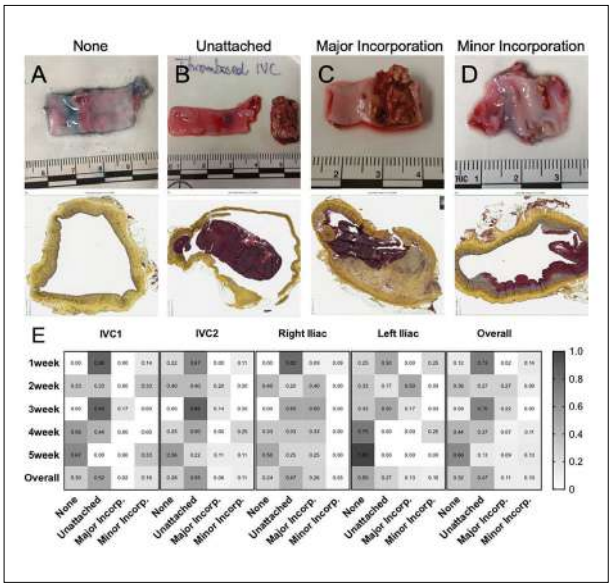

Figure 2: Thrombus classifications by gross evaluations as described in the text **(A-D)**. In the middle row, Movat stains collagen yellow, proteoglycans and glycosaminoglycans blue, elastin black, and fibrin and smooth muscle cells red. The proportion of samples that fell into each category for each location and timepoint **(E)**.

IVC1 = infrarenal inferior vena cava 1;
IVC2 = infrarenal inferior vena cava 2.

Thickness of Vessel Wall

In healthy veins, the wall thickness of the SH was greater than that of the other segments (each: p<0.0001; Figure 3A). There was no significant differences in thickness otherwise. The wall thickness was greater in the DVT veins than for healthy veins, both overall (p= 0.0005; Figure 3C) and specifically at 2 and 3 weeks (each: p<0.0001; Figure 3D). Moreover, the venous wall at 2 weeks was thicker for all other timepoints (1 week, 4 week: p<0.0001; 5 week: p=0.0024). The vessel wall at 3 weeks was also thicker than that of the 1 week (p<0.0001) and 4 week (p=0.0184) timepoints. Unlike the healthy veins, the DVT veins showed no differences in thickness between locations (Figure 3E). Over time, the thicknesses of the IVC2 and LI changed significantly. The thickness of IVC2 at 2 and 3 weeks was greater than both healthy (2 weeks: p=0.0311; 3 weeks: p=0.0050) and 1 week (2 weeks: p=0.0280; 3 weeks: p=0.0052) tissue (Figure 3F). The thickness of LI at 2 weeks was greater than healthy (p<0.0001) and all other time points (1 week: p=0.0002; 4 weeks: p=0.0237; 5 weeks: p=0.0034), except 3 weeks.

When analyzing the samples according to the thrombus classification, the thickness of the major incorporation group was greater than the remaining three classifications (each p<0.0001; Figure 3B). Therefore, the comparison of thickness between groups was repeated after censoring all samples classified as major incorporation to assess the effects of thrombosis on wall thickness independent of these extreme samples. Even after this censoring, the DVT veins were thicker than those of healthy pigs (p= 0.0003; Figure 3G). Additionally, the thickness of the venous wall at 2, 3, and 5 weeks was increased compared to healthy (2 week, 3 week: p<0.0001; 5 week: p=0.0003) and 1 week (2 week, 3 week: p<0.0001; 5 week: 0.0005; Figure 3H). At the 4 week timepoint, IVC2 (p=0.0268) and RI (p=0.0025) were thinner than IVC1. This censoring also revealed differences between anatomical locations (Figure 3I). SH was thicker than IVC2 (p<0.0001), RI (p=0.0011), and LI (p<0.0001). IVC1 was thicker than IVC2 (p=0.0016) and LI (p=0.0013). IVC1 increased in thickness compared to healthy at 2 weeks (p=0.0222), 4 weeks (p=0.0003), and 5 weeks (p=0.0413), and it was thicker at 4 weeks than at 1 week (p=0.0060; Figure 3J).

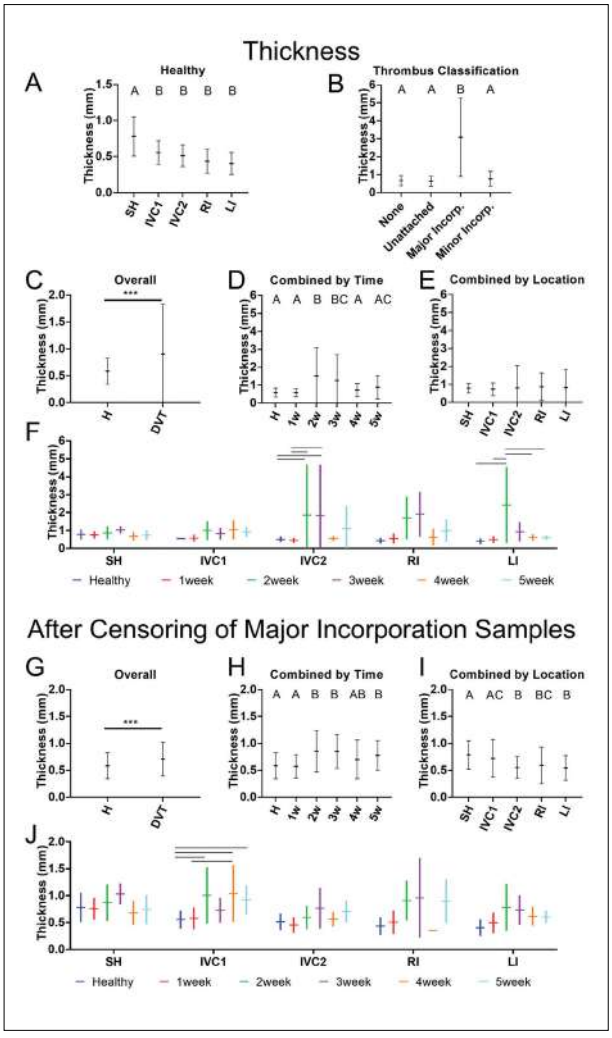

Figure 3: Thickness of the venous wall. In healthy veins, SH was thicker than other anatomical regions **(A)**. Major incorporation samples were thicker than those in other classifications **(B)**. The venous wall in the DVT model was thicker overall than for healthy pigs **(C)**. The thickness was greatest at 2 and 3 weeks in the DVT model **(D)**. Thickness did not differ between anatomical locations **(E)**. IVC2 and LI displayed significant differences between timepoints **(F)**. After censoring the major incorporation samples, the DVT wall remained thicker overall than that in healthy pigs **(G)**.

After censoring, thickness increased at timepoints 2 weeks and later compared to healthy and 1 week **(H)**. Censoring revealed new differences between anatomical locations **(I)**. IVC1 thickness was different between timepoints **(J)**. Groups that do not share a letter are significantly different from one another.

***= p<0.001. A bar indicates significant difference between the groups at the two endpoints. H = healthy; DVT = deep vein thrombosis model; w = weeks; SH = suprahepatic inferior vena cava; IVC1 = infrarenal inferior vena cava 1; IVC2 = infrarenal inferior vena cava 2; RI = right iliac vein; LI = left iliac vein.

Mechanical Behavior of Healthy Veins

The longitudinal stiffness (IVC1: p=.0014; IVC2: p<0.0001) and failure strength (each p<0.0001) of SH was lower than that of both infrarenal IVCs but not that of the iliac veins (Figure 4A,B). LI was less stiff longitudinally than IVC2 (p=0.0051) and had a lower longitudinal failure strength than IVC1 (p=0.0008) and IVC2 (p=0.0007).

In the circumferential direction, SH showed the reverse trend in that it was stiffer (IVC1: p=0.0007; IVC2: p=0.0002) and stronger (IVC1: p=0.0103; IVC2: p=0.0076) than the infrarenal IVCs (Figure 4C,D). When comparing circumferential to longitudinal orientations, SH (stiffness: p<0.0001; strength: p=0.0088) and IVC2 (stiffness: p=0.0027; strength: p=0.0006) showed anisotropy for both stiffness (Figure 4E) and failure strength (Figure 4F), whereas IVC1 was only different for failure strength (p=0.0009). However, the SH and infrarenal IVCs were anisotropic in opposite ways with SH stiffer circumferentially and the IVCs stiffer longitudinally.

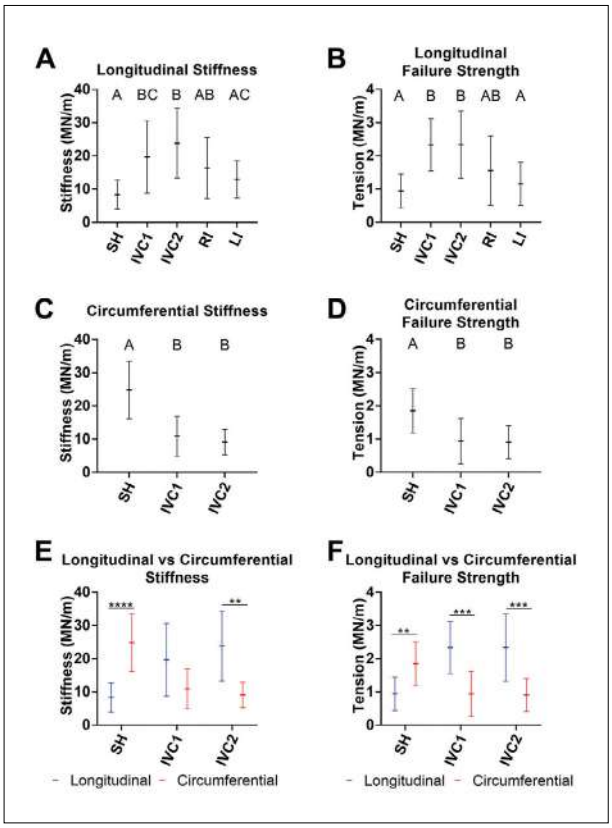

Figure 4: Mechanical properties of healthy veins. The stiffness and failure strength of SH was lower in the longitudinal direction **(A,B)** and higher in the circumferential direction **(C,D)** than IVC1 and IVC2. SH and IVC2 displayed anisotropy in stiffness **(E)**. SH, IVC1, and IVC2 displayed anisotropy in failure strength **(F)**. Groups that do not share a letter are significantly different from one another.

** = p<0.01; *** = p<0.001; **** = p<0.0001. SH = suprahepatic inferior vena cava; IVC1 = infrarenal inferior vena cava 1; IVC2 = infrarenal inferior vena cava 2; RI = right iliac vein; LI = left iliac vein.

Longitudinal Material Behavior

Overall, the longitudinal stiffness of the venous wall in the thrombosis models was greater than for healthy pigs (p=0.0277; Figure 5A). Over time, the longitudinal stiffness displayed an increasing trend, becoming stiffer than healthy at 4 weeks (p=0.0154) with a nearly significant increase at 5 weeks (p=0.1092; Figure 5B).

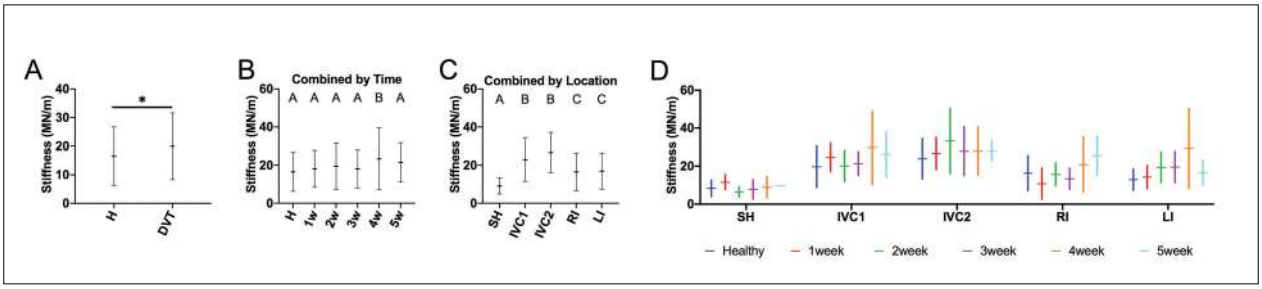

Figure 5: Longitudinal stiffness in the DVT model. The DVT venous wall was stiffer overall than in healthy pigs **(A)**. The stiffness had an increasing trend over time **(B)**. SH was the least stiff, and IVC1 and IVC2 were the stiffest of the regions **(C)**. There were no significant changes in stiffness for the individual locations **(D)**. In B and C, groups that do not share a letter are significantly different from one another.

*= p<0.05. H = healthy; DVT = deep vein thrombosis model; w = weeks; SH = suprahepatic inferior vena cava; IVC1 = infrarenal inferior vena cava 1; IVC2 = infrarenal inferior vena cava 2; RI = right iliac vein; LI = left iliac vein.

The suprahepatic IVC was the least stiff (IVC1, IVC2: p<0.0001; RI: p=0.0049; LI: p=0.0010), while IVC1 (RI: p=0.0095; LI: p=0.0184) and IVC2 (RI, LI: p<0.0001) were the stiffest (Figure 5C). There were no differences between the IVC1 and IVC2, nor between the two iliac veins.

There were no significant differences in failure strength between the healthy and DVT veins overall or over time (data not shown). However, IVC1 and IVC2 were both stronger than SH, RI, and LI (each: p<0.0001).

Circumferential Material Behavior

There were no significant differences in circumferential stiffness (Figure 6A) or failure strength (data not shown) detected over time. However, the suprahepatic IVC was stiffer (Figure 6B,C) and stronger than IVC1 and IVC2 (each: p<0.0001).

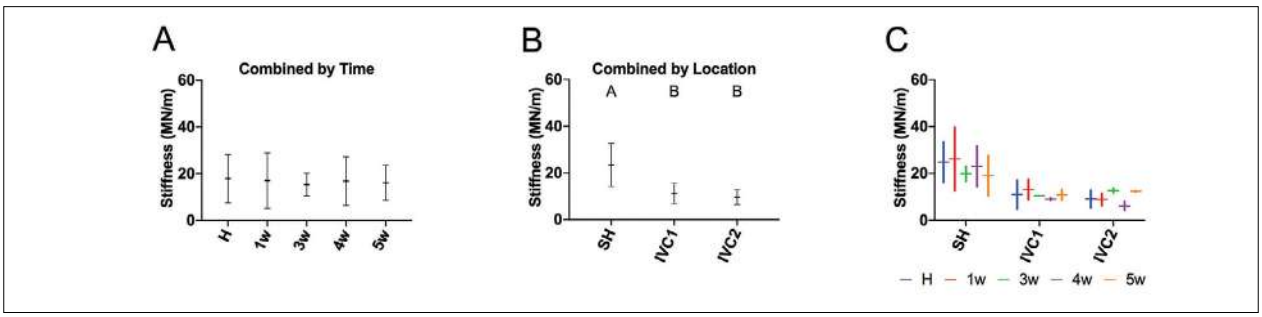

Figure 6: Circumferential stiffness of the venous wall in the DVT model. No differences were detected over time **(A)**. SH was stiffer than IVC1 and IVC2 **(B)**. No differences were found between time points for each location **(C)**. Groups that do not share a letter are significantly different from one another.

H = healthy; w = weeks; SH = suprahepatic inferior vena cava; IVC1 = infrarenal inferior vena cava 1; IVC2 = infrarenal inferior vena cava 2.

Material Behavior Based on Thrombus Classification

When the venous samples were classified according to the presence of thrombus, there were no significant differences detected in longitudinal stiffness or failure strength between groups (data not shown). However, the unattached (p=0.0801) and minor incorporation (p=0.0817) groups trended toward being stiffer than the none group. There were not enough samples per group to perform a similar circumferential analysis.

Discussion

This work describes the first analysis of altered material properties in a clinically relevant porcine model of DVT with comparison to healthy venous tissue. This model demonstrated the progression of thrombosis observed clinically, with fibrin clot formation, fibrotic transformation and vessel wall incorporation, and resolution,[21] which underscores the significance of our findings. Our study revealed differences in thickness, stiffness, and failure strength between anatomical sites in healthy and DVT model pigs. Additionally, we found the venous wall becomes thicker and stiffer longitudinally over the course of DVT. These results provide valuable information for the design of endovascular devices specific to the central venous system.

Our analysis of healthy tissue showed region-specific differences in material properties and significant anisotropy in the venous wall. Within the IVC, stiffness increased longitudinally and decreased circumferentially with distance from the heart. The SH, which is closer to the heart than the infrarenal IVC and iliac veins, is thicker than the more distal locations, a pattern also reported in the canine superior vena cava (SVC).[22] The canine SVC study, however, found that circumferential stiffness increased over a 5 cm distance from the right heart.[22] Here, both the SH and the IVC regions showed a pronounced anisotropy, but in an opposite manner. The SH region was stiffer circumferentially than longitudinally, which has previously been reported in the thoracic IVC.[3] The reversal of this pattern for the infrarenal IVC may reflect the different mechanical loading environment between the locations. The SH is intrathoracic and is thus exposed to negative pressure during inhalation, which would increase the blood load in the SH, while the infrarenal IVC is abdominal and thus exposed to positive pressure during this process. Together, these data illuminate the regional inhomogeneity within the venous system.

The venous wall thickness increased in the DVT model compared to healthy, changes that were evident regardless of whether the incorporated thrombus was considered. In the initial analysis, it was noted that the wall thickness was much greater at 2 and 3 weeks, which were the timepoints with the most major incorporation samples. Because it was not possible to measure the venous wall thickness without including the thrombus in these samples, we censored the data from the major incorporation samples. This removal of 5% of the samples decreased the overall mean thickness by 21% while decreasing the standard deviation by 66%, enabling detection of smaller differences in the remaining samples. The censored analysis still shows venous thickening at 2 weeks and later, indicative of progression from acute to chronic stage thrombosis. Increased thickness of the venous wall over the progression of thrombosis, even after resolution, has been noted both clinically[23,24] and in rat models.[5] The censored analysis also showed similar anatomic variation in thickness to that observed in healthy veins, suggesting that despite increases in thickness, the overall physiological patterns between regions are maintained.

The venous wall was stiffer in the DVT model than in healthy pigs. The increase in longitudinal stiffness over the progression of thrombosis was expected due to reports of fibrosis of the thrombus, stiffening of fibers embedded in the venous wall, and activation of matrix remodeling enzymes such as Matrix Metalloproteinase-9.[17,18,23] Increased stiffness in DVT has also been reported in murine models[16–18] and is consistent with reports of decreased venous compliance during the disease.[25] It should be noted that the stiffness and failure strength in this study were obtained by normalizing to the width of the test tissue instead of the cross-sectional area, since the thrombus-driven thickening was thought not to contribute to the load-bearing capacity of the venous wall. Nonetheless, this stiffening should be considered in the development of venous endovascular devices for the treatment of DVT. Interestingly, the relationships between locations in the DVT model for stiffness and failure strength (*e.g.*, SH < iliac veins < IVC1 and IVC2 for longitudinal parameters) closely mirrored those in healthy veins. In addition, IVC1 and IVC2 displayed similar trends in thrombus classification proportions, despite different roles in the initiation of the DVT model, and also did not differ in their material properties over time. This similarity suggests that the effects of thrombin may spread to immediately neighboring regions. In contrast, the left and right iliac veins in the DVT model had similar longitudinal material behavior, but very different presentations of thrombus. The effect of thrombosis on venous wall remodeling may depend more on the biological response to thrombosis, such as inflammation and hypoxia, than on the direct presence of thrombus. Additionally, the relatively stable mechanics of the SH over time suggests that DVT does not affect the venous wall mechanics of distant regions. Overall, the similarities in the relationships between locations in the DVT model and in healthy tissue suggest a uniformity in the tissues' responses to thrombosis.

Although this characterization of porcine venous material behavior in health and DVT is novel, there are notable limitations to the study. First, the presentation of DVT in this porcine model mimicked the clinical condition, but the results may not be fully generalizable to humans. Additionally, there were only small number of pigs at each timepoint as this was a pilot evaluation of the DVT model.[19] The use

of different commercial suppliers for the DVT and healthy pigs likely contributed to greater pig-to-pig variation than normal. Furthermore, the thin, floppy nature of veins in their planar state[26] made it difficult to measure the width and thickness, so the tissue was gently pulled taut until all folding was removed and the tissue laid flat. Lastly, the ex vivo tensile testing methods required sacrificing animals at each timepoint. Non-invasive methods, such as ultrasound elastography,[27] would enable the measurement of DVT-driven changes to the venous wall mechanics in the same animal at multiple timepoints.

In conclusion, this porcine model of DVT induced gradual increases in the thickness and longitudinal stiffness of the venous wall, even after thrombus resolution. Despite these pathological alterations, the DVT veins showed the same location-based patterns of material behavior and thickness found in healthy veins. Together, these findings broaden our understanding of venous mechanics and provide guidance for designing venous-specific endovascular devices to treat DVT.

Acknowledgements

This work was supported by the National Science Foundation Graduate Research Fellowship (1450681) to DPV. The authors thank Dr. Jonathan Stewart for statistical guidance, Drs. Jennifer Connell for critical review, and Judit E. Markovits, Courtney Vallien, and the Houston Methodist Department of Veterinary Pathology for histological staining.

References

1. Benjamin EJ, Muntner P, Alonso A, Bittencourt MS, Callaway CW, Carson AP, *et al.* Heart disease and stroke statistics—2019 update: A report from the American Heart Association. *Circulation* 2019; 139: e56-e528.

2. Silver FH, Snowhill PB, Foran DJ. Mechanical behavior of vessel wall: A comparative study of aorta, vena cava, and carotid artery. *Ann Biomed Eng* 2003; 31: 793-803.

3. Mattson JM, Zhang Y. Structural and functional differences between porcine aorta and vena cava. *J Biomech Eng* 2017; 139: 0710071.

4. Schwein A, Georg Y, Lejay A, Nicolini P, Hartung O, Contassot D, *et al.* Endovascular treatment for venous diseases: where are the venous stents? *Methodist Debakey Cardiovasc J* 2018; 14: 208-13.

5. Diaz JA, Obi AT, Myers DD, Wrobleski SK, Henke PK, Mackman N, *et al.* Critical review of mouse models of venous thrombosis. *Arterioscler Thromb Vasc Biol* 2012; 32: 556-62.

6. Faulkner Besancon M, Kyles AE, Griffey SM, Gregory CR. Evaluation of the characteristics of venous occlusion after placement of an ameroid constrictor in dogs. *Vet Surg* 2004; 33: 597-605.

7. Foster ED, Dobell AR. Evaluation of rigid prosthetic rings as *in vivo* intravascular thrombogenic models. *J Surg Res* 1971; 11: 550–8.

8. Diaz JA, Wrobleski SK, Alvarado CM, Hawley AE, Doornbos NK, Lester PA, *et al.* P-selectin inhibition therapeutically promotes thrombus resolution and prevents vein wall fibrosis better than enoxaparin and an inhibitor to von willebrand factor. *Arterioscler Thromb Vasc Biol* 2015; 35: 829-37.

9. Downing LJ, Wakefield TW, Strieter RM, Prince MR, Londy FJ, Fowlkes JB, *et al.* Anti-p-selectin antibody decreases inflammation and thrombus formation in venous thrombosis. *J Vasc Surg* 1997; 25: 816-27.

10. Wakefield TW, Wrobleski SK, Sarpa MS, Taylor FB, Esmon CT, Cheng A, *et al.* Deep venous thrombosis in the baboon: an experimental model. *J Vasc Surg* 1991; 14: 588-98.

11. Barbash IM, Schenke WH, Halabi M, Ratnayaka K, Faranesh AZ, Kocaturk O, *et al.* Experimental model of large pulmonary embolism employing controlled release of subacute caval thrombus in swine. *J Vasc Interv Radiol* 2011; 22: 1471-7.

12. Geier B, Muth-Werthmann D, Barbera L, Bolle I, Militzer K, Philippou S, *et al.* Laparoscopic ligation of the infrarenal vena cava in combination with transfemoral thrombin infusion: a new animal model of chronic deep venous thrombosis. *Eur J Vasc Endovasc Surg* 2005; 29: 542-8.

13. Hosaka J, Roy S, Kvernebo K, Enge I, Laerum F. Induced thrombosis in the pig inferior vena cava: a model of deep venous thrombosis. *J Vasc Interv Radiol* 1996; 7: 395-400.

14. Ichiki M, Sakai Y, Nango M, Nakamura K, Matsui H, Cho H, *et al.* Experimental venous thrombi: MRI characteristics with histopathological correlation. *Br J Radiol* 2012; 85: 331-8.

15. Geier B, Barbera L, Muth-Werthmann D, Siebers S, Ermert H, Philippou S, *et al.* Ultrasound elastography for the age determination of venous thrombi. *Thromb Haemost* 2005; 93: 368-74.

16. Vekilov DP, Grande-Allen KJ. Mechanical Properties of Diseased Veins. *Methodist Debakey Cardiovsc* J 2018; 14: 1-6.

17. McGilvray KC, Sarkar R, Nguyen K, Puttlitz CM. A biomechanical analysis of venous tissue in its normal and post-phlebitic conditions. J Biomech 2010; 43: 2941-7.

18. Nguyen KP, McGilvray KC, Puttlitz CM, Mukhopadhyay S, Chabasse C, Sarkar R. Matrix metalloproteinase 9 (MMP-9) regulates vein wall biomechanics in murine thrombus resolution. *PLoS One* 2015; 10: e0139145.

19. Schwein A, Magnus L, Markovits J, Chinnadurai P, Autry K, Jenkins L, *et al.* A new porcine model of acute and chronic central deep venous thrombosis mimicking human pathology. *Eur J Vasc Endovasc Surg* (In review)

20. Puperi DS. Biomimetic heterogeneous scaffolds for a layered tissue engineered heart valve. *Rice University* 2016; 17: 1766-75.

21. Kumar V, Abbas A, Fausto N, Aster JC. Robbins and Cotran Pathologic Basis of Disease 8th edition. Philadelphia, PA; 2010.

22. Minten J, Verheyen A, Cornelissen F, Rombauts W, Dequeker J, De Geest H. Correlation between mechanical properties and wall composition of the canine superior vena cava. *Arch Int Physiol Biochim* 1986; 94: 349-62.

23. Deatrick KB, Elfline M, Baker N, Luke CE, Susan B, Stabler C, *et al.* Post thrombotic vein wall remodeling. J Vasc Surg 2011; 53:139-46.

24. Chandrashekar A, Garry J, Sikalas N, Gasparis A, Labropoulos N. Heterogeneity in post-thrombotic vein wall remodeling. J Vasc Surg Venous Lymphat Disord 2017; 5: 145.

25. Neglén P, Raju S. Compliance of the normal and post-thrombotic calf. *J Cardiovasc Surg* 1995; 36: 225-31.

26. Desch GW, Weizsäcker HW. A model for passive elastic properties of rat vena cava. *J Biomech* 2007; 40: 3130-45.

27. Mumoli N, Mastroiacovo D, Giorgi-Pierfranceschi M, Pesavento R, Mochi M, Cei M, *et al.* Ultrasound elastography is useful to distinguish acute and chronic deep vein thrombosis. *J Thromb Haemost* 2018; 16: 2482-91.

Mechanics of small diameter arteries and dedicated vascular grafts: a short review

34

Lucie GERNEZ, Mélissandre ASFAZADOURIAN, Didier LETOURNEUR, Isabelle BATAILLE, Frédéric CHAUBET

There is a need to develop small-diameter (<6mm) vascular vessels for bypass surgery and other vascular reconstructive procedures. Up to now, no artificial small diameter vascular graft is good enough to be used as gold-standard because of poor long-term patency, mainly due to mechanical properties mismatch. Because of their composition, small arteries are viscoelastic with delayed elasticity, anisotropic and compliant. The development of relevant vascular grafts needs the determination of the mechanical properties performed with both native arteries and the dedicated graft, what is rarely presented in the literature. This review highlights first the main mechanical parameters of interest: the Young's modulus, a major index of the material elasticity, loss and storage moduli to characterize the viscoelastic behavior, compliance which is a direct description of arterial distensibility, and burst pressure related to the capacity of the artery to withstand pressure. Some of the most relevant studies are presented and a guideline is proposed for mechanics study in order to help designing vascular graft able to closely mimic the mechanical properties of small native arteries.

Introduction

For over 50 years, researchers are trying to find a satisfactory vascular substitute with diameter lower than 6 mm. Indeed, arteries are complex structures and the composition of the vascular wall impart particular mechanical properties which are difficult to imitate with artificial prostheses. Today, the gold-standard remains autologous vessels, including saphenous vein or intern mammary artery and no artificial vascular graft was found good enough to be used because of poor long-term patency. Even if the obstacle of thrombogenicity is avoided, sooner or later the mismatch between the mechanical properties of the vascular substitute and the native arterial tissue leads to catastrophic lumen obstruction. To design a mechanically suitable vascular substitute it is essential (i) to know the main mechanical parameters and values of native healthy arteries and (ii) to characterize the small arteries and their dedicated substitutes. In this short review, we will first focus on the mechanics of native small diameter arteries to get a better understanding of the required specifications and the current challenges faced in the design of artificial substitutes. Then some mechanical values of studied artificial prosthesis will be presented and recommendations will be proposed.

Physiological mechanical behaviors of arteries and intrinsic properties of the arterial wall

Arteries are made up of three superimposed layers: the intima, a monolayer of endothelial cells in contact with the blood; the media, made up of smooth muscle cells (SMC) in a matrix of elastin and collagen fibers and the adventitia, a peripheral layer of fibrous tissue mainly constituted of fibroblasts in a network of collagen and elastin fibers. Layers are separated by a basal lamina of connective tissue. The media and the adventitia form the largest part of the artery wall and are determinant for the mechanical properties of arteries [1–3]. The composition of arteries depends on their diameter. Medium and small arteries are mostly made up of SMC making them part of the muscular artery family, they are not very stretchy, unlike larger arteries which contain more elastin than collagen. The arterial wall is heterogeneous, mechanically anisotropic, incompressible, highly deformable and shows non-linear stress-strain characteristics with a viscoelastic behavior [4].

In the body, arteries are stretched and undergo different mechanical stresses due to the blood flow pressure. Going out the heart, the pressure during the systole is up to 120mmHg in larger arteries. The pressure progressively reduces in medium and small arteries. The systolic pressure is cushioned by the arteries which store 70% of the blood volume by stretching the wall. During the diastole, the stored blood is released and the blood flow becomes continuous to irrigate the tissues. The change in volume of arteries induced by a change in pressure is known as the compliance which could be considered as the storage capacity of the artery. Compliance values differ following the composition, the structure and the size of arteries.

During the heart cycle, the artery is stretched and pass through different mechanical phases (Figure 1A). At the start, elastin and collagen fibers of the vascular wall are disorganized. During the first phase, related to a very small load, the stress-strain relationship is linear: all elastin fibers are solicited giving the elastic behavior to the tissue. During the second phase, with an increasing load, related to the physiological range of the blood pressure, collagen fibers start to straighten. The material has a hyperelastic behavior: both elastin and collagen fibers are recruited. During the third phase, under high stress, collagen fibers are extended. The mechanical behavior is controlled by the rigid collagen fibers that prevent the damage or the rupture of the artery if the load is increased. The stress-strain relationship is linear again [5].

This global non-linear behavior is common with viscoelastic materials which response to a stress is an elastic deformation (storing energy) and a viscous flow (dissipating energy) [6]. But, there is no permanent viscosity in arteries. After a delay to return to their original shape they fully recover from deformation, a phenomenon known as hysteresis. The viscoelastic aspect of arteries has been widely investigated and characterized [2,7].

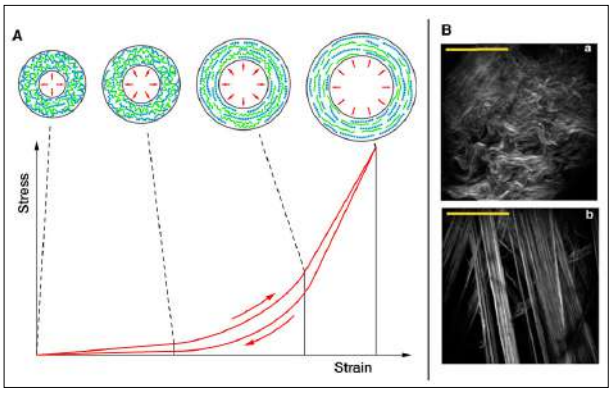

Figure 1: Physiological behavior of blood vessels under stress.

A) Stress-strain relationship with delayed elasticity and gradual differentiated recruitment of wall fibers.

B) Straightening of adventitial collagen fibers during mechanical loading at strains of (a) 0% and (b) 40% by second-harmonic imaging (scale bar 180µm) from Turcotte *et al.* [9].

Elastin and collagen organization, realignment and recruitment are essential for a proper functioning of arteries. Chow *et al.* performed experiments on artery segments in order to evidence the role of each component in response to mechanical loading. The media layer of arteries contains a great fraction of type III collagen whereas the adventitia layer is mainly composed of type I collagen. The latter is less extensible than the former. Thus, when stretched, the medial collagen continues to straighten throughout the mechanical loading, whereas the adventitial collagen shows a delay in the straightening of the fibers (Figure 1). Medial fibers are involved at the onset of mechanical loading up to 20% strain, which confirms the major load bearing role of collagen[8].

Multiphoton imaging provides information about the fiber alignment under mechanical loading[9]. The fibers of the adventitia are naturally aligned in the circumferential direction (low or no mechanical loading). Indeed, at rest, the fibers are wavy up to 20% strain (figure 1B). The same goes for medial fibers, whose circumferential orientation intensifies when stretched under high stress. This behavior shows that both adventitial and medial collagen fibers realign in the direction of loading during deformation.

On the contrary, elastin fibers form a dense interconnected network which is more uniformly distributed compared with collagen. They are not significantly affected by mechanical deformations. This uniform and dense network allows to evenly distribute mechanical loading through the arterial wall thanks to the elastin/collagen interactions. In their study Chow *et al.*, suggest that there are strong intrinsic interactions between elastin and collagen. The elastin network exerts a compressive stress on the collagen network allowing a proper mechanical functioning of arteries[8].
Finally, all studies evidenced a dependence of mechanical properties on the direction of the stress as a consequence of the structural anisotropy of the arterial wall[10].

Mechanical measures to characterize small arteries and their substitutes

The mechanical behavior of arteries being viscoelastic and anisotropic, their characterization is complex. Through the past decades, researchers used multiple variables to mechanically characterize native arteries and vascular grafts. The main parameters used are presented below.

Elastic Modulus

The elastic modulus, or Young's Modulus (E), characterizes the stiffness of a solid material by linking stress and strain in the elastic regime which is the area where the deformed material goes back to its initial state when forces are removed[6]. This relation is proportional for very small deformations: the higher the modulus, the higher the stiffness.
Blood vessels undergo large deformations *in vivo*, so, the nonlinear stress-strain relationship suggests the use of a more suitable modulus, called incremental elastic modulus[2,4]. This modulus is defined as a specific point M by the tangent slope to the curve at this point. It is not constant and depends on the previous stress state[11].

Viscoelastic parameters of arteries: E' and E''

Viscoelastic parameters of the material are the storage and loss moduli, respectively E' and E''. Storage modulus is associated to the elastic response by measuring the stored energy. The loss modulus is related to the viscous response by measuring the dissipated energy.

These variables can be assessed by a dynamic mechanical analysis (DMA) in vitro allowing to determine the viscoelastic properties of a material at physiologically relevant frequencies. Nevertheless, publications on specific mechanical tests for arteries using this method are rare [12].
These parameters can also be assessed by either observing the strain as a function of time at constant stress or the stress relaxation at constant strain. Both tests can be performed with a uniaxial tensile testing system [13].

Compliance

Arterial compliance describes a change in the volume of arteries following a change in blood pressure. The arterial lumen volume is pressure-dependent because of the elastin and collagen composition of arteries. The compliance concept is a direct description of arterial distensibility. Regarding arteries, compliance is the ratio of the change in volume (dV) resulting from a change in transmural distending pressure (dP) or dV/dP, it is the slope of the pressure-volume relationship. There is not a unique definition of compliance in literature. Some authors define it as a relationship between a change in volume and a change in pressure influenced by wall thickness, wall stiffness or arterial size and expressed in m^3/kPa [14,15]. Some others describe it as a relationship between a change in cross-sectional area and change in pressure expressed in m^2/kPa, assuming a perfectly homogeneous arterial segment without changes in arterial segment length [16,17]. This definition suggests that compliance is linked to a change in diameter and not length of the vessel. Sarkar *et al.* expressed the compliance as a parameter homogeneous with the inverse of a pressure by linking it to the Young's modulus and wall thickness [18].

Burst pressure

Burst pressure is the pressure causing the rupture of the artery. With a constant strength, the burst pressure is inversely proportional to the arterial diameter and proportional to the wall thickness [19]. Burst pressure tests are conducted by cannulating and pressurizing vessel segments with physiological solutions until failure.

Main systems used to assess mechanical measures

Tensile tests system

The most widely spread mechanical tests to determine stress-strain relationship, Young's modulus or viscoelastic parameters are uniaxial and biaxial tensile tests.

In uniaxial tensile test, a rectangular strip of an artery is pulled along the longest direction of the sample (Figure 2A). The sample must be cut in a dog bone shape to limit boundaries effect, although in general the lack of tissue led to use rectangular strips. The minimum ratio between length and width considered to limit boundary effect is 5:1. The sample needs to undergo several loading and unloading cycles at a constant stretch rate for preconditioning and the stress-strain data is recorded on the last cycle [13].

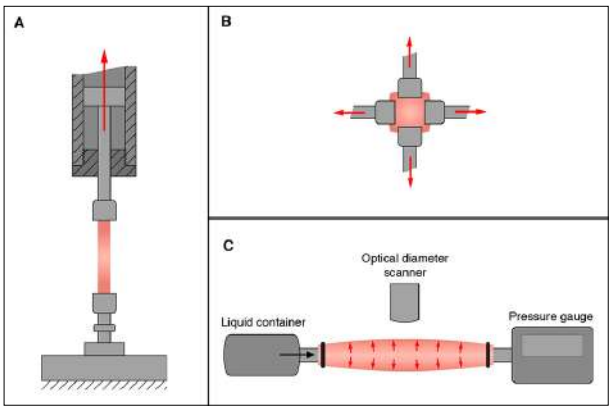

Figure 2: Main mechanical tests.
A) Uniaxial tensile test with a rectangle shaped sample.
B) Biaxial tensile test with a square shaped sample.
C) Pressurized of inflation test with a tubular sample.

With uniaxial tensile test, elastic modulus can be collected, but also elongation and strength at break where a force is applied until the sample's break[6]. In a cyclic mode (DMA), the viscoelastic parameters are obtained as well. However, uniaxial tests give a stress-strain relationship only in one direction which is not representative of physiological conditions.

For a biaxial tensile test, a rectangular or square, thin, flat sample of artery is pulled in two directions simultaneously. In arteries, circumferential and longitudinal directions are considered (Figure 2B). The tissue is initially marked in its central region and the strain is obtained optically by measuring the relative displacement of this indentation. The forces can be measured in each direction and linked to the strain. This test is preferred to consider the artery anisotropy but experimentally it is difficult to grip the sample in both directions without damaging the tissue[13].

Pressurized tests

Pressurized or inflation test is an in vitro test where a tubular sample is put under pressure (and possibly under tension) with a physiological solution. The diameter of the artery at variable pressures is measured by imaging[20] (Figure 2C). Pressurized tests are used to obtain compliance and also burst pressure, where an increasing pressure is applied until the rupture of the sample. When tension is applied as well as pressure, this type of test could be performed to get elastic modulus.

Compliance can be estimated *in vivo*, by measuring the lumen size is at diastole and systole with ultrasonography. Since 1980's, this method is frequently found in literature, given that there is no harvest needed and ultrasound machines are common[21,22].

References values for healthy arteries

In order to design suitable vascular grafts for *in vivo* implantation, it is important to know the order of magnitude of the previously highlighted mechanical properties in the arteries of interest. The most studied small arteries in literature are the coronary artery and the internal mammary artery. These arteries have a mean diameter of 4 mm and 1 mm respectively.

In this section, we aim at presenting some common mechanical properties values that can be found in literature and discussing them regarding the relevance of experimental conditions. Data are summarized in Table 1.

The difficulty to find reliable results lays on the wide range of mechanical characterization. Indeed, values could be very different from a study to another due to the test type, the protocol or preloading conditions. Moreover, sometimes, there is a lack of information about the protocols, if tensile values are obtained longitudinally or circumferentially for instance.

Values of small vascular grafts

Although large arteries have had efficient grafts for decades, smaller ones are still the focus of cardiovascular research. Expanded-polytetrafluoroethylene (Teflon®) and polyethylene terephthalate (Dacron®) materials show satisfying results for replacing large arteries but they are poorly qualified regarding small arteries. Indeed, these materials have a low compliance compared to native small arteries, causing a mechanical mismatch with the connected tissue. To overcome this issue, biomaterials are investigated to obtain a mechanically suitable small diameter vascular graft.

In Table 2, we aim at reporting current properties of some of the developed small synthetic vascular grafts through their in vitro studies. We focus our study on synthetic grafts, in this context, tissue engineered grafts will not be investigated.

Table 1: Some mechanical properties of healthy small arteries in literature.

Model	Artery	Young's Modulus (MPa)	Maximum modulus (MPa)	Storage and Loss Modulus (MPa)	Compliance	Burst pressure (mmHg)	Ultimate strength (MPa)	Strain at break (%)
Human	Coronary	**1.48 ± 0.24** [23] (UTT) **1.76 ± 0.22** [24] (UTT) **0.90 – 4.11** [25] (PT) **1.21** [26] (BTT) **3.12 ± 0.29** [24] (UTT)			**14.8%** / 100mmHg^{-1} [27] (US) **0.010 – 0.052** mm^2/mmHg [28] (US)		**1.44 ± 0.87** [23] (UTT)	**54 ± 25** [23] (UTT)
Human	Intern mammary artery	**0.22 ± 0.023** [29] (UTT) **8 ± 3** [30] (circ) (UTT) **16.8 ± 7.1** [30] (axial) (UTT)			**11.5%** / 100mmHg^{-1} [20] (PT)	**3196** [20]	**4.1 ± 0.9** [30] (circ) (UTT) **4.3 ± 1.8** [30] (axial) (UTT)	**134 ± 28** [30] (circ) (UTT) **59 ± 15** [30] (axial) (UTT)
Human	Middle cerebral artery		**18.2** [31] (UTT)				**3.23** [31] (UTT)	**141** [31] (UTT)
Human	Cortical artery		**19.9** [31] (UTT)				**4.07** [31] (UTT)	**142** [31] (UTT)
Human	Internal thoracic artery	**1.17** [32] (UTT) **1.15** [26] (BTT)			**11.5%** / 100mmHg^{-1} [20] (PT)	**3073** [33]		
Pig	Left anterior descending artery			Storage : **22.16 - 17.40** [12] (UTT) Loss : **2.10 ± 0.33** [12] (UTT)				

(UTT: uniaxial tensile test; BTT: biaxial tensile test; PT: pressurized test; US: ultrasound)

Table 2: Main mechanical properties of some small vascular grafts in literature.

Author	Type of graft	Young's Modulus	Ultimate strength	Strain at break	Compliance	Burst pressure
-	PET (Dacron®)	**14000** MPa [34]	**139** MPa (long) [35] **128** MPa (circ) [35] 170-**180** MPa [34]		**0.019-0.075%** / mmHg [34] **1.9 ± 0,3%**. mmHg x 10^{-2} [36]	
-	PTFE (Teflon®)	**0.5** GPa [36]	**66.7** Mpa (long) [35] **85.2** MPa (circ) [35] **140** MPa [37]		**0.016%** / mmHg [35] **1.6 ± 0.2%** mmHg x 10^{-2} [36]	
Stitzel [38]	Collagen / elastin / PLGA			**40%** (axial and circ)	**12-14%** / 100mmHg	1425 mmHg
Hong [39]	PEUU / PMBU	**5**-7 MPa	**9 ± 1** MPa	388 ± 58%	**2.2-4.4%** / 100mmHg	
Behr [40]	PCL	2-286 MPa			0.94-4.79% / $mmHg^{-2}$	600-2000 mmHg
Chaouat [41]	PVA	**2x10⁸** N/m^2 (DMA)			**3 ± 0.2%** (80-120mmHg)	507 ± 25 mmHg
Chen [42]	SPEU		**16.0-13.7** MPa (long) **15.9-13.6** MPa (circ)	**1650-980%** (long) **1510-890%** (circ)	**4.2-9.7%** (50-200mmHg)	1748-2050 mmHg
Aussel [43]	Chitosan	5.1-7.2 MPa	**1.3-2.3** MPa (long) **0.66-1.2** MPa (circ)		**3.3-11.5%** / $100mmHg^{-1}$	840-1313 mmHg
Wise [33]	Elastin / polycaprolactone	269 ± 12 kPa			**0.006** kPa^{-1}	**1900** mmHg
Wise [33]	PET (Dacron®)	**2100** kPa			**0.001** kPa^{-1}	

(PET : Polytéréphtalate d'éthylène; PTFE : Polytétrafluoroéthylène; PLGA : Poly(lactic-co-glycolic acid); PEUU : poly(esterurethane) urea; PMBU : poly(2-methacryloyloxyethylphosphorylcholine-co-methacryloyloxyethyl butylurethane); PCL : Polycaprolactone; PVA : Alcool polyvinylique; SPEU : Segmented polytherurethane)

Compliance can be tailored by modifying the processing parameters [38], the grafts dimensions [40] or the polymer's bulk density [42]. The wall thickness was a key parameter to adjust compliance: thicker tubes are much less compliant than thinner ones [40]. On one hand a thin wall can achieve the compliance requirement, but not the burst pressure causing leakage more easily. There is nothing like a fitting result in literature, all is about making choices and compromises: a compliant graft but likely to have a lower lifetime because of adjustments or a less compliant graft with a risk of mismatch but that can last for years.

Burst pressure in current small vascular grafts is much lower than the native burst pressure of arteries which is between 2000 and 4000 mmHg in human. The burst pressure of small vascular graft does not need to be the same as native arteries but it needs to be high enough to support systolic arterial pressure in human (~120 mmHg) even in case of hypertension (>180mmHg). Numerous researchers attained a consensus about the reference burst pressure to achieve, for vascular grafts, which is, at least, the saphenous vein one's [20,44].

Young's modulus is representative of the graft stiffness. If it is too high, the graft will be much stiffer than the native artery leading to a mechanical mismatch at the anastomoses between stiff artificial graft and native vessel.

Wise *et al.* obtained close results to native arteries with their elastin/polycaprolactone based graft, demonstrating in the meantime the incapacity of the commercialized Dacron® material to replace small arteries. It has a modulus six times higher and a compliance ten times lower than a native internal mammary artery [33] (Figure 3). This study highlights, once more, that polyethylene terephthalate is not a suitable candidate for artificial small vascular substitutes.

Recommendations about mechanical characterization

As evidenced in the previous sections, characterizing arteries is hard. The specific mechanical behavior of arteries makes the choice of relevant mechanical variables difficult. Indeed, the obtained values can be strongly different depending on the location of the portion studied and model, the assumptions made and the theoretical and experimental approaches definitely influence the results [4].

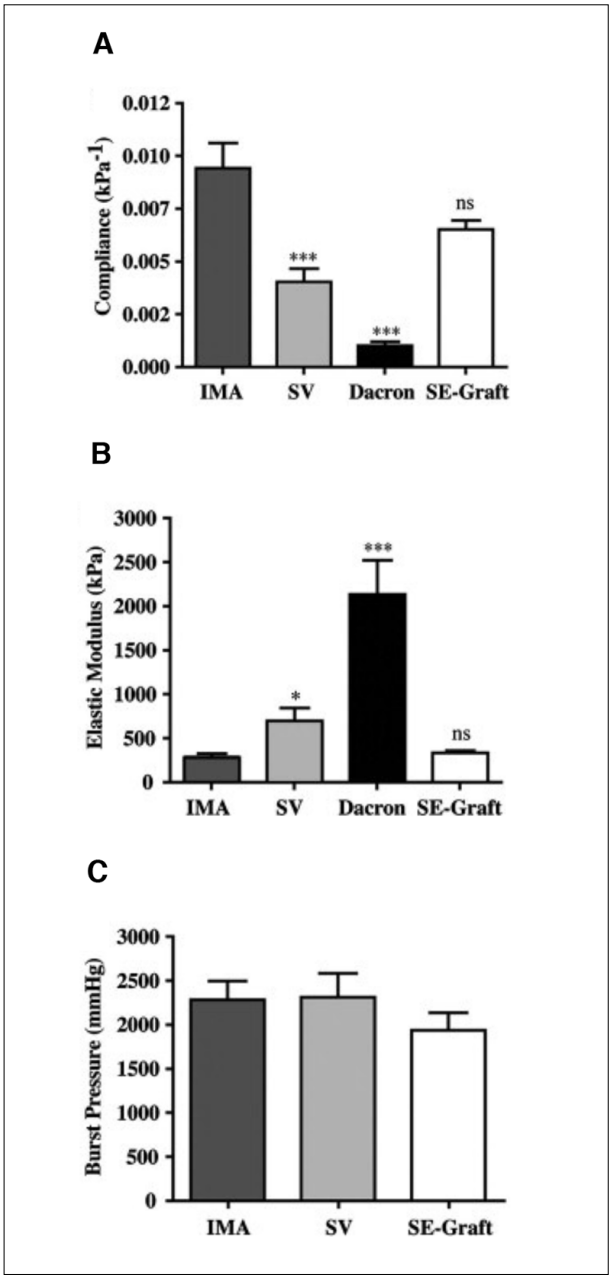

Figure 3: Mechanical properties of blood vessels often used as vascular graft (Intern Mammary Artery and Saphenous Vein) and synthetics grafts (Dacron® and Synthetic Elastin/Polycaprolactone) from Wise *et al.* [33].

Very few publications in literature propose a protocol to mechanically characterize small arteries or small arterial substitutes [45]. Some recommendations to assess mechanical characterizations are given in this review.

Before characterizing samples, it is mandatory to properly manipulate them. To this purpose, the shape, the size, the model, the type of artery, the source and the stocking conditions must be carefully chosen. Moreover, mechanical testing should be performed as quickly as possible and samples should be stored at physiological conditions, as far as possible, to preserve the material structure and properties.

The mechanical characterization must not be the same if it is a simple characterization of native arteries or if it is a comparison between native arteries and arterial substitutes. To characterize and compare arteries between them, all mechanical measures are relevant. But, to compare a vascular graft with arteries, all mechanical measures don't have the same relevance. As said before, arteries, as well as most of vascular substitutes, present anisotropic properties.

The most important property of a vascular graft is its compliance. Vascular grafts must have the same capacity to react to blood pressure than native arteries in order to avoid flow disruption. It is well known that compliance mismatch between host artery and the vascular graft leads to the graft failure [22]. Moreover, vascular grafts are not sutured with an axial tension to the host artery. That is why, the radial properties of the graft are more important than its axial properties.

The most relevant test to compare arterial substitute and native arteries are the pressurized tests, because they reproduce the radial forces applied *in vivo*. But they are more complex tests to set up. In this light, a first test could be conducted, a DMA test. This test performed on native arteries and the arterial substitute provide axial viscoelastic parameters. If the arterial substitute present similar properties as the native arteries, the pressurized tests must be performed. The compliance values obtained will be a key parameter to characterize the arterial substitute.

Even though uniaxial and biaxial tests on flat samples are still a gold standard to characterize mechanical properties of arterial walls, some authors as Hayashi *et al.*, already claimed that pressure-diameter data obtained from a tubular segment undergoing an inflation test are more representative and realistic [4]. Vascular grafts could be axially characterized anyway, but if only these parameters are considered to adapt the mechanical properties of the graft, these will not assure a successful implantation. Young's Modulus is more relevant than incremental modulus to characterize vascular grafts. Vascular grafts are not stretched lengthwise and subject to stresses at the same level as native arteries *in vivo*. Arteries *in vivo*, are stretched longitudinally about 30% while vascular grafts usually have the same length than the distance between the two remaining portions to connect. That is why, in the case of native arteries, the notion of incremental modulus is important since they are subject to high deformations. And, Young's modulus is more appropriate to longitudinally study vascular grafts.

Burst pressure and stress and strain at break are not the most relevant since arteries and vascular grafts will not burst or tear *in situ*. Nevertheless, it is important to assess for vascular grafts in order to certify that the substitute can safely withstand physiological pressures.

Moreover, to have the best chance to obtain a mechanically suitable arterial substitute, same tests with the same parameters have to be done with the arterial substitute and the reference native artery. Use mechanical values found in literature as reference values for its vascular grafts is not relevant. Indeed, measures could be assessed with different tests, for *e.g.*, Young's modulus could be obtained with tensile test or pressurized test, which can influence the value obtained. To limit this error, tests have to be done on both native arteries of reference and arterial substitute. In this way, references values will be relevant and so the targeted values of the graft will be accurate and precise.

Conclusion

This review aimed at creating a guideline for mechanics study in order to help designing vascular graft which closely mimic the mechanical properties of small native arteries.

A set of the most relevant mechanical parameters was first considered as Young's modulus, storage and loss modulus, compliance and burst pressure It is recommended to perform these tests both with the native artery and the dedicated vascular graft to build suitable substitutes.

Eventually, this review proposes a brief guideline for the design of vascular grafts whose mechanical properties are as close as possible to those of the small native arteries that they must replace.

Acknowledgements

The authors are grateful for the PhD fellowship for Lucie Gernez from Université Sorbonne Paris Nord.

Funding

This research was funding by INSERM, Université de Paris and Université Sorbonne Paris Nord. The PhD fellowship was funded by Université Sorbonne Paris Nord (contract number SB/2018-2613).

References

1. Bauer RD, Busse R, Schabert A, Wetterer E. The Role of the Elastic and the Viscous Wall Properties in the Mechanics of Elastic and Muscular Arteries. In: Kenner T, Busse R, Hinghofer-Szalkay H (eds). Cardiovascular System Dynamics: Models and Measurements. *Springer US: Boston,* MA, 1982, pp 373-82.

2. Bergel DH. The static elastic properties of the arterial wall. *J Physiol* 1961; 156: 445-57.

3. Mcveigh GE, Hamilton PK, Morgan DR. Evaluation of mechanical arterial properties: clinical, experimental and therapeutic aspects. Clin Sci 2001; 102: 51-67.

4. Hayashi K. Experimental Approaches on Measuring the Mechanical Properties and Constitutive Laws of Arterial Walls. *J Biomech Eng* 1993; 115: 481-8.

5. Holzapfel GA. Biomechanics of Soft Tissue in Cardiovascular System. *Springer* 2003.

6. Tanzi MC, Farè S, Candiani G. Foundations of Biomaterials Engineering. *Academic Press* 2019.

7. Imura T, Yamamoto K, Satoh T, Kanamori K, Mikami T, Yasuda H. *In vivo* viscoelastic behavior in the human aorta. *Circ Res* 1990; 66: 1413-9.

8. Chow M-J, Turcotte R, Lin CP, Zhang Y. Arterial Extracellular Matrix: A Mechanobiological Study of the Contributions and Interactions of Elastin and Collagen. *Biophys J* 2014; 106: 2684-92.

9. Turcotte R, Mattson JM, Wu JW, Zhang Y, Lin CP. Molecular Order of Arterial Collagen Using Circular Polarization Second-Harmonic Generation Imaging. *Biophys J* 2016; 110: 530-3.

10. Cox R. Arterial wall mechanics and composition and the effects of smooth muscle activation. *Am J Physiol* 1975; 229: 807-12.

11. Comolet R. Généralités sur la circulation sanguine, ch. 2. Bioméc Circ MASSON Paris 1984; pp. 34-52.

12. Burton HE, Freij JM, Espino DM. Dynamic Viscoelasticity and Surface Properties of Porcine Left Anterior Descending Coronary Arteries. *Cardiovasc Eng Technol* 2017; 8: 41-56.

13. Tian L, Chester NC. *In Vivo* and *in Vitro* Measurements of Pulmonary Arterial Stiffness: A Brief Review. *Pulm Circ* 2012; 2: 505-17.

14. Spencer M, Denison A. Pulsatile blood flow in the vascular system. In: Handbook of physiology. *American Physiology Society: Washington,* DC, 1963, pp. 842.

15. Simon AC, Levenson J, Bouthier J, Safar ME, Avolio AP. Evidence of early degenerative changes in large arteries in human essential hypertension. *Hypertension* 1985; 7: 675-80.

16. Chirinos JA. Arterial Stiffness: Basic Concepts and Measurement Techniques. *J Cardiovasc Transl Res* 2012; 5: 243-55.

17. Chamiot-Clerc P, Copie X, Renaud JF, Safar M, Girerd X. Comparative reactivity and mechanical properties of human isolated internal mammary and radial arteries. *Cardiovasc Res* 1998; 37: 811-9.

18. Sarkar S, Salacinski HJ, Hamilton G, Seifalian AM. The Mechanical Properties of Infrainguinal Vascular Bypass Grafts: Their Role in Influencing Patency. *Eur J Vasc Endovasc Surg* 2006; 31: 627-36.

19. Sarkar S, Hillery C, Seifalian A, Hamilton G. Critical parameter of burst pressure measurement in development of bypass grafts is highly dependent on methodology used. *J Vasc Surg* 2006; 44: 846-52.

20. Konig G, McAllister TN, Dusserre N, Garrido SA, Iyican C, Marini A *et al.* Mechanical properties of completely autologous human tissue engineered blood vessels compared to human saphenous vein and mammary artery. *Biomaterials* 2009; 30: 1542-50.

21. Laogun AA, Gosling RG. *In vivo* arterial compliance in man. *Clin Phys Physiol Meas* 1982; 3: 201-12.

22. Hasson JE, Megerman J, Abbott WM. Increased compliance near vascular anastomoses. *J Vasc Surg* 1985; 2: 419-23.

23. Karimi A, Navidbakhsh M, Shojaei A, Faghihi S. Measurement of the uniaxial mechanical properties of healthy and atherosclerotic human coronary arteries. *Mater Sci Eng C* 2013; 33: 2550-4.

24. Faturechi R, Hashemi A, Abolfathi N, Solouk A. Mechanical guidelines on the properties of human healthy arteries in the design and fabrication of vascular grafts: experimental tests and quasi-linear viscoelastic model. *Acta Bioeng Biomech* 2019; 21: 13-21.

25. Ozolanta I, Tetere G, Purinya B, Kasyanov V. Changes in the mechanical properties, biochemical contents and wall structure of the human coronary arteries with age and sex. *Med Eng Phys* 1998; 20: 523-33.

26. Kamenskiy AV, Dzenis YA, Kazmi SAJ, Pemberton MA, Pipinos II, Phillips NY *et al.* Biaxial mechanical properties of the human thoracic and abdominal aorta, common carotid, subclavian, renal and common iliac arteries. *Biomech Model Mechanobiol* 2014; 13: 1341-59.

27. Shaw JA, Kingwell BA, Walton AS, Cameron JD, Pillay P, Gatzka CD *et al.* Determinants of coronary artery compliance in subjects with and without angiographic coronary artery disease. *J Am Coll Cardiol* 2002; 39: 1637-43.

28. Williams MJA, Stewart RAH, Low CJS, Wilkins GT. Assessment of the mechanical properties of coronary arteries using intravascular ultrasound: an *in vivo* study. *Int J Card Imaging* 1999; 15: 287-94.

29. Kajbafzadeh AM, Khorramirouz R, Kameli SM, Hashemi J, Bagheri A. Decellularization of Human Internal Mammary Artery: Biomechanical Properties and Histopathological Evaluation. *BioResearch Open Access* 2017; 6: 74-84.

30. Stekelenburg M, Rutten MCM, Snoeckx LHEH, Baaijens FPT. Dynamic Straining Combined with Fibrin Gel Cell Seeding Improves Strength of Tissue-Engineered Small-Diameter Vascular Grafts. *Tissue Eng Part A* 2009; 15: 1081-9.

31. Monson KL, Goldsmith W, Barbaro NM, Manley GT. Significance of source and size in the mechanical response of human cerebral blood vessels. *J Biomech* 2005; 38: 737-44.

32. Pietrabissa R. Biomateriali per protesi e organi artificiali : introduzione alla biocompatibilità, alla scienza e alla applicazione dei materiali per dispositivi biomedici. 1996.

33. Wise SG, Byrom MJ, Waterhouse A, Bannon PG, Ng MKC, Weiss AS. A multilayered synthetic human elastin/polycaprolactone hybrid vascular graft with tailored mechanical properties. *Acta Biomater* 2011; 7: 295-303.

34. Boss A, Stierli P. [Dacron prosthesis dilatation. Case report and review of the literature]. *Helv Chir Acta* 1993; 60: 153-6.

35. How TV. Mechanical Properties of Arteries and Arterial Grafts. In: Hastings GW (ed). Cardiovascular Biomaterials. *Springer: London*, 1992, pp. 1-35.

36. Salacinski HJ, Goldner S, Giudiceandrea A, Hamilton G, Seifalian AM, Edwards A *et al.* The Mechanical Behavior of Vascular Grafts: A Review. *J Biomater Appl* 2001; 15: 241-78.

37. Kannan RY, Salacinski HJ, Butler PE, Hamilton G, Seifalian AM. Current status of prosthetic bypass grafts: A review. *J Biomed Mater Res B Appl Biomater* 2005; 74B: 570-81.

38. Stitzel J, Liu J, Lee SJ, Komura M, Berry J, Soker S , *et al.* Controlled fabrication of a biological vascular substitute. *Biomaterials* 2006; 27: 1088-94.

39. Hong Y, Ye SH, Nieponice A, Soletti L, Vorp DA, Wagner WR. A small diameter, fibrous vascular conduit generated from a poly(ester urethane)urea and phospholipid polymer blend. *Biomaterials* 2009; 30: 2457-67.

40. Behr JM, Irvine SA, Thwin CS, Shah AH, Bae MCK, Zussman E *et al.* Matching Static and Dynamic Compliance of Small-Diameter Arteries, with Poly(lactide-co-caprolactone) Copolymers: *In Vitro* and *In Vivo* Studies. *Macromol Biosci* 2020; 20: 1900234.

41. Chaouat M, Visage CL, Baille WE, Escoubet B, Chaubet F, Mateescu MA *et al.* A Novel Cross-linked Poly(vinyl alcohol) (PVA) for Vascular Grafts. *Adv Funct Mater* 2008; 18: 2855-61.

42. Chen J-H, Laiw R-F, Jiang S-F, Lee Y-D. Microporous segmented polyetherurethane vascular graft: I. Dependency of graft morphology and mechanical properties on compositions and fabrication conditions. *J Biomed Mater Res* 1999; 48: 235-45.

43. Aussel A, Montembault A, Malaise S, Foulc MP, Faure W, Cornet S *et al. In Vitro* Mechanical Property Evaluation of Chitosan-Based Hydrogels Intended for Vascular Graft Development. *J Cardiovasc Transl Res* 2017; 10: 480-8.

44. Chan-Park MB, Shen JY, Cao Y, Xiong Y, Liu Y, Rayatpisheh S *et al.* Biomimetic control of vascular smooth muscle cell morphology and phenotype for functional tissue-engineered small-diameter blood vessels. *J Biomed Mater Res A* 2009; 88A: 1104-21.

45. Camasão DB, Mantovani D. The mechanical characterization of blood vessels and their substitutes in the continuous quest for physiological-relevant performances. A critical review. *Mater Today Bio* 2021; 10: 100106.

Tissue Engineering Vascular Graft: current status and clinical application

35

Toshiharu SHINOKA

Cardiovascular disease (CVD) is still the leading cause of death in western countries. Surgical outcomes for CVD had been improving with the development of surgical techniques, medications, and perioperative management strategies, however, adverse postoperative events related to the use of artificial prosthetic materials are still problematic. In pediatric patients, using these artificial materials make future re-intervention inevitable due to their lack of growth potential. This review focuses on the most current tissue-engineering (TE) technologies to treat congenital cardiovascular diseases and discusses their limitations through reports ranging from animal studies to clinical trials. Unlike prosthetic materials, tissue engineered structures are hypothetically more biocompatible and provide growth potential, saving patients from additional or repetitive interventions.

In conclusion, while there are many methods being investigated to develop TE technologies in the hopes of finding better options to treat CVD, most of these approaches are not ready for clinical use or trials. However, tissue engineering has great promise to potentially provide better treatment options to vastly improve cardiovascular surgical outcomes.

Introduction

With advances in surgical techniques, medicine, materials science, and device fabrication, surgical outcomes for CVD have dramatically improved. Synthetic grafts have played in major role in improving CVD outcomes, and are widely used to reconstruct, replace, or bypass occluded arterial vessels. However, postoperative adverse events associated with the use of artificial prosthetic materials in cardiovascular surgery, such as stenosis, thromboembolism or calcification still exist. These shortcomings are especially apparent in the repair of small diameter vessels (< 6 mm in diameter). Additionally, the lack of growth potential in current prosthetic materials necessitate repeat interventions to the pediatric population.[1]

Tissue engineering (TE) is a new discipline that offers the potential to create replacement structures using autologous cells and/ or biodegradable polymer scaffolds (Figure 1). Tissue engineered structures, can be implanted to provide mechanical function similar to non-diseased tissue. However, unlike prosthetic materials, tissue engineered structures are hypothetically more biocompatible and provide growth potential, saving patients from additional or repetitive interventions.[2] Therefore, the TE approach may provide a groundbreaking alternative to the usage of prosthetic materials in cardiovascular surgery.

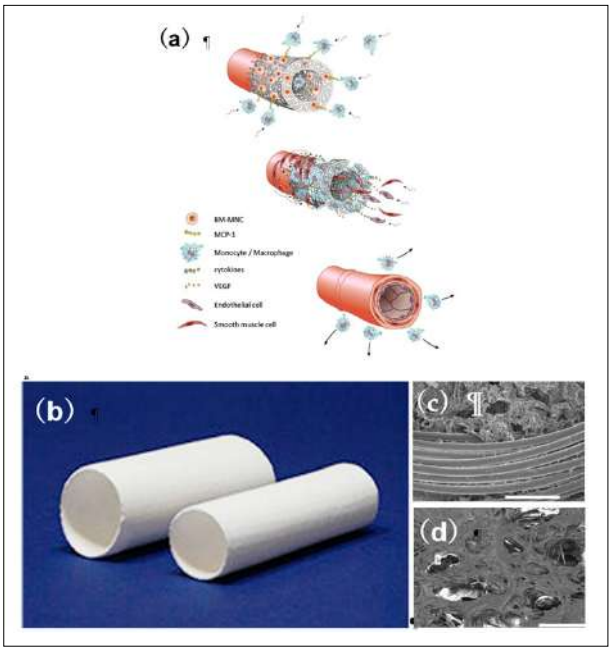

Figure 1

(a) Proposed mechanism of neovessel formation after implantation of a cell-seeded biodegradable scaffold. Early pulse of monocyte chemoattractant protein-1 (MCP-1) and related cytokines from seeded bone marrow-derived mononuclear cells (BM-MNCs) enhances early monocyte recruitment to the scaffold. Infiltrating monocytes release multiple angiogenic cytokines and growth factors (*e.g.*, vascular endothelial growth factor (VEGF)), which recruit smooth muscle cells.

(b) Appearance of tissue engineered vascular graft (TEVG). TEVG has a thickness of 1 mm, and mainly has a length of 13 cm; they are trimmed and implanted according to the anatomy of the patient.

(c) SEM image of Woven poly (glycolic acid) (PGA).

(d) SEM image of luminal PCLA; the bar shows 100 μm adopted with permission from Shinoka et al.

Methods

Many variables of tissue engineered vascular graft (TEVG) design have been studied to date. An ideal scaffold must provide the desired shape and sufficient strength to withstand mechanical stress. Additionally, a scaffold must promote the correct vascular cell phenotype and offer enough surface area to stimulate cell attachment.[3] To encourage cell migration and tissue growth, scaffold structures should be highly porous and provide an area for cells to adhere.[4] Within the scaffold, its porous network provides channels for nutrient delivery, waste removal, cell migration, and cellular and molecular signaling.[3] Initially, scaffolds can be biostable to provide long-term support, and then eventually degrade at a rate equal to tissue regeneration. Additionally, because the regenerated tissue is native to the patient, it would be inherently able to remodel, as well as, non-thrombogenic, -immunogenic, and -destructive to blood cell, and corresponding electrolytes. As this technology continues to advance, these patient friendly devices will provide an affordable and off the shelf ready alternative to prosthetic grafts.[5]

Fabrication Techniques

Scaffolds are often made to mimic the fibrous structure of natural extracellular matrices. Fabrication techniques play an important role during scaffold development.[6] Among fabrication techniques, electrospinning appears to hold the most promising results for TE applications[6], and is the most widely studied method as evidenced by a survey of publications papers worldwide since the 1990s. The Electrospinning technique has been the most common means to develop small diameter grafts. These grafts have similar extracellular matrix of vessels and the ability to incorporate autologous cells into the scaffold. However, it does not have enough strength to withstand the arterial pressure environment. Additionally, there are limited long-term studies on the performance of electrospun scaffolds as vascular grafts.[6]

Using a mold to fabricate a collagen and fibroblast based biotube, is one unique way to create biological material-based scaffolds. One study's histologic examination revealed a graft that mainly comprised of collagen fibers, and lacked fibroblasts, elastic fiber formation, and SMCs. Additionally, these scaffolds were reported to have high mechanical properties.[7] It is possible that this type of graft will soon be available clinically.

Materials

One main scaffold component are the materials it is constructed from. A wide range of materials have been researched as a component for vessel scaffolds. Scaffolds may be made out of individual natural or synthetic polymers, blends, autologous or stem-cell-derived cells, and decellularized tissues.

Synthetic scaffolds (Table 1.)

In vascular tissue engineering, various biodegradable synthetic polymer scaffolds have been studied and created. In terms of materials, four biodegradable materials are commonly used: Poly (glycolic acid) (PGA), Poly (lactic acid) (PLA), Poly (ε-caprolactone) (PCL), Poly (glycerol) sebacate (PGS). Although, the degradation periods were affected surrounding environment such as PH and temperature, these four materials have degradation periods of approximately 2-6 weeks, 6-12 months, 2-3 years, and 4 weeks, respectively.[8]

Table 1: Characteristics of Synthetic materials

	Degradation period	Advantages	Disadvantages
Poly (glycerol) sebacate (PGS)	4 weeks	+ Biocompatible. + Nonthrombogenic. + High elasticity.	- Rapid biodegradation. - Acidic degradation products may cause tissue inflammation.
Poly (glycolic acid) (PGA)	6-8 weeks	+ High flexibility; + Lack of inflammatory reaction. + High mechanical properties.	- Higher cost. - Rapid biodegradation. - High level of crystallinity makes it difficult to process.
Poly (lactic acid) (PLA)	6-12 months	+ High mechanical properties. + Non immunogenic. + Hydrolysis product (lactic acid) can be eliminated through renal excretion and are not bio-accumulative in a body.	- Hydrophobicity contributes to: low cell adhesion and low degradation rate. - Thrombogenicity. - Stimulate bacterial adhesion and form biofilms.
Poly (ε-caprolactone) (PCL)	2-3 years	+ Slow degradation rate relates to high mechanical properties. + High stability during processing and storage. + Low cost.	- Hydrophobicity contributes to: low cell adhesion, low proliferation low degradation rate. - Hydrophobicity contributed to low cell adhesion, proliferation and low degradation rate. - Thrombogenicity. - Develops intimal hyperplasia.

These materials work as temporary blood vessel scaffolds and is eventually replaced by neotissue derived from autologous cells.[9] These synthetic polymers are highly attractive for clinical use due to their availability, controllable properties, and affordability. Numerous reports have shown their potential as small-diameter vascular grafts in animal studies.[10] Some reports showed that vascular grafts made from only biodegradable synthetic materials, can remodel *in situ* into native artery-like tissues with long-term stability.10 However, there are several limitations preventing their widespread clinical adoption.

One major limitation of completely biodegradable synthetic vascular grafts relates to their lack of cell migration or adhesion.[11] To address this limitation, cell-adhesion peptides, such as autologous extracellular matrix (ECM) or bone marrow cells, can be incorporated onto the polymer surface to encourage cell migration and vessel regeneration.[11] Another limitation is graft durability, which is related to the rate at which polymers degrade. For example, fast degradation of polyurethane leads to graft dilation and limits its use in the clinic.[12] To address graft durability limitations, the concept to blend materials was developed, where different polymer combinations are formed to obtain desired graft characteristics.[1] In arterial scaffolds, PCL, a strong yet slow degrading polymer, is often blended with weaker materials in order to maintain appropriate mechanical strength while neotissue forms.

In a recent report, Fu *et al.* designed a composite biodegradable synthetic vascular graft with fast-degrading PGS cores and slow-degrading PCL sheaths. Their composite biodegradable synthetic vascular graft was scaffold free at 3-months and patent out to 1-year as a sheep carotid artery conduit. Although this composite synthetic vascular graft was able to maintain appropriate mechanical properties, the design needs to be validated with a larger sample size before human translation.

From a clinical viewpoint, tissue-engineered blood vessels are particularly appealing for pediatric patients, who often outgrow non-degradable synthetic vascular grafts and can require additional operations. In fact, a tissue-engineered vessel was first used to treat a pediatric patient with a congenital single ventricle in 2001.[13]
Subsequently, an additional 25 grafts, made of woven PGA fabric and seeded with autologous bone marrow cells, were successfully implanted as extracardiac conduits for total cavopulmonary connection (TCPC) procedures. Long-term results of these grafts showed no evidence of aneurysm formation, rupture, infection, or ectopic calcification. While stenosis was the primary mode of graft complication, the narrowing were successfully treated with balloon angioplasty or stenting (Figure 2).[14,15]
Furthermore, histology of the remodeled TEVG was similar to that of native pulmonary artery (Figure 3). Following the excellent results of Shinoka *et al.*, Breuer and colleagues are currently performing the first FDA-approved human clinical trial investigating the use of TEVGs in children.

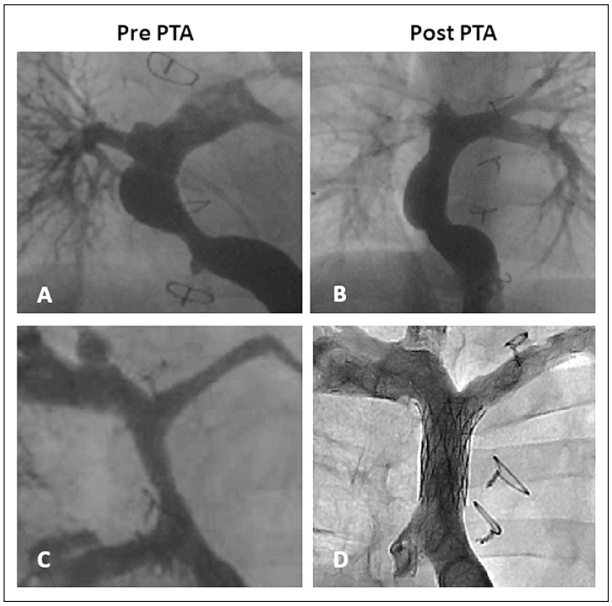

Figure 2: Stenotic TEVGs were treated with balloon dilatation (A, B) or stent implantation (C,D)

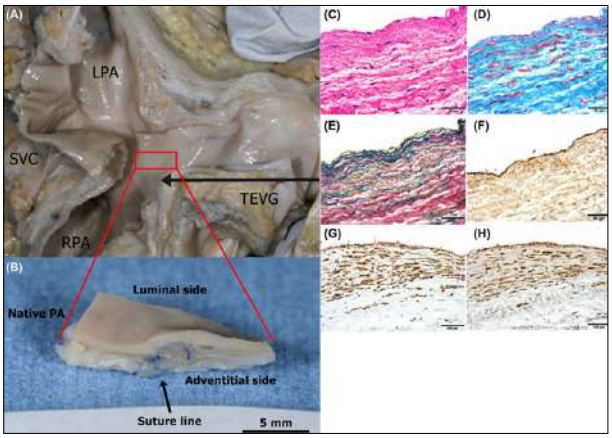

Figure 3: Histological finding of explanted human TEVG (Autopsy).

(A) Gloss image of explanted tissue showed no significant differences between native PA and TEVG.

(B) Cross-sectional view of the border between native PA and TEVG.

(C) Hematoxylin-eosin staining.

(D) Masson trichrome staining.

(E) Victoria blue-van Gieson staining.

(F) Factor VIII–positive cells (brown).

(G) α-Smooth muscle actin–positive cells (brown).

(H) Calponin-positive cells (brown).

LPA, left pulmonary artery; PA, pulmonary artery; RPA, right pulmonary artery; SVC, superior vena cava; TCPC, total cavopulmonary connection; TEVG, tissue engineered vascular graft. Modified from Matsumura G, Shinoka T. First report of histological evaluation of human tissue-engineered vasculature. J Biotechnol Biomater 2015; 5:200 Adopted with permission from Shinoka et al.

Biological scaffolds

Scaffolds fabricated from biologically derived materials offer the potential of improved biocompatibility through enhanced cellular interactions and the reduced likelihood of a foreign body reaction. From the time Weinberg and Bell first created their vessel conduits [16], a large variety of materials have been adopted to fabricate vascular networks that mimic the complex, unique structures and functionality of human blood vessels. [1] Collagen and elastin are two widely used biomaterials that are major arterial components responsible for an artery's characteristic mechanical properties.

Using a mold to fabricate a collagen and fibroblast based biotube, is one unique way to create biological material-based scaffolds. Recently, Fujita *et al.* reported successful biotube implantations as human pulmonary arterial grafts in two children. Interestingly, the in-vitro burst pressure of the biotube was 3057 mmHg, which is strong enough to withstand human arterial pressures. [7] Although the sample size was small, and long-term results have yet to be reported, this approach may be able to address the tissue shortages seen in cardiovascular surgery.

Vascular endothelium has a significant role in controlling circulatory functions such as homeostasis, permeability, defense and remodeling. These abilities strongly relate to long-term lumen vascular graft patency. Utilizing autologous endothelial cells (ECs), smooth muscles (SMCs) or a combination of these cells have been commonly utilized. *In vitro* endothelialization where ECs or SMCs are cultured and seeded on scaffolds prior to implantation has been well investigated. Other cell sources that have been investigated to achieve appropriate endothelialization include: umbilical vein ECs, mesenchymal stem cells, endothelial progenitor cells, embryonic stem cells and Induced pluripotent stem cells. [17] However, the viability, bioactivity and stability of these seeded cells is not guaranteed once the graft is implanted. Moreover, *in vitro* cell culture consumes precious time, is cost prohibitive, and have greater risks of contamination. [18] Therefore, the *in situ* endothelialization of TEVGs is thought of as a feasible option. However, to date, a viable solution to the challenge of complete endothelialization has yet to be developed.

One promising scaffold fabrication method utilizes autologous ECM. [19] Developing decellularization techniques is encouraged to generate autologous ECM scaffolds [19] (these studies will be touched on in the following section). However, limitations to utilize autologous tissues include: technical challenges in harvesting cells, prolonged *ex vivo* expansion due to reduced proliferative capacity, or overall lack of available cells. Therefore, to address that lack of available cells, investigations have focused on stem cells as a possible means to provide an unlimited cell source. [20]

Hybrid scaffolds

TEVGs display poor mechanical strength and often need to be combine with synthetic materials for additional support. For example, composite scaffolds, which blend together collagen, elastin, and several other bioresorbable polymers, have been developed. By blending the correct ratio of multiple materials, the resulting scaffold is able to be dimensionally stable, biocompatible, and present mechanical properties suitable for *in vivo* applications.[21] Stem cell-based vascular cells, in conjunction with composite scaffolds, have recently received more focus in research. Recently, Generali *et al.* succeeded in creating autologous endothelialized TEVGs from blood-derived iPSCs, which were harvested from donor's peripheral blood *in vitro*. To create the graft, SMCs were seeded onto tubular scaffolds and cultured under pulsatile flow. The resulting TEVGs were structurally similar to small diameter vessels.[19]

Going further, Luo *et al.* developed human iPSC TEVGs and implanted them into a mouse abdominal aorta model. Human iPSCs were differentiated into vascular SMCs, and then were seeded onto PGA scaffolds. The resulting construct was then incubated in an incremental pulsatile stretching bioreactor. In *in vitro* testing, the human iPSC TEVGs displayed mechanical strength comparable to that of native vessels (human saphenous vein) used for arterial bypass grafting procedures. The grafts were implanted in mouse abdominal aortas and were patent for 30 days patency without dilation, while effectively maintaining mechanical and contractile function.[22]

Lawson *et al.* developed a clinically relevant 6 mm graft by seeding human vascular SMCs onto a PLA polymer scaffold, that was then cultured in a pulsatile bioreactor for 8 weeks. Afterwards the resulting structure was decellularized to remove immunogenic cellular antigens, and the grafts were implanted into patient arms for hemodialysis access in a 60 patient clinical trial. Although the grafts did not dilatate, and rarely bled post-cannulation, only 38% achieved primary patency, with thrombosis being the most common cause of failure.[23] To expand the use of this graft to other cardiovascular procedures, the thrombogenicity of this technology should be addressed.

Decellularized-matrix scaffolds

Decellularization methods aim to eliminate immunogenicity or thrombogenicity by removing native cells and genetic material from an ECM.[24] The remaining construct is thought to maintain its structural, biochemical, and biomechanical properties. Decellularized tissues and organs can then be repopulated with a patient's own cells to produce their own neo-tissue.[25] There are several decellularization techniques that involve chemical, physical, or a combination of methods to achieve appropriate removal of cells and genetic material.[25]

In 2006, Cabotari *et al.* developed decellularization protocols for donated human heart valves, and implanted the resulting structure into two pediatric patients as pulmonary valves with favorable early-term results. In the time since, both decellularized xenogenic and allogeneic materials have been clinically used in both pediatric and adult patients.[25]

For pulmonary valve reconstruction, implantation of decellularized pulmonary homograft (DPH) showed promising results compared to non-decellularized cryopreserved pulmonary homograft (CH). Sarikouch *et al.* reported mid-term results of pulmonary valve replacement with DPH for 93 pediatric patients. DPH was superior to CH and bovine jugular vein (BJV) conduits, showing a 100% freedom from explantation rate compared to 84.2 and 84.3% for CH and BJV conduits respectively ($P = 0.01$).[26] In a separate report, Boethig *et al.* reported 123 DPH implantations which showed significantly better freedom from explantation rates (DPH 96.7 ± 2.1%, CH 84.4 ± 3.2%, $P = 0.029$ and BJV 82.7 ± 3.2%, $P = 0.012$), and less structural valve degeneration at 10 years when compared to CH, $n = 235$ and BJV conduits, $n = 235$ (DPH 61.4 ± 6.6%, CH 39.9 ± 4.4%, n.s., BJV 47.5 ± 4.5%, $P = 0.029$).[27]

For aortic valve reconstruction, Horke et al, reported results of aortic valve replacement (AVR) with decellularized aortic homografts (DAHs). They implanted 106 DAHs in pediatric patients. The DAHs had 5-year freedom from death and explantation rates at 97.8 ± 1.6 and 85.0 ± 7.4, respectively. While expected adverse events for DAH was similar to mechanical AVR (12.8 years), they were lower when compared to cryopreserved homograft patients (mean age 8.9 years) and Ross patients (9.4 years).[28] In terms of using decellularized xenomaterials, Bell et al, reported experiences of 500 implantations of decellularized bovine pericardium for 377 pediatric patients from 2012 to 2017. The decellularized bovine pericardium resulted in 96% overall freedom from reintervention 5-years post-implantation. Additionally, there was no evidence of patch calcification in any patient based on echocardiographic and radiologic imaging.[29]

While we have mainly discussed valves in this section, Tong *et al.* investigated decellularized porcine arteries in below-knee bypass surgery for diabetic lower extremity ischemia.[30] They demonstrated 100% (3/3) patency of these grafts at both 1- and 6-months after implantation graft insertion. Although, the number of cased are sample size was small, this is a promising result which can addresses reperfusion for lower limb ischemia.

Discussion

Tissue-engineering techniques have great potential for clinical applications in reconstructive cardiac surgery, and numerous ideas and techniques have been developed. However, there are several limitations preventing their clinical translation.

One major limitation is the difficulty to develop ideal bioabsorbable grafts which are durable enough and can remain patent in high pressure arterial environments until they appropriately regenerate into autologous tissues. In this aspect, the ideal fiber diameter and pore size encourages both adequate cell migration into the scaffold and tissue formation that is capable of withstanding arterial pressure once the scaffold material loses its mechanical integrity. Recently, we investigated finding the ideal pore size of synthetic tissue-engineering arterial grafts (TEAGs) composed of outer electrospun PCL and inner heparin conjugated 50:50 poly (l-lactide-co-ε-caprolactone) copolymer (PLCL) with an inner diameter of 5 mm. The study specifically focused on what pore size of the outer electrospinning PCL layer best facilitated cell migration. In the study, a 2-cm grafts of differing pore sizes (4um, 7um, 10um and 15um) were implanted into a total of 14 sheep's carotid artery. Grafts were explanted at 8 weeks post-implantation and histologically evaluated. The results showed that grafts with pore diameters larger than 4 μm promoted macrophage infiltration and neo-tissue formation but were unable to resist dilation caused by high arterial pressures. On the other hand, grafts with pore diameters of 4 μm could resist dilation, but also delayed neo-tissue formation.[31] To date, this was the first large animal study to evaluate appropriate pore size. While more investigation is necessary, these results suggest that arterial grafts with pore sizes between 4-7 μm provide the best balance between appropriate cell migration and scaffold degradation.

Another limitation is insufficient graft biocompatibility. Insufficient biocompatibility may present as graft stenosis, obstruction due to thrombosis, intimal hyperplasia or calcification. To address this limitation, pharmaceutical and chemical conjugation to synthetic grafts has been proposed. Heparin conjugation is one promising method to prevent thrombosis in small-diameter arterial grafts. Ye *et al.* developed a PCL–heparin conjugated scaffold and implanted it into canines as a femoral interposition graft. The results showed graft patency one-month after implantation with cell infiltration into the scaffold walls, collagen formation, and the presence of an endothelial layer. Additionally, no calcification or thrombotic event was seen in the scaffold during the experimental period.[32] Recently, we separately

published longer-term data of a heparin-conjugated PCL graft implanted into sheep. In the study, all five heparinized PCL graft were patent at 8 weeks after implantation. In contrast, three out of five non-heparinized PCL grafts thrombosed.[33] Although further longer-term results are necessary to evaluate graft safety and efficacy, heparin conjugation appears to be a promising modification in the development of small-diameter arterial grafts.

To prevent intimal hyperplasia, Rapamycin conjugation has recently been investigated in small-diameter arterial grafts. Rapamycin is an FDA-approved drug and has demonstrated to therapeutically prevent restenosis and thrombosis when conjugated to drug eluting stents for coronary artery disease. Zou. *et al.* developed venous grafts which consist of Poly (lactic-co-glycolic acid) (PLGA) with rapamycin contained nanoparticles. Grafts were explanted 21 days after implantation in rat's extra jugular vein and authors presented results which showed significantly less intima-media sickness in rapamycin-loaded grafts when compared to control grafts (a reduction of intimal-media thickness of 150.2 ± 62.5 μm, $p = 0.001$).[34] Yang *et al.* developed a rapamycin conjugated PCL vascular graft. PCL nanofibers, blended with rapamycin, were electrospun outside a decellularized vascular graft, and the resulting hybrid TEVG was implanted into rat abdomen as aortic interposition grafts that were functional up to 8 weeks *in vivo*. Additionally, histological analysis of explanted 12-week rapamycin conjugated grafts, demonstrated significant decreases in neo-intimal hyperplasia when compared with non-conjugated grafts.[35] From these results, Rapamycin has an ability to prevent intima to medial hyperplasia which is induced by inflammatory reaction in both venous and arterial pressure environments. Recently, we conducted implantation model of rapamycin conjugated TEVG into sheep IVC. In this research, we intend to evaluate both rapamycin's short-term ability to prevent inflammatory reaction and its long-term impact for tissue regeneration in large animal model. Although, the results have not yet been revealed, we believe that the result will be worthful to consider the clinical implementation of rapamycin utilization un this field.
Despite rapid development of TE science, there are many hurdles to overcome before TE materials can be routinely used in cardiovascular surgery. First, the safety of such technologies needs to be ensured by defining how the success of implantation and the function of the TE materials is controlled. Therefore, specific clinical protocols or guidelines are necessary. Second, the utilization of TE materials should be straightforward to allow for broad clinical adoption. In order to prevent any potential error during its use, the product should be easy to handle compared to the current standard cardiovascular prostheses used clinically. Additionally, the regulation of the manufacturing process and quality control is essential to have a standardized and controlled outcome.[36]

In conclusion, while there have been numerous trials to develop TEVGs, the ideal design is yet to be discovered. Experts in medicine, developmental biology, stem cells, vascular biology, and immunology are needed to study graft infiltrating cells and identify ways to control their function. Should the current clinically investigated grafts prove safe and effective, they will likely reach more patients than current prosthetic grafts and open the possibility to further modifications. Therefore, further development of TE technologies are merited for their potential translational benefits and the scientific insight they will provide.

Additional information

Dr. Shinoka is financially supported by Gunze ltd under Grant number 820342-0322-00.

References

1. Matsuzaki Y, Kelly J, Shoji T, Shinoka T. The Evolution of Tissue Engineered Vascular Graft Technologies: From Preclinical Trials to Advancing Patient Care. *Appl Sci (Basel)* 2019; 9: 1274

2. Tissue engineered vascular grafts for pediatric cardiac surgery. T Shoji, T Shinoka. *Transl Pediatr* 2018; 7: 188-95.

3. Vats A, Tolley NS, Polak JM, Gough JE. Scaffolds and biomaterials for tissue engineering: a review of clinical applications. *Clin Otolaryngol Allied Sci* 2003; 28: 165-72.

4. Berglund JD, Galis ZS. Designer blood vessels and therapeutic revascularization. *Br J Pharmacol* 2003; 140: 627-36.

5. Chan BP, Leong KW. Scaffolding in tissue engineering: general approaches and tissue-specific considerations. *Eur Spine J* 2008;17: 467-79.

6. Asadian M, Chan KV, Norouzi M, Grande S, Cools P, Morent R, *et al.* Fabrication and Plasma Modification of Nanofibrous Tissue Engineering Scaffolds. *Nanomaterials (Basel)* 2020; 10: 119.

7. Fujita S, Yamagishi M, Kanda K, Maeda Y, Inoue T, Yamanami M, *et al.* Histology and Mechanics of *In Vivo* Tissue-Engineered Vascular Graft for Children. *Ann Thorac Surg* 2020; 110: 1050-4.

8. Zhang F, King MW. Biodegradable Polymers as the Pivotal Player in the Design of Tissue Engineering Scaffolds. *Adv Healthc Mater* 2020; 9: e1901358.

9. Hashi CK, Zhu Y, Yang GY, Young WL, Hsiao BS, Wang K; *et al.* Antithrombogenic property of bone marrow mesenchymal stem cells in nanofibrous vascular grafts. *Proc Natl Acad Sci USA* 2007; 104:11915-20.

10. Yao Y, Wang J, Cui Y, Xu R, Wang Z, Zhang J, *et al.* Effect of sustained heparin release from PCL/chitosan hybrid small-diameter vascular grafts on anti-thrombogenic property and endothelialization. *Acta Biomater* 2014; 10: 2739-49.

11. Fu J, Ding X, Stowell CET, Wu YL, Wang Y. Slow degrading poly(glycerol sebacate) derivatives improve vascular graft remodeling in a rat carotid artery interposition model. *Biomaterials* 2020; 257: 120251.

12. Tiwari A, Salacinski H, Seifalian AM, Hamilton G. New prostheses for use in bypass grafts with special emphasis on polyurethanes. *Cardiovasc Surg* 2002; 10: 191-7.

13. Shin'oka T, Imai Y, Ikada Y. Transplantation of a tissue-engineered pulmonary artery. *N Engl J Med* 2001; 344: 532-3.

14. Hibino N, McGillicuddy E, Matsumura G, Ichihara Y, Naito Y, Breuer C, *et al.* Late-term results of tissue-engineered vascular grafts in humans. *J Thorac Cardiovasc Surg* 2010; 139: 431-6.

15. Sugiura T, Matsumura G, Miyamoto S, Miyachi H, Breuer CK, Shinoka T. Tissue-engineered Vascular Grafts in Children with Congenital Heart Disease: Intermediate Term Follow-up. *Semin Thorac Cardiovasc Surg* 2018; 30: 175-9.

16. Weinberg CB, Bell E. A blood vessel model constructed from collagen and cultured vascular cells. *Science* 1986; 231: 397-400.

17. Qingjin C, Wanshan L, Fangchao X, Wang X, Zhou W, Li Y, *et al.* Selection of different endothelialization modes and different seed cells for tissue-engineered vascular graft. *Bioact Mater* 2021; 6: 2557-68.

18. Zhuang Y, Zhang C, Cheng M, Huang J, Liu Q, Yuan G, *et al.* Challenges and strategies for *in situ* endothelialization and long-term lumen patency of vascular grafts. *Bioact Mater* 2020; 6: 1791-809.

19. Edri R, Gal I, Noor N, Harel T, Fleischer S, Asasi N, *et al.* Personalized Hydrogels for Engineering Diverse Fully Autologous Tissue Implants. *Adv Mater* 2019; 31: e1803895.

20. Klein D. iPSCs-based generation of vascular cells: reprogramming approaches and applications. *Cell Mol Life Sci* 2018; 75: 1411-33.

21. Qin K, Wang F, Simpson RML, Zheng X, Wang H, Hu Y, *et al.* Hyaluronan promotes the regeneration of vascular smooth muscle with potent contractile function in rapidly biodegradable vascular grafts. *Biomaterials* 2020; 257: 120226.

22. Luo J, Qin L, Zhao L, Gui L, Ellis MW, Huang Y, *et al.* Tissue-Engineered Vascular Grafts with Advanced Mechanical Strength from Human iPSCs. *Cell Stem Cell* 2020; 26: 251-61.

23. Lawson JH, Glickman MH, Ilzecki M, Jakimowicz T, +Jaroszynski A, Peden EK, *et al.* Bioengineered human acellular vessels for dialysis access in patients with end-stage renal disease: two phase 2 single-arm trials. *Lancet* 2016; 387: 2026-34.

24. Ilanlou S, Khakbiz M, Amoabediny G, Mohammadi J, Rabbani H. Carboxymethyl kappa carrageenan-modified decellularized small-diameter vascular grafts improving thromboresistance properties. *J Biomed Mater Res A* 2019; 107: 1690-701.

25. García-Gareta E, Abduldaiem Y, Sawadkar P, Kyriakidis C, Lali F, Greco KV. Decellularized scaffolds: just a framework? Current knowledge and future directions. *J Tissue Eng* 2020; 11: 2041731420942903.

26. Sarikouch S, Horke A, Tudorache I, Beerbaum P, Westhoff-Bleck M, Boethig D, *et al.* Decellularized fresh homografts for pulmonary valve replacement: a decade of clinical experience. *Eur J Cardiothorac Surg* 2016; 50: 281-90.

27. Boethig D, Horke A, Hazekamp M, Meyns B, Rega F, *et al.* A European study on decellularized homografts for pulmonary valve replacement: initial results from the prospective ESPOIR Trial and ESPOIR Registry data. *Eur J Cardiothorac Surg* 2019; 56: 503-9.

28. Horke A, Tudorache I, Laufer G, Andreas M, Polmar JL, Pereda D, *et al.* Early results from a prospective, single-arm European trial on decellularized allografts for aortic valve replacement: the ARISE study and ARISE Registry data. *Eur J Cardiothorac Surg* 2020; 58: 1045-53.

29. Bell D, Betts K, justo R, Forde N, Venugopal P, Corno AF, *et al.* Multicenter Experience With 500 CardioCel Implants Used for the Repair of Congenital Heart Defects. *Ann Thorac Surg* 2019; 108: 1883-8.

30. Tong Z, Xu Z, Tong Y, Qi L, Guo L, Guo J, Gu Y. Effectiveness of distal arterial bypass with porcine decellularized vascular graft for treating diabetic lower limb ischemia. *Int J Artif Organs* 2021; 44: 580-6.

31. Matsuzaki Y, Iwaki R, Reinhardt JW, Chang YC, Miyamoto S, Kelly J, *et al.* The effect of pore diameter on neo-tissue formation in electrospun biodegradable tissue-engineered arterial grafts in a large animal model. *Acta Biomater* 2020; 115: 176-84.

32. Ye L, Wu X, Duan HY, Geng X, Chen B, Gu YQ, *et al.* The *in vitro* and *in vivo* biocompatibility evaluation of heparin-poly(ε-caprolactone) conjugate for vascular tissue engineering scaffolds. *J Biomed Mater Res A* 2012; 100: 3251-8.

33. Matsuzaki Y, Miyamoto S, Miyachi H, Iwaki R, Shoji T, Blim K, *et al.* Improvement of Novel Small-Diameter Tissue Engineered Arterial Graft with Heparin Conjugation. *Ann Thorac Surg* 2021; 111: 1234-41.

34. Zou J, Zhang X, Yang H, Zhu Y, Ma H, Wang S. Rapamycin-loaded nanoparticles for inhibition of neointimal hyperplasia in experimental vein grafts. *Ann Vasc Surg* 2011; 25: 538-46.

35. Yang Y, Lei D, Zou H, Huang S, Yang Q, Li S, *et al.* Hybrid electrospun rapamycin-loaded small-diameter decellularized vascular grafts effectively inhibit intimal hyperplasia. *Acta Biomater* 2019; 97: 321-332.

36. Emmert MY, Fioretta ES, Hoerstrup SP. Translational Challenges in Cardiovascular Tissue Engineering. *J Cardiovasc Transl Res* 2017; 10: 139-49.

Xeltis: towards grafts from supramolecular materials

36

Martijn. A. J. COX, Hannah S. BAUER, Mohammed S. EL-KURDI

Synthetic grafts have yet to overcome challenges associated with small diameter clinical application. The functional restoration of natural tissues through Endogenous Tissue Restoration (ETR) is emerging as a potential solution. Recent progress in the development of biocompatible, biodegradable, and tunable biomaterials with unprecedented properties allows the next step from laboratory studies to clinical studies. Supramolecular polymers are uniquely qualified for ETR because they offer independent control over mechanical properties and biodegradability, provided by the combination of covalent and non-covalent bonds. This paper aims to provide an overview on the preclinical and clinical application of supramolecular polymers for ETR, with a specific focus on vascular applications, and demonstrating the potential of supramolecular technology in bringing ETR to patients.

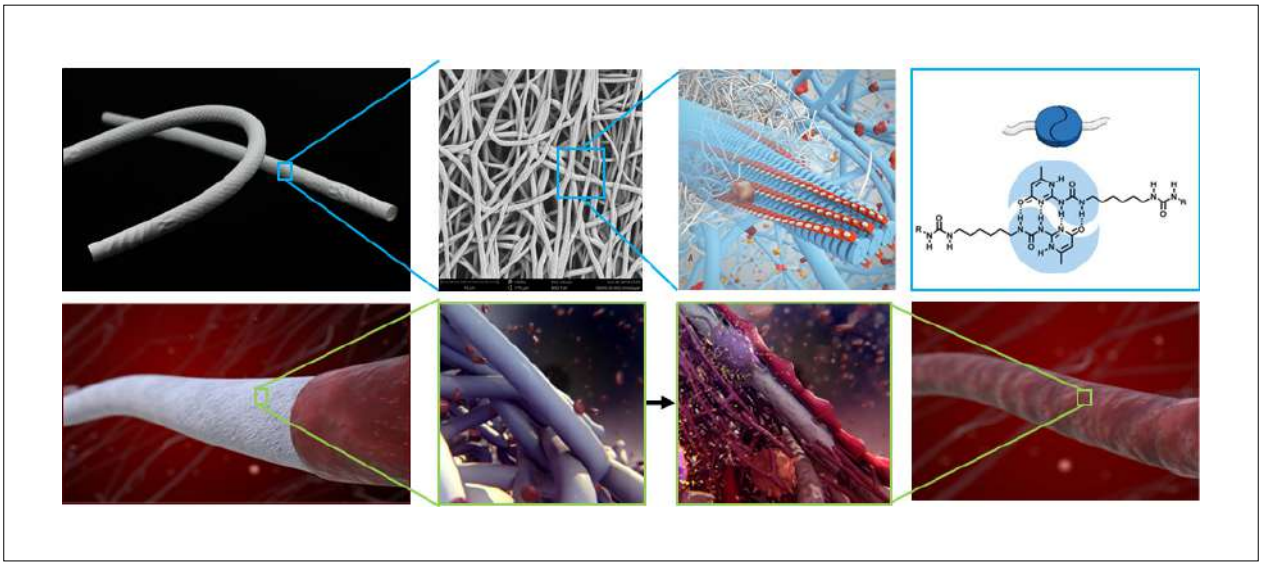

Graphical abstract - Adapted from [1].

Introduction

Coronary artery bypass grafting (CABG) after myocardial infarction constitutes 52% of all open-heart surgeries performed annually worldwide. Despite recent advances with full arterial revascularization, 80% of these procedures involve painful harvesting of patient's saphenous veins. Saphenous vein grafts (SVG) are associated with significant co-morbidity due to harvest, and most importantly suboptimal

performance in CABG, with reported SVG failure rates at 10-30% at one year and approximately 50% at 10 years[2-4]. For dialysis patients a native arteriovenous fistula is still considered the gold standard, despite an average of 3.5 months maturation time with 40% maturation failure[5] and only 72% primary patency by 6 months[6]. Despite these limitations, synthetic grafts have failed to offer adequate alternatives. There is currently no synthetic CABG on the market nor regulatory approved. Synthetic access grafts for dialysis are being used, although performance is poor due to associated infection risks of up to 17%[7] and further compromised functionality with a primary patency at 6 months of 58%[6].

The development of new organic-based biomaterials has opened the creation of new biomedical devices with unprecedented properties[8]. While in the early days biomaterials have mainly been used in more basic applications such as dialysis tubing or in dentistry, modern biomaterials are increasingly being found in more demanding medical applications such as controlled drug delivery systems or regenerative applications[9]. In the latter, the biomaterials are typically used as scaffolds for (functional) tissue growth whereby the scaffold provides the necessary mechanical support and enables the new tissue to grow within the desired geometry. In this paper, we present a novel modular biomaterial platform based on supramolecular polymer chemistry, and its potential for restoring natural and functional tissue in vascular applications.

Endogenous Tissue Restoration

The classic approach to natural tissue restoration is the *in vitro* tissue engineering approach, as postulated by Langer and Vacanti in their 1993 landmark paper[10]. Using the *in vitro* tissue engineering method, cells are harvested from the patient and seeded onto a temporary carrier. The combination is placed in a bioreactor in which it is typically exposed to physiological stresses and strains to stimulate production of autologous tissue. Despite initial successes, such as the first clinical application of a tissue engineered Fontan conduit in 2001[11], mainstream clinical adoption is lacking. This is largely due to the complexities and costs associated with prolonged periods of ex vivo cell and tissue manipulation. The company Humacyte has partly overcome these challenges by incorporating a decellularization step in the final phase of manufacturing, thus improving scale-up by using an allogeneic approach and enabling long term storage[12,13]. Humacyte late stage clinical trials with dialysis access grafts are well underway. The company Vascudyne recently announced start of clinical trials with a dialysis access graft[14], using the fibrin-based *in vitro* tissue engineering approached developed by Tranquillo *et al.*[15]. The common denominator for these approaches is that the success hinges on the creation of sufficiently strong neo-tissue prior to implantation, using extensive and prolonged ex vivo cell manipulation.

An alternative approach is to implant a device that is capable of providing functionality while gradually being permeated with cells and neo-tissue, which eventually take over functionality. In this endogenous tissue restoration (ETR) approach, fully synthetic polymeric scaffolds are implanted, without any additional cells or growth factors[16]. A key advantage of ETR over other regenerative approaches is the pure synthetic composition of the implant, which enacts the well-known regulatory framework of medical devices.

A schematic overview of the ETR process is provided in Figure 1. Firstly, the device is made using biorestorative polymer materials and implanted at the intended position in the patient. At this point in time, the functionality is fully carried by the device. Secondly, the device is infiltrated with cells that start forming neo-tissue, which gradually takes over functionality. In the final phase, the neo-tissue is strong enough to take over functionality completely, and the remnants of the polymeric devices are gradually absorbed. Clearly, an appropriate balance between tissue restoration and device absorption is essential for ensuring adequate functionality throughout the ETR process. As this balance is different

for every application, and even different in different parts of the same device, it is evident that these properties cannot be obtained with one single material. Therefore, the versatility of supramolecular polymer chemistry may be instrumental in creating a material platform that enables ETR.

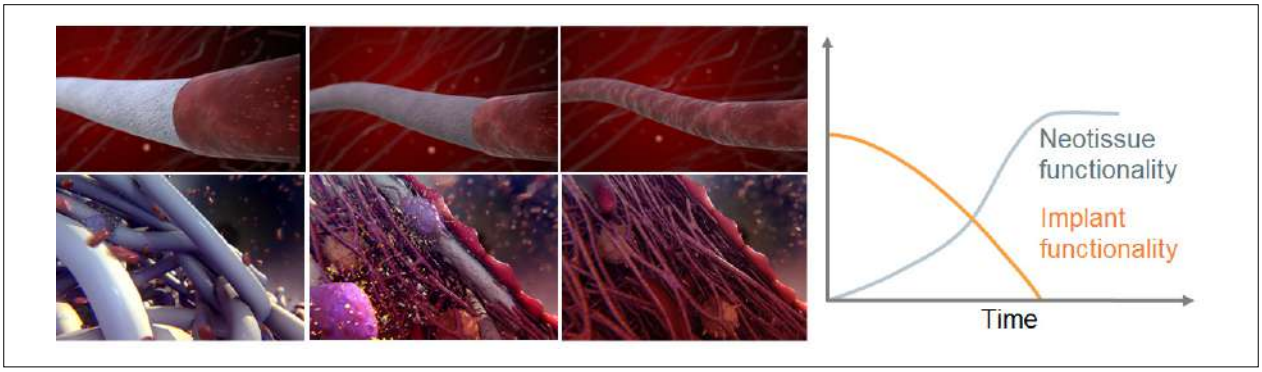

Figure 1: Schematic view of endogenous tissue restoration process in a conduit at macroscopic (top) and microscopic level (bottom). While the implant gradually loses functionality, neotissue builds up and takes over (right). The balance between those 2 processes is crucial for ETR to be successful.

Electrospinning

An important element in ETR is the creation of a three-dimensional matrix that is sufficiently porous to allow cell infiltration and subsequent ETR, while also providing adequate shape and function to allow the ETR process to yield a functional body part. A promising technique for this purpose is electrospinning, due its versatility and control over the scaffold microstructure. With this technique, the polymer is dissolved, and an electrostatic charge is applied between a syringe containing the polymer solution and a rotating collector target. The electric charge pulls fibers of polymer towards the rotating target, where it forms a microporous mesh, which can be molded into a three-dimensional shape such as a blood vessel. While the first report on electrospun vascular grafts dates back to 1978 [17], the approach regained popularity more recently, see *e.g.* [18-21].

Supramolecular polymers

The key to success for ETR is the development of biorestorative materials which are characterized by high strength, elasticity, durability, and controlled bio-absorption [22]. This has galvanized the development of a new modular biomaterial platform built on supramolecular polymers comprising ureidopyrimidinone (UPy) hydrogen bonding units [23-25]. This unique hydrogen bonding supramolecular unit has been developed at Eindhoven University of Technology and is responsible for the strong non-covalent and reversible (supramolecular) interactions between the supramolecular polymers due to its unprecedented high self-association strength [26,27]. Because the supramolecular hydrogen bonding interactions can be modulated with polar organic solvents, these polymers can relatively easily be processed into porous implant structures using solvent processing techniques like electrospinning. The development of this platform has been more extensively described by Mes *et al.* [28], a short summary is provided below.

In 1988, Lehn described supramolecular chemistry as “chemistry beyond the molecule” in which well-defined non-covalent interactions determine the (dis)-assembly, conformation, and function of the molecular system[29]. Initially, supramolecular chemistry was focused on the development of well-defined aggregates or supramolecular assemblies in solution as pioneered by Cram, Lehn, and Pedersen, which was honored with a Nobel Prize in 1987. The unit that has been most successful in bringing this field to everyday reality, is the self-complementary quadruple hydrogen bond unit as developed by Sijbesma and Meijer in 1997[25]. The key to its success was the use of hydrogen-bonding arrays in which cooperative hydrogen-bonding interactions are present. Consequently, their self-complementary quadruple hydrogen bonding units based on 2-ureido-4[1*H*]-pyrimidinones (UPy) display a strong self-association and resulted for the first time in a supramolecular H-bonding unit that was strong, stable and synthetically easily accessible[30]. Moreover, this strong self-association allowed for the first time the formation of supramolecular polymers with high degrees of polymerization.

Since the first introduction of UPy-polymers, several improvements have been proposed (low molecular weight telechelic polymer backbones, linker molecules, and chain-extending UPy-units) each of which contribute to the chemical, physical and biological properties of the resulting materials[31-33]. The polymer backbone is typically a biocompatible and biodegradable aliphatic polyester or aliphatic polycarbonate with a relatively low molecular weight (< 5 kDa). By changing the composition of the polymer ingredients, a wide range of mechanical properties can be obtained from soft to elastic, and even stiff, while keeping materials that are easily processable, biodegradable and biocompatible[23]. An additional advantage of the UPy-polymers is their processability using solution-based techniques such as electrospinning. In solution, the reversible UPy cross-links can be temporarily removed by using a polar, hydrogen-bonding competitive, co-solvent which will result in a formulation with sufficiently low viscosity as needed for electrospinning. Upon evaporation of the polar solvent, hydrogen bonds are reformed, and the mechanical strength of the polymer is restored. Figure 2 illustrates the hierarchical architecture of an electrospun UPy-polymer scaffold.

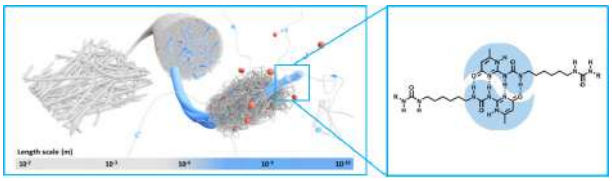

Figure 2: Illustration of hierarchical structure of an electrospun supramolecular polymer scaffold, with an illustration of the self-complementary UPy-motif (inset). Figure adapted from[1,34].

Preclinical studies and clinical outlook

Supramolecular polymers have been evaluated in range of preclinical models and applications. It is of interest to note that significant advances have been made with supramolecular polymer heart valves. Several studies have demonstrated the potential of restoring a functional pulmonary valve[35-38], with longest follow-up out to 2 years in an ovine pulmonary interposition model[39]. First studies indicating potential for aortic valve application have recently been published as well[40,41]. Current review will focus on vascular graft applications.

Small animal model - tissue remodeling & biocompatibility

To better understand the potential of the UPy-platform, Cramer *et al.*[42] implanted electrospun UPy-polymer discs in a subcutaneous rat model. Results revealed a mild inflammatory response associated with macrophage influx and extensive formation of neocapillaries within 2 weeks after implantation. Calcification potential was low compared to cross-linked bovine pericardium controls. Interestingly, the

materials consistently demonstrated a dominant M2-macrophage response throughout follow-up (Figure 3) in contrast to typical M1-dominant behavior reported for synthetic materials [43,44]. Generally, M2 macrophages are associated with a pro-healing response, while M1 macrophages are pro-inflammatory[45-47]. Whether this pro-healing response is another unique feature of the UPy-platform or rather an effect of the electrospun microstructure remains to be elucidated in future more mechanistic studies.

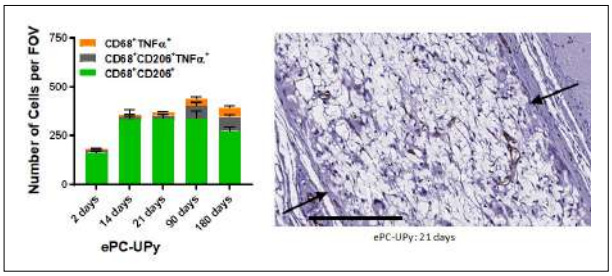

Figure 3:

A) Electrospun UPy-discs trigger more pro-healing (M2, CD206 positive) than pro-inflammatory (M1, TNFα positive) macrophages in a subcutaneous rat model.

B) Neocapillary ingrowth illustrated by CD31 stain (brown) within UPy implant (implant margins marked by black arrow) at 3 weeks follow-up. Adapted from [42], with permission.

Small animal model - functional

The rat aortic interposition graft model has been well-established for first-order functional evaluation of novel materials or grafts [48]. Using this model, UPy-based grafts enhanced with stromal cell derived factor 1-alpha (SDF-1a) were demonstrated to increase CD68+ cell concentration at 7 days follow-up compared to non-enhanced UPy-grafts. Studies with a fast-degrading bisurea-based supramolecular polymer demonstrated the potential of ETR with this platform, although premature dilatation remained a concern [49,50]. It is suggested that a more gradually absorbing material may be required to allow sufficient time for functional tissue restoration. The most extensive study has been reported by Besseling *et al.*, who evaluated graft performance out to 3 months in a chronic kidney disease (CKD) rat model (5/6 nephrectomy)[51]. Their results demonstrated 100% patent grafts (n=20 sham, n=21 CKD) with rapid cell ingrowth, increased mechanical strength and apparent endothelialization by 8 weeks (Figure 4). No differences were found between sham and CKD animals, which is an important indicator for the potential of these materials for dialysis in CKD patients.

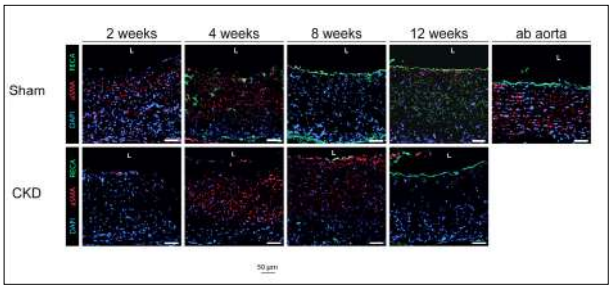

Figure 4: Vascular Tissue formation in Sham and CKD animals in grafts explanted at 2, 4, 8, and 12 weeks. Stained with rat endothelial marker, RECA (green) and smooth muscle cell marker, aSMA (red), with cell nuclei in blue (DAPI). Lumen is indicated by L. Scale bars represent 50μm. Figure adapted from Besseling et al, with permission [51].

Large animal model – low pressure circulation

A first demonstration of ETR in a chronic large animal model was reported by Schoen *et al.* [52], in a pulmonary artery interposition model in 9 adult sheep using an electrospun conduit, composed of a polycaprolactone-based UPy polymer. Follow-up ranged from 5 days to 1 year. Mechanical testing performed on the explanted grafts showed that no mechanical contribution could be measured from the implanted polymer beyond 11 weeks, and the burst pressure of the newly formed tissue was well above safety requirements for commercial conduits. Upon implantation, the device is infiltrated with inflammatory cells, predominantly macrophages, which release growth factors that attract endothelial

cells, (myo)fibroblasts and smooth muscle cells that take care of neotissue formation. While neotissue forms, polymer absorption is governed by macrophages secreting enzymes and oxygen radicals. In areas where the implant is absorbed, the inflammatory trigger is resolved as well, and the inflammatory cells disappear, thus leaving a quiescent, natural tissue that has taken over functionality from the original polymeric implant. Figure 5 illustrates the progression of ETR with time in this study.

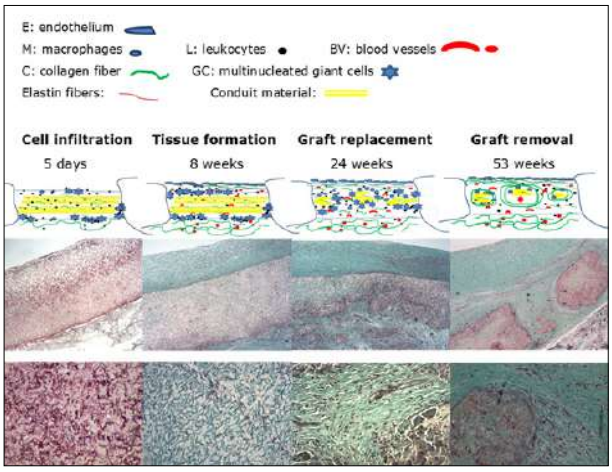

Figure 5: Histopathological progression of ETR with time in an ovine pulmonary artery interposition model. Left cell infiltration (red dots) is shown within 5 days after implantation. At 8 weeks, new tissue (blue-green) has formed at the luminal side and within the implant. At 24 weeks the implant starts fragmenting and is progressively replaced with tissue, which continues at 53 weeks. Adapted with permission from Bockeria *et al.*[53].

Large animal model – peripheral applications

While the small animal models and the pulmonary interposition model provide positive indications, it is of crucial importance to evaluate performance in the more challenging combination of high pressure and small diameter in large animals. A first indication was provided using an ovine carotid interposition model[54]. Electrospun polycarbonate-UPy grafts (4-5cm long, 6 or 7mm inner diameter) were implanted unilaterally as a straight inter-position graft in the native ovine carotid artery. Patency was 100% at 6 months (n=3) and 12 months (n=3) follow-up with no indications of stenosis. By 12 months the original implant is largely fragmented, embedded within collagen-rich connective tissue, and overlaying a stable neointima (Figure 6). There are abundant neocapillaries and the graft lumen is lined with vWf-positive cells, suggesting endothelialization.

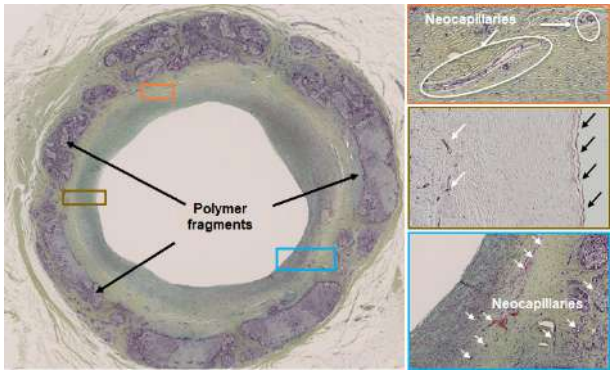

Figure 6: 12m ovine carotid explant. Left: mid graft cross section (Movat pentachrome) illustrating collagen-rich (green-yellow) neointima. Absorption of the fragmented polymer is ongoing (black arrows). High magnification (orange & brown box) insets further illustrate neocapillary formation in neointima and in between polymer fragments. Middle inset (brown box) shows vWf-positive cells lining the lumen of the graft as well as intragraft neocapillaries.

Endothelialization is an important indicator for late stage healing, however in a 5cm long carotid interposition model it is likely attributable to trans-anastomotic ingrowth. Clinically, transanastomotic ingrowth is limited to 1-2cm and therefore of limited relevance for complete healing. An excellent review on the topic of preclinical model translation has been provided by Zilla *et al.*[55] who postulate a rat loop model with anastomotic isolation for assessing clinically relevant endothelialization.

A drawback of the model is the small caliber graft required, which therefore does not allow testing of clinical size devices. As an alternative, we have used an ovine arteriovenous shunt loop model, connecting the carotid artery to the jugular vein. Electrospun polycarbonate-UPy grafts (20cm long, 6mm inner diameter) were reinforced with an embedded braided nitinol microskeleton to enhance kink-resistance in a unilateral model and demonstrated superior aggregated patency compared to

size-matched commercially available ePTFE controls up to 12 months follow-up: 6 of 9 patent UPy-grafts *vs.* 1 of 3 ePTFE controls (data on file). In addition, UPy grafts were punctured biweekly between 1 and 12 months to simulate dialysis without any issues. As illustrated in Figure 7, UPy grafts demonstrated nearly complete absorption by 12 months, with a thin mature neointima and a cellular lining of the lumen. Note that the nitinol microskeleton required plastic embedding, thus limiting possibilities for staining specific cell types. Given long graft length, it seems reasonable to assume that the observed cellular lining is not resulting from anastomotic ingrowth, which is promising towards clinical translation.

Large animal model – coronary artery bypass grafting

An ovine coronary artery bypass graft model provides a very challenging environment, partly illustrated by the scarcity of literature data in comparison to peripheral models [56-58]. Despite these challenges, we recently completed a one-year study with an electrospun polycarbonate UPy graft (15cm long, 4mm inner diameter) with an embedded nitinol microskeleton, which was used as a bypass graft from the descending aorta to the left anterior descending artery (LAD) in a sheep model. Graft patency was demonstrated out to 1 year with generally uniform graft lumen and widely patent and well-healed anastomoses. A combination of SEM and von Willebrand factor staining suggests mid graft coverage with endothelial-like cells at 12 months follow-up (Figure 8). A manuscript with further details on the study is currently under preparation.

Clinical outlook

Besides various preclinical applications as mentioned above, the first clinical applications of supramolecular polymers have been reported as well. Bockeria *et al.* performed a world-first clinical feasibility trial, in which five children (aged 4 to 12 years) received an electrospun polycaprolactone-based UPy polymer conduit as part of a Fontan procedure [53,59]. This procedure is performed on children with a congenital heart defect, possessing

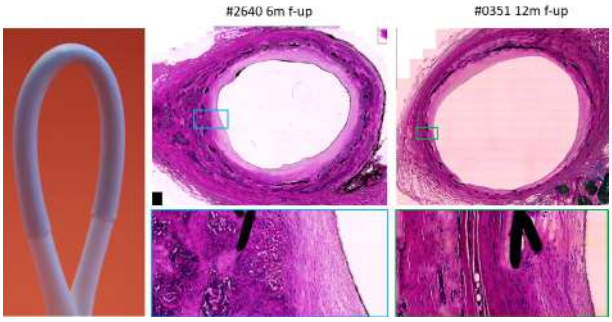

Figure 7: Left: Photograph of supramolecular access graft.

Middle: H&E mid graft 6m ovine access graft explant. High magnification inset shows cellular lining of lumen and advanced fragmentation of polymer implant.

Right: H&E mid graft 6m ovine access graft explant. High magnification inset shows cellular lining of lumen. Polymer implant absorption is substantially completed.

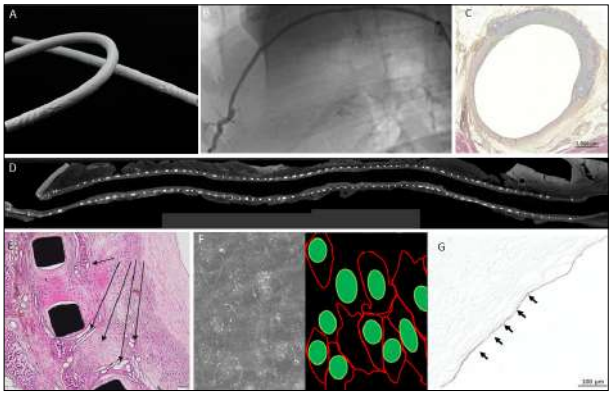

Figure 8: Imaging at 12m f-up in an ovine CABG model.

A) photographic impression of graft

B) Angio with fully patent graft (15cm long, 4mm diameter, descending aorta to LAD).

C) Movat-pentachrome stain of explant distal anastomosis illustrating smooth transition from implant (10-4 o'clock) to native LAD (4-10 o'clock).

D) MicroCT longitudinal cross-section of explant from aorta (left) to LAD (right) with uniform lumen and nitinol microskeleton in white.

E) H&E high magnification mid graft illustrating transmural capillaries (black arrows) as potential source of mid graft endothelialization.

F) Mid graft Scanning electron microscopy of explant showing confluent endothelial cell lining with tight cell to cell junction, graphically illustrated as red lines with cell nucleus in green.

G) Mid graft section of neointima (paraffin embedding) showing positive von Willebrand factor staining at lumen (black arrows) indicative of endothelial lining.

only a single functional ventricle. All patients received an 18 mm or 20 mm diameter conduit to create the extracardiac total cavopulmonary connection (EC-TCPC) during the final stage of the Fontan procedure.

All procedures were successful and a significant improvement in patients' general conditions were reported at 1 and 2 years, with no (adverse) changes to the grafts compared to early postoperative data[59,60]. Good haemodynamics, and anatomical and functional stability of the graft was demonstrated using MRI (Figure 9). While the number of patients was small, this first clinical study provides important data on the initial clinical safety and feasibility of restoring cardiovascular function using a supramolecular polymer-based approach.

In addition to the extracardiac conduit, a pulmonary valved conduit has progressed into clinical evaluation. Xeltis currently has 2 clinical feasibility trials ongoing with a pulmonary valved conduit, showing promising results [61-64]. Based on this encouraging data, Xeltis recently announced the start of a worldwide pivotal trial as a final step towards market approval [65].

While reoperation rates have been low for these patients, Figure 10 provides histological images of the conduit portion of a supramolecular PV obtained from a patient who was reoperated after 4 years. Fragments of the polymer are still visible, although functionality has clearly been taken over by natural tissue. Furthermore, there are no indications of calcification, thrombus or other adverse remodeling responses. Note resemblance with preclinical findings (Figure 6) including abundant neocapillary formation.

While it is very exciting to see a first-ever clinical application of supramolecular polymer-based heart valves, longer term data will need to be awaited to confirm the potential of supramolecular chemistry enabling ETR to provide the much-needed improvement in this and other clinical applications. Initial clinical trials with supramolecular coronary artery bypass grafts [66] as well as dialysis access grafts [67] are currently in preparation.

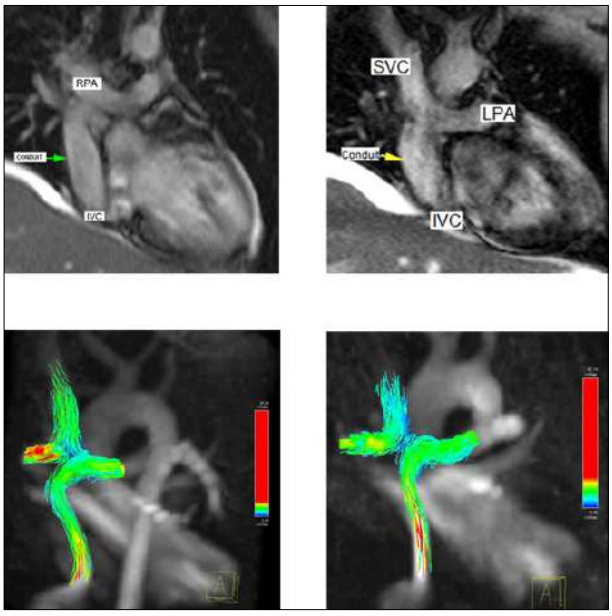

Figure 9: One and two-year MRI controls on frontal views showing the EC-TCPC connecting Inferior Vena Cava to the left and right pulmonary artery. 4D flow evaluation shows good laminar flow in the vascular graft with no turbulence. (Adapted with permission from Bockeria *et al.* [59])

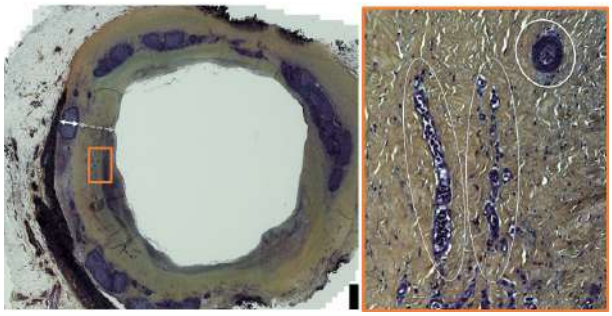

Figure 10: Movat-pentachrome stain of 4-year follow-up clinical PV conduit, which was explant for redo surgery. Left: conduit only cross-section (subvalvular) showing neointima (dashed gray arrow) and fragmented polymer dispersed with neomedia (solid white arrow). High magnification inset (orange box) shows neocapillaries and arterioles (white circles) in neointima section.

Conclusions

Almost 35 years after the Nobel prize for supramolecular chemistry, the versatility of the concept is making it emerge as a potential enabler of restorative cardiovascular applications, specifically small diameter vascular grafts. A range of preclinical models with varying complexity support the use of supramolecular polymer platforms for ETR. In addition to various reports on chronic studies in large animal models, various clinical studies with large diameter (pulmonary valve) conduits also support the safety of the platform. First clinical trials with small caliber vascular grafts are underway. In our view it is only the beginning of using supramolecular materials as biomaterials for ETR to overcome traditional challenges with synthetic grafts.

References

1. Besseling PJ, Mes T, Bosman AW, Peeters JW, Janssen HM, Bakker MH, *et al.* The in-vitro biocompatibility of ureido-pyrimidinone compounds and polymer degradation products, *J Polym Sci* 2021; 59: 1257-67.
2. Alexander JH, Ferguson TB, Joseph DM, Mack MJ, Wolf RK, Gibson CM, *et al.* The PRoject of Ex-vivo Vein graft ENgineering via Transfection IV (PREVENT IV) trial: study rationale, design, and baseline patient characteristics., *Am Heart J* 2005; 150: 643-9.
3. Fitzgibbon GM, Kafka HP, Leach AJ, Keon WJ, Hooper GD, Burton JR. Coronary bypass graft fate and patient outcome: angiographic follow-up of 5,065 grafts related to survival and reoperation in 1,388 patients during 25 years. *J Am Coll Cardiol* 1996; 28: 616-26.
4. Yun KL, Wu YX, Aharonian V, Mansukhani P, Pfeffer TA, Sintek CF, *et al.* Randomized trial of endoscopic *vs.* open vein harvest for coronary artery bypass grafting: Six-month patency rates, *J Thorac Cardiovasc Surg* 2005; 129: 496-503.
5. Lawson JH, Niklason LE, Roy-Chaudhury P. Challenges and novel therapies for vascular access in haemodialysis, *Nat Rev Nephrol* 2020; 16: 586–602.
6. Huber TS, Carter JW, Carter RL, J.M. Seeger JM. Patency of autogenous and polytetrafluoroethylene upper extremity arteriovenous hemodialysis accesses: A systematic review *J Vasc Surg* 2003; 38: 1005-1.
7. Lawson JH, Glickman MH, Ilzecki M, Jakimowicz T, Jaroszynski A, Peden EK, *et al.* Bioengineered human acellular vessels for dialysis access in patients with end-stage renal disease: two phase 2 single-arm trials. *Lancet* 2016; 387: 2026-34.
8. Webber MJ, Appel EA, Meijer EW, Langer R, Supramolecular biomaterials. *Nat Mater* 2015; 15: 13-26.
9. Langer R. Biomaterials in drug delivery and tissue engineering: One laboratory's experience. *Acc Chem Res* 2000; 33: 94-101.
10. Sodian R, Hoerstrup SP, Sperling JS, Daebritz SH, Martin DP, Schoen FJ, *et al.* Tissue engineering of heart valves: *In vitro* experiences, *Ann Thorac Surg* 2000; 70: 140-4.
11. Shin'oka T, Imai Y, Ikada Y. Transplantation of a tissue-engineered pulmonary artery. *N Engl J Med* 2001; 344: 532-3.
12. Lawson JH, Glickman MH, Ilzecki M, Jakimowicz T, Jaroszynski A, Peden EK, *et al.* Bioengineered human acellular vessels for dialysis access in patients with end-stage renal disease: Two phase 2 single-arm trials, *Lancet* 2016; 387: 2026-34.
13. Niklason LE, Lawson JH. Bioengineered human blood vessels. Science 2020; 370: eaaw8682.
14. Preliminary Safety of The TRUE Vascular Graft for Hemodialysis Access (TRUE HD I Study) ClinicalTrials.gov Identifier: NCT04905511, (2021).
15. Syedain ZH, Graham ML, Dunn TB, O'Brien T, Johnson SL, Schumacher RJ, *et al.* A completely biological "off-the-shelf" arteriovenous graft that recellularizes in baboons. *Sci Transl Med* 2017; 9: eean4209.
16. Serruys PW, Miyazaki Y, Katsikis A, Abdelghani M, Leon MB, Virmani R, *et al.* Restorative valve therapy by endogenous tissue restoration: Tomorrow's world? Reflection on the EuroPCR 2017 session on endogenous tissue restoration, *EuroIntervention* 2017; 13: AA68-AA77.
17. Annis D, Bornat A, Edwards RO, Higham A, Loveday B, Wilson J. An elastomeric vascular prosthesis. *Trans Am Soc Artif Intern Organs* 1978; 24: 209-14.
18. Hu ZJ, Li ZL, Hu LY, He W, Liu RM, Sen Qin S, *et al.* The *in vivo* performance of small-caliber nanofibrous polyurethane vascular grafts, *BMC Cardiovasc Disord* 2012; 12: 115.
19. Bergmeister H, Strobl M, Grasl C, Liska R, Schima H. Tissue engineering of vascular grafts. *Eur Surg* 2013; 45: 187-93.
20. Wang Z, Cui Y, Wang J, Yang X, Wu Y, Wang K, *et al.* The effect of thick fibers and large pores of electrospun poly(ε-caprolactone) vascular grafts on macrophage polarization and arterial regeneration. *Biomaterials* 2014; 35: 5700-10.
21. Ong CS, Zhou X, Huang CY, Fukunishi T, Zhang H, Hibino N. Tissue engineered vascular grafts: current state of the field. *Expert Rev Med Devices* 2017; 14: 383-92.

22. Wissing TB, Bonito V, Bouten CVC, Smits AIPM. Biomaterial-driven *in situ* cardiovascular tissue engineering—a multi-disciplinary perspective. *Npj Regen Med* 2017; 2: 1-19.

23. Dankers PYW, Maria G, Gemert LHV, Janssen HM, Meijer EW, Bosman AW, US8883188B2 - Modular bioresorbable or biomedical, biologically active supramolecular materials - Google Patents, 2006. https://patents.google.com/patent/US8883188B2/en (accessed June 2, 2021).

24. Dankers PYW, van Leeuwen ENM, van Gemert GML, Spiering AJH, Harmsen MC, Brouwer LA, *et al.* Chemical and biological properties of supramolecular polymer systems based on oligocaprolactones. *Biomaterials* 2006; 27: 5490-501.

25. Goor OJGM, Hendrikse SIS, Dankers PYW, Meijer EW. From supramolecular polymers to multi-component biomaterials. *Chem Soc Rev* 2017; 46: 6621.

26. Sijbesma RP, Beijer FH, Brunsveld L, Folmer BJB, Hirschberg JHKK, Lange RFM, *et al.* Reversible polymers formed from self-complementary monomers using quadruple hydrogen bonding. *Science* 1997; 278: 1601-4.

27. Brunsveld L, Folmer BJB, Meijer EW, Sijbesma RP. Supramolecular polymers. *Chem Rev* 2001; 101: 4071-97.

28. Mes T, Serrero A, Bauer HS, Cox MAJ, Bosman AW, Meijer EW. Supramolecular polymer materials bring restorative heart valve therapy to patients - in preparation, Mater. *Today.* (n.d.).

29. Lehn LM. Supramolecular Chemistry—Scope and Perspectives Molecules, Supermolecules, and Molecular Devices (Nobel Lecture). *Angew Chemie Int Ed English* 1988; 27: 89-112.

30. Beijer FH, Sijbesma RP, Kooijman H, Spek AL, Meijer EW. Strong dimerization of ureidopyrimidones via quadruple hydrogen bonding. *J Am Chem Soc* 1998; 120: 6761-9.

31. Dankers PYW, Harmsen MC, Brouwer LA, Van Luyn MJA, Meijer EW. A modular and supramolecular approach to bioactive scaffolds for tissue engineering. *Nat Mater* 2005; 4: 568-74.

32. Folmer BJB, Sijbesma RP, Versteegen RM, van der Rijt JAJ, Meijer EW. Supramolecular Polymer Materials: Chain Extension of Telechelic Polymers Using a Reactive Hydrogen-Bonding Synthon. *Adv Mater* 2000; 12: 874-8.

33. Dankers PYW. Supramolecular Biomaterials: Introducing a Modular Approach, 2006.

34. Mori da Cunha MGMC, Arts B, Hympanova L, Rynkevic R, Mackova K, Bosman AW, *et al.* Functional supramolecular bioactivated electrospun mesh improves tissue ingrowth in experimental abdominal wall reconstruction in rats. *Acta Biomater* 2020; 106: 82-91.

35. Kluin J, Talacua H, Smits AIPM, Emmert MY, Brugmans MCP, Fioretta ES, *et al. In situ* heart valve tissue engineering using a bioresorbable elastomeric implant – From material design to 12 months follow-up in sheep. Biomaterials 2017; 125: 101-117.

36. Bennink G, Torii S, Brugmans M, Cox M, Svanidze O, Ladich E, *et al.* A novel restorative pulmonary valved conduit in a chronic sheep model: Mid-term hemodynamic function and histologic assessment, *J Thorac Cardiovasc Surg* 2018; 155: 2591-601.e3.

37. Soliman OI, Miyazaki Y, Abdelghani M, Brugmans M, Witsenburg M, Onuma Y, *et al.* Midterm performance of a novel restorative pulmonary valved conduit: Preclinical results. *EuroIntervention* 2017; 13: e1418-e1427.

38. Uiterwijk M, Smits AIPM, van Geemen D, van Klarenbosch B, Dekker S, Cramer MJ, *et al. In Situ* Remodeling Overrules Bioinspired Scaffold Architecture of Supramolecular Elastomeric Tissue-Engineered Heart Valves. *JACC Basic Transl Sci* 2020; 5: 1187-206.

39. De Kort BJ, Marzi J, Brauchle E, Lichauco AM, Bauer HS, Serrero A, *et al.* Inflammatory and regenerative processes in bioresorbable synthetic pulmonary valves up to 2 years in sheep: Spatiotemporal insights augmented by Raman microspectroscopy. *Acta Biomateriala* 2021; in press.

40. Serruys PW, Kawashima H, Chang CC, Modolo R, Wang R, de Winter RJ, *et al.* Chronic Hemodynamic Performance of a Biorestorative Transcatheter Heart Valve in an Ovine Model - *EuroIntervention* 2021; in press.

41. Miyazaki Y, Soliman OI, Abdelghani M, Katsikis A, Naz C, Lopes S, *et al.* Acute performance of a novel restorative transcatheter aortic valve: Preclinical results. *EuroIntervention* 2017; 13: e1410-e1417.

42. Cramer M, Chang J, Li H, Serrero A, El-Kurdi M, Cox M, *et al.* Tissue response, macrophage phenotype, and intrinsic calcification induced by cardiovascular biomaterials: Can clinical regenerative potential be predicted in a rat subcutaneous implant model? *J Biomed Mater Res Part A* 2021, in press.

43. Brown BN, Valentin JE, Stewart-Akers AM, McCabe GP, Badylak SF, Macrophage phenotype and remodeling outcomes in response to biologic scaffolds with and without a cellular component. *Biomaterials* 2009; 30: 1482-91.

44. Wolf MT, Vodovotz Y, Tottey S, Brown BN, Badylak SF. Predicting *in vivo* responses to biomaterials via combined *in vitro* and in silico analysis. *Tissue Eng Part C Methods* 2015; 21: 148-59.

45. Bonito V, Smits AIPM, Goor OJGM, Ippel BD, Driessen-Mol A, Münker TJAG, *et al.* Modulation of macrophage phenotype and protein secretion via heparin-IL-4 functionalized supramolecular elastomers, *Acta Biomater* 2018; 71: 247-60.

46. Wissing TB, Bonito V, van Haaften EE, van Doeselaar M, Brugmans MM, Janssen HM, *et al.* Macrophage-driven biomaterial degradation depends on scaffold microarchitecture. *Front Bioeng Biotechnol* 2019; 7: 87.

47. Badylak SF, Valentin JE, Ravindra AK, McCabe GP, Stewart-Akers AM, Macrophage phenotype as a determinant of biologic scaffold remodeling, *Tissue Eng Part A* 2008; 14: 1835-42.

48. Gregory EK, Vercammen JM, Flynn ME, Kibbe MR. Establishment of a rat and guinea pig aortic interposition graft model reveals model specific patterns of intimal hyperplasia. *J Vasc Surg* 2016; 64:1835-43.

49. Duijvelshoff R, van Engeland NCA, Gabriels KMR, Söntjens SHM, Smits AIPM, Dankers PYW, *et al.* Host response and neo-tissue development during resorption of a fast degrading supramolecular electrospun arterial scaffold, *Bioengineering*. 2018; 5: 1-16.

50. Duijvelshoff R, di Luca A, van Haaften EE, Dekker S, Söntjens SHM, Janssen HM, *et al.* Inconsistency in Graft Outcome of Bilayered Bioresorbable Supramolecular Arterial Scaffolds in Rats. *Tissue Eng Part A* 2021; 27: 894-904.

51. Besseling PJ, Krebber MM, Fledderus JO, Teraa M, den Ouden K, van de Kaa M, *et al.* Chronic kidney disease does not impair long-term tissue formation in *in situ* tissue-engineered vascular grafts. In preparation.

52. Brugmans M, Serrero A, Cox M, Svanidze O, F.J. Schoen, Morphology and mechanisms of a novel absorbable polymeric conduit in the pulmonary circulation of sheep. *Cardiovasc Pathol* 2019; 38: 31-8.

53. Bockeria LA, Svanidze O, Kim A, Shatalov K, Makarenko V, Cox M, *et al.* Total cavopulmonary connection with a new bioabsorbable vascular graft: First clinical experience. *J Thorac Cardiovasc Surg* 2017; 153: 1542-50.

54. Marzi J, Brauchle EM, Serrero A, Bosman AW, Cox MAJ, Schenke-Layland K. Monitoring of tissue maturation and polymer absorption in a restorative polymeric graft as a carotid interposition in a sheep model. *Termis, Maastricht,* 2021.

55. Zilla P, Bezuidenhout D, Human P. Prosthetic vascular grafts: Wrong models, wrong questions and no healing, *Biomaterials* 2007; 28: 5009-27.

56. Fang S, Ellman DG, Andersen DC. Review: Tissue Engineering of Small-Diameter Vascular Grafts and Their *In Vivo* Evaluation in Large Animals and Humans. *Cells* 2021; 10: 713.

57. Byrom MJ, Bannon PG, White GH, Ng MKC. Animal models for the assessment of novel vascular conduits. *J Vasc Surg* 2010; 52: 176-95.

58. Ben-Gal Y, Taggart DP, Williams MR, Orion E, Uretzky G, Shofti R, *et al.* Expandable external support device to improve Saphenous Vein Graft Patency after CABG, *J Cardiothorac Surg* 2013; 8: 1-9.

59. Bockeria L, Carrel T, Lemaire A, Makarenko V, Kim A, Shatalov K, *et al.* Total cavopulmonary connection with a new restorative vascular graft: Results at 2 years. *J Thorac Dis* 2020; 12: 4168-73.

60. Safety and Performance of the COR-VG-001 Conduit in Pediatric Patients for Extracardiac Total Cavopulmonary Connection - Full Text View - ClinicalTrials.gov, (n.d.). https://clinicaltrials.gov/ct2/show/NCT02377674 (accessed June 2, 2021).

61. Study to Assess Safety of the Pulmonary Valved Conduit (PV-001) in Subjects Undergoing Right Ventricular Outflow Tract Reconstruction - Full Text View - ClinicalTrials.gov, (n.d.). https://clinicaltrials.gov/ct2/show/NCT02700100 (accessed June 2, 2021).

62. Xeltis Bioabsorbable Pulmonary Valved Conduit Early Feasibility Study - Full Text View - ClinicalTrials.gov, (n.d.). https://clinicaltrials.gov/ct2/show/NCT03022708 (accessed January 26, 2021).

63. Morales DL, Herrington C, Bacha EA, Morell VO, Prodán Z, Mroczek T, *et al.* A Novel Restorative Pulmonary Valve Conduit: Early Outcomes of Two Clinical Trials. *Front Cardiovasc Med* 2021; 7: 583360.

64. Prodan Z, Mroczek T, Sivalingam S, Bennink G, Asch FM, Cox M, *et al.* Initial Clinical Trial of A Novel Pulmonary Valved Conduit. *Semin Thorac Cardiovasc Surg* 2021, in press.

65. Xeltis Bioabsorbable Pulmonary Valved Conduit Pivotal Study (Xplore2) ClinicalTrials.gov Identifier: NCT03022708, (2017). https://clinicaltrials.gov/ct2/show/NCT03022708?term=Xeltis&draw=2&rank=2.

66. Xeltis Coronary Artery Bypass Graft (XABG) First in Human (FIH) (XABG-FIH) ClinicalTrials.gov Identifier: NCT04545112, (2020). https://clinicaltrials.gov/ct2/show/NCT04545112?term=Xeltis&draw=2&rank=5.

67. First-in-Human (FIH) Study of the Xeltis Hemodialysis Access Graft (aXess-FIH) ClinicalTrials.gov Identifier: NCT04898153, (2021). https://clinicaltrials.gov/ct2/show/NCT04898153?term=Xeltis&draw=2&rank=3.

Bioresorbable synthetic Heart Valves to induce *In Situ* tissue regeneration: recent advances and current challenges

37

Anthal I.P.M. SMITS

There is a growing clinical demand for heart valve replacements with growth and remodeling potential. Resorbable synthetic heart valves are emerging as attractive materials to effectively induce endogenous heart valve tissue regeneration. Such valves are designed to instantaneously take over valve function upon implantation, followed by a gradual replacement of the synthetic starter material by endogenous valvular tissue. This process, known as *in situ* tissue regeneration, is driven by the inflammatory response to the implanted artificial scaffold material. With proof-of-concept in preclinical models established over the past years and the recent release of the first reports on ongoing clinical trials, the technology of *in situ* tissue engineering is entering a new developmental stage. This concise review describes the most recent advances for using resorbable synthetic heart valves and pinpoints three important current challenges in the field, namely: (1) harnessing the inflammatory response, (2) the restoration of native-like tissue organization, and (3) centering patient-specific characteristics. Reflecting on these specific challenges, an integral perspective is provided on the steps to take towards robust and safe clinical application.

Introduction

Tissue engineering of an autologous living heart valve replacement has been pursued for almost three decades[1]. For pediatric patients with congenital cardiac defects in particular, a living valve replacement is essential to avoid otherwise inevitable reinterventions during somatic growth. With respect to heart valve replacements in adults, the benefit of having a living valve replacement as an adult is evident from studies comparing outcome of an autologous pulmonary valve as aortic valve replacement (Ross procedure) with non-viable grafts, which show that a pulmonary autograft significantly improves the patient quality of life with a reduced risk of reintervention, as well as life expectancy[2]. Consequently, both for pediatric and adult patients, there is a strong clinical need for cost-effective heart valve prostheses that are capable of growth and remodeling, similar to their native counterpart. Considering the large patient population in need of a heart valve replacement as a consequence of rheumatic heart disease in developing countries, it is particularly important that any new technology is affordable and broadly applicable[3].

Although technically feasible, the tissue engineering of an autologous valve *in vitro* has proven complex and the process is subject to several intrinsic limitations for clinical translation, including the long culture periods required for cell expansion and tissue formation, and the logistical and financial cost at which that comes. To avoid these limitations, attention has shifted to the more direct approach of *in situ* heart valve tissue engineering. Rather than culturing a valve *in vitro*, the approach of *in situ* tissue engineering makes use of acellular degradable valvular grafts (*i.e.* scaffolds) that act as a template for the body to endogenously regenerate a new valve, directly in the valve's functional site[4,5] (Figure 1). Such scaffolds can be of natural (*e.g.* decellularized tissues) or synthetic origin, or a combination of both. After degradation and/or remodeling of the initially implanted scaffold material and replacement by endogenously formed new tissue, the patient is left with an autologous living heart valve that is capable of growth and remodeling. The benefits for clinical translation of *in situ* heart valve tissue engineering are that such valves are off-the-shelf available and do not come with the costs and logistical complexity associated with culturing valves in the laboratory.

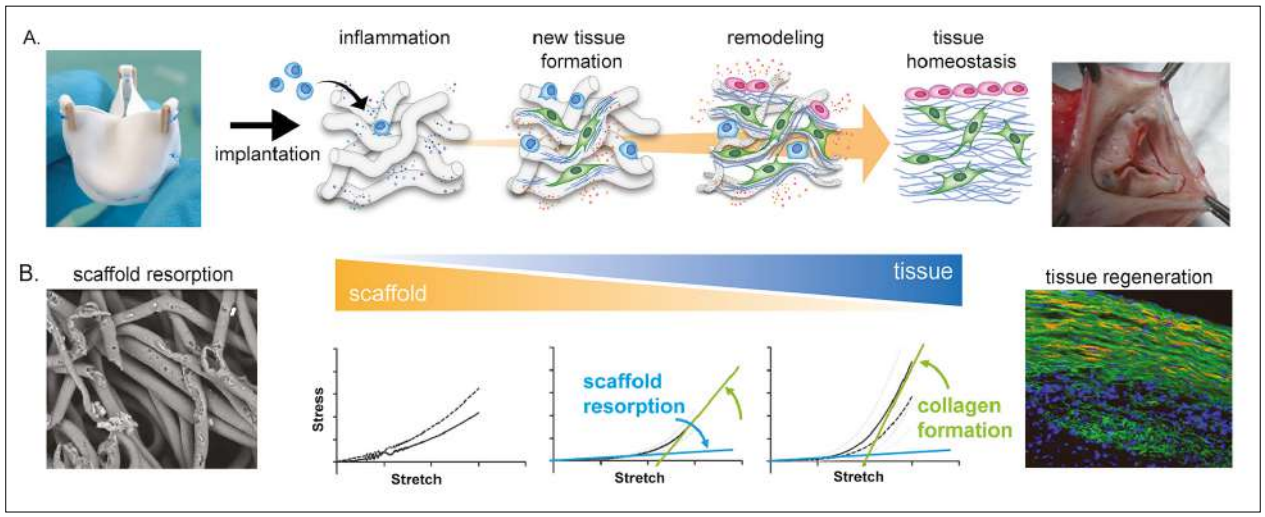

Figure 1: Concept of in situ heart valve tissue engineering.

(A) The process of in situ regeneration is hypothesized to be analog to the wound healing cascade, starting from an inflammatory response to the synthetic scaffold upon implantation, which leads to the recruitment of tissue-forming cells. The final goal is to achieve a functional living heart valve in a state of tissue homeostasis.

(B) The mutually interdependent processes of scaffold resorption and new tissue formation lead to a gradual change in scaffold-dominated mechanical properties to tissue-dominated mechanical properties. The immunostaining displays collagen in green, elastin in red and cell nuclei in blue (courtesy of Sylvia Dekker).

Figure (A) is adapted from Wissing and Bonito et al. npj Regen Med. 2017[5], with valve pictures adapted from Uiterwijk and Smits et al. JACC Basic Transl Sci 2020[27]. Figure (B): SEM image is adapted from Wissing et al. Front. Bioeng and Biotechnol. 2019[19].

While the scaffolds used for *in situ* heart valve tissue engineering are relatively simple devices, the biological events that occur *in vivo* in response to implantation of such a scaffold and that drive tissue regeneration are complex and difficult to control. The aim of this concise review is to delineate the recent achievements in the field of *in situ* heart valve tissue engineering using resorbable synthetic scaffolds and to pinpoint some of the key imminent challenges that the field is facing. Notwithstanding the exciting results gained with decellularized biological tissues, here the focus specifically is on synthetic-based scaffolds as these do not require any donor tissue, nor *in vitro* culture. It should be noted that this is an opinionated review that is by no means complete. To gain an overview of the field of *in situ* heart valve tissue engineering, both using natural and synthetic scaffolds, the reader is referred to recent comprehensive reviews[6,7].

State-of-the-art and recent advances

The use of resorbable synthetic scaffolds to replace heart valves is a relatively recent scientific avenue, yet, it builds on the tremendous body of knowledge gained from decades of *in vitro* tissue engineering research. In fact, some of the most exciting recent findings are achieved with acellular valves that are created from cell-produced de novo tissue-engineered extracellular matrix, which is decellularized prior to implantation to enable on-shelf storage [8,9] One downside of these approaches is that they still require a cell source as well as costly *in vitro* culture.

With respect to valves based purely on resorbable synthetic scaffolds, proof-of-concept was demonstrated in a study by Kluin *et al.* [10]. This study was the first to demonstrate the sustained functionality of a resorbable synthetic valve up to 12 months *in vivo*. The valves were produced via electrospinning of a resorbable supramolecular elastomer, polycarbonate-bisurea, resulting in a highly porous fibrous mesh with relatively large microfibers and large pores to facilitate endogenous cell infiltration. The infiltrating cells gradually degraded the synthetic scaffold material and replaced it with new extracellular matrix, without compromising valve functionality [10]. Bennink *et al.* reported comparable results for a preclinical study of electrospun pulmonary valved conduits of a supramolecular elastomer from the company Xeltis (Xeltis-XPV) [11]. These valved conduits have since been tested in ongoing clinical trials as pulmonary valve replacement in pediatric patients with congenital valvular defects. A recent report describes encouraging results of the first two clinical trials (12 patients group 1, median age 5 (2 to 12) years; 6 patients group 2, median age 5 (3 to 9) years), with 17/18 treated children being free of reintervention at 1 year follow-up [12]. Five patients in the first group were reported to develop severe valvular insufficiency due to prolapse of at least one leaflet. This led to a modification of the valve's geometrical design, after which this complication was no longer observed in the second group [12].

While preclinical and clinical results using resorbable synthetic valves emphasize the proof-of-principle and the clinical potential of this technology, relatively little is known about the *in vivo* processes that underly *in situ* valve regeneration. Recently reported inter-subject variabilities in outcome and cases of failure after subtle changes in valve design parameters, emphasize that there is much to be gained in terms of predictability and robustness for *in situ* heart valve tissue engineering using resorbable synthetic scaffolds. The following section elaborates on three of the most important current challenges to overcome in order to facilitate true control over the *in situ* tissue regenerative processes, namely: (1) harnessing the inflammatory response, (2) the restoration of native-like tissue organization, and (3) centering patient-specific characteristics.

Current challenges

Harnessing the paradoxical influence of the inflammatory response

Whenever an artificial material is implanted into the body, the body's immune system will recognize and respond to it. This immunological reaction by the host is an important mechanism by which acellular synthetic scaffolds are populated by cells and a kick-starter for the formation of new tissue. The host response to a synthetic implant is a cascade of interdependent events that is ignited by the tissue injury induced by the implantation procedure, as elaborately described elsewhere [5] (Figure 1A). In brief, the iatrogenic tissue injury leads to the release of danger signals and pro-inflammatory cytokines, triggering the recruitment of inflammatory cells, such as neutrophils and macrophages. The end-stage manifestation of the inflammatory response is the foreign body response (FBR), which is a protective mechanism to shield any foreign material from the rest of the body by fibrotic encapsulation, driven by fused macrophages, the multinucleated giant cells (MNGCs), in cross-talk with myofibroblasts.

The FBR is typically regarded as a pathological event that causes fibrosis. Indeed, recent analyses by our group show that the prolonged presence of pro-inflammatory cytokines and pro-inflammatory M1-type macrophages, lead to fibrotic tissue encapsulation, leading to leaflet thickening and valve regurgitation (Figure 2). On the other hand, the inflammatory response to the implanted scaffold is absolutely essential to start scaffold cellularization *in situ* and progress the tissue regenerative response. This is evident for example from previous studies on vascular grafts, which show that *in situ* tissue regeneration is completely abrogated if there is no macrophage response [13]. Interestingly, macrophages have also been identified as essential cellular mediators of physiological development and remodeling in native valves [14,15]. Macrophages and MNGCs play essential active roles in the resorption of the synthetic scaffold material [16]. This poses a paradoxical challenge for the development of resorbable heart valve scaffolds for *in situ* tissue engineering: on the one hand, a scaffold should induce inflammation to ignite the regenerative response, while on the other hand, prolonged inflammation may lead to progressive fibrosis. Hence, the question arises how the initially induced inflammation can be modulated and at which stage(s) of the regenerative process this should actively be regulated.

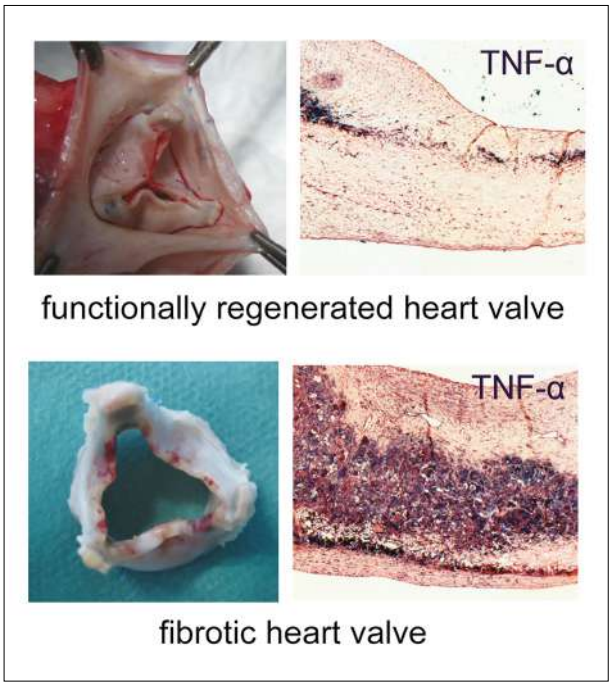

Figure 2: Macroscopic photographs and microscopic section of explanted valves after 12 months of implantation in the pulmonary position in sheep. Regurgitation in one of the valves due to fibrotic leaflet encapsulation and shortening (bottom panel) was associated with excess persistent presence of pro-inflammatory cells in contrast to a functionally regenerated valve (top panel). Displayed is staining for the pro-inflammatory cytokine tumor necrosis factor alpha (TNFα) (positive staining in purple).
Valves adapted from Kluin et al. Biomaterials 2017 [10]. Stainings courtesy of Sylvia Dekker.

Analog to wound healing, the reciprocal interactions between macrophages and MNGCs with myofibroblasts have been identified as an important determinant between functional tissue regeneration and pathological fibrosis [17]. Moreover, the timely switching of macrophages to a pro-regenerative M2 phenotype, has been pinpointed as a predictor for successful tissue integration and regeneration [18]. *In vivo*, these cellular processes are however dynamic and complex, and dominantly influenced by other immune cells, such as neutrophils and T helper-cells. Scaffold design features, such as fiber diameter and pore size have been shown to dictate the macrophage response and with that, the rate of scaffold resorption and the maturity of the newly formed tissue *in situ* [19–21].

There is little *in vivo* evidence on the tissue-specific inflammatory processes in resorbable synthetic heart valves, as opposed to other, more elaborately investigated tissues such as vascular grafts. This is certainly not trivial as heart valves have a geometrically complex shape and they are exposed to complex hemodynamic loading patterns. Motta *et al.* recently described the heterogeneous presence of inflammatory cells in explanted heart valves based on decellularized tissue-engineered extracellular matrix, with a proposed correlation to the local mechanical strains [22]. Recent *in vitro* studies show that the macrophage response to a synthetic scaffold is dependent on hemodynamic loads, including shear stress and cyclic strain [23,24]. Our group recently reported on the comprehensive analysis of inflammation and tissue formation in electrospun pulmonary valved conduits of resorbable supramolecular elastomers up to 24 months of implantation in sheep [16]. We observed strong spatiotemporal heterogeneities in influx

of inflammatory cells, scaffold resorption and tissue maturation in the valves. Specifically, scaffold resorption and tissue maturation occurred more rapidly in the pulmonary wall and hinge region of the valvular leaflet, when compared to the mid and free edge regions of the leaflet [16]. Together, these findings suggest that in heart valves, the local inflammation and tissue maturation is dominantly dictated by the local hemodynamic loads on the one hand, and the cellular influx from surrounding tissue on the other.

Restoring native-like tissue composition and organization

Native heart valves have a well-known three-layered structure, in which the collagen has a specific anisotropic alignment that develops and matures post-natally in response to the hemodynamic loads on the valve [25]. These specific tissue microarchitectures of native heart valves are key determinants of long-term functionality in the stringent hemodynamic environment, and disturbances of the organization are associated with valvular pathologies and degeneration. The restoration of the native-like architecture in replacement valves using *in situ* tissue engineering approaches is highly challenging. Inducing endogenous tissue regeneration has proven feasible, but there is still little control over the spatial deposition of extracellular matrix components and the tissue remodeling process *in situ*. Regenerating mature elastic fibers is notoriously challenging and typically not observed at native-like levels in regenerating heart valves [10,11,16,26]. Reproducing the typical three-layered structure with a well-defined collagen alignment has not yet been achieved.

In a recent study, we aimed to use the principle of contact guidance to promote the restoration of a native-like collagen alignment in resorbable synthetic pulmonary valves [27]. To that end, valves were produced with a predefined alignment of the synthetic fibers in the circumferential direction of the valvular leaflets via electrospinning (Figure 3). The predefined fiber structure was aimed to act as a template for the cells to deposit new collagen by providing contact guidance to the infiltrating cells. However, when implanted in the pulmonary position in sheep, surprisingly, the predefined mechanical anisotropy was lost already after 1 month *in vivo*, pointing to breakage or accelerated degradation of the circumferentially aligned fibers [27]. Consequently, the newly formed tissue was deposited in an uncontrolled

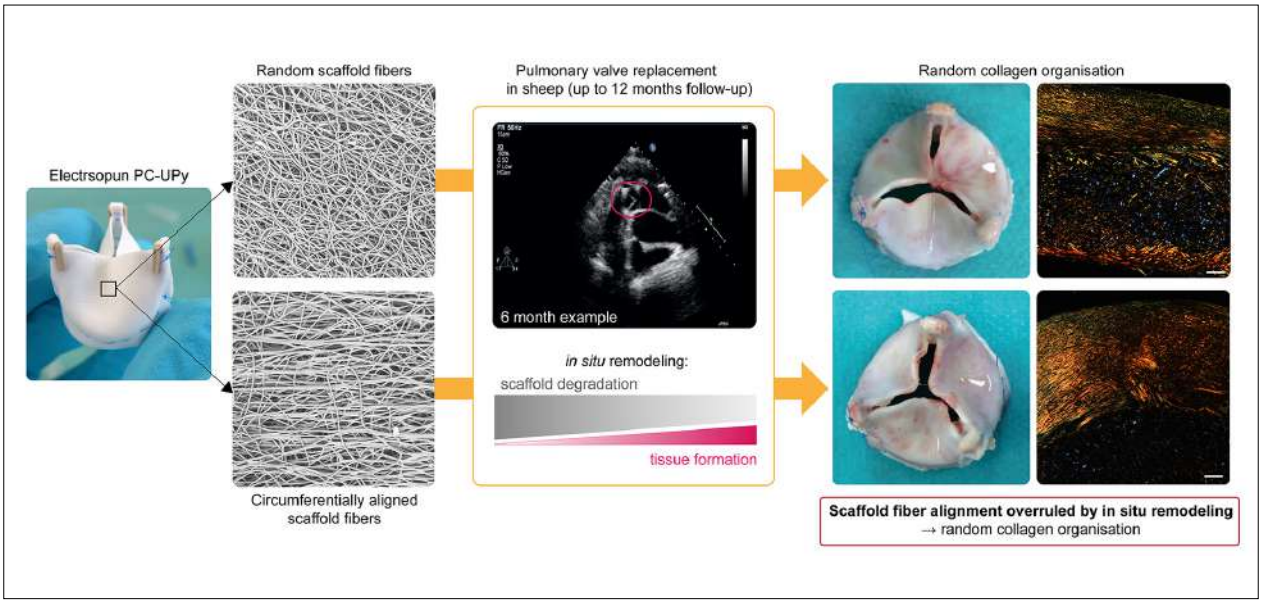

Figure 3: Visual summary of a recent study, which reported that in vivo remodeling processes overruled a pre-imposed bio-inspired organization of synthetic scaffold fibers in the circumferential direction of the leaflets when surgically implanted as valve replacement in the pulmonary position in sheep. As a result, alignment of the newly formed collagen followed a random orientation (far right, picrosirius red staining imaged with polarized light). *From Uiterwijk and Smits et al. JACC Basic Transl Sci 2020* [27].

and generally non-native like manner. We hypothesized that any contact guidance by the predefined fiber structure had been overruled by the local mechanical loads on the cells, acting as the dominant determinant of tissue remodeling [27]. While further long-term *in vivo* data for synthetic heart valves is limited, some interesting parallels can be observed when studying resorbable synthetic vascular grafts. For example, Krynauw *et al.* reported on the reduced mechanical anisotropy and lack of control over neotissue organization for polyurethane scaffolds with highly aligned fibers in the circumferential direction, due to the *in situ* tissue ingrowth and remodeling processes [28]. Li *et al.* and Zhu *et al.* showed that a predefined circumferential fiber alignment only led to a native-like well-organized collagen alignment and mechanical behavior in arterial grafts in rats when fabricated from elastic and compliant material [29], but not from stiff, non-compliant polycaprolactone [30]. The former was accompanied by a favorable temporal course of the inflammatory response [29].

Although the native-like valvular tissue organization has represented the blue-print for heart valve tissue engineering since decades [31], these studies highlight that recreating a native-inspired scaffold microstructure is not sufficient to induce native-like tissue organization, but rather that the interplay between the microstructural and mechanical cues is key. Also in this respect the dominant influence of the inflammatory response *in vivo* should not be overlooked. Along this line, more sophisticated biomimicking designs have been proposed as heart valve grafts for *in situ* tissue engineering, in which not only the microstructural organization of the native valve is recreated, but also the mechanical behavior. One example is a study by Saidy *et al.* in which melt-electrowriting was used to create polycaprolactone microfibrous valves with precisely defined native-like non-linear mechanical properties [32]. D'Amore *et al.* and Capulli *et al.* described the engineering of various types of resorbable synthetic heart valves using electrodeposition and jet-spinning techniques, respectively, which allow for the multi-scale control over macro-and micro-structural, as well as mechanical designs [33,34]. These developments in fabrication technologies open up new possibilities in multi-scale valve design and it will be exciting to learn how such valves that are biomimicking on a more holistic level will perform in long-term *in vivo* experiments. In addition, the application of in silico models to optimize valve design are an indispensable tool to accelerate design steps by enabling the prediction of the influence of valve design parameters on long-term *in vivo* remodeling [9].

Centering patient-specific characteristics

The principle of *in situ* tissue engineering is based on endogenous tissue regeneration. This means that the success or failure of this approach is fundamentally dependent on the regenerative capacity and immunological state of the patient themselves. Consequently, the intensity and rate of key biological processes for *in situ* tissue engineering, such as inflammation, scaffold resorption and tissue formation, is likely to strongly vary between individual patients.

Obvious patient characteristic that might influence outcome are patient sex and age. With respect to age, so far, *in situ* tissue-engineered valves have been applied as pulmonary valves for pediatric patients. Pediatric patients represent a relatively small age range and are generally considered to possess a high intrinsic regenerative capacity when compared to adults. As such, from a purely biological perspective, early intervention in pediatric patients may represent the ideal conditions for successful *in situ* tissue regeneration. Interesting studies by Weber *et al.* and Zakko *et al.* show technical feasibility of transcatheter delivery of tissue-engineered valves even before birth, in a fetal ovine model [35,36]. When looking ahead at applications in adults, apart from scaling considerations regarding valve size and resulting flows, the expected biological diversity among patients (*e.g.* due to differences in lifestyle and general health) is much larger. Patients in need of an aortic valve replacement due to calcific valve disease are often elderly patients, who may suffer from common multifactorial diseases, such as diabetes or hyperlipidemia. Patients in need of valve replacement due to rheumatic heart disease are of a much broader age range [37], suggesting an even larger variability among patients. The potential

influence of age is evident from studies on the foreign body response in animals. For example, Johnson *et al.* reported on adverse remodeling of polycaprolactone-based aortic grafts in old rats [38]. Metabolic disorders, such as diabetes, generally lead to an increased inflammatory response to artificial implants and less fibrogenic capacity, compromising the intrinsic regenerative capacity [39].

In addition to age, there is an increased recognition of the potential influence of patient sex on cardiovascular disease manifestation, but also outcome after treatment. Generally, males have a higher risk of developing calcific aortic valve disease, while post-menopausal females more often suffer from valvular fibrosis [40]. Little direct data is available on how sex-specific biases may influence *in situ* tissue engineering. A recent study by Blum *et al.* reports on subtle, yet significant sex-specific foreign body response to resorbable vascular grafts [41].

These observations raise the question whether synthetic scaffolds for *in situ* heart valve tissue engineering should be designed in a 'one-size-fits-all' manner, or whether a more tailored approach is needed, and, in case of the latter, how to predict outcome in a clinically relevant manner.

Outlook & Conclusion

Taken together, the exciting preclinical and clinical findings when using resorbable synthetic scaffolds to replace malfunctioning heart valves underline the potential for this technology. The use of a relatively simple synthetic device offers a translational benefit in terms of costs and logistics, as well as regulatory complexity when compared to other tissue engineering strategies. This is illustrated by the relatively rapid progression from the bench to the first clinical trials using this technology.

While much research is dedicated to designing the 'ideal' resorbable heart valve prosthesis, it remains to be established whether such a design exists that robustly serves a broad patient population or whether a more tailored approach is required. To achieve that, it is essential to improve our fundamental understanding of the biological mechanisms that occur *in vivo*, as these still remain, to a large extent, a black box. What is clear is that the challenges as delineated in this review share several common denominators that are reciprocally interdependent, the immunological response, the balance between scaffold resorption and tissue formation, and the influence of hemodynamics. The local mechanical loads experienced by the recruited cells at any time during the regenerative process are determined by the summative mechanical properties of the degrading scaffold and the newly formed tissue (Figure 1B). In turn, the local loads drive the processes of tissue remodeling, as well as inflammation and scaffold resorption. Hence, there is no 'ideal' scaffold degradation rate, but rather, the initial mechanical and microstructural design of the scaffold should promote a favorable start of the tissue regenerative process. It remains to be determined whether downstream inflammation and tissue formation are self-regulating processes in the long run, which ensure an adequate balance between scaffold resorption and tissue formation at all times without intervention.

One important aspect in unraveling the *in vivo* mechanisms is to perform dedicated analyses on explanted valve material. Long-term animal experiments on resorbable synthetic heart valves are scarce, so it is essential to maximize the knowledge from such long-term *in vivo* studies. One example is the establishment of a comprehensive sheep-specific antibody panel by our group to enable the detailed analysis of tissue composition and the cellular phenotypes that orchestrate inflammation and regeneration [42]. Although a very simple tool, this panel has proven effective in pinpointing the spatiotemporal distributions of the endogenous cell types infiltrating a valve in recent studies by us and others [16,22]. In this respect, it should be emphasized that such findings may be biased by animal model-specific regenerative and inflammatory processes, for example in terms of cellularization routes and immunological mechanisms. Moreover, taking into account relevant patient-specific characteristics

(*e.g.* age or metabolic disorders) is only limitedly possible, particularly in large animal models. The use of reductionist, potentially personalized human *in vitro* models, in parallel to animal experiments, can aid in systematically unravelling specific mechanisms by isolating specific environmental cues in a well-controlled laboratory setting [43,44]. Moreover, experimental data can fuel in silico models, which have increasingly demonstrated to be tremendously effective tools for the prediction of long-term *in vivo* remodeling events [9,45].

To date, (pre)clinical experiences with resorbable synthetic valves are still limited and with relatively short follow-up, and it is highly relevant to investigate what the remodeling capacity and durability of these valves after extended periods of implantation beyond the lifetime of traditional biological valve replacements (> 10 years). The most impactful recent findings have resulted from team-efforts by tissue engineers, biologists, materials scientists, and clinicians closely collaborating using *in vivo*, *in vitro* and in silico models in a complementary way. Such inter-disciplinary research is essential in dealing with, arguably, the most challenging anticipated future hurdle for *in situ* heart valve tissue engineering: to provide a safe and robust regenerative heart valve replacement for a broad variety of patients, each with their own patient-specific immunological state and regenerative capacity.

Acknowledgements

I gratefully acknowledge the Gravitation Program "Materials Driven Regeneration", funded by the Netherlands Organization for Scientific Research (024.003.013).

References

1. Shinoka T, Breuer CK, Tanel RE, Zund G, Miura T, Ma PX, *et al.* Tissue engineering heart valves: valve leaflet replacement study in a lamb model. *Ann Thorac Surg* 1995; 60: S513-6.

2. El-Hamamsy I, Eryigit Z, Stevens L-M, Sarang Z, George R, Clark L, *et al.* Long-term outcomes after autograft versus homograft aortic root replacement in adults with aortic valve disease: a randomised controlled trial. *Lancet* 2010; 376: 524-31.

3. Zilla P, Bolman RM, Yacoub MH, Beyersdorf F, Sliwa K, Zühlke L, *et al.* The Cape Town Declaration on Access to Cardiac Surgery in the Developing World. *Ann Thorac Surg* 2018; 106: 930-3.

4. Bouten CVC, Smits AIPM, Baaijens FPT. Can We Grow Valves Inside the Heart? Perspective on Material-based *In Situ* Heart Valve Tissue Engineering. *Front Cardiovasc Med* 2018; 5: 54.

5. Wissing TB, Bonito V, Bouten CVC, Smits AIPM. Biomaterial-driven *in situ* cardiovascular tissue engineering—a multi-disciplinary perspective. *NPG Regen Med* 2017; 2: 18.

6. Fioretta ES, Motta SE, Lintas V, Loerakker S, Parker KK, Baaijens FPT, *et al.* Next-generation tissue-engineered heart valves with repair, remodelling and regeneration capacity. *Nat Rev Cardiol* 2021;18: 92-116.

7. Mela P, Hinderer S, Kandail HS, Bouten CVC, Smits AIPM. Tissue-engineered heart valves. In: Principles of Heart Valve Engineering. *Elsevier* 2019. p. 123-76.

8. Syedain ZH, Haynie B, Johnson SL, Lahti M, Berry J, Carney JP, *et al.* Pediatric tri-tube valved conduits made from fibroblast-produced extracellular matrix evaluated over 52 weeks in growing lambs. *Sci Transl Med* 2021; 13: eabb7225.

9. Emmert MY, Schmitt BA, Loerakker S, Sanders B, Spriestersbach H, Fioretta ES, *et al.* Computational modeling guides tissue-engineered heart valve design for long-term *in vivo* performance in a translational sheep model. *Sci Transl Med* 2018; 10: eaan4587.

10. Kluin J, Talacua H, Smits AIPM, Emmert MY, Brugmans MCP, Fioretta ES, *et al. In situ* heart valve tissue engineering using a bioresorbable elastomeric implant – From material design to 12 months follow-up in sheep. *Biomaterials* 2017; 125: 101-17.

11. Bennink G, Torii S, Brugmans M, Cox M, Svanidze O, Ladich E, *et al.* A novel restorative pulmonary valved conduit in a chronic sheep model: Mid-term hemodynamic function and histologic assessment. *J Thorac Cardiovasc Surg* 2018; 155: 2591-601.e3.

12. Morales DL, Herrington C, Bacha EA, Morell VO, Prodán Z, Mroczek T, *et al.* A Novel Restorative Pulmonary Valve Conduit: Early Outcomes of Two Clinical Trials. *Front Cardiovasc Med* 2021; 7: 583360.

13. Hibino N, Yi T, Duncan DR, Rathore A, Dean E, Naito Y, *et al.* A critical role for macrophages in neovessel formation and the development of stenosis in tissue-engineered vascular grafts. *FASEB J* 2011; 25: 425363.

14. Shigeta A, Huang V, Zuo J, Besada R, Nakashima Y, Lu Y, *et al.* Endocardially Derived Macrophages Are Essential for Valvular Remodeling. *Dev Cell* 2019; 48: 617-30.e3.

15. Hulin A, Anstine LJ, Kim AJ, Potter SJ, DeFalco T, Lincoln J, *et al.* Macrophage Transitions in Heart Valve Development and Myxomatous Valve Disease. *Arterioscler Thromb Vasc Biol* 2018; 38: 636-44.

16. De Kort BJ, Marzi J, Brauchle EE, Lichauco AM, Bauer H, Serrero A, *et al.* Inflammatory and regenerative processes in bioresorbable synthetic pulmonary valves up to 2 years in sheep: Spatiotemporal insights augmented by Raman microspectroscopy. *Acta Biomater* 2021; in press.

17. Barron L, Wynn T a. Fibrosis is regulated by Th2 and Th17 responses and by dynamic interactions between fibroblasts and macrophages. *Am J Physiol Gastrointest Liver Physiol* 2011; 300: G723-8.

18. Brown BN, Londono R, Tottey S, Zhang L, Kukla KA, Wolf MT, *et al.* Macrophage phenotype as a predictor of constructive remodeling following the implantation of biologically derived surgical mesh materials. *Acta Biomater* 2012; 8: 978-87.

19. Wissing TB, Bonito V, van Haaften EE, van Doeselaar M, Brugmans MMCP, Janssen HM, *et al.* Macrophage-Driven Biomaterial Degradation Depends on Scaffold Microarchitecture. *Front Bioeng Biotechnol* 2019; 7: 87.

20. Fu J, Wang M, De Vlaminck I, Wang Y. Thick PCL Fibers Improving Host Remodeling of PGS-PCL Composite Grafts Implanted in Rat Common Carotid Arteries. *Small* 2020; 16: 1-15.

21. Tylek T, Blum C, Hrynevich A, Schlegelmilch K, Schilling T, Dalton PD, *et al.* Precisely defined fiber scaffolds with 40 µm porosity induce elongation driven M2-like polarization of human macrophages. *Biofabrication* 2020; 12: 025007

22. Motta SE, Fioretta ES, Lintas V, Dijkman PE, Hilbe M, Frese L, *et al.* Geometry influences inflammatory host cell response and remodeling in tissue-engineered heart valves in-vivo. *Sci Rep* 2020; 10: 19882.

23. Bonito V, de Kort BJ, Bouten CVC, Smits AIPM. Cyclic Strain Affects Macrophage Cytokine Secretion and Extracellular Matrix Turnover in Electrospun Scaffolds. *Tissue Eng Part A* 2019 ; 25: 1310-25.

24. Wissing TB, van Haaften EE, Koch SE, Ippel BD, Kurniawan NA, Bouten CVC, *et al.* Hemodynamic loads distinctively impact the secretory profile of biomaterial-activated macrophages–implications for *in situ* vascular tissue engineering. *Biomater Sci* 2020; 8: 132-47.

25. Oomen PJA, Loerakker S, van Geemen D, Neggers J, Goumans M-JTH, van den Bogaerdt AJ, *et al.* Age-dependent changes of stress and strain in the human heart valve and their relation with collagen remodeling. *Acta Biomater* 2016; 29: 161-9.

26. Fioretta ES, Lintas V, Mallone A, Motta SE, von Boehmer L, Dijkman PE, *et al.* Differential Leaflet Remodeling of Bone Marrow Cell Pre-Seeded Versus Nonseeded Bioresorbable Transcatheter Pulmonary Valve Replacements. *JACC Basic Transl Sci* 2020; 5: 15-31.

27. Uiterwijk M, Smits AIPM, van Geemen D, van Klarenbosch B, Dekker S, Cramer MJ, *et al. In Situ* Remodeling Overrules Bioinspired Scaffold Architecture of Supramolecular Elastomeric Tissue-Engineered Heart Valves. *JACC Basic Transl Sci* 2020; 5: 1187-206.

28. Krynauw H, Buescher J, Koehne J, Verrijt L, Limbert G, Davies NH, *et al.* Tissue Ingrowth Markedly Reduces Mechanical Anisotropy and Stiffness in Fibre Direction of Highly Aligned Electrospun Polyurethane Scaffolds. *Cardiovasc Eng Technol* 2020; 11: 456-68.

29. Zhu M, Wu Y, Li W, Dong X, Chang H, Wang K, *et al.* Biodegradable and elastomeric vascular grafts enable vascular remodeling. *Biomaterials* 2018; 183: 306-18.

30. Li W, Chen J, Xu P, Zhu M, Wu Y, Wang Z, *et al.* Long-term evaluation of vascular grafts with circumferentially aligned microfibers in a rat abdominal aorta replacement model. *J Biomed Mater Res Part B Appl Biomater* 2018; 106: 2596-604.

31. Chester AH, Grande-Allen KJ. Which Biological Properties of Heart Valves Are Relevant to Tissue Engineering? *Front Cardiovasc Med* 2020; 7: 63.

32. Saidy NT, Wolf F, Bas O, Keijdener H, Hutmacher DW, Mela P, *et al.* Biologically Inspired Scaffolds for Heart Valve Tissue Engineering via Melt Electrowriting. *Small* 2019; 15: 1900873.

33. D'Amore A, Luketich SK, Raffa GM, Olia S, Menallo G, Mazzola A, *et al.* Heart valve scaffold fabrication: Bioinspired control of macro-scale morphology, mechanics and micro-structure. *Biomaterials* 2018; 150: 25-37.

34. Capulli AK, Emmert MY, Pasqualini FS, Kehl D, Caliskan E, Lind JU, *et al.* JetValve: Rapid manufacturing of biohybrid scaffolds for biomimetic heart valve replacement. *Biomaterials* 2017; 133: 229-41.

35. Weber B, Emmert MY, Behr L, Schoenauer R, Brokopp C, Drögemüller C, *et al.* Prenatally engineered autologous amniotic fluid stem cell-based heart valves in the fetal circulation. *Biomaterials* 2012; 33: 4031-43.

36. Zakko J, Blum KM, Drews JD, Wu Y-L, Hatoum H, Russell M, *et al.* Development of Tissue Engineered Heart Valves for Percutaneous Transcatheter Delivery in a Fetal Ovine Model. *JACC Basic Transl Sci* 2020; 5: 815-28.

37. Zilla P, Brink J, Human P, Bezuidenhout D. Prosthetic heart valves: catering for the few. *Biomaterials* 2008; 29: 385-406.

38. Johnson R, Rafuse M, Selvakumar PP, Tan W. Effects of recipient age, heparin release and allogeneic bone marrow-derived stromal cells on vascular graft remodeling. *Acta Biomater* 2021; 125: 172-82.

39. Wang Z, Zheng W, Wu Y, Wang J, Zhang X, Wang K, *et al.* Differences in the performance of PCL-based vascular grafts as abdominal aorta substitutes in healthy and diabetic rats. *Biomater Sci* 2016; 4: 1485-92.

40. Simard L, Côté N, Dagenais F, Mathieu P, Couture C, Trahan S, *et al.* Sex-Related Discordance Between Aortic Valve Calcification and Hemodynamic Severity of Aortic Stenosis Is Valvular Fibrosis the Explanation ? *Circ Res* 2017; 120: 681-91.

41. Blum KM, Roby LC, Zbinden JC, Chang Y-C, Mirhaidari GJM, Reinhardt JW, *et al.* Sex and Tamoxifen confound murine experimental studies in cardiovascular tissue engineering. *Sci Rep* 2021; 11: 8037.

42. Dekker S, van Geemen D, van den Bogaerdt AJ, Driessen-Mol A, Aikawa E, Smits AIPM. Sheep-Specific Immunohistochemical Panel for the Evaluation of Regenerative and Inflammatory Processes in Tissue-Engineered Heart Valves. *Front Cardiovasc Med* 2018; 5: 105.

43. Van Haaften EE, Wissing TB, Kurniawan NA, Smits AIPM, Bouten CVC. Human *In Vitro* Model Mimicking Material-Driven Vascular Regeneration Reveals How Cyclic Stretch and Shear Stress Differentially Modulate Inflammation and Matrix Deposition. *Adv Biosyst* 2020; 4: 1900249.

44. Enayati M, Eilenberg M, Grasl C, Riedl P, Kaun C, Messner B, *et al.* Biocompatibility Assessment of a New Biodegradable Vascular Graft via *In Vitro* Co-culture Approaches and *In Vivo* Model. *Ann Biomed Eng* 2016; 44: 3319-34.

45. Szafron JM, Ramachandra AB, Breuer CK, Marsden AL, Humphrey JD. Optimization of Tissue-Engineered Vascular Graft Design Using Computational Modeling. *Tissue Eng Part C Methods* 2019; 25: 561-70.

Tissue-Engineered Vascular Grafts: the promise of the Textile-Inspired approach

38

Fabien KAWECKI, Nicolas L'HEUREUX

Cardiovascular diseases are the leading cause of mortality in the world and encompass several blood circulatory system pathologies, including atherosclerosis. In the cases of severe vessel occlusion, surgical intervention using bypass grafts may be required. Synthetic vascular grafts can be used but provide poor patency for small diameter applications. In very small vessels, such as coronary arteries, outcomes are unacceptable and are only acceptable in larger vessels used for peripheral bypass and hemodialysis access. Autologous (native) vessels are the best conduits for small diameter applications, but their accessibility may be limited. There is a clear clinical need for a small diameter vascular graft that can provide outcomes similar to that of native vessels. Tissue-engineering approaches based on the use of biological scaffolds associated with living cells have been developed to provide native-like tissue with the appropriate mechanical and biological properties and overcome the limitations of synthetic and autologous grafts. This non-exhaustive review gives a brief overview of the most known methods developed to produce tissue-engineered vascular grafts (TEVGs) with a specific focus on the promising textile-inspired approach. Indeed, this assembly method shows a reduced production time compared to biological scaffolding or cell-assembled extracellular matrix approaches, which require maturation steps. Another advantage of the textile-inspired approach is that it provides much better directional and regional control of the TEVG mechanical strengths. Finally, this approach would allow the production of tapered TEVGs, which will display clinically relevant outcomes.

Introduction

According to the American Heart Association (AHA), cardiovascular diseases (CVDs) are the leading cause of mortality in the United States in 2019.[1] The most common CVD is atherosclerosis. This pathology is a progressive inflammatory disease developed within the vascular media and causes hyperplasia and calcification of blood vessels.[2,3] The progressive obstruction of the vessel lumen is often asymptomatic until the spontaneous formation of a thrombus.[2] In addition, at an advanced stage of development, the atheromatous plaque can break and release clots into the blood circulation. These can lead to the occlusion of smaller arteries, such as the brain arterioles, and thus causes ischemia of the downstream areas. Currently, no medications are available to cure atherosclerosis. One surgical option preferred by the surgeons to restore the blood circulation is the percutaneous angioplasty that consists of introducing a balloon within a peripheral artery, bringing it to the pathological artery, inflate through the blood circulation, compress the atheromatous plaque, and restore the artery lumen. This operation is usually associated with the use of a guide for the positioning of a stent that keeps open the lumen of the vessel. Nevertheless, in response to the injury caused by the passage of the guide and the positioning of the stent, the vessel is exposed to late restenosis. Although more costly and risky, a more long-term solution is to bypass the blockage with a conduit.

Synthetic vascular grafts (SVGs) are commercially available and have been successfully used as large and medium internal diameter (ID) prosthetics (ID ≥ 6 mm).[4] Generally, these SVGs are composed of expanded polytetrafluoroethylene (e-PTFE or Goretex®) or woven/knitted polyethylene terephthalate (PET or Dacron®) fibers with patency rates ranging from 40 to 50% for lower limb bypass.[4,5] Unfortunately, when applied to small diameter vessels (ID < 6 mm), these artificial grafts displayed far lower patency (*e.g.*, 20 to 25% for 1 mm diameter PTFE vessel).[4,6] Indeed, these materials, recognized as foreign bodies by the host's innate immune system, cause a chronic inflammatory environment that promotes fibrosis, intimal hyperplasia, calcification, and thrombosis.[7] Despite new surface treatments designed to reduce thrombogenicity, current commercial SVGs are made from rigid materials that cannot be remodeled by the patient's cells and are susceptible to infection.[8] As a result, these synthetic conduits perform very poorly in small diameter applications (coronary bypass or lower limb bypass) or arteriovenous shunts.

Autologous vascular grafts, such as internal mammary arteries or saphenous veins, remain the "gold standard" for vascular repairs. For example, it was demonstrated that saphenous vein grafts display a low occlusion rate (10 to 15%) after one year in the context of coronary artery bypass surgery, and 50% of these conduits fail after ten years of implantation.[9] However, the availability of these grafts is limited due to previous use or poor quality of the vessel because of the cardiovascular pathology itself. In addition, these grafts cause substantial donor site morbidity that can be particularly significant with elderly and/or diabetic patients. Consequently, there is a critical clinical need for a long-lasting but readily available small-diameter vascular conduit.

An alternative to using synthetic prosthesis or autografts is to use tissue-engineered blood vessels made from biological scaffolds associated with living cells to provide native-like tissue with adequate mechanical and biological properties to be remodeled by the host into a functional blood vessel. Since several research groups have studied tissue-engineered vascular grafts (TEVGs), this non-exhaustive review provides a brief overview of the methods used to produce TEVGs with a specific focus on the textile-inspired approach.

The First Tissue-Engineered Vascular Graft

Tissue engineering is a multidisciplinary field of research that aims to produce biological tissues by combining cells and biomaterials.[10] The first TEVG was developed in 1986 by Weinberg and Bell using a multi-step process.[11] Firstly, a collagen gel was mixed with bovine smooth muscle cells (SMCs) and placed within a tubular mold. The tubular tissue was obtained after one week of maturation around a mandrel. Subsequently, a Dacron® mesh was slipped over the tissue to provide mechanical support, and a second gel was cast around the first, this time containing bovine fibroblasts. After two additional weeks of maturation, the tissue was removed from the mandrel and cannulated to inject a suspension of bovine endothelial cells within the luminal surface. Finally, a three-layered TEVG was obtained after one more week of dynamic maturation (rotation around a longitudinal axis at 1 rev.min^{-1}). While transmission electron microscopy images showed a well-organized endothelial layer covering the luminal surface, the TEVG had a burst pressure that was ten times lower than that of native arteries (≈300 mmHg). Mechanical properties of the vessel were entirely dependent on the synthetic mesh as the bust pressure without the mesh was < 10 mmHg. Despite the poor mechanical properties of this model, they demonstrated the possibility to reproduce *in vitro* the general architecture of a muscular artery.

Approaches for Vascular Tissue Engineering

Biodegradable synthetic scaffolding

Because of the limitations associated with non-degradable synthetic vascular grafts and autologous vessels, many research groups began to develop vascular grafts using alternative tissue engineering approaches in the late 1990s. One popular approach was to use degradable polymers (*e.g.*, polylactic acid (PLA) or polyglycolic acid (PGA)) associated with living cells. This approach has the advantage of having a chemically and physically well-defined matrix, which can be tailored to specific mechanical and geometric requirements. However, the downside of this approach is that the degradation of this matrix creates an inherently unstable tissue with changing properties. The outcome largely depends on the right balance between degradation of the scaffold and *in vivo* ECM production. These processes can be complicated to predict since they vary between the patients due to age, disease, or unknown variables. In blood vessels or other tissues playing important mechanical roles, a temporary lack of mechanical strength can lead to catastrophic graft failure.

Currently, Dr. Niklason's group leads this approach and uses long-term culture (ten weeks) in a complex bioreactor to avoid this uncertainty.[12] During the culture period, the biomaterial constituted of a PGA mesh is largely degraded and replaced by ECM produced by the cells themselves. Blood vessels produced using this method have shown acceptable mechanical properties, good mid-term results in animal studies, and promising preliminary results in a clinical trial.[13-16] One of the limitations of this approach is that the subproducts of this synthetic matrix degradation create a microenvironment that negatively affects cell growth and ECM production.[17] In addition, incomplete degradation of this matrix could lead to adverse *in vivo* effects. Furthermore, the specific approach of Dr. Niklason's group is based on the early-passage use of pooled smooth muscle cells from the human aorta collected from deceased donors, which complicates cell sourcing and approval from regulatory agencies. The most important challenge for this approach is achieving a graft performance-to-price ratio that will support successful commercialization.

Biological scaffolding

Based on the previous works of Weinberg and Bell, Dr. L'Heureux developed in 1993 a tubular vascular model exclusively composed of human cells and collagen.[18] This equivalent was formed with the three main cell types composing native vessels: SMCs, fibroblasts, and endothelial cells. Briefly, a media-like tissue was formed by seeding the human SMCs (2x106 cells.mL^{-1}) onto a tubular structure composed of a human collagen gel (3 mg.mL^{-1}) molded within a plastic tube containing a glass mandrel on its center. The SMCs exposed contractile behavior that compacted the collagen around the mandrel for two days. After that, an additional layer of human collagen containing human fibroblast cells was added at a concentration of 5.10^{5} cells.mL^{-1} onto the outer part of the media tissue to formed an adventitia-like structure. To reconstruct the endothelium layer, the tubular structure was slipped off the mandrel and cannulated at one extremity. Then, a solution containing human endothelial cells at 1.10^{6} cells.mL^{-1} was injected into the lumen of the vessel. Subsequently, the vessel was closed and placed within an incubator and frequently rotated. The cannulas were removed after one day, and the artificial blood vessel was matured *in vitro* for one to two additional weeks.[18] Due to its completely biological composition and its human origin, this first model has initiated a strong enthusiasm for developing autologous TEVG for translational applications. However, this graft displayed relatively weak mechanical properties.

Dr. Tranquillo's group combined living cells with a bovine fibrin gel to produce completely biological vascular substitutes.[19] To overcome the low mechanical strength of this type of construct, they chose a long period culture approach (seven to nine weeks) in a complex bioreactor to induce the ECM production by the cells.[20] They reported that vascular substitutes produced from sheep cells had shown good mechanical resilience and good results after implantation in sheep for up to six months.[21] More recently, Vascudyne Inc. company announced the successful first-in-human use of its TRUE™ Vascular Graft produced using Dr. Tranquillo's technology.[22] This first procedure was performed in ten end-stage diseases patients requiring hemodialysis access with a completion date of their phase 1 clinical trial estimated in 2022. Although their preliminary results are promising, this approach has limitations associated with the use of a complex bioreactor system, exposed to contamination risks, over a long period of culture.

Cell-Assembled Extracellular Matrix Approach

Another method that does not rely on the exogenous scaffold for TEVG production was developed by Dr. L'Heureux's group in 1998.[23] This approach, sometimes referred to as Tissue Engineering by Self-Assembly (TESA), aims at producing Cell-Assembled extracellular Matrix (CAM) by channeling the ability of mesenchymal cells to secrete and assemble endogenous ECM in the presence of ascorbic acid and serum.[23,24] The accumulation of ECM within the culture flask allows the formation of a robust, yet completely biological, sheet (Figure 1). To produce a TEVG, SMCs or fibroblasts were cultured in the presence of 50 µg.mL^{-1} sodium L-ascorbate for approximately 30 days.[23] Both cell types formed cell sheets that could be detached from the culture flask and rolled around an inert mandrel (3 mm diameter) to produce a cylinder composed of concentric sheet layers (Figure 1). After an additional maturation period, the layers fused and formed a cohesive TEVG composed of vascular media and adventitia. Thereafter, TEVG was removed from the mandrel, and endothelial cells were seeded within the lumen. The resulting biological tubular structure displayed comparable burst strength (≈ 2,500 mmHg) to native vessels, as well as good suturability characteristics.[23] Unlike matrices made of proteins chemically extracted from living tissue, the CAM has a native-like organization and composition, which gives it mechanical strength and supports a better *in vivo* integration.

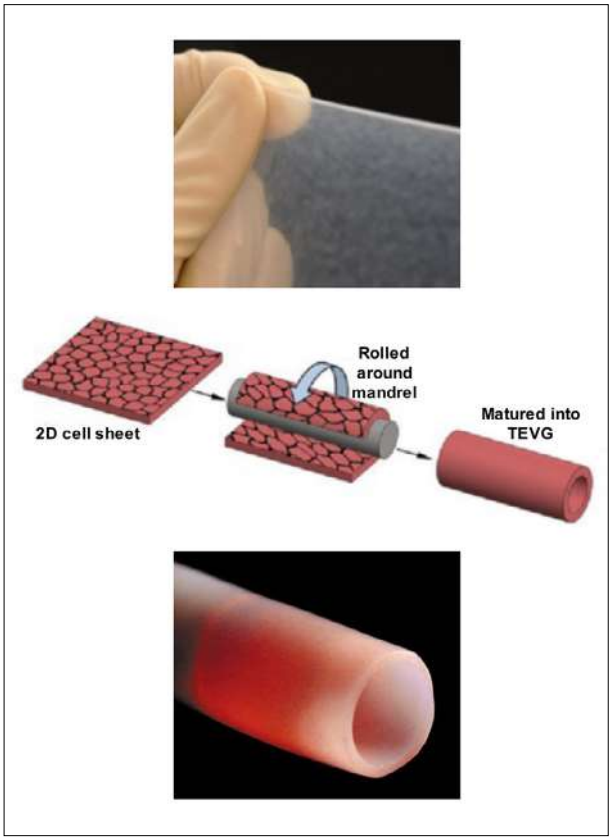

Figure 1: Tissue-engineered vascular graft (TEVG) production process using scaffold-free approaches. A sheet of Cell-Assembled extracellular Matrix is produced and rolled around a mandrel to form a tubular structure. Then, a TEGV is obtained after a period of maturation. Adapted under the terms of the Creative Commons Attribution License (CC-BY).[25]
Copyright 2015, Mary Ann Liebert, Inc. Adapted with permission.[26] Copyright 2007, Massachusetts Medical Society.

These substitutes have been implanted in ten patients with end-stage renal failure and have shown a high luminal permeability rate (up to three years).[26-28] Clinical results support the hypothesis that a TEVG free of synthetic material can integrate with the native tissue, be remodeled by host cells, and resist infection. The durability of autologous TEVGs shows that the CAM does not trigger an innate immune response. Finally, non-living TEVGs composed of CAM produced by allogeneic fibroblasts were implanted in three patients without eliciting a specific immune response.[27] In agreement with the literature, the data demonstrated that allogeneic (dead) fibroblasts alone do not create a specific immune response.[29-31] This opens the door to a strategy for the large-scale production of allogeneic substitutes that can be stored until needed (off-the-shelf). However, this production process required more than four months and necessitated multiple processing steps of maturation. In addition, the rolling approach of the CAM has limited ability to control the geometry and mechanical properties of the TEVG.

Textile-Inspired Approach

The collagenous thread remains the raw material of the textile-inspired approach. In 1994, Cavallaro & Kemp reported an innovative method for the fabrication of collagen threads.[32] These biological threads were produced by the extrusion of denatured bovine collagen (solubilized in 8.8 mM acetic acid) into a buffered solution of 20% polyethylene glycol (pH 7.55), where the collagen precipitate into filaments. These threads were used to fabricate various collagenous structures using textile-inspired methods such as knitting, weaving, or braiding. Braided and bundled structures composed of collagen threads were used to replace an anterior cruciate ligament in a dog model. While an inflammatory response was immediately identified after implantation, the immune reaction was resolved after 12 weeks of tissue remodeling, and the implanted structures preserved their required functions. They also demonstrated that knitted collagen threads could be used to repair herniation after 12 weeks of implantation in a rat abdominal repair model. However, these biological threads presented a low ultimate tensile strength (UTS) of 1.2 MPa (wet collagen thread).

In 2008, Zeugolis *et al.* evaluated the influence of cross-linking methods (chemical, physical, and biological) on the mechanical properties of extruded collagen threads.[33] Their results demonstrated that bifunctional agents, such as epoxy and hexamethylene diisocyanate (HMDC), improve the mechanical resilience of wet collagen threads (stress at break; untreated: 3 MPa, epoxy: 30.2 MPa, and HMDC: 17.3 MPa) by the creation of linear cross-linking within the collagenous matrix. Cornwell *et al.* also investigated the effects of various cross-linking strategies on the mechanical properties and the *in vitro* rate of new tissue ingrowth on bundle threads extruded from type I collagen.[34] Their results indicate that while physical cross-linking techniques (dehydrothermal or ultraviolet light) increase thread mechanical strengths, these treatments significantly reduce the migration rate of fibroblast cells. Only carbodiimide chemical cross-linking achieved sub-optimal strength generation with a similar cell migration rate compared to uncross-linked threads. While these treatments interestingly enhanced the strength of the threads, cross-links are not natural and cause the tissue to be seen as foreign/denatured. Indeed, it is reasonable to imagine that these molecules could create an intense inflammatory reaction that will results in partial or complete degradation of the thread once implanted. In addition, these biological threads are composed of denatured collagen that was renatured during its extrusion. This type of denatured collagenous material could be aggressively degraded after implantation.

In 2014, Younesi *et al.* developed interesting biological threads using electrochemically aligned collagen (ELAC) fibers that enable the fabrication of woven biotextile scaffolds.[35] These threads were fabricated by a kinematically rotating linear electrode pair and chemically cross-linked (0.625% genipin in 90% v/v ethanol solution at 37°C) for three days. Their results demonstrated that a reduction of the thread diameter increases the UTS (150 µm Ø: ≈ 21 MPa , 130 µm Ø: ≈ 35 MPa, and 100 µm Ø: ≈ 51 MPa). By twisting three threads as a yarn, they provided a significant gain of the UTS (≈ 65 MPa) comparable to those of the native tendon. In addition, they showed that these threads support cell adhesion and differentiation

(tendogenesis), as well as ECM deposition *in vitro*. Recent *in vivo* biomechanical, histochemical, and immunohistochemical metrics showed interesting outcomes after three months of functional loading of this ELAC scaffold in critical-size tendon defects (New Zealand white rabbits).[36] ELAC threads have been originally developed for tendon repairs. More recently, these collagenous filaments have been used to produce a hybrid vascular graft using the circular knitting method.[37] The ELAC threads were plied together with traditional PLA yarns. The collagen component promoted endothelial cell adhesion and proliferation *in vitro*, and the PLA provided sufficient mechanical properties and structural stability. Once knitted to form a tubular structure, the vessel exhibited excellent bursting strength (≈ 1.9 MPa), suture retention strength (≈ 10.9 N), and comparable compliance (≈ 4%/100 mmHg) to that of the coronary artery (3.8%/100 mmHg) under normotensive pressure. However, the knitting method generated a structure with ≈ 250 µm pore size. While a high porosity may facilitate cell infiltration necessary for tissue remodeling, this macro-scale pore size may lead to a lack of hemostasis and ultimately result in blood leakage. In addition, the *in vivo* success of this type of graft will depend on the right balance between degradation and ECM neoformation since it is composed of biodegradable synthetic PLA.

Also inspired by the textile industry methods, Nicolas L'Heureux's group is developing a model of woven TEVG, using CAM-based threads, which is completely biological, human, and displays appropriate biological and mechanical properties.[38] This promising method can reduce the CAM-based TEVG production time by three, by eliminating the maturation step (fusion) of the sheets and allowing precise adjustment of its mechanical properties. Among the main textile industry methods, weaving has been identified as being the most promising for its ability to generate tubular structures with low porosity walls (unlike knitting) and whose diameters are not drastically affected by the longitudinal tension (unlike braiding) (Figure 2A and B).[38] In this process, a set of longitudinal CAM-based threads can be woven with a single circumferential thread to generate a completely biological, human, textile-inspired TEVG that can be sutured and implanted in the carotid of a sheep (Figure 2C-H). The graft was leak-proof and allowed to restore normal blood flow immediately post-implantation. This process allows greater applicability of the CAM for TEVG production by developing a faster, cheaper, and more versatile method. Based on the clinical results with TEVGs made with rolled CAM sheets, the host immune system will accept these woven CAM-based TEVGs and completely integrate with the native tissue in long-term implantation (> one year).

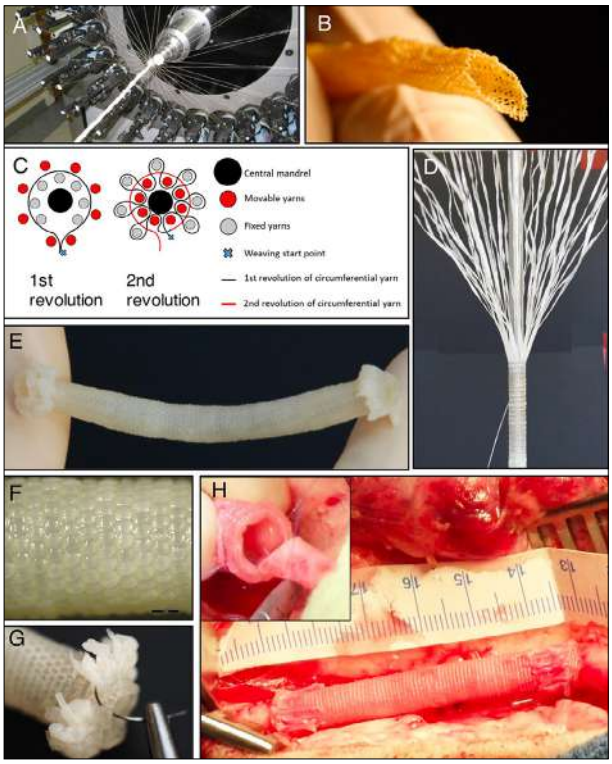

Figure 2: Engineering of completely biological, human, textile-inspired vascular grafts.

A and B) Automated braiding of a vascular graft using 48 human threads.

C) Schematic representation of the basic weaving technique used for a manual circular loom.

D) Macroscopic observation of a TEVG partially woven using 49 longitudinal ribbons and one circumferential thread.

E) Macroscopic observation of a completely woven TEVG.

F) The wall of the woven vessel is composed of tightly packed biological yarns (scale bar = 1 mm).

G) The graft can be easily sutured using 6–0 Prolene® at its extremities.

H) As a proof of concept, a human woven TEVG (internal diameter 4.2 mm) was implanted in the carotid of a sheep using standard surgical techniques. Reuse with permission.[38] Copyright 2020, Elsevier.

Conclusion

The development of a small-caliber arterial substitute by a tissue engineering approach represents a pivotal step in cardiovascular surgery to provide a functional conduit for coronary and peripheral bypass when autologous vessels are not available.[39] Before attempting the clinical translation of TEVGs, they must have specific characteristics to withstand the vascular environment. The ANSI/AAMI/ISO 7198:1998/2001 standard describes the methodology for validating various properties of vascular prostheses.[40] The parameters evaluated include the structural characteristics of the wall (thickness, composition, porosity, transmural permeability, and diameter), mechanical properties (tensile strength, suture retention, compliance, and bending radius), and biocompatibility. This standard has been established for synthetic vascular prostheses. However, it does not consider the immunological aspect of the graft integration in the host, which is particularly important for tissue reconstruction. It also does not specify minimum or acceptable values for each of the parameters under evaluation. While both CAM-based and biological scaffold-based TEVGs showed promising clinical results, the time and cost of production, governmental regulations, and ethical considerations continue to challenge their development.

While a non-living allogeneic approach is an important step towards making production more commercially viable, TEVGs produced by CAM sheet rolling/fusion can be prohibitively costly and somewhat unreliable. The mechanical integrity of this TEVG depends on the fusion of sheet layers during a lengthy maturation process (8-12 weeks). With two steps of rolling/maturation, the production time of the TEVGs used in the clinical trial was about 6-7 months. In addition, the maturation step is a cell-driven process that can be unreliable due to patient-to-patient variability and high sensitivity to culture conditions. A textile-inspired assembly method does not require maturation steps, which cuts the production time by three and avoids the possible delamination of layers due to incomplete fusion.

Another advantage of a textile-inspired approach is that it provides much better control over the mechanical properties of the TEVG, including directional and regional control. This would allow, among other things, the production of tapered TEVGs, which are clinically relevant. Unlike the CAM-based approach, it allows the control of wall permeability/density, which can influence, for example, the flexibility of the graft and its ability to be colonized by cells. Finally, textile-inspired approaches are not limited to the creation of TEVGs. They can also lead to innovation in many other applications, such as a simple non-inflammatory suturing material to a support mesh, a ligament, or a hollow structure to support organ development.

Acknowledgements

The authors thank the European Research Council (ERC) [Advanced grant number 785908] and the “Fondation pour la Recherche Médicale (FRM)” [Post-doctoral fellowship grant number SPF202004011810] for their financial supports.

References

1. Benjamin EJ, Muntner P, Alonso A, Bittencourt MS, Callaway CW, Carson AP, *et al.* Heart Disease and Stroke Statistics-2019 Update: A Report From the American Heart Association. *Circulation* 2019; 139: e56-66.

2. Lusis AJ. Atherosclerosis. *Nature* 2000; 407: 233-41.

3. Hansson GK. Mechanisms of disease: Inflammation, atherosclerosis, and coronary artery disease. *N Engl J Med* 2005; 352: 1685-95.

4. Kannan RY, Salacinski HJ, Butler PE, Hamilton G, Seifalian AM. Current status of prosthetic bypass grafts: a review. *J Biomed Mater Res B Appl Biomater* 2005; 74: 570-81.

5. Lau H, Cheng SW. Is the preferential use of ePTFE grafts in femorofemoral bypass justified ? *Ann Vasc Surg* 2001; 15: 383-7.

6. Budd JS, Allen KE, Hartley G, Bell PR. The effect of preformed confluent endothelial cell monolayers on the patency and thrombogenicity of small calibre vascular grafts. *Eur J Vasc Surg* 1991; 5: 397-405.

7. Brossollet LJ. Mechanical issues in vascular grafting: a review. *Int J Artif Organs* 1992; 15: 579-84.

8. Shemesh D, Goldin I, Hijazi J, Zaghal I, Berelowitz D, Verstandig A, *et al.* A prospective randomized study of heparin-bonded graft (Propaten) *versus* standard graft in prosthetic arteriovenous access. *J Vasc Surg* 2015; 62: 115-22.

9. Harskamp RE, Lopes RD, Baisden CE, De Winter RJ, Alexander JH. Saphenous vein graft failure after coronary artery bypass surgery: Pathophysiology, management, and future directions. *Ann Surg* 2013; 257: 824-33.

10. Langer R, Vacanti J. Tissue engineering. *Science 1*993; 260: 920-6.

11. Weinberg CB, Bell E. A blood vessel model constructed from collagen and cultured vascular cells. *Science* 1986; 231: 397-400.

12. Niklason LE, Gao J, Abbott WM, Hirschi KK, Houser S, Marini R, *et al.* Functional arteries grown *in vitro*. Science 1999; 284: 489-93.

13. Quint C, Kondo Y, Manson RJ, Lawson JH, Dardik A, Niklason LE. Decellularized tissue-engineered blood vessel as an arterial conduit. *Proc Natl Acad Sci USA* 2011; 108: 9214-9.

14. Dahl SLM, Kypson AP, Lawson JH, Blum JL, Strader JT, Li Y, *et al.* Readily available tissue-engineered vascular grafts. *Sci Transl Med* 2011; 3: 68ra9.

15. Lawson JH, Glickman MH, Ilzecki M, Jakimowicz T, Jaroszynski A, Peden EK, *et al.* Bioengineered human acellular vessels for dialysis access in patients with end-stage renal disease: Two phase 2 single-arm trials. *Lancet* 2016; 387: 2026-34.

16. Gutowski P, Gage SM, Guziewicz M, Ilzecki M, Kazimierczak A, Kirkton RD, *et al.* Arterial reconstruction with human bioengineered acellular blood vessels in patients with peripheral arterial disease. *J Vasc Surg* 2020; 72: 1247-58.

17. Higgins SP, Solan AK, Niklason LE. Effects of polyglycolic acid on porcine smooth muscle cell growth and differentiation. *J Biomed Mater Res - Part A* 2003; 67: 295-302.

18. L'Heureux N, Germain L, Labbé R, Auger FA. *In vitro* construction of a human blood vessel from cultured vascular cells: A morphologic study. *J Vasc Surg* 1993; 17: 499-509.

19. Grassl ED, Oegema TR, Tranquillo RT. A fibrin-based arterial media equivalent. *J Biomed Mater Res - Part A* 2003; 66: 550-61.

20. Syedain ZH, Meier LA, Bjork JW, Lee A, Tranquillo RT. Implantable arterial grafts from human fibroblasts and fibrin using a multi-graft pulsed flow-stretch bioreactor with noninvasive strength monitoring. *Biomaterials* 2011; 32: 714-22.

21. Syedain ZH, Meier LA, Lahti MT, Johnson SL, Tranquillo RT. Implantation of completely biological engineered grafts following decellularization into the sheep femoral artery. *Tissue Eng - Part A* 2014; 20: 1726-34.

22. Vascudyne Announces Successful First Human Use of TRUE Vascular Graft for Hemodialysis Access | News Direct 2021.

23. L'Heureux N, Pâquet S, Labbé R, Germain L, Auger FA. A completely biological tissue-engineered human blood vessel. *FASEB J* 1998; 12: 47-56.

24. Chan D, Lamande SR, Cole WG, Bateman JF. Regulation of procollagen synthesis and processing during ascorbate-induced extracellular matrix accumulation *in vitro*. *Biochem J* 1990; 269: 175-81.

25. Pashneh-Tala S, MacNeil S, Claeyssens F. The tissue-engineered vascular graft - Past, present, and future. *Tissue Eng - Part B Rev* 2016; 22: 68-100.

26. L'Heureux N, McAllister TN, De La Fuente LM. Tissue-engineered blood vessel for adult arterial revascularization. *N Engl J Med* 2007; 357: 1451-3.

27. Wystrychowski W, McAllister TN, Zagalski K, Dusserre N, Cierpka L, L'Heureux N. First human use of an allogeneic tissue-engineered vascular graft for hemodialysis access. *J Vasc Surg* 2014; 60: 1353-7.

28. McAllister TN, Maruszewski M, Garrido SA, Wystrychowski W, Dusserre N, Marini A, *et al.* Effectiveness of haemodialysis access with an autologous tissue-engineered vascular graft: a multicentre cohort study. *Lancet* 2009; 373(9673): 1440–6.

29. Sher SE, Hull BE, Rosen S, Church D, Friedman L, Bell E. Acceptance of allogeneic fibroblasts in skin equivalent transplants. *Transplantation* 1983; 36: 552-7.

30. Hull BE, Sher SE, Rosen S, Church D, Bell E. Fibroblasts in isogeneic skin equivalents persist for long periods after grafting. *J Invest Dermatol* 1983; 81: 436-8.

31. Magnan L, Kawecki F, Labrunie G, Gluais M, Izotte J, Marais S, *et al. In vivo* remodeling of human cell-assembled extracellular matrix yarns. Biomaterials 2021; 273: 120815.

32. Cavallaro JF, Kemp PD, Kraus KH. Collagen fabrics as biomaterials. *Biotechnol Bioeng* 1994; 44: 146.

33. Zeugolis DI, Paul GR, Attenburrow G. Cross-linking of extruded collagen fibers-A biomimetic three-dimensional scaffold for tissue engineering applications. *J Biomed Mater Res - Part A* 2009; 89: 895-908.

34. Cornwell KG, Lei P, Andreadis ST, Pins GD. Crosslinking of discrete self-assembled collagen threads: Effects on mechanical strength and cell-matrix interactions. *J Biomed Mater Res - Part A* 2007; 80: 362-71.

35. Younesi M, Islam A, Kishore V, Anderson JM, Akkus O. Tenogenic Induction of Human MSCs by Anisotropically Aligned Collagen Biotextiles. *Adv Funct Mater* 2014; 24: 5762-70.

36. Learn GD, McClellan PE, Knapik DM, Cumsky JL, Webster-Wood V, Anderson JM, *et al.* Woven collagen biotextiles enable mechanically functional rotator cuff tendon regeneration during repair of segmental tendon defects *in vivo*. *J Biomed Mater Res - Part B* Appl Biomater 2019; 107: 1864-76.

37. Zhang F, Bambharoliya T, Xie Y, Liu L, Celik H, Wang L, *et al.* A hybrid vascular graft harnessing the superior mechanical properties of synthetic fibers and the biological performance of collagen filaments. *Mater Sci Eng C* 2021; 118: 111418.

38. Magnan L, Labrunie G, Fénelon M, Dusserre N, Foulc MP, Lafourcade M, *et al.* Human textiles: A cell-synthesized yarn as a truly "bio" material for tissue engineering applications. *Acta Biomater* 2020; 105:111-20.

39. Seifu DG, Purnama A, Mequanint K, Mantovani D. Small-diameter vascular tissue engineering. *Nat Rev Cardiol* 2013; 10: 410-21.

40. ANSI/AAMI/ISO 7198:1998/2001. Cardiovascular implants - Tubular vascular prostheses 1998:54.

Biohybrid Vascular Graft – Reduction of production time through the integration of textile reinforcement systems

39

Alicia FERNÁNDEZ-COLINO, Christian APEL, Christian BOEHM, F. WOLF, Stefan JOCKENHOEVEL

Many research is focused nowadays in the development of vascular substitutes to address the unmet clinical need of small-caliber grafts.The classical tissue engineering approach has aimed to develop fully autologous prosthesis with the mechanisms of adaptation, remodeling and self-repair. However, not many tissue-engineered concepts have found their way into clinic due to mechanical weakness of the final construct and due to the limited producibility, or even more importantly limited reproducibility. The following chapter deals with the combination of the principles of tissue engineering and the development of technical components into biohybrid vascular prostheses, which strive for (i) sufficient biomechanical stability, (ii) (re)producibility and an (iii) optimal biological performance. Herefore, a fundamental understanding of the design principles that govern native tissue functionality and their translation to the development of bioinspired vascular grafts represent an attractive approach. The native vessels are textile-reinforced entities, and therefore textile technologies constitute a very attractive tool to developed bioinspired vascular replacements. The combination of biomimetic textiles with cell-interactive matrices constitutes the main pillar of the biohybrid concept.

Clinical and Technological Background

Cardiovascular diseases (CVD) are the most common causes of mortality worldwide (Townsend *et al.* 2016). The vascular diseases are characterized by increasing reduction of the lumen, which is accompanied by increasing stiffness of the vessel wall. This leads to local changes in vascular compliance (ΔV/ΔP), which sets in motion a vicious circle that promotes further narrowing of the lumen and ultimately leads to total vascular occlusion. Clinical intervention to treat CVD can involve minimally invasive procedures (*e.g.* endovascular stenting, angioplasty) or more invasive treatment options (*e.g.* bypass). While the latter is associated with a higher perioperative mobility, it is the option of choice for those patients requiring long term solutions (*i.e.* life expectancy >2 years). Up to date, the benchmark bypass grafts are autologous arteries or veins. Unfortunately, in addition to the aforementioned patient morbidity intrinsically associated with the use of autologous material, the failure rate associated with this graft is also significant. Specifically, the use of vena saphena magna (SV) grafts (either for coronary artery or for femoropopliteal bypass) is linked to a 50% of failure at 10 years due to suboptimal patency [1,2]. While the use of arteries is associated to a higher patency rates when compared to veins, the use of these grafts also increase the likehood of severe complications due to the removal from the native location [3].

Material science has the potential (and the responsibility) to seek for alternative concepts to the use of native tissues. Indeed, many efforts have been made to use synthetic materials to fabricate off-the shelf vascular prostheses with patency rates comparable to natural graft materials. These efforts have resulted in synthetic vascular grafts made of *e.g.* (i) PET (polyethylene terephthalate, Dacron), which is used for larger vessels (ID 10 mm), or (ii) ePTFE (expanded polytetrafluoroethylene, GORE-TEX) which is preferred for medium-sized vessels[4]. Unfortunately, the patency rates in small caliber grafts (ID< 6mm) are still unsatisfactory. In other words, no suitable graft exists for vessels such as coronary arteries, infrainguinal arteries and infrageniculate arteries, and a synthetic conduit is only suggested as a choice for those locations if no other suitable autologous vessel is available. The failure of the synthetic grafts is based on multi-factorial causes like (i) lack of endothelialisation, (ii) implant-associated infections, (iii) compliance mismatch at the anastomosis side, (iv) local stress concentration of the suture line inducing hyper-proliferation and (v) general inflammation induced by the surgical trauma.

In principle, tissue engineering approaches have the potential to overcome the current hurdles of both synthetic and autologous bypass grafts[5]. There are many factors to be considered in the development of a tissue-engineered vascular prosthesis. Those range from the choice of scaffold material and (micro) structure, scaffold processing, and selection of the cell sources. Additionally, the fundamental question of whether pre-seeding and pre-conditioning in bioreactor systems (*in vitro* tissue engineering) is preferable to a cell-free (*in situ* tissue engineering) approach or not is an open topic and a matter of ongoing debate. The design of native vessels obeys to the functional requirement of encompassing both mechanical strength and elasticity. From the material´s science perspective, the consecution of a design that balances both properties is not trivial, as strength and elasticity are very often inversely correlated[6]. Indeed, the fascinating combination of structural integrity and material elasticity can only be produced to a very limited extent with today's materials and manufacturing processes[7]. In order to advance in the pursuit of a lab-made graft able to match the endopoints that the functionality requires, it is necessary to have a close-up look to the nature, and to learn from the native vessel design (as a blue print and source of inspiration).

An important design aspect of human being in general and native tissues in particular is the fact that they are "fibre-reinforced composites". The native vessels can be considered as a network composite, in which a water-based matrix is reinforced with a fibrous anisotropic pattern. That means that the biomechanical properties of native tissues are mainly defined by fibers like, elastin, collagen etc. Therefore textile engineering offers a multi-scale toolbox for mimicking natural structures and properties on the level of (i) polymers, (ii) fibres, (iii) spinning (e-spinning, wet and dry spinning, melt spinning) and (iv) textile fabric processing (non-wovens, wovens, warp-knitting, braiding etc.). The combination of such technologies with other manufacturing techniques and materials enables the development of unique hierarchical and composite designs[8].

In this chapter, we will describe the development of textile-reinforced vascular grafts for clinical applications and as *in vitro* test systems for biomedical engineering.

From Classical Tissue Engineering towards Biohybrid Implants

Classical tissue engineering aims at the production of completely autologous prostheses by means of *in vitro* cell culture and bioreactor conditioning. In doing so, classical tissue engineering must mimic in the lab the process of tissue regeneration. Taking into account that tissue regeneration is closely linked to the process of haemostasis, and that fibrin is a kind of natural substrate to stimulate tissue regeneration, the application of such material for the development of vascular implants results highly appealing.

Indeed, fibrin offers a number of properties for an ideal scaffold, including (i) precise time-control over the polymerization, (ii) modulation of the degradation rate by the administration of protease inhibitors both *in vitro* and *in vivo*, which can consequently be adapted to the individual tissue maturation, (iii) highly efficiency for cell seeding and embedding, which avoids time-consuming cell migration processes, and (iv) excellent processability by a wide variety of biofabrication approaches [9, 10], (*e.g.* bioprinting, injection moulding, dip-coating, laser-induced forward transfer (LIFT), electrospinning, etc.), enabling the development of complex 3-dimensional structures both as monocultures and in hierarchical layered assemblies in co-cultures. However, fibrin has one major disadvantage: the low initial mechanical stability. Therefore, either (i) prolonged pre-cultivation phases or (ii) reinforcing structures embedded into the fibrin matrix are necessary to achieve sufficient stability as a vascular prosthesis.

As mentioned above, textile engineering offers a multiscale toolbox to mimic the native fibrillar structure of blood vessels and reinforce the fibrin matrix. We have witnessed how in the last decades, textile technologies (*e.g.* weaving, knitting and electrospinning) have expanded their horizons, from the development of daily application products (*e.g.* cloths) to the development of high-value devices (*i.e.* biomedical implants). In this regard, textile technologies provide a very attractive avenue to manufacture 2D and 3D constructs with a proper control over their structure (*e.g.* size, shape, and porosity)[11].

In additional, emerging technologies such as melt electrospinning (also known as melt electrowriting, MEW), illustrate the evolution of fiber-processing technologies and the advances in developing fully controlled implants that can mimic the functionality of native tissues.
In order to avoid a compliance mismatch between the native vessel and the vascular prosthesis, knitted fabrics are particularly suitable for textile reinforcement. They allow pulsatile volume changes through the material elasticity via a specifically adjustable structural elasticity, but prevent unrestricted lumen expansion in the sense of aneurysm formation. In this case, the effective technology is particularly suitable, as on the one hand it allows for suture-free tubular structures and on the other hand it avoids for the formation of an aneurysm.

The production of biohybrid vascular prostheses as a textile-reinforced scaffold that combines (i) fibrin as a cell carrier and (ii) a warp-knitted basic structure was intensively researched by us. We were able to achieve sufficient strength through the textile base structure and excellent biologisation of the overall structure through the fibrin-hydrogel component [12] (see Figure 1 A-C). In our preclinical study in the ovine carotid artery model over 6 months, we were able to demonstrate the significant superiority of the biohybrid prosthesis with regard to the openness rate compared to the clinical gold standard in synthetic vessel replacement (ePTFE). The textile probation made of a long-term biodegradable warp-knitted structure of degradable poly (L/D)lactide 96:4 P(L/D)LA 96/4 successfully prevented aneurysm formation [13] (see Figure 1 D-F).

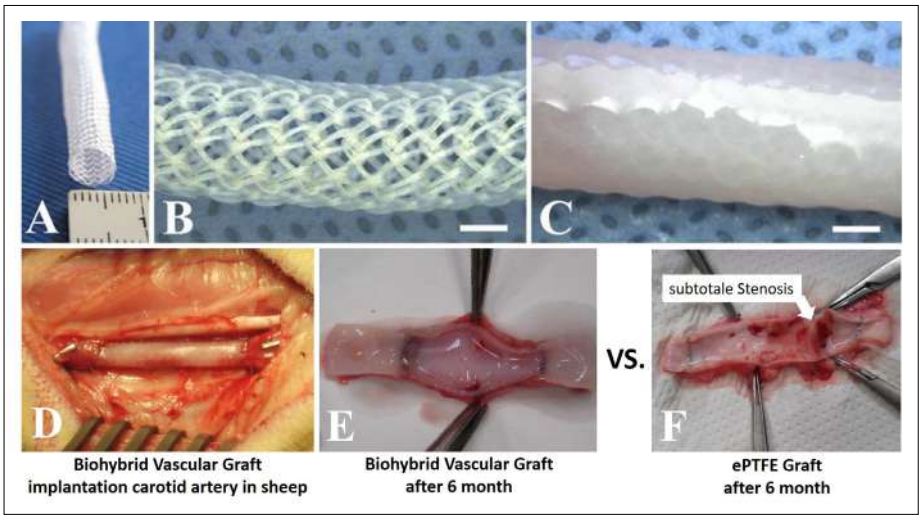

Figure 1: Production of Biohybrid Vascular Prosthesis based on a textile-reinforced warp-knitted mesh and a fibrin-gel-matrix as cell carrier in an injection molding technique **[A-C]** [Adapted from [12]] and the *in vivo* evaluation in the ovine carotid artery model for 6 month **[D, E]** in comparison with a ePTFE graft, which already demonstrated subtotal stenosis in nearly all control grafts **[F].**

Theoretically, the used of a degradable textile embedded within a degradable matrix allows for the fully resorption of the implant and ideally its transformation into an autologous-like graft after remodeling. The success of such a degradable implant relies on a perfect equilibrium between the remodeling and the degradation rates, so that the mechanical properties of the implant during the entire reabsorption/ remodeling process meet the minimum requirements for a functional implant.

These efforts were supported by the valuable experience of the working group around L'Heureux *et al.*, who were able to achieve an outstanding initial stability of the vascular prostheses with regard to their radial burst strength through their scaffold-free production of vascular prostheses. However, some prostheses failed in the clinical trial due to their aneurysm development. This is most likely caused by remodelling of the extracellular matrix post implantationem.

We therefore decided to switch from degradable to non-degradable textile reinforcements and finally opted for polyvinylidene fluoride (PVDF). This is based, among other things, on the preliminary work of Klinge *et al.* who intensively investigated the outstanding and long-term stable properties of PVDF for biomedical applications[14]. Under optimized culture conditions, we were able to show that an excellent bursting strength of 870 mmHg could already be achieved after an *in vitro* cultivation time of 2 weeks[15] (Wolf *et al.* 2019). In the animal studies performed later in sheep (dialysis shunt model carotid artery to jugular vein), no signs of a foreign body reaction could be detected. It appears that *in vitro* pre-cultivation leads to complete encapsulation of the materials under non-inflammatory conditions.

Despite these successes, a concept that requires 2-3 weeks of cell cultivation followed by 2 weeks of *in vitro* preconditioning in the bioreactor system is difficult to translate clinically, as there is an acute to subacute need for vascular prosthesis. In order to be able to significantly reduce the production time, we have changed the selected primary cells to adipose derived mesenchymal stem cells and also further strengthened the textile structure. Therefore, we combined the non-degradable PVDF warp-knitted structure with an e-spun degradable PLGA nonwoven. Thus, we were able to ensure the long-term stability of the vascular prosthesis via the PVDF on the one hand and achieve temporary mechanical support via the e-spun PLGA on the other. With the PLGA, we chose a material that degrades in the short to medium term. By that the degradation can take place in parallel with the increasing extracellular matrix development *in situ* after implantation. Immediately after production of the prosthesis by injection moulding, we were able to achieve already an average radial bursting strength of approx. 450 mmHg with PLGA coating *vs.* 200 mmHg without. After 4 days of pre-cultivation in the bioreactor system, the radial burst strength of the prostheses reinforced with an e-spun PLGA fleece had increased to an average of 590 mmHg, with a suture tear strength of 2.2 N, so that implantation was possible already after such a short time. In this way, the production time could thus be reduced from previously around 42 days to 4 days and for the first time also becomes clinically relevant in the sense of a peri-operative approach (see Figure 2).

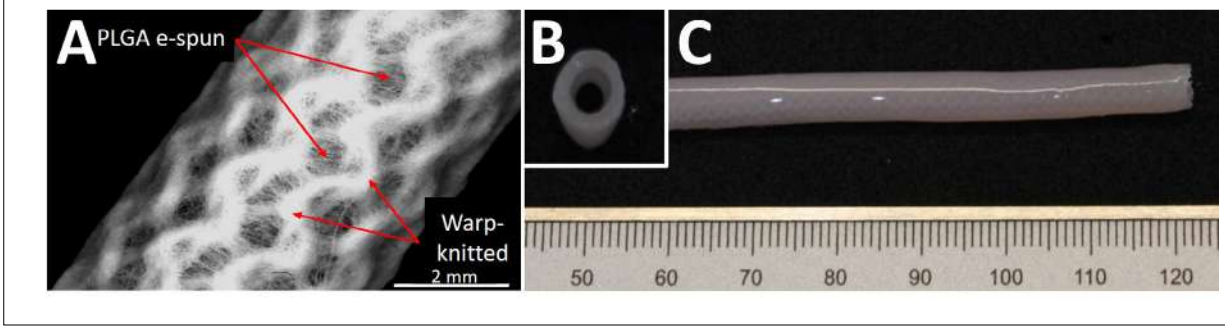

Figure 2: Biohybrid vascular prosthesis **[B, C]** with warp-knitted textile-reinforcement structure and additional PLGA e-spun layer on top **[A]**

The PVDF mesh has also been exploited to create biohybrid grafts envisioned as cell-free implants for *in situ* tissue engineering. Specifically, the PVDF mesh was used as a reinforment of an artificial elastin-like matrix, made out of elastin-like recombinamers (ELRs) [16] (Figure 3). The ELRs are artificial polypeptides, bioinspired in the sequence of the elastin and produced by the genetic engineering techniques [17]. Because of this mimicry, the ELR has an outstanding capability to stretch and recoil, which makes them highly attractive for engineering cardiovascular implants. Additionally, many studies [18, 19], including ours [20, 16], have shown minimal platelet adhesion to this kind of materials, which further supports their used for the fabrication of blood-contacting materials. The unique combination of the textile reinforcement with the ELR-based matrix resulted in an anisotropic elasto-mechanical behavior of the graft, mirroring the behaviour of the native arteries.

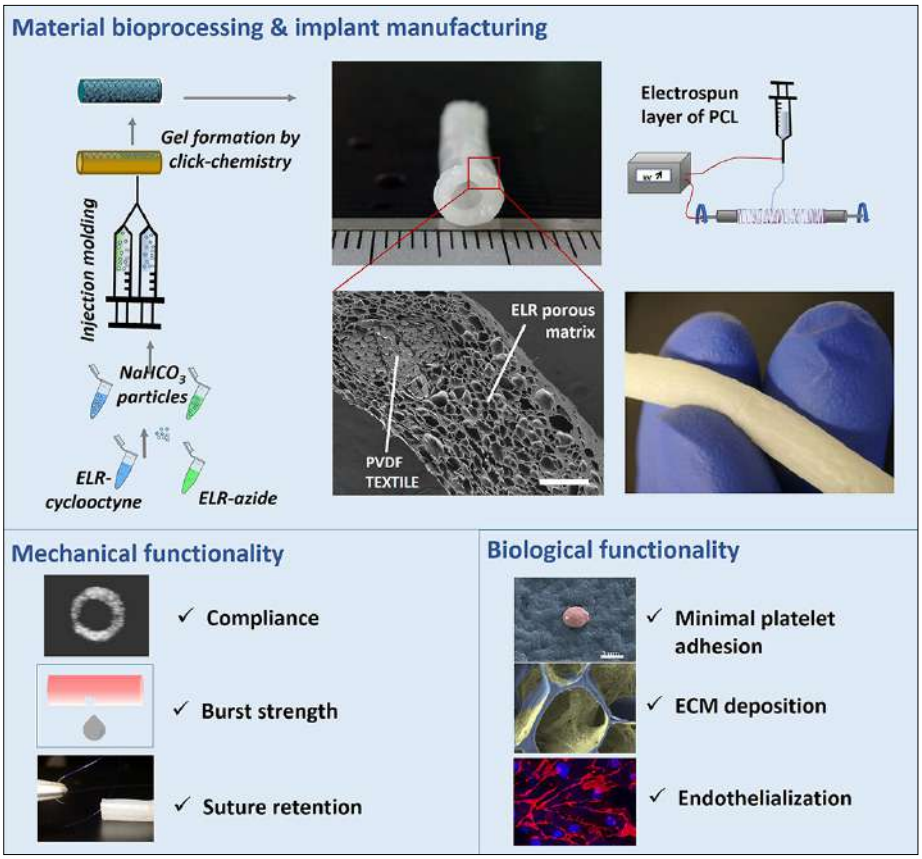

Figure 3: Biofabrication approach resulting functionality of textile-reinforced vascular grafts based on ELRs. *Adapted with permission from (Fernández-Colino et al. 2019). Copyright © 2019 Fernández-Colino, Wolf, Rütten, Schmitz-Rode, Rodríguez-Cabello, Jockenhoevel and Mela*

Conclusions

In summary, there is still a great clinical need for small-caliber vascular prostheses with long-term patency rates. Although classical tissue engineering has in principle the potential to overcome the biological hurdles in bypass surgery, long production times and insufficient short- and especially long-term stability are obstacles to clinical application. With the development of textile-reinforced biohybrid vascular prostheses, we were able to demonstrate that these are clearly superior to the current synthetic clinical gold standard (ePTFE) in terms of their patency rates. The combination of a non-degradable

active structure (for long-term stability) and a degradable e-spun nonwoven structure (for temporary reinforcement until replacement by ECM *in situ*) has significantly reduced the production time to currently 4 days. This facilitates the clinical use as a peri-operatively manufactured and patient-individualized implant. With the use of elastin-like recombinamers (ELRs) in biohybrid implant research, Fernandez-Colino *et al.* introduced an hydrogel matrix with minimal platelet adhesion. Future research will investigate whether this will enable us to create off-the-shelf biohybrid implants that are clinically superior in terms of their mechanical and biological function.

References

1. Harskamp RE, Lopes RD, Baisden CE, de Winter RJ, Alexander JH. Saphenous vein graft failure after coronary artery bypass surgery: pathophysiology, management, and future directions. *Ann Surg* 2013; 257: 824-33.
2. Klinkert P, Post PN, Breslau PJ, van Bockel JH. Saphenous vein versus PTFE for above-knee femoropopliteal bypass. A review of the literature. *Eur J Vasc Endovasc Surg* 2004; 27: 357-62.
3. Masden DL, Seruya M, Higgins JP. A systematic review of the outcomes of distal upper extremity bypass surgery with arterial and venous conduits. *J Hand Surg* 2012; 37: 2362-7.
4. van Lith R, Ameer GA. Biohybrid Strategies for Vascular Grafts. In: Pallua N, Suscheck CV, editors. Tissue Engineering: From Lab to Clinic. Berlin, Heidelberg: Springer Berlin Heidelberg 2011. pp. 279-316.
5. Pashneh-Tala S, MacNeil S, Claeyssens F. The Tissue-Engineered Vascular Graft-Past, Present, and Future. *Tissue Eng Part B Rev* 2016; 22: 68-100.
6. Sarkar S, Schmitz-Rixen T, Hamilton G, Seifalian AM. Achieving the ideal properties for vascular bypass grafts using a tissue engineered approach: a review. *Med Biol Eng Comput* 2007; 45: 327-36.
7. Eble JA, Niland S. The extracellular matrix of blood vessels. *Curr Pharma Des* 2009; 15: 1385-400.
8. Bas O, Catelas I, De-Juan-Pardo EM, Hutmacher DW. The quest for mechanically and biologically functional soft biomaterials via soft network composites. *Adv Drug Deliv Rev* 2018; 132: 214-34.
9. Koroleva A, Gittard S, Schlie S, Deiwick A, Jockenhoevel S, Chichkov B. Fabrication of fibrin scaffolds with controlled microscale architecture by a two-photon polymerization-micromolding technique. *Biofabrication* 2012; 4: 015001.
10. Weber M, Gonzalez de Torre I, Moreira R, Frese J, Oedekoven C, Alonso M, *et al.* Multiple-Step Injection Molding for Fibrin-Based Tissue-Engineered Heart Valves. *Tissue Eng Part C Methods* 2015; 21: 832-40.
11. Fernández-Colino A, Jockenhoevel S. Textile-Reinforced Scaffolds for Vascular Tissue Engineering. In: Walpoth BH, Bergmeister H, Bowlin GL, Kong D, Rotmans JI, Zilla P, editors. Tissue-Engineered Vascular Grafts. *Cham: Springer International Publishing* 2020. pp. 339-63.
12. Tschoeke B, Flanagan TC, Koch S, Harwoko MS, Deichmann M, Ellå V, *et al.* Tissue-Engineered Small-Caliber Vascular Graft Based on a Novel Biodegradable Composite Fibrin-Polylactide Scaffold. *Tissue Eng Part A* 2009; 15: 1909-18.
13. Koch S, Flanagan TC, Sachweh JS, Tanios F, Schnoering H, Deichmann T, *et al.* Fibrin-polylactide-based tissue-engineered vascular graft in the arterial circulation. *Biomaterials* 2010; 31: 4731-9.
14. Klinge U, Klosterhalfen B, Ottinger AP, Junge K, Schumpelick V. PVDF as a new polymer for the construction of surgical meshes. *Biomaterials* 2002; 23: 3487-93.
15. Wolf F, Paefgen V, Winz O, Mertens M, Koch S, Gross-Weege N, *et al.* MR and PET-CT monitoring of tissue-engineered vascular grafts in the ovine carotid artery. *Biomaterials* 2019; 216: 119228.
16. Fernández-Colino A, Wolf F, Rütten S, Schmitz-Rode T, Rodríguez-Cabello JC, Jockenhoevel S, *et al.* Small Caliber Compliant Vascular Grafts Based on Elastin-Like Recombinamers for *in situ* Tissue Engineering. *Front Bioeng Biotechnol* 2019; 7: 340.
17. Ibanez-Fonseca A, Flora T, Acosta S, Rodriguez-Cabello JC. Trends in the design and use of elastin-like recombinamers as biomaterials. *Matrix Biol* 2019; 84: 111-26.
18. Woodhouse KA, Klement P, Chen V, Gorbet MB, Keeley FW, Stahl R, *et al.* Investigation of recombinant human elastin polypeptides as non-thrombogenic coatings. *Biomaterials* 2004; 25: 4543-53.
19. Jordan SW, Haller CA, Sallach RE, Apkarian RP, Hanson SR, Chaikof EL. The effect of a recombinant elastin-mimetic coating of an ePTFE prosthesis on acute thrombogenicity in a baboon arteriovenous shunt. *Biomaterials* 2007; 28: 1191-7.
20. Fernández-Colino A, Wolf F, Moreira R, Rütten S, Schmitz-Rode T, Rodríguez-Cabello JC, *et al.* Layer-by-layer biofabrication of coronary covered stents with clickable elastin-like recombinamers. *Eur Polym J* 2019; 121: 109334.

Relationship between hemodynamics and in-stent restenosis in femoral arteries

40

Anna CORTI, Monika COLOMBO, Diego GALLO, Josè Felix Rodriguez MATAS, Francesco MIGLIAVACCA, Stefano CASARIN, Claudio CHIASTRA

Although percutaneous transluminal angioplasty with stenting is one of the preferred treatments of lower extremity peripheral artery disease, this procedure suffers from a 66% 1-year primary patency rate. The unfavorable outcome is mostly attributable to in-stent restenosis, an inflammatory-driven arterial response, characterized by excessive smooth muscle cell proliferative and synthetic activity ultimately leading to lumen re-narrowing. The etiology of in-stent restenosis is multifactorial, involving different systemic, biological and biomechanical drivers. Among the biomechanical factors, a key role has been recognized to the stent-induced hemodynamic alteration, influencing smooth muscle cell activity both directly and through endothelium-dependent mechanisms. In this scenario, computational fluid dynamics simulations of stented femoral arteries allowed quantifying the local hemodynamics and identifying wall shear stress-based hemodynamic predictors of in-stent restenosis. This contributed to enhance the current knowledge of the fluid dynamic-related mechanisms of post-stenting lumen remodeling. However, given the multiscale and multifactorial nature of in-stent restenosis, multiscale mechanobiological modeling relating the intervention-induced mechanical stimuli to the complex network of biological events has recently emerged as a fundamental approach to decipher the underlying pathological pathways. This involves the analysis of interactions, cause-effect relationships, feedback mechanisms and cascade signaling pathways across different spatial and temporal scales, thus allowing tracking the effect of the intervention-induced perturbation to the molecular, cellular and finally tissue response. The present chapter examines the state-of-the-art of computational fluid dynamics studies of in-stent restenosis in femoral arteries and provides an overview on the emerging field of multiscale mechanobiological modeling of arterial adaptation following endovascular procedures.

Introduction

In-stent restenosis in femoral arteries

Percutaneous transluminal angioplasty (PTA) followed by stent placement is a common minimally invasive procedure used to open narrowed atherosclerotic femoral arteries and to restore the correct blood flow to the lower limbs. Nowadays, this procedure is performed and recommended for those patients who are susceptible to surgical risk and in presence of lesions with stenosis/occlusions shorter than 25 cm.[1] The incidence of adverse events is still high. In particular, in-stent restenosis (ISR), consisting in the re-narrowing of the stented segment in the months after intervention, is a major adverse event, with an incidence ranging from 15% to 32%, with a peak between 9 and 15 months post-intervention.[2]

ISR, often recalcitrant, is caused by excessive neointima growth and unfavorable inward vascular remodeling. PTA with stenting causes severe vascular injury including endothelial denudation. The healing process that begins after the endovascular treatment involves the activation of inflammatory and vascular cells leading to re-endothelialization, neointimal growth and remodeling.[3] However, this process can degenerate into a sustained inflammatory state and abnormal smooth muscle cell proliferation and extracellular matrix (ECM) deposition, potentially leading to neointima hyperplasia and ISR.[4–6] The mechanisms for the pathogenesis of ISR are not completely understood. ISR is promoted by several interrelated factors, including patient, biological, biomechanical, and operator-related factors.[7] Among the biomechanical factors, the stent-induced flow disturbances seem to play an important role on ISR development.[8–10]

Role of computer simulations in the study of in-stent restenosis

Over the past two decades, mathematical and computational modeling has emerged as a powerful tool to help elucidate the role of hemodynamic flow disturbances on ISR development. Such research has predominantly focused on two approaches. The first approach adopts computational fluid dynamics (CFD) modeling on three-dimensional (3D) patient-specific femoral artery geometries reconstructed from clinical images to address the impact of the altered hemodynamics after stent implantation on ISR. This approach has provided evidence on the role of stent-induced flow disturbances on ISR development.[8–10] In particular, the stent struts cause blood flow separation, creating recirculation and stagnation zones and expose the lumen to low and oscillatory wall shear stress (WSS), which promotes neointima regrowth.[8–10] The second approach aims to simulate the biological response of the artery following stent deployment, through a mechanobiological, multiscale model. The majority of the studies following this approach adopts agent-based models (ABMs) (*e.g.*[11–13]), whereby a natural description of cellular systems is obtained through the definition of a set of rules governing the agents' activities.[14] Thanks to this bottom-up approach, a complete understanding of the whole system is not needed but its behavior will naturally emerge from the imposed rules. ABMs easily capture spatial-related aspects such as tissue heterogeneity, composition and morphology, and can integrate phenomena at different scales within multiscale frameworks.[15] Moreover, ABMs can be coupled with hemodynamic models,[11,13,16-18] enabling the replication of hemodynamic-related cellular behaviors through the inclusion of rules depending on quantitative descriptors of flow disturbances, like the exposure to low and oscillatory WSS. In this way, it is possible to gain insights into the hemodynamic-driven mechanisms of tissue remodeling and ISR following stent deployment.

Chapter contents

The present chapter reviews the state-of-the-art in computational research on ISR of femoral arteries treated by endovascular intervention. In the first part of the work, the studies elucidating the relationship between altered hemodynamics and ISR via a CFD-based approach are described. In the second part, the general concept of vascular adaptation is introduced and the way in which multiscale models are revolutionizing the related research towards clinical translation is presented. Finally, the innovative approach, based on a multiscale computational framework, that our research group is pursuing to investigate the interdependent factors promoting ISR is presented.

Hemodynamics modeling of in-stent restenosis in femoral arteries

Recently, CFD models have been proposed to elucidate the direct link between the post-intervention altered hemodynamics and ISR in femoral arteries. Table 1 summarizes the aim of the studies, the clinical data available and the main characteristics of the developed models.

Table 1: Recent published studies on patient-specific hemodynamic modeling of in-stent restenosis in femoral arteries

First author, year [reference]	Aim	Arterial model (no. patient-specific cases)	Imaging data	Follow-ups	Analysis type (solver)	Boundary conditions	Blood model
Gokgol *et al.*, 2019 [19]	Impact of leg configuration (i.e. straight, flexed) on restenosis	3D patient-specific, FPA (20)	2D angiography (geometry), MRI (boundary conditions)	Baseline + Outcome (6M)	CFD (ANSYS CFX)	I: parabolic velocity profile O: zero pressure	Newtonian (μ=0.004 Pa·s), ρ=1050 kg/m^3
Colombo *et al.*, 2021 [20]	Impact of altered hemodynamics on restenosis progression	3D patient-specific, SFA with CFA bifurcation (10)	CT (geometry), DUS (boundary conditions)	Baseline, Follow-up (1M, 6M, 1Y) + Outcome (2Y)	CFD (ANSYS Fluent)	I: parabolic velocity profile O: flow-split	Non-Newtonian Carreau (μ_0= 0 Pa·s μ_∞=0.0035 Pa·s, λ=25 s, n=0.25), ρ=1060 kg/m^3
Colombo *et al.*, 2021 [22]	Restenosis prediction based on altered hemodynamics	3D patient-specific, SFA with CFA bifurcation (10)	CT (geometry), DUS (boundary conditions)	Baseline, Follow-up (1Y) + Outcome (2Y)	CFD (ANSYS Fluent)	I: parabolic velocity profile O: flow-split	Non-Newtonian Carreau (μ_0= 0 Pa·s μ_∞=0.0035 Pa·s, λ=25 s, n=0.25), ρ=1060 kg/m^3

Gokgol *et al.*[19] performed CFD simulations in patient-specific femoropopliteal artery models both in straight and flexed leg configuration. Twenty lesions were analyzed, half treated with PTA and the other half with self-expandable stents. The vessel models were reconstructed from two-dimensional X-ray angiographic images acquired immediately after the endovascular intervention. The lumen areas affected by low time-averaged wall shear stress (TAWSS) were larger in case of leg flexion (Figure 1) and also of lesions classified for restenosis at 6-month follow-up. However, none of the investigated hemodynamic descriptors

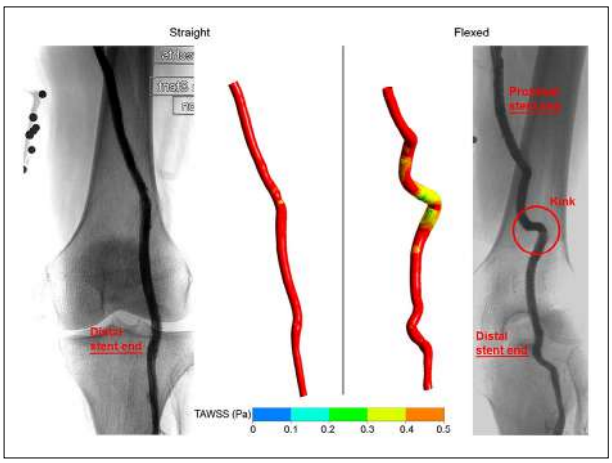

Figure 1: Time-averaged wall shear stress (TAWSS) distribution in an explanatory model of stented femoral artery exhibiting kinking during leg flexion. The X-ray images were acquired in the straight (left) and flexed (right) leg position and show the locations of the stented region and the kink when the leg is flexed. The lumen area exposed to low TAWSS (< 0.5 Pa) were located next to the kink or highly curved segment.

Reprinted with permission from Biomechanics and Modeling in Mechanobiology, 2019, Vol. 18(6), Gökgöl C et al., Prediction of restenosis based on hemodynamical markers in revascularized femoro-popliteal arteries during leg flexion, 1883-1893 (http://creativecommons.org/licenses/by/4.0/).

resulted significantly related to restenosis, possibly due to the limited resolution of the imaging modality used for the vessel reconstruction or by the lack of patient-specific boundary conditions imposed in the CFD simulations. Furthermore, the evaluation of success/failure of the endovascular treatment was based on a dichotomous information about the absence/presence of restenosis at 6-month follow-up. Thus, a local quantification of the lumen remodeling leading to restenosis was not possible.

To analyze the lumen remodeling trajectory over time after stent placement and to investigate the impact of altered hemodynamics on ISR initiation and progression, Colombo *et al.* [20] performed a longitudinal study by considering the data of 10 superficial femoral artery (SFA) lesions of 7 patients at multiple follow-ups, namely at post-operative 1 week, 1 month, 6 months and 1 year. Following the framework depicted in Figure 2, the patient-specific SFA models, semi-automatically reconstructed from computed tomography (CT) at the different follow-ups, [21] were used (i) to perform a morphological analysis (all the follow-ups), quantifying the lumen area change between the time-points, and (ii) to analyze the hemodynamics by means of transient CFD simulations (1-week, 1-month and 6-month follow-ups), computing several WSS-based descriptors.

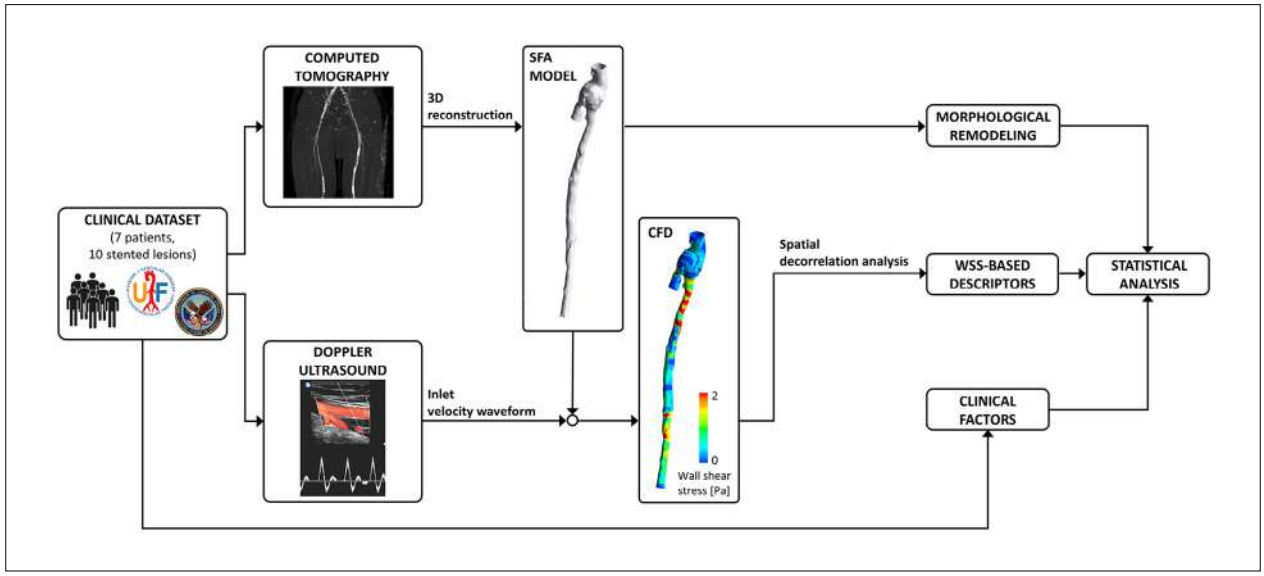

Figure 2: Schematic overview of the computational workflow adopted in the studies of Colombo *et al.* [20,22] to investigate the link between hemodynamics and in-stent restenosis in human superficial femoral arteries.

Reprinted with permission from Annals of Biomedical Engineering, 2021, in press, Colombo M et al., In-stent restenosis progression in human superficial femoral arteries: dynamics of lumen remodeling and impact of local hemodynamics. (http://creativecommons.org/licenses/by/4.0/)

Colombo and colleagues observed that the largest lumen remodeling occurred in the first post-operative month, with significantly larger inward remodeling in the fringe segments of the stented lesions, whereas focal re-narrowing frequently occurred after 6 months (Figure 3A-C). In exploring the impact of hemodynamics, the authors found that abnormal patterns of multidirectional WSS were significantly associated with lumen remodeling occurring both in the first- and last-time intervals (Figure 3D). In particular, TAWSS at 1 week was negatively correlated with lumen area change in the first-time interval (1-week:1-month), suggesting that for low TAWSS an inward remodeling occurred. Also, positive trends between oscillatory shear index (OSI) and relative residence time (RRT) and the lumen area change were observed at both first-and last-time intervals.

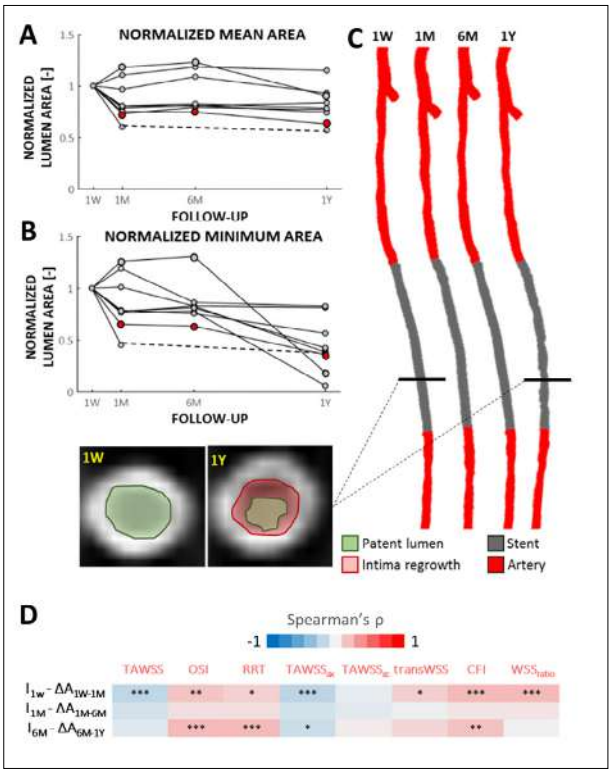

Figure 3:

A-B) Remodeling trajectory over time of the human superficial femoral artery (SFA) lesions analyzed in Colombo et al.20, reported as mean and minimum lumen area normalized with respect to the 1-month (1M) lumen area.

C) Reconstructed SFA models at 1-week (1W), 1M, 6-month (6M) and 1-year (1Y) follow-up and corresponding cross-sectional computed tomography images of one explanatory case.

D) Spearman's correlations between the lumen area change (ΔA) in the current time interval and the wall shear stress (WSS)-based descriptors (I) computed at the beginning of that time interval. TAWSS: time-averaged WSS; OSI: oscillatory shear index; RRT: relative residence time; TAWSSax: axial component of TAWSS; TAWSSsc: secondary component of TAWSS; transWSS: transverse WSS; CFI: cross-flow index; WSSratio: ratio between the cycle-averaged magnitude of the secondary and the axial WSS components; *: p<0.05; **: p<0.01; ***: p<0.001.

Adapted with permission from Annals of Biomedical Engineering, 2021, in press, Colombo M et al., In-stent restenosis progression in human superficial femoral arteries: dynamics of lumen remodeling and impact of local hemodynamics.
(http://creativecommons.org/licenses/by/4.0/)

Following the previous findings on the association between altered hemodynamics and lumen remodeling, Colombo *et al.*[22] evaluated the power of the WSS-based descriptors computed at 1 week to predict the inward lumen remodeling at 1 year (quantified as the lumen area change occurring during the time interval 1-week:1-year). From the findings of the study, it emerged that the TAWSS was strongly negatively correlated to the lumen area change (ρ = -0.75, p = 0.013), suggesting that low TAWSS is related to a large lumen area change. Furthermore, a positive strong correlation was found between the lumen area exposed to low TAWSS and the lumen area change (ρ = 0.69, p = 0.026), suggesting that the larger the lumen area exposed to low TAWSS is, the larger the lumen area change at 1 year is expected to be. Conversely, OSI and RRT were not correlated to the lumen area change (p > 0.05). Moreover, compared to the other WSS-based descriptors, the TAWSS was the best predictive marker with a positive predictive value (*i.e.* the probability that the lumen area subjected to altered hemodynamics can successfully identify corresponding regions of larger lumen area change) of ~45%.

In all reviewed studies, the image resolution of angiography and CT did not allow to detect the stent struts and, hence, to reconstruct the 3D stent geometry (*i.e.* detailed stent geometry with struts and links) and include it within the computational models. Moreover, the CFD simulations were performed assuming rigid arterial walls and fixed leg configuration (either straight/flexed in Gokgol *et al.*[19] or straight in Colombo *et al.*[20,22]). In the future, intravascular images could be combined with angiography or CT to reconstruct the stent geometry[23] and the leg movement could be simulated by using a methodology recently proposed for idealized femoral artery models.[24]

Multiscale computational modeling of in-stent restenosis in femoral arteries

Multiscale models of vascular adaptation: general concepts

Vascular adaptation is driven by a complex network of heterogeneous and interconnected mechanisms (*e.g.* mechanotransduction, gene pattern alterations),[25] a deep understanding of which is crucial to deliver personalized treatment, yet lacking. To cope with it, researchers have lately revolved to a "systems biology" approach, for which a biological system is seen as an interconnected web involving environmental conditions and mutual interactions among its components.[26–28] Multiscale models are the computational translation of the "systems biology" concept and thus they are suitable to bridge in-vitro models of single-scale phenomena to *in-vivo* models of whole systems of interest.[25,29] Such a detail level, together with late progress in biomedical technology, offers a powerful instrument for personalized medicine and fosters the establishment of *in-silico* models to drive biomedical research in a more robust fashion.

ABMs are a class of computational models well-fitting to represent heterogeneous populations and capture the behavior of systems with an intrinsic discrete nature, as systems of cells.[30,31] They are convenient in a multiscale optic since they replicate complex systems' behavior that directly emerges from (i) agent individual dynamics, (ii) interactions among agents, and (iii) environmental conditions. ABMs easily incorporate stochasticity, consistently with the real observations of the phenomena of interest. Additionally, they capture spatial-related aspects as tissue heterogeneity and composition, and can integrate phenomena at different scales within a multiscale framework. These integrated frameworks have a twofold advantage: (i) they can augment the knowledge we have on complex systems, thanks to their bottom-up structure, and (ii) they can act as a therapy/intervention outcome predictor, since they are able to track the propagation of perturbation (therapy/intervention) across the multiscale network and quantify its effect at tissue/organ level.

Agent-based multiscale frameworks have been largely adopted to describe the complexity of vascular pathologies (*e.g.* atherosclerosis[32,33]) and depict the driving mechanisms of response to endovascular procedures or surgical interventions, from stenting (*e.g.*[11,12]) to vein graft bypass (*e.g.*[34,35]). In the specific arena of ISR, several studies have been presented until now, even though none of them has been applied to femoral arteries. Hoekstra's research group proposed a multiscale framework to dissect the hemodynamic and mechanical effects of stenting on the pathological process of ISR and the benefit of eluting antiproliferative drugs to reduce neointimal growth.[11,13,16–18,36] The following four modules were integrated: (i) a Lattice-Boltzman-based module for hemodynamic computation, (ii) a finite difference scheme to solve the set of partial differential equations of drug transport, (iii) an ABM of tissue mechanics to compute the stress and strain state within arterial wall, and (iv) an ABM of cellular dynamics to replicate cellular activities. The stent deployment acted as a perturbation from the model equilibrium and propagated to the other sub-modules, driving the system towards its adaptation. In the last improvements of the framework, the ECM was included and a validation against data from porcine coronary arteries was conducted.[11] On a different perspective, an Irish research group focused on the arterial wall damage induced by PTA and stenting.[12,37–39] The triggering action on cellular proliferation employed by arterial injury was studied by means of an agent-based multiscale framework characterized by three modules: (i) a finite element method module of stent deployment, (ii) a module based on the solution of ordinary differential equations to compute inflammatory cues, and (iii) an ABM of cellular dynamics.

Multiscale model of in-stent restenosis of femoral arteries: an example of agent-based computational framework

Our research group is currently developing a patient-specific multiscale computational framework of ISR of femoral arteries able to integrate the effects of hemodynamics and monocyte gene expression on the cellular dynamics (Figure 4). The framework is characterized by the integration of the following two modules: (i) a hemodynamic module computing the WSS along the stented region of the vessel coupled with (ii) an ABM of cellular dynamics replicating arterial wall remodeling in response to local WSS and gene expression inputs.

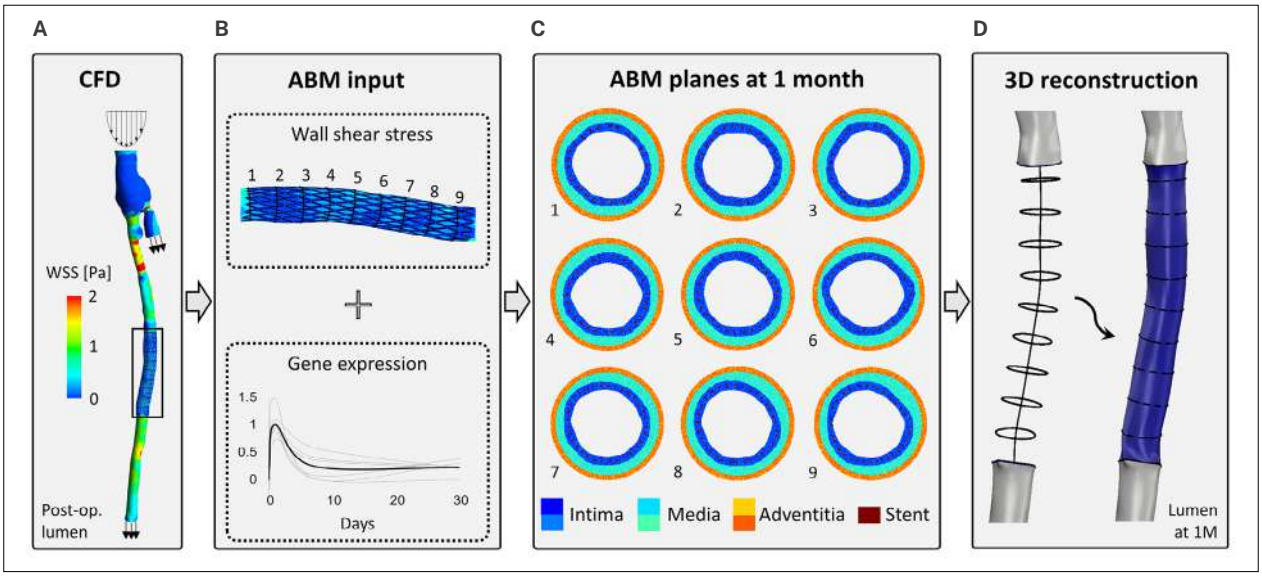

Figure 4: Workflow of a multiscale agent-based computational framework of in-stent restenosis in superficial femoral arteries, able to link hemodynamics, monocyte gene expression and cellular dynamics.

A) A computational fluid dynamics simulation (CFD) of a patient-specific stented superficial femoral artery is performed to compute the wall shear stress (WSS) along the stented segment.

B) The WSS profile for each selected cross-sectional plane within the stented region as well as monocyte gene expression data are used to initialize two-dimensional agent-based models (ABMs) simulating the arterial wall remodeling after stent implantation.

C) ABM-simulated intimal regrowth at 1-month follow-up. All cross-sectional planes are characterized by increased intima thickness with coverage of the stent struts, caused by perturbed cell and extracellular matrix activities, while media and adventitia preserve their initial areas.

D) The ABMs are stopped. The vessel geometry is updated by reconstructing the lumen from the ABM outputs at 1-month follow-up. Then, a new CFD analysis can be performed considering the updated vessel geometry and the entire cycle can be repeated for simulating the time period of interest.

To develop the framework, the CT images (at 1 week and 1 month after the intervention) and monocyte gene expression (measured at 1 hour before, and 2 hours, 1, 7 and 28 days after intervention) of one case of diseased SFA treated with self-expanding stent at the Malcom Randall VA Medical Center (Gainesville, FL, USA) were considered. The study was conducted in accordance with the ethical standards of the local institutional review board, and with the 1964 Helsinki Declaration and its later amendments. Informed consent was obtained from the patient. A 3D stented SFA geometry was reconstructed from the CT images using a validated reconstruction algorithm[21] and the stent was deployed with morphing procedure. A steady-state CFD simulation was performed with Fluent (Ansys Inc., USA) to compute the average hemodynamics along the stented area (Figure 4A), extracting the WSS at specific equally-spaced vessel

cross-sections (Figure 4B). A two-dimensional ABM simulating the arterial wall remodeling by replicating cell and ECM dynamics was implemented in Matlab (MathWorks, USA) for each cross-section (Figure 4C). Each ABM was generated on a hexagonal grid and filled with smooth muscle cells, fibroblasts, ECM, and stent strut agents. The behavior of cell and ECM agents was simulated by assigning probabilistic rules to the following events: cell mitosis/apoptosis and ECM production/degradation. Constant activities were set in the media and adventitia layers to preserve homeostasis.[33] Cell mitosis and ECM production in the intima depended on the local WSS and patient-specific gene expression. Specifically, only those genes for which a statistically significant correlation was found with the intervention outcome were used as input of the ABM.[40,41] The process of intimal growth was preliminary simulated for a time period of 1 month (Figure 4C). After that period, the ABM simulations were stopped and an updated vessel geometry was reconstructed by smoothly connecting the ABM lumen contours at 1 month (Figure 4D). Potentially, new CFD simulations can be performed and the cycle can be then repeated to simulate the arterial wall remodeling for longer time periods.

Despite the work being preliminary and a validation of the model is still ongoing, the proposed framework was able to capture the process of intimal growth in a patient-specific stented region at 1-month follow-up in response to different stimuli (Figure 4C-D). In perspective, the application of such a framework to other patient-specific cases will enable elucidating the role and the interdependence of the different factors promoting ISR in femoral arteries.

Conclusions and future perspectives

This chapter reviewed the recent CFD studies that have sought to establish a direct link between the post-stenting altered hemodynamics and ISR in femoral arteries. Furthermore, it provided an overview about multiscale computational approaches that could allow elucidating the underlying pathological mechanisms, by integrating biological and biomechanical stimuli at different spatiotemporal scales.

The number of patient-specific hemodynamic studies in the context of femoral arteries is still limited. In addition to the studies reported in Table 1, it is worth mentioning those by Conti *et al.*[42] and Ferrarini *et al.*[43]. However, here the focus was on the relationship between hemodynamics and thrombus formation after stent-graft placement rather than hemodynamics and ISR. Moreover, the clinical dataset analyzed in each study was small (20 lesions in Gokgol *et al.*[19] and 10 lesions in Colombo *et al.*[20,22]). Thus, further investigations on larger datasets are strongly required to confirm the present findings.

Further experimental research, in tandem with computational multiscale modeling, is required to better understand the hemodynamic-driven mechanisms leading to ISR of femoral arteries. Future experimental and modeling work should seek to address some of the limitations highlighted here by considering the analysis of interactions, cause-effect relationships, feedback mechanisms and cascade signaling pathways across different spatial and temporal scales. Ideally, to assess the credibility of the computational models, future experimental protocols should allow quantitative comparison with the simulation outputs. In this way, it will be possible to confirm the potential of computational models as a tool able to (i) elucidate the mechanistic link between hemodynamic disturbances and clinical outcomes after femoral artery stenting, (ii) provide patient-specific predictions of the risk of ISR, and (iii) support the design, optimization and evaluation of femoral artery stents.

Acknowledgements

This work has been supported by Fondazione Cariplo, Italy (Grant number 2017-0792, TIME). The authors are grateful to Jared M. Rozowsky, Dr. Yong He and Prof. Scott Berceli (University of Florida, Gainesville, FL, USA) for their contribution to the multiscale agent-based modeling framework.

References

1. Aboyans V, Ricco J, Bartelink M, Björck M, Brodmann M, Cohnert T, *et al.* 2017 ESC Guidelines on the Diagnosis and Treatment of Peripheral Arterial Diseases, in collaboration with the European Society for Vascular Surgery (ESVS). *Eur Heart J* 2018; 39: 763-816.

2. Kim W, Choi D. Treatment of Femoropopliteal Artery In-stent Restenosis. *Korean Circ J* 2018; 48: 191-7.

3. Chaabane C, Otsuka F, Virmani R, Bochaton-Piallat ML. Biological responses in stented arteries. *Cardiovasc Res* 2013; 99: 353-63.

4. Marx S, Totary-Jain H, Marks A. Vascular smooth muscle cell proliferation in restenosis. *Circ Cardiovasc Interv* 2011; 4: 104-11.

5. Welt FG, Rogers C. Inflammation and restenosis in the stent era. *Arter Thromb Vasc Biol* 2002; 22: 1769-76.

6. Chung I, Gold H, Schwartz S, Ikari Y, Reidy M, Wight T. Enhanced extracellular matrix accumulation in restenosis of coronary arteries after stent deployment. *J Am Coll Cardiol* 2002; 40: 2072-81.

7. Shlofmitz E, Iantorno M, Waksman R. Restenosis of Drug-Eluting Stents: A New Classification System Based on Disease Mechanism to Guide Treatment and State-of-the-Art Review. *Circ Cardiovasc Interv* 2019; 12: e007023.

8. Koskinas KC, Chatzizisis YS, Antoniadis AP, Giannoglou GD. Role of endothelial shear stress in stent restenosis and thrombosis: Pathophysiologic mechanisms and implications for clinical translation. *J Am Coll Cardiol* 2012; 59: 1337-49.

9. Wang J, Jin X, Huang Y, Ran X, Luo D, Yang D, *et al.* Endovascular stent-induced alterations in host artery mechanical environments and their roles in stent restenosis and late thrombosis. *Regen Biomater* 2018; 5: 177-87.

10. Ng J, Bourantas C V., Torii R, Ang HY, Tenekecioglu E, Serruys PW, *et al.* Local hemodynamic forces after stenting: implications on restenosis and thrombosis. *Arterioscler Thromb Vasc Biol* 2017; 37: 2231-42.

11. Zun PS, Narracott AJ, Chiastra C, Gunn J, Hoekstra AG. Location-specific comparison between a 3D in-stent restenosis model and micro-CT and histology data from porcine *in vivo* experiments. *Cardiovasc Eng Technol* 2019; 10: 568-82.

12. Nolan DR, Lally C. An investigation of damage mechanisms in mechanobiological models of in-stent restenosis. *J Comput Sci* 2018; 24: 132-42.

13. Tahir H, Bona-Casas C, Hoekstra AG. Modelling the effect of a functional endothelium on the development of in-stent restenosis. *PLoS One* 2013; 8: e66138.

14. Hwang M, Garbey M, Berceli S, Tran-Son-Tay R. Rule-based simulation of multi-cellular biological systems-A review of modeling techniques. *Cell Mol Bioeng* 2009; 2: 285-94.

15. Glen C, Kemp M, Voit E. Agent-based modeling of morphogenetic systems: Advantages and challenges. *PLoS Comput Biol* 2019; 15: e1006577.

16. Tahir H, Hoekstra AG, Lorenz E, Lawford P V, Hose DR, Gunn J, *et al.* Multi-scale simulations of the dynamics of in-stent restenosis: impact of stent deployment and design. *Interface Focus* 2011; 1: 365-73.

17. Tahir H, Bona-Casas C, Narracott A, Iqbal J, Gunn J, Lawford P, *et al.* Endothelial repair process and its relevance to longitudinal neointimal tissue patterns: comparing histology with in silico modelling. *J R Soc Interface* 2014; 11: 20140022.

18. Zun P, Anikina T, Svitenkov A, Hoekstra A. A comparison of fully-coupled 3D in-stent restenosis simulations to *in-vivo* data. *Front Physiol* 2017; 8: 284.

19. Gökgöl C, Diehm N, Räber L, Büchler P. Prediction of restenosis based on hemodynamical markers in revascularized femoro-popliteal arteries during leg flexion. *Biomech Model Mechanobiol* 2019; 18: 1883-93.

20. Colombo M, He Y, Corti A, Gallo D, Ninno F, Casarin S, *et al.* In-Stent Restenosis Progression in Human Superficial Femoral Arteries: Dynamics of Lumen Remodeling and Impact of Local Hemodynamics. *Ann Biomed Eng* 2021; 49; 2349-64..

21. Colombo M, Bologna M, Garbey M, Berceli S, He Y, Rodriguez Matas JF, *et al.* Computing patient-specific hemodynamics in stented femoral artery models obtained from computed tomography using a validated 3D reconstruction method. *Med Eng Phys* 2020; 75: 23-35.

22. Colombo M, He Y, Corti A, Gallo D, Casarin S, Rozowsky JM, *et al.* Baseline local hemodynamics as predictor of lumen remodeling at 1-year follow-up in stented superficial femoral arteries. *Sci Rep* 2021; 11: 1613.

23. Chiastra C, Migliori S, Burzotta F, Dubini G, Migliavacca F. Patient-Specific Modeling of Stented Coronary Arteries Reconstructed from Optical Coherence Tomography: Towards a Widespread Clinical Use of Fluid Dynamics Analyses. *J Cardiovasc Transl Res* 2018; 11: 156-72.

24. Colombo M, Luraghi G, Cestariolo L, Ravasi M, Airoldi A, Chiastra C, *et al.* Impact of lower limb movement on the hemodynamics of femoropopliteal arteries: A computational study. *Med Eng Phys* 2020; 81: 105-17.

25. Qu Z, Garfinkel A, Weiss J, Nivala M. Multi-scale modeling in biology: how to bridge the gaps between scales? *Prog Biophys Mol Biol* 2011; 107: 21-31.

26. Kesić S. Systems biology, emergence and antireductionism. *Saudi J Biol Sci* 2016; 23: 584-91.

27. Mazzocchi F. Complexity and the reductionism-holism debate in systems biology. *Wiley Interdiscip Rev Syst Biol Med* 2012; 4: 413-27.

28. Kohl P, Crampin E, Quinn T, Noble D. Systems biology: an approach. *Clin Pharmacol Ther* 2010; 88: 25-33.

29. Walpole J, Papin J, Peirce S. Multiscale computational models of complex biological systems. *Annu Rev Biomed Eng* 2013; 15: 137-54.

30. Bonabeau E. Agent-based modeling: methods and techniques for simulating human systems. *Proc Natl Acad Sci* 2002; 99: 7280-7.

31. An G, Mi Q, Dutta-Moscato J, Vodovotz Y. Agent-based models in translational systems biology. *Wiley Interdiscip Rev Syst Biol Med* 2009; 1: 159-71.

32. Bhui R, Hayenga HN. An agent-based model of leukocyte transendothelial migration during atherogenesis. *PLOS Comput Biol* 2017; 13: e1005523.

33. Corti A, Chiastra C, Colombo M, Garbey M, Migliavacca F, Casarin S. A fully coupled computational fluid dynamics–agent-based model of atherosclerotic plaque development: Multiscale modeling framework and parameter sensitivity analysis. *Comput Biol Med* 2020; 118: 103623.

34. Garbey M, Casarin S, Berceli SA. A versatile hybrid agent-based, particle and partial differential equations method to analyze vascular adaptation. *Biomech Model Mechanobiol* 2019; 18: 29-44.

35. Garbey M, Casarin S, Berceli SA. Vascular adaptation: pattern formation and cross validation between an agent based model and a dynamical system. *J Theor Biol* 2017; 429: 163.

36. Caiazzo A, Evans D, Falcone JL, Hegewald J, Lorenz E, Stahl B, *et al.* A Complex Automata approach for in-stent restenosis: two-dimensional multiscale modelling and simulations. *J Comput Sci* 2011; 2: 9-17.

37. Boyle C, Lennon A, Early M, Kelly D, Lally C, Prendergast P. Computational simulation methodologies for mechanobiological modelling: a cell-centred approach to neointima development in stents. *Philos Trans A Math Phys Eng Sci* 2010; 368: 2919-35.

38. Boyle C, Lennon A, Prendergast P. In silico prediction of the mechanobiological response of arterial tissue: application to angioplasty and stenting. *J Biomech Eng* 2011; 133: 081001.

39. Zahedmanesh H, Van Oosterwyck H, Lally C. A multi-scale mechanobiological model of in-stent restenosis: deciphering the role of matrix metalloproteinase and extracellular matrix changes. *Comput Methods Biomech Biomed Engin* 2014; 17: 813-28.

40. DeSart K, O'Malley K, Schmit B, Lopez M, Moldawer L, Baker H, *et al.* Systemic inflammation as a predictor of clinical outcomes after lower extremity angioplasty/stenting. *J Vasc Surg* 2016; 64: 766-78.e5.

41. Rehfuss J, DeSart K, Rozowsky J, O'Malley K, Moldawer L, Baker H, *et al.* Hyperacute Monocyte Gene Response Patterns Are Associated With Lower Extremity Vein Bypass Graft Failure. *Circ Genomic Precis Med* 2018; 11: e001970.

42. Conti M, Ferrarini A, Finotello A, Salsano G, Auricchio F, Palombo D, *et al.* Patient-specific computational fluid dynamics of femoro-popliteal stent-graft thrombosis. *Med Eng Phys* 2020; 86: 57-64.

43. Ferrarini A, Finotello A, Salsano G, Auricchio F, Palombo D, Spinella G, *et al.* Impact of leg bending in the patient-specific computational fluid dynamics of popliteal stenting. *Acta Mech Sin* 2021; 37: 279-91.

Growth assessment of Engineered Vascular Grafts and Heart Valves

41

Zeeshan H. SYEDAIN, Robroy MACIVER, Robert T. TRANQUILLO

Growth is the holy grail of tissue implants in pediatrics. Following a perspective on what is the appropriate definition of growth for a pediatric tissue implant, preclinical and clinical pediatric studies of implanted vascular grafts (unvalved conduits) and heart valves (valved conduits) are reviewed with respect to a proposed definition based on functional regenerative growth. Metrics of growth from these studies are tabulated for comparison. Analysis reveals substantial evidence for regenerative tissue growth among the various methods used.

Introduction

Growth is the holy grail of tissue implants in pediatrics. In the absence of implant growth, most simply defined as an increase in physical size over time, the patient must undergo consecutive surgeries to upsize the implant to match their somatic growth and metabolic demand. In the case of implants for congenital heart disease, this necessitates recurrence of open-heart surgery that presents repeated trauma to the patient as multiple cardiovascular bypass episodes and extensive post-operative care amounting to multiple significant interruptions of normal growth and development. These are compelling factors for developing implants with growth capacity even if risk is not clearly increased with subsequent sternotomies[1,2]. Table 1 summarizes procedures that could benefit from an implanted material possessing growth capacity and degeneration/ calcification resistance[3]. This includes valved and unvalved conduits, and vascular and cardiac patches. Beyond reduction of patient morbidity and mortality risk of multiple open-heart surgeries, grafts that grow would present a substantial cost savings to the healthcare system.

Growth must be further delineated and defined. A key distinction in growth of implants for congenital tissue defect repair is “somatic growth” *versus* “growth accommodation”. Somatic growth can be defined as an increase in physical size (dimensions) and mass of the implant due to activity of cells within the implant, implying growth of tissue. In contrast, growth accommodation is simply an increase in size of the implant that accommodates growth of the surrounding anatomy, with no requirement for mass increase or cellular activity within the implant, that is, no tissue growth. For example, Feins *et al.* reported a growth-accommodating valve annuloplasty ring comprising a biodegradable core and a tubular braided sleeve. The biodegradable core constrains the diameter of the sleeve, and gradual core degradation following implantation enabled sleeve and overall ring elongation to accommodate growth of the tricuspid valve annulus in piglets[4]. Though an impressive application of growth accommodation, most congenital heart defect repairs would benefit from somatic growth that more closely simulates normal tissue growth regulation and hemodynamic properties.

Table 1: Number of Procedures/Repairs in the 2015-2018 STS Database by Category*

Procedure/Repair	N
Vasculoplasty	
VSD repair, Patch	7,577
ASD repair, Patch	3,814
AVC (AVSD) repair, Complete (CAVSD)	3,348
Coarctation repair, End to end, Extended	2,635
RVOT procedure	2,489
TOF repair, Ventriculotomy, Transannular patch	2,423
Aortic arch repair	2,349
PA, reconstruction (plasty), Branch, Central (within the hilar bifurcation)	2,280
Valved Conduit	
Valve replacement, Pulmonic (PVR)	1,682
Conduit placement, RV to PA	1,601
Non-Valved Conduit	
Fontan, TCPC, External conduit, Fenestrated	1,860
Fontan, TCPC, External conduit, Nonfenestrated	1,385
Other (Patch or Conduit)	
TAPVC repair	1,608
Aortic stenosis, Subvalvar, Repair	1,395
Superior Cavopulmonary anastomosis(es) + PA reconstruction	1,357
Conduit reoperation	1,047

* Data from: STS Congenital Heart Surgery Data Executive Summary, Primary Procedures, All Patients (Jan 2015 - Dec 2018)

A further distinction for somatic growth must be made. “Normal tissue growth”, as occurs in development, is tissue growth leading to normal composition, that is, concentrations and structure of constituents (cellular and extracellular matrix) and normal physico-chemical properties, such as stress-strain behavior. Hormonal regulation is key to normal tissue growth, and hormonal variation is a hallmark of development. “Regenerative tissue growth”, which is defined herein for growth of implants in repair of cardiovascular tissues, always entails a critical role of immune regulation [5] in addition to hormonal regulation. Biomechanicians distinguish tissue growth (mass increase) from remodeling (changes in properties) [6], but these both occur in both normal and regenerative tissue growth, and so this distinction is not discussed further.

Growth of implants for congenital heart defect repair entails regenerative tissue growth, for most repairs. Whereas normal tissue growth is well characterized, regenerative tissue growth is not; in fact, unintended consequences of regenerative growth can occur. For example, a physiological increase in diameter of an unvalved conduit resulting from increasing mass of collagen deposited by host cells that repopulate the conduit is not a desired outcome if supra-physiological stiffness with sequalae of anastomotic intimal hyperplasia results. Other examples of undesirable outcomes peculiar to pediatrics include a supra-physiological increase in diameter of the conduit despite physiological wall thickness and physiological stiffness of the developing tissue, or, a rate of diameter increase that lags or leads the adjacent vessel. These outcomes could compromise function by creating adverse pressure gradients across the conduit and associated adverse wall shear stresses.

Thus, it is important to define and delineate the preservation of function in regenerative tissue growth. "Functional growth" is defined as regenerative growth that preserves tissue function even if histological structure is not completely normal. As examples, the diameter of the conduit increases at a physiological rate and the stiffness/compliance is physiological even though the tissue does not possess the normal concentration of elastin, or, the elastin is not organized as normal lamellae. While the stress-strain behavior of the tissue (and pressure-diameter behavior of the conduit) would almost surely be different from the average behavior of the target vessel in this example, it is sufficiently similar to yield the required function – distention and recoil comparable to the adjacent vessel (and without tissue failure, of course). While there is ambiguity with this definition, it conveys what most would consider to be successful regenerative tissue growth:

i. the implant increases in critical physical dimension(s) at normal developmental rate

ii. the increase occurs via tissue growth (increase in mass of tissue)

iii. the implant maintains required function

As specific cardiovascular implant examples, required function would be acceptable pressure gradient for non-valved conduits, and acceptable systolic gradient and insufficiency in the case of valved conduits. Notably, the tissue does not necessarily attain normal composition and physico-chemical properties in all respects, that is, does not necessarily become a normal tissue. Critical physical dimensions would be (lumen) diameter and length for non-valved conduits, and, in addition, leaflet area or leaflet height and free edge length for valved conduits. Thickness of the conduit wall (and leaflets) is not considered critical in terms of growth and would not necessarily increase to confer required function during growth of the host; in fact, thinning might result from regeneration of the implanted graft.

With that proposed definition to guide assessment of implant growth, pre-clinical and clinical studies of implants intended to exhibit growth (in children or growing large animals) are reviewed, first "tissue-engineered vascular grafts" (non-valved conduits) and then "tissue-engineered heart valves" (valved conduits). Note the proposed definition can be applied to the variety of implants used in these studies, including decellularized tissue grown *in vitro*, decellularized native tissues, and acellular and cell-seeded synthetic polymers. While the definition can be rigorously applied to pre-clinical studies, it cannot be fully applied to the clinical studies since all the conclusive evidence of tissue growth, including increase of mass of the implant due to activity of cells within the implant, is unavailable without explantation. A recent, broader review of cardiovascular tissue engineering relevant to congenital heart defect repair is available [7]; here the focus is on the most recent data reported in children and large animal growth models for the various types of tissue-engineered vascular grafts and heart valves developed.

Tissue-engineered Vascular Graft studies

The published preclinical (large animal) and clinical (pediatric) studies of tissue-engineered vascular graft (TEVG) relevant for growth potential are summarized in Table 2. When available, graft diameter and length are presented based on imaging conducted immediately post-implantation and at the longest timepoint. Four methods in terms of graft types are encompassed, illustrated in Figure 1:

(G1) a resorbable polymer graft (PGA fiber mesh embedded with a PCL/PLLA co-polymer matrix) seeded with autologous BMMC, both preclinical [8, 9] and clinical [9, 10] studies,

(G2) a degradable polymer graft (PGA fiber mesh coated with P4HB) sequentially seeded with autologous myofibroblasts and endothelial cells implanted in growing sheep [11],

(G3) an acellular resorbable graft (chain-extending PCL) in clinical study [12], and

(G4) a collagenous matrix from a decellularized donor fibroblast tissue grown *in vitro* implanted in growing sheep [13]; see Figure 2 for an example image.

While G1, G2 & G4 all used a growing sheep model, they also are distinguished by the anatomical location for the interpositional grafting: the inferior vena cava for G1 and G3, and the main pulmonary artery for G2 and G4. G4 is also distinguished both in being a biological matrix and acellular at implantation.

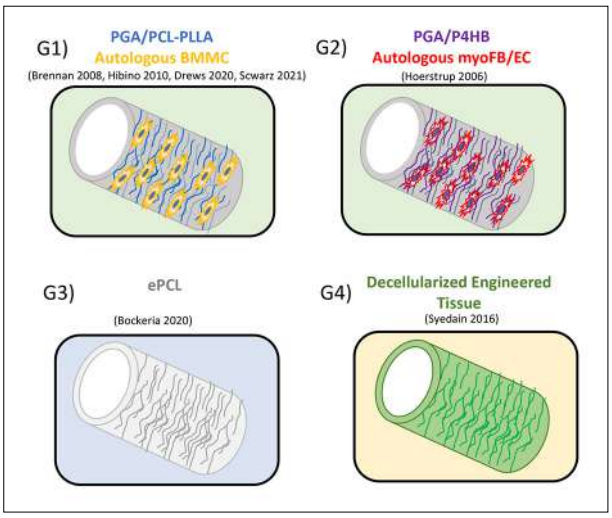

Figure 1: Illustration of methods for the TEVG reviewed:

(G1) a resorbable polymer graft (PGA fiber mesh embedded with a PCL/PLLA co-polymer matrix) seeded with autologous BMMC, both preclinical (Brennan 2008, Drews 2020) and clinical (Hibino 2010, Schwarz 2021) studies,

(G2) a degradable polymer graft (PGA fiber mesh coated with P4HB) sequentially seeded with autologous myofibroblasts and endothelial cells implanted in growing sheep (Hoerstrup 2006),

(G3) an acellular resorbable graft (chain-extending PCL) in clinical study (Bockeria 2020), and

(G4) a collagenous matrix from a decellularized donor fibroblast tissue grown in vitro implanted in growing sheep (Syedain 2016).

Figure 2: Photograph of a TEVG produced using G4, a tube of collagenous matrix from a decellularized donor fibroblast tissue grown in vitro (Syedain 2016).

Regarding preclinical studies, they all present evidence of collagen deposition over the duration (ranging from 26 to 100 weeks of maximum duration) and so meet the criterion of tissue growth, but the difference in anatomical location (and associated hemodynamic factors) might explain, in part, the differences in growth based on the criterion of increase in critical dimension. In terms of graft diameter, there was an increase of 30% reported for G2 and 50% reported for G4 for their grafts implanted into the main pulmonary artery over 100 and 42 weeks, respectively, but a transient stenosis without recovery of the initial diameter over 52 weeks reported for G[19], an occurrence not reported in their earlier study (8). Only G2 and G4 reported the (longitudinal) modulus of the explanted grafts, which were ~9 MPa and ~1.5 MPa (circumferential), respectively, comparable to ~1 MPa for the native pulmonary artery also measured in G4. In terms of graft length, increases of 49% and 130% were reported by G2 and G4, respectively.

Regarding clinical studies, the preclinical results of G1 using the PGA - PCL/PLLA graft seeded with autologous BMMC align with the clinical results of G1 to date as a Fontan conduit. There were some occurrences of graft stenosis in both patients and sheep[9,14] with a 45% graft diameter decrease relative to 6 months post-op after 5 years in patients[10] and a 0.37-fold change (decrease) in graft diameter over 52 weeks in sheep[9]. However, a 13.9% increase in the graft length occurred after 5 years in patients[10]. In a prior clinical study of G1 as a Fontan conduit, there was a 3% graft diameter increase relative to one year post-op after a mean follow-up of 5.8 years in patients[14], noting the abstract of an earlier report of the same clinical trial states a mean 10% increase of the graft diameter over the implanted value during a mean follow-up of 490 days[15], and the graft length increased by 52.3% over 10 years for one reported patient[9]. Importantly, although no graft diameters are reported in the most recent report of this 25 patient cohort after a mean follow-up of 11.1 years to assess graft growth, still no graft-related deaths have occurred. The clinical results of G3 to date, also as a Fontan conduit, indicate a 6.9% increase in graft diameter from 12 months to 24 months[12]; graft lengths were not reported.

Table 2: TEVG Growth Studies

	Preclinical Studies			
Method	G1	G1	G2	G4
Study	Brennan (2008)	Drews (2020)	Hoerstrup (2006)	Syedain (2016)
Species	sheep	sheep	sheep	sheep
Age / Weight at Implantation	n/a ("juvenile")	n/a ("juvenile")	28 kg	15 kg (8 wk)
Implantation Site	intrathoracic IVC (interposition)	intrathoracic IVC (interposition)	main PA (interpositional)	main PA (interpositional)
Initial Graft Composition	Non-woven PGA fibers embedded with a PCL/PLLA copolymer porous matrix	PGA fibers embedded with a PCL/PLLA copolymer porous matrix	nonwoven polyglycolic-acid (PGA) mesh heat wielded to poly-4-and coated with hydroxybutyrate (P4HB)	decellularized donor fibroblast matrix grown in vitro
Initial Cell Content	autologous bone marrow mononuclear cells (1M cells/cm^2)	autologous bone marrow mononuclear cells (1400M cells/ graft)	autologous-myofibroblasts (5M cells/cm^2) and endothelial cells (1M cells/cm^2) seeded sequentially	none

Implant Duration (longest)	26 wk	52 wk	100 wk (> 2x animal weight gain)	42 wk
Initial Graft Diameter	13 mm (pre-implant)	n/a	18 mm (pre-implant)	16 mm (pre-implant)
"Final" Graft Diameter	n/a (127% increase in graft volume by MRI at 6mo over 1mo[1]) (n=6)	0.37 fold decrease (n=14)	(30% increase by CTA at 100wk over 20wk[4]) (n=4)	24 mm (50% increase by TTE at 50wk over 8wk[6]) (n=3)
Initial Graft Length	30 mm	130 mm	~17.5 mm	16-19 mm
"Final" Graft Length	n/a	n/a	~25 mm (45% increase by TEE at 100wk over p.o.[5]) (n=4)	37-41 mm (130% increase by TTE at 50wk over 8wk[7]) (n=3)
Initial Graft Wall Thickness	1.5mm (pre-implant)	1.5 mm^2 (1wk IVUS)	1mm (pre-implant)	1.2 mm (pre-implant)
"Final" Graft Wall Thickness	1.1 mm	1.9 mm^3 52wk IVUS)	n/a	0.85 mm
Increase in ECM Content	(0) to 21 µg HPRO / mg dry weight	(apparent from histology)	~5 to ~50 µg HPRO / mg dry weight	111% / 465% increase in graft collagen concentration / content

[1] Figure 1 related text / [2] Table S6, for the 14 animals with 1wk and 52wk values / [3] Table S6, for the 14 animals with 1wk and 52wk values / [4] Figure 4 and related text / [5] Figure 4 and related text / [6] Table 1 / [7] Table 1

Table 2: TEVG Growth Studies

	Clinical Studies		
Method	G1	G3	G1
Study	Hibino (2010)	Bockeria (2020)	Schwarz (2021)
Species	human	human	human
Age / Weight at Implantation	1-24 years (mean 7.3 years)	4–12 years (mean 6.2 years)	
Implantation Site	extracardiac total cavopulmonary connection (Fontan conduit)	extracardiac total cavopulmonary connection (Fontan conduit)	extracardiac total cavopulmonary connection (Fontan conduit)
Initial Graft Composition	polyglycolic acid (PGA) or poly-L-lactide (PLLA) woven fabric embedded with a poly caprolactone (PCL) and PLLA copolymer porous matrix	Fiber matrix of chain-extending PCL with 2-ureido-4[1H]-pyrimidinone	PGA fibers embedded with a PCL/PLLA copolymer porous matrix
Initial Cell Content	autologous bone marrow mononuclear cells (0.32M cells/cm^2)	none	autologous bone marrow mononuclear cells (340M cells/graft)

Implant Duration (longest)	4.3–7.3 yr (mean 5.8 yr)	2 yr	5 yr
Initial Graft Diameter	12–24 mm (mean 17.2 mm at Y1)[8]	18-/ 20 mm (pre-implant)	16-18 mm (pre-implant)
"Final" Graft Diameter	12–24 mm (mean 17.7 mm) [9] (n=21)	18-20 mm [11] (6.9% increase by MRI [12] and 5% decrease by TTE at 24mo over 12mo [13]) (n=5)	8.8-11.5 mm [15] (minimum diameter) (45% decrease by MRI at 60mo over 6mo [16]) (n=4)
Initial Graft Length	32.5 (n=1)	n/a	33-40 mm
"Final" Graft Length	49.4 (52% increase by angiography over 10yr [10]) (n=1)	n/a	36-45 mm (13.9% increase by MRI at 60mo over 6mo [17]) (n=4)
Initial Graft Wall Thickness	0.6-0.7 mm (pre-implant)	n/a	0.7 mm (pre-implant)
"Final" Graft Wall Thickness	n/a	0.5 mm (7% increase by TTE [14] at 24mo over 12mo)	n/a
Increase in ECM Content	n/a	n/a	n/a

[8] Table 1, for the 21 of 25 surviving patients at late-term / [9] Table 2, for the 21 of 25 surviving patients at late-term / [10] Fig. S13 of Drews (2020) / [11] Table 3, for the 4 patients with 12mo and 24mo values / [12] Table 3, for the 4 patients with 12mo and 24mo values / [13] Table 2, for the 4 patients with 12mo and 24mo values / [14] Table 2, for the 4 patients with 12mo and 24mo values / [15] Table 1 (for the 3 patients with 60mo values) / [16] Figure 2b (estimated) / [17] Figure S2c,d (based on reported average slope)

Tissue-engineered Heart Valve Studies

The published preclinical (large animal) and clinical (pediatric) studies of tissue-engineered heart valve (TEHV) relevant for growth potential are summarized in Table 3. Four methods in terms of graft types are encompassed, illustrated in Figure 3:

(V1) a decellularized pulmonary valve allograft implanted in growing sheep [16],

(V2) a valve constructed from porcine small intestinal submucosa (SIS) implanted in growing baboons [17],

(V3) an acellular resorbable polymer valve (chain-extending PCL and PC) in pediatric clinical trial [18], and

(V4) a valve constructed from tubes of collagenous matrix from a decellularized donor fibroblast tissue grown *in vitro* implanted in growing sheep [19]; see Figure 4 for an example image.

V3 and V4 involve the same investigators utilizing the same material as for G3 and G4 for TEVG. V3 does not have a published preclinical study in a growth model to include in Table 3. V1 is also in pediatric clinical trial but the results are reported in aggregate for patients aged age 21.3 ± 14.4 years and valve diameter 24.4 ± 2.8 mm[20], and cannot be included here lacking stratification into a pediatric age group. A study reported for V1 focused on a pediatric population does not include comparative data needed for Table 2 and indicates that despite a successful long-term outcome, a z score tending to zero reflects minimal graft shrinkage and not real growth[21]. V4 is again distinguished both in being a biological matrix and acellular at implantation.

While V1 and V4 used a similar growing sheep model, they differ in the implant location (pulmonary annulus and pulmonary artery, resp.) and duration (80 weeks and 52 weeks, respectively). The difference in implant location and/or the differences between decellularized valve tissue and decellularized biologically-engineered tissue likely account for the greater increase in valve diameter (12% *vs.* 32%, resp.). While these two studies present data showing an increase in valve diameter, only V4 presents data showing an increase in leaflet dimensions (i.e. free edge length). None of the studies present data supporting leaflet growth per the proposed definition. All of the valves in these studies exhibited some level of insufficiency, although classified no worse than mild (index 2). Another key metric of valve function, mean systolic pressure gradient, was only reported in two of the studies, V3 and V4, which was clinically acceptable at 15.8 and 4.3 mmHg, respectively Thus, while the number of studies is small, the results to date are promising, but somatic growth potential of the valves, primarily regarding leaflet growth, has not been clearly demonstrated.

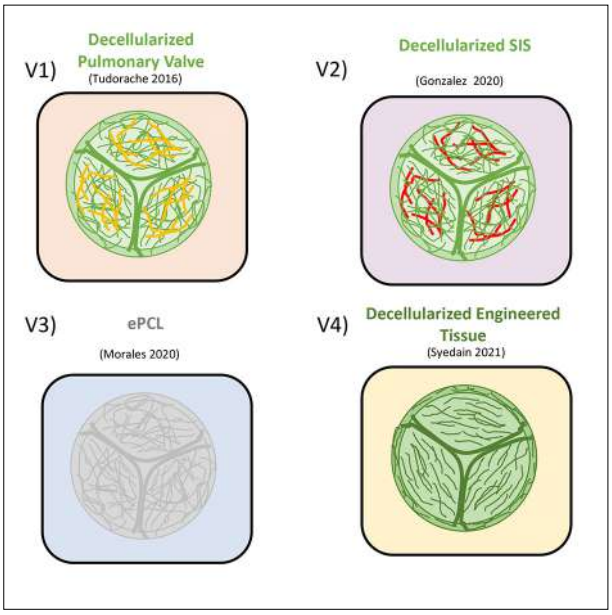

Figure 3: Illustration of lines of research for TEHV reviewed:

(V1) a decellularized pulmonary valve allograft implanted in growing sheep (Tudorache 2016),

(V2) a valve constructed from porcine small intestinal submucosa implanted in growing baboons (Gonzalez 2020),

(V3) an acellular resorbable polymer valve (chain-extending PCL and PC) in pediatric clinical trial (Morales 2020), and

(V4) a valve constructed from tubes of collagenous matrix from a decellularized donor fibroblast tissue grown in vitro implanted in growing sheep (Syedain 2021).

Figure 4: Photograph of a TEHV produced using V4, three tubes of collagenous matrix from a decellularized donor fibroblast tissue grown in vitro sewn together with degradable suture (Syedain 2021).

Table 3: TEHV Growth Studies : **Preclinical Studies and Clinical Studies**

	Preclinical Studies			Clinical Studies
Method	V1	V2	V4	V3
Study	Tudorachea (2016)	Gonzalez (2020)	Syedain (2021)	Morales (2020)
Species	sheep	babbon	sheep	human
Age / Weight at Implantation	25 ± 3.4 kg (n=5)	13.50 ± 0.76 mo (n=3)	3.5 mo 32 kg (n=3)	3 – 9 years (median 5 years) 14 to 29 kg (median 21 kg) (n=6)
Implantation Site	Pulmonary (valve replacement)	Mitral (valve replacement)	Main PA (interpositional, Gen2 design)	RVOT (valved pulmonary conduit, modified design)
Initial Graft Composition	decellularized pulmonary valve allograft	porcine small intestinal submucosa (PSIS), fatigued 2ply	decellularized donor ovine fibroblast matrix grown in vitro	wall PCL-UPy, leaflets PC-UPy 2-ureido-4[1H]-pyrimidone (UPy) polycaprolactone (PCL), polycarbonate (PC)
Initial Cell Content	none	none	none	none
Implant Duration (longest assessment timepoint)	80 wk (43.4 ± 10.6 kg)	11.6 wk (9.5% increase in BSA)	52 wk (79 kg)	48 wk
Initial Valve Diameter	17.0 ± 0.7 mm [1] (“implantation” TTE) (n=5)	n/a	19 mm (pre-implant)	16.6 mm [4] (7d TTE) (n=5)
“Final” Valve Diameter	19.0 ± 2.1 mm [2] (80wk TTE) (n=5)	n/a	25.3 mm (52wk TTE) (n=3)	17.0 mm [5] (48wk TTE) (n=5)
Initial Leaflet Area	n/a	n/a	n/a	n/a
“Final” Leaflet Area	n/a	n/a	n/a (27% increase in free edge length)	n/a
Initial Leaflet Thickness	n/a	110 µm	540 µm	n/a
“Final” Leaflet Thickness	n/a	n/a	490 µm	n/a
Increase in Leaflet ECM Content	n/a (recellularization by cells positive for intracellular pro-collagen type I)	n/a (“minimal infiltration of new cells”)	n/a (“leaflet cellularity ~33% of native leaflets”)	n/a

	Preclinical Studies			Clinical Studies
"Final" Leaflet Modulus	n/a	n/a	10 MPa (circumferential)	n/a
"Final" Mean Systolic Gradient		n/a	4.3 mm Hg (n=3)	15.8 mm Hg [6] (n=5)
"Final" Insufficiency Index	1.5 [3]	1.5 ("sporadic trivial to mild valve regurgitation") (n=3)	2	1.4 [7] (n=5)

[1] Table 1, DPVA group / [2] Table 1, DPVA group / [3] Table 1, DPVA group (conversion: <10=trace=1, 1o=mild=2, 2o= moderate=3) / [4] Table 1, Group 2 (RVOT diameter, see Fig. 4) / [5] Table 1, Group 2 (RVOT diameter, see Fig. 4) / [6] Table 1, Group 2 / [7] Table 1, Group 2 (conversion: none=0, trace=1, mild=2, moderate=3, severe=4)

Conclusions

There is no broadly accepted definition of growth in the context of an implant that is intended to grow. The proposed definition is a minimalist definition and does not address many other criteria that should be met, including immuno-, hemo-, and bio-compatibility, calcification-resistance, durability, and tissue integration; however, these are all related to the third criterion of maintaining required function.

This survey of the literature reveals few large animal preclinical studies of TEVG and TEHV in a growth model, and even fewer pediatric clinical trials accordingly. Comparisons across these studies, even with this minimalist definition, is very limited because of differences in the types of measurements reported compounded by the restricted nature of measurements in human trials compared to animal studies. Overall, more compelling evidence of growth exists in the preclinical studies compared to the clinical studies to date based on increase of diameter as the critical physical dimension. That may reflect the nature of the anatomical site and/or study durations further convoluted disparate growth rates among species; the substantial difference in growth rates between sheep and humans is a confounding variable for extrapolating most of the preclinical results to the clinical trials given the critical role of recellularization, which might be a limiting rate for implant regeneration in sheep relative to the (high) growth rate of sheep. That also may reflect graft diameter as the critical dimension, the only one reported across all studies for comparison, further complicated by limited information from trans thoracic echography relative to magnetic resonance imaging when grafts become non-circular post-implantation. The most recent clinical trial reporting shows growth results can be contradictory based on a single critical dimension, with an increase in length of Fontan grafts observed concurrently with a decrease in their diameter [10]. Interestingly, an increase in graft length occurred across all the studies reporting length despite graft diameter decreases in some studies.

Given the essential role of the immune system in tissue regeneration [5], another potential explanation for any difference between preclinical and clinical outcomes with the same graft are differences in the immune responses of humans and sheep to these regenerative implants. Note some studies reviewed lacked measurements to assess the proposed growth criterion of tissue growth (increase in mass of tissue), in which case successful regenerative tissue growth of the implant cannot be clearly distinguished from growth accommodation.

Most importantly, the clinical trials to date have positive outcomes overall and the preclinical studies portend achievement of successful regenerative tissue growth of valved and non-valved conduits. It is expected that regulatory approval of conduit implants will lead to their use in various vasculopathy applications as well, which would also benefit from a regenerative material that provides functional tissue growth.

Abbreviations

BMMC – Bone Marrow Mononuclear Cells
PC – Polycarbonate
PCL – Polycaprolactone
PGA – Poly(glycolic acid)
PLLA – Poly(lactic acid)
P4HB – Poly(4-Hydroxybutyrate)
STS – Society of Thoracic Surgeons
TEVG – Tissue-engineered Vascular Graft
TEHV – Tissue-engineered Heart Valve

Acknowledgements

The authors acknowledge funding from NIH R01 HL107572 (to R.T.T).

Declarations

ZS, RT: financial interest in Vascudyne, Inc., licensee of related University of Minnesota patents

References

1. Yin CH, Yan J, Li SJ, Li DY, Wang Q, Wang ES. Effect analysis of repeat sternotomy in pediatric cardiac operations. *J Cardiothorac Surg* 2015; 10: 179.

2. Jacobs JP, Mavroudis C, Quintessenza JA, Chai PJ, Pasquali SK, Hill KD, *et al.* Reoperations for pediatric and congenital heart disease: an analysis of the Society of Thoracic Surgeons (STS) congenital heart surgery database. *Semin Thorac Cardiovasc Surg Pediatr Card Surg Annu* 2014; 17: 2-8.

3. STS. Congenital Heart Surgery National Database. *The Society of Thoracic Surgeons* 2018.

4. Feins EN, Lee Y, O'Cearbhaill ED, Vasilyev NV, Shimada S, Friehs I, *et al.* A Growth-Accommodating Implant for Paediatric Applications. *Nat Biomed Eng* 2017; 1: 818-25.

5. Dziki JL, Huleihel L, Scarritt ME, Badylak SF. Extracellular Matrix Bioscaffolds as Immunomodulatory Biomaterials. *Tissue Eng Part A* 2017; 23: 1152-9.

6. Taber LA. Biomechanics of growth, remodeling, and morphogenesis. *Appl Mech Rev* 1995; 48: 487-545.

7. Blum KM, Mirhaidari GJM, Breuer CK. Tissue engineering: Relevance to neonatal congenital heart disease. *Semin Fetal Neonatal Med* 2021: 101225.

8. Brennan MP, Dardik A, Hibino N, Roh JD, Nelson GN, Papademitris X, *et al.* Tissue-engineered vascular grafts demonstrate evidence of growth and development when implanted in a juvenile animal model. *Ann Surg* 2008; 248: 370-7.

9. Drews JD, Pepper VK, Best CA, Szafron JM, Cheatham JP, Yates AR, *et al.* Spontaneous reversal of stenosis in tissue-engineered vascular grafts. *Sci Transl Med* 2020; 12: eaax6919.

10. Schwarz EL, Kelly JM, Blum KM, Hor KN, Yates AR, Zbinden JC, *et al.* Hemodynamic performance of tissue-engineered vascular grafts in Fontan patients. *NPJ Regen Med* 2021; 6: 38.

11. Hoerstrup SP, Cummings Mrcs I, Lachat M, Schoen FJ, Jenni R, Leschka S, *et al.* Functional growth in tissue-engineered living, vascular grafts: follow-up at 100 weeks in a large animal model. *Circulation* 2006; 114: I159-66.

12. Bockeria LA, Svanidze O, Kim A, Shatalov K, Makarenko V, Cox M, *et al.* Total cavopulmonary connection with a new bioabsorbable vascular graft: First clinical experience. *J Thorac Cardiovasc Surg* 2017; 153: 1542-50.

13. Syedain Z, Reimer J, Lahti M, Berry J, Johnson S, Tranquillo RT. Tissue engineering of acellular vascular grafts capable of somatic growth in young lambs. *Nat Commun* 2016; 7: 12951.

14. Hibino N, McGillicuddy E, Matsumura G, Ichihara Y, Naito Y, Breuer C, *et al.* Late-term results of tissue-engineered vascular grafts in humans. *J Thorac Cardiovasc Surg* 2010; 139: 431-6.

15. Shin'oka T, Matsumura G, Hibino N, Naito Y, Watanabe M, Konuma T, *et al.* Midterm clinical result of tissue-engineered vascular autografts seeded with autologous bone marrow cells. *J Thorac Cardiovasc Surg* 2005; 129: 1330-8.

16. Tudorache I, Theodoridis K, Baraki H, Sarikouch S, Bara C, Meyer T, *et al.* Decellularized aortic allografts *versus* pulmonary autografts for aortic valve replacement in the growing sheep model: haemodynamic and morphological results at 20 months after implantation. *Eur J Cardiothorac Surg* 2016; 49: 1228-38.

17. Gonzalez BA, Pour Issa E, Mankame OV, Bustillos J, Cuellar A, Rodriguez AJ, *et al.* Porcine Small Intestinal Submucosa Mitral Valve Material Responses Support Acute Somatic Growth. *Tissue Eng Part A* 2020; 26: 475-89.

18. Morales DL, Herrington C, Bacha EA, Morell VO, Prodan Z, Mroczek T, *et al.* A Novel Restorative Pulmonary Valve Conduit: Early Outcomes of Two Clinical Trials. *Front Cardiovasc Med* 2020; 7: 583360.

19. Syedain ZH, Haynie B, Johnson SL, Lahti M, Berry J, Carney JP, *et al.* Pediatric tri-tube valved conduits made from fibroblast-produced extracellular matrix evaluated over 52 weeks in growing lambs. *Sci Transl Med* 2021; 13: eabb7225.

20. Boethig D, Horke A, Hazekamp M, Meyns B, Rega F, Van Puyvelde J, *et al.* A European study on decellularized homografts for pulmonary valve replacement: initial results from the prospective ESPOIR Trial and ESPOIR Registry datadagger. *Eur J Cardiothorac Surg* 2019; 56: 503-9.

21. da Costa FDA, Etnel JRG, Torres R, Balbi Filho EM, Torres R, Calixto A, *et al.* Decellularized Allografts for Right Ventricular Outflow Tract Reconstruction in Children. *World J Pediatr Congenit Heart Surg* 2017; 8: 605-12.

Sponsors

We thank our sponsor for their financial support to the 12th European Symposium on Vascular Biomaterials.

DIAMOND

BD

BARD

GORE

GOLD

TERUMO Aortic

COOK MEDICAL

Boston Scientific
Advancing science for life™

caresyntax

relyens

SILVER

Medtronic
Further, Together

VYGON
Value Life

BRONZE

bioprotec
BANQUE DE TISSUS

BIOTRONIK
excellence for life

LSO Medical
Light Solution, Solution for Life

LeMaitre

Johnson & Johnson
MEDICAL DEVICES COMPANIES

Edwards Lifesciences

GETINGE

Bentley

START-UP

MedSynApps

BONE 3D
PERSONALIZED MEDICINE

Therenva
Share medical innovation

surgicalscience
Simbionix Simulators

OTHERS

STRASBOURG EVENTS.

Grand Est
ALSACE CHAMPAGNE-ARDENNE LORRAINE
L'Europe s'invente chez nous

STRASBOURG EUROPTIMIST

france BIOVALLEY
l'innovation santé

esvs

Freedom to find your fit.

Every patient has a different story. Each unique aorta, a unique challenge. Terumo Aortic empowers your team to collaborate with patient-driven solutions based on our preferred approach. With your expertise and our comprehensive portfolio, we help you find the right fit for your patient - and their aorta.

TERUMO Aortic

Continuing the pattern of PERFORMANCE

Continue to count on the GORE® EXCLUDER® Device family to help you move EVAR forward.

Built on a foundation of best-in-class ePTFE technology, proven outcomes data, and decades of real-world experience. Inspired by your commitment to performance.

Discover more:
goremedical.com/eu/excluder-family

NEW indication

GORE® EXCLUDER® Iliac Branch Endoprosthesis is now indicated for the use with **GORE® EXCLUDER® Conformable AAA Endoprosthesis with ACTIVE CONTROL System*.**

* The GORE® EXCLUDER® Conformable AAA Endoprosthesis with ACTIVE CONTROL System is CE Mark approved. Caution: Investigational device in United States. Limited by United States law to investigational use.

W. L. Gore & Associates, Inc. | Flagstaff, AZ 86004 | goremedical.com

Consult Instructions for Use
eifu.goremedical.com

Refer to *Instructions for Use* at eifu.goremedical.com for a complete description of all applicable indications, warnings, precautions and contraindications for the markets where this product is available. ℞ Only

Products listed may not be available in all markets.

GORE, ACTIVE CONTROL, EXCLUDER and designs are trademarks of W. L. Gore & Associates.
© 2020 W. L. Gore & Associates GmbH AY3363-EN2 DECEMBER 2020

GORE

WavelinQ™

EndoAVF System

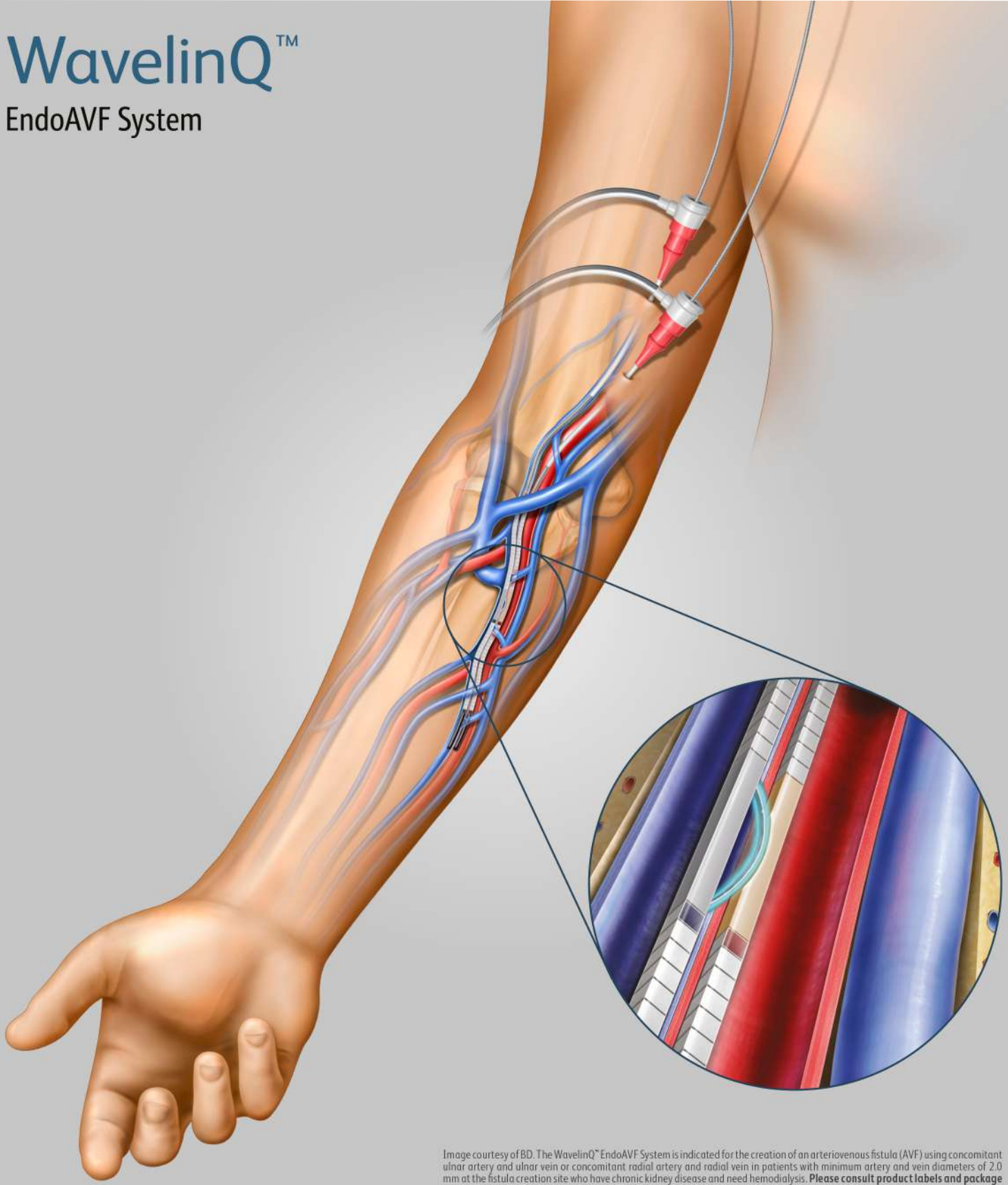

Image courtesy of BD. The WavelinQ™ EndoAVF System is indicated for the creation of an arteriovenous fistula (AVF) using concomitant ulnar artery and ulnar vein or concomitant radial artery and radial vein in patients with minimum artery and vein diameters of 2.0 mm at the fistula creation site who have chronic kidney disease and need hemodialysis. **Please consult product labels and package inserts for indications, contraindications, hazards, warnings, cautions, and information for use.**

crbard.com/peripheral-vascular | bd.com

BD, Tempe, AZ, USA, 1 800 321 4254

© 2020 BD. BD, the BD Logo, and WavelinQ are trademarks of Becton, Dickinson and Company or an affiliate. Illustrations by Mike Austin.
Copyright 2020.All Rights Reserved. BD-15658

BD

esvb 2021

12th european symposium on vascular biomaterials

NEW ENDOVASCULAR TECHNOLOGIES | FROM BENCH TEST TO CLINICAL PRACTICE

Freedom to find your fit.

Every patient has a different story. Each unique aorta, a unique challenge. Terumo Aortic empowers your team to collaborate with patient-driven solutions based on our preferred approach. With your expertise and our comprehensive portfolio, we help you find the right fit for your patient - and their aorta.

TERUMO Aortic

GEPROVAS

Groupe Européen de Recherche sur les Prothèses Appliquées à la Chirurgie Vasculaire

Published by: GEPROVAS Strasbourg, France
Realized by: Arborescence - Schiltigheim, France

All rights reserved. No part of this publication may be reproduced, stored in a retrieval system, or transmitted, in any form or by any means, electronic, mechanical, photocopying, recording, or otherwise, without either the prior written permission of the publishers.